This is to certify that the
dissertation entitled

THE DEVELOPMENT OF A NOVEL ASYMMETRIC
HALOLACTONIZATION
AND THE INVESTIGATION OF PEPTIDIC LIGANDS FOR OSMIUM
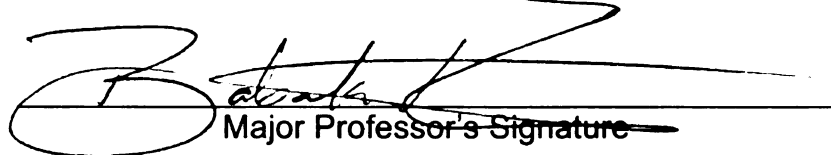TETROXIDE MEDIATED TRANSFORMATIONS

presented by

Daniel Charles Whitehead

has been accepted towards fulfillment
of the requirements for the

__Doctoral__   degree in   _____Chemistry_____

Major Professor's Signature

4/27/2009

Date

PLACE IN RETURN BOX to remove this checkout from your record.
TO AVOID FINES return on or before date due.
MAY BE RECALLED with earlier due date if requested.

DATE DUE	DATE DUE	DATE DUE

THE DEVELOPMENT OF A NOVEL ASYMMETRIC HALOLACTONIZATION
AND THE INVESTIGATION OF PEPTIDIC LIGANDS FOR OSMIUM
TETROXIDE MEDIATED TRANSFORMATIONS

VOLUME I

By

Daniel Charles Whitehead

A DISSERTATION

Submitted to
Michigan State University
in partial fulfillment of the requirements
for the degree of

DOCTOR OF PHILOSOPHY

Chemistry

2009

ABSTRACT

THE DEVELOPMENT OF A NOVEL ASYMMETRIC HALOLACTONIZATION AND THE INVESTIGATION OF PEPTIDIC LIGANDS FOR OSMIUM TETROXIDE MEDIATED TRANSFORMATIONS

By

Daniel Charles Whitehead

The work presented in this thesis includes the development of two novel

approaches towards the development of an organocatalytic asymmetric

halolactonization reaction of alkenoic acid starting materials. The first approach

(Chapter 2) focused on a combinatorial strategy whereby a number of peptide-

based bromoiodinane catalysts were prepared and screened as effective

catalysts for a novel bromolactonization of 4-phenylpentenoic acid. The optimal

catalyst system returned the desired chiral bromo-δ-lactone in up to 15% ee

when employed in 0.1 equivalents and 24% ee when employed in 1.11

equivalents.

On addressing the limitations of this first generation approach, an

analogous asymmetric chlorolactonization was developed, employing a $Cinchona$

alkaloid-based organocatalyst and N-chlorinated hydantoins as the terminal

chlorenium source (Chapter 3). This second generation strategy returned the

desired chloro-δ-lactones in good yield in up to 90% ee. A limited substrate

scope of several 4-substituted pentenoic acids was conducted. Additionally,

some initial mechanistic studies were conducted.

Furthermore, an operationally simple and expedient preparation of N-

chlorohydantoins was borne out of the chlorolactonization strategy.

Trichloroisocyanuric acid (TCCA) was found to promote the chlorination of various hydantoins (Chapter 4). Ten examples were prepared including three of the first known examples of chiral N-chlorohydantoins. Additionally, a compendium of hitherto scarce physical data was assembled for these compounds.

Chapter 5 describes efforts aimed at developing peptidic ligands for osmium tetroxide. A number of peptide β-turn sequences were prepared and screened as competent ligands for the asymmetric dihydroxlyation of α-methylstyrene. The peptides were screened under three separate co-oxidant systems, returning the desired glycol in excellent yields as the racemate.

Chapter 6 describes the extension of the oxidative cleavage of olefins with osmium tetroxide and oxone to include alternate osmium sources. Osmium trichloride, potassium osmate, polymer-bound osmium tetroxide, and OsEnCat proved effective in promoting the oxidative cleavage of a number of olefinic starting materials. Additionally, the ability to recycle OsEnCat was investigated.

For Kristi, who makes it all worthwhile.

ACKNOWLEDGEMENTS

There are a number of people who have helped me throughout my journey in graduate school. This thesis would be incomplete without conveying my heartfelt thanks for the help and support I have received.

First and foremost, I would like to thank my advisor, Babak Borhan. During my time in your lab I have learned a great deal from you, and much of who I am as a scientist is directly due to your influence. Thank you for helping me to learn how to think critically and to have the confidence to put my ideas into practice. I am particularly grateful for the freedom you granted me in allowing me to pursue my own ideas, both in the lab and in our research proposals. Thanks for everything you have done for me.

I would also like to thank the members of my committee: Professor Jetze Tepe, Professor William Wulff, and Professor Aaron Odom. Thank you for your guidance and support during my time here at MSU.

I am very proud to have been a member of one of the greatest groups, not only here at MSU but in the whole country. It has been my great pleasure to work with such a dedicated group of scientists. I have learned a great deal from each of you. Additionally, I have thoroughly enjoyed getting to know each of you. I will not soon forget the entertaining discussions we have had during our long hours in the lab together. I would particularly like to thank Chrysoula for keeping us all sane, Aman and Xiaoyong for keeping us laughing, and Roozbeh and Arvind for being good sports!

v

A number of people have been extremely helpful to me during the course of my studies. Particularly, I would like to thank Chrysoula and Sing for collecting lots of MALDI data, Aman for her marathon HRMS session, and Matt Fhaner for his considerable efforts in making a bunch of peptides. Additional thanks goes to Dr. Richard Staples, who has met only a few crystals he cannot solve!

I have been very lucky to make a number of friends during my studies here at MSU. In particular, Adam, Thu, Stewart, and Jason have become some of the closest friends I've ever had. Thank you all for the good times we've shared and the fun we've had together. The memories will last a lifetime. Thanks also for being a great support group during the difficult times too!

I would also like to extend my thanks to the Britton lab in the MMG department, my "second group". It has been a great pleasure to get to know all of you. Thanks for including me as one of your own at lab functions and parties. Particularly, I would like to thank Rob and Laura for your support and advice during these six years. Thanks also to Phil and Jess for keeping Kristi and me young!

I would also like to thank my family for their unwavering love and support. Thank you for making the countless trips across the country to visit us. You guys really made our graduate school experience much more bearable. Thank you for always believing in us! We love you both very much and can't wait to be closer to home!

Finally, I would like to thank my wonderful wife, Kristi. The eleven years we have spent together have been the greatest of my life. Thank you for your

support, for making me laugh, and for putting up with me! I cannot wait to see

where life will take us from here. What a great journey it has been so far. I love

you with all my heart!

TABLE OF CONTENTS

LIST OF TABLES

x

LIST OF FIGURES

Images in this dissertation are presented in color.

LIST OF SCHEMES

Chapter 1: A Brief Overview of Asymmetric Organocatalysis

1.1: Introduction

Asymmetric organocatalysis might be broadly defined as any transformation that is accelerated by the presence of a substoichiometric amount of a chiral small molecule promoter that is composed mainly of carbon, hydrogen, nitrogen, sulfur, or phosphorus. As opposed to transition metal-mediated transformations, the catalytic activity of organocatalysts is not dependent upon the presence of metal atoms to carry out the reaction.

Most, although not all, organocatalytic transformations can be roughly divided into two broad mechanistic manifolds, covalent or non-covalent catalysis.[1] Covalent catalysis proceeds by the formation of a covalent complex between a substrate or reagent and the organocatalyst, which on collapse effects the particular transformation in an asymmetric fashion. Scheme I-1 indicates three such interactions. Equation 1 depicts the covalent activation of acetone (I-2) by action of proline (I-1), so generating the activated enamine nucleophile I-3 as popularized by Barbas and List.[2-5] In contrast, equation 2 and 3 indicate the generation of chiral electrophiles by action of covalent catalysis. MacMillan's imidazolidinone catalyst of general type I-4, on reaction with α,β-unsaturated ketone I-5 generates the activated, chiral iminium ion I-6 (equation 3).[6,7] Alternatively, alkyl histidine containing peptides (I-7) popularized by Miller and co-workers participate in covalent catalysis by activating a reagent (in lieu of the substrate), thus generating the chiral acyl transfer catalyst I-9.[8-11]

Scheme I-1. Covalent asymmetric organocatalysis.
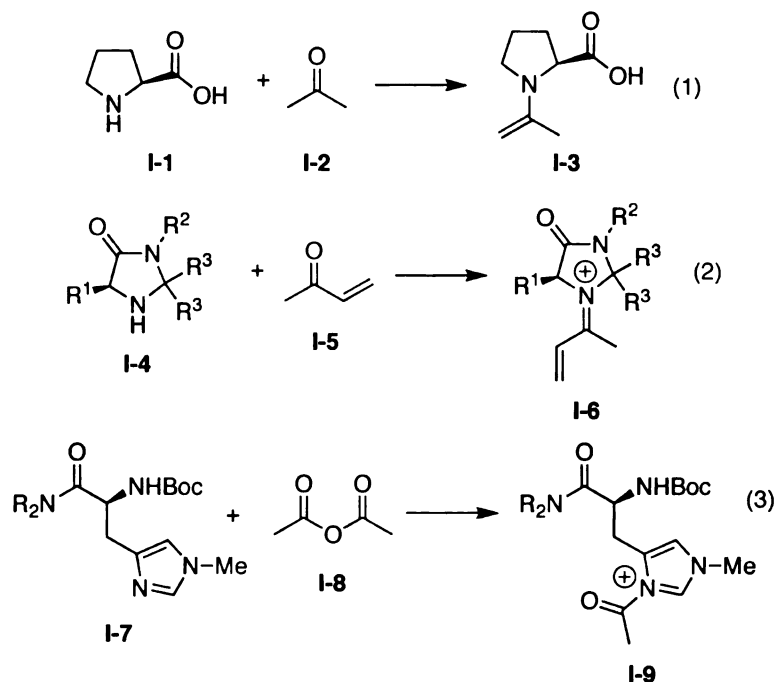
In addition to covalent catalysis, there are also a number of organocatalytic transformations that allow for asymmetric induction by non-covalent catalysis. Two examples are depicted in Scheme I-2. Thiourea catalysts **I-10**, popularized by Jacobsen and co-workers, activate various carbonyl-derived electrophiles by acting as hydrogen bond donors, in lieu of activation by the formation of covalent bonds.[12,13] The chiral H-bond governed complexes **I-12** serve to activate the electrophile, while shielding one prochiral face, allowing for asymmetric induction on interaction with an achiral nucleophile. Similarly, chiral phase transfer catalysts (PTCs) such as the alkylated cinchonidine derivative **I-13** developed by O'Donnell, govern the asymmetric

2

induction of various alkylation reactions by the formation of chiral ion pairs like complex I-15.[14]

Scheme I-2. Non-covalent organocatalysis.

$$(1)$$

$$(2)$$
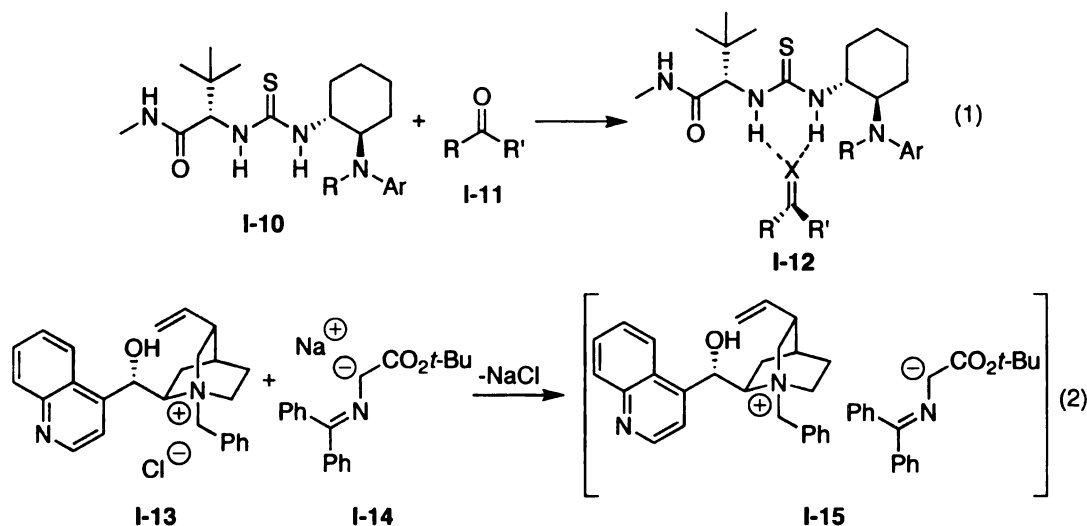
The majority of known asymmetric organocatalytic processes fit into one of these two catalytic domains. In each case, these two broad mechanistic considerations have paved the way for new, yet still related modes of catalysis. For example, MacMillan and co-workers have recently extended their iminium catalysis framework (**I-6**, Scheme 1, eq. 2), to include SOMO activation (*i.e.* singly occupied molecular orbital activation in lieu of LUMO activation).[15-17] Similarly, the Jacobsen group has recently introduced a new activation mode employing their thiourea catalysts (**I-10**) using chiral counterion catalysis.[18]

Although reported as early as 1912,[19] organocatalysis has only been a defined, active area of research since the late 1990s. Currently, however, the field is burgeoning, with at least 1500 manuscripts detailing over one hundred distinct transformations appearing in the relatively short period between 1998

3

and 2008.[7] Given the abundance of examples in the field, an exhaustive review of the prior art is beyond the scope of this chapter. In addition, a number of excellent and thorough books[1] and reviews[2,4,6,7,9,10,12,20-26] have recently appeared. The reader is directed to these publications in the event that the treatment herein is found lacking in certain areas. In the interest of brevity, the salient features of several of the most popular organocatalysts are illustrated with only a relatively few examples. In some cases, only seminal disclosures are illustrated as an overall paradigm for a particular set of organocatalysts, while in other cases the author has deferred to personal favorites within a particular subset of catalysts. Within this particular context, added emphasis has been placed on the most closely related catalyst systems to the ones developed during the course of the work described in this thesis (e.g. peptide and Cinchona alkaloid catalysis). As a trade-off, certain organocatalytic scaffolds will not be discussed, most notably the asymmetric epoxidation catalysts developed by Shi[27] and Yang,[28] as well as the planar DMAP catalysts developed by Fu and co-workers.[29] While not discussed herein, their contribution to the field of organocatalysis certainly warrants their mention.

1.2.1: Proline Enamine Catalysis

Since the very early days of organocatalysis, proline (I-1) has undoubtedly emerged as one of the most versatile catalyst scaffolds.[4,5,22] In 1971, two research groups independently reported that proline promoted an asymmetric cyclization of various di- and tri-ketones (e.g. I-16). The so-called Hajos-Parrish-

Eder-Sauer-Wiechert protocol[30,31] returned bicylic diketones like **I-17** in high yield

and enantiomeric excess (Scheme I-3, eq. 1). Interestingly, however, the broad

applicability of this strategy to more general intermolecular aldol condensations

did not emerge for another thirty years. In 2000, the analogous intermolecular

asymmetric aldol reaction mediated by proline was reported by List, Lerner, and

Barbas (Scheme I-3, eq. 2).[32] In this seminal report, acetone underwent the aldol

condensation with several aryl and alkyl aldehyde acceptors on activation with 30

mol% of proline. Aldol adducts such as **I-19** were generated in yields ranging

from 54 to 97% with enantioselectivities ranging from 60 to 96%. The

transformation is proposed to proceed via a closed transition state organized by

the proline carboxylic acid (see **I-20**). The crucial hydrogen bond between the

aldehyde acceptor and the carboxylic acid proton serves to properly orient and

activate the aldehyde for attack by the enamine nucleophile.[4]

Scheme I-3. Proline catalyzed intra and intermolecular asymmetric aldol reactions.
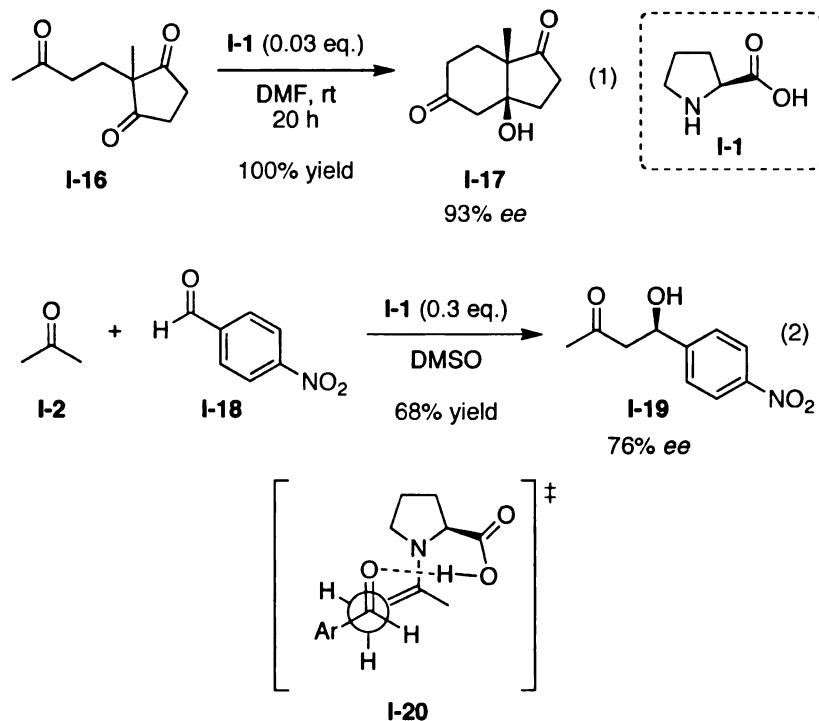
Since the initial disclosure by List, Lerner, and Barbas, a veritable

explosion of research by numerous groups has followed, resulting in the

application of the generalized approach to asymmetric transformations by

enamine catalysis to a number of organic transformations. Furthermore a

number of proline derivatives and analogs have been prepared and applied in

enamine based asymmetric processes. Figure I-1 indicates a few of the various

structural perturbations of the scaffold.

In addition to the expansion of the asymmetric inter and intramolecular

aldol reaction,[22] proline based catalysts have been employed subsequently in

related transformations such as the asymmetric Mannich and Michael reactions.[4]

Important strides have been made in applying both ketones and aldehydes as

enamine precursors, as well as applying a range of enamine acceptors including aldehydes, ketones, aldimines, ketimines, α,β-unsaturated carbonyl compounds, nitro-olefins, and vinyl sulfones.[4,22,25]

In addition to extensions of aldol-like processes, the asymmetric enamine catalysis afforded by proline and derivatives/analogues thereof has also been applied to various other asymmetric α-substitution reactions. List and co-workers have reported the asymmetric intermolecular α-alkylation of aldehydes.[4,33,34] Additionally, a number of hetero-atom functional groups can be installed in an asymmetric fashion using proline-based catalysts. Such transformations include α-amination, α-aminoxylation, α-sulfenylation, α-selenylation, and various α-halogenations.[4,23] Subsequently, Jørgensen and co-workers have extended the enamine promoted heterofuntionalization to the installation of amino moieties at the γ-position by the generation of a vinylogous enamine.[4,35]

Figure I-1. Various proline-like catalysts for asymmetric enamine catalysis.

I-21   I-22   I-23   I-24

I-25   I-26   I-27   I-28

I-29   I-30   I-31

I-32   I-33   I-34
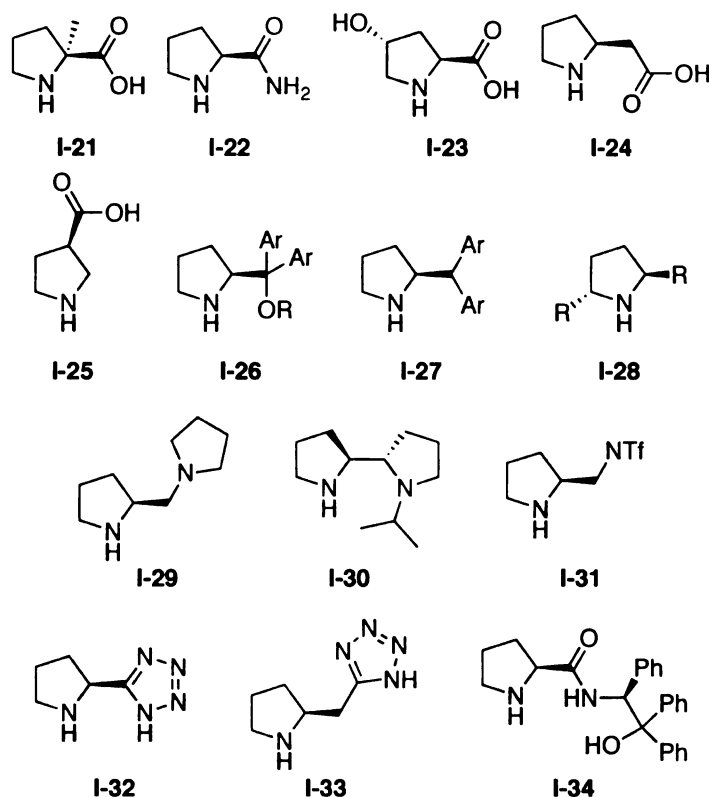
1.2.2: Imidazolidinone Iminium Catalysts

Contemporary with the advent of asymmetric enamine catalysis, the MacMillan group introduced a novel imidazolidinone catalyst scaffold that has subsequently found application in a number of asymmetric transformations.[6,7] The hallmark of these catalysts (e.g. **I-4**, Scheme I-4) is their ability to form reactive iminium ion intermediates (**I-6**), thus lowering the energy level of the LUMO of the electrophilic component of the reaction similar to Lewis acid activation (*cf.* **I-35**).

8

Scheme I-4. Lewis acid-like activation by imidazolidinone iminium catalysis.
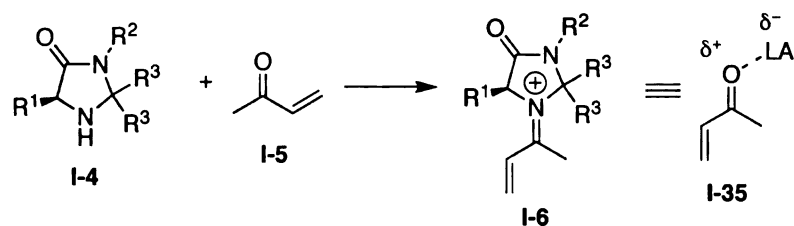
1st generation catalyst   2nd generation catalyst

I-36   I-37
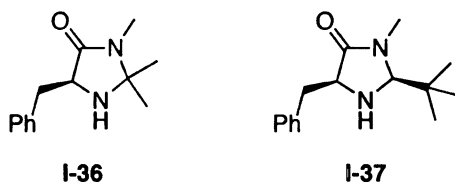
From the outset these catalysts were exquisitely designed such that groups at the R^3 position (*gem*-dimethyl in **I-36** and *tert*-butyl in **I-37**) would favor the generation of a particular, defined iminium geometry. In practice, the *E*-iminium geometry depicted in **I-6** is favored in order to minimize non-bonding interactions between the substrate olefin and the *gem*-dimethyl (**I-36**) or *tert*-butyl moiety (**I-37**). Distal to the R^3 position is the stereodefining R^1 group (benzyl for both **I-36** and **I-37**). The projection of this group over one enantioface (*Si* face in **I-6**) of the substrate olefin directs the introduction of the incoming nucleophile from the more accessible *Re* face in a stereocontrolled fashion.

Two illustrative examples of iminium catalysis are described below in Scheme I-5. In their seminal disclosure, the MacMillan group applied catalyst **I-36** to effect the iminium catalyzed Diels-Alder cyclization of α,β-unsaturated aldehydes with assorted dienes (eq. 1). For example, on treatment of 1,3-

cyclohexadiene and acrolein with 0.05 equiv. of catalyst **I-36**, the chiral bicyclic

adduct **I-40** was returned in an 82% yield (14:1 endo/exo selectivity) with 94%

ee.[6,36] Subsequently the same group extended the methodology to include the

use of α,β-unsaturated ketone dienophiles by employing the perchlorate salt of I-

41.[37] Later, catalyst **I-37** was utilized as the catalyst for several intramolecular

Diels-Alder applications.[38] Additionally, iminium catalysts were applied in 1,3-

dipolar cycloadditions between α,β-unsaturated aldehydes and nitrones

(MacMillan)[39] and the [4+3] cycloaddition of dienes with silyloxypentadienals

(Harmata).[40]

Scheme I-5. Select examples of asymmetric iminium catalysis.
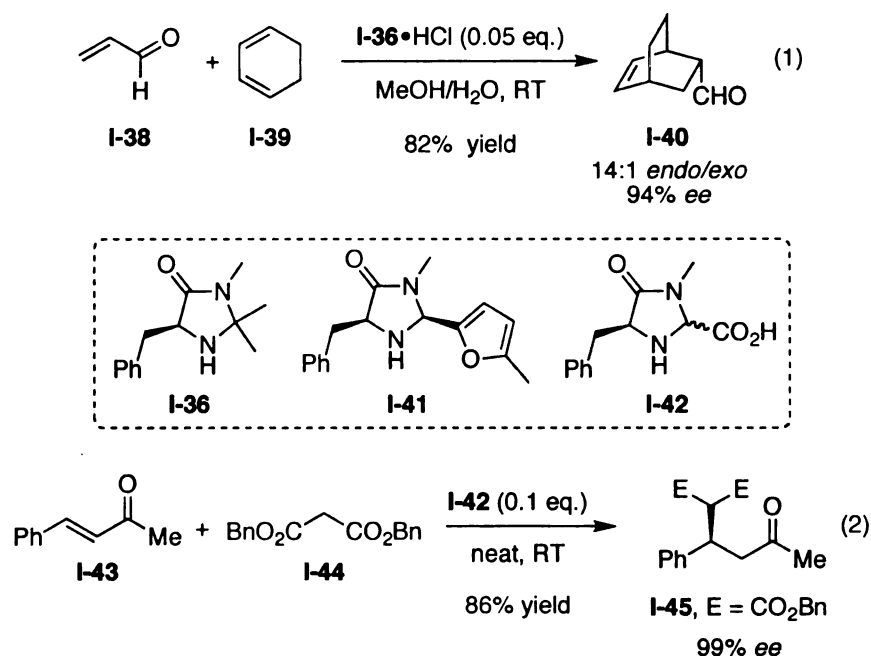
In addition to cycloadditions, iminium catalysis has also been exceptionally

useful in promoting various 1,4 additions to α,β-unsaturated aldehydes and

ketones.[6] The first examples of iminium catalyzed 1,4-additions were

10

demonstrated by Taguchi[41] and later Hanessian[42] with proline. Subsequently the

MacMillan group applied iminium catalysis to various 1,4-addition reactions

including the asymmetric Friedel-Crafts alkylation of unsaturated aldehydes with

pyrroles,[43] indoles,[44] anilines,[45] and siloxyfurans.[46] Additionally, the Jørgensen

group has pioneered several Michael addition reactions catalyzed by iminium

catalyst I-42 and analogues thereof.[47-51] Scheme I-5, eq. 2 illustrates one such

example where the Michael addition of dibenzyl malonate I-44 to α,β-unsaturated

ketone I-43 is promoted by iminium organocatalyst I-42.[49] In the event, Michael

adduct I-45 is returned in 86% yield and 99% ee.

Although cycloadditions and 1,4-additions are by far the most prevalent

examples, iminium catalysts have also been employed in various other

applications including transfer hydrogenations[52] and several cascade

processes.[53,54] Finally, the design principles of the iminium catalysts described

above have been extended to include an entirely new activation mode, SOMO

catalysis.[15-17]

1.2.3: Peptide-Mediated Nucleophilic Asymmetric Organocatalysis

Short peptide sequences have been a fertile source of highly effective

catalysts for asymmetric group transfer reactions (i.e. acylation, phosphorlyation,

etc.).[8,11] Unlike other organocatalytic scaffolds, peptide-based catalysts are

typically discovered and optimized through a randomized, combinatorial

approach.[55] Peptides are ideally suited for such an approach owing to their facile

preparation by well-established solid-phase peptide synthesis (Fmoc SPPS).[56]

Additionally the subsequent development of split-and-pool synthesis[57-59] and

various methods for the rapid assay[60] of large catalyst libraries has allowed for

the processing of literally thousands of potential catalysts at once.

The Miller group has developed as series of highly selective β-turn[61-68]

peptide catalysts for various asymmetric organocatalytic transformations.[8,11]

Their initial efforts were focused on the generation of β-hairpin peptides equipped

with an N-terminal nucleophilic N-alkyl histidine (e.g. I-47) for the kinetic

resolution of various amino alcohols such as I-46 by catalytic acyl transfer

(Scheme I-6).[69-73]

Scheme I-6. Miller's organocatalytic acylation.
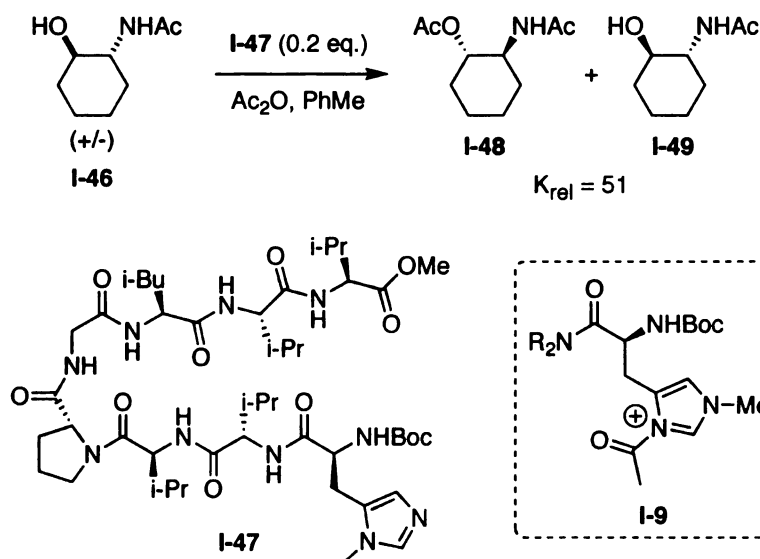
Catalyst I-47 was the culmination of the combinatorial preparation of a

number of N-methyl hisitidine peptides designed around the well-known D-Pro-

Gly[68,74] β-turn sequence. Their efforts in this regard were greatly accelerated by

the development of a fluorescent-based screening approach, allowing for the on-

12

bead evaluation of potential catalysts prepared by SPPS.[75,76] Ultimately I-47 was

discovered, thus allowing for the kinetic resolution of racemic mixtures of amino-

alcohol I-46, allowing for the generation of ester I-48 with a K_{rel} of 51.[77] The

putative active catalyst proceeds by the asymmetric delivery of the activated acyl

group from the N-terminal N-methyl histidine moiety (see I-9).

Subsequently, they have applied a similar peptide-mediated site-selective

acylation to a number of applications including: the preparation of a key

intermediate en route to an aziridinomitosane anti-cancer target;[78] the site-

selective acylation of carbohydrates,[79] glycerols,[80] and Erythromycin A;[81] as well

as the remote desymmetrization of meso-alcohols that were separated by a

remarkably large distance (~1 nm).[82,83] A similar approach was also applied to

the development of a related resolution of tert-butanesulfinyl chloride, thus

facilitating the preparation of chiral sulfinate esters.[84] Importantly, each of the

subsequently developed applications alluded to above relied upon a different

optimal peptide catalyst, indicating that catalysts from the same family can be

tailored for specific niche applications within the broader reaction class.[8,11]

In addition to their efforts in the development of peptide-base acyl transfer

catalysts, the Miller group has also developed a large library of peptide catalysts

for the asymmetric phosphorylation of alcohols.[85] These efforts have culminated

in the development of a series of peptide catalysts that can selectively

phosphorylate a singular alcohol position of myo-inositol (Scheme I-7).[85-90]

The preparation of 3-P and 1-P myo-inositol derivatives via the

desymmetrization of meso-form I-48 described in Scheme I-7 serves to highlight

another interesting nuance of their combinatorial approach to peptide catalyst discovery. Namely, two structurally very different peptide structures emerged as the ideal organocatalysts for the preparation of the two enantiomeric phosphorylated products I-49 and I-50.

Scheme I-7. Miller's peptide-based phosphorylation catalysts.
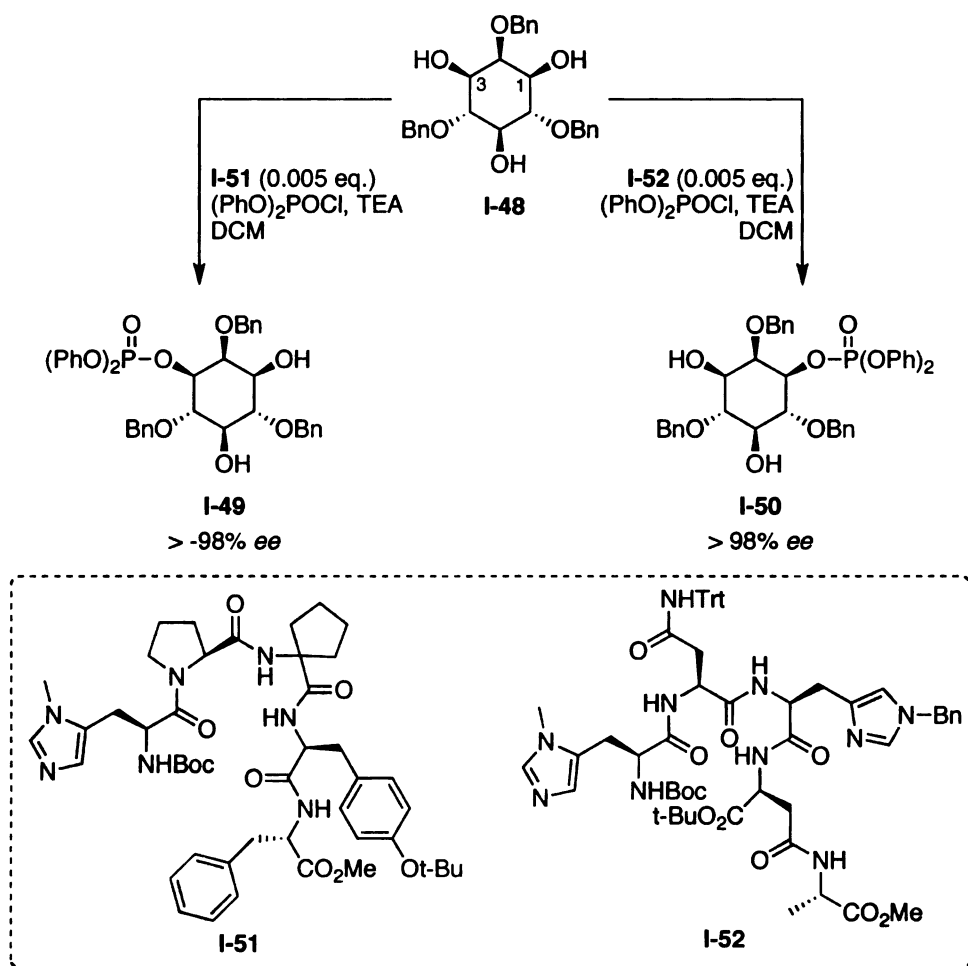
In the event, a combinatorial screen of 178 catalyst candidates returned the β-turn peptide **I-51** that efficiently returned the 3-P phosphorylated product **I-49** in greater than -98% *ee*. Additionally, a second peptide from the library (**I-52**)

14

allowed equally selective access to the enantiomeric 1-P derivative **I-50**.

Interestingly the hit peptide catalyst for the preparation of **I-50** is markedly

different from that used to prepare its enantiomer **I-49**. Even more remarkable is

the fact that the stereochemistry of active site N-methyl histidine residue is the

same! This example highlights the necessity for a randomized approach to

peptide catalyst design. Furthermore, since the structural features that govern

the stereodivergence of **I-51** and **I-52** are non-obvious, the results depicted in

Scheme I-7 also serve to underscore the difficulty inherent in attempting to

employ a rationalized, design-based approach to the development of peptide-

based catalysts.

In addition to applications in acyl and phosphoryl transfer, the Miller group

has also applied short oligopeptides to other non-related transformations.[8,11]

Shorter β-turn analogues of catalysts **I-47** and **I-51** that still maintain the critical

N-terminal N-methyl histidine residue have been applied to the conjugate

addition of azide ion to α,β-unsaturated carbonyl compounds.[91-94] Similarly, N-

terminal N-methyl histidine β-turn peptides were also used to catalyze

asymmetric Baylis-Hillman reactions[95,96] (with proline as a cocatalyst) and the

asymmetric Michael addition of α-nitroketones.[97] Finally, the Miller group has

employed related β-turn scaffolds containing an N-terminal thiazolylalanine

residue (Taz) in several applications of the asymmetric Stetter reaction.[98,99]

1.2.4: Non-Covalent Catalysis Mediated by Peptides

In addition to nucleophilic catalysis (*i.e.* covalent catalysis, Scheme I-1, *vide supra*), peptides have also been sparsely applied in several applications relying on non-covalent catalysis (Scheme I-2, *vide supra*). Chief among these transformations is the Juliá-Colonna epoxidation reaction.[1,100,101] In the early 1980s, these researchers reported the highly enantioselective epoxidation of various chalcone derivatives by action of a poly-*L*-alanine in basic 30% H_2O_2/toluene mixtures, thus returning the desired epoxyketones in high yield and enantiopurity.[102-106] Subsequently, the reaction was modified to allow for the asymmetric epoxidation of chalcones in non-aqueous media employing the poly-L-leucine catalyst introduced by Roberts and co-workers (Scheme I-8, eq. 1).[107-116] In their approach, chalcone was epoxidized by action of poly-*L*-leucine in the presence of urea-hydroperoxide (UHP) and DBU in THF, thus yielding epoxyketone **I-54** in 90% yield and 92% *ee*.[111] Currently, however, the methodology is hamstrung by a relatively limited substrate scope; typically only substituted chalcones are effective substrates.

The mechanistic underpinnings of the transformation are still a matter of some debate. A hydrogen bond-driven binding of the chalcone substrate at the terminus of the α-helix of the polypeptide has been invoked by some.[100] Alternatively, others suggest a similar binding of the peroxide nucleophile in lieu of a substrate-peptide complex.[101,117] What is apparent, however, is that the induction afforded by the poly-peptide catalyst results from a non-covalent reagent/catalyst association instead of covalent activation.

Scheme I-8. Non-covalent chiral catalysis by peptides.

(1)

I-53

poly-*L*-leucine

UHP, DBU, THF

90% yield

I-54

92% *ee*

(2)

HO⟶OH

I-55

I-57 (0.3 eq.)

TBSCl, DIPEA
PhMe, -78 °C

82% yield

TBSO⟶OH

I-56

96% *ee*

I-57
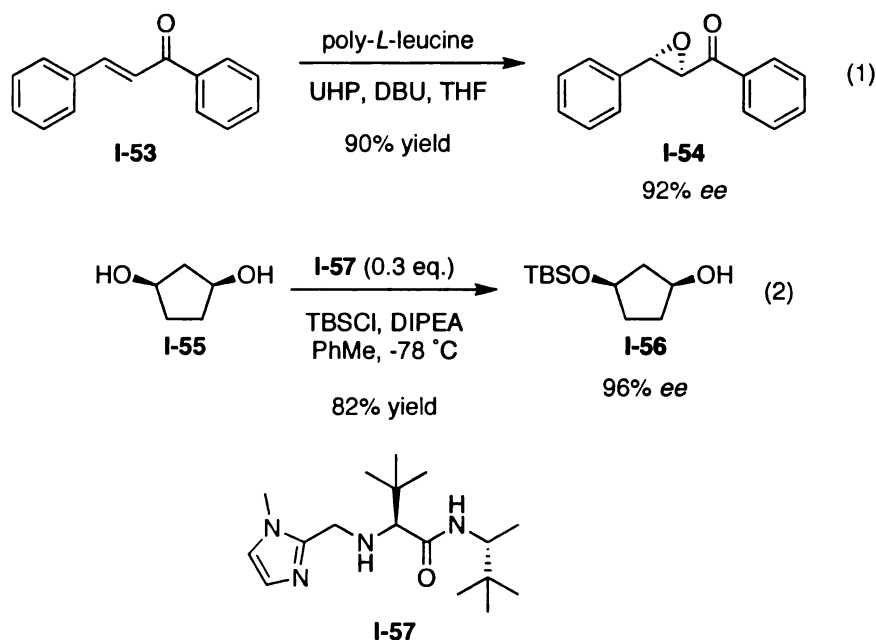
A second example of non-covalent catalysis by peptide-like molecules is indicated in Scheme I-8. In 2006, Hoveyda and Snapper introduced the small peptide catalyst **I-57**, which promoted the desymmetrization of *meso*-diols by selective mono-silyl protection. For example, *meso*-1,3-cyclopentanediol **I-55** was selectively protected, thus generating mono-TBS protected **I-56** in high yield with excellent enantiopurity (Scheme I-8, eq. 2). Interestingly, a covalent complex between **I-57** and the silicon source does not form on incubation of the catalyst with TBSCl under the reaction conditions. Therefore, these authors proposed that catalyst **I-57** confers its enantioselectivity by a non-covalent coordination event between the pendant imidazole on the catalyst and the silicon atom of TBSCl.[118]

1.2.5: Jacobsen Thio-Urea Catalysis

A number of catalyst manifolds have been discovered that confer asymmetric induction by means of a hydrogen bond mediated pre-organization between the catalyst and electrophile, thus facilitating an asymmetric approach from an incoming nucleophile. Transformations of this sort have been described in detail in several excellent reviews.[12,13] Although a complete treatment of these processes in this chapter is not practical, a brief discussion of the family of thiourea catalysts developed by Jacobsen and co-workers will serve as a salient example of the class as a whole.

In a series of publications ranging from early 1998 to mid 2002, the Jacobsen group described the initial discovery and optimization of a set of thiourea-Schiff base catalysts for the asymmetric Strecker reaction (*i.e.* addition of cyanide ion to imines).[119-122] The culmination of these efforts resulted in the discovery of catalyst I-62 that facilitates the addition of HCN to a number of different aldimines and ketoimines (Scheme I-9, eq. 2). In the presence of just 0.01 equivalent of second generation catalyst I-62, Strecker product I-59 was generated from N-benzylaldimine I-58 in 95% *ee*. The journey culminating in the development I-62 as the catalyst of choice in this transformation was one based on equal measures of an initial focus on a high throughput screening approach followed by painstaking mechanistic investigations. Owing to their modular nature, initial attempts to develop an asymmetric Strecker catalyst focused on the preparation of parallel libraries of a number of potential catalysts by varying the amino acid, diamine, and salicylaldimine units of the scaffold.[119] This initial

screening intensive approach returned a 1st generation system (**I-60**) that

returned the Strecker products with aldimine[119,120] and ketoimine[121] substrates

with enantioselectivities ranging from approximately 70 to 90% *ee*. Some

substrates, however, returned less satisfactory enantioselectivities. For instance,

the conversion of **I-58** to **I-59** by action of **I-61** proceeded in a less selective 79%

ee (Scheme I-9, eq. 1).

Scheme I-9. Jacobsen's thiourea Strecker catalyst.
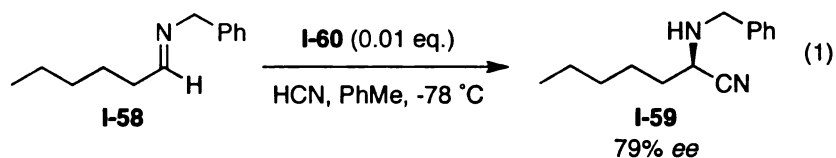
First Generation:
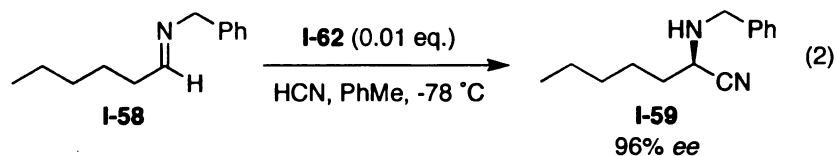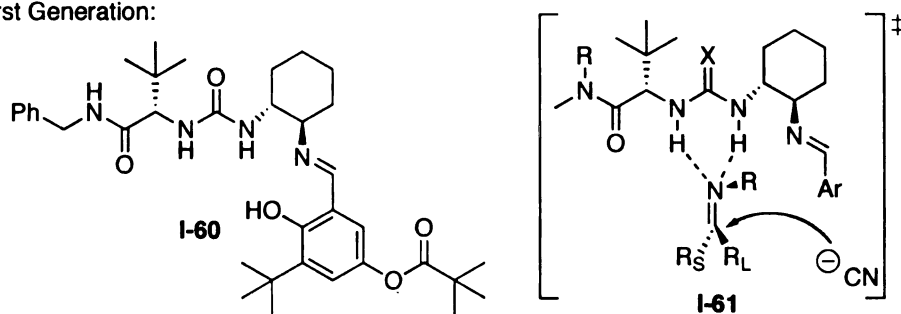
Second Generation:
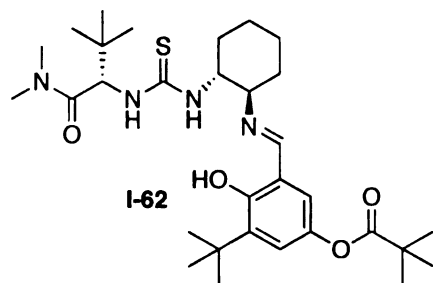
At the culmination of these efforts the researchers had arrived at a selective 1st generation catalyst scaffold **I-60** with an excellent substrate scope, yet they had gained very little knowledge about the mechanistic underpinnings of the transformation. They correctly surmised that the realization of the full potential of the catalyst scaffold would likely require a thorough understanding of the mechanism by which the catalyst confers its selectivity. In that vein, they next undertook an extensive mechanistic investigation of the transformation. The culmination of kinetic experiments, NMR studies, and molecular modeling revealed a consistent mechanistic hypothesis that accounted for the high level of enantioselectivity and broad substrate scope observed for the reaction. As depicted in transition state **I-61**, the stereochemical course of the reaction is governed by hydrogen bond organization and activation of exclusively the Z-imine isomer (available from rapid E to Z imine intercoversion) by action of a dual H-bonding event from both NH hydrogens of the urea or thiourea moiety. The binding occurs in such a way as to direct the more sterically demanding imine substituent away from the catalyst projecting into the solvent. In this arrangement, cyanide ion is delivered from the same side of the catalyst as the diamine/salicylaldimine groups.[122] The careful understanding of this mechanism facilitated the *rational* (as opposed to randomized) structural modifications that led to a more broadly applicable 2nd generation catalyst **I-62**. In particular, the incorporation of a secondary amide in lieu of the benzyl amide in **I-61** allowed for a more finely tuned discrimination of the steric environment about the two

20

enantiofaces of the substrate imine, while the more active thiourea moiety allowed for tighter substrate binding and more active catalyst.[12,13,122]

The additional insight proffered by the extensive mechanistic studies for the Strecker catalysts subsequently facilitated the application of similar urea and thiourea based scaffolds to a number of other transformations. The applications include the asymmetric Mannich reaction of silyl ketene acetals with imines,[123,124] the asymmetric nitro-Mannich reaction,[125] the acyl-Mannich reaction of isoquinolines,[126] the acyl-Pictet-Spengler reaction,[127] the hydrophosphonylation of imines,[128] and aza-Baylis-Hillman reactions.[129]

The lasting legacy of the Jacobsen thiourea catalyst system is that it serves as an exquisite example of the delicate interplay between the initial screening intensive efforts toward catalyst design and later stage detail-oriented studies directed at understanding and fine tuning the catalyst system. It seems likely that the development of subsequent thiourea promoted transformations would have proceeded much more slowly without the guiding principles gleaned from carefully understanding the mechanistic drivers of the Strecker process. The efforts of the Jacobsen group serve to highlight the need for both approaches to catalyst development. A less-rational initial foray into hitherto unexplored reactivity regimes is necessary to drive innovation in asymmetric catalysis. Nonetheless, one must take care to fully appreciate the mechanistic underpinnings of those processes developed by screening intensive efforts, thus allowing a new catalyst scaffold to realize its full potential.

1.2.6: *Cinchona* Alkaloid Mediated Organocatalysis

1.2.6.1: Historical Perspective

The *Cinchona* alkaloids and derivatives thereof have been prominent members of the organocatalyst arsenal since the very beginning of the field. Indeed, quinine and quinidine were employed as catalysts in the very first example of asymmetric organocatalysis. In 1912, Bredig and Fiske reported the generation of chiral mandelonitriles by the quinine or quinidine catalyzed addition of hydrogen cyanide to benzaldehydes. The resulting cyanohydrins were produced with selectivities of less than 10% *ee*.[1,19] More recent pioneering work was conducted by Pracejus[1,130,131] and later Wynberg[1,132-134] (Scheme I-10).

Scheme I-10. Early examples of *Cinchona* alkaloid asymmetric organocatalysis
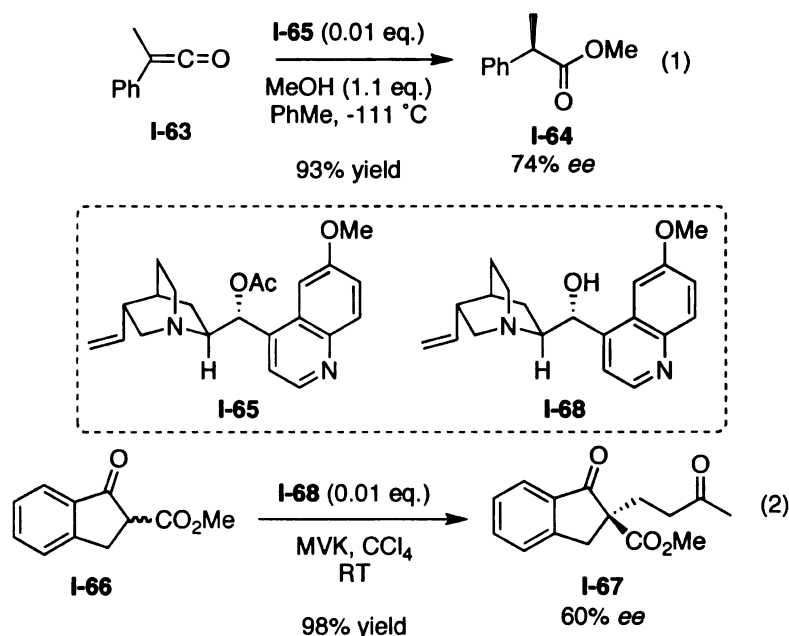
In the mid-1960s, Pracejus employed acylated quinine **I-65** to catalyze the addition of methanol to methyl phenyl ketene **I-63** (Scheme I-10, eq. 1). In what

is likely one of the first examples of *Cinchona* alkaloid mediated nucleophilic catalysis (*vide infra*), the desired α-chiral methyl ester was isolated in excellent yield with 74% *ee*.[1,130,131] In the late 1970s and early 1980s, Wynberg and coworkers applied quinine **I-68** as well as other *Cinchona* alkaloids to effect several conjugate addition reactions.[1,132-134] For example, β-ketoester **I-66** underwent an efficient Michael addition to methyl vinyl ketone (MVK) on treatment with a catalytic amount of quinine (**I-68**). The resulting adduct **I-67** was generated in 98% yield with 60% *ee*.[133] This example is likely one of the earliest examples of asymmetric induction by chiral H-bond donors.[12,13]

1.2.6.2: Non-Covalent Asymmetric Catalysis With *Cinchona* Alkaloids

Chiral *Cinchona* alkaloid phase transfer catalysts (PTCs) have been a well known class of organocatalysts whose use in an number of transformations has been detailed extensively in a number of excellent reviews.[1,24,135,136] As an illustrative example, we will turn to a discussion of the asymmetric alkylation of imines catalyzed by *Cinchona* alkaloid PTCs.[1,14,135-138]

Initially investigated by O'Donnell in the late 1980s,[14,135,136,139] and later perfected by Corey[140,141] and Lygo,[137,142,143] the asymmetric alkylation of benzophenone imines has emerged as a powerful method for the asymmetric synthesis of chiral, non-natural amino acids. The reactions rely upon the use of N,O-bisalkylated *Cinchona* alkaloid PTCs (among others)[1,135] to preorganize, through non-covalent interactions, an enolate generated by action of a non-chiral base. An example of such a transformation is depicted in Scheme I-11.[1,140]

Scheme I-11. *Cinchona* alkaloid PTCs of asymmetric alkylations.
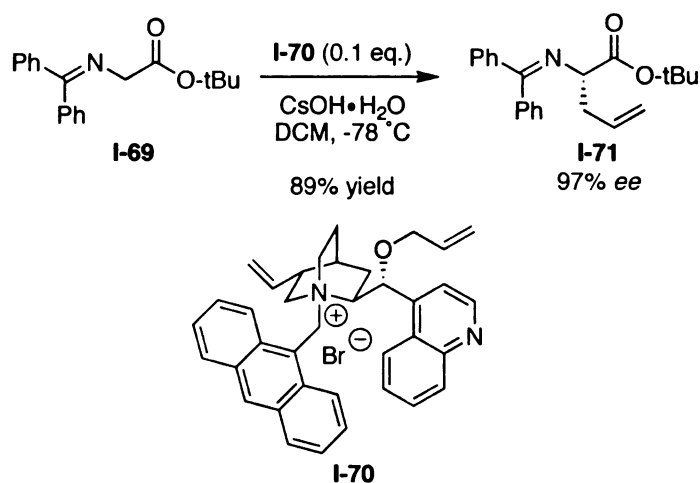
In a typical experiment, cinchonidine derivative **I-70** promotes the highly enantioselective allylation of **I-69**, thus generating allyl glycine derivative **I-71** in high yield and excellent enantioselectivity.[1,140] In addition to these types of alkylation reactions, *Cinchona* alkaloid PTCs have also been employed as effective asymmetric organocatalysts for a number of other transformations including other enolate alkylation applications, aldol reactions, nucleophilic epoxidations, Michael reactions, hydrosilane and borohydride reductions, trifluoromethylations, enantioselective S_NAr substitutions, Strecker reactions, Henry reactions, aza-Henry reactions, Mannich reactions, aziridinations, Horner-Wadsworth-Emmons reactions and the Darzens reaction.[1,24,135,136] Interestingly, some studies have shown that in addition to the nature of the alkyl group on the quaternary ammonium center, even the halide counterion of the PTC can play a profound role in influencing the selectivity of the transformation. In particular, *Cinchona* alkaloid PTCs with fluoride counterions have been extensively studied

in promoting the aldol condensation of silyl enol ethers and ketene acetals.

These reactions are initiated by the fluoride induced collapse of the silylated reagents.[138]

Similar to the PTCs in function, a number of transformations utilizing non-alkylated *Cinchona* alkaloids have been described that are proposed to promote asymmetric catalysis by means of non-covalent interactions. In these cases, the basic quinuclidine ring of the alkaloid is protonated, thus generating a hydrogen bond donor, through which non-covalent activation can occur. Alternatively, the quinuclidine engages as a hydrogen bond acceptor with a protonated nucleophile. The transformations based on this mode of activation are many, and have been thoroughly reviewed. Some of the transformations include: enantioselective conjugate additions, aldols, Mannich reactions, Henry reactions, asymmetric Friedel-Crafts alkylations of heterocyclic aromatics, hydrazinations, hydrophosphorylations, α-sulfenylations, and aza-Baylis-Hillman reactions.[1,12,13,23-25]

1.2.6.3: *Cinchona* Alkaloid-Mediated Nucleophilic Catalysis

Relative to the large number of applications as PTCs as well as the many examples of non-covalent activation by non-alkylated alkaloids, there are notably fewer applications of *Cinchona* alkaloids as nucleophilic catalysts (*i.e.* covalent catalysis). The majority of reports in this arena proceed via the formation of chiral alkaloid enolates by activation of acid chloride starting materials (see Scheme I-12).[1,9,144]

Scheme I-12. General mode of nucleophilic catalysis by *Cinchona* alkaloids.
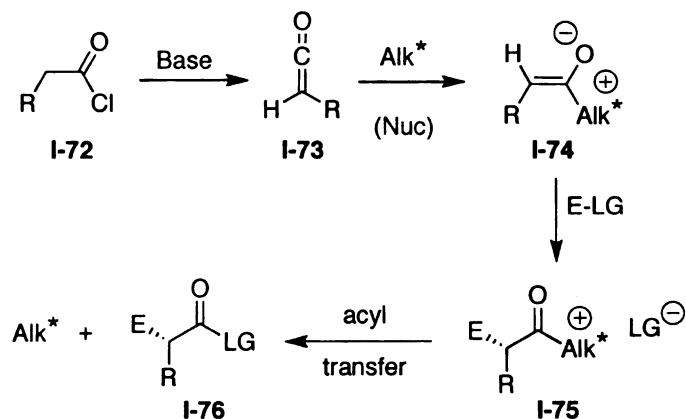
The general sequence depicted in Scheme I-12 typically begins by the *in situ* generation of a ketene electrophile (**I-73**) by the deprotonation of acid chloride **I-72** by action of a non-chiral base. Subsequently, ketene **I-73** suffers attack from the chiral alkaloid catalyst, thus generating a chirally disposed enolate (i.e. **I-74**). On encountering an appropriate electrophile (E-LG), the collapse of enolate **I-74** generates the chiral α-substituted acyl alkaloid species **I-75**. Finally, the alkaloid catalyst is regenerated after an acyl transfer reaction with the leaving group (LG) from the electrophile, so generating the α-chiral acyl derivative **I-76**.[1]

The general activation paradigm described in Scheme I-12 has been applied to a number of transformations.[1,9,23] Two salient examples are described *below* in Scheme I-13.

Scheme I-13. Applications of nucleophilic *Cinchona* alkaloid organocatalysis.

$$I\text{-}80 \ (0.1 \ \text{eq.})$$

NaHCO$_3$
15-crown-5
PhMe, -10 °C

(1)

58% yield

dr (cis/trans) = 12:1
93% *ee*

I-80

$$I\text{-}80 \ (0.1 \ \text{eq.})$$

proton sponge
PhMe, -78 °C

(2)

40% yield

I-82

95% *ee*
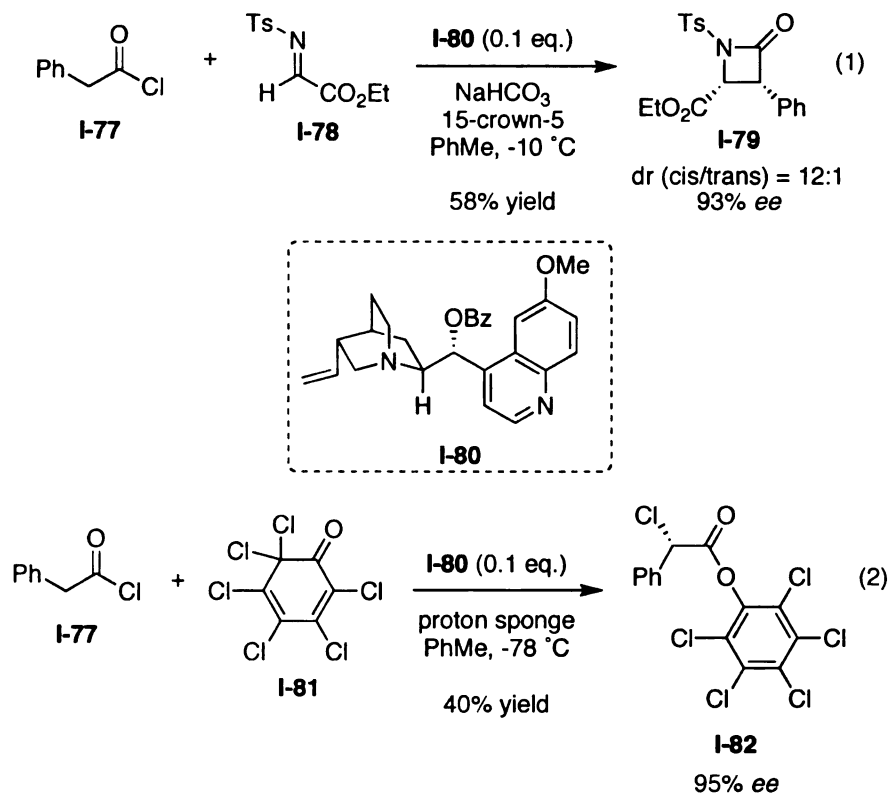
Building on pioneering efforts by Wynberg in the development of *Cinchona* alkaloid promoted formal [2+2] cyclizations leading to chiral β-lactones,[1,145] Lectka and coworkers developed a highly selective variant leading to chiral β-lactam products (Scheme I-13, eq. 1).[9,144,146,147] In the event, the chiral enolate (*i.e.* **I-74**, *vide supra*) derived from the ketene congener of **I-77** and **I-80** undergoes a step-wise cyclization with N-tosylimine **I-78** to return chiral β-lactam **I-79** with excellent diastereo and enantioselectivity, albeit in moderate yield. This transformation has been extended to other related transformations including ketene dimerizations.[9]

Founded on similar mechanistic principles, Lectka and co-workers have extended the chiral activation of ketenes to include α-halogenation reactions.[9] For example, on treating the chiral enolate from **I-80** and the *in situ* generated ketene (from **I-77**) with chlorine source **I-81**, α-chloroester **I-82** is generated in moderate yield with excellent enantioselectivity. In this case, the active catalyst is regenerated on acyl transfer (see conversion of **I-75** to **I-76** in Scheme I-12) by the reduced per-chlorinated phenol product from **I-81**.[9,23]

In addition to these examples of nucleophilic catalysis promoted by *Cinchona* alkaloids, other examples include the desymmetrization of diols and anhydrides as well as asymmetric Baylis-Hillman and aza-Baylis-Hillman transformations.[1,9,148]

1.3: Conclusions and Significance

Since the early 1990s, the explosion of new developments in the arena of asymmetric organocatalysis has thrust the field to the forefront of asymmetric catalysis. Currently the art is emerging into a fully mature subdivision of organic chemistry, where the initially disclosed transformations are slowing becoming more and more well understood, thus allowing for the further development of new applications. Not surprisingly, the catalyst manifolds that currently enjoy the largest applicability to a variety of transformations are those whose mechanistic nuances are the most clearly delineated. This fact underscores the necessity for a thorough mechanistic understanding of a newly discovered transformation or

catalyst scaffold. It seems likely that only after such efforts can a particular catalyst scaffold or transformation realize its true potential.

The efforts described in this thesis have been directed at extending the current scope of asymmetric organocatalysis to include the delivery of chirally disposed halenium ions (Cl^+, Br^+, etc.) to olefins. Such transformations are conspicuously absent in the context of asymmetric organocatalysis (as well as metal mediated processes for that matter). A brief review of the sparse examples known to date is given at the beginning of the following chapter. The culmination of the efforts described in this thesis has resulted in the first example of an organocatalytic asymmetric chlorolactonization of alkenoic acids that returns the desired chloro-γ-lactones in good yield with useful enantioselectivity. What follows is an account of the initial discoveries and subsequent optimization that led to this new entry into asymmetric organocatalysis.

1.4: References

1. Berkessel, A.; Groger, H. *Asymmetric Organocatalysis - From Biomimmetic Concepts to Applications in Asymmetric Synthesis*; Wiley-VCH: Morlenbach, 2005.

2. List, B. *Synlett* **2001**, 1675-1686.

3. List, B. *Acc. Chem. Res.* **2004**, *37*, 548-557.

4. Mukherjee, S.; Yang, J. W.; Hoffmann, S.; List, B. *Chem. Rev.* **2007**, *107*, 5471-5569.

5. Notz, W.; Tanaka, F.; Barbas, C. F. *Acc. Chem. Res.* **2004**, *37*, 580-591.

6. Lelais, G.; MacMillan, D. W. C. *Aldrichim. Acta* **2006**, *39*, 79-87.

7. MacMillan, D. W. C. *Nature* **2008**, *455*, 304-308.

8. Blank, J. T.; Miller, S. J. *Biopolymers* **2006**, *84*, 38-47.

9. France, S.; Guerin, D. J.; Miller, S. J.; Lectka, T. *Chem. Rev.* **2003**, *103*, 2985-3012.

10. Jarvo, E. R.; Miller, S. J. *Tetrahedron* **2002**, *58*, 2481-2495.

11. Miller, S. J. *Acc. Chem. Res.* **2004**, *37*, 601-610.

12. Doyle, A. G.; Jacobsen, E. N. *Chem. Rev.* **2007**, *107*, 5713-5743.

13. Taylor, M. S.; Jacobsen, E. N. *Angew. Chem., Int. Ed.* **2006**, *45*, 1520-1543.

14. O'Donnell, M. J. *Acc. Chem. Res.* **2004**, *37*, 506-517.

15. Kim, H.; MacMillan, D. W. C. *J. Am. Chem. Soc.* **2008**, *130*, 398-399.

16. Jang, H. Y.; Hong, J. B.; MacMillan, D. W. C. *J. Am. Chem. Soc.* **2007**, *129*, 7004-7005.

17. Beeson, T. D.; Mastracchio, A.; Hong, J. B.; Ashton, K.; MacMillan, D. W. C. *Science* **2007**, *316*, 582-585.

18. Reisman, S. E.; Doyle, A. G.; Jacobsen, E. N. *J. Am. Chem. Soc.* **2008**, *130*, 7198-7199.

19.   Bredig, G.; Fiske, P. S. *Biochem. Z.* **1912,** *46,* 7-23.

20.   Dalko, P. I.; Moisan, L. *Angew. Chem., Int. Ed.* **2001,** *40,* 3726-3748.

21.   Dalko, P. I.; Moisan, L. *Angew. Chem., Int. Ed.* **2004,** *43,* 5138-5175.

22.   Guillena, G.; Najera, C.; Ramon, D. J. *Tetrahedron: Asymmetry* **2007,** *18,* 2249-2293.

23.   Guillena, G.; Ramon, D. J. *Tetrahedron: Asymmetry* **2006,** *17,* 1465-1492.

24.   Kacprzak, K.; Gawronski, J. *Synthesis* **2001,** 961-998.

25.   Pellissier, H. *Tetrahedron* **2007,** *63,* 9267-9331.

26.   *Special Issue on Asymmetric Organocatalysis - Acc. Chem. Res.* **2004,** *37 (8),* 487-631.

27.   Shi, Y. *Acc. Chem. Res.* **2004,** *37,* 488-496.

28.   Yang, D. *Acc. Chem. Res.* **2004,** *37,* 497-505.

29.   Fu, G. C. *Acc. Chem. Res.* **2004,** *37,* 542-547.

30.   Eder, U.; Sauer, G.; Weichert, R. *Angew. Chem., Int. Ed.* **1971,** *10,* 496-497.

31.   Hajos, Z. G.; Parrish, D. R. *J. Org. Chem.* **1974,** *39,* 1615-1621.

32.   List, B.; Lerner, R. A.; Barbas, C. F. *J. Am. Chem. Soc.* **2000,** *122,* 2395-2396.

33.   Fu, A. P.; List, B.; Thiel, W. *J. Org. Chem.* **2006,** *71,* 320-326.

34.   Vignola, N.; List, B. *J. Am. Chem. Soc.* **2004,** *126,* 450-451.

35.   Bertelsen, S.; Marigo, M.; Brandes, S.; Diner, P.; Jorgensen, K. A. *J. Am. Chem. Soc.* **2006,** *128,* 12973-12980.

36.   Ahrendt, K. A.; Borths, C. J.; MacMillan, D. W. C. *J. Am. Chem. Soc.* **2000,** *122,* 4243-4244.

37.   Northrup, A. B.; MacMillan, D. W. C. *J. Am. Chem. Soc.* **2002,** *124,* 2458-2460.

38. Wilson, R. M.; Jen, W. S.; MacMillan, D. W. C. *J. Am. Chem. Soc.* **2005,** *127*, 11616-11617.

39. Jen, W. S.; Wiener, J. J. M.; MacMillan, D. W. C. *J. Am. Chem. Soc.* **2000,** *122*, 9874-9875.

40. Harmata, M.; Ghosh, S. K.; Hong, X. C.; Wacharasindhu, S.; Kirchhoefer, P. *J. Am. Chem. Soc.* **2003,** *125*, 2058-2059.

41. Kawara, A.; Taguchi, T. *Tetrahedron Lett.* **1994,** *35*, 8805-8808.

42. Hanessian, S.; Pham, V. *Org. Lett.* **2000,** *2*, 2975-2978.

43. Paras, N. A.; MacMillan, D. W. C. *J. Am. Chem. Soc.* **2001,** *123*, 4370-4371.

44. Austin, J. F.; MacMillan, D. W. C. *J. Am. Chem. Soc.* **2002,** *124*, 1172-1173.

45. Paras, N. A.; MacMillan, D. W. C. *J. Am. Chem. Soc.* **2002,** *124*, 7894-7895.

46. Brown, S. P.; Goodwin, N. C.; MacMillan, D. W. C. *J. Am. Chem. Soc.* **2003,** *125*, 1192-1194.

47. Halland, N.; Hazell, R. G.; Jorgensen, K. A. *J. Org. Chem.* **2002,** *67*, 8331-8338.

48. Halland, N.; Hansen, T.; Jorgensen, K. A. *Angew. Chem., Int. Ed.* **2003,** *42*, 4955-4957.

49. Halland, N.; Aburel, P. S.; Jorgensen, K. A. *Angew. Chem., Int. Ed.* **2003,** *42*, 661-665.

50. Halland, N.; Aburel, P. S.; Jorgensen, K. A. *Angew. Chem., Int. Ed.* **2004,** *43*, 1272-1277.

51. Pulkkinen, J.; Aburel, P. S.; Halland, N.; Jorgensen, K. A. *Adv. Synth. Catal.* **2004,** *346*, 1077-1080.

52. Ouellet, S. G.; Tuttle, J. B.; MacMillan, D. W. C. *J. Am. Chem. Soc.* **2005,** *127*, 32-33.

53. Austin, J. F.; Kim, S. G.; Sinz, C. J.; Xiao, W. J.; MacMillan, D. W. C. *Proc. Natl. Acad. Sci. U. S. A.* **2004,** *101*, 5482-5487.

54. Huang, Y.; Walji, A. M.; Larsen, C. H.; MacMillan, D. W. C. *J. Am. Chem. Soc.* **2005,** *127*, 15051-15053.

55. Berkessel, A. *Curr. Opin. Chem. Biol.* **2003,** *7*, 409-419.

56. Chan, W. C.; White, P. D. *Fmoc Solid Phase Peptide Synthesis*; Oxford University Press: Oxford, 2004.

57. Furka, A.; Sebestyen, F.; Asgedom, M.; Dibo, G. *Int. J. Pept. Protein Res.* **1991,** *37*, 487-493.

58. Houghten, R. A.; Pinilla, C.; Blondelle, S. E.; Appel, J. R.; Dooley, C. T.; Cuervo, J. H. *Nature* **1991,** *354*, 84-86.

59. Lam, K. S.; Salmon, S. E.; Hersh, E. M.; Hruby, V. J.; Kazmierski, W. M.; Knapp, R. J. *Nature* **1991,** *354*, 82-84.

60. Reetz, M. T. *Angew. Chem., Int. Ed.* **2002,** *41*, 1335-1338.

61. Imperiali, B.; Fisher, S. L.; Moats, R. A.; Prins, T. J. *J. Am. Chem. Soc.* **1992,** *114*, 3182-3188.

62. Imperiali, B.; Kapoor, T. M. *Tetrahedron* **1993,** *49*, 3501-3510.

63. Amblard, M.; Raynal, N.; Averlant-Petit, M. C.; Didierjean, C.; Calmes, M.; Fabre, O.; Aubry, A.; Marraud, M.; Martinez, J. *Tetrahedron Lett.* **2005,** *46*, 3733-3735.

64. Banerji, B.; Bhattacharya, M.; Madhu, R. B.; Das, S. K.; Iqbal, J. *Tetrahedron Lett.* **2002,** *43*, 6473-6477.

65. Banerji, B.; Mallesham, B.; Kumar, S. K.; Kunwar, A. C.; Iqbal, J. *Tetrahedron Lett.* **2002,** *43*, 6479-6483.

66. Haque, T. S.; Little, J. C.; Gellman, S. H. *J. Am. Chem. Soc.* **1996,** *118*, 6975-6985.

67. Prasad, B. V. V.; Balaram, H.; Balaram, P. *Biopolymers* **1982,** *21*, 1261-1273.

68. Raghothama, S. R.; Awasthi, S. K.; Balaram, P. *J. Chem. Soc.-Perkin Trans. 2* **1998,** 137-143.

69. Miller, S. J.; Copeland, G. T.; Papaioannou, N.; Horstmann, T. E.; Ruel, E. M. *J. Am. Chem. Soc.* **1998,** *120*, 1629-1630.

70. Copeland, G. T.; Jarvo, E. R.; Miller, S. J. *J. Org. Chem.* **1998,** *63*, 6784-6785.

71. Fierman, M. B.; O'Leary, D. J.; Steinmetz, W. E.; Miller, S. J. *J. Am. Chem. Soc.* **2004,** *126*, 6967-6971.

72. Jarvo, E. R.; Vasbinder, M. M.; Miller, S. J. *Tetrahedron* **2000,** *56*, 9773-9779.

73. Vasbinder, M. M.; Jarvo, E. R.; Miller, S. J. *Angew. Chem., Int. Ed.* **2001,** *40*, 2824-2827.

74. Stanger, H. E.; Gellman, S. H. *J. Am. Chem. Soc.* **1998,** *120*, 4236-4237.

75. Copeland, G. T.; Miller, S. J. *J. Am. Chem. Soc.* **1999,** *121*, 4306-4307.

76. Copeland, G. T.; Miller, S. J. *J. Am. Chem. Soc.* **2001,** *123*, 6496-6502.

77. Miller, S. J. *Biopolymers* **2005,** *80*, 488-488.

78. Papaioannou, N.; Blank, J. T.; Miller, S. J. *J. Org. Chem.* **2003,** *68*, 2728-2734.

79. Griswold, K. S.; Miller, S. J. *Tetrahedron* **2003,** *59*, 8869-8875.

80. Lewis, C. A.; Sculimbrene, B. R.; Xu, Y. J.; Miller, S. J. *Org. Lett.* **2005,** 7, 3021-3023.

81. Lewis, C. A.; Miller, S. J. *Angew. Chem., Int. Ed.* **2006,** *45*, 5616-5619.

82. Lewis, C. A.; Chiu, A.; Kubryk, M.; Balsells, J.; Pollard, D.; Esser, C. K.; Murry, J.; Reamer, R. A.; Hansen, K. B.; Miller, S. J. *J. Am. Chem. Soc.* **2006,** *128*, 16454-16455.

83. Lewis, C. A.; Gustafson, J. L.; Chiu, A.; Balsells, J.; Pollard, D.; Murry, J.; Reamer, R. A.; Hansen, K. B.; Miller, S. J. *J. Am. Chem. Soc.* **2008,** *130*, 16358-16365.

84. Evans, J. W.; Fierman, M. B.; Miller, S. J.; Ellman, J. A. *J. Am. Chem. Soc.* **2004,** *126*, 8134-8135.

85. Sculimbrene, B. R.; Morgan, A. J.; Miller, S. J. *Chem. Commun.* **2003,** 1781-1785.

86. Morgan, A. J.; Komiya, S.; Xu, Y. J.; Miller, S. J. *J. Org. Chem.* **2006,** *71*, 6923-6931.

87.   Sculimbrene, B. R.; Miller, S. J. *J. Am. Chem. Soc.* **2001,** *123*, 10125-10126.

88.   Sculimbrene, B. R.; Morgan, A. J.; Miller, S. J. *J. Am. Chem. Soc.* **2002,** *124*, 11653-11656.

89.   Sculimbrene, B. R.; Xu, Y. J.; Miller, S. J. *J. Am. Chem. Soc.* **2004,** *126*, 13182-13183.

90.   Xu, Y. J.; Sculimbrene, B. R.; Miller, S. J. *J. Org. Chem.* **2006,** *71*, 4919-4928.

91.   Guerin, D. J.; Horstmann, T. E.; Miller, S. J. *Org. Lett.* **1999,** *1*, 1107-1109.

92.   Horstmann, T. E.; Guerin, D. J.; Miller, S. J. *Angew. Chem., Int. Ed.* **2000,** *39*, 3635-3638.

93.   Guerin, D. J.; Miller, S. J. *J. Am. Chem. Soc.* **2002,** *124*, 2134-2136.

94.   Tsuboike, K.; Guerin, D. J.; Mennen, S. M.; Miller, S. J. *Tetrahedron* **2004,** *60*, 7367-7374.

95.   Imbriglio, J. E.; Vasbinder, M. M.; Miller, S. J. *Org. Lett.* **2003,** *5*, 3741-3743.

96.   Aroyan, C. E.; Vasbinder, M. M.; Miller, S. J. *Org. Lett.* **2005,** *7*, 3849-3851.

97.   Linton, B. R.; Reutershan, M. H.; Aderman, C. M.; Richardson, E. A.; Brownell, K. R.; Ashley, C. W.; Evans, C. A.; Miller, S. J. *Tetrahedron Lett.* **2007,** *48*, 1993-1997.

98.   Mennen, S. M.; Blank, J. T.; Tran-Dube, M. B.; Imbriglio, J. E.; Miller, S. J. *Chem. Commun.* **2005,** 195-197.

99.   Mennen, S. M.; Gipson, J. D.; Kim, Y. R.; Miller, S. J. *J. Am. Chem. Soc.* **2005,** *127*, 1654-1655.

100.   Berkessel, A.; Koch, B.; Toniolo, C.; Rainaldi, M.; Broxterman, Q. B.; Kaptein, B. *Biopolymers* **2006,** *84*, 90-96.

101.   Kelly, D. R.; Roberts, S. M. *Biopolymers* **2006,** *84*, 74-89.

102.   Julia, S.; Masana, J.; Vega, J. C. *Angew. Chem., Int. Ed.* **1980,** *19*, 929-931.

103. Julia, S.; Guixer, J.; Masana, J.; Rocas, J.; Colonna, S.; Annuziata, R.; Molinari, H. *J. Chem. Soc.-Perkin Trans. 1* **1982**, 1317-1324.

104. Colonna, S.; Molinari, H.; Banfi, S.; Julia, S.; Masana, J.; Alvarez, A. *Tetrahedron* **1983,** *39*, 1635-1641.

105. Julia, S.; Masana, J.; Rocas, J.; Colonna, S.; Annunziata, R.; Molinari, H. *Quimica* **1983,** *79*, 102-104.

106. Banfi, S.; Colonna, S.; Molinari, H.; Julia, S.; Guixer, J. *Tetrahedron* **1984,** *40*, 5207-5211.

107. Adger, B. M.; Barkley, J. V.; Bergeron, S.; Cappi, M. W.; Flowerdew, B. E.; Jackson, M. P.; McCague, R.; Nugent, T. C.; Roberts, S. M. *J. Chem. Soc.-Perkin Trans. 1* **1997**, 3501-3507.

108. Allen, J. V.; Cappi, M. W.; Kary, P. D.; Roberts, S. M.; Williamson, N. M.; Wu, L. E. *J. Chem. Soc.-Perkin Trans. 1* **1997**, 3297-3298.

109. Bentley, P. A.; Bergeron, S.; Cappi, M. W.; Hibbs, D. E.; Hursthouse, M. B.; Nugent, T. C.; Pulido, R.; Roberts, S. M.; Wu, L. E. *Chem. Commun.* **1997**, 739-740.

110. Cappi, M. W.; Chen, W. P.; Flood, R. W.; Liao, Y. W.; Roberts, S. M.; Skidmore, J.; Smith, J. A.; Williamson, N. M. *Chem. Commun.* **1998**, 1159-1160.

111. Allen, J. V.; Bergeron, S.; Griffiths, M. J.; Mukherjee, S.; Roberts, S. M.; Williamson, N. M.; Wu, L. E. *J. Chem. Soc.-Perkin Trans. 1* **1998**, 3171-3179.

112. Gillmore, A. T.; Roberts, S. M.; Hursthouse, M. B.; Malik, K. M. A. *Tetrahedron Lett.* **1998,** *39*, 3315-3318.

113. Chen, W. P.; Roberts, S. M. *J. Chem. Soc.-Perkin Trans. 1* **1999**, 103-105.

114. Geller, T.; Roberts, S. M. *J. Chem. Soc.-Perkin Trans. 1* **1999**, 1397-1398.

115. Allen, J. V.; Drauz, K. H.; Flood, R. W.; Roberts, S. M.; Skidmore, J. *Tetrahedron Lett.* **1999,** *40*, 5417-5420.

116. Ray, P. C.; Roberts, S. M. *Tetrahedron Lett.* **1999,** *40*, 1779-1782.

117. Mathew, S. P.; Gunathilagan, S.; Roberts, S. M.; Blackmond, D. G. *Org. Lett.* **2005,** *7*, 4847-4850.

118. Zhao, Y.; Rodrigo, J.; Hoveyda, A. H.; Snapper, M. L. *Nature* **2006**, *443*, 67-70.

119. Sigman, M. S.; Jacobsen, E. N. *J. Am. Chem. Soc.* **1998,** *120*, 4901-4902.

120. Sigman, M. S.; Vachal, P.; Jacobsen, E. N. *Angew. Chem., Int. Ed.* **2000,** *39*, 1279-1281.

121. Vachal, P.; Jacobsen, E. N. *Org. Lett.* **2000,** *2*, 867-870.

122. Vachal, P.; Jacobsen, E. N. *J. Am. Chem. Soc.* **2002,** *124*, 10012-10014.

123. Wenzel, A. G.; Jacobsen, E. N. *J. Am. Chem. Soc.* **2002,** *124*, 12964-12965.

124. Wenzel, A. G.; Lalonde, M. P.; Jacobsen, E. N. *Synlett* **2003**, 1919-1922.

125. Yoon, T. P.; Jacobsen, E. N. *Angew. Chem., Int. Ed.* **2005,** *44*, 466-468.

126. Taylor, M. S.; Tokunaga, N.; Jacobsen, E. N. *Angew. Chem., Int. Ed.* **2005,** *44*, 6700-6704.

127. Taylor, M. S.; Jacobsen, E. N. *J. Am. Chem. Soc.* **2004,** *126*, 10558-10559.

128. Joly, G. D.; Jacobsen, E. N. *J. Am. Chem. Soc.* **2004,** *126*, 4102-4103.

129. Raheem, I. T.; Goodman, S. N.; Jacobsen, E. N. *J. Am. Chem. Soc.* **2004,** *126*, 706-707.

130. Pracejus, H. *Justus Liebig Ann. Chem.* **1960,** *634*, 9-22.

131. Pracejus, H.; Matje, H. *J. Prakt. Chem.* **1964,** *24*, 195-205.

132. Wynberg, H.; Helder, R. *Tetrahedron Lett.* **1975**, 4057-4060.

133. Hermann, K.; Wynberg, H. *J. Org. Chem.* **1979,** *44*, 2238-2244.

134. Hiemstra, H.; Wynberg, H. *J. Am. Chem. Soc.* **1981,** *103*, 417-430.

135. O'Donnell, M. J. In *Catalytic Asymmetric Synthesis;* Ojima, I. Ed.; Wiley-VCH: New York, 2000; pp. 727-755.

136. O'Donnell, M. J. *Aldrichim. Acta* **2001,** *34*, 3-15.

137. Lygo, B.; Andrews, B. I. *Acc. Chem. Res.* **2004,** *37*, 518-525.

138. Ooi, T.; Maruoka, K. *Acc. Chem. Res.* **2004,** *37,* 526-533.

139. O'Donnell, M. J.; Bennett, W. D.; Bruder, W. A.; Jacobsen, W. N.; Knuth, K.; Leclef, B.; Polt, R. L.; Bordwell, F. G.; Mrozack, S. R.; Cripe, T. A. *J. Am. Chem. Soc.* **1988,** *110,* 8520-8525.

140. Corey, E. J.; Xu, F.; Noe, M. C. *J. Am. Chem. Soc.* **1997,** *119,* 12414-12415.

141. Corey, E. J.; Noe, M. C. *Org. Syn.* **2003,** *80,* 38-45.

142. Lygo, B.; Crosby, J.; Lowdon, T. R.; Wainwright, P. G. *Tetrahedron Lett.* **1997,** *38,* 2343-2346.

143. Lygo, B.; Wainwright, P. G. *Tetrahedron Lett.* **1997,** *38,* 8595-8598.

144. France, S.; Weatherwax, A.; Taggi, A. E.; Lectka, T. *Acc. Chem. Res.* **2004,** *37,* 592-600.

145. Wynberg, H.; Staring, E. G. J. *J. Am. Chem. Soc.* **1982,** *104,* 166-168.

146. Hafez, A. M.; Taggi, A. E.; Wack, H.; Drury, W. J.; Lectka, T. *Org. Lett.* **2000,** *2,* 3963-3965.

147. Taggi, A. E.; Hafez, A. M.; Wack, H.; Young, B.; Drury, W. J.; Lectka, T. *J. Am. Chem. Soc.* **2000,** *122,* 7831-7832.

148. Tian, S. K.; Chen, Y. G.; Hang, J. F.; Tang, L.; McDaid, P.; Deng, L. *Acc. Chem. Res.* **2004,** *37,* 621-631.

Chapter 2: The Development of Peptide-based Catalyst for Asymmetric Bromolactonizations

2.1: Introduction

2.1.1: Specific Aims

The broad aim of the research program detailed in this and the following chapter is to develop new methodologies for the asymmetric organocatalytic halogenation of a number of olefinic substrates. Our overarching goal is the development of catalytic systems that will provide rapid access to myriad functionalities based upon the simple principle of a subsequent nucleophilic attack upon a preceding chiral halonium ion, whose stereochemistry is generated by a *reagent-controlled* asymmetric delivery to an olefinic starting material.

As discussed in Chapter 1, perusal of any major journal devoted to organic chemistry reveals asymmetric organocatalytic processes as a cornerstone of modern reagent-controlled stereoselective transformations. A recent push to develop asymmetric methodologies that are cheap, environmentally friendly, and safe has exacerbated the explosion of new chemistries in this arena. Literally hundreds of different transformations have been explored in an organocatalytic context and the library of available "designer" organocatalysts seems to grow almost daily. As alluded to in the first chapter, perhaps the largest subset of organocatalytic transformations is devoted to the exploitation of various chiral enamine/enolate equivalents as a nucleophile in reactions with a number of electrophiles such as electron-deficient olefins, carbonyls, and imines/iminium ions.[1-7] Other applications have included

cycloadditions and chiral protonation. Aside from enolate α-halogenations,[8-10] asymmetric organocatalytic electrophilic halogenations are rare, and with only a few exceptions the examples in the literature typically proceed with mediocre enantioselectivities (*vide infra*).

It warrants emphasis that the successful enolate α-halogenations, with few exceptions, rely on generating a chiral enolate equivalent as opposed to a chiral halogen source. This fact ultimately indicates that viable solutions to asymmetric olefin halogenation perhaps do not lie within previously described catalyst systems for enolate halogenations. The fundamentally different enantiodetermining step of both enolate and olefin halogenation reactions is illustrated in Scheme II-1. Equation 1 illustrates a general schematic that represents the majority of successful enolate halogenation protocols. The enantiodetermining step is achieved by an *achiral halogen source* (**II-2**) suffering attack by a *chiral nucleophile* (**II-1**) in the form of a chiral enamine (enolate equivalent). In contrast, since a chiral olefin equivalent is typically untenable, asymmetric olefin halogenations must proceed via the generation of a *chiral halogen source* (**II-6**), which is attacked by an *achiral nucleophile* (**II-5**). This striking difference in the enantiodetermining step of these two protocols clearly indicates the need for a strategically different approach to asymmetric olefin halogenation. While impressive gains have been made in the arena of enolate halogenations, this strategy will likely not succeed for enantioselective olefin *halogenations*. One might speculate that the most difficult task in generating a chiral halogen source of type **II-6** in a catalytic framework will be regenerating the

active catalyst from the reduced organocatalyst **II-8** while quelling any

contribution from non-catalyzed (and inherently racemic) background

halogenation by the terminal halogen source.

Scheme II-1. The dichotomy between asymmetric enolate and olefin halogenations.

- General schematic of asymmetric enolate halogenations

II-1	II-2	II-3	II-4
chiral enolate equivalent	achiral halogen source	chiral halogenated product	chiral organocatalyst

(chiral nucleophile) (achiral electrophile)

- General schematic of asymmetric olefin halogenations

II-5	II-6	II-7	II-8
achiral olefin substrate	chiral halogen source	chiral halogenated product	chiral organocatalyst

(achiral nucleophile) (chiral electrophile)
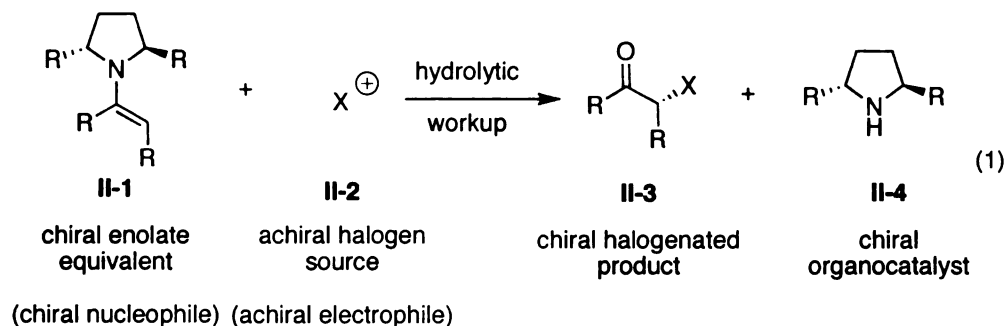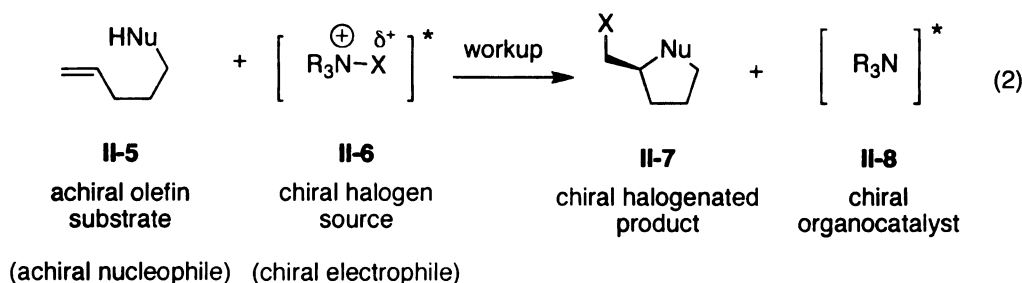
What follows is a brief review of the state of the art of various asymmetric

halogenation reactions of olefin nucleophiles. Subsequent to that treatment is a

brief discussion of the design principles applied to the development of our first

generation of peptide-based catalysts that led to a marginally selective

bromolactonization reaction. The initial discoveries discussed in this chapter

ultimately paved the way for the development of a highly selective

chlorolactonization mediated by a commercially available *Cinchona* alkaloid

dimer (see Chapter 3).

41

2.1.2: Enantioselective Halolactonizations

In sharp contrast to the large number of known examples of substrate controlled stereoselective halolactonizations,[11,12] *reagent-controlled* processes are exceptionally rare, and have only begun to emerge within the last 15 to 20 years. The advantages of a successful approach to a reagent controlled halolactonization are obvious, since such a methodology would provide rapid access to richly functionalized halolactones in one step from achiral congeners. The first enantioselective halolactonization was reported in 1992 by Taguchi and coworkers when a single alkenoic acid substrate (**II-9**) was cyclized by treatment with iodine and a stoichiometric amount of a chiral titanium complex, generated from titanium (IV) *iso*-propoxide and ligand **II-10**, returning iodolactone **II-11** in 67% yield with 65% *ee* (Scheme II-2, eq. 1).[13] This report was subsequently followed by a number of reports employing stoichiometric or super-stoichiometric amounts of a chiral amine promoter to effect an iodolactonization. Nearly all of these methodologies rely upon the formation of a dimeric iodonium salt (*i.e.* [(L*)$_2$I$^+$]Y$^-$, where L* is a chiral amine promoter, and Y is a non-nucleophilic counterion, see **II-17**).[13-17] Two of the most highly selective variants of this strategy were presented by Wirth[16,15] (eq. 2) and Rousseau[17] (eq. 3). Aside from the obvious disadvantage of committing up to ~5 equivalents of chiral promoter in some cases, these approaches were marred by poor enantioselectivities (15 to 45% *ee*) and limited substrate scope. It is also important to emphasize that all of these methodologies proceed via an iodocyclization; reports on analogous chloro and bromolactonizations are absent, except for a singular example reported by

Cui and Brown where a bromolactone was produced in only 5% *ee* by action of

an analogous chiral bromonium/pyridine dimer.[18]

Scheme II-2. Asymmetric halolactonization protocols.

Taguchi:

1. Ti(O*i*-Pr)$_4$
   II-10 (1 eq.)

Py, iodine
2. PTSA, PhH

II-9   II-11   (1)

67% , dr = 58:1, 65% *ee*

Wirth:

II-13 (2 eq.), ICl

DCM, -78 °C

II-12   II-14   (2)

82%, 45% *ee*

Rousseau:

N-methylephedrine (4.8 eq.)

AgSbF$_6$, I$_2$, DCM, -78 °C

II-15   II-16   (3)

92% yield (from I$_2$), 45% *ee*

II-10   II-13   II-17

X = SbF$_6$
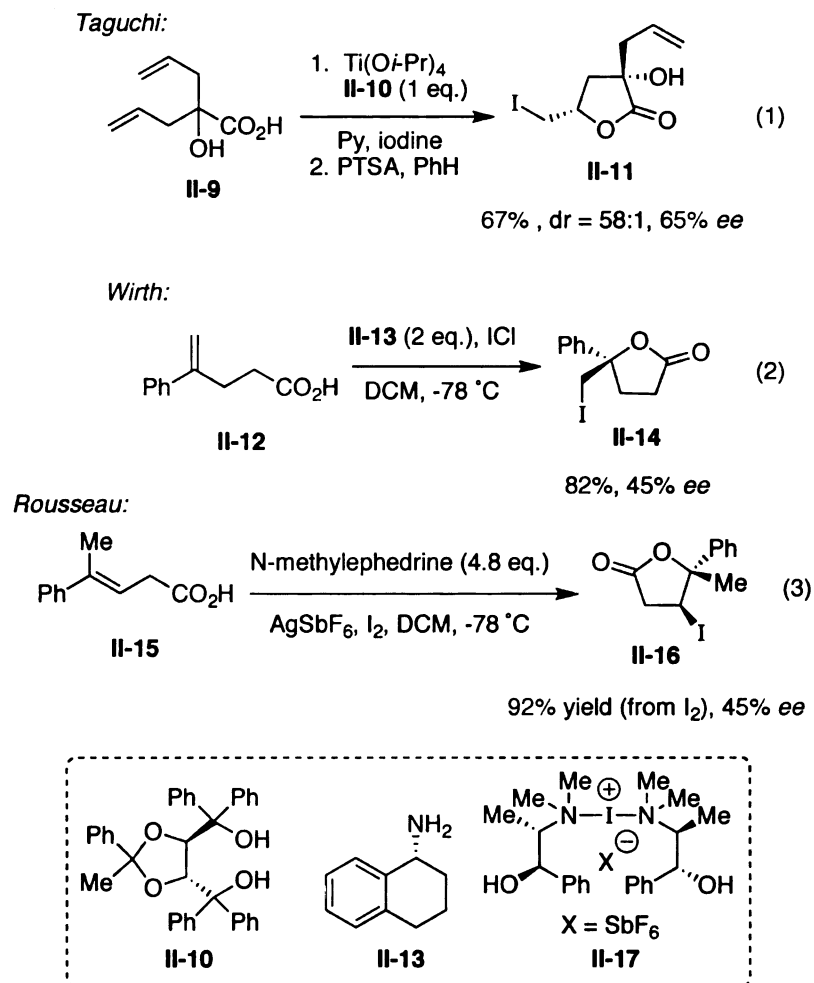
Recently, Gao and coworkers reported the first and only published

catalytic protocol whereby *trans*-5-aryl-4-pentenoic acids such as **II-18** were

cyclized in the presence of iodine and 30 mol% of a quaternary ammonium salt

derived from cinchonidine **II-19** (Scheme II-3).[19,20] The desired iodolactones

were returned in nearly a 1:1 ratio of *exo* **II-20** and *endo* **II-21** isomers with

marginal enantioselectivities (*exo* = 16% *ee*, *endo* = 31% *ee*). Finally, Braddock

and coworkers have attempted to catalyze the formation of chiral bromolactones

by action of a chiral amidine organocatalyst, but racemic products were

isolated.[21]

Scheme II-3. Gao's organocatalytic iodolactonization.

II-18

II-19 (0.3 eq.), I_2

aq. NaHCO$_3$
DCM, 0 °C

II-20

16% *ee*

II-21

31% *ee*

80% combined yield

II-20:II-21 = 47:53

II-19
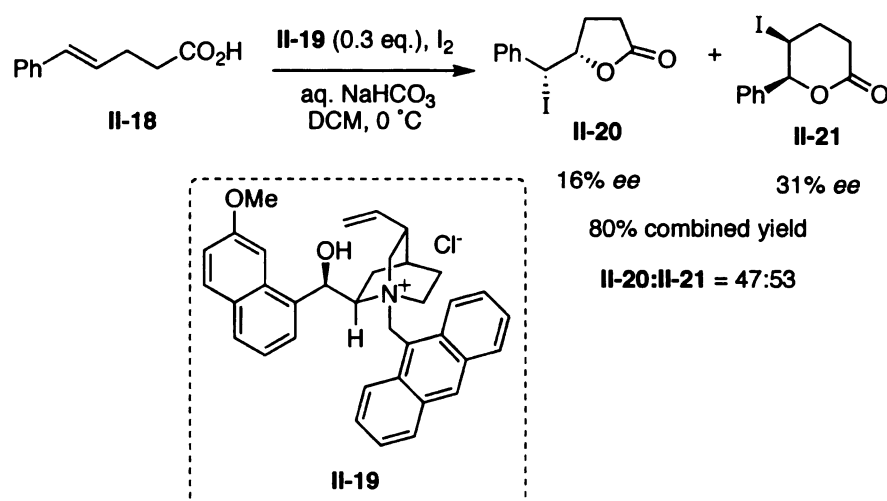
2.1.3: Reagent-Controlled Enantioselective Haloetherifications

As compared to their halolactone cousins, reagent controlled

enantioselective haloetherifications have enjoyed somewhat more success. The

first example was again reported by Taguchi's group in 1992, employing a

stoichiometric amount of a (+)-DIPT/titanium complex in the presence of iodine.[13]

Subsequently, Cui and Brown disclosed a stoichiometric chiral pyridine

bromonium dimer that returned a cyclic bromo-THF compound in 2.4% *ee*.[18]

Kang's group has presented an elegant series of transition metal catalysts

for the iodocyclization of γ-hydroxy-*cis*-alkenes **II-23** (Scheme II-4). With a

BINOL-titanium (IV) complex (20 mol% loading), the desired iodocyclized

products were produced in high yield with selectivities up to 65% *ee*.[22] Their

salen-cobalt (II) catalysts **II-22** (30 mol% loading) return iodo-THF products such

as **II-24** with enantioselectivities ranging from 67 to 90% *ee*.[23,24] To date, these

catalyst systems have been studied primarily with γ-hydroxy-*cis*-alkenes,

indicating that a system that is applicable to a larger substrate scope is perhaps

currently elusive.

Scheme II-4. Kang's cobalt catalyzed iodoetherification.

1. NCS, PhMe
   RT, 0.5 h
2. I₂, -78 °C

3.

II-22

0.3 eq.
relative to alkenol

-78 °C, 20 h

II-23

II-24

94%, 86% *ee*
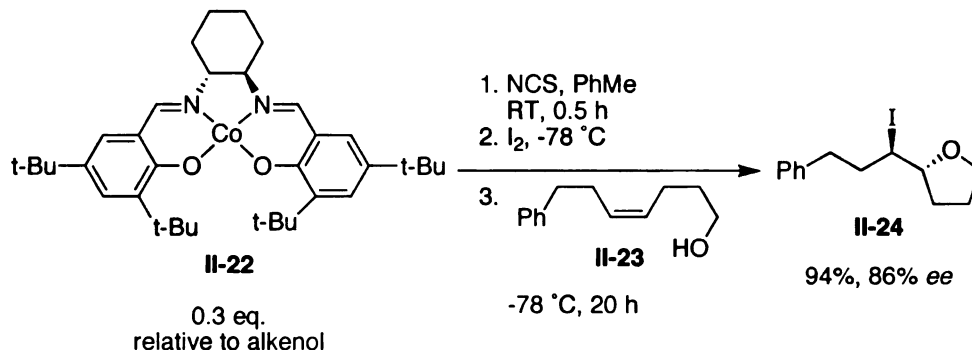
2.1.4: Reagent Controlled Enantioselective Halocarbocyclizations

Halocarbocyclizations have been relatively less explored than

lactonizations and etherifications. Again, Taguchi and coworkers applied a

titanium (IV) TADDOL complex **II-26** in 20-30 mol% to effect the enantioselective

cyclization of a series of malonate esters like **II-25** onto an iodonium ion to return

the desired carbocycles in high yield and selectivities ranging from 62 to 94% *ee*

(Scheme II-5).[25,26] More recently, Ishihara and coworkers disclosed an

enantioselective polyprenoid iodocyclization promoted by phosphoramidite **II-30**.

Polyene **II-29** was cyclized to provide tricyclic compound **II-31** in 95% *ee* and

57% yield. This elegant methodology allows for the formation of 2 to 3 rings and up to 5 stereogenic centers as a single diastereomer. This impressive protocol currently, however, relies upon a stoichiometric amount of chiral phosphoramidite promoter II-30.[27]

Scheme II-5. Reagent controlled asymmetric iodocarbocyclizations.

86% , 94% *ee*

57% , 95% *ee*
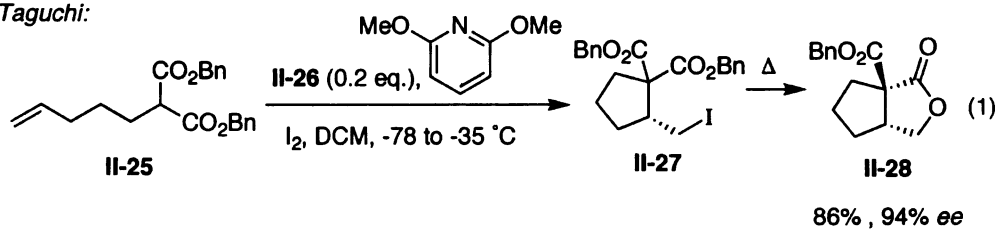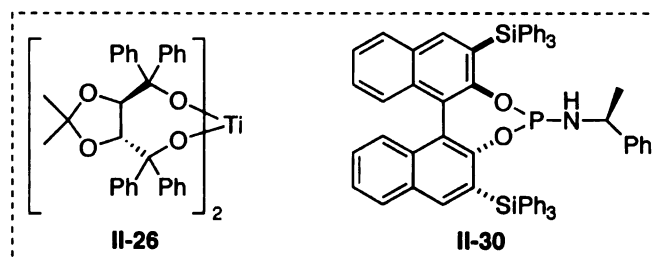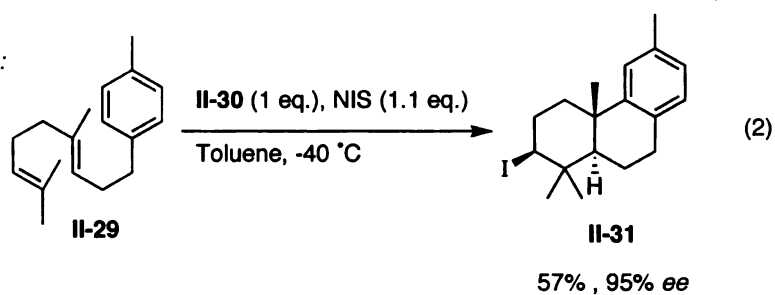
2.1.5: Enantioselective Gem-Dihalogen and Halohydrin Formation

Exploration of the organocatalytic enantioselective dihalogenation of olefinic substrates has to date met with little success. Early attempts relying on stoichiometric chiral ammonium perbromide salts (*e.g.* II-33) returned dibromoalkanes, bromohydrins or bromoethers (depending on solvent) with less than 33% *ee* (Scheme II-6).[28-32] Subsequently, Henry and coworkers disclosed a promising palladium (II) BINAP complex II-36 that returns chiral chlorohydrins (e.g. II-37) from various allyl ether starting materials.[33] This group has also reported an analogous dibromination reaction employing the same catalyst system.[34]

Scheme II-6. Asymmetric approaches to geminal dihaloalkanes and halohydrins.
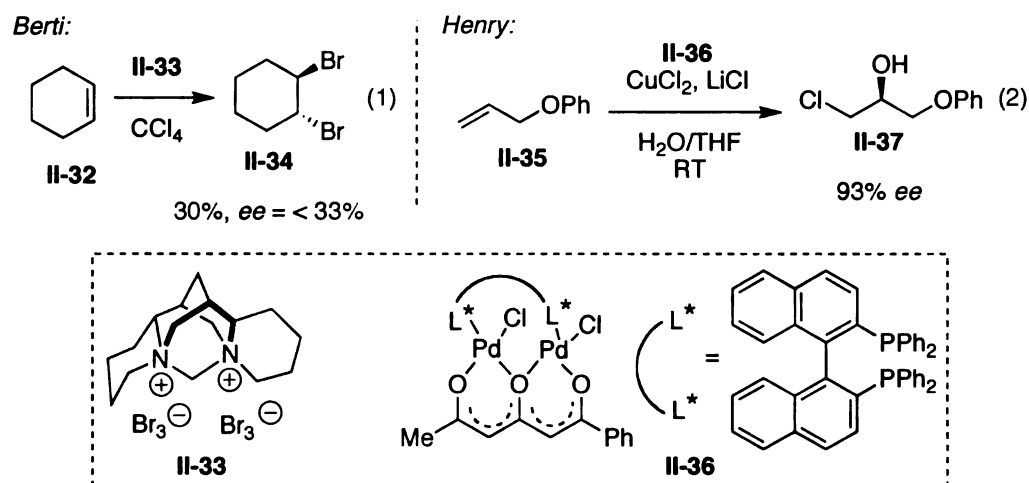
2.1.6: The Braddock-Cansell-Hermitage Bromolactonization

Our initial entry into the field was based upon a strategy where we sought to develop an asymmetric variant of a known organocatalytic protocol for effecting the bromolactonization of alkenoic acids. The general principles of this

transformation are described in this section. In 2006, Braddock and coworkers

developed two novel bromoiodinanes containing a rare I(III)-Br bond (**II-39**,

Scheme II-7). These reagents were conveniently prepared by treating the

appropriate *ortho*-iodo tertiary benzyl alcohols **II-38** with N-bromosuccinimide in

chloroform. The resulting crystalline products **III-39** have been characterized by

X-ray crystallography.

Scheme II-7. Braddock's bromoiodinane reagent **II-39**.
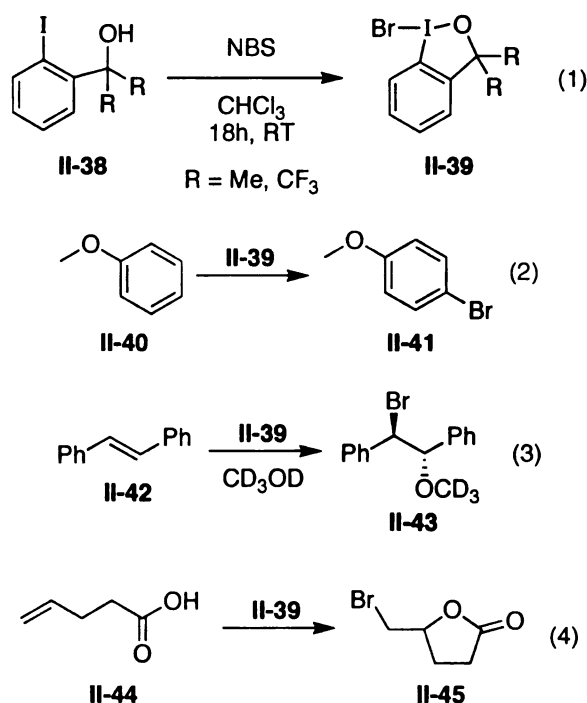
Subsequently, it was found that reagents of type **II-39** are effective

sources of electrophilic bromine (Br$^+$). The reagents proved useful as

stoichiometric bromenium sources for the bromination of anisole (eq. 2), the

intermolecular bromoetherification of *trans*-stilbene with methanol-d_4 (eq. 3), and

the bromolactonization of 4-pentenoic acid (eq. 4).[35] Importantly, control

experiments attempting the bromolactonization of 4-pentenoic acid with

molecular bromine provide significant amounts of the competing 4,5-dibromopentanoic acid, indicating that bromoiodinanes **II-39** are not generating molecular bromine *in situ*.[36]

A short time later, the same group reported a catalytic variant of the bromoiodinane reagents that were effective catalysts for the bromolactonization of a number of alkenoic acids. In particular, a number of aryl iodides with *ortho* nucleophilic groups were evaluated as effective organocatalysts (Scheme II-8). The presence aryl iodides with carboxylic acid, amide, or amidine *ortho* substituents all proved to be effective catalysts for the halolactonization of 4-pentenoic acid, showing enhanced rates and conversions compared to the background reaction with NBS alone. Not surprisingly, the most active catalysts were those substituted with more nucleophilic *ortho* substituents. The amidine catalyst **II-53**, along with the secondary and tertiary amides **II-50** and **II-51**, were the most active catalysts, completing the halolactonization of **II-44** in less than half an hour. Importantly, the uncatalyzed background reaction with NBS alone returned **II-45** in 2% conversion after 30 minutes and just 20% conversion after 15 hours. In total, seven alkenoic acids of various substitution patterns were cyclized using organocatalyst **II-53** and NBS. The desired bromolactones were isolated in yields ranging between 81 and 98%.[37]

Scheme II-8. The Braddock-Cansell-Hermitage Bromolactonization.

II-44 → NBS (1.2 eq.) / organocatalyst (0.1 eq.) / CDCl₃ RT → II-45

II-46
100% conv.
6 h

II-47
100% conv.
3 h

II-48
53% conv.
19 h

II-49
72% conv.
2 h

II-50
100% conv.
0.5 h

II-51
100% conv.
0.33 h

II-52
100% conv.
> 1.5 h

II-53
100% conv.
> 0.5 h
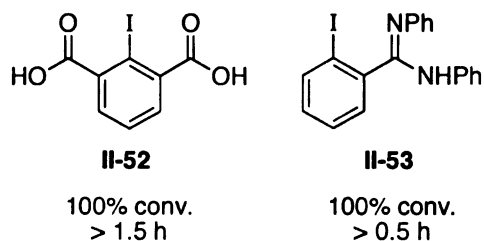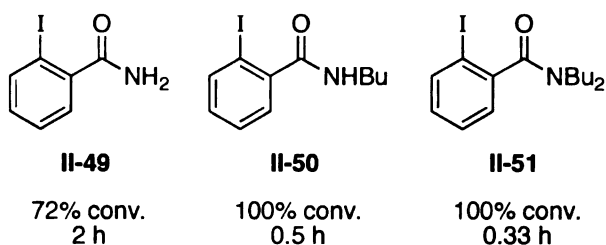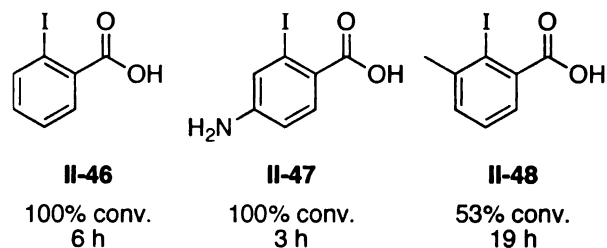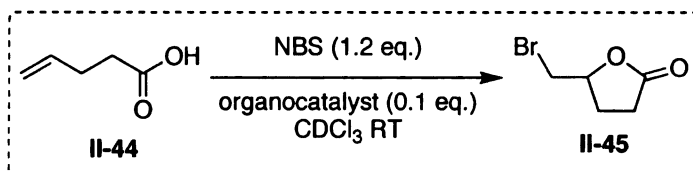
Intrigued by the ability of *ortho*-iodo secondary and tertiary aryl amides to catalyze the halolactonization and aware of the lack of a selective approach to asymmetric reagent controlled halolactonizations, a program to develop an enantioselective variant of the bromoiodinane-catalyzed bromolactonization reaction was initiated. For an initial investigation, we envisioned incorporating an *ortho*-iodoarylamido moiety within a chiral peptide framework. As discussed in

Chapter 1, chiral peptides with reactive functionality have enjoyed a large degree of success within the realm of asymmetric organocatalysis.[5] Several potential peptide-based scaffolds that embed the *ortho*-iodoarylamido active site within a chiral framework are shown in Figure II-1. Peptide **II-54** is perhaps the simplest of these scaffolds, and is reminiscent of scaffolds popularized by Hoveyda and Snapper used for enantioselective metal-mediated processes[38-41] and organocatalysis[42] (See Chapter 5 for a brief review). Scaffold **II-56** incorporates the well-established β-turn motif, nucleated by the presence of a Pro-D-Aaa sequence.[43,44] Short peptides incorporating this motif have been used previously as highly enantioselective organocatalysts[5,45,46] and as ligands for transition metal-catalyzed[47] enantioselective processes. Importantly, scaffolds **II-54** and **II-56** are amenable to preparation via well-established solid phase protocols (SPPS)[48,49] in a combinatorial sense. While scaffolds **II-54** and **II-56** only allow for the incorporation of the catalytically active site on the end of the peptide sequence, catalysts of the general type **II-55** allow for the incorporation of the crucial *ortho*-iodoarylamido motif within the heart of the chiral peptide chain. Catalyst **II-55** is a C2 symmetric catalyst that is readily accessible via the condensation of amino acid amides or esters with an iodo-isophthalic acid derivative. This scaffold is similar in nature to the bis-amino acid pyridine compounds employed for various chiral recognition applications.[50,51] Similarly, N-oxides of the bis-amino acid pyridine motif have been applied for the asymmetric alkylation of aldehydes with diethylzinc.[52]

Figure II-1. Peptide scaffolds incorporating the o-iodoarylamide site.

II-54

II-55

II-56
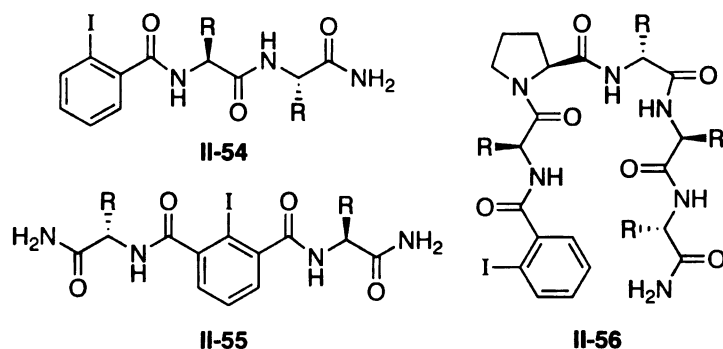
Detailed herein is an account of the application of a combinatorial strategy to develop a competent peptide-based organocatalyst based upon the general scaffolds described above. Most of our efforts have focused on the investigation of structure **II-54**. Scaffolds **II-55** and **II-56** have been investigated to a lesser degree. Although this approach did not return a highly selective catalyst, some gains were made. Ultimately, the lessons learned from the work detailed in this chapter laid an important foundation that culminated in the discovery of a related, highly selective chlorolactonization reaction (See Chapter 3).

2.2: Results and Discussion

2.2.1: Establishment of a Test Reaction and Appropriate Screening Scale

Initial efforts were geared towards establishing a test reaction to screen the peptide organocatalysts for asymmetric induction. The initial driver for the choice of a test substrate was to settle on a substrate whose enantiomers were readily separated by chiral HPLC, so as to establish a high-throughput screen to judge the extent of asymmetric induction afforded by potential organocatalysts.

We arrived at 4-phenyl-4-pentenoic acid (**II-12**) (Scheme II-9) owing to the fact

that it was readily prepared in quantity from commercially available methyl 3-

benzoylpropionate **II-57** by sequential Wittig olefination and saponification.[37]

Compound **II-12** is readily converted to the desired γ-bromolactone **II-58** under

racemic organocatalytic conditions with 10 mol % *ortho*-iodobenzoic acid (**II-46**)

and NBS as reported by Braddock and coworkers. The enantiomers of **II-58** are

conveniently separated by chiral HPLC (Chiralcel OD-H). In addition to these

operational conveniences, the choice of compound **II-12** was also driven by the

fact that some of the most recent attempts at the development of an asymmetric

reagent-controlled halolactonization reaction focused on the 4-arylpentenoic acid

substrate class (see Scheme II-2).[15,16] It seemed that initially targeting this

substrate class would provide a convenient standard to which we might

benchmark our progress. Furthermore, the lactonization of this class of alkenoic

acids proceeds cleanly to provide the γ-lactone as the sole product without

undergoing competing *endo* cyclization (*i.e.* δ-lactone formation).

     With regards to the scale of the screening protocol, we elected to perform

reactions in microscale, screening the peptides for the asymmetric

bromolactonization on a 0.05 mmol scale with respect to substrate **II-12** (9 mg

loading). This approach was taken in order to facilitate a high-throughput

screening approach, allowing the processing of between eight to ten samples per

day. On this scale, product purification could be carried out by performing silica

gel chromatography using packed Pastuer pipets allowing for the simultaneous

purification of up to ten samples at once.

Additionally, this scale allowed for the judicious application of only a few milligrams of the relatively more precious and expensive peptide catalysts. The trade-off for such a small scale approach, however, was that tracking isolated yields on the scale of a few milligrams was untenable. As a result, we chose to optimize the catalyst scaffold and reaction conditions based upon the perturbations observed for the enantioselectivity of the transformation as the sole variable. *Nonetheless, it warrants emphasis that all of the transformations described in this chapter proceeded to completion as judged by TLC analysis prior to work-up.*

Scheme II-9. Preparation of substrate **II-12** and lactone **II-58**.
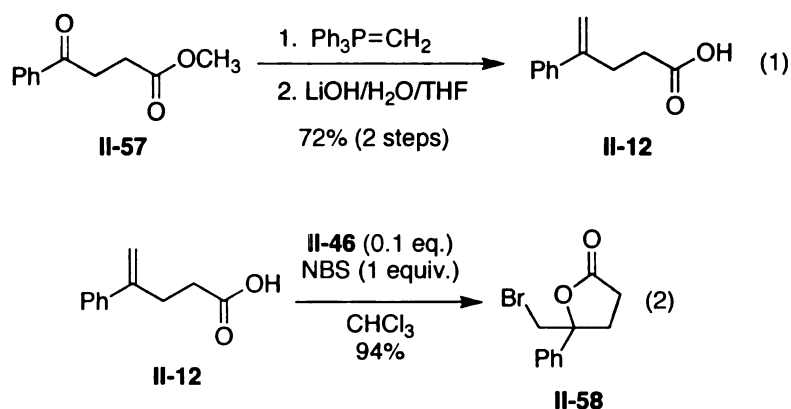
2.2.2: Preparation and Screening of the Initial Peptide Libraries

With substrate **II-12** in hand, a series of organocatalysts of general structure **II-54** (Figure II-1, *vide supra*) were prepared by solid phase peptide synthesis employing the Rink amide MBHA resin and standard coupling conditions (HOBt/DIC).[49] (For a discussion of the general principles and strategy of solid phase peptide synthesis, please see Chapter 5.) Initially, nine peptides were prepared whereby two amino acids were assembled from the C-terminus

54

and finally capped with the *ortho*-iodoaryl amide active site by capping the N-terminus with *o*-iodobenzoic acid (Figure II-2). The isolated peptides were subsequently characterized by MALDI-TOF mass spectrometry.

Figure II-2. Initial peptide library (**II-59** through **II-67**)
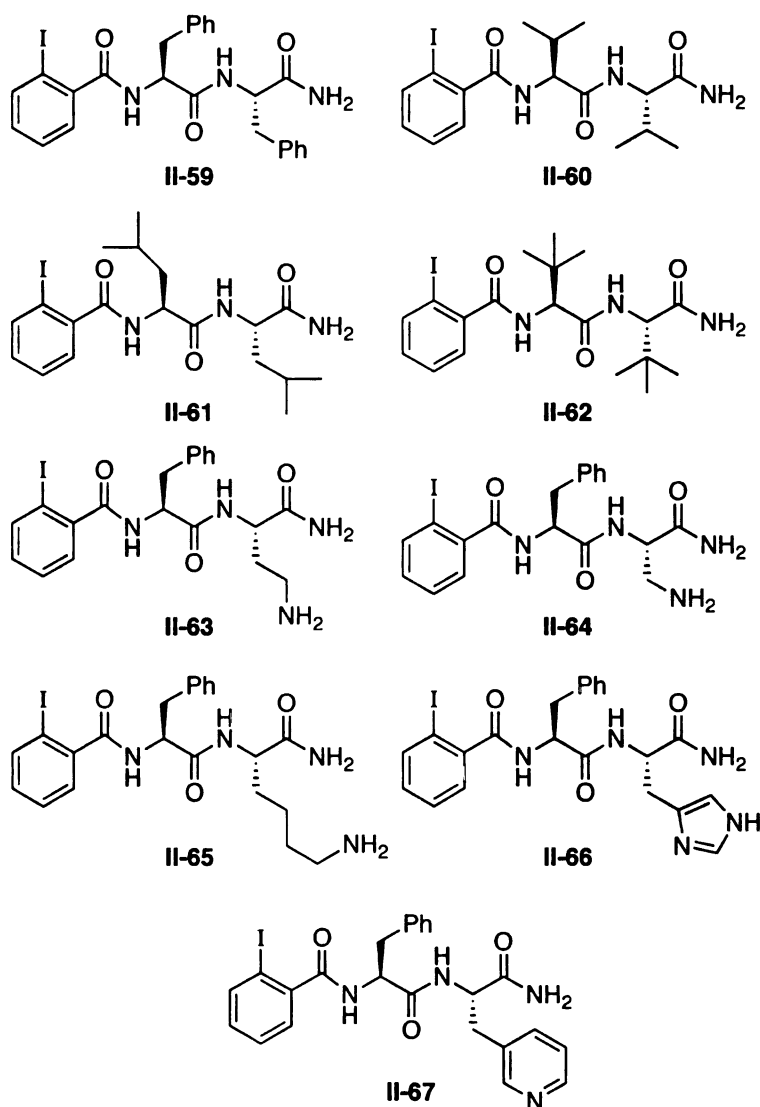
Peptide **II-59** incorporated an aromatic side chain, while peptides **II-60**, **II-61**, and **II-62** incorporated various aliphatic side chains of increasing steric bulk. Peptides **II-63** through **II-67** incorporate a basic residue on the C-terminus

separated from the aryliodo active site by a phenylalanine residue. The basic residues in organocatalysts II-63 through II-67 were incorporated in the hopes that they might serve to either deprotonate and thus activate the carboxylic acid nucleophile or to coordinate and thus orient the substrate in proximity with the active aryliodo site.

After their preparation, catalysts II-59 through II-67 were screened in the conversion of II-12 to II-58 with a 10 mol% catalyst loading (Table II-1). In the event, the conversion of substrate II-12 to II-58 proceeded in quantitative conversion by TLC in the presence of all of the organocatalysts described in Figure II-2. Initially, peptide II-59 was screened in the test reaction in a number of different solvents, with little selectivity regardless of solvent. After this initial screen, all other peptides were screened in only DCM and chloroform (owing mainly to solubility concerns). It was surmised that a more comprehensive solvent screen could be performed later with a lead scaffold. Peptides II-60, II-61, and II-63 through II-67 also proved to be unselective organocatalysts for the asymmetric halolactonization in both DCM and chloroform returning II-58 with less than 2% ee in all cases. In contrast, while organocatalyst II-62 performed poorly in chloroform, an enantiomeric excess of 7% was realized when the reaction was conducted in dichloromethane. Since this initial result was found to be reproducible, peptide II-62 was then taken to be an initial "hit" catalyst for the halolactonization. In that vein, efforts were then focused on the optimization of this lead based upon further manipulation of the organocatalyst structure.

Table II-1. Initial screening of peptides **II-59** through **II-67**.
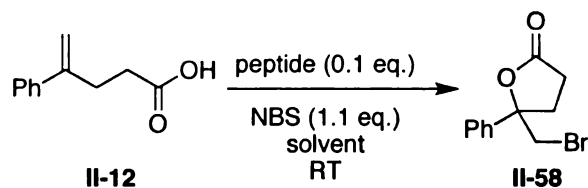
Peptide	Solvent	% *ee* (II-58)
II-59	chloroform	0
II-59	DCM	0
II-59	toluene	0
II-59	benzene	0
II-59	DMF	0
II-59	DMF/DCM (1:1)	1
II-59	ACN	3
II-59	EtOAc	0
II-60	chloroform	0
II-60	DCM	-2
II-61	chloroform	0
II-61	DCM	1
II-62	chloroform	0
II-62	DCM	7
II-63	DCM	2
II-64	DCM	0
II-65	DCM	0
II-66	DCM	-1
II-67	DCM	0

Note: All reactions were complete by TLC

Given that catalyst **II-62** emerged as an initial hit scaffold, a directed library was generated whereby ten new catalysts were prepared by modulating the C-terminal amino acid distal from the aryl iodoamide moiety. This residue was targeted for optimization on the assumption that the proximal *tert*-leucine residue in **II-62** would be a crucial structural element for maintaining the selectivity that was initially realized. Figure II-3 indicates the next ten peptides resulting from the directed library screen around the initial hit scaffold **II-62**.

Figure II-3. Analogs from positional scanning of hit scaffold II-62.

II-68

II-69

II-70

II-71

II-72

II-73

II-74

II-75

II-76

II-77
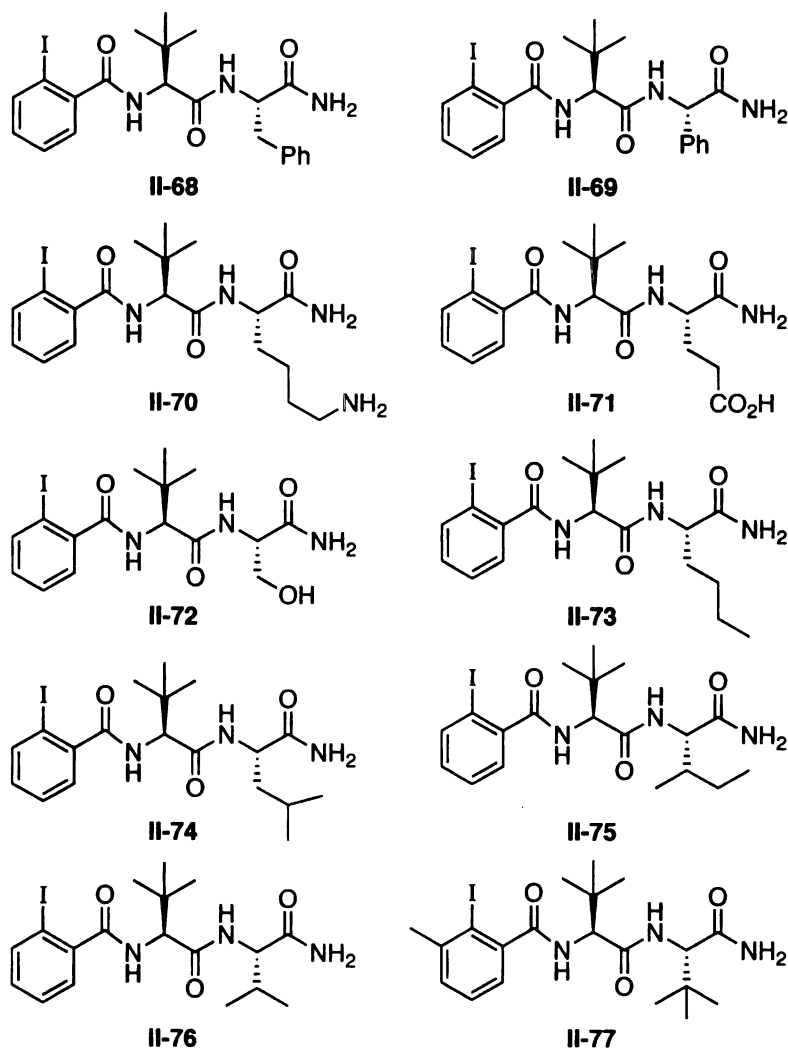
These organocatalysts were screened in the test reaction at room temperature in dichloromethane (Table II-2). While none of the peptides from this directed library outperformed organocatalyst **II-62**, it is interesting to note some of the minute structural changes that result in reduced selectivity. Simply put, it appears that both *tert*-leucine residues found in **II-62** are necessary to maintain the 7% *ee*. Modulating the C-terminal *tert*-leucine to benzyl (**II-68**), phenyl (**II-69**), basic (**II-70**), acidic (**II-71**) or carbinol (**II-72**) side chains proved to be detrimental to the minimal selectivity garnered from **II-62**.

More interesting still are the changes observed by modulating the C-terminal *tert*-leucine to other aliphatic side chains. Incorporating unbranched aliphatic chains (**II-73**) or removing the site of branching farther away from the peptide backbone (**II-74**) resulted in inferior catalysts. Even those catalysts that maintained branching at the 1 position on the side chain (**II-75** and **II-76**) were less selective. Finally, incorporating a methyl group at the 3 position on the aryl iodoamide residue (**II-77**) resulted in a poorly selective catalyst. This result is in keeping with the initial findings disclosed by Braddock and co-workers.[37] In their work, an sp^3 hybridized substituent flanking the iodine atom resulted in a less active catalyst (*cf.* **II-46** vs. **II-48**, Scheme II-8).

Table II-2. Screen of peptides **II-68** through **II-77**.
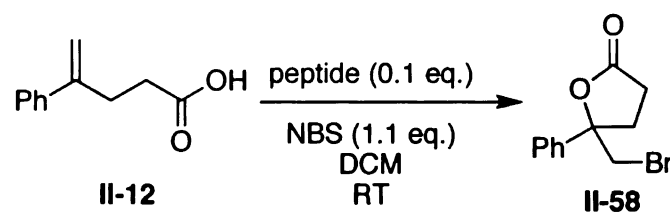
Peptide	% *ee* (II-58)
II-68	2
II-69	3
II-70	2
II-71	1
II-72	2
II-73	0
II-74	2
II-75	2
II-76	4
II-77	2

Note: All reactions were complete by TLC

Having established that both the proximal as well as the distal *tert*-leucine

residues were necessary for the 7% *ee* observed with catalyst **II-62**, a longer

analogue was prepared, thus incorporating a third *tert*-leucine moiety. When

screened in the test reaction (**II-12** to **II-58**), second generation catalyst **II-78**

proved to be twice as selective as its shorter cousin **II-62**, thus returning **II-58** in

14% *ee* (Table II-3, entry 9). Upon discovery of this catalyst a number of

experiments were undertaken in an effort to enhance the selectivity of **II-78** by

optimizing the reaction conditions. Initially, a relatively limited solvent screen was

undertaken (Table II-3, entries 1-8). Again the initially discovered conditions,

employing dichloromethane were the most selective. Changing the solvent to

Table II-3. Screen of peptide **II-78**.
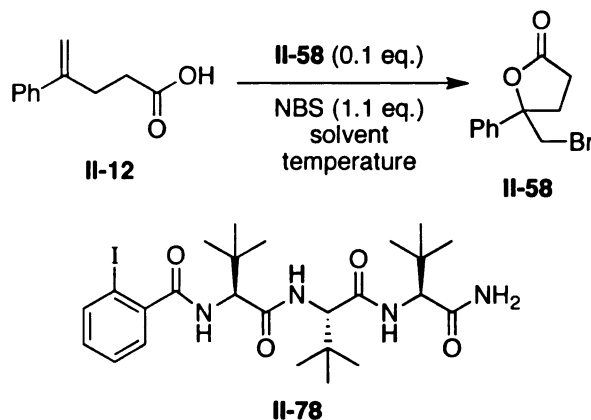
Entry	Solvent	Temp. (°C)	% ee (II-58)
1	chloroform	RT	3
2	toluene	RT	1
3	benzene	RT	0
4	THF	RT	-2
5	DMF	RT	0
6	DMSO	RT	0
7	ACN	RT	1
8	1,2-DCE	RT	8
9	DCM	RT	14
10	DCM	4	12
11	DCM	-20	12
12	DCM	-78 to RT	12

Note: All reactions were complete by TLC.

61

chloroform, toluene, benzene, N,N-dimethylformamide, dimethylsulfoxide, or acetonitrile resulted in inferior reactions with almost no selectivity. The only other solvent to show any appreciable enantioselectivity was dichloroethane, providing the desired bromolactone **II-58** in 8% *ee* (entry 8).

Somewhat surprisingly, lowering the reaction temperature also failed to improve the selectivity of the halolactonization in the presence of **II-78** (entries 10-12). While the reaction proceeded to completion in all cases, running the reaction a 4 °C, -20 °C and even -78 °C resulted in selectivities that were comparable to the screen run at room temperature.

Next a moisture study was undertaken to ascertain whether the exclusion of water from the reaction mixture would enhance the selectivity of the reaction. The initial data collected for peptide **II-78** (14 % *ee*, entry 9, Table II-3) resulted from a reaction conducted in freshly distilled dichloromethane under non-anhydrous conditions (*i.e.* run in a non-flame dried screw-top vial). In order to completely preclude water from the system, two experiments were conducted. First, the reaction was run under strictly anhydrous conditions in a sealed, flame-dried round-bottomed flask with freshly distilled dichloromethane, under a nitrogen atmosphere. Simultaneously, a second experiment was conducted under analogous conditions with the addition of activated 4 Å molecular sieves. Both of these screens resulted in a less selective bromolactonization, yielding 6% and 4% *ee*, respectively. This data might suggest that some serendipitous water is necessary to maintain the initially observed 14% *ee*.

Having noted the apparent necessity for some ambient water present in

the reaction, a second set of experiments were conducted to evaluate the effect

of added moisture on the selectivity of the reaction (Table II-4). Seven

experiments were conducted simultaneously whereby water was added to the

reaction mixture in equivalencies ranging for 1 to 500 equivalents. While some

water (up to 1 equivalent) allows for selectivities in the ballpark of the initial

screen (10% *ee* vs. 14% *ee*), extra equivalents of water (5, 10, 20, 50, 100, and

500 equivalents) proved to cause a less selective process.

Table II-4. Water equivalency study with peptide **II-78**.
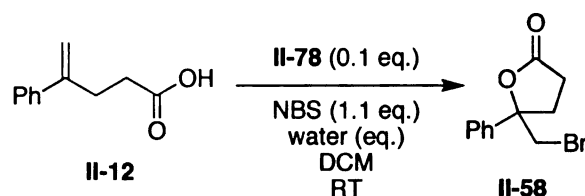
Entry	water (eq.)	% ee (II-58)
1	1	10
2	5	4
3	10	5
4	20	7
5	50	5
6	100	2
7	500	3

Note: All reactions were complete by TLC

Next, the effect of the equivalency of the peptide organocatalyst on the

selectivity of the reaction was evaluated (Table II-5). The goals of this trial of

experiments were two-fold. First, it was of interest to evaluate whether or not the

selectivity of the initial reaction (0.1 equivalents of peptide) could be maintained

when lower catalyst loading was employed. Secondly, it was also interesting to

evaluate whether or not the selectivity of the reaction could be increased by

increasing the catalyst loading beyond 0.1 equivalents. In particular, the

evaluation of the stoichiometric variant might provide some insight into the

"ceiling" selectivity for organocatalyst **II-78**.

Table II-5. Equivalency study for II-78.
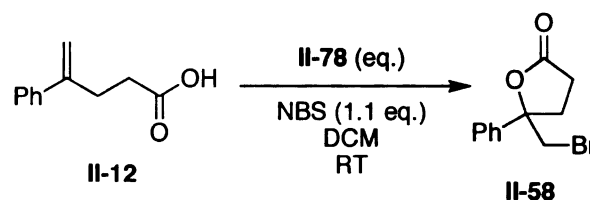
Entry	II-78 (eq.)	% *ee* (II-58)
1	0.01	2
2	0.05	7
3	0.10	14
4	0.20	14
5	1.11	24

Note: All reactions were complete by TLC

Unfortunately, the initial selectivity of the reaction with 0.1 equivalents of

II-78 (14% *ee*) could not be maintained on decreasing the loading to 0.01 (5%

ee) or even 0.05 equivalents (7% *ee*). On increasing the catalyst loading 0.2

equivalents, the same selectivity (14% *ee*) was observed. Finally, the

stoichiometric variant of the reaction was evaluated employing 1.11 equivalents

of catalyst **II-78**. For this particular experiment, **II-78** was pre-stirred in DCM with

1 equivalent of NBS for 30 minutes. This initial catalyst aging process was employed in order to insure the (assumed) complete conversion of the organocatalyst into the active iodinane reagant **II-79** (Scheme II-10). After this initial incubation, substrate **II-12** was added in solid form in one portion. After work-up, this particular experiment yielded the desired bromolactone **II-58** with an enantiomeric excess of 24%. This low level of selectivity under stoichiometric conditions was disheartening, and potentially sounded the death knell for this particular strategy towards asymmetric halolactonization. Several possible explanations for the result came to light. First, it is possible that the conversion to the putative active bromoiodinane catalyst **II-79** was sufficiently slow to allow for the uncatalyzed background reaction. In other words, if the formation of bromoiodinane moiety is not facile, there may only be a small portion **II-79** at equilibrium mixture. Alternatively, the formation of **II-79** might be favored at equilibrium, but might be a less active bromenium source than NBS. A final possibility is that **II-79** could be adequately reactive, but requires more structural tuning to result in a truly selective catalyst.

Scheme II-10. Potential equilibrium between **II-78** and **II-79**.

II-78   II-79
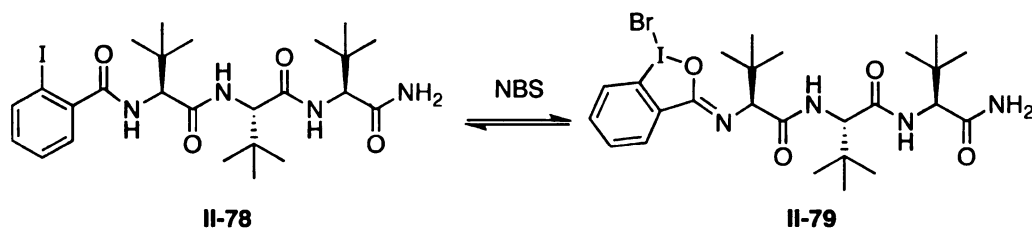
Subsequent to these experiments, a final condition screen included an evaluation of the selectivity of the reaction at various concentrations. The initial

result with peptide **II-78** (14% *ee*, Table II-5, entry 3) was obtained at a

concentration of 0.05 M in substrate (9 mg of **II-12** in 1 mL DCM). To evaluate

the fate of the reaction at higher and lower concentrations in substrate, two

experiments were performed (Table II-6). First, the effect of dilution on the

selectivity of the reaction was evaluated. An analogous reaction was run at

0.025 M concentration (entry 1), and the desired lactone **II-58** was isolated in

10% ee. The effect of higher concentration on the reaction selectivity was more

pronounced: when the reaction was conducted at 0.1 M in substrate the reaction

provided products with 6% ee (entry 3). Once again, the initially discovered

reaction conditions proved to be optimal (entry 2).

Table II-6. Concentration study with catalyst **II-78**.
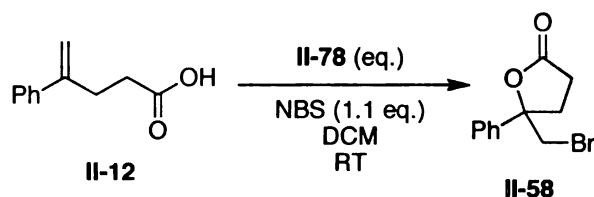
Entry	Conc. (M)	% ee (II-58)
1	0.025	10
2	0.05	14
3	0.5	6

Note: All reactions were complete by TLC

Having demonstrated a relative inability to improve upon the selectivity of

the initially discovered reaction conditions, a new round of peptides were

synthesized in an attempt to drive the selectivity higher by modifying scaffold **II-78** by positional scanning. Applying this strategy, eleven new peptides were

prepared (Figure II-4). Peptides **II-80** through **II-82** were developed in order to

determine if all three amino acids in the peptide chain necessarily needed to be *tert*-leucine residues. Peptides were therefore constructed whereby the amino acids in the peptide were sequentially replaced with valine residues starting at the C-terminus (**II-80**) and moving towards the N-terminus (**II-81** and **II-82**). Peptide **II-83** was constructed to probe the necessity of the C-terminal amide, and was easily prepared using a valine-loaded Wang resin. Peptides **II-84** and **II-85** were assembled to evaluate the consequences of increasing the length of the peptide by the installation of a fourth amino acid residue on the C-terminus. Catalysts **II-86** and **II-87** were designed to evaluate the course of the reaction using a catalyst with even bulkier residues than those found in **II-78**. In this case *tert*-butyl threonine units were installed in lieu of the *tert*-butyl groups resident in **II-78**. These structures were assembled on the Val-Wang resin and cleaved using the MeOH/TEA/DCM (9:1:1) cleavage cocktail that returns fully side-chain protected peptide methyl esters. Simultaneously, **II-88** was prepared on the Rink amide MBHA resin to provide the fully deprotected amide variant of **II-87**. Finally, **II-89** and **II-90** were assembled to probe the effects of installing an intervening proline residue between the *o*-iodoarylamide active site and the *tert*-leucine residues.

Figure II-4. Analogues of peptide II-78.
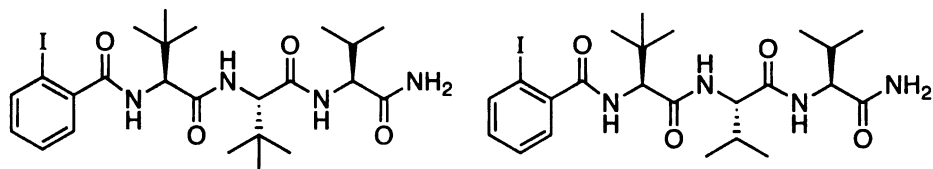
II-80

II-81
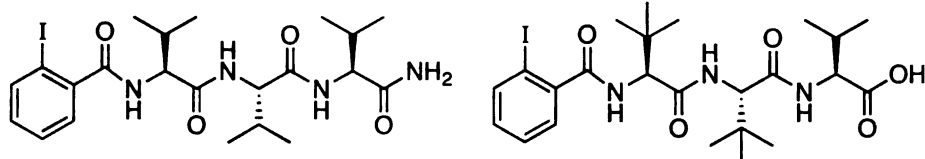
II-82

II-83
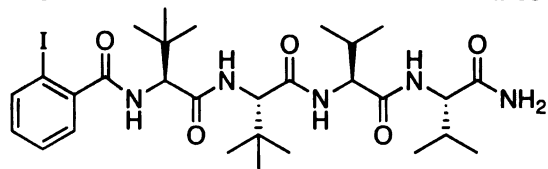
II-84
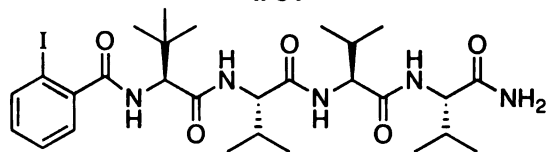
II-85
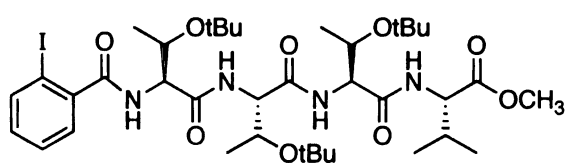
II-86
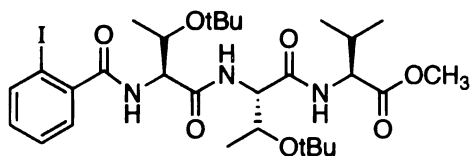
II-87

II-88

II-89

II-90

68
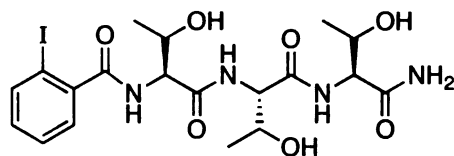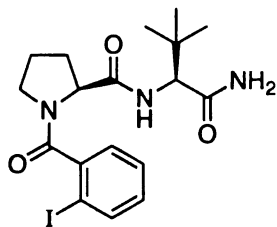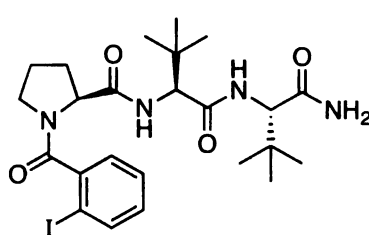
Peptides **II-80** through **II-90** were screened in the bromolactonization of II-12 (Table II-7). As the C-terminal residues were sequentially modulated from *tert*-leucine to valine, a definite decline in selectivity was realized. While changing the C-terminal *tert*-leucine farthest removed from the iodoarylamido active site was tolerated (*cf.* 13% *ee* for **II-80** vs. 14% *ee* for **II-78**), further changes closer to the N-terminus of the scaffold resulted in poorly selective catalysts (Table II-7, entries 2 and 3). Switching all of the *tert*-leucine moieties with valine resulted in a completely unselective catalyst while retaining only one *tert*-leucine returned the lactone in 7% *ee*. These data are in excellent agreement with the initial experiments that lead to the discovery of **II-78** as a lead scaffold (Tables II-1 and II-2, *vide supra*), and serve to confirm the assertion that two flanking *tert*-leucine residues represent a minimal structrual element for stereoinduction. Modulating the C-terminal amide in **II-80** to a C-terminal carboxylic acid (**II-83**) had no effect on the selectivity of the bromolactonization (Table II-7, entries 1 and 4).

On incorporating a fourth amino acid residue (valine) on the C-terminus, a negligible increase to 15% *ee* was realized with peptide **II-84**. Peptide **II-85** again confirms the necessity of the two *tert*-leucine residues proximal to the iodoarylamido site (2% *ee*, entry 6).

Further increasing the steric bulk of the catalyst by incorporating *tert*-butyl threonine residues in lieu of *tert*-leucine resulted in inferior catalysts (peptides **II-86** and **II-87**, entries 7 and 8). Similarly the unprotected threonine analogue **II-88** was completely unselective (entry 9).

The incorporation of a proline residue in between the iodoarylamido active site and the crucial neighboring *tert*-leucine produced peptides **II-89** and **II-90**, which were inferior to the second generation catalyst **II-78**. These experiments further underscore the necessity for the two *tert*-leucine residues neighboring the active site aryliodoamido moiety as a minimal scaffold for a selective peptide.

Table II-7. Screen of peptides **II-80** through **II-90**.
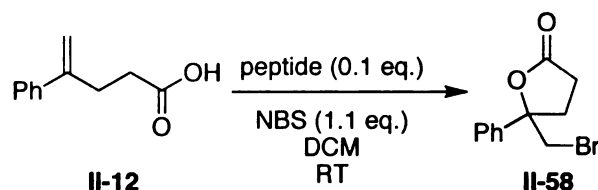
Entry	Peptide	% *ee* (II-58)
1	**II-80**	13
2	**II-81**	7
3	**II-82**	0
4	**II-83**	13
5	**II-84**	15
6	**II-85**	2
7	**II-86**	0
8	**II-87**	0
9	**II-88**	0
10	**II-89**	0
11	**II-90**	4

Note: All reactions were complete by TLC

Overall the analogues of **II-78** (**II-80** through **II-90**) failed to provide a new lead compound. The only peptide that offered an enhanced selectivity was **II-84**,

and even in this case, the addition of a fourth amino acid only earned an increase of 1% in enantiomeric excess. Perhaps the only benefit of peptide **II-84** over **II-78** is the existence of an additional potential site for positional scanning.

Given that we had reached an initial roadblock with scaffold **II-54**, we sought to investigate the other scaffolds described in Figure II-1 (*vide supra*). The discussion will now turn to a limited investigation of β-turn scaffold **II-56**, as well as the investigation of the bis-amino acid scaffold **II-55**.

2.2.3: Investigation of β-Turn (II-56) and Bis-Amino Acid Scaffolds (II-55)

Initially, two hexapeptide β-turn catalysts were prepared by incorporating the well-known Pro-D-Aaa sequence (where D-Aaa is any D configured amino acid).[43,44] Catalyst **II-91** was capped on its N-terminus with *o*-iodobenzoic acid while **II-92** was capped with 2-iodo-3-methylbenzoic acid (Figure II-5).

Figure II-5. β-turn catalysts **II-91** and **II-92**.

II-91   II-92
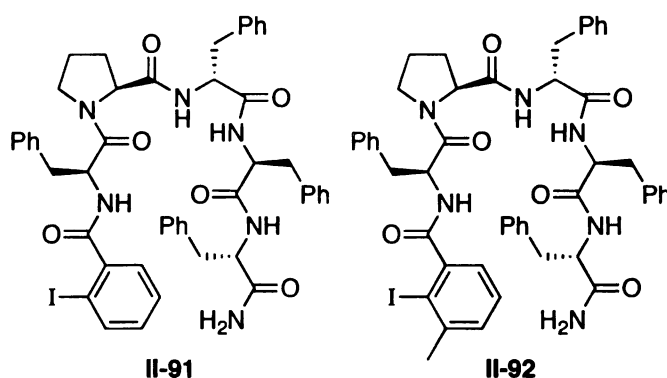
Catalysts **II-91** and **II-92** were subsequently screened in the bromolactonization of **II-12** (Table II-8). While peptide **II-91** was completely unselective in both DCM and ACN, peptide **II-92** returned lactone **II-58** in 5% *ee*

71

in DCM at room temperature. Perhaps a positional scanning regime originating

from **II-92** would eventually yield a useful catalyst, but the size of these

molecules might somewhat detract from their potential usefulness. For instance

a 0.1 equivalent loading of **II-92** requires the use of 10 mg of catalyst to convert

only 17 mg of substrate **II-12**!

Table II-8. Screen of β-turn catalysts **II-91** and **II-92**.
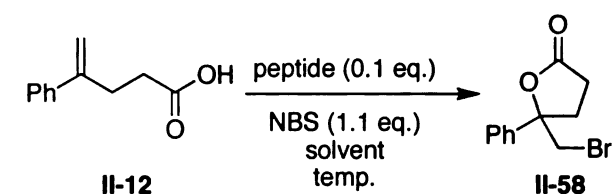
Peptide	Temp. (°C)	Solvent	% *ee* (II-58)
II-91	RT	DCM	1
II-91	RT	DCM	0
II-91	4	ACN	0
II-92	RT	DCM	5

Note: All reactions were complete by TLC

In addition to investigating the β-turn scaffold **II-56** (Figure II-1), we

envisioned targeting the bis-amino acid based scaffold **II-55** by conventional

synthesis. We applied a similar synthetic strategy as that used by Moriuchi and

coworkers in their preparation of bis-amino acid pyridine scaffolds for chiral

recognition applications (Scheme II-11).[50,51] Namely, the bis acid chloride of 2-

iodo-*iso*-phthalic acid (**II-94**) was subsequently treated with 2 equivalents of the

appropriate amino acid methyl ester hydrochloride salt (**II-95**) in the presence of

triethyl amine and dichloromethane thus generating the desired bis-amino acid

scaffold **II-96** (*i.e.* the methyl ester analogue of amide **II-55**, Figure II-1). The

required 2-iodo-*iso*-phthalic acid was prepared from the commercially available 2-amino-*iso*-phthalic acid (**II-93**) according to known methodology.[53] Applying this strategy, the corresponding bis valine (**II-97**, 46%), *tert*-leucine (**II-98**, 62%), phenylglycine (**II-99**, 12%), and proline (**II-100**, 35%) catalysts were prepared.

Scheme II-11. Preparation of bis-amino acid catalysts **II-97** through **II-100**.
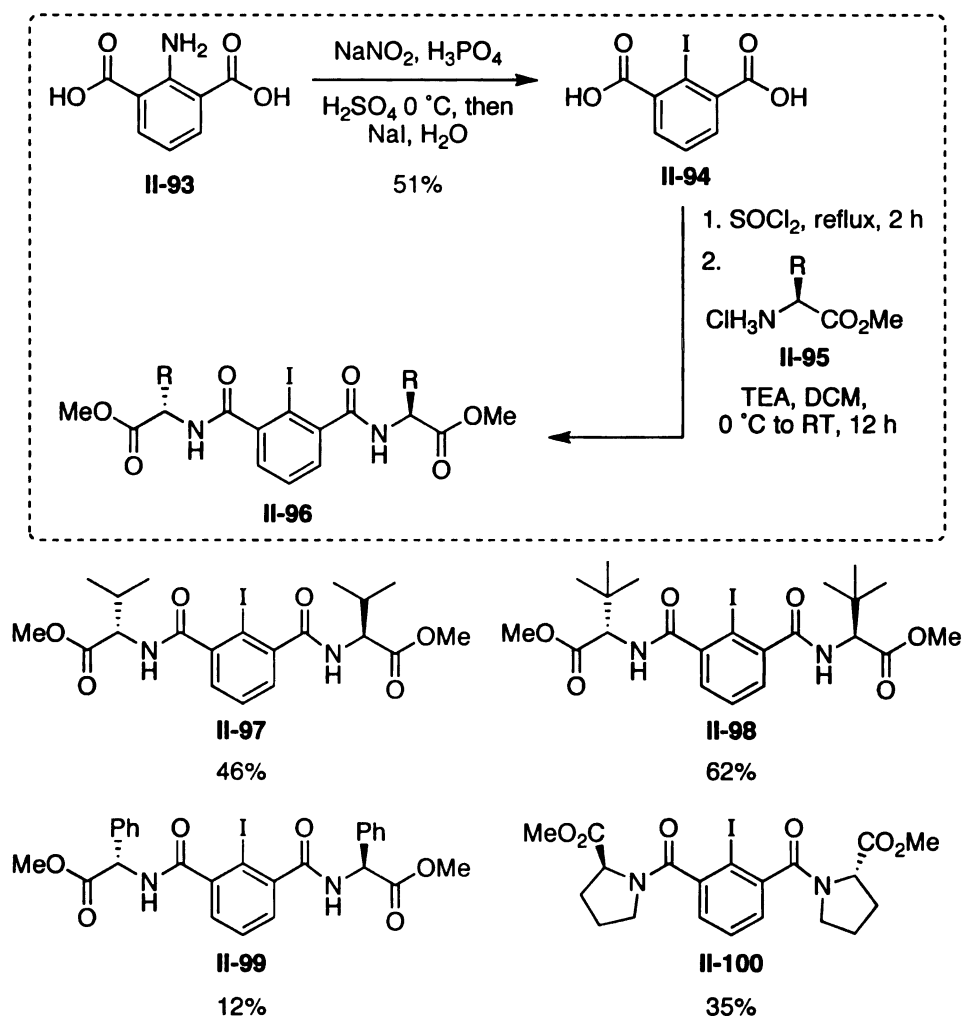
Although the yields were poor in some cases, these catalysts were prepared in sufficient quantity for screening in the test lactonization of **II-12**. In

73

addition to screening at room temperature, these peptides were also screened at -40 °C. The experiments described in Table II-9 were contemporaries of fruitful low temperature studies in the analogous *Cinchona*-alkaloid mediated chlorolactonization work (see Chapter 3). They are included here for completeness.

As is evident from Table II-9, the bis-amino acid catalysts performed poorly. In each case, a selectivity of greater than 4% *ee* was never realized regardless of solvent or temperature. In one case, a stoichiometric experiment (entry 9) also returned racemic **II-58**. Although only speculative, one might suggest that these catalysts are too sterically crowded around the iodo active site, thus preventing the generation of the active bromoiodinane reagent.

Table II-9. Screen of bis-amino acid catalysts **II-97** through **II-100**.
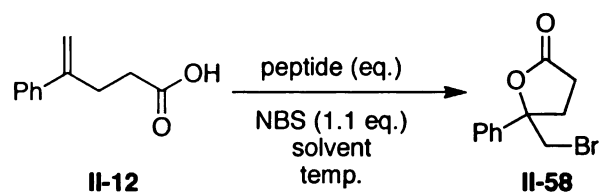
Entry	Peptide	Cat. (eq.)	Temp. (°C)	Solvent	% *ee* (II-58)
1	**II-97**	0.1	RT	DCM	0
2	**II-97**	0.1	RT	chloroform	0
3	**II-97**	0.1	-40	DCM	0
4	**II-97**	0.1	-40	chloroform	4
5	**II-98**	0.1	RT	DCM	0
6	**II-98**	0.1	RT	chloroform	0
7	**II-98**	0.1	-40	DCM	0
8	**II-98**	0.1	-40	chloroform	0
9	**II-98**	1.0	-40	chloroform	0
10	**II-99**	0.1	RT	DCM	0
11	**II-99**	0.1	RT	chloroform	0
12	**II-99**	0.1	-40	DCM	0
13	**II-99**	0.1	-40	chloroform	0
14	**II-100**	0.1	RT	DCM	0
15	**II-100**	0.1	RT	chloroform	1
16	**II-100**	0.1	-40	DCM	0
17	**II-100**	0.1	-40	chloroform	1

Note: All reactions were complete by TLC

75

2.2.4: Investigation of Alternative Bromine Sources

At this juncture, peptide organocatalyst **II-78** had emerged as the catalyst

of choice, and represented the best results under the initial screening conditions

employing substrate **II-12** and NBS as the terminal bromenium source.

Purification (recyrstallization) of NBS or the slow addition of NBS over 7 hours

failed to improve the selectivity of the reaction, returning **II-58** in 13 and 12% *ee*,

respectively. Focus then shifted to efforts aimed at discovering an alternative

bromine source. A literature survey revealed many possible alternative sources

of electrophilic bromine. Figure II-6 details several sources or reagent

combinations that were commercially available.

Figure II-6. Commerically available bromine sources or reagent combinations.
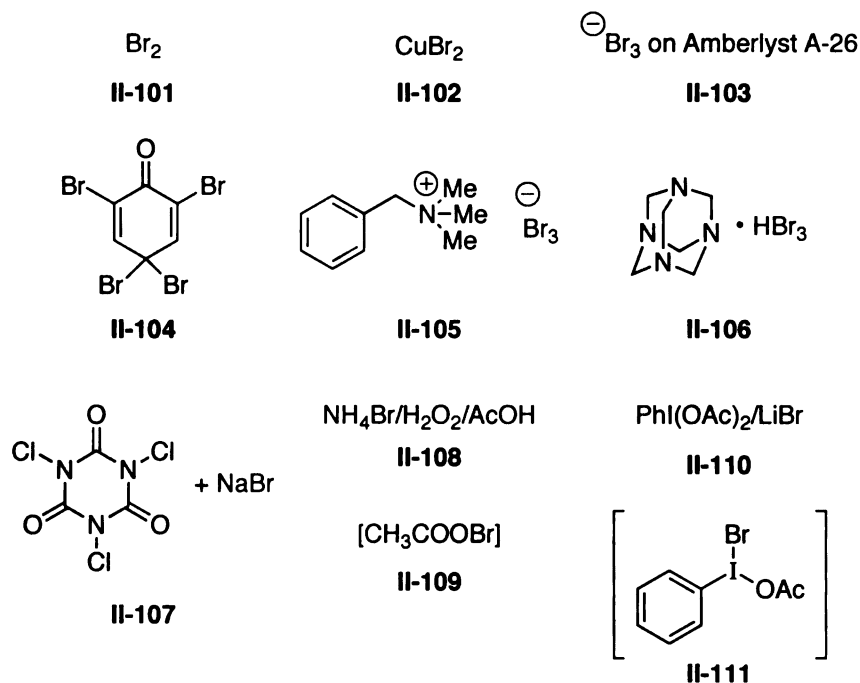
In addition to molecular bromine (**II-101**), perhaps the most well-known

bromenium sources include the organic ammonium tribromides (OATBs).[54]

Those purchased for this study include benzyltrimethylammonium tribromide (II-105),[54] hexamethylenetetramine tribromide (II-106), and tribromide on Amberlyst A-26 resin (II-103). In addition to these tribromide sources, two were synthesized (*vide infra*). Other commercial sources included 2,4,4,6-tetrabromo-2,5-cyclohexadienone (TABCO, II-104)[55,56] and cupric bromide (II-102).[57] TABCO has found use as an electrophilic bromine source for the deprotection of thioacetals.[55,56] Cupric bromide has been used sparsely as a bromenium source for the bromination of electron-rich aryls.[57] In addition to these sources, several cocktails prepared from commercial reagents have been shown to serve as electrophilic bromine sources. Tetrachloroisocyanuric acid (TCCA) and sodium bromide (II-107) is an effective bromine source for the bromination of activated aromatics.[58,59] The combination of ammonium bromide and hydrogen peroxide in acetic acid (II-108) is an effective bromine source for the bromination of anilines. This cocktail is thought to generate bromenium acetate (II-109) as the active bromine source.[60] Finally, Braddock and coworkers discovered that a combination of bis(acetoxy)iodobenzene and lithium bromide (II-110) could catalyze a number of bromination reactions such as the bromination of aryls, bromolactonization, and the addition of dibromide across an olefin. These reagents are thought to produce intermediate II-111, containing a rare I(III)-Br bond, via the displacement of one acetoxy group form the iodine by bromide ion.[36]

In addition to these commercial sources of electrophilic bromine (Br$^+$), six additional sources were prepared (Scheme II-12). Some of these synthetic

sources are themselves commercially available, but were cheaply and conveniently prepared in house.

Scheme II-12. Preparation of various electrophilic bromine sources.
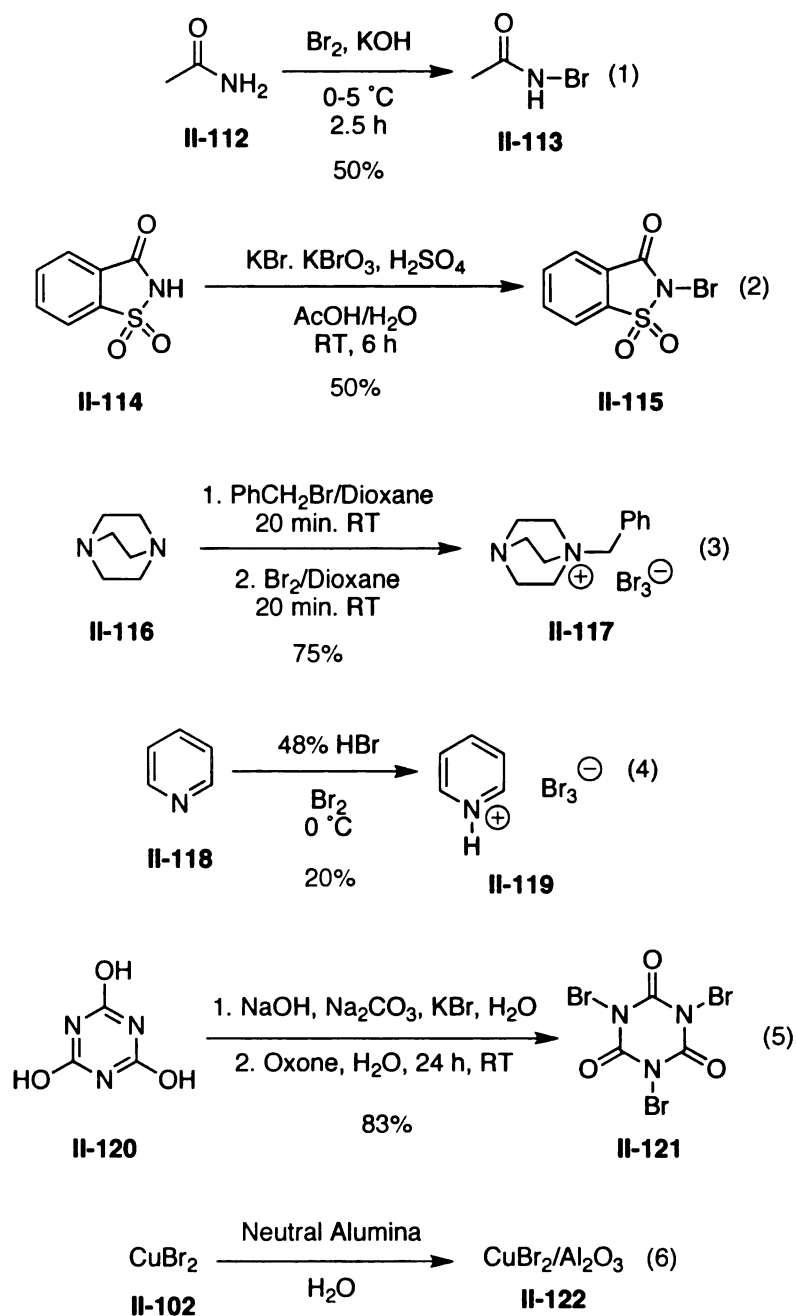
N-bromoacetamide (NBA, **II-113**)[61] and N-bromosaccharin (NBSac, II-

115)[62,63] were prepared as analogues of NBS. Pyridinium tribromide (**II-119**) was

prepared easily by the method of Fieser and Fieser.[64] A final tribromide source,

N-benzyl-DABCO tribromide **II-117** was readily prepared by Moghaddam's

protocol.[65,66] N-benzyl-DABCO tribromide has been employed previously as a

bromine source for the deprotection of thioacetals[66] and the oxidative cyclization

of benzothioamides to benzothiazoles[65].

Tribromoisocyanuric acid (TBCA) (**II-121**), a useful reagent for the

bromination of activated aryls, was easily prepared from commercially available

cyanuric acid.[58,59] Finally, cupric bromide on alumina (**II-122**) is a known source

of electrophilic bromine that is useful in the bromolactonization of alkenoic acids[67]

and the bromination of aryls.[68]

With these new bromine sources in hand, they were quickly screened as

halogen sources for the lactonization of **II-12** in the presence of 0.1 equivalents

of **II-78** at room temperature in DCM. Table II-12 summarizes the data for this

screen. Note that all transformations described in Table II-12 proceeded to

completion as judged by TLC analysis, with the exception of entry 14 (see text,

vide infra).

Table II-12. Screen of alternative bromine sources.
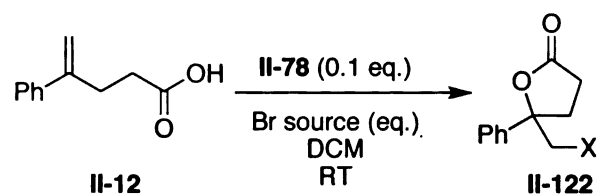
Entry	Br Source	Equiv.	% *ee* (II-122)	X (II-122)
1	II-113	1.1	2	Br
2	II-113	2.2	1	Br
3	II-115	1.1	9	Br
4	II-103	1.1	0	Br
5	II-105	1.1	0	Br
6	II-106	1.1	7	Br
7	II-116	1.1	7	Br
8	II-119	1.1	0	Br
9	II-119	2.2	0	Br
10	II-101	1.1	0	Br
11	II-104	1.1	4	Br
12	II-121	1.1	5	Br
13	II-121	0.6	7	Br
14	II-121	0.3	6	Br
15	II-107	1.1/6.6	0	Cl
16	II-122	2 g/mmol	0	Br
17	II-102	1.1	11	Br
18	II-102	2.2	12	Br
19	II-110	1.1	0	Br
20	II-108	1.1	0	Br

On screening the analogues of NBS, the selectivity was not improved. Switching to N-bromoacetamide returned the desired bromolactone in 2 (1.1 eq., entry 1) and 1% *ee* (2.2 eq., entry 2). N-bromosaccharin (entry 3) returned the desired lactone with 9% *ee*.

Perhaps owing to their enhanced reactivity, the tribromide sources as a whole (entries 4-9) proved to be unselective. Most of them provided completely racemic products with the notable exceptions of hexamethylenetetramine tribromide (7% *ee*, entry 6) and N-benzyl-DABCO tribromide **II-117** that also provided the desired lactone in 7% *ee* (entry 7). Molecular bromine (entry 10) not only suffered from poor enantioselectivity, but also poor chemoselectivity, as evidenced by the appearance of several additional spots on the TLC. TABCO (**II-104**) returned the lactone product with 4% *ee* (entry 11), but also, like bromine, suffered from chemoselectivity issues.

Next, the trihaloisocyanuric acids developed by de Mattos and coworkers,[58,59] were screened (entries 12-15). The perbrominated analog (TBCA, **II-121**) could in principle donate each of its three bromine atoms, and thus might be employed in substoichiometric amounts relative to the substrate. In the event, TBCA was employed in 1.1 equivalents (entry 12), 0.6 equivalents (entry 13), and 0.3 equivalents (entry 14). Not surprisingly, the reaction was slowed considerably when less equivalents of TBCA was employed. When 1.1 equivalents was employed the reaction proceeded to completion in 30 hours (notably slower than reactions catalyzed by NBS or other bromenium sources). When the equivalency of TBCA was reduced to 0.6 equivalents, the reaction was

slower still, proceeding to completion after 42 h. When 0.3 equivalents of TBCA

is employed the reaction is impractically slow, not completing even after stirring

for 42 hours. This last result is not surprising, since completing the reaction with

0.3 equivalents of TBCA requires that a molecule of TBCA transfer each of its

three bromine atoms. In each case, TBCA proved to be marginally selective

providing products with 5% *ee* with 1.1 equivalent (entry 12), 7% *ee* with 0.6

equivalents (entry 13), and 6% *ee* with 0.3 equivalents (entry 14).

In the same communication, de Mattos *et al.* employed a combination of

trichloroisocyanuric acid (TCCA) and sodium bromide as a bromenium source.

When this combination was employed (entry 15, 1.1 equivalents TCCA and 6.6

equivalents of NaBr), the corresponding chlorolactone was isolated as the

racemate. Evidently, substrate **II-12** suffers chlorination by action of TCCA prior

to the generation of the bromenium source *in situ*.

While cupric bromide on alumina complex (employed in a 2 g/mmol

loading), reported to be effective for halolactonizations,[67] proved to be

unselective (entry 16), cupric bromide alone emerged as the most selective of

the alternative bromine sources. Employing 1.1 or 2.2 equivalents of cupric

bromide as the bromenium source produced similar results, providing the lactone

product in 11% and 12% *ee*, respectively (entries 17 and 18).

Braddock's combination of bis(acetoxy)iodobenzene and lithium bromide

(**II-110**) provided racemic products (entry 19).[36] Finally, the ammonium

bromide/hydrogen peroxide combination in acetic acid (**II-108**) developed by

Kulkarni and coworkers was evaluated.[60] While the reaction cleanly provided the desired lactone, the product was returned as the racemate (entry 20).

The extensive bromine source screen detailed above confirmed NBS to be the bromine source of choice. Given the discouraging results of the halogen source screen detailed above, this particular approach to asymmetric halolactonization was abandoned in lieu of a more promising approach employing a *Cinchona* alkaloid catalyst system.

2.3: Conclusions and Future Directions

The inability to increase the selectivity of the initial hit scaffold **II-78** above 14% *ee* (0.1 equiv.) and 24% *ee* (1.1 equiv.) irrespective of the reaction conditions indicates that perhaps the most difficult obstacle preventing further optimization of the bromoiodinane strategy is taming the uncatalyzed background reaction due to the terminal bromine source. Indeed, the uncatalyzed lactonization of **II-12** to provide **II-58** by action of NBS alone is complete within just five minutes at room temperature by TLC analysis (Scheme II-13). That fact, coupled with a relatively slow generation of the putative active catalyst **II-79** suggests that a highly selective bromolactonization mediated by iodoarylamido peptides might be difficult if not impossible to achieve. Indeed, attempts to observe the conversion of a secondary *o*-iodo amide **II-123** into its corresponding bromoiodinane **II-124** by action of NBS showed no new peaks in the ^{13}C NMR after 1 day. The bromoiodinane reagents developed by Braddock show a distinctive change in the ^{13}C chemical shift of the iodine's α-carbon (*cf.* **II-125** vs.

II-126, $\Delta\delta = 18.8$ ppm).[35] It was hoped that a similar diagnostic peak would appear in the ^{13}C NMR of **II-123** on treatment with NBS. That no change was observed after 1 day of incubation indicates that either the formation of **II-124** is highly reversible or prohibitively slow to be observed in the NMR. Either of these situations when extrapolated to scaffold **II-78**, coupled with facile background reaction (Scheme II-13, equation 1), indicates that only an exceedingly active third generation bromoiodinane catalyst might overcome the limitations of **II-78**.

Scheme II-13. Difficulties associated with bromoiodinane catalysis.
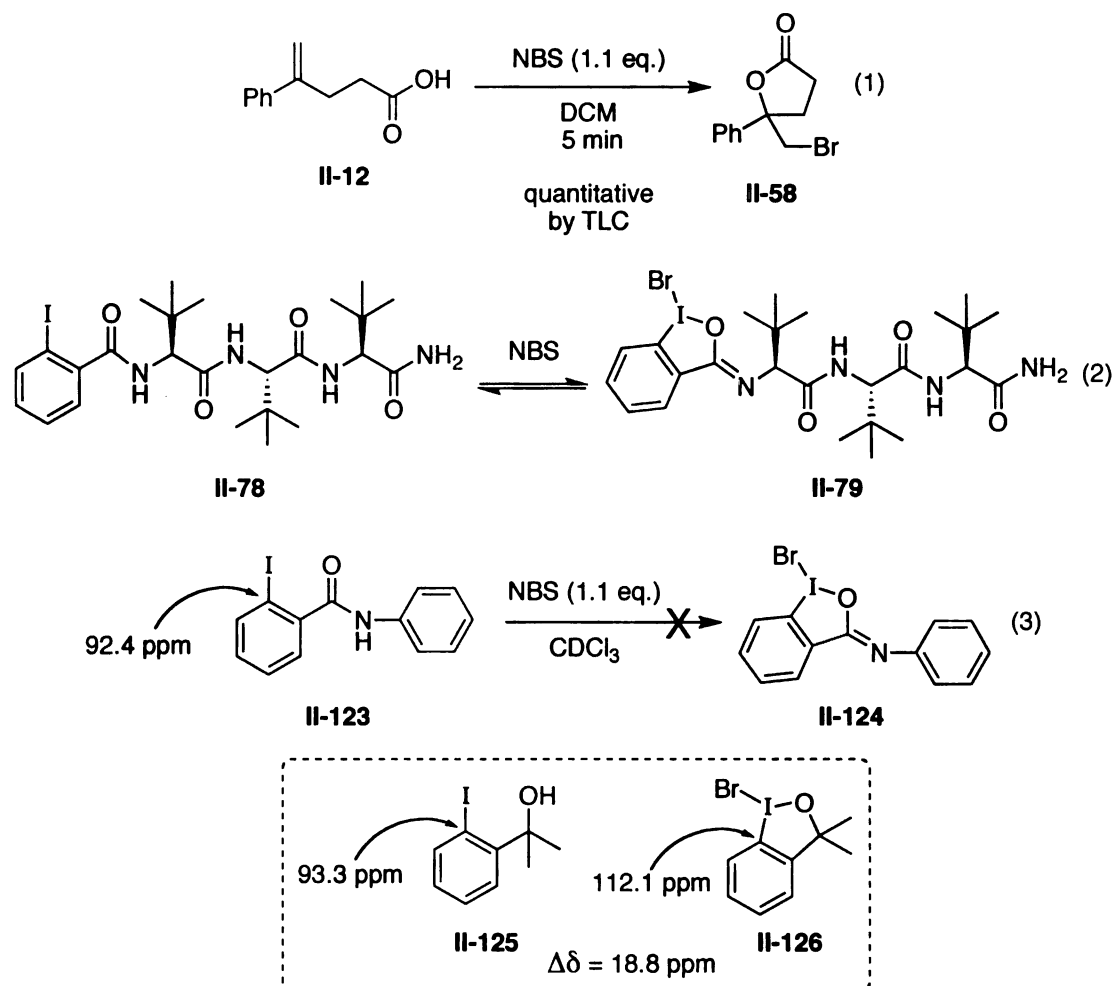
A few potential solutions might guide future attempts at developing peptide based scaffolds for halogenations. Ultimately, future catalyst iterations for chiral halogenation applications ought to incorporate more nucleophilic moieties, thus generating more reactive catalyst systems that can effectively out-compete the prevailing background reaction. In the context of the bromoiodinane scaffold described herein, a logical extension would be to incorporate even more nucleophilic *ortho*-aryliodo active sites such as amidines (see **II-127**, Figure II-7). This group might be readily installed by capping the N-terminus of the appropriate peptide with N-phenyl *o*-iodobenzimidoyl chloride **II-128**. Reagent **II-128** could be generated analogously to the known N-phenyl benzimidoyl chloride.[69]

Figure II-7. Potential third generation peptide scaffolds for chiral halogenations.
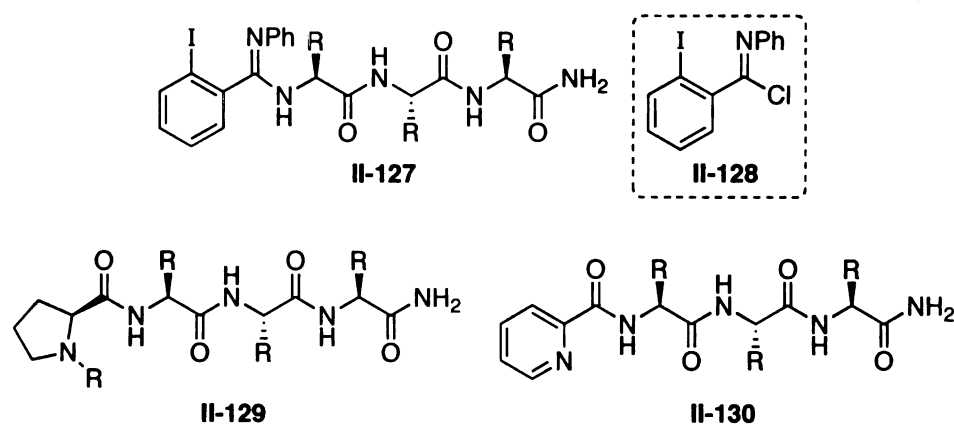
In addition, several scaffolds can be imagined that incorporate other nucleophilic residues such as tertiary amines (**II-129**) and pyridines (**II-130**) and might be readily prepared by solid phase synthesis (SPPS). These compounds would be readily accessible by capping the N-terminus of the growing peptide with N-alkyl proline derivatives (**II-129**) or picolinic acid (**II-130**) and nicotinic acid.

Ultimately, these scaffolds might prove more generally useful, given that they can be coupled with other halogen sources (*i.e.* iodo or chloro sources). It is important to note that an analogous chlorolactonization approach (*i.e.* replacing NBS with NCS) fails to produce any chlorolactone products when catalyst **II-78** is employed. Evidently, an analogous iodine-chlorine bond is not accessible (*cf.* **II-79**).

In conclusion, a number of peptides containing *o*-iodoarylamide active sites were prepared and screened as catalysts for the asymmetric bromolactonization of 4-phenyl-4-pentenoic acid (**II-12**). Peptide **II-78** provided the highest selectivity, returning lactone **II-58** in 14% *ee* when 0.1 equiv. catalyst was employed and 24% *ee* when employed in a stoichiometric amount. Perhaps the most overarching lesson learned from these experiments is that the pairing of a sufficiently active organocatalyst with an appropriately attenuated halogen source will be key to the success of future attempts. Indeed, as will become evident in Chapter 3, careful tuning of the terminal halogen source ultimately proved crucial in the development of a novel asymmetric chlorolactonization protocol mediated by a *Cinchona* alkaloid organocatalyst.

2.4. Acknowledgement

described in this chapter under my guidance. Their efforts in this regard are highly appreciated.

2.5: Experimental Details

The solid phase peptide synthesis of the peptides described herein was conducted following well-established protocols that can be found in *Fmoc Solid Phase Peptide Synthesis: A Practical Approach* by W.C. Chan and P.D. White.[49] Additional protocols can be found in the appendix of the Novabiochem product catalogue. Peptides were prepared in disposable 5 or 10 mL fritted syringes purchased from CSPS Pharmaceuticals, Inc. All Fmoc protected amino acids were purchased from Novabiochem, CSPS Pharmaceuticals, Inc. or Aldrich and used without purification. Wang and Rink Amide MBHA resins were purchased from Novabiochem. All other reagents and solvents were purchased from commercial sources and used without purification. C-terminal carboxylic acid and methyl ester peptides were synthesized using a commercially available Wang resin that was preloaded with Fmoc-valine (Fmoc-Val-Wang resin). C-terminal amide peptides were synthesized using the Rink Amide MBHA resin which was loaded with the first amino acid of the desired sequence. Peptide ligands were characterized by MALDI-TOF mass spectrometry (Figure II-8, *vide infra*). A sample of 2-iodo-*iso*-phthalic acid was prepared by previously disclosed methodology.[53] Synthetic halogen sources were prepared by known methodology: N-bromoacetamide (**II-113**) was prepared by the method of Oliveto and Gerold,[61] N-bromosaccharin (**II-115**) was prepared by the method of

87

Zajc,[63] N-benzyl DABCO perbromide (**II-117**) was prepared by the method of

Moghaddam,[65] pyridinium tribromide (**II-119**) was prepared by the method of

Fieser and Fieser,[64] TBCA (**II-121**) was prepared by the method of de Mattos,[58]

and $CuBr_2$ on alumina (**II-122**) was prepared by the method of Kodomari *et. al.*[68]

Compounds **II-12** and **II-58** had ^1H and ^{13}C NMR data in full agreement with

samples prepared previously.[37]

   Crude peptides were then screened as catalysts for the asymmetric

bromolactonization of **II-12**. HPLC separation of the two enantiomeric

bromolactones (Chiralcel OD-H column, 5% IPA/hexane, 0.8 mL/min, 245 nm UV

detection) provided the extent of selectivity emparted by the catalyst. Given

below is a general protocol for each step in the solid phase synthesis along with

a general protocol for the lactonization reaction.

General Procedures for Solid Phase Peptide Synthesis

Bead Loading

   Rink Amide MBHA resin (87 mg, 0.06 mmol, 0.69 mmol/g loading) was

pre-swelled in a 5 mL disposable syringe equipped with a frit by rotating with

DCM (3 mL) for 1h. The resin was then washed with DMF (5 X 4 mL). The

Fmoc protecting group on the bead was removed by treatment with 5 bed

volumes (ca. 4 mL) of a 20% piperidine solution in DMF for 20 minutes.

   Meanwhile, Fmoc-Phe-OH (116 mg, 0.3 mmol, 5 eq.) was dissolved in

DMF (3 mL) along with HOBt (41 mg, 0.3 mmol, 5 eq.). Diisopropyl carbodiimide

(DIC) (50 μL, 0.3 mmol, 5 eq.) was then added and the resulting mixture was stirred at room temperature for 20 min.

After 20 minutes, the resin was washed with DMF (5 X 4 mL). To the thoroughly washed resin bed, was added the coupling solution (Fmoc-Phe-OH, HOBt, and DIC), and the resulting mixture was rotated for 12 hours. The loaded resin was then washed with DMF (5 X 4 mL) and used in subsequent Fmoc solid phase peptide synthesis as described below.

Fmoc removal

The Fmoc group of the terminal amino acid of the growing peptide chain was deprotected by treating the resin beads (0.69 mmol/g loading) with a 20% solution of piperidine in DMF (ca. 4 mL) with rotation for three minutes. The deprotection cocktail was then discharged from the syringe and the resin beads were treated with a fresh portion of 20% piperidine in DMF for three minutes. This protocol is repeated until the resin beads have been treated with four aliquots of 20% piperidine in DMF. The final portion is then discharged from the syringe and the deprotected beads are washed with DMF (5 X 4 mL). The washed, deprotected resin beads were then immediately coupled with the next amino acid in the sequence.

HOBt-Mediated Coupling

The next amino acid in a desired sequence was activated as the HOBt ester by dissolving the desired amino acid (0.3 mmol, 5 equivalents relative to

the 0.69 mmol/g resin loading) along with HOBt (41 mg, 0.3 mmol, 5 eq.) in DMF/DCM (1:1) (3 mL). To the resulting solution was added DIC (50 μL, 0.3 mmol, 5 eq.) and the resulting solution was stirred at room temperature for twenty minutes (usually while the terminal amino acid of the resin bound sequence is deprotected).

The resulting solution of HOBt ester was added to the N-terminal deprotected, resin-bound, peptide sequence and the mixture was rotated for one hour. The resin beads were then thoroughly washed with DMF (5 X 4 mL). The resulting N-terminal, Fmoc-protected, resin-bound peptide sequence was then resubjected to the Fmoc removal protocol and subsequent HOBt couplings until the desired sequence had been assembled.

N-Terminal o-Iodobenzoate Capping

The N-terminus of the peptide was capped with the o-iodoarylamido active site by the HOBt active ester methodology. The o-iodobenzoic acid (0.3 mmol, 5 equivalents relative to the 0.69 mmol/g resin loading) was dissolved along with HOBt (41 mg, 0.3 mmol, 5 eq.) in DMF/DCM (1:1) (3 mL). To the resulting solution was added DIC (50 μL, 0.3 mmol, 5 eq.) and the resulting solution was stirred at room temperature for twenty minutes (usually while the terminal amino acid of the resin bound sequence is deprotected).

The resulting solution of HOBt ester was added to the N-terminal deprotected, resin-bound, peptide sequence and the mixture was rotated for one hour. The resin beads were then thoroughly washed with DMF (5 X 4 mL).

TFA Cleavage/Global Side-chain Deprotection of Peptides

Peptides were cleaved from the resin beads by employing the following protocol:

The fully assembled, resin-bound peptides were prepared for cleavage by washing the beads with DMF (5 X 4 mL), DCM (5 X 4 mL), and methanol (5 X 4 mL). The syringe plunger was removed from the barrel and the resin beads were dried overnight in the vacuum oven at 25 °C. The following day, the resin was treated with a cleavage cocktail comprised of a mixture of TFA/H_2O/TIS (95:2.5:2.5) (3 mL) for 2.5 hours with minimal, intermittent agitation. The cleavage cocktail, containing the solvated, resin-free peptide was then ejected into a 5 mL pear-shaped flask and the solvent was removed under a stream of nitrogen to give a thick oil. The crude peptide was then precipitated by the addition of ice-cold diethyl ether. The solid peptide was then isolated by vacuum filtration and washed with copious amounts (*ca.* 15-20 mL) of cold ethyl ether. The solid peptide was then dried *in vacuo*. The identity of the desired sequence was verified by MALDI-TOF mass spectrometry (Figure II-8, *vide infra*).

MeOH/TEA/DMF Cleavage of Peptides (peptide methyl esters)

The fully assembled, side-chain protected, resin-bound peptides were readied for cleavage by washing the beads with DMF (5 X 4 mL), DCM (5 X 4 mL), and methanol (5 X 4 mL). The syringe plunger was removed from the barrel and the resin beads were dried overnight in the vacuum oven at 25 °C. The following day, the resin was treated with a cleavage cocktail comprising methanol/TEA/DMF (9:1:1) (3 mL) with rotation for four days. The cleavage

cocktail, containing the solvated, resin-free peptide was then ejected into a 5 mL

pear-shaped flask and the solvent was removed under a stream of nitrogen to

give a thick oil. The crude peptide was then precipitated by the addition of ice-

cold ethyl ether. The solid peptide was then isolated by vacuum filtration and

washed with copious amounts (*ca.* 15-20 mL) of cold ethyl ether. The solid

peptide was then dried *in vacuo*. The identity of the desired sequence was

verified by MALDI-TOF mass spectrometry (Figure II-8, *vide infra*).

Figure II-8. MALDI-TOF data for peptides **II-59** through **II-78** and **II-80** through **II-92**.

II-59

Calc.: 541.38   Found: 564.2 (M+Na)
564.37 (M+Na)

II-60

Calc.: 445.30   Found: 468.0 (M+Na)
468.29 (M+Na)

II-61

Calc.: 473.35   Found: 495.9 (M+Na)
496.34 (M+Na)   511.9 (M+K)
512.45 (M+K)

II-62

Calc.: 473.35   Found: 496.3 (M+Na)
496.34 (M+Na)

II-63

Calc.: 494.33   Found: 516.7 (M+Na)
517.23 (M+Na)   532.7 (M+K)
533.43 (M+K)

II-64

Calc.: 480.30   Found: 480.8
502.99 (M+Na)   502.7 (M+Na)

II-65

Calc.: 522.38   Found: 522.8

II-66

Calc.: 531.35   Found: 532.4 (M+H)
532.36 (M+H)

93

Figure II-8. (Cont'd)

II-67
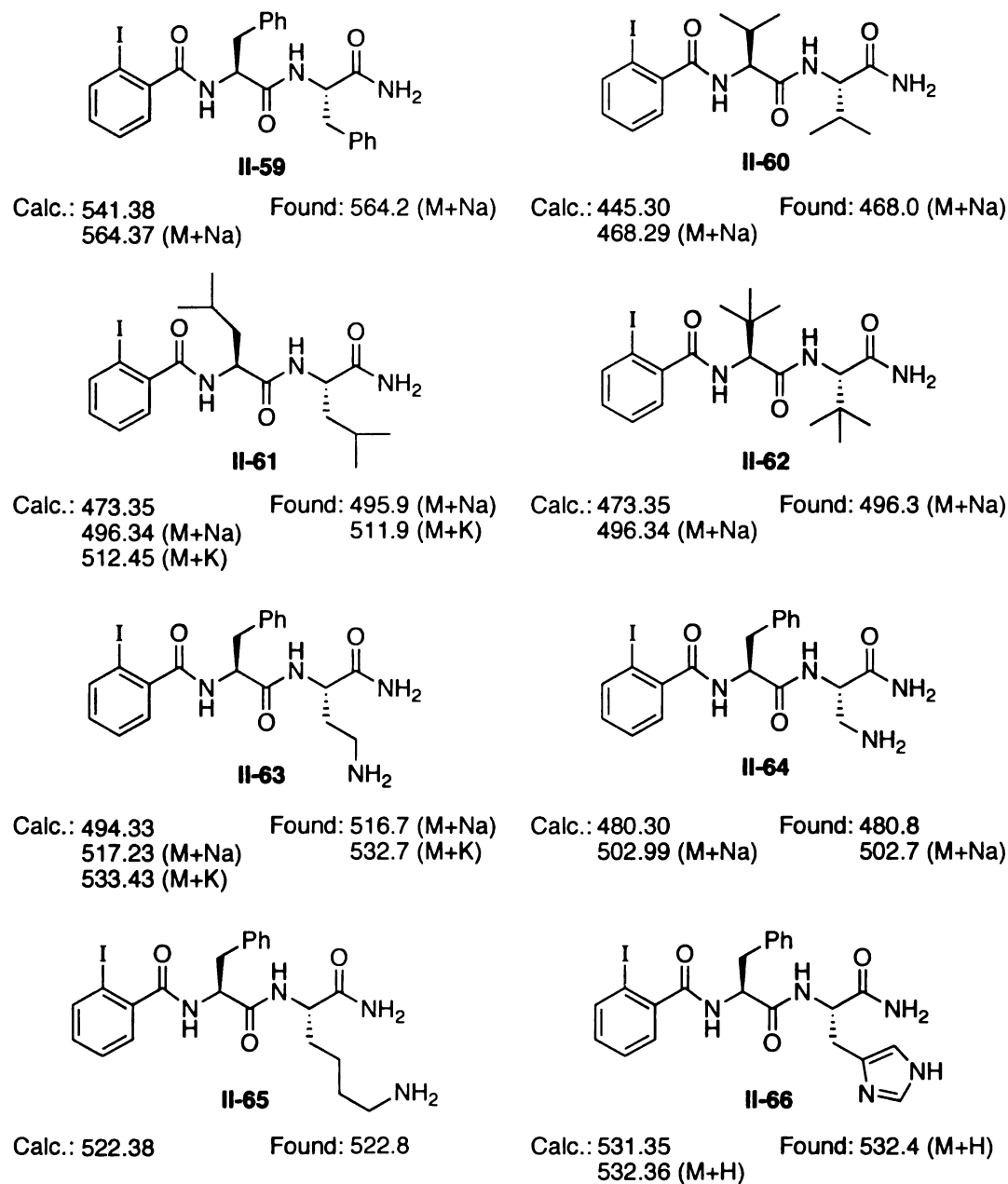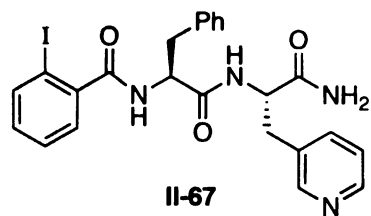
Calc.: 542.37   Found: 542.9
565.36 (M+Na)   565.8 (M+Na)

II-68
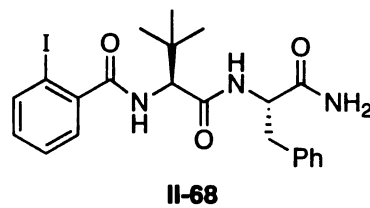
Calc.: 507.10   Found: 530.3 (M+Na)
530.00 (M+Na)

II-69
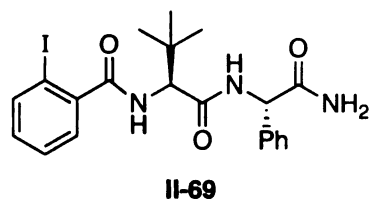
Calc.: 493.09   Found: 516.0 (M+Na)
515.99 (M+Na)   532.0 (M+K)
532.19 (M+K)

II-70
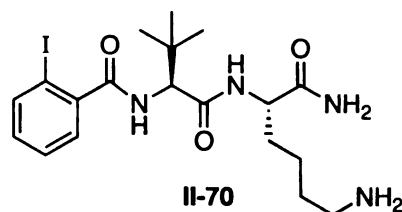
Calc.: 488.13   Found: 488.7

II-71
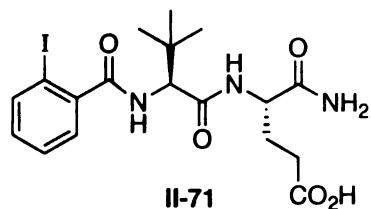
Calc.: 489.08   Found: 511.6 (M+Na)
511.98 (M+Na)

II-72
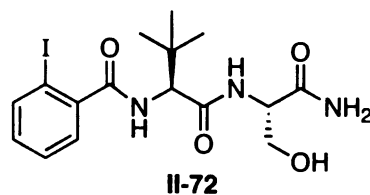
Calc.: 447.07   Found: 470.3 (M+Na)
470.06 (M+Na)

II-73
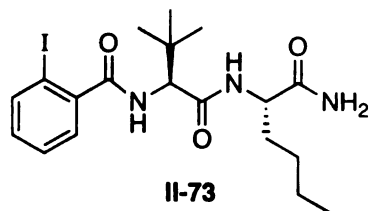
Calc.: 473.12   Found: 496.3 (M+Na)
496.11 (M+Na)

II-74
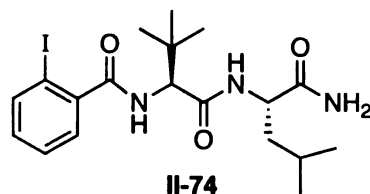
Calc.: 473.12   Found: 496.4 (M+Na)
496.11 (M+Na)

94

Figure II-8. (Cont'd)
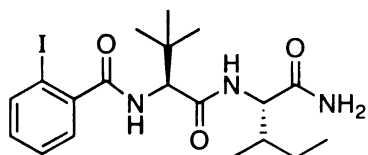
II-75

Calc.: 473.12   Found: 496.0 (M+Na)
496.02 (M+Na)
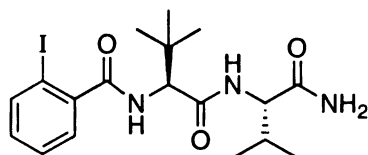
II-76

Calc.: 459.10   Found: 482.3 (M+Na)
482.09 (M+Na)
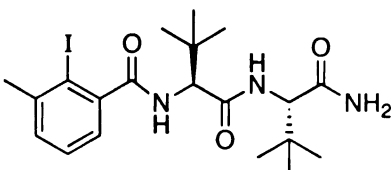
II-77

Calc.: 487.13   Found: 510.0 (M+Na)
510.12 (M+Na)   526.0 (M+K)
526.23 (M+K)
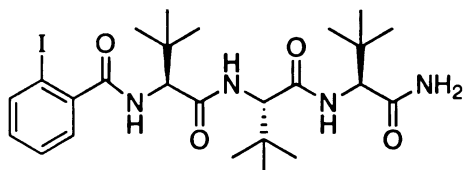
II-78

Calc.: 586.20   Found: 609.4 (M+Na)
609.19 (M+Na)
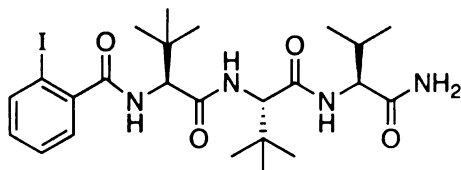
II-80

Calc.: 572.19   Found: 595.2 (M+Na)
595.18 (M+Na)
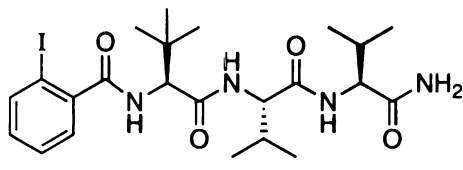
II-81

Calc.: 558.17   Found: 580.7 (M+Na)
581.16 (M+Na)
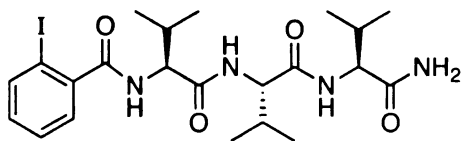
II-82

Calc.: 544.15   Found: 567.1 (M+Na)
567.16 (M+Na)
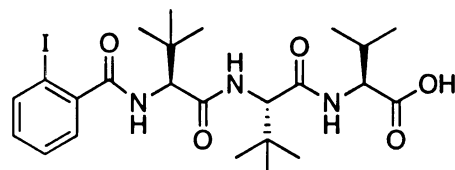
II-83

Calc.: 576.46   Found: 599.6 (M+Na)
599.45 (M+Na)

95
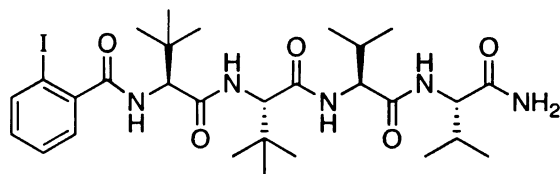
Figure II-8. (Cont'd)

II-84

Calc.: 671.25   Found: 694.5 (M+Na)
694.24 (M+Na)
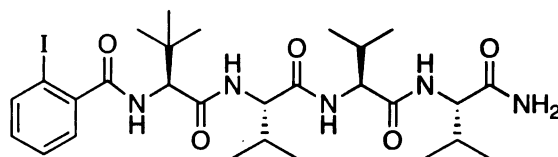
II-85

Calc.: 657.24   Found: 680.7 (M+Na)
680.14 (M+Na)
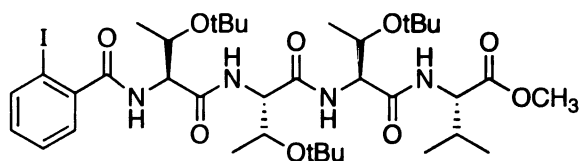
II-86

Calc.: 832.35   Found: 832.5
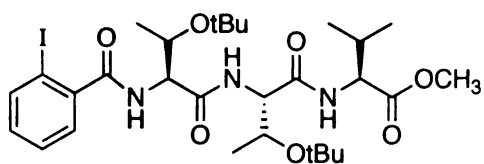
II-87

II-88

Calc.: 675.24   Found: 698.4 (M+Na)   Calc.: 550.09   Found: 573.2 (M+Na)
698.23 (M+Na)   573.08 (M+Na)

96

Figure II-8. (Cont'd)

II-89

Calc.: 457.09
496.19 (M+K)

Found: 495.8 (M+K)

II-90

Calc.: 570.17

Found: 569.2

II-91

Calc.: 932.84
955.83 (M+Na)
971.5 (M+K)

Found: 955.5 (M+Na)
971.5 (M+K)

II-92

Calc.: 947.87
970.86 (M+Na)
986.97 (M+K)

Found: 969.6 (M+Na)
985.6 (M+K)
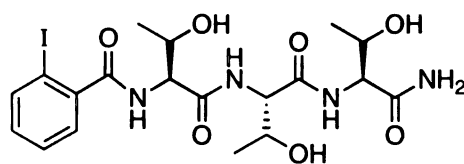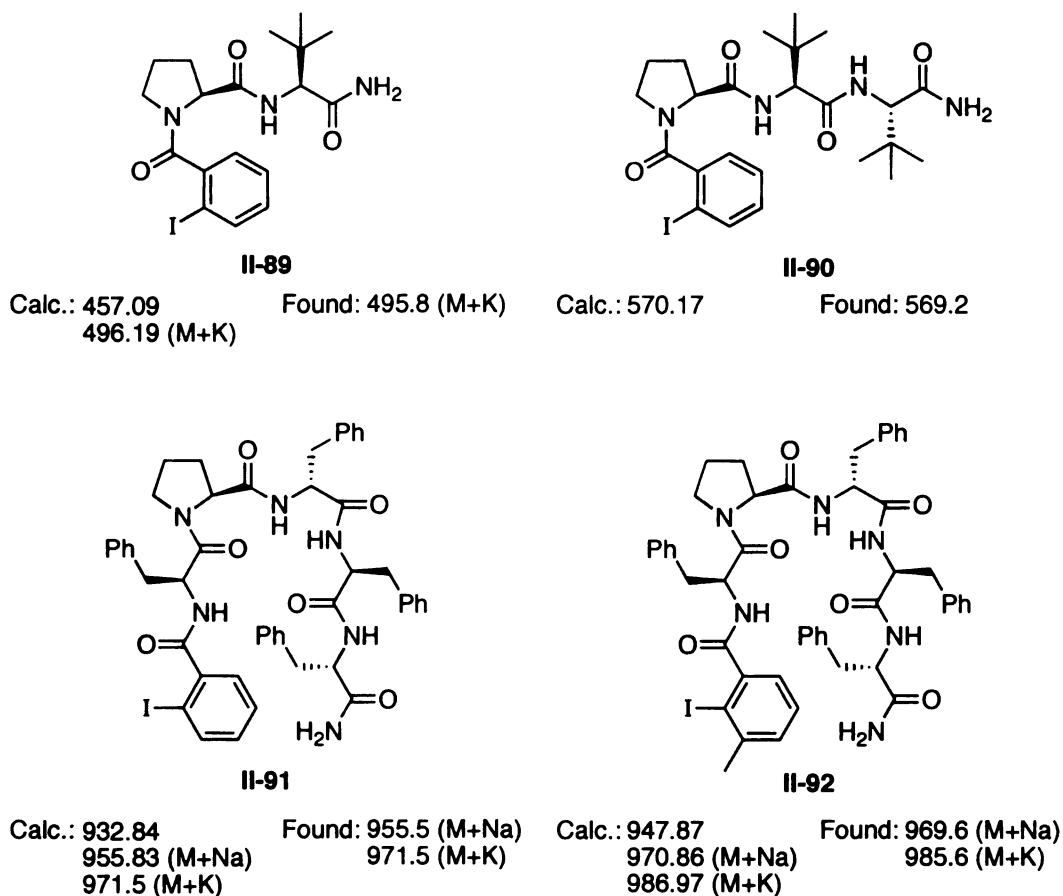
Procedure for the Bromolactonization of II-12 with Peptide Catalysts

$$\text{Ph} \underset{\text{O}}{\overset{}{\longrightarrow}} \text{OH} \xrightarrow[\substack{\text{NBS (1.1 eq.)} \\ \text{DCM} \\ \text{RT}}]{\text{peptide (0.1 eq.)}} \text{II-58}$$

II-12

II-58
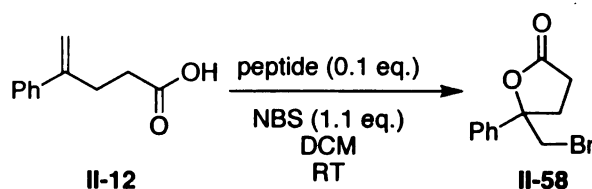
A 3.7 mL screw-top vial equipped with a magnetic stir bar was charged

with 4-phenyl-4-pentenoic acid II-12 (9 mg, 0.05 mmol), N-bromosuccinimide (10

mg, 0.055 mmol) and peptide organocatalyst (typically *ca.* 4 mg, 0.005 mmol).

The solids were then taken up in 1 mL of freshly distilled dichloromethane. The

vial was sealed with the screw-top and the reaction mixture was stirred overnight

and monitored by TLC (20% ethyl acetate in hexanes, KMnO$_4$ burn). Upon

completion, the reaction mixture was poured into a 60 mL separatory funnel

along with 5 mL of water. The resulting solution was extracted twice with 5 mL of

dichloromethane. The combined organics were then dried (anhydrous Na$_2$SO$_4$)

and concentrated in the presence of a small portion of silica gel via rotary

evaporation. The resulting silica plug was then placed on top of a Pasteur pipet

packed with silica gel. The desired lactone product (II-58) was eluted from the

pipet column with 20% ethyl acetate in hexanes which on concentration returned

a clear oil. The enantiomeric excess of the product was determined by HPLC

(Chiralcel OD-H, 5% iso-propyl alcohol in hexanes, 0.8 mL/min, 254 nm, RT$_1$ =

24.38 min, RT$_2$ = 27.42 min).

II-58, 5-(bromomethyl)-5-phenyldihydrofuran-2(3H)-one[37]

^{1}H NMR (300 MHz, CD$_3$Cl): δ 7.34 (m, 5H), 3.71 (d, J = 11.1 Hz, 1H), 3.67 (d, J =

11.1 Hz, 1H), 2.77 (m, 2H), 2.52 (m, 2H); ^{13}C NMR (75 MHz, CD$_3$Cl): δ 175.4,

140.6, 128.7, 128.5, 124.7, 86.3, 40.9, 32.2, 28.9.

Preparation of 4-phenyl-4-pentenoic acid (II-12)[37]
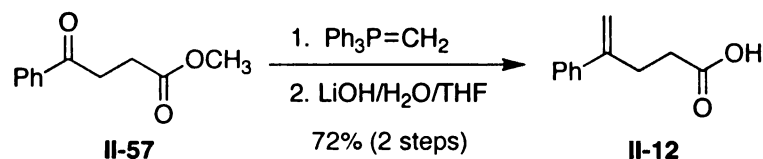
Methyltriphenylphosphonium bromide (1.96 g, 5.6 mmol, 1.08 equivalent)

was suspended in freshly distilled toluene (30 mL) and cooled to ca. 0 °C on an

ice bath. Sodium bis(trimethylsilyl)amide (5.4 mL, 5.4 mmol, 1.04 equivalents, 1

M solution in THF) was added dropwise by syringe and the resulting solution was

stirred for 30 minutes. The solution was then lowered to -78 °C and methyl 3-

benzoylpropionate (II-57) (1.0 g, 5.2 mmol, 1 equivalent) was added dropwise by

syringe. The resulting solution was then stirred while warming to room

temperature. The reaction mixture was then refluxed for 40 hours. On cooling,

the reaction was quenched by the addition of saturated ammonium chloride (40

mL) and the resulting slurry was diluted with 50 mL of water and extracted with

ethyl acetate (3X 50 mL). The combined organics were washed with brine (100

mL), dried over anhydrous Na_2SO_4, and concentrated by rotary evaporation. The

residue was purified by column chromatography on silica gel (10% ethyl acetate

in hexanes) to give 762 mg (77% yield) of the desired methyl 4-phenylpent-4-

enoate. This substance was used immediately without characterization in the

following saponification reaction.

The ester (536 mg, 2.82 mmol, 1 equivalent) was dissolved in THF (20

mL) and cooled to *ca.* 0 °C on an ice bath. A solution of lithium hydroxide

monohydrate (600 mg, 14.30 mmol, 5.07 equivalents) in 20 mL of water was

added dropwise over about 5 minutes via an addition funnel. The resulting

solution was allowed to warm to room temperature while stirring for 18 hours.

The solution was acidified to pH <4 with 1N HCl and then extracted with diethyl

ether (3X 20 mL). The combined organics were then washed with water (60 mL)

and brine (60 mL), and then dried over anhydrous Na_2SO_4. The organics were

concentrated by rotary evaporation to give the desired compound **II-12** (467 mg, 94% yield). This crude isolate was sufficiently pure by ^{1}H and ^{13}C NMR analysis.

II-12, 4-phenyl-4-pentenoic acid[37]

^{1}H NMR (300 MHz, acetone-d_6): δ 7.46 (m, 2H), 7.37-7.27 (m, 3H), 5.32 (m, 1H), 5.12 (m, 1H), 2.82 (m, 2H), 2.46 (m, 2H); ^{13}C NMR (75 MHz, acetone-d_6): δ 171.2, 148.1, 141.5, 129.2, 128.4, 126.8, 112.7, 33.2, 30.9.

Preparation of bis-amino acid catalysts II-97 through II-100.
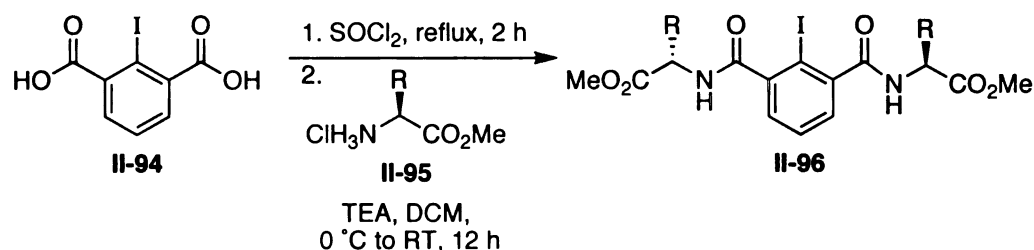
General procedure for the preparation of scaffold **II-96**:

A flame-dried 25 mL round-bottomed flask was charged with a magnetic stir bar, 2-iodo-*iso*-phthalic acid[53] (**II-94**) (219 mg, 0.75 mmol, 1 equiv.) and thionyl chloride (5 mL, 69 mmol). The resulting suspension was refluxed for 2 hours, after which time the brown solution was concentrated to a thick oil by rotary evaporation. The acid chloride, so generated, was then reconstituted in dry DCM (10 mL) and was added dropwise to an ice-cold solution of the appropriate amino acid methyl ester hydrochloride (**II-95**) (1.6 mmol, 2.1 equiv.) and triethylamine (558 mL, 4 mmol, 5.3 equiv.) in dry DCM (10 mL). The

resulting slurry was stirred overnight while warming to room temperature. The reaction mixture was then diluted with DCM (20 mL) and washed with 1N HCl (50 mL) and saturated brine (50 mL). The organics were then dried over anhydrous sodium sulfate and concentrated by rotary evaporation. The desired bis-amino acid catalysts **II-96** were isolated after purification by silica gel chromatography (ethyl acetate/hexanes (1:1)).

II-97, bis-valine organocatalyst
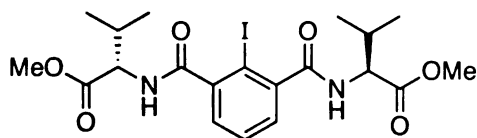
^{1}H NMR (300 MHz, CD$_3$Cl): δ 7.33 (m, 3H), 6.65 (d, J = 8.7 Hz, 2H), 4.70 (dd, J_1 = 4.8 Hz, J_2 = 8.7 Hz, 2H), 3.76 (s, 6H), 2.30 (septet of doublets, J_1 = 4.8 Hz, J_2 = 6.9 Hz, 2H), 1.05 (d, J = 6.9 Hz, 6H), 0.98 (d, J = 6.9 Hz, 6H); ^{13}C NMR (75 MHz, CD$_3$Cl): δ 171.8, 169.1, 143.8, 128.6, 128.3, 90.2, 57.6, 52.1, 31.2, 19.0, 17.9; IR (vcm^{-1}, KBr): 3279, 1744, 1651. HRMS (C$_{20}$H$_{27}$N$_2$O$_6$I) Calc. (M+H): 519.0992 Found (M+H): 519.0990; [α]$_D^{20}$ = -5.7° (c =0.5, CHCl$_3$); mp = 201-203 °C

II-98, bis-*tert*-leucine organocatalyst
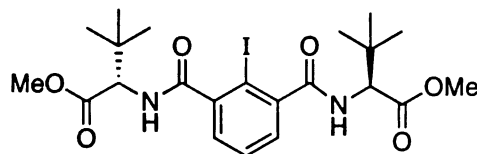
^{1}H NMR (300 MHz, CD$_3$Cl): δ 7.33 (m, 3H), 6.49 (d, J = 9.0 Hz, 2H), 4.62 (d, J = 9.0 Hz, 2H), 3.74 (s, 6H), 1.07 (s, 9H); ^{13}C NMR (75 MHz, CD$_3$Cl): δ 171.2,

168.8, 143.9, 128.7, 128.3, 90.0, 60.6, 51.7, 34.8, 26.7; IR (vcm^{-1}, KBr): 3319,

1740, 1657. HRMS (C$_{22}$H$_{31}$N$_2$O$_6$I) Calc. (M+H): 547.1305 Found (M+H):

547.1300; [α]$_D^{20}$ = -20.1° (c =0.5, CHCl$_3$); mp = 95-97 °C.

II-99, bis-phenylglycine organocatalyst
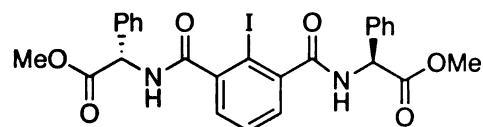
^{1}H NMR (300 MHz, CD$_3$Cl): δ 7.45-7.25 (m, 13H), 6.88 (d, *J* = 7.2 Hz, 2H), 5.73

(d, *J* = 7.2 Hz, 2H), 3.74 (s, 6H); ^{13}C NMR (75 MHz, CD$_3$Cl): δ 170.8, 168.3,

143.3, 135.8, 129.0, 128.7, 128.4, 127.5, 90.4, 56.8, 52.9; IR (vcm^{-1}, KBr): 3277,

1744, 1653. HRMS (C$_{26}$H$_{23}$N$_2$O$_6$I) Calc. (M+H): 587.0679 Found (M+H):

587.0675; [α]$_D^{20}$ = +57.0° (c =0.5, CHCl$_3$); mp = 245-246 °C (decomp.).

II-100, bis-proline organocatalyst
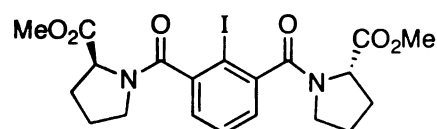
^{1}H NMR (300 MHz, CD$_3$Cl): δ 7.53-7.15 (m, 3H), 4.69 (m, 2H), 3.94-3.48 (m,

10H, CH$_3$+CH$_2$), 2.35-1.91 (m, 8H) ; ^{13}C NMR (75 MHz, CD$_3$Cl): δ 172.2, 168.4,

144,2, 129.1, 128.7, 88.9, 58.3, 52.0, 48.5, 29.3, 24.6; IR (vcm^{-1}, KBr): 1745,

1647. HRMS (C$_{20}$H$_{23}$N$_2$O$_6$I) Calc. (M+H): 515.0679 Found (M+H): 515.0682;

[α]$_D^{20}$ = -54.7° (c =0.5, CHCl$_3$); mp = 139-141 °C.

Figure II-9. X-ray crystal structure of bis-proline catalyst II-100.
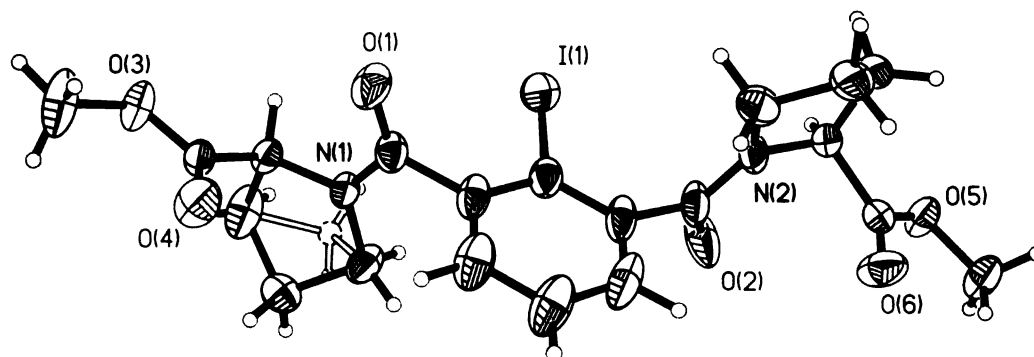
Table II-13. Crystal data and structure refinement for II-100.

Identification code	bb13_0m
Empirical formula	C20 H23 I N2 O6
Formula weight	514.30
Temperature	173(2) K
Wavelength	0.71073 Å
Crystal system	Orthorhombic
Space group	P2(1)2(1)2(1)
Unit cell dimensions	a = 7.7111(2) Å a= 90°.
	b = 11.0395(3) Å b= 90°.
	c = 25.1892(8) Å g = 90°.
Volume	2144.27(11) Å^3
Z	4
Density (calculated)	1.593 Mg/m^3
Absorption coefficient	1.531 mm^{-1}
F(000)	1032
Crystal size	0.27 x 0.24 x 0.06 mm^3
Theta range for data collection	1.62 to 27.89°.
Index ranges	-10<=h<=10, -13<=k<=14, -26<=l<=33
Reflections collected	29760
Independent reflections	5104 [R(int) = 0.0365]
Completeness to theta = 25.00°	100.0 %
Absorption correction	Semi-empirical from equivalents
Max. and min. transmission	0.9137 and 0.6790
Refinement method	Full-matrix least-squares on F^2
Data / restraints / parameters	5104 / 0 / 274
Goodness-of-fit on F^2	1.056
Final R indices [I>2sigma(I)]	R1 = 0.0429, wR2 = 0.0887
R indices (all data)	R1 = 0.0663, wR2 = 0.1006
Absolute structure parameter	0.00(2)
Largest diff. peak and hole	0.933 and -1.711 e.Å^{-3}

103

Table II-14. Atomic coordinates (x 10^4) and equivalent isotropic displacement parameters (Å^2x 10^3) for **II-100**. U(eq) is defined as one third of the trace of the orthogonalized U^{ij} tensor.

	x	y	z	U(eq)
I(1)	965(1)	3466(1)	-283(1)	71(1)
O(1)	-110(4)	3281(4)	1134(1)	56(1)
O(2)	133(5)	6164(4)	-1096(2)	77(2)
O(3)	3243(4)	2656(3)	2249(1)	46(1)
O(4)	1777(6)	4391(3)	2184(1)	62(1)
O(5)	-2272(4)	6582(3)	-2370(1)	43(1)
O(6)	-3417(6)	7356(3)	-1633(1)	59(1)
N(1)	2325(4)	4413(3)	1086(1)	31(1)
N(2)	-2495(5)	5282(4)	-1071(2)	48(1)
C(1)	-278(6)	4962(5)	72(2)	45(1)
C(2)	-208(6)	5096(5)	615(2)	41(1)
C(3)	-947(7)	6107(5)	847(2)	53(1)
C(4)	-1812(7)	6971(6)	542(2)	62(2)
C(5)	-1891(7)	6804(5)	-2(2)	60(2)
C(6)	-1112(6)	5824(5)	-244(2)	50(1)
C(7)	660(6)	4173(4)	970(2)	37(1)
C(8)	-1084(7)	5757(5)	-842(2)	55(1)
C(9)	3337(6)	5449(4)	899(2)	45(1)
C(10A)	4717(9)	5563(7)	1334(3)	41(2)
C(10B)	5139(16)	4695(13)	820(6)	42(4)
C(11)	5156(6)	4178(5)	1409(2)	55(1)
C(12)	3333(5)	3618(4)	1428(2)	31(1)
C(13)	2661(5)	3630(4)	1989(2)	33(1)
C(14)	2806(8)	2581(7)	2807(2)	70(2)
C(15)	-4093(7)	4823(5)	-822(2)	53(1)
C(16)	-5389(6)	4808(5)	-1267(2)	55(1)
C(17)	-4293(7)	4548(4)	-1751(2)	52(1)
C(18)	-2603(6)	5256(4)	-1655(2)	40(1)
C(19)	-2798(6)	6532(4)	-1868(2)	38(1)
C(20)	-2610(8)	7692(4)	-2655(2)	50(1)

Table II-15. Bond lengths [Å] and angles [°] for **II-100**.

I(1)-C(1)	2.109(6)
O(1)-C(7)	1.223(5)
O(2)-C(8)	1.223(6)
O(3)-C(13)	1.336(5)
O(3)-C(14)	1.447(5)
O(4)-C(13)	1.188(5)
O(5)-C(19)	1.330(5)
O(5)-C(20)	1.444(5)
O(6)-C(19)	1.186(5)
N(1)-C(7)	1.343(6)
N(1)-C(12)	1.455(5)
N(1)-C(9)	1.463(5)
N(2)-C(8)	1.339(6)
N(2)-C(15)	1.472(6)
N(2)-C(18)	1.472(6)
C(1)-C(2)	1.378(6)

Table II-15. (Cont'd)

C(1)-C(6)	1.397(6)
C(2)-C(3)	1.383(7)
C(2)-C(7)	1.510(6)
C(3)-C(4)	1.396(7)
C(3)-H(3)	0.9500
C(4)-C(5)	1.384(8)
C(4)-H(4)	0.9500
C(5)-C(6)	1.380(8)
C(5)-H(5)	0.9500
C(6)-C(8)	1.507(7)
C(9)-C(10A)	1.533(8)
C(9)-C(10B)	1.632(13)
C(9)-H(9A)	0.9900
C(9)-H(9B)	0.9900
C(10A)-C(11)	1.578(9)
C(10A)-H(10A)	0.9900
C(10A)-H(10B)	0.9900
C(10B)-C(11)	1.589(14)
C(10B)-H(10C)	0.9900
C(10B)-H(10D)	0.9900
C(11)-C(12)	1.537(7)
C(11)-H(11A)	0.9900
C(11)-H(11B)	0.9900
C(12)-C(13)	1.507(5)
C(12)-H(12)	1.0000
C(14)-H(14A)	0.9800
C(14)-H(14B)	0.9800
C(14)-H(14C)	0.9800
C(15)-C(16)	1.502(7)
C(15)-H(15A)	0.9900
C(15)-H(15B)	0.9900
C(16)-C(17)	1.509(8)
C(16)-H(16A)	0.9900
C(16)-H(16B)	0.9900
C(17)-C(18)	1.539(6)
C(17)-H(17A)	0.9900
C(17)-H(17B)	0.9900
C(18)-C(19)	1.514(6)
C(18)-H(18)	1.0000
C(20)-H(20A)	0.9800
C(20)-H(20B)	0.9800
C(20)-H(20C)	0.9800
C(13)-O(3)-C(14)	116.3(4)
C(19)-O(5)-C(20)	117.0(4)
C(7)-N(1)-C(12)	121.4(3)
C(7)-N(1)-C(9)	126.4(3)
C(12)-N(1)-C(9)	112.2(3)
C(8)-N(2)-C(15)	129.1(4)
C(8)-N(2)-C(18)	119.0(4)
C(15)-N(2)-C(18)	111.8(4)
C(2)-C(1)-C(6)	120.8(5)
C(2)-C(1)-I(1)	119.2(4)
C(6)-C(1)-I(1)	120.0(4)

Table II-15. (Cont'd)

C(1)-C(2)-C(3)	119.3(5)
C(1)-C(2)-C(7)	122.1(5)
C(3)-C(2)-C(7)	118.5(4)
C(2)-C(3)-C(4)	121.0(5)
C(2)-C(3)-H(3)	119.5
C(4)-C(3)-H(3)	119.5
C(5)-C(4)-C(3)	118.4(6)
C(5)-C(4)-H(4)	120.8
C(3)-C(4)-H(4)	120.8
C(6)-C(5)-C(4)	121.6(5)
C(6)-C(5)-H(5)	119.2
C(4)-C(5)-H(5)	119.2
C(5)-C(6)-C(1)	118.8(5)
C(5)-C(6)-C(8)	119.1(4)
C(1)-C(6)-C(8)	122.0(5)
O(1)-C(7)-N(1)	123.3(4)
O(1)-C(7)-C(2)	121.9(4)
N(1)-C(7)-C(2)	114.8(4)
O(2)-C(8)-N(2)	122.8(4)
O(2)-C(8)-C(6)	121.1(4)
N(2)-C(8)-C(6)	116.0(4)
N(1)-C(9)-C(10A)	101.8(4)
N(1)-C(9)-C(10B)	95.4(6)
C(10A)-C(9)-C(10B)	62.5(6)
N(1)-C(9)-H(9A)	111.4
C(10A)-C(9)-H(9A)	111.4
C(10B)-C(9)-H(9A)	153.1
N(1)-C(9)-H(9B)	111.4
C(10A)-C(9)-H(9B)	111.4
C(10B)-C(9)-H(9B)	56.3
H(9A)-C(9)-H(9B)	109.3
C(9)-C(10A)-C(11)	98.9(5)
C(9)-C(10A)-H(10A)	112.0
C(11)-C(10A)-H(10A)	112.0
C(9)-C(10A)-H(10B)	112.0
C(11)-C(10A)-H(10B)	112.0
H(10A)-C(10A)-H(10B)	109.7
C(11)-C(10B)-C(9)	94.4(7)
C(11)-C(10B)-H(10C)	112.8
C(9)-C(10B)-H(10C)	112.8
C(11)-C(10B)-H(10D)	112.9
C(9)-C(10B)-H(10D)	112.8
H(10C)-C(10B)-H(10D)	110.3
C(12)-C(11)-C(10A)	101.4(4)
C(12)-C(11)-C(10B)	99.6(6)
C(10A)-C(11)-C(10B)	62.5(6)
C(12)-C(11)-H(11A)	111.5
C(10A)-C(11)-H(11A)	111.5
C(10B)-C(11)-H(11A)	54.1
C(12)-C(11)-H(11B)	111.5
C(10A)-C(11)-H(11B)	111.5
C(10B)-C(11)-H(11B)	148.8
H(11A)-C(11)-H(11B)	109.3
N(1)-C(12)-C(13)	111.6(3)

Table II-15. (Cont'd)

N(1)-C(12)-C(11)	103.2(3)
C(13)-C(12)-C(11)	109.9(4)
N(1)-C(12)-H(12)	110.7
C(13)-C(12)-H(12)	110.7
C(11)-C(12)-H(12)	110.7
O(4)-C(13)-O(3)	124.1(4)
O(4)-C(13)-C(12)	126.2(4)
O(3)-C(13)-C(12)	109.7(4)
O(3)-C(14)-H(14A)	109.5
O(3)-C(14)-H(14B)	109.5
H(14A)-C(14)-H(14B)	109.5
O(3)-C(14)-H(14C)	109.5
H(14A)-C(14)-H(14C)	109.5
H(14B)-C(14)-H(14C)	109.5
N(2)-C(15)-C(16)	104.0(4)
N(2)-C(15)-H(15A)	110.9
C(16)-C(15)-H(15A)	110.9
N(2)-C(15)-H(15B)	110.9
C(16)-C(15)-H(15B)	110.9
H(15A)-C(15)-H(15B)	109.0
C(15)-C(16)-C(17)	103.4(4)
C(15)-C(16)-H(16A)	111.1
C(17)-C(16)-H(16A)	111.1
C(15)-C(16)-H(16B)	111.1
C(17)-C(16)-H(16B)	111.1
H(16A)-C(16)-H(16B)	109.1
C(16)-C(17)-C(18)	104.5(4)
C(16)-C(17)-H(17A)	110.8
C(18)-C(17)-H(17A)	110.8
C(16)-C(17)-H(17B)	110.8
C(18)-C(17)-H(17B)	110.8
H(17A)-C(17)-H(17B)	108.9
N(2)-C(18)-C(19)	110.0(4)
N(2)-C(18)-C(17)	102.4(4)
C(19)-C(18)-C(17)	109.4(4)
N(2)-C(18)-H(18)	111.6
C(19)-C(18)-H(18)	111.6
C(17)-C(18)-H(18)	111.6
O(6)-C(19)-O(5)	124.5(4)
O(6)-C(19)-C(18)	125.2(4)
O(5)-C(19)-C(18)	110.2(4)
O(5)-C(20)-H(20A)	109.5
O(5)-C(20)-H(20B)	109.5
H(20A)-C(20)-H(20B)	109.5
O(5)-C(20)-H(20C)	109.5
H(20A)-C(20)-H(20C)	109.5
H(20B)-C(20)-H(20C)	109.5

Table II-16. Anisotropic displacement parameters $(\text{Å}^2 \times 10^3)$ for **II-100**. The anisotropic displacement factor exponent takes the form: $-2p^2[\,h^2 a^{*2} U^{11} + \ldots + 2\,h\,k\,a^*\,b^*\,U^{12}\,]$

	U^{11}	U^{22}	U^{33}	U^{23}	U^{13}	U^{12}
I(1)	124(1)	49(1)	42(1)	4(1)	-23(1)	-14(1)
O(1)	49(2)	64(3)	56(2)	30(2)	-8(2)	-20(2)
O(2)	63(2)	122(4)	45(2)	36(2)	-22(2)	-57(2)
O(3)	46(2)	59(2)	34(2)	18(2)	3(1)	12(2)
O(4)	97(3)	52(2)	38(2)	-2(2)	16(2)	20(2)
O(5)	53(2)	39(2)	38(2)	6(2)	0(1)	16(2)
O(6)	105(3)	33(2)	40(2)	-3(1)	6(2)	-1(2)
N(1)	31(2)	35(2)	27(2)	7(1)	-3(1)	1(2)
N(2)	42(2)	52(2)	49(2)	21(2)	-24(2)	-18(2)
C(1)	45(3)	50(3)	40(2)	18(2)	-12(2)	-18(2)
C(2)	29(2)	56(3)	37(2)	20(2)	-4(2)	-10(2)
C(3)	40(3)	77(3)	43(2)	23(2)	9(2)	6(3)
C(4)	39(3)	80(4)	67(4)	33(3)	6(3)	13(3)
C(5)	40(3)	75(4)	65(3)	43(3)	-11(3)	-3(3)
C(6)	37(2)	66(3)	47(2)	31(2)	-17(2)	-23(2)
C(7)	38(2)	46(2)	27(2)	7(2)	-1(2)	-4(2)
C(8)	53(3)	67(3)	44(2)	31(2)	-25(2)	-26(3)
C(9)	38(2)	42(2)	54(3)	20(2)	-6(2)	-6(2)
C(10A)	32(4)	49(4)	43(4)	-3(3)	3(3)	-6(3)
C(10B)	27(6)	47(8)	51(8)	12(6)	6(6)	5(6)
C(11)	30(2)	82(4)	52(3)	28(3)	4(2)	5(2)
C(12)	37(2)	30(2)	27(2)	4(2)	1(2)	7(2)
C(13)	35(2)	35(2)	28(2)	5(2)	-5(2)	-1(2)
C(14)	61(4)	109(5)	39(3)	29(3)	3(3)	18(4)
C(15)	43(3)	53(3)	64(3)	11(2)	-12(3)	-21(3)
C(16)	37(3)	46(3)	83(4)	6(3)	-17(3)	-9(2)
C(17)	48(3)	32(2)	75(3)	3(2)	-30(3)	-4(2)
C(18)	44(3)	32(2)	45(2)	6(2)	-19(2)	-5(2)
C(19)	46(2)	33(2)	35(2)	-2(2)	-14(2)	-3(2)
C(20)	67(3)	45(3)	40(2)	9(2)	2(2)	17(3)

Table II-17. Hydrogen coordinates ($\times 10^4$) and isotropic displacement parameters $(\text{Å}^2 \times 10^3)$ for **II-100**.

	x	y	z	U(eq)
H(3)	-864	6216	1221	64
H(4)	-2335	7658	703	74
H(5)	-2495	7377	-214	72
H(9A)	2616	6190	875	54
H(9B)	3869	5286	548	54
H(10A)	4243	5928	1662	50
H(10B)	5737	6033	1213	50
H(10C)	5045	4051	548	50
H(10D)	6144	5225	743	50

Table II-17. (Cont'd)

H(11A)	5837	3859	1106	66
H(11B)	58004032	1743	66	
H(12)	3347	2774	1284	38
H(14A)	3293	3280	2994	105
H(14B)	3287	1833	2956	105
H(14C)	1542	2578	2847	105
H(15A)	-4478	5364	-532	64
H(15B)	-3914	3998	-678	64
H(16A)	-5982	5600	-1300	66
H(16B)	-6268	4167	-1212	66
H(17A)	-4878	4832	-2078	62
H(17B)	-4058	3670	-1783	62
H(18)	-1581	4835	-1815	48
H(20A)	-3230	8258	-2423	76
H(20B)	-3321	7516	-2968	76
H(20C)	-1510	8054	-2767	76

Table II-18. Torsion angles [°] for **II-100**.

C(6)-C(1)-C(2)-C(3)	-1.2(7)
I(1)-C(1)-C(2)-C(3)	176.8(4)
C(6)-C(1)-C(2)-C(7)	179.1(4)
I(1)-C(1)-C(2)-C(7)	-2.9(6)
C(1)-C(2)-C(3)-C(4)	2.2(8)
C(7)-C(2)-C(3)-C(4)	-178.0(4)
C(2)-C(3)-C(4)-C(5)	-1.1(8)
C(3)-C(4)-C(5)-C(6)	-1.2(8)
C(4)-C(5)-C(6)-C(1)	2.2(8)
C(4)-C(5)-C(6)-C(8)	-173.8(5)
C(2)-C(1)-C(6)-C(5)	-1.0(7)
I(1)-C(1)-C(6)-C(5)	-179.0(3)
C(2)-C(1)-C(6)-C(8)	174.9(4)
I(1)-C(1)-C(6)-C(8)	-3.1(6)
C(12)-N(1)-C(7)-O(1)	-0.9(7)
C(9)-N(1)-C(7)-O(1)	179.1(5)
C(12)-N(1)-C(7)-C(2)	179.2(4)
C(9)-N(1)-C(7)-C(2)	-0.8(6)
C(1)-C(2)-C(7)-O(1)	-86.0(6)
C(3)-C(2)-C(7)-O(1)	94.2(6)
C(1)-C(2)-C(7)-N(1)	93.8(5)
C(3)-C(2)-C(7)-N(1)	-85.9(5)
C(15)-N(2)-C(8)-O(2)	-176.2(5)
C(18)-N(2)-C(8)-O(2)	-0.6(8)
C(15)-N(2)-C(8)-C(6)	0.7(8)
C(18)-N(2)-C(8)-C(6)	176.3(4)
C(5)-C(6)-C(8)-O(2)	92.0(7)
C(1)-C(6)-C(8)-O(2)	-83.9(7)
C(5)-C(6)-C(8)-N(2)	-84.9(6)
C(1)-C(6)-C(8)-N(2)	99.2(6)
C(7)-N(1)-C(9)-C(10A)	155.1(5)
C(12)-N(1)-C(9)-C(10A)	-24.9(5)

Table II-18 (Cont'd)

C(7)-N(1)-C(9)-C(10B)	-142.0(6)
C(12)-N(1)-C(9)-C(10B)	38.1(6)
N(1)-C(9)-C(10A)-C(11)	42.4(5)
C(10B)-C(9)-C(10A)-C(11)	-47.6(6)
N(1)-C(9)-C(10B)-C(11)	-53.9(7)
C(10A)-C(9)-C(10B)-C(11)	46.5(6)
C(9)-C(10A)-C(11)-C(12)	-45.7(5)
C(9)-C(10A)-C(11)-C(10B)	49.2(6)
C(9)-C(10B)-C(11)-C(12)	53.1(7)
C(9)-C(10B)-C(11)-C(10A)	-44.8(5)
C(7)-N(1)-C(12)-C(13)	-66.7(5)
C(9)-N(1)-C(12)-C(13)	113.2(4)
C(7)-N(1)-C(12)-C(11)	175.3(4)
C(9)-N(1)-C(12)-C(11)	-4.7(5)
C(10A)-C(11)-C(12)-N(1)	31.4(5)
C(10B)-C(11)-C(12)-N(1)	-32.3(7)
C(10A)-C(11)-C(12)-C(13)	-87.6(5)
C(10B)-C(11)-C(12)-C(13)	-151.3(6)
C(14)-O(3)-C(13)-O(4)	-2.8(7)
C(14)-O(3)-C(13)-C(12)	175.9(4)
N(1)-C(12)-C(13)-O(4)	-19.8(6)
C(11)-C(12)-C(13)-O(4)	94.0(5)
N(1)-C(12)-C(13)-O(3)	161.6(3)
C(11)-C(12)-C(13)-O(3)	-84.6(4)
C(8)-N(2)-C(15)-C(16)	161.6(5)
C(18)-N(2)-C(15)-C(16)	-14.3(6)
N(2)-C(15)-C(16)-C(17)	31.8(5)
C(15)-C(16)-C(17)-C(18)	-37.8(5)
C(8)-N(2)-C(18)-C(19)	-68.9(6)
C(15)-N(2)-C(18)-C(19)	107.5(4)
C(8)-N(2)-C(18)-C(17)	174.8(4)
C(15)-N(2)-C(18)-C(17)	-8.8(5)
C(16)-C(17)-C(18)-N(2)	28.5(5)
C(16)-C(17)-C(18)-C(19)	-88.1(5)
C(20)-O(5)-C(19)-O(6)	-5.1(7)
C(20)-O(5)-C(19)-C(18)	171.2(4)
N(2)-C(18)-C(19)-O(6)	-26.5(6)
C(17)-C(18)-C(19)-O(6)	85.2(6)
N(2)-C(18)-C(19)-O(5)	157.3(4)
C(17)-C(18)-C(19)-O(5)	-91.0(5)

2.6: References

1. Pellissier, H. *Tetrahedron* **2007,** *63*, 9267-9331.

2. Taylor, M. S.; Jacobsen, E. N. *Angew. Chem., Int. Ed.* **2006,** *45*, 1520-1543.

3. Dalko, P. I.; Moisan, L. *Angew. Chem., Int. Ed.* **2004,** *43*, 5138-5175.

4. Dalko, P. I.; Moisan, L. *Angew. Chem., Int. Ed.* **2001,** *40*, 3726-3748.

5. Jarvo, E. R.; Miller, S. J. *Tetrahedron* **2002,** *58*, 2481-2495.

6. France, S.; Guerin, D. J.; Miller, S. J.; Lectka, T. *Chem. Rev.* **2003,** *103*, 2985-3012.

7. Kacprzak, K.; Gawronski, J. *Synthesis* **2001,** 961-998.

8. Guillena, G.; Ramon, D. J. *Tetrahedron: Asymmetry* **2006,** *17*, 1465-1492.

9. Oestreich, M. *Angew. Chem., Int. Ed.* **2005,** *44*, 2324-2327.

10. Muniz, K. *Angew. Chem., Int. Ed.* **2001,** *40*, 1653-1656.

11. Dowle, M. D.; Davies, D. I. *Chem. Soc. Rev.* **1979,** *8*, 171-197.

12. Cardillo, G.; Orena, M. *Tetrahedron* **1990,** *46*, 3321-3408.

13. Kitagawa, O.; Hanano, T.; Tanabe, K.; Shiro, M.; Taguchi, T. *Chem. Commun.* **1992,** 1005-1007.

14. Grossman, R. B.; Trupp, R. J. *Can. J. Chem.* **1998,** *76*, 1233-1237.

15. Haas, J.; Bissmire, S.; Wirth, T. *Chem., Eur. J.* **2005,** *11*, 5777-5785.

16. Haas, J.; Piguel, S.; Wirth, T. *Org. Lett.* **2002,** *4*, 297-300.

17. Garnier, J. M.; Robin, S.; Rousseau, G. *Eur. J. Org. Chem.* **2007,** 3281-3291.

18. Cui, X. L.; Brown, R. S. *J. Org. Chem.* **2000,** *65*, 5653-5658.

19. Wang, M.; Gao, L. X.; Mai, W. P.; Xia, A. X.; Wang, F.; Zhang, S. B. *J. Org. Chem.* **2004,** *69*, 2874-2876.

20. Wang, M.; Gao, L. X.; Yue, W.; Mai, W. P. *Synth. Commun.* **2004,** *34,* 1023-1032.

21. Ahmad, S. M.; Braddock, D. C.; Cansell, G.; Hermitage, S. A.; Redmond, J. M.; White, A. J. P. *Tetrahedron Lett.* **2007,** *48,* 5948-5952.

22. Kang, S. H.; Park, C. M.; Lee, S. B.; Kim, M. *Synlett* **2004,** 1279-1281.

23. Kang, S. H.; Lee, S. B.; Park, C. M. *J. Am. Chem. Soc.* **2003,** *125,* 15748-15749.

24. Kang, S. H.; Kang, S. Y.; Park, C. M.; Kwon, H. Y.; Kim, M. *Pure Appl. Chem.* **2005,** *77,* 1269-1276.

25. Inoue, T.; Kitagawa, O.; Kurumizawa, S.; Ochiai, O.; Taguchi, T. *Tetrahedron Lett.* **1995,** *36,* 1479-1482.

26. Inoue, T.; Kitagawa, O.; Ochiai, O.; Shiro, M.; Taguchi, T. *Tetrahedron Lett.* **1995,** *36,* 9333-9336.

27. Sakakura, A.; Ukai, A.; Ishihara, K. *Nature* **2007,** *445,* 900-903.

28. Berti, G.; Marsili, A. *Tetrahedron* **1966,** *22,* 2977-2988.

29. Bellucci, G.; Giordano, C.; Marsili, A.; Berti, G. *Tetrahedron* **1969,** *25,* 4515-4522.

30. Bellucci, G.; Berti, G.; Marioni, F.; Marsili, A. *Tetrahedron* **1970,** *26,* 4627-4633.

31. Bellucci, G.; Berti, G.; Bianchini, R.; Orsini, L. *Gazz. Chim. Ital.* **1986,** *116,* 77-81.

32. Dauphin, G.; Kergomard, A.; Scarset, A. *Bull. Chim. Soc. Fr.* **1976,** 862-866.

33. El-Qisairi, A.; Hamed, O.; Henry, P. M. *J. Org. Chem.* **1998,** *63,* 2790-2791.

34. El-Qisairi, A. K.; Qaseer, H. A.; Katsigras, G.; Lorenzi, P.; Trivedi, U.; Tracz, S.; Hartman, A.; Miller, J. A.; Henry, P. M. *Org. Lett.* **2003,** *5,* 439-441.

35. Braddock, D. C.; Cansell, G.; Hermitage, S. A.; White, A. J. P. *Chem. Commun.* **2006,** 1442-1444.

36. Braddock, D. C.; Cansell, G.; Hermitage, S. A. *Synlett* **2004**, 461-464.

37. Braddock, D. C.; Cansell, G.; Hermitage, S. A. *Chem. Commun.* **2006**, 2483-2485.

38. Hoveyda, A. H. *Chem. Biol.* **1998,** *5,* R187-R191.

39. Shimizu, K. D.; Snapper, M. L.; Hoveyda, A. H. *Chem., Eur. J.* **1998,** *4,* 1885-1889.

40. Hoveyda, A. H.; Hird, A. W.; Kacprzynski, M. A. *Chem. Commun.* **2004**, 1779-1785.

41. Kuntz, K. W.; Snapper, M. L.; Hoveyda, A. H. *Curr. Opin. Chem. Biol.* **1999,** *3,* 313-319.

42. Zhao, Y.; Rodrigo, J.; Hoveyda, A. H.; Snapper, M. L. *Nature* **2006,** *443,* 67-70.

43. Imperiali, B.; Fisher, S. L.; Moats, R. A.; Prins, T. J. *J. Am. Chem. Soc.* **1992,** *114,* 3182-3188.

44. Imperiali, B.; Kapoor, T. M. *Tetrahedron* **1993,** *49,* 3501-3510.

45. Miller, S. J. *Acc. Chem. Res.* **2004,** *37,* 601-610.

46. Blank, J. T.; Miller, S. J. *Biopolymers* **2006,** *84,* 38-47.

47. Agarkov, A.; Greenfield, S. J.; Ohishi, T.; Collibee, S. E.; Gilbertson, S. R. *J. Org. Chem.* **2004,** *69,* 8077-8085.

48. Fields, G. B.; Noble, R. L. *Int. J. Pept. Protein Res.* **1990,** *35,* 161-214.

49. Chan, W. C.; White, P. D. *Fmoc Solid Phase Peptide Synthesis*; Oxford University Press: Oxford, 2004.

50. Moriuchi, T.; Shen, X. L.; Hirao, T. *Tetrahedron* **2006,** *62,* 12237-12246.

51. Moriuchi, T.; Nishiyama, M.; Yoshida, K.; Hirao, T. *Heterocycles* **2006,** *67,* 375-383.

52. Derdau, V.; Laschat, S.; Hupe, E.; Konig, W. A.; Dix, I.; Jones, P. G. *Eur. J. Inorg. Chem.* **1999**, 1001-1007.

53. Rewcastle, G. W.; Denny, W. A. *Synthesis* **1985**, 217-220.

54. Jordan, A. D.; Luo, C.; Reitz, A. B. *J. Org. Chem.* **2003,** *68*, 8693-8696.

55. Iranpoor, N.; Firouzabadi, H.; Shaterian, H. R. *J. Org. Chem.* **2002,** *67*, 2826-2830.

56. Iranpoor, N.; Firouzabadi, H.; Shaterian, H. R. *Tetrahedron Lett.* **2003,** *44*, 4769-4773.

57. Nonhebel, D. C. *J. Chem. Soc.* **1963**, 1216-1220.

58. de Almeida, L. S.; Esteves, P. M.; de Mattos, M. C. S. *Synlett* **2006**, 1515-1518.

59. de Almeida, L. S.; Esteves, P. M.; de Mattos, M. C. S. *Synthesis* **2006**, 221-223.

60. Mohan, K.; Narender, N.; Srinivasu, P.; Kulkarni, S. J.; Raghavan, K. V. *Synth. Commun.* **2004,** *34*, 2143-2152.

61. Oliveto, E. P.; C., G. *Org. Synth. Coll.* **1963,** *4*, 104.

62. de Souza, S. P. L.; da Silva, J. F. M.; de Mattos, M. C. S. *Synth. Commun.* **2003,** *33*, 935-939.

63. Zajc, B. *Synth. Commun.* **1999,** *29*, 1779-1784.

64. Fieser, L. F.; Fieser, M. *Reagents for Organic Synthesis*; Vol. 1.

65. Moghaddam, F. M.; Boeini, H. Z. *Synlett* **2005**, 1612-1614.

66. Moghaddam, F. M.; Boeini, H. Z.; Zargarani, D.; Bardajee, G. R. *Synth. Commun.* **2006,** *36*, 1093-1096.

67. Rood, G. A.; DeHaan, J. M.; Zibuck, R. *Tetrahedron Lett.* **1996,** *37*, 157-158.

68. Kodomari, M.; Satoh, H.; Yoshitomi, S. *Bull. Chem. Soc. Jpn.* **1988,** *61*, 4149-4150.

69. Hontz, A. C.; Wagner, E. C. *Org. Syn.* **1951,** *31*, 48-52.

Chapter 3: Development of a *Cinchona* Alkaloid Promoted Asymmetric Chlorolactonization of Alkenoic Acids

3.1: Introduction

The relative inability to improve upon our first generation peptide-based bromiodinane catalyst system (**III-1**, Scheme III-1) in the bromolactonization of **III-2**, brought to light several damning limitations that ultimately led us to explore alternate means towards realizing our goals of a highly selective halolactonization protocol. As detailed in Chapter 2, the catalyst from our 1st generation library returned bromolactone **III-3** in 14% *ee* when 0.1 equivalents of catalyst **III-1** was employed. More disappointingly, **III-3** was generated in just 24% *ee* when a stoichiometric amount of **III-1** was employed (eq. 1). We surmised that the poorly selective stoichiometric reaction might in part be explained by a sluggish initial reaction between **III-1** and NBS, thus leading to a relatively small equilibrium concentration of active bromoiodinane catalyst **III-4**. This fact, coupled with an exceptionally rapid background reaction (*i.e.* complete generation of **III-3** by action of NBS alone in less than 5 minutes; eq. 3) ultimately suggested that only an exceedingly active catalyst within the bromoiodinane approach would be able to effectively outstrip the background reaction. Ultimately, the problem would be much simpler if one had access to a more nucleophilic catalyst manifold as well as the ability to explore alternate and hopefully less active terminal halogen sources. Initial experiments aimed at coupling the existing peptide scaffold containing the *ortho*-iodoarylamido active

site with a terminal chlorine source in lieu of a bromine source failed to return any

desired chlorolactone (Scheme III-1, eq. 4).

Scheme III-1. Limitations of first generation catalyst system **III-1**.

14% *ee* (0.1 eq. **III-1**)

24% *ee* (1.1 eq. **III-1**)
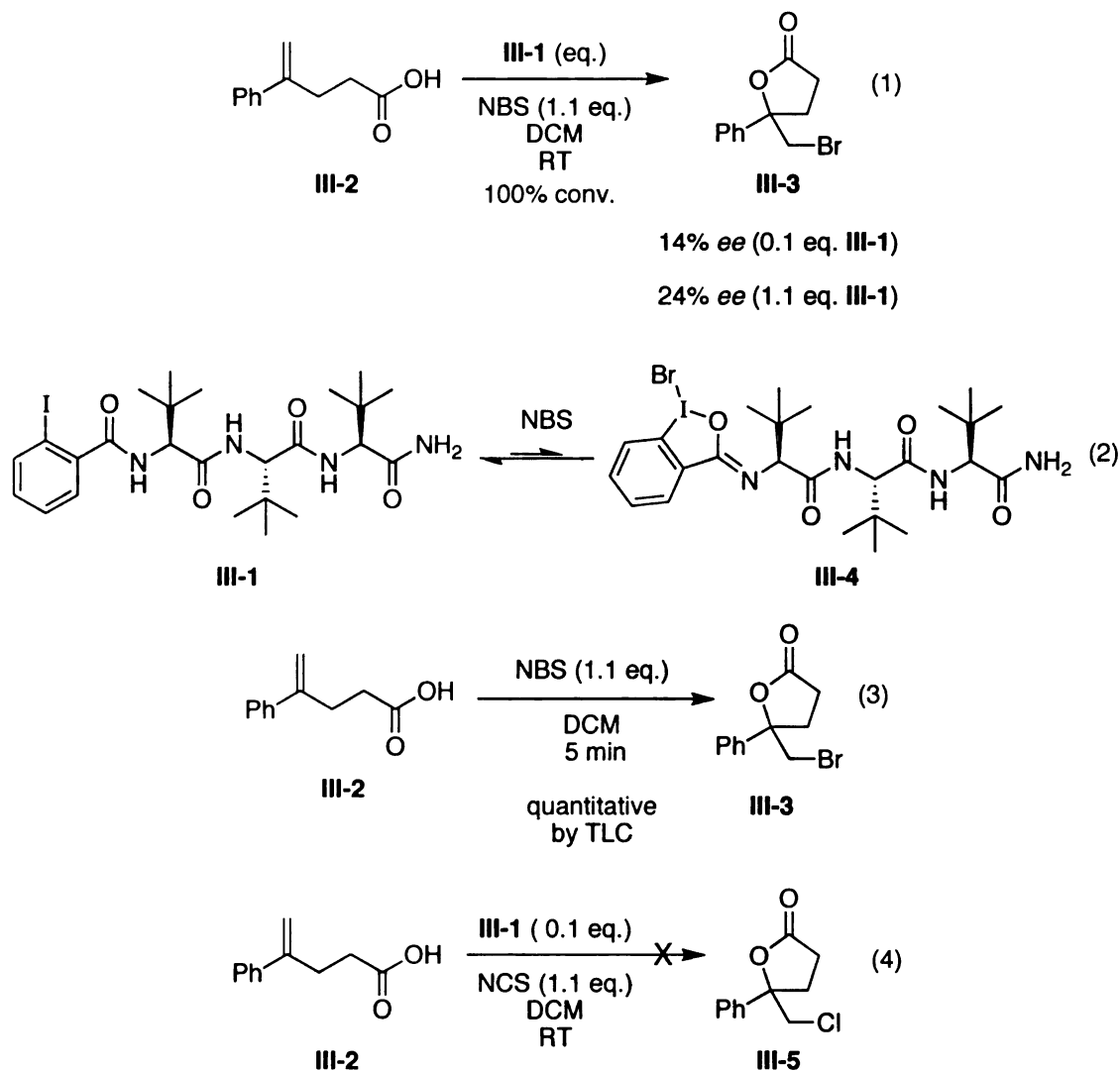
Having sufficiently exhausted the available options toward optimizing the

initial hit scaffold **III-1** past the initially discovered 14% *ee*, we again turned to the

work of Braddock and co-workers for inspiration.[1,2] Their second generation

approach to effecting an organocatalytic bromolactonization reaction originated

from the discovery that the addition of a catalytic amount of N,N-

dimethylformamide to a CDCl$_3$ solution of pentenoic acid **III-6** and NBS led to a significant rate enhancement in the generation of bromolactone **III-7** (Scheme III-2). In the presence of 0.2 equiv. of **III-8**, the cyclization of **III-6** proceeded with 43% conversion after just 2 hours, whereas the uncatalyzed reaction mediated by NBS alone proceeded to only 15% conversion after 15 hours. The rate of conversion to **III-7** was further enhance by employing 0.1 equiv. of N,N-dimethylacetamide **III-9** (100% conversion in 30 minutes). Faster still was the transformation in the presence of just 0.01 equiv. of tetramethylguanidine **III-10** (100% conversion in less than 15 minutes).[1] Subsequent to these studies, they also disclosed that various amidines can accelerate the conversion of **III-6** to **III-7** in the presence of NBS in CDCl$_3$. Namely, they discovered that 0.01 equiv. of racemic amidine **III-11** allowed for the reaction to proceed to 90% conversion within 1 hour. Finally, they employed chiral amidines **III-12** and **III-13** to promote the bromolactonization of substrate **III-6** as well as substrate **III-14**, in an attempt at developing an asymmetric variant of the reaction. In the event, the corresponding bromolactones were produced in adequate yield in racemic form. In addition to the bromolactonization reaction, amidines **III-12** and **III-13** were screened for asymmetric induction in the bromoacetoxylation of several 1,2-*trans* olefins with equally discouraging results.[2]

Scheme III-2. Braddock's second generation bromolactonization organocatalysts.
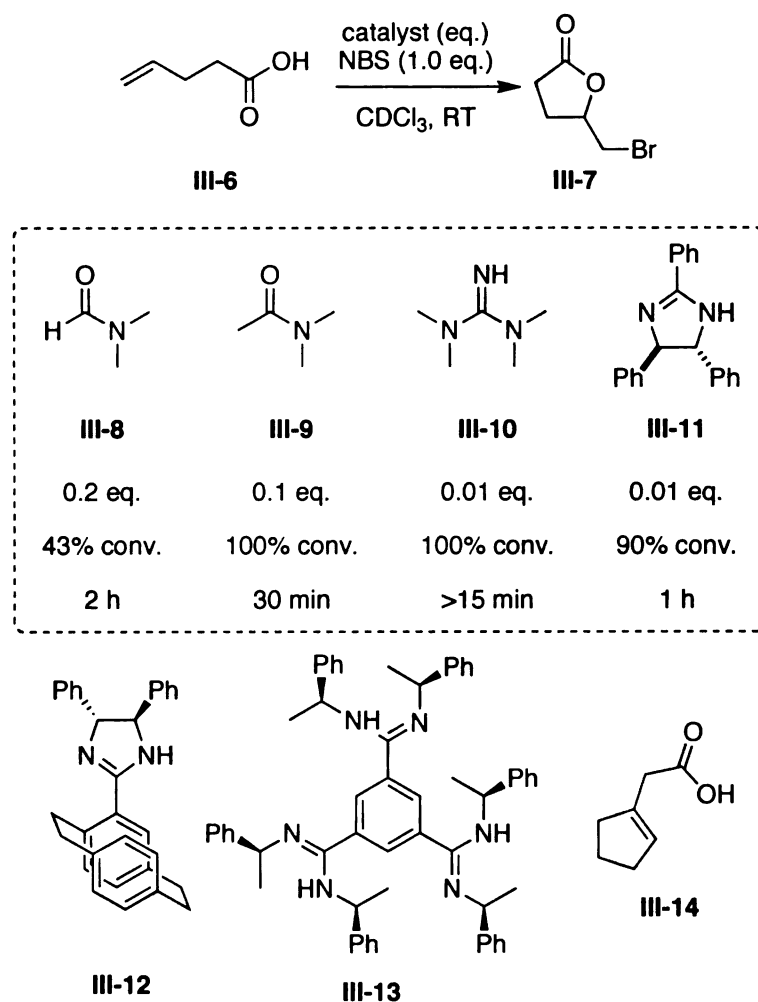
Although their initial entry into an enantioselective approach was unsuccessful, we were emboldened by the knowledge that other organic functionalities could promote an accelerated halolactonization in lieu of relying on the iodinane approach described earlier. Braddock's second generation organocatalytic system was inherently more general than the bromoiodinane[3,4] approach. Distilled to its most basic principles, their second generation approach required a terminal halenium source (importantly not necessarily limited to bromine) and an a appropriate chiral nucleophile promoter. We envisioned that

118

the second requirement, the chiral nucleophile, need not necessarily be limited to chiral amidines or amides. In that vein, our initial departure from the bromoiodinane strategy was to screen several commercially available chiral nucleophiles and well-known chiral ligands/catalysts for activity in the bromolactonization of our established test substrate III-2. Presented below is the detailed account of how these initial experiments ultimately led to the discovery of an enantioselective chlorolactonization reaction.

3.2: Results and Discussion

3.2.1: Initial Catalyst Screen

An initial screen was conducted whereby a number of commercially available chiral molecules were assayed in the test reaction (conversion of III-2 to III-3). The reactions were conducted in microscale, employing 0.05 mmol of III-2 and 0.1 equivalent of the putative catalyst. As with the experiments conducted in Chapter 2, we evaluated the enantioselectivity of the reaction and did not determine isolated yields. *It warrants emphasis that all of the transformations described in this chapter proceeded to completion by TLC analysis, unless otherwise noted.*

As mentioned earlier, we conceptualized the organocatalysis observed in the Braddock second generation system by action of amides, guanidines, and amidines to be potentially more broadly applicable to any number of nucleophilic moieties. As such we elected to screen a number of chiral promoters containing amine, phosphine, alcohol, and oxazoline nucleophiles. We hoped that an initial

assay of a subset of chiral promoters might reveal a marginally selective initial

scaffold that could be subsequently optimized to a highly selective catalyst. The

structures of the potential catalysts for the initial screen are shown in Figure III-1.

Figure III-1. Potential organocatalysts for the halolactonization of **III-2**.

pyroglutamic acid

III-15

(-)-sparteine

III-16

(*1S,2S*)-1,2-diphenylethylenediamine

III-17

(*1S,2S*)-1,2-diaminocyclohexane

III-18

(*S*)-1,1'-binaphthyl-2,2'-diamine

III-19

L-*tert*-leucine

III-20

(*R*)-1-(1-naphthyl)-ethylamine

III-21

(*S*)-2-(diphenylmethyl)pyrrolidine

III-22

(DHQD)$_2$PHAL

III-23

Bisoxazoline (BOX)

III-24

PyBox

III-25

(*S*)-BINAP

III-26

121

Figure III-1. (Cont'd)

(*1R, 2R, 3S,5R*)- pinanediol

III-27

TADDOL

III-28

(*R*)-BINOL

III-29

(*R*)-VAPOL

III-30

(*S*)-VANOL

III-31

Jacobsen SALEN Ligand
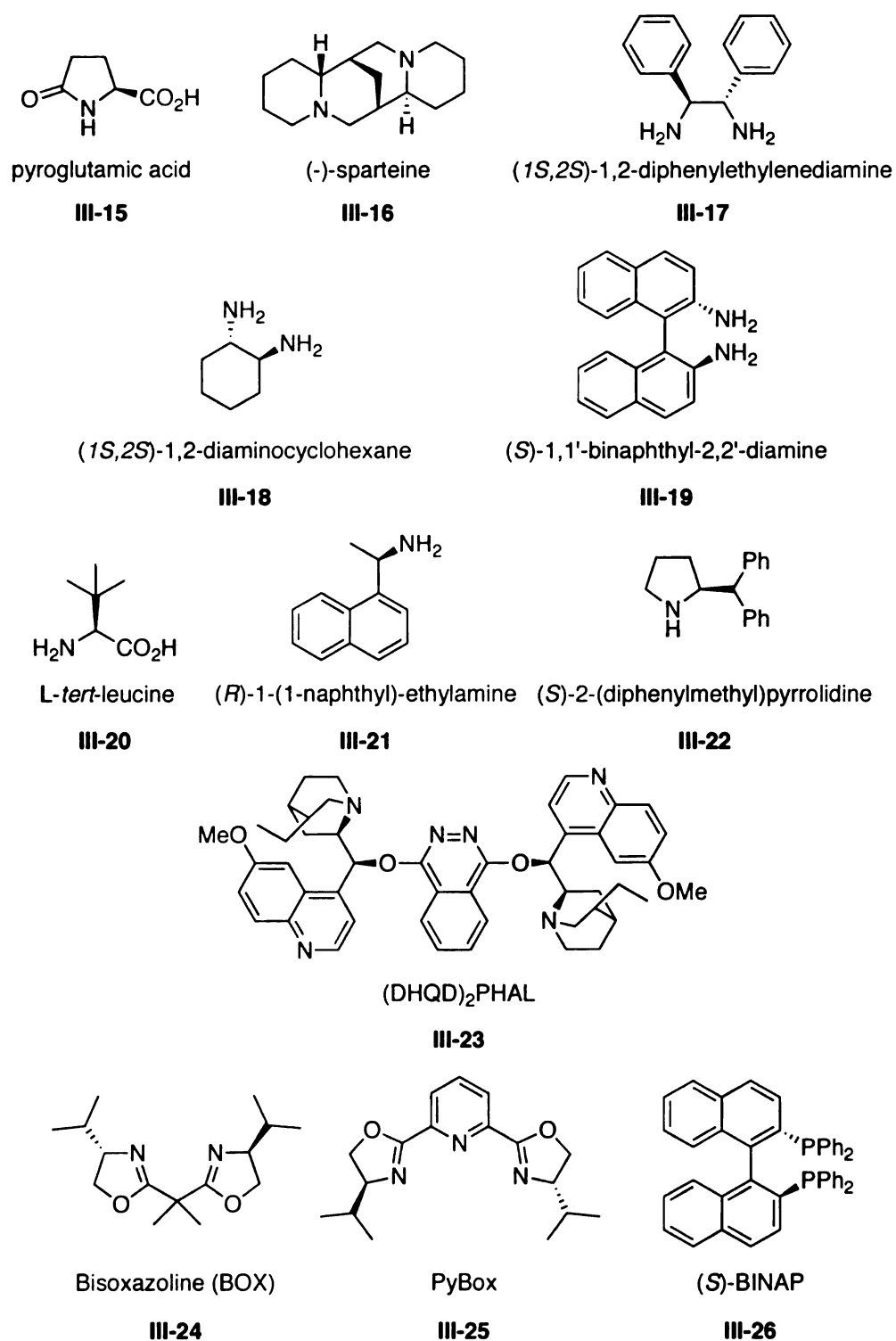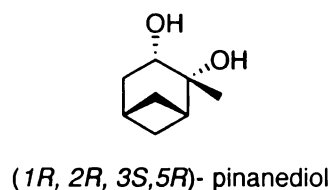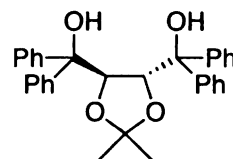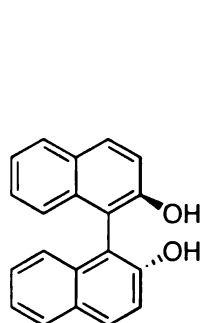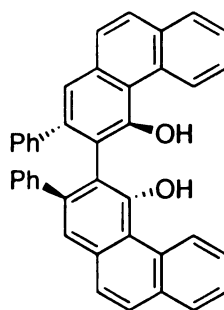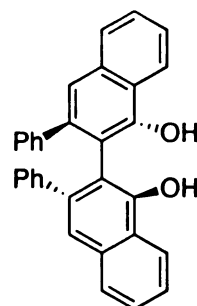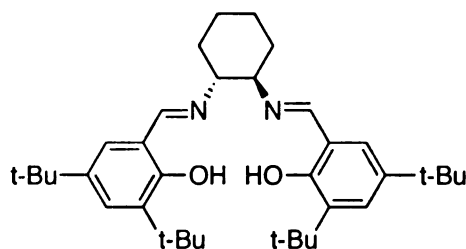
III-32

Our initial screen included eighteen potential catalysts. Pyroglutamic acid (**III-15**) served as a single example of a chiral amide. Four chiral diamines were screened in the lactonization of substrate **III-2**. These examples included the alkaloid sparteine (**III-16**),[5] two vicinal diamines (**III-17**[6] and **III-18**), and the axially chiral binaphthyldiamine **III-19**.[7] Monoamine catalysts included the amino acid, *tert*-leucine (**III-20**), along with 1-(1-napthyl)ethylamine (**III-21**) and

diphenylmethylenepyrrolidine catalyst **III-22**.[8-11] In addition to these amine based catalysts, (DHQD)$_2$PHAL[12] (**III-23**) served as the sole example of the *Cinchona* alkaloid catalyst class.[13,14]

In addition to amine based catalysts, the well known bis(oxazoline) (BOX, **III-24**),[15,16] Pybox (**III-25**),[17] and BINAP (**III-26**)[18,19] ligands were screened. Five diols were screened including pinanediol **III-27**, Seebach's TADDOL[20] ligand (**III-28**), along with three axially chiral diols. In addition to BINOL **III-29**,[21-23] the vaulted ligands VAPOL (**III-30**) and VANOL (**III-31**) developed by Wulff and coworkers were investigated.[24-26] Finally, **III-32** represents an example of the salen ligands popularized by Jacobsen as well as others.[27]

In the event, amide **III-15** and amines **III-16** through **III-22** proved poorly selective, returning **III-3** in less than 4% *ee* (Table III-1, entries 1-8). BOX ligand **III-24** and Pybox **III-25** returned the bromolactone in 1 and 0% *ee*, respectively while BINAP **III-26** returned **III-3** in 5% *ee* (entries 10-12). Pinanediol **III-27** and TADDOL (**III-28**) also returned racemic bromolactone (entries 13 and 14). The axially chiral diols BINOL (**III-29**), VAPOL (**III-30**), and VANOL (**III-31**) returned bromolactone **III-3** in -4, -3, and 0% *ee*, respectively (entries 15-17). Salen ligand **III-32** returned the desired bromolactone product in 6% *ee* (entry 18).

While the results with these seventeen potential catalysts were uninspiring, (DHQD)$_2$PHAL (**III-23**) returned the desired bromolactone **III-3** in 20% *ee* as judged by HPLC analysis (entry 9). This initial result was exciting and bested in a single experiment, the hard-won 14% *ee* realized by peptide **III-1** after several months of optimization.

Table III-1. Screen of potential catalysts **III-15** through **III-32.**
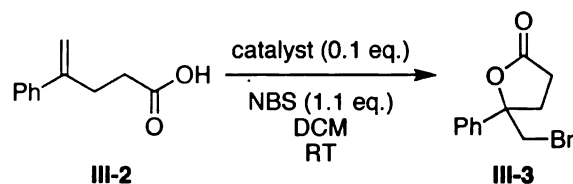
Entry	Catalyst	% ee (III-3)	Entry	Catalyst	% ee (III-3)
1	III-15	0	10	III-24	1
2	III-16	0	11	III-25	0
3	III-17	0	12	III-26	5
4	III-18	0	13	III-27	0
5	III-19	4	14	III-28	0
6	III-20	2	15	III-29	-4
7	III-21	0	16	III-30	-3
8	III-22	0	17	III-31	0
9	III-23	20	18	III-32	6

Note: All reactions were complete by TLC.

3.2.2: Initial Optimization Experiments

With the discovery that *Cinchona* alkaloid based ligand **III-23** was effective

in providing bromolactone **III-3** with marginal enantioselectivities (Table III-1,

entry 9), a series of experiments were conducted to improve the selectivity of this

catalyst system to hopefully provide a more selective process. Initial efforts

focused on evaluating the selectivity of the reaction when the temperature was

lowered, as well as when the equivalency of the organocatalyst was changed

(Table III-2).

Table III-2. Temperature and catalyst equivalent study.
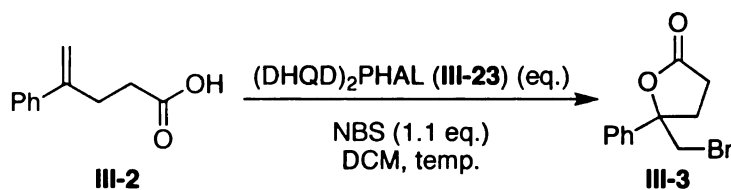
Entry	III-23 (eq.)	Temp. (˚C)	% ee (III-3)
1	0.1	-20	14
2	0.1	4	19
3	0.1	RT	22
4	0.05	RT	20
5	0.01	RT	22
6	1.1	RT	12
7	5.0	RT	3

Note: All reactions were complete by TLC.

A control experiment with the initially discovered reaction conditions employing 0.1 equivalents of **III-23** at room temperature (Table III-2, entry 3), returned bromolactone **III-3** in 22% *ee*. Lowering the temperature below room temperature resulted in a less selective transformation (entries 1 and 2). In the event, lowering the temperature to -20 ˚C returned **III-3** in 14% *ee*, while conducting the reaction in a 4 ˚C cold room produced the bromolactone in a slightly improved 19% *ee*.

Modulating the catalyst equivalency also failed to improve the selectivity of the reaction. Excitingly, the catalyst loading could be lowered to 0.05 or even 0.01 equivalents without a detrimental loss in enantioselectivity (entries 4 and 5). Curiously, however, increasing the catalyst loading to 1.1 or 5 equivalents

resulted in an inferior reaction with respect to enantioselectivity (entries 6 and 7), returning **III-3** in 12 and 3% *ee*, respectively. The stoichiometric and super-stoichiometric results were curious, given that at first blush one might expect for the enantioselectivity of the transformation to increase when additional chiral catalyst was employed. Indeed, this axiom was borne out in our 1st generation system (*vide supra*, Scheme III-1). The reasons for the decrease in selectivity in the system at hand are not clear. It is intriguing, however, to note that *Cinchona* alkaloids (most notably quinine and dihydroquinine) have been known to exhibit auto-aggregation to form dimeric complexes in concentrated solutions.[28,29] A similar event in this system might account for the poor selectivity when a large excess of catalyst is employed (*vide infra*, Section 3.2.6).

Although catalyst **III-23** could maintain a selectivity of *ca.* 20-22% *ee* at 0.05 and 0.01 equivalents (entries 4 and 5), the initially discovered catalyst loading of 0.1 equivalents was maintained in subsequent optimization experiments. It was reasoned that optimization of the other reaction parameters (*i.e.* solvent, halogen source, etc.) might result in a less active catalyst system that could be swamped by a prevailing background reaction at such low loadings. In short, it was felt that we could return to tuning the catalyst loading at a later stage in the optimization of the system after the enantioselectivity had been driven to more synthetically useful levels.

Having investigated lower temperatures and catalyst loading, we next turned to evaluating the selectivity of the reaction on increasing the concentration of the reaction. Concentrations ranging from the initially discovered conditions

(0.05 M) to 1 M (relative to substrate **III-2**) were evaluated. As is indicated in

Table III-3 below, the selectivity of the reaction was only marginally affected

when the reaction was conducted under more concentrated conditions, ranging

from 19 to 21% *ee*.

Table III-3. Concentration study with **III-23**/NBS system.
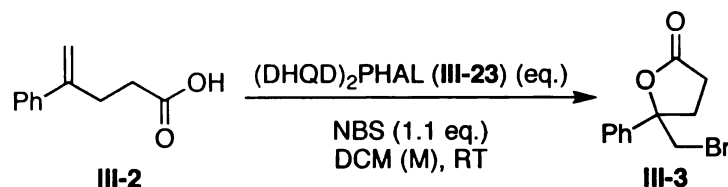
Entry	Conc. (M)	% *ee* (III-3)
1	0.05	20
2	0.1	21
3	0.5	20
4	1.0	19

Note: All reactions were complete by TLC.

Subsequent to the concentration experiments, a few alternate bromine

sources were investigated. Given that a more comprehensive bromine source

screen had proven fruitless in the course of the optimization of our first

generation scaffold **III-1**, we were hesitant to undertake such a thorough screen

with the system at hand. Hence, we chose the four best bromine sources from

the bromine source screen with **III-1** and rapidly screened them with catalyst **III-23**. Namely, we chose to investigate N-bromoacetamide[30] (NBA, **III-33**), N-bromosaccharin[31,32] (NBSac, **III-34**), TABCO[33,34] (**III-35**) and cupric bromide[35] (**III-36**). As indicated in Table III-4, while NBA (entry 1) and TABCO (entry 3)

allowed for an equally selective transformation as the initially discovered

127

conditions with NBS (20-23% *ee*), NBSac (entry 2) and cupric bromide (entry 4) resulted in a virtually unselective reaction. In the end, we elected to retain NBS as the halogen source of choice for subsequent experiments.

Table III-4. Bromine source screen with catalyst III-23.
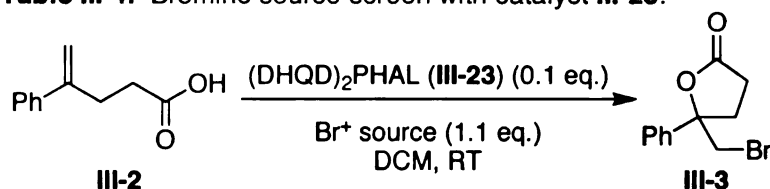
Entry	Br$^+$ source	% *ee* (III-3)
1	III-33	23
2	III-34	0
3	III-35	22
4	III-36	2
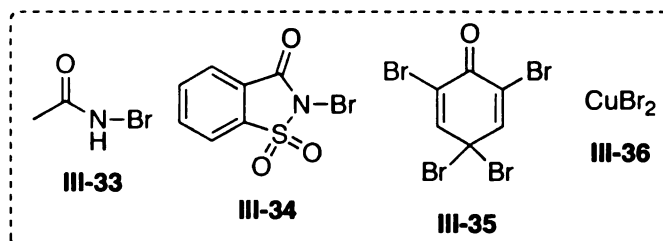
Note: All reactions were complete by TLC.

As a final attempt at optimization of the initially discovered reaction conditions (*vide supra*, Table III-1, entry 9) the reaction was attempted in the presence of other *Cinchona* alkaloid based catalysts.[12,13] Other commercially available ligands including the parent alkaloid hydroquinidine (DHQD, III-37), and the various O-aryl and O-acyl derivatives thereof (III-38 through III-40) were screened in the bromolactonization of III-2 (Figure III-2 and Table III-5). Also, two dimeric structures, (DHQD)$_2$PYR (III-41) and (DHQ)$_2$AQN (III-42) were evaluated.

Figure III-2. Various *Cinchona* alkaloid-based cataysts.
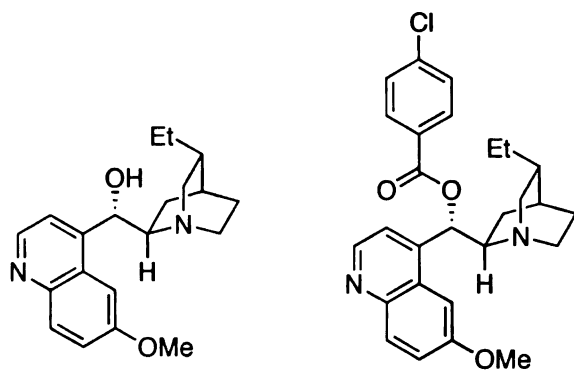
hydroquinidine (DHQD)

III-37

DHQD-CLB

III-38
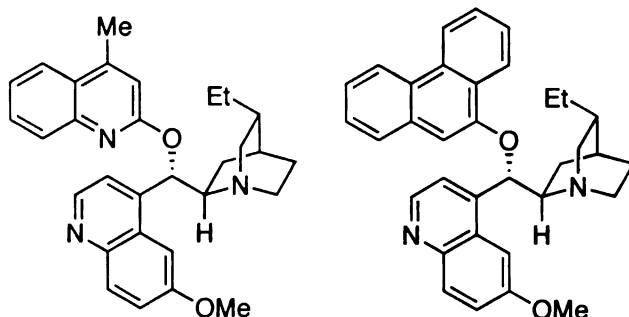
DHQD-MEQ

III-39

DHQD-PHN

III-40
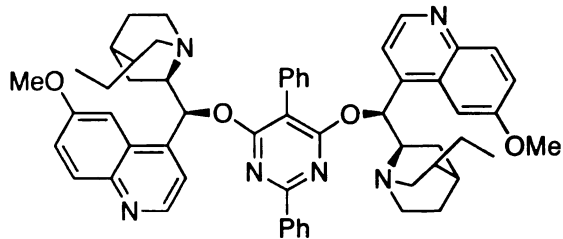
$(DHQD)_2Pyr$

III-41
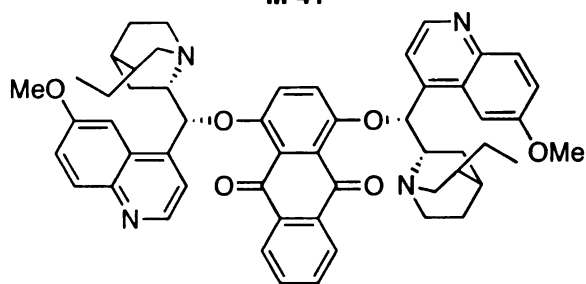
$(DHQ)_2AQN$

III-42

Interestingly, while the initially discovered conditions employing

(DHQD)₂PHAL (**III-23**) provided lactone **III-3** with an enantiomeric excess of 22%

(in favor of the first enantiomer to elute from the HPLC) the parent hydroquinidine

(**III-37**) by itself returned the **III-3** in 15% *ee* in favor of the opposite enantiomer

(Table III-5, entry 1). (Note: negative *ee* values in Table III-5 indicate a

preference for the second enantiomer to elute from the HPLC.) Similarly, the

chlorobenzoate derivative of DHQD (**III-38**) also returned lactone **III-3** in -16 *ee*

(entry 2). This reversal in enantioselectivity at the hands of monomeric catalysts

of the same quasienantiomeric configuration as **III-23** is remarkable, and strongly

indicates that a different mode of catalysis is occurring for the transformation.

Table III-5. Screen of various *Cinchona* alkaloid catalysts.
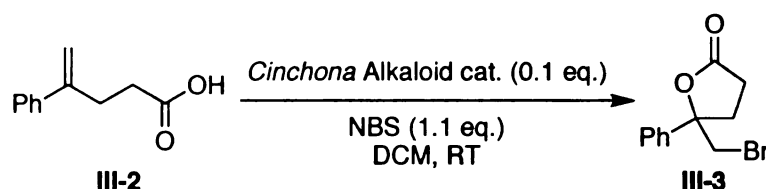
Entry	Cat.	% ee (III-3)
1	III-37	-15
2	III-38	-16
3	III-39	0
4	III-40	7
5	III-41	-7
6	III-42	-2

Note: All reactions were complete by TLC.

The 4-methylquinoloyl ether **III-39** returned **III-3** as the racemate (entry 3)

and the phenanthroyl ether **III-40** returned the bromolactone in just 7% *ee* (entry

130

4). The diphenylpyrimidine dimer of DHQD (**III-41**) returned **III-3** in -7% *ee* (entry 5). Finally, the dihydroquinine anthraquinone dimer **III-42** generated **III-3** in -2% ee (entry 6). Although the switch in selectivity observed for the monomeric DHQD variants was intriguing, none of the catalysts supplanted the (DHQD)$_2$PHAL system that was initially discovered.

In the end, all of the initial attempts made to increase the selectivity of the initially discovered reaction conditions were fruitless.   At this point we still had failed to address the exceptionally fast, uncatalyzed background reaction at the hands of NBS alone (*vide supra*, Scheme III-1, eq. 3). Nonetheless, the efforts detailed above had brought to light a catalyst system that was not hamstrung by the limitation that led us away from our first generation peptide-based approach. Namely, in the case at hand, the terminal halogen source need not necessarily be limited to a bromine-based system. The most logical extension of this methodology was to replace NBS with NCS, to investigate whether an analogous chlorolactonization was possible. Initially, we were encouraged by the fact that the uncatalyzed chlorolactonization of **III-2** by NCS alone showed no evidence of chlorolactone **III-43** after 24 hours at room temperature (Scheme III-3, eq. 1). Conversion to chlorolactone **III-43** was only observed after the inclusion of 0.1 equiv. of DMAP (eq. 2).   Even after the incorporation of an amine nucleophile, the reaction was sufficiently sluggish to allow for the detection of starting material by TLC after 24 hours. Emboldened by the substantially slower background reaction in the presence of NCS, we attempted the asymmetric reaction in the presence of (DHQD)$_2$PHAL. Excitingly, the desired chlorolactone **III-43** was

produced in 100% conversion by TLC with an enantiomeric excess of 39% (Scheme III-3, dashed box). What follows is a detailed account of the optimization strategy that eventually led to a synthetically useful asymmetric chlorolactonization protocol.

Scheme III-3. An analogous chlorolactonization reaction increases selectivity.
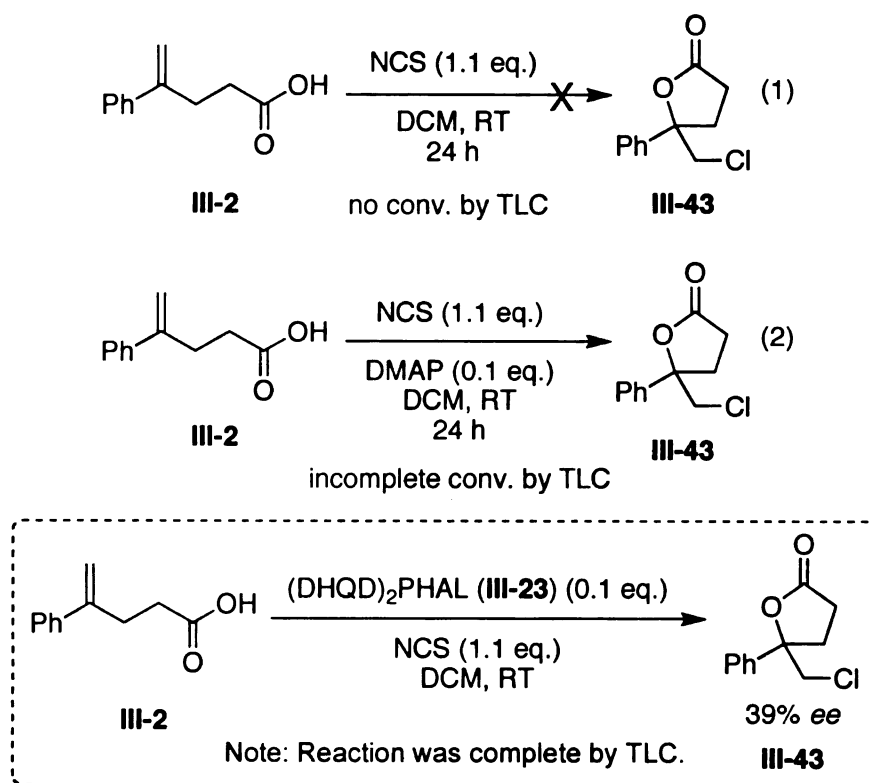
3.2.3: Optimization of the (DHQD)$_2$PHAL/NCS Chlorolactonization Protocol

On roughly doubling the selectivity of the (DHQD)$_2$PHAL mediated halolactonization by employing NCS in lieu of NBS, a number of experiments were undertaken aiming to further increase the selectivity of the transformation. First, we investigated the equivalency of NCS as well as a few other chlorine sources (Table III-6). Specifically, the selectivity of the reaction was evaluated when 3, 5 and 10 equivalents of NCS were employed. Additionally, the

stoichiometric variant of the reaction was evaluated with 1.1 equivalents of both

NCS and (DHQD)$_2$PHAL. Finally, the chlorolactonization of **III-2** was performed

with chloramine-T **(III-45)**, chloroamine-B **(III-46)** and

hexachlorocyclohexadienone **III-47**.

Table III-6. Screen of NCS equivalents and other chlorine sources.

Entry	Eq. (III-23)	Eq. (Cl⁺)	Cl⁺ source	% ee (III-3)
1	0.1	3	**III-44**	44
2	0.1	5	**III-44**	43
3	0.1	10	**III-44**	45
4	1.1	1.1	**III-44**	39
5	0.1	1.1	**III-45**	0
6	0.1	1.1	**III-46**	4
7	0.1	1.1	**III-47**	8
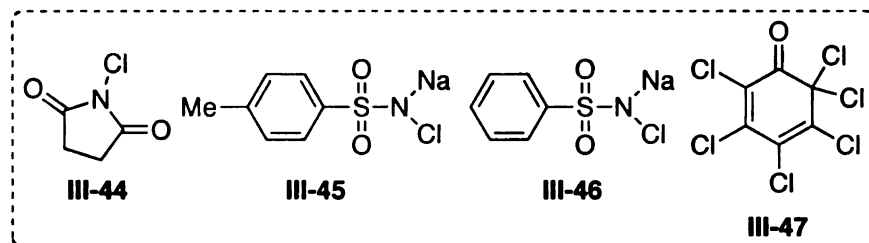
Note: All reactions were complete by TLC.

The enantioselectivity of the reaction increased (*cf.* Scheme III-3) as the

loading of NCS was increased (entries 1-3). Compared to the 39% *ee* realized

when 1.1 equivalents of NCS were used, increasing the loading to 3, 5 and 10

equivalents returned **III-43** in 44, 43, and 45% *ee*, respectively. Although this

trend was interesting, the gain in selectivity was deemed insufficient to warrant such an excessive loading of NCS. Additionally, these results serve to further highlight the insignificant contribution made by the uncatalyzed background reaction. Entry 4 describes the stoichiometric variant of the reaction, indicating that employing 1.1 equivalents of (DHQD)$_2$PHAL does not improve upon the selectivity of the catalytic reaction, although the reaction is not less selective as was the case for the analogous bromolactonization (*vide supra*, Table III-2, entry 6). Finally, neither the chloramines **III-45** and **III-46**, nor **III-47** allowed for a more selective chlorolactonization (entries 5-7).

Next, a comprehensive solvent screen was undertaken in an attempt to drive the enantioselectivity of the reaction higher. Eighteen different solvents were screened in the test reaction (**III-2** to **III-43**) in microscale. In the event, 0.05 mmol of **III-2** was cyclized in 1 mL of the appropriate solvent (0.05 M in substrate). A range of solvents were screened including protic, aprotic, non-polar and polar examples (Table III-7). DMSO (entry 1) and DMF (entry 2) returned lactone **III-43** in 3 and 10% *ee*, respectively. The poor results with DMSO and DMF was not entirely unexpected, as sulfoxides[36,37] and amides[1,38] are known to react with electrophilic halogen sources. Interestingly, nitromethane returned chlorolactone in -22 % *ee*, a net change of 61 percentage points! The reason for this dramatic reversal in selectivity due to solvent is not clear, but is nonetheless not without precendent.[39] Alcoholic solvents proved to be less selective than DCM (entry 7), returning products with 21% *ee* in methanol (entry 4), 29% *ee* in ethanol (entry 5), and 30% *ee* in *iso*-propyl alcohol (entry 6).

Table III-7: Solvent screen with **III-23**/NCS catalyst system.
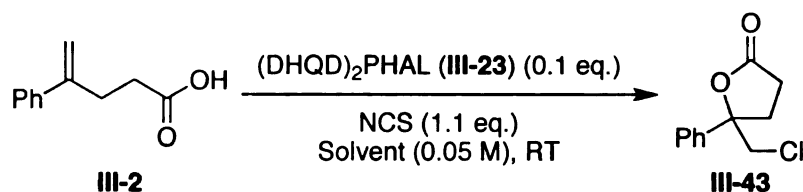
Entry	Solvent	% ee (III-43)	Entry	Solvent	% ee (III-43)
1	DMSO	3	12	ethyl acetate	28
2	DMF	10	13	acetone	-
3	nitromethane	-22	14	acetonitrile	4
4	methanol	21	15	diethyl ether	40
5	ethanol	29	16	1,4-dioxane	29
6	IPA	30	17	THF	4
7	DCM	39	18	benzene	40
8	chloroform	65	19	toluene	22
9	1,2-dichloroethane	43	20	hexane	34
10	1,1,1-trichloroethane	42	21	cyclohexane	34
11	o-dichlorobenzene	39	22	pentane	34

Note: All reactions were complete by TLC after 18 h, except entries 13 and 18-22.

Other highly polar solvents, including ethyl acetate (28% *ee,* entry 12), acetone (no conversion to **III-43**, entry 13), and acetonitrile (4% *ee,* entry 14) were also inferior solvents. Regarding ethereal solvents, diethyl ether returned the desired lactone in 40% *ee,* however the reaction was exceedingly slow owing to poor substrate and catalyst solubility. Other ethers, included 1,4-dioxane (29% *ee,* entry 16) and THF (4% *ee,* entry 17). Nonpolar solvents including benzene (40% *ee,* entry 18), toluene (22% *ee,* entry 19), hexane (34% *ee,* entry 20), cyclohexane (34% *ee,* entry 21), and pentane (34% *ee,* entry 22) were all

found to be slightly less selective than DCM, but in all cases suffered from poor conversion due to unacceptable solubility.

Substantial gains in selectivity were realized, however, on investigating other chlorinated solvents. As compared to DCM (39% *ee*, entry 7), 1,2-dichloroethane, 1,1,1-trichloroethane, and *o*-dichlorobenzene were equally as selective (entries 9-11). Nonetheless, the reaction in chloroform (entry 8) proceeded to completion by TLC and importantly returned lactone **III-43** in a substantially improved 65% *ee*. We subsequently found that the selectivity could be further enhanced to 70% *ee* when the NCS was purified by recrystallization from chloroform prior to use (Scheme III-4). Interestingly, employing chloroform also increases the selectivity of the NBS reaction, increasing the selectivity from 20% *ee* (*vide supra*, Table III-1, entry 9) to 35% *ee* for the production of bromolactone **III-3**.

Scheme III-4. A further increase in selectivity using purified NCS.

III-2

(DHQD)₂PHAL (**III-23**) (0.1 eq.)

recrystallized NCS (1.1 eq.)
CHCl₃, RT

Note: Reaction was complete by TLC.

70% *ee*

III-43
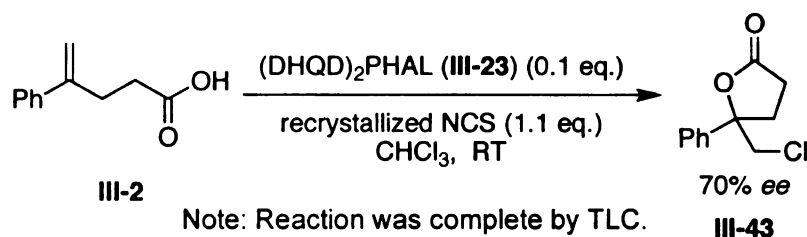
We initially wondered whether the increased selectivity with chloroform relative to DCM was due to the decreased polarity, or due to trace amounts of ethanol in the unpurified chloroform. This latter explanation seemed suspect given the poor selectivity of the reaction in alcoholic solvents (Table III-7, entries 4-6). Nonetheless, we undertook two studies aimed at discerning the effect of

136

added ethanol and water to the newly discovered reaction conditions (*i.e.*

recrystallized NCS in chloroform). The results of these studies are presented in

Table III-8.

Table III-8. Ethanol and water study with **III-23**/NCS system in chloroform.
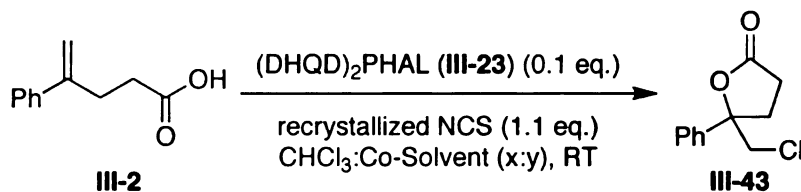
Entry	CHCl$_3$:EtOH	% ee (III-43)		Entry	CHCl$_3$:H$_2$O	% ee (III-43)
1	95:5	57		12	95:5	65
2	90:10	56		13	90:10	63
3	80:20	50		14	80:20	64
4	70:30	42		15	70:30	63
5	60:40	38		16	60:40	62
6	50:50	32		17	50:50	62
7	40:60	32		18	40:60	66
8	30:70	39		19	30:70	63
9	20:80	26		20	20:80	60
10	10:90	43		21	10:90	61
11	5:95	39		22	5:95	61

Note: All reactions were complete by TLC.

Regarding the addition of ethanol, although the data is somewhat variable,

an overall trend of decreased selectivity with a larger percentage of ethanol is

evident (entries 1-11). These data are in agreement with the relatively poor

selectivity of the reaction in ethanol alone (*vide supra*). A similar, but less

pronounced trend is evident on the addition of larger volumes of water to the reaction mixture (entries 12-22).

We also suspected that the additional selectivity garnered from running the reaction in chloroform could be due to residual acid (*i.e.* HCl) in the unpurified solvent. We sought to probe this theory by screening a number of acid additives.[40] Included in the screen were ammonium acetate, ammonium chloride, PPTS, camphorsulfonic acid, citric acid, phenol, *p*-nitrophenol, 2,4,6-trichlorophenol, PTSA, sulfuric acid, hydrochloric acid, acetic acid, TFA, silica gel, and acidic alumina. In each case 1.1 equivalent of the acid additive was employed relative to the substrate. Silica gel and acid alumina were added in a 200 mg/mmol loading (roughly 10 mg relative to 0.05 mmol of **III-2**). The results of this study are presented in Table III-9.

Ammonium acetate (entry 1) returned lactone **III-43** in 51% ee, while the addition of 1.1 equivalents of ammonium chloride (entry 2) shut down the reaction completely. PPTS also caused the complete arrest of the reaction (entry 3). The reaction proceeded to complete conversion in the presence of camphorsulfonic acid (entry 3, 1% *ee*) and citric acid (50% *ee*, entry 5), however, the transformation was less selective. An equivalent of phenol was well tolerated, returning **III-43** in 70% *ee*, although this additive failed to improve the selectivity of the reaction (entry 5). Nonetheless, more acidic phenols such as *p*-nitrophenol (33% *ee*, entry 6) and 2,4,6-trichlorophenol (7% *ee*, entry 8) were much less selective. Stronger acids including PTSA (8% *ee*, entry 9), sulfuric acid (14% *ee*, entry 10), and hydrochloric acid (5% *ee*, entry 11) were also

detrimental to the enantioselectivity of the transformation. An equivalent of acetic

acid additive returned lactone **III-43** in a slightly lower 65% *ee* (entry 12).

Conversely, the addition of TFA was poorly tolerated (20% *ee*, entry 13). Finally

Table III-9. Acid additive study with **III-23**/NCS system.
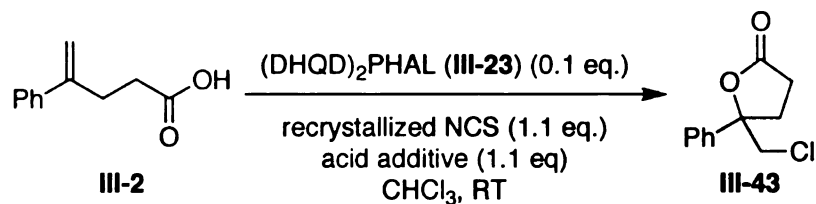
Entry	acid additive	% *ee* (III-43)
1	NH$_4$OAc	51
2	NH$_4$Cl	-
3	PPTS	-
4	(+/-)-CSA	1
5	citric acid	50
6	phenol	70
7	*p*-nitrophenol	33
8	2,4,6-trichlorophenol	7
9	PTSA	8
10	sulfuric acid	14
11	hydrochloric acid	5
12	acetic acid	65
13	trifluoroacetic acid	20
14	silica gel	51
15	acidic alumina	56

Note: All reactions were complete by TLC after 18 h, except entries 2 and 3.

the addition of heterogeneous acid sources like silica gel and acidic alumina did not improve upon the selectivity of the reaction, returning **III-43** in 51 and 56% *ee*, respectively (entries 14 and 15).

Lastly, a final variable was evaluated in attempts to improve upon the selectivity of the (DHQD)$_2$PHAL/NCS catalyst combination. Namely, we surmised that lowering the reaction temperature might enhance the selectivity of the transformation. Given the relatively high melting temperature of chloroform (mp = -63 °C), the course of the reaction was probed when the temperature was maintained at -40 °C with the aid of an immersion cooler. Disappointingly, at this temperature the reaction was exceedingly slow, indicating the presence of no products by TLC after 24 hours (Scheme III-5). On concentration and injection of the reaction mixture into the HPLC, trace amounts of the desired lactone **III-43** were detected, albeit with a reduced enantiopurity of just 43% *ee*. This result was potentially devastating with respect to further optimization experiments and seemed to suggest the need for a more reactive halogen source relative to NCS that might allow for the reaction to be conducted at cooler temperatures. In fact, the ideal halogen source evidently needed to be couched some where in between NCS and NBS in reactivity.

Scheme III-5. Poor conversion and selectivity of the **III-23**/NCS system at lower temperatures.

III-2

(DHQD)$_2$PHAL (**III-23**) (0.1 eq.)

recrystallized NCS (1.1 eq.)
CHCl$_3$, -40 °C

No conversion by TLC

trace by HPLC
43% *ee*

III-43
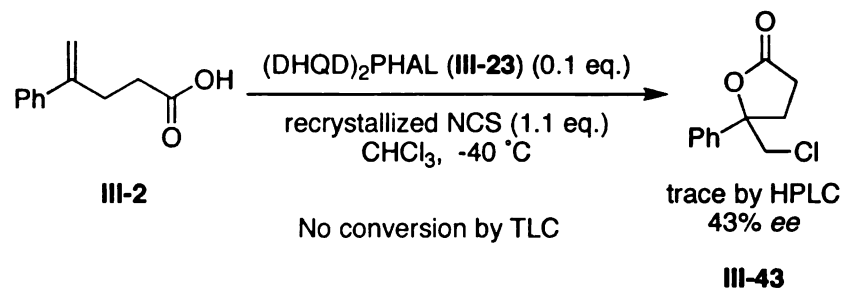
This significant limitation of NCS as the terminal halogen source in the transformation represented the first major impasse that was encountered after the deviation from our first generation peptide-based approach (see Chapter 2). The solution for this crippling result was ultimately discovered after a literature scan that revealed a new chlorenium source, 1,3-dichloro-5,5-dimethylhydantoin (III-48, DCDMH), possessing an exquisitely tuned reactivity profile for our purposes. What follows below is a detailed account of the application and optimization of this variant of the chlorolactonization reaction.

3.2.4: Optimization of the (DHQD)₂PHAL/Chlorohydantoin System

A literature scan revealed a commercially available chlorenium source that we had not evaluated for our purposes. Namely, 1,3-dichloro-5,5-dimethylhydantoin (DCDMH, III-48) has found use in number of organic chlorination and oxidation reactions.[41] A brief review of various organic transformations mediated by DCDMH can be found in Chapter 4. As an initial foray into its use in the transformation at hand, DCDMH was screened as the terminal chlorenium source in the chlorolactonization of III-2 at various temperatures in a few chlorinated solvents and solvent combinations (Table III-10).

Table III-10. Screen of **III-23/III-48** catalyst system.
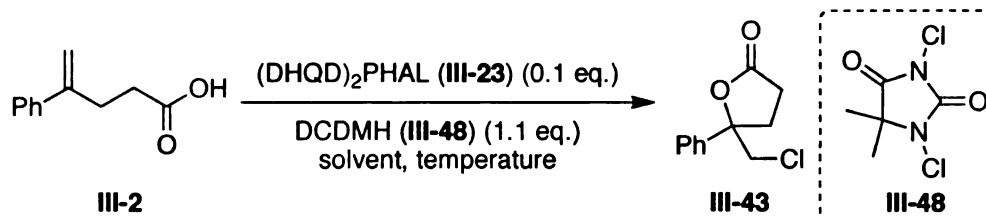
Entry	Solvent	Temp. ($^\circ$C)	% ee (III-43)
1	CHCl$_3$	RT	71
2	CCl$_4$	RT	71
3	CHCl$_3$	4	72
4	CHCl$_3$	-30	82
5	CHCl$_3$	-40	83
6	CHCl$_3$	-50	81
7	DCM	-40	49
8	CHCl$_3$/DCM (9:1)	-40	76
9	CHCl$_3$/DCM (8:2)	-40	76
10	CHCl$_3$/DCM (7:3)	-40	72
11	CHCl$_3$/DCM (6:4)	-40	64
12	CHCl$_3$/DCM (9:1)	-78	48
13	CHCl$_3$/DCM (8:2)	-78	64
14	CHCl$_3$/DCM (1:1)	-78	55
15	DCM	-78	43

Note: All reactions were complete by TLC.

Initial experiments at room temperature in chloroform and carbon tetrachloride revealed DCDMH to be marginally more selective than NCS in the chlorolactonization of **III-2**, returning **III-43** in 71% *ee* in both cases (entry 1 and

142

2). Unlike NCS, however, the reaction proceeded to completion at lower

temperatures.   At 4 °C in chloroform, **III-43** was produced in 72% *ee* (entry 3).

On lowering the temperature further, however, the selectivity of the reaction was

substantially increased, returning the desired lactone in 82% *ee* at -30 °C (entry

4). Lowering the temperature further to -40 and -50 °C returned **III-43** in 83 and

81% ee, respectively (entries 5 and 6). Indeed, the 83% *ee* in chloroform at -40

°C represents an initial ceiling selectivity realized on changing from NCS to

DCDMH. It is also noteworthy that, similar to the NCS system, chloroform is

required to maintain a high selectivity, evidenced by the fact that conducting the

reaction in DCM at -40 °C results in a cholorolactonization in 49% *ee*. Given the

relatively high melting point of chloroform (mp = -63 °C), we elected to conduct

the reaction in several mixtures of chloroform and dichloromethane aiming to

investigate solvent mixtures that were amenable to lower temperatures. Initially,

mixtures ranging from 90% to 60% $CHCl_3$ in DCM were evaluated at -40 °C to

assess the amount of DCM that was tolerated without significantly eroding the

selectivity of the transformation (entries 9-11). Mixtures comprised of 90% and

80% chloroform were less selective than chloroform alone (76% *ee*, entries 8 and

9) but significantly more selective than DCM. Increased amounts of DCM,

however, resulted in a less selective reaction (entries 10 and 11). On lowering

the temperature to -78 °C in both 90% and 80% chloroform, the reaction was in

fact less selective than the corresponding reactions conducted at -40 °C.

Specifically, a 9:1 mixture of chloroform and DCM returned **III-43** in 48% *ee*

(entry 12) while an 8:2 mixture produced the lactone in 64% *ee* (entry 13).

Additionally, conducting the reaction in either a 1:1 mixture of CHCl$_3$/DCM (entry 14) or in DCM alone (entry 15) at -78 °C were also less selective (55 and 43% *ee*, respectively).

After generating lactone **III-43** in 83% ee with the (DHQD)$_2$PHAL/DCDMH reagent combination at -40 °C in chloroform, we returned briefly to the other *Cinchona* alkaloid derivatives described in Figure III-2 along with their natural cousins quinine (**III-49**), quinidine (**III-50**), and cinchonidine (**III-51**) (Figure III-3). These catalysts were screened in order to investigate their influence on the stereochemical course of the transformation employing the optimized halogen source (**III-48**) and solvent.

Figure III-3. Additional *Cinchona* alkaloid catalysts.

| quinine | quinidine | cinchonidine |
| **III-49** | **III-50** | **III-51** |
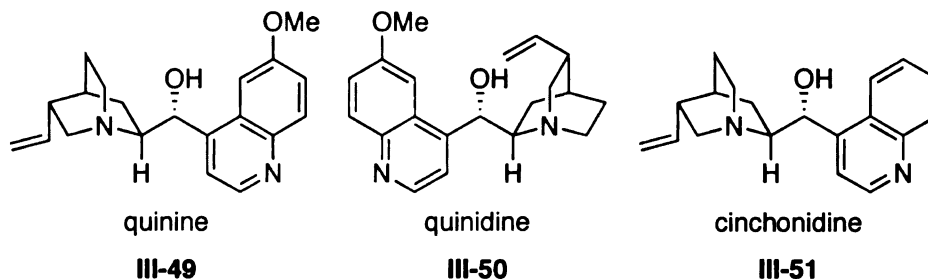
In the event, when the other *Cinchona* alkaloids depicted in Schemes III-2 and III-3 were applied in the presence of DCDMH (**III-48**) at -40 °C in chloroform, they all proved to be less selective than (DHQD)$_2$PHAL (Table III-11). Although less selective overall, the results with these alternative *Cinchona* alkaloid catalysts are interesting nevertheless. In the presence of DHQD (**III-37**, entry 1), the lactone **III-43** was produced in -14% *ee* (*i.e.* favoring the second enantiomer to elute from the HPLC). The ester and ether analogues of DHQD all favored the production of the opposite enantiomer, returning **III-43** with 17% (catalyst **III-38**,

entry 2), 13% (catalyst **III-39**, entry 3), and 3% ee (catalyst **III-40**, entry 4)

respectively. Although the dimeric catalysts **III-41** and **III-42** are

quasienantiomeric, they both returned the desired chlorolactone in -14 and -12%

ee, respectively (entries 5 and 6).

Table III-11. Screen of alternate *Cinchona* alkaloid catalysts with DCDMH.
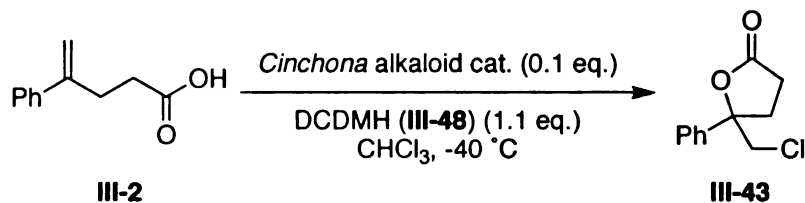
Entry	Catalyst	% *ee* (III-43)
1	III-37	-14
2	III-38	17
3	III-39	13
4	III-40	3
5	III-41	-14
6	III-42	-12
7	III-49	-18
8	III-50	0
9	III-51	22

Note: All reactions were complete by TLC.

On screening the natural product congeners of the catalysts depicted in

Figure III-2 (see Figure III-3), seemingly small structural changes produced

relatively drastic changes in enantioselectivity. Quinine (**III-49**) returned the

lactone in -18% *ee* (entry 7). Conversely, cinchonidine (**III-51**) which differs from

quinine only by the absence of the 6-methoxy group on the quinoline moiety,

returned **III-43** in 22% *ee*, in spite of the fact that **III-49** and **III-51** share the same stereochemical relationship (entry 9). Such a complete reversal of selectivity on changing from quinine to cinchonidine is rare in organocatalysis, although the phenomenon has been documented previously in unrelated transformations.[39,42,43] Quinidine (**III-50**, entry 8) returned racemic lactone products, notably less selective than its saturated analogue **III-37** (entry 1).

After reaffirming (DHQD)$_2$PHAL (**III-23**) to be uniquely selective in the chlorolactonization of **III-2**, we next turned to a more in depth investigation into the nature of the chlorohydantoin component. In principle, an equivalent of DCDMH (**III-48**) could donate each of its two chlorine atoms during the course of the reaction. In that vein, the influence of lowered loadings of **III-48** was evaluated (Table III-12).

Table III-12. DCDMH (**III-48**) equivalency study.

Entry	Eq. (III-48)	% *ee* (III-43)
1	1	83
2	0.75	83
3	0.5	84

Note: All reactions were complete by TLC after 24 h except entry 3.

As indicated above in Table III-12, decreasing the loading of DCDMH does not substantially influence the stereochemical course of the reaction. As compared to the initially employed 1 equivalents of **III-48** (83% *ee*, entry 1),

reducing the loading to 0.75 or 0.5 equivalents returned lactone **III-43** with effectively the same degree of stereoinduction (83 and 84% *ee*, respectively). It is noteworthy, however, that the reaction is substantially slower when 0.5 equivalents of **III-48** is used (*i.e.* incomplete reaction after 24 h).

In addition to evaluating the loading of the terminal chlorine source, it was also interesting to investigate the enantioselectivity of the chlorolactonization reaction when the gross structure of the chlorohydantoin reagent was modified. Efforts in this regard ultimately culminated in the development of an efficient methodology for the preparation of N-chlorinated hydantoins (see Chapter 4).[41] In the task at hand, we investigated four new chlorohydantoins in the conversion of **III-2** to **III-43** (Table III-13). Namely, we investigated 1,3-dichloro-5,5-diphenylhydantoin (**III-52**, DCDPH), 1,3-dichloro-5-methyl-5-phenylhydantoin (**III-53**, DCMPH), 3-chloro-1,5,5-trimethylhydantoin (**III-54**, CTMH), and 1,3-dichlorohydantoin (**III-55**, DCH). Chlorohydantoins **III-52**, **III-53**, and **III-55**, were meant to probe the effects of varying the substitution at the hydantoin 5 position, while **III-54** sought to evaluate the influence of the N-1 chlorine.

Interestingly, the structural features of the terminal chlorine source seemed to have a profound effect on the selectivity of the reaction in some cases. While a high degree of selectivity was maintained in the lactonization of **III-2** with **III-52** (81% *ee*, entry 1) and **III-53** (81% *ee*, entry 2), the removal of the C-5 substitution on the chlorohydantoin returned **III-43** in a substantially lowered 65% *ee* (entry 4). Similarly, on replacing the N-1 chlorine in DCDMH with a methyl group (**III-54**) produced an inferior result (61% *ee*, entry 3). It is also

noteworthy that the transformation in the presence of CTMH **III-54** did not

proceed to completion after 24 hours.

Table III-13. Screen of other N-chlorohydantoins with catalyst **III-23**.
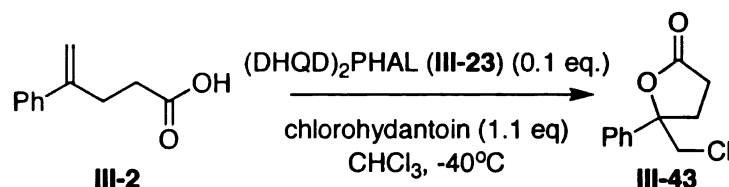
Entry	Cl⁺ Source	% ee (III-43)
1	III-52	81
2	III-53	81
3	III-54	61
4	III-55	65
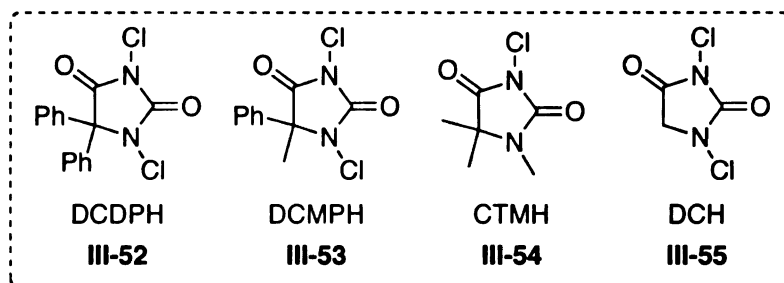
Note: All reactions were complete by TLC, except entry 3.

The dramatic changes in enantioselectivity in some cases, on employing

different N-chlorohydantoins is interesting, and seems to indicate a more intimate

interaction between the terminal chlorine source and the catalyst. A cursory

mechanistic suggestion for the course of the reaction might include simply the

transfer of a chlorenium equivalent from the chlorohydantoin onto the

quinuclidine nitrogen of the organocatalyst, thus generating a fully dissociated

amino-chlorenium species like **III-56** (Figure III-4). If **III-56** were operative, one

would expect that the selectivity of the reaction would not depend appreciably

upon the gross structure of the chlorohydantoin. That the selectivity drops in some instances might, however suggest the prevalence of a more tightly associated complex between the organocatalyst and the terminal chlorine source. Three possible complexes that invoke such a situation are also depicted in Figure III-4. Complex **III-57** invokes a hydrogen bond-mediated association between the organocatalyst and the chlorohydantoin. On the other hand, complex **III-58** is similar in nature to **III-56**, except that it invokes a tight ion pair between the amino chlorenium catalyst and the hydantoin counteranion. Finally, **III-59** suggests the formation of a dimeric chloronium species, generated on coordination of the quinuclidine of the organocatalyst with the N-3 chlorine atom of the chlorohydantoin. At this point it is unclear which, if any, of the proposed active catalysts depicted in Figure III-4 is operative. What seems clear is that the catalyst system is most likely not proceeding via the simplified model **III-56**. We will return to a discussion of these structures proposed in Figure III-4 shortly.

Figure III-4. Potential active catalyst species.

| III-57 | III-58 | III-59 |
| hydrogen bonded framework | tight ion pair framework | chloronium dimer framework |
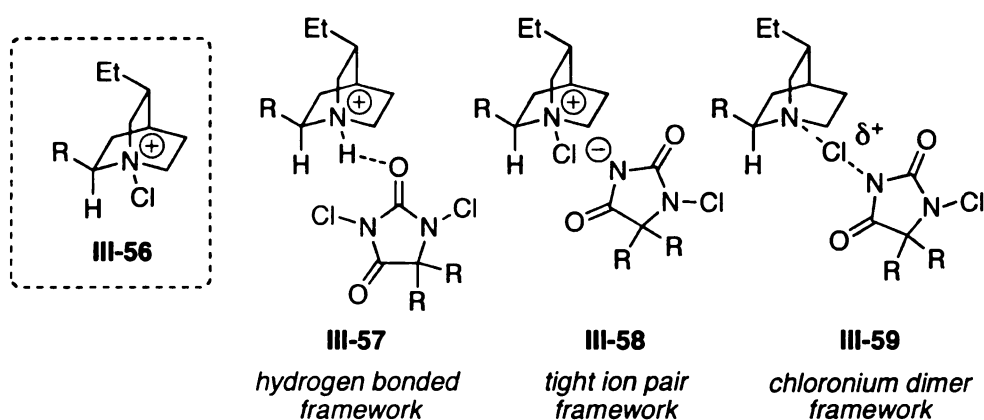
Although the investigation of alternative chlorohydantoin terminal chlorine sources raised a few interesting questions about the reaction mechanism, it

149

failed to provide a more selective transformation than the initially optimized (DHQD)$_2$PHAL/DCDMH (**III-23/III-48**) catalyst system in chloroform at -40 °C (*vide supra*, Table III-10, entry 5). With this in mind, an extensive screen of various co-solvents was undertaken aiming to further enhance the selectivity of the transformation. Sixteen different co-solvents of varying polarity were evaluated ranging from 5, 10, 20, 30, 40 and 50% v/v in chloroform. It was surmised that on increasing the percentage of co-solvent a trend in the enantioselectivity of the transformation would emerge. Those co-solvents returning positive gains in selectivity were screened in further combinations ranging from 60 to 100% v/v. The co-solvents evaluated in this study include: methanol, ethanol, dichloromethane, 1,2-dichloroethane, ethyl acetate, acetone, acetonitrile, nitromethane, tetrahydrofuran, 1,4-dioxane, diethyl ether, pentane, cyclohexane, benzene, toluene, and *n*-hexanes. In the case of DCM, toluene, THF, and acetonitrile, the solvents were freshly distilled prior to use. Similarly, 1,4-dioxane was collected from a dry still prior to use. When available, HPLC or reagent grade solvents were used in all other cases. The data for the co-solvent screen described above is presented in Table III-14.

Table III-14. Co-solvent study with **III-23/III-48** catalyst system.
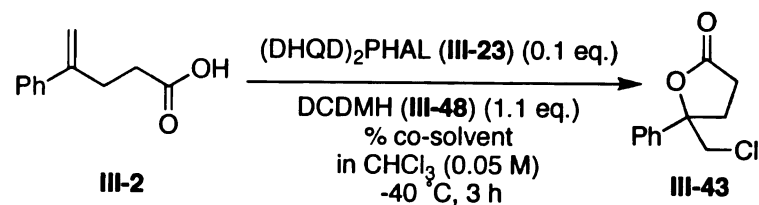
Entry	Co-Solvent	% Co-Solvent	% ee (III-43)
1	methanol	5	56
2	methanol	10	50
3	methanol	20	43
4	methanol	30	42
5	methanol	40	40
6	methanol	50	38
7	ethanol	5	73
8	ethanol	10	72
9	ethanol	20	62
10	ethanol	30	55
11	ethanol	40	49
12	ethanol	50	48
13	DCM	5	82
14	DCM	10	80
15	DCM	20	78
16	DCM	30	75
17	DCM	40	72
18	DCM	50	69

Note: All reactions were complete by TLC.

Table III-14. (Cont'd)
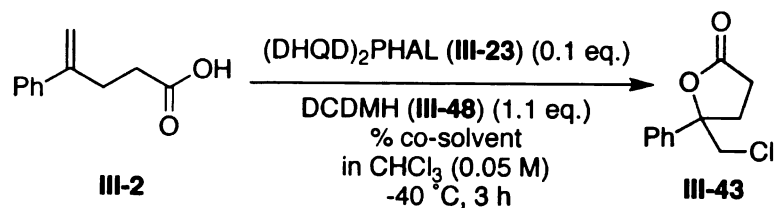
Entry	Co-Solvent	% Co-Solvent	% ee (III-43)
19	1,2-dichloroethane	5	81
20	1,2-dichloroethane	10	82
21	1,2-dichloroethane	20	79
22	1,2-dichloroethane	30	77
23	1,2-dichloroethane	40	73
24	1,2-dichloroethane	50	69
25	ethyl acetate	5	82
26	ethyl acetate	10	82
27	ethyl acetate	20	81
28	ethyl acetate	30	80
29	ethyl acetate	40	79
30	ethyl acetate	50	77
31	acetone	5	79
32	acetone	10	73
33	acetone	20	55
34	acetone	30	47
35	acetone	40	35
36	acetone	50	28

Note: All reactions were complete by TLC.

152

Table III-14. (Cont'd)
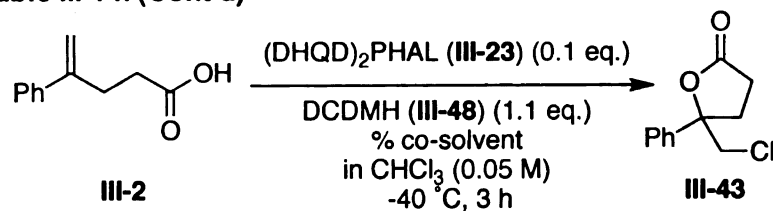
Entry	Co-Solvent	% Co-Solvent	% ee (III-43)
37	acetonitrile	5	74
38	acetonitrile	10	63
39	acetonitrile	20	54
40	acetonitrile	30	28
41	acetonitrile	40	17
42	acetonitrile	50	12
43	nitromethane	5	73
44	nitromethane	10	60
45	nitromethane	20	40
46	nitromethane	30	27
47	nitromethane	40	18
48	nitromethane	50	11
49	THF	5	81
50	THF	10	78
51	THF	20	50
52	THF	30	14
53	THF	40	0
54	THF	50	0

Note: All reactions were complete by TLC.

153

Table III-14. (Cont'd)
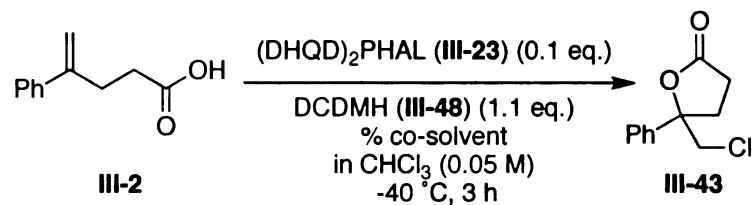
Entry	Co-Solvent	% Co-Solvent	% ee (III-43)
55	1,4-dioxane	5	82
56	1,4-dioxane	10	84
57	1,4-dioxane	20	84
58	1,4-dioxane	30	85
59	1,4-dioxane	40	85
60	1,4-dioxane	50	81
61	diethyl ether	5	83
62	diethyl ether	10	84
63	diethyl ether	20	83
64	diethyl ether	30	84
65	diethyl ether	40	84
66	diethyl ether	50	83
67	diethyl ether	60	83
68	diethyl ether	70	83
69	diethyl ether	80	81
70	diethyl ether	90	82
71	diethyl ether	100	78

Note: All reactions were complete by TLC.

Table III-14. (Cont'd)
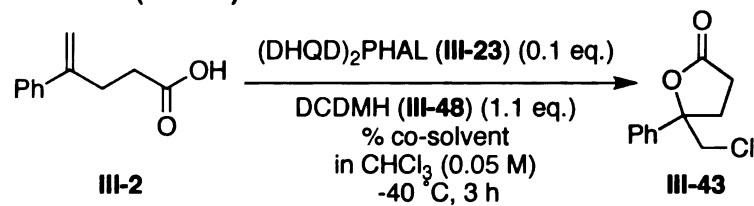
Entry	Co-Solvent	% Co-Solvent	% ee (III-43)
72	pentane	5	84
73	pentane	10	85
74	pentane	20	85
75	pentane	30	86
76	pentane	40	86
77	pentane	50	86
78	cyclohexane	5	83
79	cyclohexane	10	84
80	cyclohexane	20	85
81	cyclohexane	30	85
82	cyclohexane	40	86
83	cyclohexane	50	87
84	benzene	5	82
85	benzene	10	82
86	benzene	20	84
87	benzene	30	84
88	benzene	40	85
89	benzene	50	85

Note: All reactions were complete by TLC.

155

Table III-14. (Cont'd)
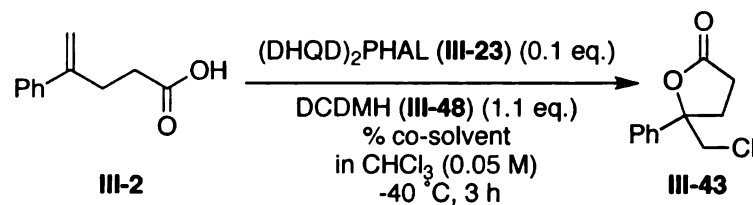
Entry	Co-Solvent	% Co-Solvent	% *ee* (III-43)
90	toluene	5	83
91	toluene	10	83
92	toluene	20	84
93	toluene	30	86
94	toluene	40	86
95	toluene	50	86
96	toluene	60	87
97	toluene	70	87
98	toluene	80	86
99	toluene	90	82
100	toluene	95	79
101	toluene	100	78
102	*n*-hexanes	5	83
103	*n*-hexanes	10	84
104	*n*-hexanes	20	85
105	*n*-hexanes	30	86
106	*n*-hexanes	40	86
107	*n*-hexanes	50	86

Note: All reactions were complete by TLC.

Table III-14. (Cont'd)
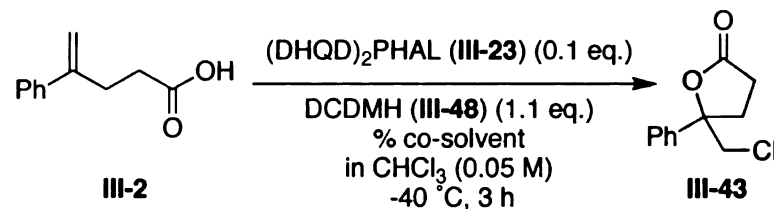
Entry	Co-Solvent	% Co-Solvent	% ee (III-43)
108	*n*-hexanes	60	82
109	*n*-hexanes	70	82
110	*n*-hexanes	80	76
111	*n*-hexanes	90	40
112	*n*-hexanes	95	29

Note: All reactions were complete by TLC.

On increasing the amount alcoholic co-solvent, the selectivity of the reaction steadily declined when both methanol and ethanol were utilized. Chlorolactone **III-43** was returned in selectivities ranging from 56% to 38% *ee* for methanol and 73% to 48% *ee* for ethanol (entries 1-12). Although the data for dichloromethane is not in total agreement with that collected earlier (*vide supra*, Table III-10, entries 8-11), the same overall trend is evident, indicating that increasing percentages of DCM relative to chloroform has a deleterious effect on the selectivity of the transformation (entries 13-18). A similar slight downward trend in selectivities were realized with both 1,2-dichloroethane (81- 69% *ee*, entries 19-24) and ethyl acetate (82-77% ee, entries 24-30). The enantioselectivity of the reaction decreased dramatically on increasing

percentages of acetone (entries 31-36), acetonitrile (entries 37-42), and nitromethane (entries 43-48).

Ethereal solvents produced mixed results. On increasing percentages of THF, the enantioselectivity of the reaction dropped precipitously, returning the racemate at 40 and 50% mixtures of THF in chloroform (entries 49-54). Alternatively, 1,4-dioxane (entries 55-60) produced a slight up-swing in enantiomeric excess, producing **III-43** in 85% *ee* when applied as 30 and 40% mixtures in chloroform. Interestingly, diethyl ether (entries 61-71) appears to be an "*ee*-neutral" solvent across a number of percentages, ranging from 5 to 90%. In all cases, the chlorolactone was produced with selectivities ranging from 81 to 83% *ee*. When the reaction was conducted in pure ether (entry 71) the selectivity dropped to 78% *ee*, partially owing to poor solubility. The neutrality of ether with respect to enantioselectivities should allow for low temperature studies to be conducted in the future below the melting point of chloroform, by employing mixtures of ether and chloroform.

The enantioselectivity was reproducibly increased by three or four percentage points when increasing percentages of pentane (entries 72-77) and cyclohexane (entries 78-83) were applied. A maximum of 86% *ee* was realized in 30, 40, and 50% mixtures of pentane and chloroform. Similarly, a 50% solution of cyclohexane in chloroform returned **III-43** in 87% *ee*.

While benzene/chloroform mixtures (entries 84-89) produced **III-43** with selectivities ranging from 82% (5% benzene) to 85% *ee* (50% benzene), the increases realized for toluene mixtures (entries 90-101) were slightly more

pronounced. Namely, **III-43** was produced in increasing *ee*, reaching a ceiling of

87% *ee* in 60 and 70% mixtures of toluene in chloroform. Increasing the

percentage of toluene past 70% produced the chlorolactone in reduced

selectivity, presumably due to poor solubility of the reaction components.

Similarly, increasing percentages of *n*-hexanes (entries 102-112) produced a

ceiling selectivity of 86% *ee* at 30, 40, and 50% *n*-hexane in chloroform.

Mixtures comprised of a majority of *n*-hexanes in chloroform, however, proved to

be less selective.

To summarize the co-solvent screen, certain mixtures of pentane (entries

75-77), cyclohexane (entries 82 and 83), toluene (entries 93-98), and *n*-hexane

(entries 105-107) all returned lactone **III-43** with 86 or 87% *ee*. We will return to

these conditions later.

Subsequent to the co-solvent screen, several additives were also

screened for their influence on the selectivity of the reaction. The beneficial

effects of achiral additives on the stereochemical course of a catalytic

asymmetric transformation have been well documented.[40] The possible mode of

action of achiral additives has been suggested to include: the deoligomerization

of non or less selective catalyst conglomerates, the promotion of the dissociation

of deleterious product-catalyst complexes, and the favorable modification of the

catalyst's geometry. Often the underlying reasons for a particular additive's

beneficial effects on the enantioselectivity of a transformation are poorly

understood. Concerning the problem at hand, we elected to screen several

additives including five amine bases, four organic acids, and select drying

agents. Loadings ranging from 0.01 equivalents to 1 equivalent were investigated for the bases and acids, while the drying agents were employed in 20% wt/wt loading relative to the substrate. The additive screen was conducted in chloroform, ignoring the results from the co-solvent study, in the hope that the additive and co-solvent effects would work in concert when combined subsequently. The five bases that were screened included triethylamine, Hünig's base, imidazole, pyridine, and di-*tert*-butyl-methylpyridine (DTMP). Acetic acid, citric acid, *p*-toluenesulfonic acid (PTSA), and benzoic acid were evaluated as acid additives. In addition to these reagents, the reaction was also conducted over 4 Å molecular sieves (20% wt/wt), sodium sulfate (20% wt/wt and 1 equiv.), and magnesium sulfate (20% wt/wt and 1 equiv.). The results of the additive study are assembled in Table III-15.

Table III-15: Additive study with **III-23/III-48** system.
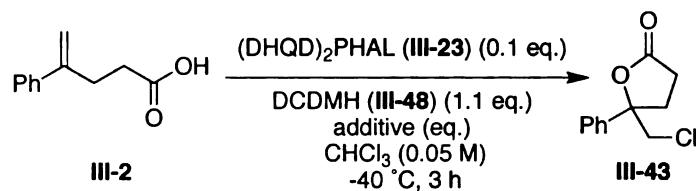
Entry	Additive	Additive (eq.)	% ee (III-43)
1	TEA	0.01	83
2	TEA	0.1	71
3	TEA	0.5	49
4	TEA	1.0	28
5	DIPEA	0.01	80
6	DIPEA	0.1	80
7	DIPEA	0.5	68
8	DIPEA	1.0	53
9	imidazole	0.01	83
10	imidazole	0.1	79
11	imidazole	0.5	3
12	imidazole	1.0	3
13	pyridine	0.01	83
14	pyridine	0.1	83
15	pyridine	0.5	82
16	pyridine	1.0	82

Note: All reactions were complete by TLC.

Table III-15. (Cont'd)
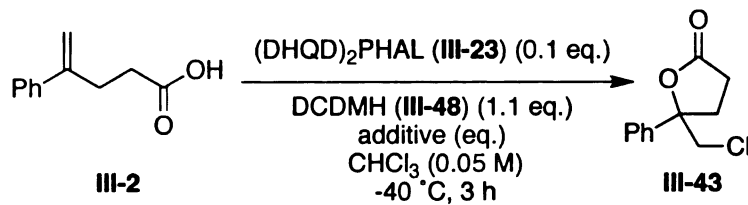
Entry	Additive	Additive (eq.)	% ee (III-43)
17	DTMP	0.01	82
18	DTMP	0.1	82
19	DTMP	0.5	83
20	DTMP	1.0	84
21	AcOH	0.01	82
22	AcOH	0.1	82
23	AcOH	0.5	80
24	AcOH	1.0	79
25	citric acid	0.01	83
26	citric acid	0.1	82
27	citric acid	0.5	81
28	citric acid	1.0	81
29	PTSA	0.01	84
30	PTSA	0.1	80
31	PTSA	0.5	63
32	PTSA	1.0	30

Note: All reactions were complete by TLC.

Table III-15. (Cont'd)
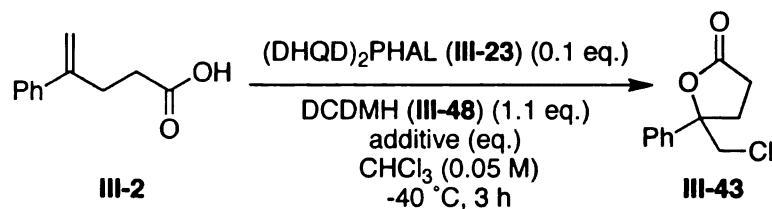
Entry	Additive	Additive (eq.)	% ee (III-43)
33	benzoic acid	0.01	83
34	benzoic acid	0.1	83
35	benzoic acid	0.5	85
36	benzoic acid	1.0	86
37	benzoic acid	2.0	86
38	benzoic acid	5.0	85
39	molecular sieves	20% wt/wt	83
40	sodium sulfate	20% wt/wt	82
41	sodium sulfate	1.0	82
42	magnesium sulfate	20% wt/wt	82
43	magnesium sulfate	1.0	84

Note: All reactions were complete by TLC.

Overall, the amine base additives resulted in decreased selectivities on increased loading. Triethyl amine was tolerated at 0.01 equivalent loading, but a significant drop in selectivity was realized when larger amounts were added (entries 1-4). Hünig's base produced similar, but less pronounced results (entries 5-8). While 0.01 and 0.1 equivalents of imidazole were tolerated relatively well, larger amounts cause a complete loss of selectivity (entries 9-12). Both pyridine (entries 13-16) and DTMP (entries 17-20) were well tolerated,

returning **III-43** with selectivities higher than 82% *ee* regardless of loading. It is curious that the more basic alkyl amines were less tolerated than pyridine additives. This result might indicate that the some degree of catalyst protonation is necessary for a selective transformation.

Regarding the acidic additives, increasing amounts of acetic acid produced a shallow decline from 82% ee with 0.01 equivalents to 79% ee with 1.0 equivalents (entries 21-24). The addition of citric acid had little effect on the selectivity of the transformation, mostly due to the compound's sparing solubility in chloroform at -40 °C (entries 25-28). Increasing amounts of PTSA (*e.g.* 0.5 and 1.0 equivalents) produced a less selective reaction, although smaller loading were tolerated (entries 29-32). Unlike the other acid additives, benzoic acid (entries 33-38) generated a reproducible increase in selectivity from 83% *ee* at 0.01 equivalents that leveled off at 86% *ee* when 1.0 equivalents was applied. Further increasing the loading of benzoic acid to 2.0 and 5.0 equivalents did not offer any additional increases in selectivity.

Drying agents had little effect on the stereochemical course of the reaction. The addition of 20 % wt/wt loading of activated 4 Å molecular sieves returned the chlorolactone in 83% *ee* (entry 39). Similarly, the addition of anhydrous sodium sulfate (entries 41 and 42) or anhydrous magnesium sulfate (entries 42 and 43) led to the production of **III-43** with effectively the same selectivity as the control. These results highlight the relative insensitivity of the protocol to adventitious water.

After demonstrating that various non-polar co-solvents (*vide supra*, Table III-14) as well as an equivalent of benzoic acid could each boost the enantioselectivity in the conversion of **III-2** to **III-43** by a few percentage points, the two conditions were combined, hoping that the effects would be additive. In the event, the chlorolactonization of **III-2** by action of the $(DHQD)_2PHAL/DCDMH$ combination was evaluated in the presence of benzoic acid in toluene/$CHCl_3$ (3:2), hexane/$CHCl_3$ (1:1), and pentane/$CHCl_3$ (1:1) mixtures (Table III-16). In addition, two substituted benzoic acids were screened to test whether or not the benzoic acid additive effect could be increased by modulating the acidity of the benzoic acid derivative.

Table III-16. Combined effect of additive and co-solvents.
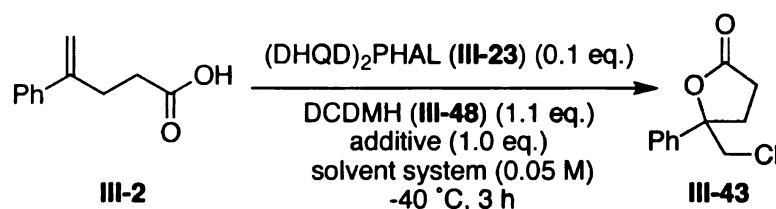
Entry	Additive	Solvent	% ee (III-43)
1	benzoic acid	Tol:CHCl$_3$ (3:2)	89
2	benzoic acid	Hex:CHCl$_3$ (1:1)	88
3	benzoic acid	Pent:CHCl$_3$ (1:1)	87
4	*p*-nitrobenzoic acid	Tol:CHCl$_3$ (3:2)	79
5	*p*-nitrobenzoic acid	Hex:CHCl$_3$ (1:1)	80
6	*p*-methoxybenzoic acid	Tol:CHCl$_3$ (3:2)	87
7	*p*-methoxybenzoic acid	Hex:CHCl$_3$ (1:1)	85

Note: All reactions were complete by TLC.

Happily, combining the best solvent systems with the appropriate additive did, in fact further enhance the selectivity of the transformation. When benzoic acid was employed as an additive in a 3:2 mixture of toluene and chloroform, lactone **III-43** was produced with 89% *ee* (entry 1). Similarly, a 1:1 mixture of *n*-hexanes and chloroform doped with the benzoic acid additive produced chlorolactone with 88% *ee* (entry 2). A 1:1 mixture of pentane and chloroform with benzoic acid returned the products with a slightly lower 87% *ee* (entry 3).

Tuning the acidity of the benzoic acid additive failed to improve upon the selectivity of the transformation. Increasing the acidity (*p*-nitrobenzoic acid) produced **III-43** in 79 and 80% *ee* in the toluene/chloroform and *n*-hexane/chloroform mixtures, respectively (entries 4 and 5). A similar, but less pronounced decrease in selectivity was realized on employing the less acidic *p*-methoxybenzoic acid (entries 6 and 7). This initial screen of the combined effects of the benzoic acid additive and the co-solvent systems indicated that a mixture of either toluene and chloroform (3:2) or *n*-hexanes and chloroform (1:1) were optimal for producing the highest enantioselectivity.

Subsequently we returned to probing the effects of altering the catalyst loading, temperature, and concentration of the reaction employing the newly discovered additive/solvent system combination. Table III-17 indicates the stereochemical outcome of the reaction as the loading of catalyst **III-23** was modulated. Loadings ranging from 0.01 equivalents to 0.30 equivalents were screened.

Table III-17. Catalyst loading study with improved conditions.
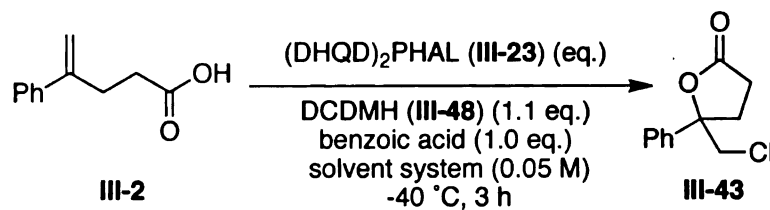
Entry	Eq. (III-23)	Solvent	% ee (III-43)
1	0.30	Tol:CHCl$_3$ (3:2)	87
2	0.20	Tol:CHCl$_3$ (3:2)	88
3	0.10	Tol:CHCl$_3$ (3:2)	89
4	0.05	Tol:CHCl$_3$ (3:2)	87
5	0.01	Tol:CHCl$_3$ (3:2)	80
6	0.30	Hex:CHCl$_3$ (1:1)	86
7	0.20	Hex:CHCl$_3$ (1:1)	87
8	0.10	Hex:CHCl$_3$ (1:1)	88
9	0.05	Hex:CHCl$_3$ (1:1)	87
10	0.01	Hex:CHCl$_3$ (1:1)	83

Note: All reactions were complete by TLC.

In short, the catalyst loading study with the improved reaction conditions confirmed the originally discovered catalyst loading of 0.1 equivalents to be optimal for maintaining enantioselectivity near 90% (entries 3 and 8). Increased catalyst loading to 0.2 and 0.3 equivalents returned **III-43** in slightly lower enantiopurity (entries 1, 2, 6, and 7). Interestingly however, the loading of the

catalyst could be reduced below 0.1 equivalents while still maintaining relatively

high selectivity. A 0.05 equivalent loading of **III-23** returned the chlorolactone in

only a slightly reduced 87% *ee* in both the toluene/chloroform and *n*-

hexane/chloroform solvent systems (entries 4 and 9, respectively). Even more

impressively, selectivities above 80% *ee* could be maintained in both solvent

systems at 0.01 equivalent loading (entries 5 and 10). A control experiment,

employing the (DHQD)$_2$PHAL/DCDMH (**III-23/III-48**) catalyst system (0.01 equiv.

loading) in chloroform alone without any additive returned lactone **III-43** in just

74% *ee* (Scheme III-6). This result serves to further underscore the significant

gains achieved on undertaking the co-solvent and additive screens detailed

above (Table III-14 and Table III-15).

Scheme III-6. Chloroform control at a lower loading of **III-23**.
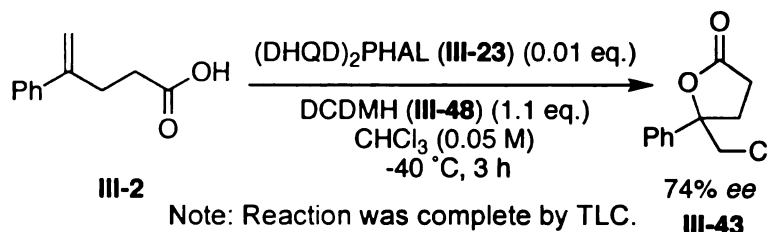
On reaffirming the initially employed 0.1 equivalent catalyst loading to be

optimal, we next turned to a study of the concentration of the reaction relative to

substrate **III-2**. So far, the best results (*vide supra*, Table III-16, entries 1-2) were

obtained at a concentration 0.05 M in substrate. Table III-18 depicts the results

of a screen of several different concentrations in both solvent systems described

earlier.

Table III-18. Concentration screen with optimized conditions.
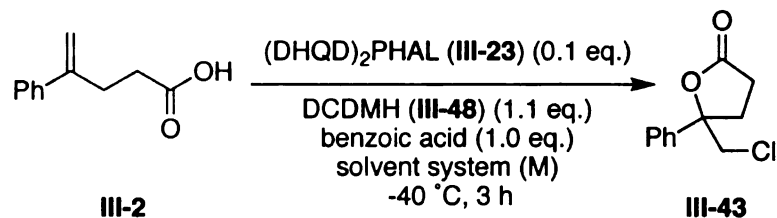
Entry	Conc. (M)	Solvent	% ee (III-43)
1	0.01	Tol:CHCl$_3$ (3:2)	89
2	0.025	Tol:CHCl$_3$ (3:2)	89
3	0.05	Tol:CHCl$_3$ (3:2)	89
4	0.10	Tol:CHCl$_3$ (3:2)	89
5	0.20	Tol:CHCl$_3$ (3:2)	87
6	0.50	Tol:CHCl$_3$ (3:2)	88
7	0.01	Hex:CHCl$_3$ (1:1)	89
8	0.025	Hex:CHCl$_3$ (1:1)	89
9	0.05	Hex:CHCl$_3$ (1:1)	89
10	0.10	Hex:CHCl$_3$ (1:1)	88
11	0.20	Hex:CHCl$_3$ (1:1)	85
12	0.50	Hex:CHCl$_3$ (1:1)	86

Note: All reactions were complete by TLC.

On the whole, the reaction is relatively insensitive to dilution or concentration when conducted in the toluene/chloroform (3:2) mixture (entries 1-6). Conversely, the enantioselectivity of the transformation was stationary on dilution of the *n*-hexane/chloroform solvent system (entries 7-9), but indicated a slight loss in selectivity on concentration of 0.20 and 0.50 M (85-86% *ee*, entries

11 and 12). Given the results described above, we elected to stay with the initially discovered concentration of 0.05 M.

Next, a final temperature study was undertaken to investigate whether the co-solvent/additive modifications would allow for enhanced selectivity at different temperatures. The reaction was conducted at 4, -20, -40, -50, -60, and -78 °C, employing both the toluene/chloroform and n-hexane/chloroform system doped with benzoic acid. The results of this study are assembled in Table III-19.

Although the reaction maintains a respectable selectivity even as warm as 4 °C (79% ee, entries 1 and 7) the enantioselectivity increases steadily until a ceiling is reached between -40 and -50 °C, returning **III-43** in the range of 87-89% ee regardless of solvent system (entries 3, 4, 9, and 10). Cooling to lower temperatures results in a less selective reaction, reaching as low as 67-68% ee at -78 °C (entries 6 and 12). These results ultimately indicate that there is relatively narrow temperature window between -40 and -50 °C that must be maintained for optimal enantioselectivity.

Table III-19. Temperature study with optimal conditions.
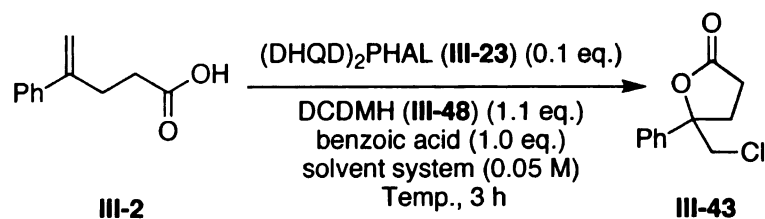
Entry	Temp (°C)	Solvent	% ee (III-43)
1	4	Tol:CHCl$_3$ (3:2)	79
2	-20	Tol:CHCl$_3$ (3:2)	83
3	-40	Tol:CHCl$_3$ (3:2)	89
4	-50	Tol:CHCl$_3$ (3:2)	88
5	-60	Tol:CHCl$_3$ (3:2)	82
6	-78	Tol:CHCl$_3$ (3:2)	68
7	4	Hex:CHCl$_3$ (1:1)	79
8	-20	Hex:CHCl$_3$ (1:1)	83
9	-40	Hex:CHCl$_3$ (1:1)	88
10	-50	Hex:CHCl$_3$ (1:1)	87
11	-60	Hex:CHCl$_3$ (1:1)	83
12	-78	Hex:CHCl$_3$ (1:1)	67

Note: All reactions were complete by TLC.

As a final screen, the reaction was evaluated using an alternative N-chlorohydantoin, 1,3-dichloro-5,5-diphenylhydantoin (DCDPH, **III-52**). Recall that DCDPH was one of only two alternative N-chlorohydantoins that returned lactone **III-43** in greater than 80% *ee* (*vide supra*, Table III-13, entry 1). We elected to screen **III-52** in the hopes that the gains earned on screening co-solvent systems

171

and additives might be further enhanced by a late stage tuning of the terminal

chlorine source. DCDPH was readily prepared in bulk using our recently

disclosed TCCA mediated chlorination protocol, which is the subject of the

following chapter.[41] On screening the optimized reaction conditions while

employing DCDPH (**III-52**), the desired lactone **III-43** was returned in a slightly

elevated 90% *ee* with the toluene/chloroform (3:2) system, and 91% *ee* with the

n-hexanes/chloroform (1:1) system (Table III-20).

Table III-20. Evaluation of **III-52** as the terminal halogen source.
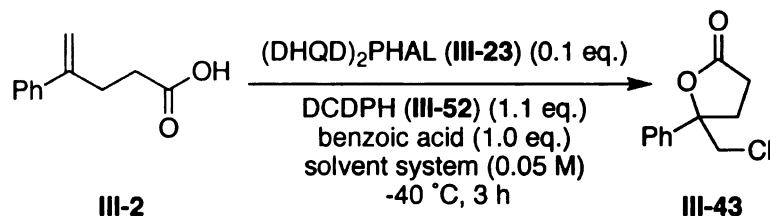
Entry	Cl⁺ Source	Solvent	% *ee* (III-43)
1	**III-52**	Tol:CHCl$_3$ (3:2)	90
2	**III-52**	Hex:CHCl$_3$ (1:1)	91

Note: All reactions were complete by TLC.

To summarize the results catalogued above in Section 3.2.4, with the

discovery that N-chlorohydantoins, particularly DCDMH (**III-48**) was sufficiently

reactive to overcome the limitations encountered with NCS at low temperatures,

a new catalyst combination arose (Table III-10). The (DHQD)$_2$PHAL/DCDMH (**III-23/III-48**) reagent combination was further tuned with respect to enantioselectivity

by evaluating a number of co-solvent combinations. This study revealed that

solvent combinations of either toluene or *n*-hexanes in chloroform caused an

increased enantioselectivity in the lactonization of **III-2** (Table II-14).

Subsequently, benzoic acid emerged as a uniquely useful additive that

contributed to a further increase in selectivity when combined with the new co-solvent systems (Tables III-15 and III-16). Later a temperature screen revealed the range between -40 to -50 °C to be optimal for the highest selectivity. Finally, the use of DCDPH (III-52) in place of DCDMH (III-48) was slightly more selective. For the most part, the two best solvent systems (toluene/chloroform (3:2) and n-hexanes:chloroform (1:1)) had performed on effectively the same level. Owing to operational simplicity, especially with regards to removal of residual solvent, we therefore deferred to the n-hexane/chloroform (1:1) solvent system for subsequent experiments.

At this point, it was surmised that most of the reasonable means towards the systematic optimization of the reaction parameters with regards to enantioselectivity had been exhausted. Furthermore, it seemed likely that substantial gains above those realized through the screening protocol delineated herein might only arise after a more intimate appreciation of the reaction mechanism was at hand. Therefore, we set out to undertake a scan of the substrate scope of the transformation (see the following section). For that study we sought to perform the reaction on a larger scale than the 0.05 mmol screening scale, in order to facilitate the more accurate determination of isolated yields. On increasing the scale of the chlorolactonization of III-2, DCDPH (III-52) quickly emerged as the terminal chlorine source of choice, consistently providing higher isolated yields and enantioselectivities 2-3% higher than DCDMH (III-48). Taking these findings into consideration, we established the conditions described

below in Scheme III-7 as the standard reaction conditions for the asymmetric

chlorolactonization of alkenoic acids.

Scheme III-7. Standard conditions for asymmetric chlorolactonization.

86% yield
89% *ee*
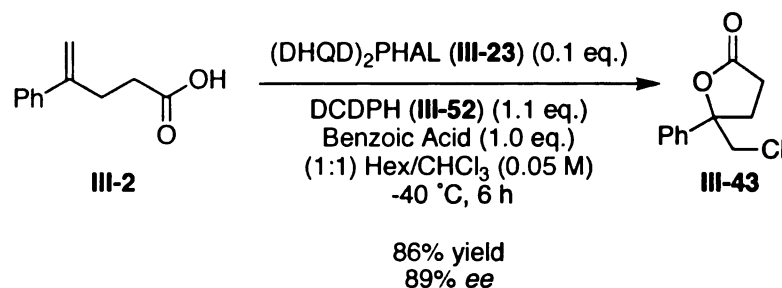
The culmination of the screening intensive approach described above

resulted in a protocol that allowed for the asymmetric chlorolactonization of

alkenoic acid **III-2** in the presence of 0.1 equivalents organocatalyst **III-23**, 1.1

equivalents of chlorine source **III-52**, and 1 equivalent of benzoic acid in a 1:1

mixture of *n*-hexanes and chloroform at -40 °C. The desired chiral chloro-γ-

lactone **III-43** was produced in 86% isolated yield with 89% *ee*. These general

conditions were applied to a substrate scope screen as detailed in the following

section.

3.2.5: Investigation of Substrate Scope

Having discovered optimal conditions for the asymmetric

chlorolactonization of **III-2**, a number of analogous alkenoic acids were prepared

and evaluated using the standard conditions described in Scheme III-7. In total,

eight additional 4-substituted pentenoic acids were prepared (Figure III-5).

Figure III-5. 4-Substituted 4-pentenoic acid substrates.

III-60

III-61

III-62

III-63

III-64

III-65

III-66

III-67
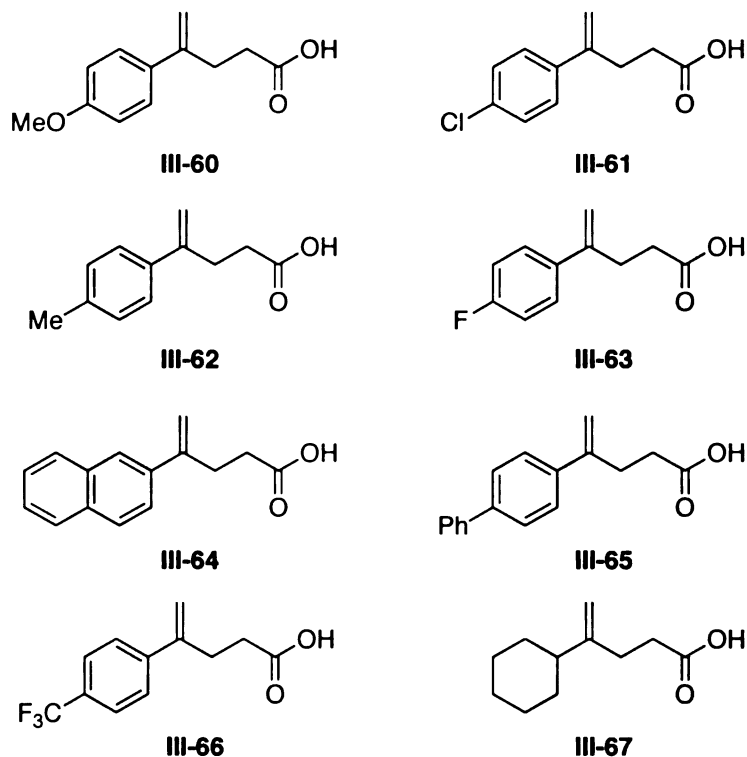
The various substrates were readily prepared by the Wittig methylenation and saponification of the corresponding keto-ester precursors (see Experimental section), with the exception of substrates **III-61** and **III-66**, which were produced via Suzuki coupling as described by Wirth and co-workers.[44]

Substrates **III-60** through **III-67** were subjected to the chlorolactonization protocol described in Scheme III-7. Reactions were conducted on a 0.1 mmol scale. The desired products were isolated after purification by silica gel column chromatography. The enantiomeric excess of the products were judged by chiral GC analysis, except for **III-70**, which was assayed by chiral HPLC. The results of this study are presented in Table III-21.

Table III-21. Investigation of the substrate scope of the chlorolactonization.
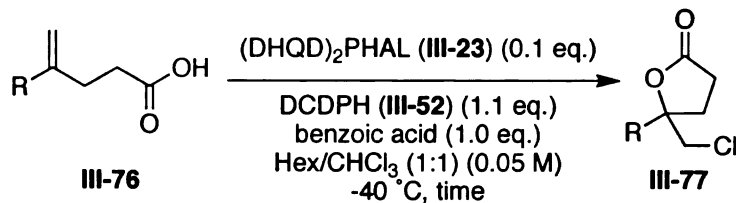
Entry	Substrate	Time (h)	Product	Yield (III-69)	% ee (III-69)
1	III-2	6	III-43	86	89
2	III-60	6	III-68	99	>5
3	III-61	6	III-69	80	88
4	III-62	6	III-70	86	80
5	III-63	6	III-71	83	87
6	III-64	12	III-72	92	72
7	III-65	12	III-73	59	70
8	III-66	12	III-74	61	90
9	III-67	6	III-75	55	43
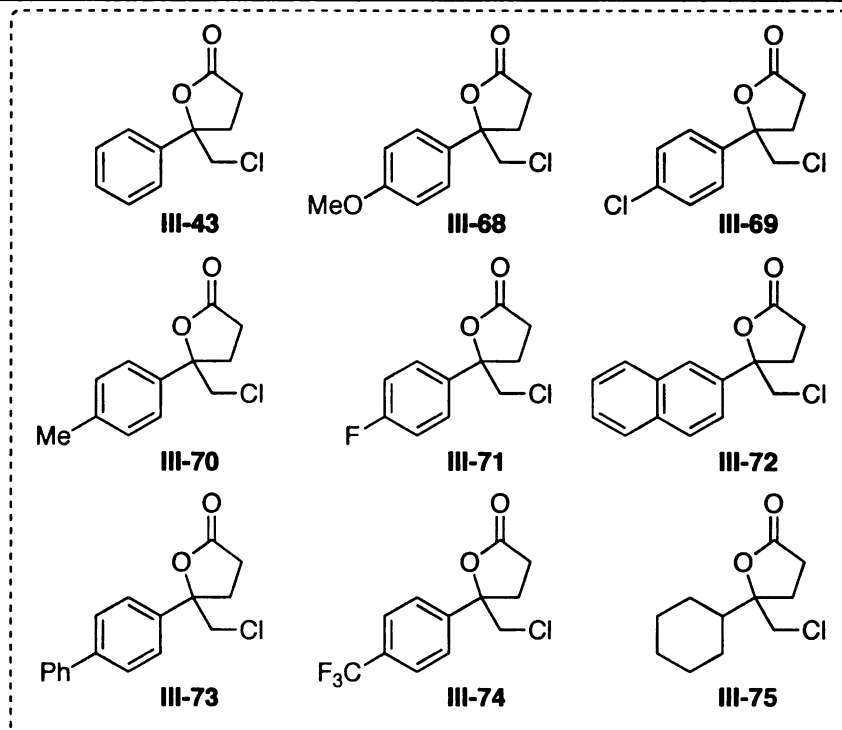
As described above in Scheme III-7, the chlorolactonization of substrate

III-2 proceeded without incident, returning lactone **III-43** in good yield and 89%

ee. Perhaps not unexpectedly, the p-methoxyphenyl subtrate **III-60** returned the

desired chlorolactone **III-68** in excellent yield, although the product was virtually

racemic (entry 2). Evidently, the strong resonance donation from the para

situated methoxy group contributes significantly to the ring opening of the

incipient chloronium intermediate **III-78**, producing oxonium ion **III-79** whose

collapse to the product lactone is inherently non-selective (Scheme III-8).

Scheme III-8. Facile chloronium ion ring opening with **III-60**.
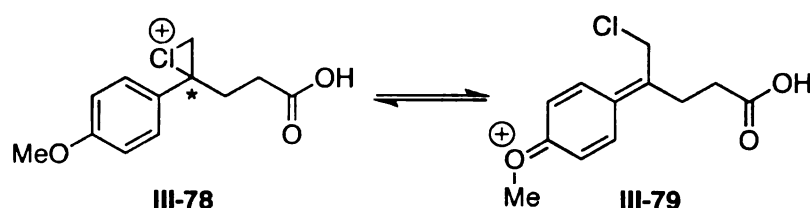
In addition the presence of the electron donating methoxy group ought to

enhance the nucleophilicity of the olefin in **III-60** relative to **III-2**, accelerating the

rate of the reaction (assuming that chlorine delivery is rate limiting). A

significantly faster reaction might also result in a less selective transformation.

Indeed, the conversion of **III-60** to **III-68** is significantly faster than the analogous

transformations depicted in Table III-21, proceeding to completion in less than 5

minutes at -40 °C! Conducting the cyclization of **III-60** at -78 °C did not improve

the selectivity.

Para substituents with somewhat tempered electron donating ability still

maintained relatively high selectivity. The para-chloro substituted substrate **III-61**

returned lactone **III-69** in 80% yield and 88% ee (entry 3). The slightly inductive

177

electron donation due to the *para*-methyl substituent in **III-62** resulted in the generation of lactone **III-70** in 86% yield, albeit with a slightly reduced 80% *ee* (entry 4). Similar to **III-61**, substrate **III-63** containing a *para*-fluoro substituent returned the corresponding lactone **III-71** in 83% yield and 87% *ee* (entry 5). Additionally, electron withdrawing substrates on the aryl ring are also tolerated. Substrate **III-66**, substituted with the electron withdrawing trifluoromethyl substituent returned lactone **III-74** in 61% yield with 90% *ee* (entry 8).

Increasing the steric bulk of the aryl ring on the substrate resulted in lactone products with somewhat reduced enantioselectivities. The 3-napthyl substrate **III-64** returned the corresponding chlorolactone **III-72** in 90% isolated yield with 70% *ee* (entry 6). Similarly, biphenyl substrate **III-65** returned lactone **III-73** in 59% yield and 70% *ee* (entry 7).

Subsequently, we sought to evaluate whether or not the presence of an aryl moiety at the 4-position of the 4-pentenoic acid substrate was necessary for high enantioselectivity. In order to probe this problem, we prepared subtrate **III-67**, containing a cyclohexyl group in the 4-position in lieu of an aryl substitutent. In the event, subjection of this substrate to the prescribed reaction conditions returned the saturated chlorolactone **III-75** in reduced yield and enantioselectivity (55% yield, 45% *ee*, entry 9).

Finally, the chlorolactonization of **III-2** was evaluated in the presence of the quasienantiomer of organocatalyst **III-23**. When (DHQ)$_2$PHAL was employed as the organocatalyst, the desired chlorolactone was returned in 75% yield with a selectivity of -77% *ee* (Scheme III-9). While the reduced selectivity in the

presence of the quasienantiomer of **III-23** is disappointing it is most likely the

result of the diastereomeric relationship between **III-23** and (DHQ)$_2$PHAL.

Scheme III-9. Cyclization of **III-2** with the quasienantiomer of catalyst **III-23**.

75% yield
-77% *ee*
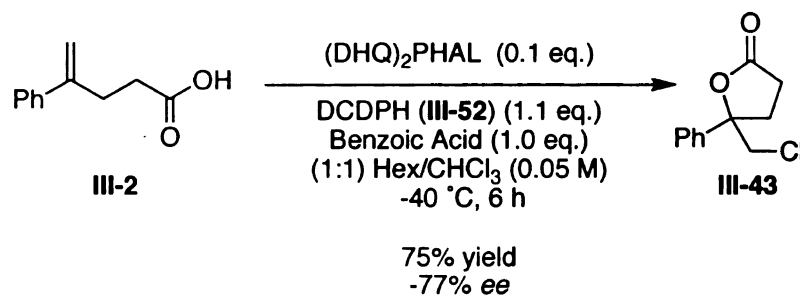
Overall, this limited investigation of the substrate scope indicates that

substitution on the *para* postion of the aryl moiety of substrate **III-76** (Table III-21)

is relatively well tolerated, provided the substituent is not a strong electron donor

(entry 2). Furthermore, reduced selectivity is realized when larger 4-substituents

are employed (*i.e.* napthyl and biphenyl, entries 6 and 7). Finally, the presence

of an aromatic group at the 4-position of **III-76** is evidently crucial for high

selectivity (entry 9). Ultimately, the substrate scan depicted in Table III-21 and

described above indicates several limitations of the methodology that may not be

easily rectified without a more thorough understanding of the mechanism by

which the (DHQD)$_2$PHAL/DCDPH (**III-23/III-52**) catalyst system confers its

enantioselectivity. Perhaps the screening intensive approach to the optimization

of the enantioselectivity with regards to a single substrate (**III-2**) has generated a

niche system that is highly tuned for the selective cyclization of a specific, limited

olefin class (**III-76**). It may be prudent for subsequent optimization attempts to

begin by revisiting some of the "milestone" conditions leading to those described

in Scheme III-7 with a small panel of compounds representing several different substrate classes. Applying such a strategy might return an alternate set of conditions that are less selective for substrates of the class of **III-76**, yet more generally applicable to a broader range of substrates. It seems clear, however, that an intimate appreciation of the mechanism of the system at hand might serve to guide the course of these subsequent optimization experiments. The following section details several initial experiments aimed at teasing out some of the mechanistic subtleties of the transformation.

3.2.6: Mechanistic Investigations

As an initial endeavor into probing the mechanism of the transformation we sought to evaluate the stereochemical course of the reaction when a full equivalent of catalyst **III-23** is employed. Owing to the more facile and quick analysis of the enantioselectivity of lactone **III-71** relative to **III-43** by chiral GC analysis, most of the mechanistic studies detailed herein were conducted with substrate **III-63** in lieu of **III-2**. The chlorolactonization of **III-63** was performed on the 0.05 mmol test scale with 1.1 equivalent of (DHQD)$_2$PHAL (**III-23**), while maintaining all of the other optimized reaction parameters. Namely, DCDPH (**III-52**) was used as the terminal chlorine source (1.1 equiv.) in a 1:1 ratio of *n*-hexanes and chloroform (0.05 M relative to **III-63**) that was maintained at -40 °C and doped with 1 equivalent of benzoic acid. As a control, the analogous catalytic (0.1 equiv. **III-23**) reaction with substrate **III-63** was conducted simultaneously. The results of this study are compiled below in Table III-22.

Table III-22. Lactonization of **III-63** with 1.1 equivalents of catalyst **III-23**.
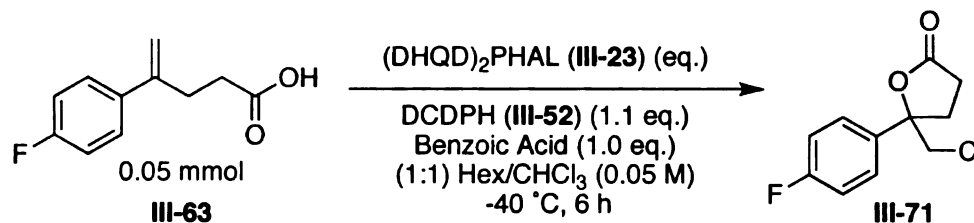
Entry	Eq. (III-23)	% ee (III-71)
1	1.1	73
2	0.1	87

Note: All reactions were complete by TLC.

Surprisingly, chlorolactone **III-71** was produced with a substantially reduced enantioselectivity of just 73% *ee* in the presence of 1.1 equivalents of **III-23**. Conversely, the control reaction in the presence of 0.1 equivalents of the organocatalyst returned **III-71** with the expected 87% *ee*, in complete agreement with the scaled experiment described in the previous section (Table III-21, entry 5). The result from the stoichiometric experiment is counterintuitive to conventional wisdom for asymmetric catalysis. One would typically expect for the selectivity of a particular asymmetric transformation to increase on increased loading of the chiral catalyst.[45,46] The decrease in selectivity observed in our system might be explained by a prevailing autoaggregation event at higher loadings of catalyst **III-23**. If catalyst aggregation is significant under stoichiometric conditions, such an event might negatively influence the stereochemical course of the transformation.

Indeed, the autoagreggation phenomena of quinine (**III-49**), a related *Cinchona* alkaloid, has be extensively characterized by Uccello-Barretta, Di Bari,

and Salvadori. They observed that the dimerization of quinine in $CDCl_3$ solutions occurs at higher concentrations as well as at lower temperatures. Specifically, on increasing the concentration of quinine from 2.6 mM to 606 mM in $CDCl_3$, they observed a significant upfield shift (up to 0.5 ppm) for the ^{1}H resonances of the two protons flanking the quinoline nitrogen atom. The authors propose a dimerization event driven by the stacking of the quinoline rings of two quinine molecules. A similar shift in the spectrum was observed on lowering the temperature of a 170 mM solution of quinine in $CDCl_3$ from 25 °C to -50 °C.[28]

Although the concentration in our study (50 mM for the stoichiometric experiment) is more dilute than those employed in their investigation, the (DHQD)₂PHAL chlorolactonization is conducted within a similar temperature regime (-40 °C). Furthermore, the presence of the less polar *n*-hexane co-solvent in our system in concert with the lower temperature might permit the auto-aggregation at lower concentrations relative to their studies. In addition to the stoichiometric experiment, the temperature study described in Table III-19 (*vide supra*, Section 3.2.4) seems to support the assertion that catalyst oligomerization might prove to be problematic with respect to enantioselectivity. Specifically, while the (DHQD)₂PHAL/DCDMH (**III-23/III-48**) system returned phenyl substituted lactone **III-43** in 88% *ee* at -40 °C in *n*-hexane/chloroform (1:1), the analogous experiment at -78 °C returned the product in just 67% *ee* (Table III-19, entries 9 and 12).

Given the results described here and in Table III-19 coupled with the documented tendency for certain *Cinchona* alkaloids to form oligomers in

solution,[28,29] further investigations into the mechanism of the $(DHQD)_2PHAL$ chlorolactonization reaction ought to consider the potential for catalyst dimerizations. Specifically, if the inferior results for the stoichiometric experiment are due to catalyst oligomerization, the trend ought to be exacerbated on further increasing the amount of catalyst (*e.g.* 5 or 10 equivalents). Alternatively, perhaps the outcome of the stoichiometric experiment can be rescued on performing the reaction under more dilute conditions.

Subsequent to the stoichiometric experiment detailed above, we next turned to a more systematic evaluation of the influence of the N-chlorohydantoin terminal chlorine source. During the course of our optimization studies, DCDMH (**III-48**) and DCDPH (**III-52**) emerged as the terminal halogen sources of choice relative to the initially discovered NBS and NCS systems. They appear to exhibit a reactivity profile that is uniquely wedged in between NBS and NCS, thus allowing for control of the uncatalyzed background reaction (unlike NBS) but also allowing for low temperature studies owing to their enhanced reactivity relative to NCS. We were particularly intrigued, however by the fact that certain N-chlorohydantoins were more selective than others in the earlier iterations of our methodology development (Table III-13). We were particularly surprised to find that the 1-methyl analogue (**III-54**, entry 3) of DCDMH (**III-48**) was less selective (*cf.* 61% *ee* for **III-54** vs. 83% *ee* for **III-48**). The expected outcome on employing **III-54** in place of DCDMH was an equally selective, but slower transformation owing to the deactivation of the remaining N-3 chlorine on replacing the N-1 chlorine with a less activating methyl group. That the selectivities drop, seemed

to indicate a more intimate relationship between the N-chlorohydantoin and catalyst **III-23** in the transition state leading to the putative chloronium intermediate. Earlier in the chapter, several possible catalyst/N-chlorohydantoin complexes were proposed in Figure III-4 that might account for these findings. In order to further probe the role of the terminal chlorenium source in our asymmetric chlorolactonization protocol, a systematic evaluation of various closely related N-chlorohydantoins was undertaken. In a series of parallel experiments, *para*-fluoro substrate **III-63** was subjected to our optimized reaction conditions while employing different terminal chlorenium sources. In addition to DCDPH (**III-52**) and DCDMH (**III-48**), we also screened several known analogues of DCDMH. Namely we evaluated 1-chloro-5,5-dimethylhydantoin (1-CDMH, **III-80**), 1-chloro-3,5,5-trimethylhydantoin (1-CTMH, **III-81**), and 3-chloro-1,5,5-trimethylhydantoin (3-CTMH, **III-54**).[47] In addition, NCS (**III-44**) and trichloroisocyanuric acid[48] (TCCA, **III-82**) were also evaluated under the optimized reaction conditions. The results of this study are presented in Table III-23. In each case the terminal chlorenium source was applied in a 1.1 equivalent loading. In addition, since TCCA harbors three active chlorenium equivalents, it was also applied in reduced loadings of 0.5 and 0.3 equivalents. The stereochemical course of the transformation was again evaluated by chiral GC analysis. Owing to the assumption that the less reactive halogen sources (*i.e.* NCS and the mono-chlorohydantoins) would result in a sluggish transformation at -40 °C, the reaction time was prolonged to 18 hours prior to work-up. The requisite N-chlorohydantoins for the study were prepared using our

TCCA mediated methodology (see Chapter 4),[41] with the exception of **III-80**, which was prepared using the method of Corral and Orazi.[47]

Table III-23. Investigation of terminal chlorenium sources in the cyclization of **III-63**.
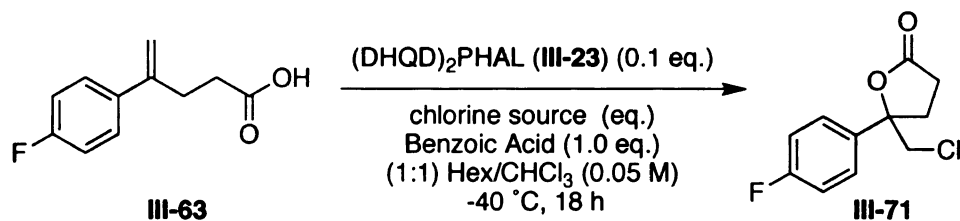
Entry	Cl⁺ Source	Eq. (Cl⁺ Source)	% ee (III-71)
1	III-52	1.1	87
2	III-48	1.1	86
3	III-80	1.1	80
4	III-81	1.1	76
5	III-54	1.1	74
6	III-44	1.1	64
7	III-82	1.1	72
8	III-82	0.5	75
9	III-82	0.3	74
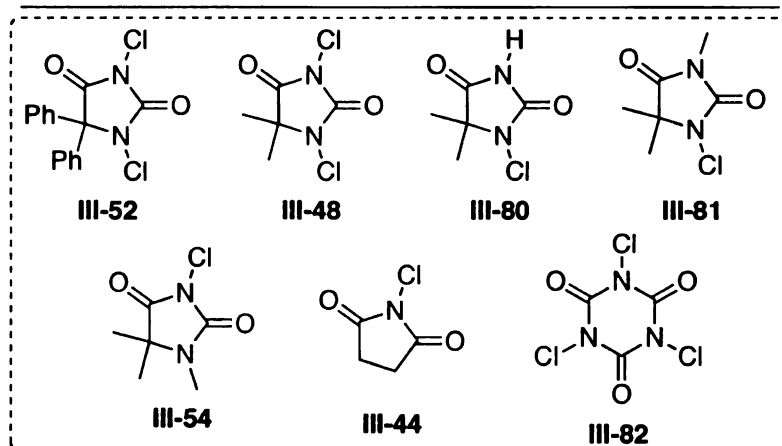
Note: All reactions were complete by TLC, except for entries 3-6.

Cyclization of **III-63** with DCDMH (**III-48**) and DCDPH (**III-52**) returned lactone **III-71** in 86 and 87% *ee*, respectively (entry 1 and 2), again in agreement with the scaled experiment detailed in Table III-21, entry 5 (*vide supra*). When 1-CDMH (**III-80**) was employed, the reaction was notably slower and did not proceed to complete conversion after 18 hours. Additionally, the chlorolactone **III-71** was returned in a reduced selectivity of 80% *ee*. The two methylated derivatives, **III-81** and **III-54** were even less selective, returning the lactone product in 76 and 74% *ee* (entries 4 and 5). These data again seem to suggest that there is some degree of association between the catalyst **III-23** and the terminal chlorenium source in lieu of a direct chlorine transfer to the alkaloid. If such a transfer were occurring, generating intermediate **III-56** (Figure III-4) for instance, one would predict that the less reactive chlorine sources would result in an equally selective, albeit slower generation of **III-71**. The data presented in Table III-23 seems to indicate that an alternative means of catalysis is occurring and that **III-56** is likely not operative. Finally, the screening of NCS (**III-44**) and TCCA (**III-82**) serve to reconfirm the dichlorinated hydantoins as the terminal chlorine sources of choice for our transformation (entries 6-9).

The data for NCS and TCCA indicate interesting nuance of the transformation. The ^{35}Cl Nuclear Quadrupole Resonance (NQR) frequency has been invoked as a quantitative marker of the chlorenium (Cl$^+$) character of a particular N-Cl bond.[49-53] In short, those N-Cl bonds with larger Cl$^+$ character resonate at higher frequencies than compounds with less active N-Cl bonds.

Figure III-6 indicates the NQR resonance frequencies for several chlorenium sources.

Figure III-6. 35-Cl NQR frequencies for various chlorenium sources.

III-52   III-48

III-44   III-82
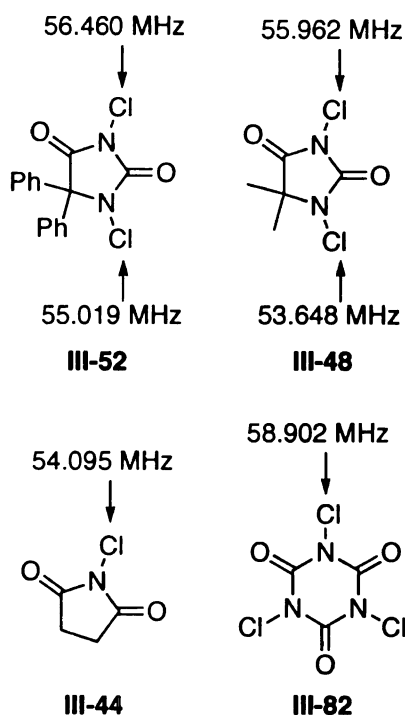
The NQR data seems to indicate that the dichlorinated hydantoins employed in our most selective conditions (*i.e.* **III-52** and **III-48**) are exquisitely positioned in between the less reactive NCS (**III-44**) and the more reactive TCCA (**III-82**). Indeed, we initially turned to the N-chlorohydantoins to correct the sluggish reactivity of NCS at lower temperatures. Furthermore, as indicated in Table III-23, employing the more reactive TCCA proved detrimental for the selectivity of the transformation returning **III-71** in 72-75% *ee* (entries 7-9). Taking the NQR data into account, this drop in enantioselectivity might be accounted for by a substantial contribution from the uncatalyzed background

reaction when TCCA is employed. In other words, the dichlorohydantoins III-52

and III-48 might be perfectly electronically tuned to overcome the sluggish

reactivity of NCS, yet still maintaining a measure of attenuation relative to the

more reactive TCCA. It seems clear that the more labile N-3 chlorine (56.460

and 55.962 MHz for III-52 and III-48, respectively) of the dichlorohydantoins is

the active chlorenium equivalent that is eventually incorporated in the lactone

products. Consequently, the less reactive N-1 chlorine, whose frequencies are

closer in nature to NCS, primarily serves to inductively activate the N-3 chlorine

towards donation. They are themselves most likely retained on the reduced

chlorohydantoin by-products.

Ultimately, the experiments described above in Table III-23 inconclusively

suggest an alternate means of catalysis in lieu of a direct transfer of an active

chlorenium equivalent to the organocatalyst (III-56). The three proposed

alternate active species depicted in Figure III-4 are reproduced below in Figure

III-7.

Figure III-7. Potential active catalyst species.

III-56	III-57	III-58	III-59
	hydrogen bonded framework	tight ion pair framework	chloronium dimer framework
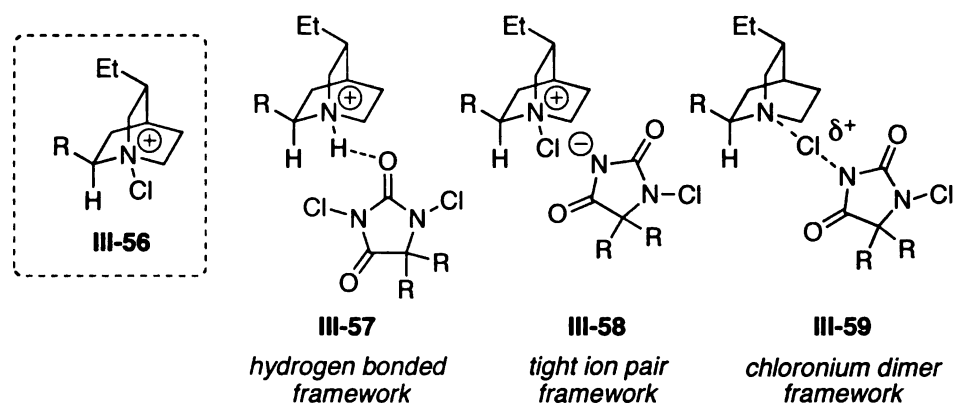
At this point, it seems unlikely that the results described in Table III-23 can be accounted for by putative intermediate **III-56**, relying on the direct donation of a chlorenium equivalent to the chiral catalyst. In fact, given that the reaction mixture includes an equivalent of the substrate acid as well as an equivalent of benzoic acid likely ensures that the quinulclidine rings of **III-23** are protonated. Although a tight ion pair (**III-58**) or chloronium dimer (**III-59**) framework might account for the dependence of the enantioselectivity of the transformation on the gross structure of the chlorohydantoin, their accessibility under the acidic reaction conditions is debatable. Alternatively, a hydrogen-bonded activation of the N-chlorohydantoin by the protonated catalyst (see **III-57**), could in principle account for the observed results. Interestingly, H-bond driven asymmetric catalysis has been invoked for transformations mediated by *Cinchona* alkaloids previously.[54] Of course, one must be careful of such conjecture; alternative means of catalysis due to the quinoline moiety of **III-23** or the association of the catalyst with the substrate cannot be ruled out. Ultimately, the data presented in Table III-23 seems to hint at a more complicated process than a simple chlorenium transfer from the hydantoin to the chiral catalyst (*i.e.* **III-56**), and begs for a more thorough investigation. Likely, only then will the limitations of the current interaction of the methodology be corrected.

As an additional probe of the effects of catalyst protonation on the selectivity of the reaction, the cyclization of the *tetra*-butylammonium salt of substrate **III-2** (**III-83**) was carried out both in the presence and absence of the

benzoic acid additive. Compound **III-83** was conveniently prepared using

Rousseau's protocol.[55] The results of this study are collected in Table III-24.

Table III-24. Cyclization of salt **III-83**.
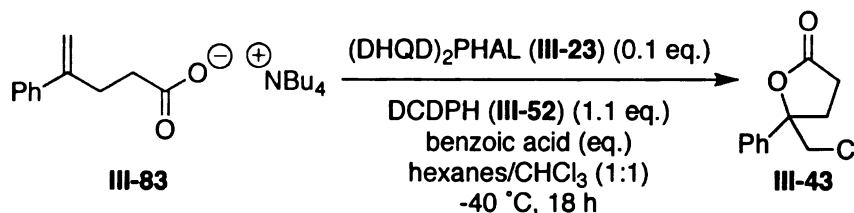
Entry	Benzoic Acid (Eq.)	% ee (III-43)
1	1.0	74
2	0.0	66

Note: Reactions were complete by TLC.

Interestingly, the cyclization of **III-83** is clearly less selective in the

absence of the benzoic acid additive. When an equivalent of benzoic acid was

included in the transformation, lactone **III-43** was returned in 74% *ee*. The

alternate reaction lacking the acid additive returned the desired product in 66%

ee. Although both transformations are markedly less selective than the

analogous cyclization of **III-2** (89% *ee*), the results may indicate a necessity for

the protonation of **III-23** as a requirement for high enantioselectivity.

As a final mechanistic probe, we re-evaluated the other *Cinchona* alkaloid

dimers that we had tested previously. Namely, the anthraquinone linked

(DHQ)$_2$AQN (**III-42**) and the diphenyl pyrimidine linked (DHQD)$_2$Pyr (**III-41**) were

evaluated as catalysts in the cyclization of **III-63** to return lactone **III-71**. The

results of this study are collected in Table III-25. Additionally, the data for the

cyclization of **III-63** by action of **III-23** (Table III-23, entry 5) and the data for the

cyclization of **III-2** by action of (DHQ)$_2$PHAL (**III-84**) (see Scheme III-9) is included

190

for comparison.　Initially, these catalysts were chosen for re-evaluation owing to

their structural similarity to the successful catalyst **III-23**.

Table III-25. Evaluation of other dimeric *Cinchona* catalysts.
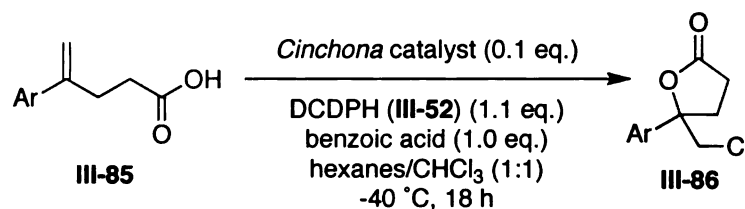
Entry	Catalyst	Ar (III-86)	% *ee* (III-86)
1	**III-41**	*p*-fluorophenyl	0
2	**III-42**	*p*-fluorophenyl	-18
3	**III-23**	*p*-fluorophenyl	87
4	**III-84**	phenyl	-77

Note: Reactions were complete by TLC.

Interestingly, the nature of the intervening aromatic linker separating the

two alkaloid units in the organocatalyst appears to have a profound effect on the

selectivity of the transformation.　For instance, on replacing the phthalazine linker

in (DHQD)$_2$PHAL (**III-23**) with the 2,5-diphenylpyrimidine linker found in

(DHQD)$_2$Pyr (**III-41**), a complete loss of induction is realized (entries 3 and 1,

respectively).　Similarly, the chlorolactonization of **III-63** by action of (DHQ)$_2$AQN

(**III-42**) is markedly less selective than the similar lactonization of **III-2** by action of

(DHQ)$_2$PHAL (**III-84**, structure not shown).　Specifically, the *p*-fluoro substituted

chlorolactone **III-71** was returned in just -18% *ee* with the anthraquinone-linked

DHQ dimer (entry 2).　Conversely, the related phenyl substituted lactone **III-43**

was produced in a much improved -77% *ee* with the phthalazine dimer (entry 4).

These data indicate that some structural feature inherent in the phthalazine linker is crucial to the relatively high stereoinduction realized by action of (DHQD)$_2$PHAL and (DHQ)$_2$PHAL. Ultimately, the data presented in Table III-25 serves to further highlight the need for an understanding of both the exact nature of the interaction between the alkaloid catalyst and the terminal chlorine source as well as the mechanism by which it governs the asymmetric delivery of a chlorenium ion.

3.3: Conclusions and Future Directions

Presented in the preceding sections, has been a full account of the initial discovery and systematic optimization of a novel asymmetric chlorolactonization reaction. This methodology was born from the lessons learned in a failed attempt to develop our 1st generation peptide-based catalyst system (see Chapter 2). The penultimate advance in this regard was arriving at a significantly more active catalyst relative the bromoiodinane peptides (e.g. III-1) that allowed for a departure from the bromolactonization protocol, thus facilitating control over the prevailing non-catalyzed background reaction. The fruits of these labors have been the development of the first example of a catalytic asymmetric chlorolactonization protocol as well as the most selective asymmetric halolactonization protocol to date. For the first time, a catalytic halolactonization protocol can be conducted with synthetically useful levels of stereoinduction.

The current state of the methodology is not without its limitations, however. As delineated in Section 3.2.5, the transformation is relatively

substrate limited, so far not tolerating significant substrate structural deviations from the initially investigated **III-2**. Hopefully, however, significant ground-work has been laid to allow for future efforts to arrive at a subsequent iteration that will be both more selective and generally applicable.

Future efforts aimed at the further optimization of the (DHQD)$_2$PHAL/DCDPH (**III-23/III-52**) catalyst system will likely benefit greatly from a more intimate understanding of the mechanistic underpinnings responsible for stereoinduction. From this point, any subsequent efforts ought to be heavily focused upon teasing out the mechanism of the transformation, especially the interaction between the catalyst and the terminal halogen source. A multi-pronged approach might be undertaken for this task. First, it would be interesting to probe the effects of using electronically different N-chlorohydantoins as the terminal halogen source in the transformation. Figure III-8 depicts several potential candidates.

Figure III-8. Alternate 5,5-aryl-N-chlorohydantoins.

III-52   III-87   III-88   III-89
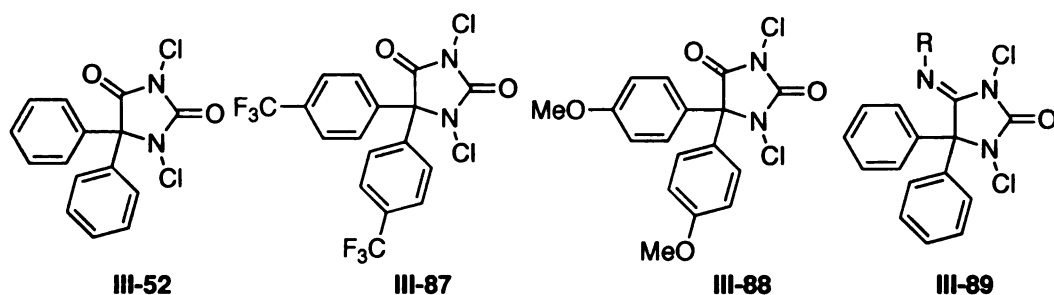
The *bis*-trifluoromethylphenyl compound **III-87** and the *bis*-methoxyphenyl compound **III-88**, ought to be electronically distinct from the parent DCDPH **III-52**. Both compounds should be readily available by applying our newly developed

chlorination protocol to the known hydantoins.[56,57] One would expect **III-87** to be slightly more activated relative to **III-52**, while **III-88** would be slightly less activated. The effects of these subtle electronic modulations on the terminal chlorine source might help to reveal the nature of the association between catalyst **III-23** and the N-chlorohydantoin. Additionally, the more amidine-like hydantoin analogue **III-89** would be interesting as well. If the association between the catalyst and the chlorine source is driven by a hydrogen bond as indicated in structure **III-57**, one would predict that chlorine sources like **III-89** would prove more apt to participate in such a situation owing to the presence of a more active H-bond acceptor, thus resulting in enhanced selectivity.

In addition to probing electronically distinct N-chlorohydantoins, an NMR evaluation of the corresponding ^{15}N labeled hydantoins (*i.e.* **III-90**) might provide insight into the nature of the hydantoin/catalyst complex. Quantitative experiments could be carried out with ^{15}N-labelled hydantoin **III-90** (Figure III-9), where the chemical shift of the labeled atom will be monitored. For example, it is expected that the chemical shift of ^{15}N in **III-90** will not be affected greatly if complex **III-57** is predominant. On the other hand, the ion pair complex depicted in **III-58** would lead to substantial shielding of the nitrogen atom. A spectroscopic ruler for the anticipated level of shielding can be established by studying the ^{15}N-NMR of **III-91** and **III-92**, the neutral and anionic analogs of **III-9**. The ^{15}N-chemical shift of compound **III-90**, if bound as depicted in complex **III-59** should be intermediate in the latter spectroscopic ruler. It should be noted that the required ^{15}N label can be readily incorporated by employing commercially

available ^{15}N labeled potassium cyanide during the course of the synthesis of III-90 via the Bucherer-Berg reaction.[58]

Figure III-9: Proposed labeled N-chlorohydantoins.

III-90   III-91   III-92

III-57   III-58   III-59
hydrogen bonded   tight ion pair   chloronium dimer
framework   framework   framework
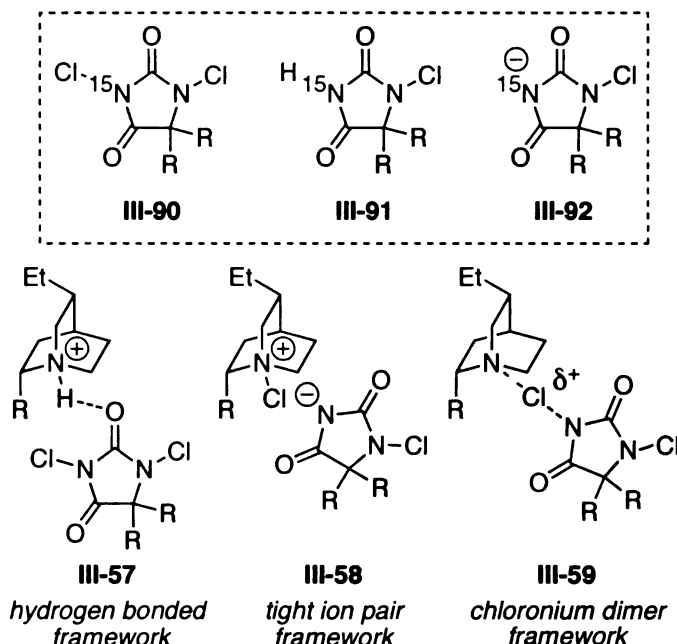
In addition to the mechanistic probes based on the hydantoin scaffold described above, one might also pursue the evaluation of a systematic library of dimeric DHQD catalysts, aiming to probe the exact influence of the phthalazine dimer in the most selective catalyst III-23. Indeed, an extensive amount of work has been undertaken by others in efforts at both tuning the selectivity and understanding the mechanistic underpinnings of the well-known SAD reaction.[12,59] Figure III-10 indicates several potential linkers that might be employed to both probe the mechanism of the chlorolactonization reaction as well as potentially further tune the selectivity of the transformation.

Figure III-10. Potential alternative catalyst scaffolds.
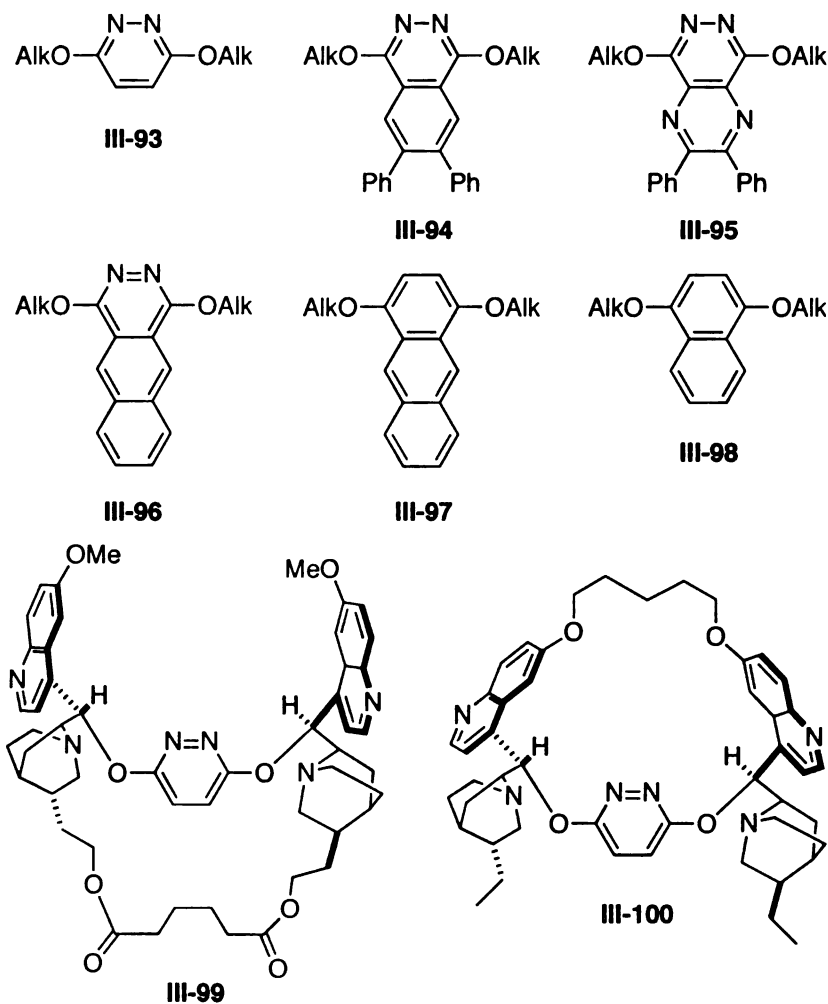
Pyridazine linker **III-93**[60,61] was introduced by Corey and co-workers while the diphenylphthalazine (**III-94**)[62] and pyrazinopyridazine (**III-95**)[63-65] were developed by Sharpless. Furthermore, dimers based on the extended aryl linker **III-96** have also been prepared.[66,67] The investigation of this small catalyst library assembled with the DHQD alkaloid moiety might both offer some insight into the exact role of the phthalazine linker in our current best catalyst (**III-23**) as well as potentially return a more selective and broadly applicable iteration of the

methodology. Additionally, it would be interesting to investigate the hydrocarbon analogues of the phthalazine dimer (**III-97** and **III-98**) to further probe the role of this heterocycle in the transformation, although their preparation would be more involved, given that they could not be prepared from the S_NAr methodology developed for the heterocyclic analogues.[12,59]

Finally, the simultaneous investigation of the conformationally constrained analogues **III-99** and **III-100** might also be instructive. The adipate bridged PYDZ dimer **III-99** was introduced by Corey and co-workers.[68,60] This catalyst conformationally restrains the catalyst by linking the two alkaloids by an intervening tether. Alternatively, the Lohray ligand **III-100** constrains the system by a linker between the two quinoline moieties.[69]

Perhaps a thorough investigation of a small library of similar catalysts related to **III-23** like those suggested in Figure III-10 would serve to shed additional light on the mechanism governing the enantioselective chlorolactonization methodology described herein. Subsequent to a clear understanding of the mechanistic underpinnings of the transformation at hand, it seems likely that continued iterative optimization might return a more broadly applicable methodology that could elevate the asymmetric halogenation of olefins to the levels of success enjoyed by asymmetric dihydroxylation, aminohydroxylation and epoxidation. The basic strategy might be applied to other related chlorenium based asymmetric transformations in the future. These would include an analogous haloetherication, haloamidation, dihalogenation, etc.

3.4: Experimental Details

All reagents were purchased from Aldrich or other commercial sources and used without purification. Anhydrous chloroform stabilized with amylenes (Aldrich) and HPLC grade 95% *n*-hexanes (Spectrum) was used for all asymmetric halolactonizations. All other solvents were purchased from either Fisher Scientific or Mallinckrodt Chemicals and used without purification. ^{1}H and ^{13}C NMR spectra were collected on a 300 MHz NMR spectrometer (VARIAN INOVA) using CD_3Cl, acetone-d_6, or DMSO-d_6. Chemical shifts are reported in parts per million (ppm). Spectra are referenced to residual solvent peaks. Infrared spectra were collected on a Mattson Galaxy Series FTIR 3000. Samples were prepared as KBr pellets or KBr discs. Optical rotations were measured on a Perkin Elmer Polarimeter 341 in chloroform. Flash silica gel (32-63 mm) from Dynamic Adsorbents, Inc. was used for column chromatography. Enantiomeric excess was judged by HPLC (chiralcel OD-H) for bromolactone **III-3** and HPLC (Chiralcel OJ-H) and later GC (GAMMA DEX) for all chlorolactones (*vide infra*).

General Procedure for Test-Scale Halolactonization
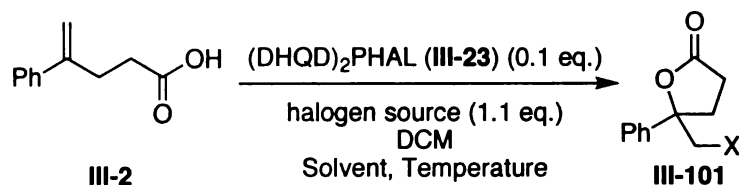
A screw-top vial equipped with a magnetic stir bar was charged with halogen source (0.055 mmol, 1.1 equiv.) and (DHQD)$_2$PHAL (**III-23**) (4 mg, 0.005 mmol, 0.1 equiv.). The solids were then taken up in the appropriate solvent or

solvent system (1 mL). The vial was sealed with the screw-top and the reaction mixture was lowered to the prescribed temperature by action of an immersion cooler. The mixture was stirred at the designated temperature and monitored by TLC (20% ethyl acetate in hexanes, $KMnO_4$ burn). Upon completion, the reaction mixture was poured into a 60 mL separatory funnel along with 0.1 M aq. NaOH (5 mL). The resulting solution was extracted twice with dichloromethane (5 mL). The combined organics were then dried (anhydrous Na_2SO_4) and concentrated in the presence of a small portion of silica gel via rotary evaporation. The resulting silica plug was then placed on top of a Pasteur pipet packed with silica gel. The desired lactone product (**III-101**) was eluted from the pipet column with 20% ethyl acetate in hexanes which on concentration returned a clear oil. The enantiomeric excess of the product was determined either by HPLC or GC (*vide infra*).

III-3, 5-(Bromomethyl)-5-phenyldihydrofuran-2(3*H*)-one[3]
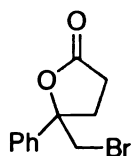
^{1}H NMR (300 MHz, CD$_3$Cl): δ 7.34 (m, 5H), 3.71 (d, *J* = 11.1 Hz, 1H), 3.67 (d, *J* = 11.1 Hz, 1H), 2.77 (m, 2H), 2.52 (m, 2H); ^{13}C NMR (75 MHz, CD$_3$Cl): δ 175.4, 140.6, 128.7, 128.5, 124.7, 86.3, 40.9, 32.2, 28.9.

General Procedure for the Scaled Chlorolactonization
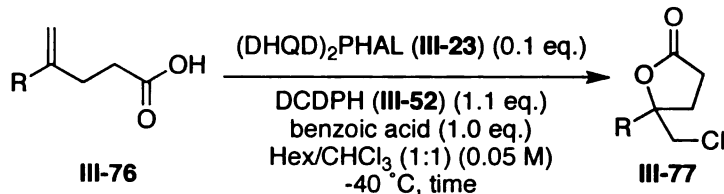
To a flame-dried screw-top vial equipped with a stir bar was added

(DHQD)$_2$PHAL (III-23) (8 mg, 0.01 mmol, 0.1 equiv.), 1,3-dichloro-5,5-

diphenylhydantoin (DCDPH, III-52) (32 mg, 0.11 mmol, 1.1 equiv.), and benzoic

acid (12 mg, 0.1 mmol, 1 equiv.). These reagents were dissolved in a 1:1

mixture of chloroform and n-hexanes (2 mL) and cooled to -40 °C with the aid of

an immersion cooler. The resulting -40 °C solution was stirred for ca. 20-30

minutes at which time the appropriate alkenoic acid III-76 (0.1 mmol, 1 equiv.)

was added in one portion in solid form. The resulting mixture was stirred at -40

°C for 6 or 12 hours as indicated in Table III-21. The reaction mixture was

poured into a 60 mL separatory funnel and diluted with chloroform (10 mL). The

organics were then washed with 0.1 M aq. NaOH (10 mL). The aqueous layer

was subsequently extracted with chloroform (10 mL). The combined organics

were dried over anhydrous sodium sulfate and concentrated by rotary

evaporation. The crude isolate was then purified by silica gel column

chromatography (20% EtOAc in hexanes, KMnO$_4$ burn). The enantiomeric

excess of the products so isolated were judged by chiral GC or HPLC (vide infra).

Analytical Data for Chlorolactones (Table III-21)

III-43, 5-(Chloromethyl)-5-phenyldihydrofuran-2(3H)-one
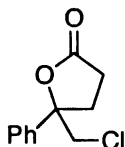
^{1}H NMR (300 MHz, CD₃Cl): δ 7.39 (m, 5H), 3.83 (d, J = 11.7 Hz, 1H), 3.75 (d, J = 11.7 Hz, 1H), 2.80 (m, 2H), 2.52 (m, 2H); ^{13}C NMR (75 MHz, CD₃Cl): δ 175.6, 140.5, 128.7, 128.5, 124.8, 87.0, 52.0, 31.3, 28.9; IR (νcm^{-1}, KBr discs): 1779; HRMS (C₁₁H₁₁O₂Cl): Calc. (M+H): 211.0526, Found (M+H): 211.0528; $[\alpha]_D^{20}$ = +39.0 ° (c = 0.605, CHCl₃) from (DHQD)₂PHAL; $[\alpha]_D^{20}$ = -30.1 ° (c = 0.51, CHCl₃) from (DHQ)₂PHAL.

III-68, 5-(Chloromethyl)-5-(4-methoxyphenyl)dihydrofuran-2(3H)-one
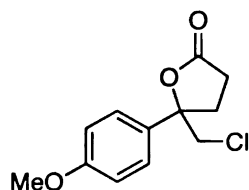
^{1}H NMR (300 MHz, CD₃Cl): δ 7.31 (m, 2H), 6.90 (m, 2H), 3.80 (s, 3H), 3.79 (d, J = 12 Hz, 1H), 3.73 (d, J = 12 Hz, 1H), 2.76 (m, 2H), 2.49 (m, 2H); ^{13}C NMR (75 MHz, CD₃Cl): δ 175.7, 159.7, 132.5, 126.2, 114.1, 87.0, 55.3, 52.1, 31.2, 29.0; IR (νcm^{-1}, KBr disc): 1784; HRMS (C₁₂H₁₃O₃Cl): Calc. (M+H): 241.0631, Found (M+H): 241.0630.

III-69, 5-(Chloromethyl)-5-(4-chlorophenyl)dihydrofuran-2(3*H*)-one
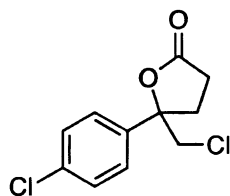
^{1}H NMR (300 MHz, CD$_3$Cl): δ 7.35 (m, 4H), 3.79 (d, *J* = 12.3 Hz, 1 H), 3.71 (d, *J* = 12.3 Hz), 2.78 (m, 2H), 2.5 (m, 2H); ^{13}C NMR (75 MHz, CD$_3$Cl): δ 175.2, 139.1, 134.8, 129.0, 126.4, 86.6, 51.8, 31.4, 28.9; IR (vcm^{-1}, KBr disc): 1786; HRMS (C$_{11}$H$_{10}$O$_2$Cl$_2$): Calc. (M+H): 245.0136, Found (M+H): 245.0138; [α]$_D^{20}$ = +26.6 ° (c = 0.67, CHCl$_3$).

III-70, 5-(Chloromethyl)-5-(4-methylphenyl)dihydrofuran-2(3*H*)-one
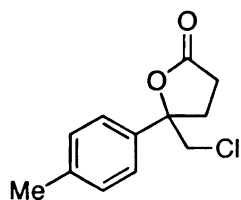
^{1}H NMR (300 MHz, CD$_3$Cl): δ 7.30 (m, 4H), 3.86 (d, *J* = 12.0 Hz, 1H), 3.78 (d, *J* = 12 Hz, 1H), 2.83 (m, 2H), 2.56 (m, 2H), 2.40 (s, 3H); ^{13}C NMR (75 MHz, CD$_3$Cl): δ 175.7, 138.6, 137.6, 129.5, 124.8, 87.1, 52.1, 31.3, 29.0, 21.0; IR (vcm^{-1}, KBr disc): 1786; HRMS (C$_{12}$H$_{13}$O$_2$Cl): Calc. (M+H): 225.0682, Found (M+H): 225.0679; [α]$_D^{20}$ = +22.9 ° (c = 0.73, CHCl$_3$).

III-71, 5-(Chloromethyl)-5-(4-fluorophenyl)dihydrofuran-2(3*H*)-one
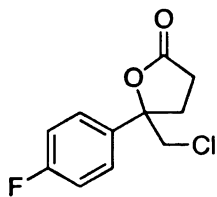
^{1}H NMR (300 MHz, CD$_3$Cl): δ 7.38 (m, 2H), 7.08 (m, 2H), 3.79 (d, *J* = 12 Hz, 1H), 3.71 (d, *J* = 12 Hz, 1H) 2.78 (m, 2H), 2.50 (m, 2H); ^{13}C NMR (75 MHz, CD$_3$Cl): δ 175.3, 162.6 (d, $^1J_{C,F}$ = 247 Hz), 136.4, 126.8 (d, $^3J_{C,F}$ = 8.6 Hz), 115.7 (d, $^2J_{C,F}$ = 21.2 Hz), 86.6, 52.0, 31.4, 28.9; IR (vcm^{-1}, KBr disc): 1786; HRMS (C$_{11}$H$_{10}$O$_2$ClF): Calc. (M+H): 229.0432, Found (M+H): 229.0436; [α]$_D^{20}$ = +29.4 ° (c = 0.57, CHCl$_3$).

III-72, 5-(Chloromethyl)-5-(naphthalen-2-yl)dihydrofuran-2(3*H*)-one
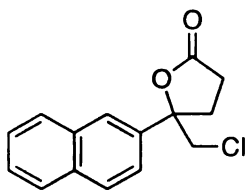
^{1}H NMR (300 MHz, CD$_3$Cl): δ 7.86 (m, 4H), 7.52 (m, 2H), 7.42 (m, 1H), 3.91 (d, *J* = 12.3 Hz , 1H), 3.86 (d, *J* = 12.3 Hz, 1H), 2.87 (m, 2H), 2.59 (m, 2H); ^{13}C NMR (75 MHz, CD$_3$Cl): δ 175.7, 137.7, 133.0, 132.9, 128.9, 128.3, 127.6, 126.9, 124.2, 122.3, 87.2, 52.0, 31.4, 29.0; IR (vcm^{-1}, KBr disc): 1782; HRMS (C$_{15}$H$_{13}$O$_2$Cl): Calc. (M+H): 261.0682, Found (M+H): 261.0677; [α]$_D^{20}$ = +8.4 ° (c = 0.61, CHCl$_3$).

III-73, 5-(Biphenyl-4-yl)-5-(chloromethyl)dihydrofuran-2(3*H*)-one
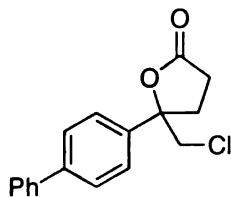
^{1}H NMR (300 MHz, CD$_3$Cl): δ 7.58 (m, 4H), 7.42 (m, 5H), 3.87 (d, *J* = 12 Hz, 1H), 3.79 (d, *J* = 12 Hz, 1H), 2.83 (m, 2H), 2.56 (m, 2H); ^{13}C NMR (75 MHz, CD$_3$Cl): δ 175.6, 141.6, 140.0, 139.5, 128.9, 127.7, 127.5, 127.1, 125.4, 87.0, 52.1, 31.4, 29.0; IR (vcm^{-1}, KBr disc): 1784; HRMS (C$_{17}$H$_{15}$O$_2$Cl): Calc. (M+H): 287.0839, Found (M+H): 287.0830; [α]$_D^{20}$ = +14.4 ° (c = 1.01, CHCl$_3$); mp = 135-137 °C.

III-74, 5-(Chloromethyl)-5-(4-(trifluoromethyl)phenyl)dihydrofuran-2(3*H*)-one
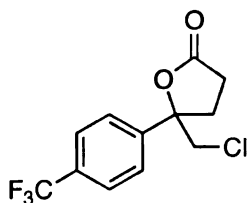
^{1}H NMR (300 MHz, CD$_3$Cl): δ 7.66 (m, 2H), 7.53 (m, 2H), 3.82 (d, *J* =12.3 Hz, 1H), 3.75 (d, *J* = 12.3 Hz, 1H), 2.82 (m, 2H), 2.53 (m, 2H); ^{13}C NMR (75 MHz, CD$_3$Cl): δ 175.0, 144.5 (q, $^4J_{C,F}$ = 1.7 Hz), 131.0 (q, $^2J_{C,F}$ = 32.6 Hz), 125.9 (q, $^3J_{C,F}$ = 3.5 Hz), 125.5, 123.7 (q, $^1J_{C,F}$ = 271 Hz), 86.5, 51.7, 31.5, 28.8; IR (vcm^{-1}, KBr disc): 1788; HRMS (C$_{12}$H$_{10}$O$_2$ClF$_3$): Calc. (M+H): 279.0400, Found (M+H): 279.0399; [α]$_D^{20}$ = +27.9 ° (c = 1.02, CHCl$_3$).

III-75, 5-(Chloromethyl)-5-cyclohexyldihydrofuran-2(3*H*)-one
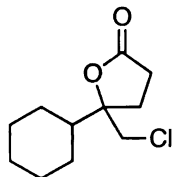
^{1}H NMR (300 MHz, CD$_3$Cl): δ 3.72 (d, *J* = 11.7 Hz, 1H), 3.65 (d, *J* = 11.7 Hz, 1H),

2.71 (m, 1H), 2.51 (m, 1H), 2.17 (m, 2H), 1.73 (m, 6H), 1.16 (m, 5H); ^{13}C NMR

(75 MHz, CD$_3$Cl): δ 176.5, 88.8, 49.8, 45.4, 29.5, 26.8, 26.5, 26.0; IR (vcm^{-1}, KBr

disc): 1774; HRMS (C$_{11}$H$_{17}$O$_2$Cl): Calc. (M+Na): 239.0815, Found (M+Na):

239.081; [α]$_D^{20}$ = -1.9 ˚ (c = 0.49, CHCl$_3$).

Methods for Enantiomer Separation

The enantiomers for all lactone products were separated on a Supelco

GAMMA DEX 225 fused silica gel capillary column (30m X 0.25mm X 0.25μm

film thickness) except for *para*-methylphenyl lactone **III-70**. Lactone **III-70** was

separated by chiral HPLC as indicated below. Listed below is the separation

protocol for each of the lactones depicted in Table III-21 as well as lactone **III-2**.

III-3, 5-(Bromomethyl)-5-phenyldihydrofuran-2(3*H*)-one:

Chiralcel OD-H; 5% *iso*-propyl alcohol in hexanes; 0.8 mL/min; 254 nm; RT$_1$ =

24.38 min, RT$_2$ = 27.42 min

III-43, 5-(Chloromethyl)-5-phenyldihydrofuran-2(3*H*)-one:

GAMMA DEX 225; 90 °C for 2 min, 90 °C to 180 °C ramp (1 °C/min), 180 °C for 1 min, 180 °C to 200 °C ramp (0.5 °C/min), 200 °C for 15 min; RT_1 = 101.96 min, RT_2 = 102.70 min.

III-68, 5-(Chloromethyl)-5-(4-methoxyphenyl)dihydrofuran-2(3*H*)-one:

GAMMA DEX 225; 90 °C for 2 min, 90 °C to 220 °C ramp (1 °C/min), 220 °C for 30 min; RT_1 = 125.74 min, RT_2 = 126.42 min.

III-69, 5-(Chloromethyl)-5-(4-chlorophenyl)dihydrofuran-2(3*H*)-one:

GAMMA DEX 225; 90 °C for 2 min, 90 °C to 220 °C ramp (10 °C/min), 220 °C for 30 min; RT_1 = 32.01 min, RT_2 = 32.44 min.

III-70, 5-(Chloromethyl)-5-(4-methylphenyl)dihydrofuran-2(3*H*)-one:

Chiralpak AS-H; 15% ethanol in hexanes; 1 mL/min; 254 nm; RT_1 = 9.91 min, RT_2 = 14.10 min.

III-71, 5-(Chloromethyl)-5-(4-fluorophenyl)dihydrofuran-2(3*H*)-one:

GAMMA DEX 225; 90 °C for 2 min, 90 °C to 220 °C ramp (5 °C/min), 220 °C for 15 min; RT_1 = 32.93 min, RT_2 = 33.25 min.

III-72, 5-(Chloromethyl)-5-(naphthalen-2-yl)dihydrofuran-2(3*H*)-one:

GAMMA DEX 225; 90 °C for 2 min, 90 °C to 225 °C ramp (1 °C/min), 225 °C for

120 min; RT_1 = 158.11 min, RT_2 = 158.91 min.

III-73, 5-(Biphenyl-4-yl)-5-(chloromethyl)dihydrofuran-2(3*H*)-one:

GAMMA DEX 225; 90 °C for 2 min, 90 °C to 225 °C ramp (1 °C/min), 225 °C for

120 min; RT_1 = 201.17 min, RT_2 = 202.69 min.

III-74, 5-(Chloromethyl)-5-(4-(trifluoromethyl)phenyl)dihydrofuran-2(3*H*)-one:

GAMMA DEX 225; 90 °C for 2 min, 90 °C to 220 °C ramp (10 °C/min), 220 °C for

15 min; RT_1 = 23.2 min, RT_2 = 23.8 min.

III-75, 5-(Chloromethyl)-5-cyclohexyldihydrofuran-2(3*H*)-one:

GAMMA DEX 225; 90 °C for 2 min, 90 °C to 220 °C ramp (2 °C/min), 220 °C for

30 min; RT_1 = 63.15 min, RT_2 = 63.52 min.

Preparation of Alkenoic Acid Substrates (Figure III-5)

All of the alkenoic acids in this chapter (compound **III-2** and those shown

in Figure III-5) were prepared by a Wittig methylenation/saponification sequence

except for *para*-chloro compound **III-61** and *para*-trifluoromethyl compound **III-66**.

These compounds were generated by Suzuki coupling as described by Wirth and

co-workers.[44] All known compounds had ^{1}H and ^{13}C NMR spectra in complete

agreement with previous reports. The Wittig methylenation/saponification

sequence for the preparation of **III-2** is presented below and can be regarded as a general protocol for the transformation.

Preparation of 4-phenyl-4-pentenoic acid (III-2)

Methyltriphenylphosphonium bromide (1.96 g, 5.6 mmol, 1.08 equivalent) was suspended in freshly distilled toluene (30 mL) and cooled to *ca.* 0 °C on an ice bath. Sodium bis(trimethylsilyl)amide (5.4 mL, 5.4 mmol, 1.04 equivalents, 1 M solution in THF) was added dropwise by syringe and the resulting solution was stirred for 30 minutes. The solution was then lowered to -78 °C and methyl 3-benzoylpropionate (1.0 g, 5.2 mmol, 1 equivalent) was added dropwise by syringe. The resulting solution was then stirred while warming to room temperature. The reaction mixture was then refluxed for 40 hours. On cooling, the reaction was quenched by the addition of saturated ammonium chloride (40 mL) and the resulting slurry was diluted with 50 mL of water and extracted with ethyl acetate (3X 50 mL). The combined organics were washed with brine (100 mL), dried over anhydrous Na_2SO_4, and concentrated by rotary evaporation. The residue was purifed by column chromatography on silica gel (10% ethyl acetate in hexanes) to give 762 mg (77% yield) of the desired methyl 4-phenylpent-4-enoate. This substance was used immediately without characterization in the following saponification reaction.

The ester (536 mg, 2.82 mmol, 1 equivalent) was dissolved in THF (20 mL) and cooled to *ca.* 0 °C on an ice bath. A solution of lithium hydroxide monohydrate (600 mg, 14.30 mmol, 5.07 equivalents) in 20 mL of water was

added dropwise over about 5 minutes via an addition funnel. The resulting solution was allowed to warm to room temperature while stirring for 18 hours. The solution was acidified to pH <4 with 1N HCl and then extracted with diethyl ether (3X 20 mL). The combined organics were then washed with water (60 mL) and brine (60 mL), and then dried over anhydrous Na_2SO_4. The organics were concentrated by rotary evaporation to give the desired compound **III-2** (467 mg, 94% yield). This crude isolate was sufficiently pure by ^{1}H and ^{13}C NMR analysis.

Analytical Data for Alkenoic Acids (III-2 and III-60 through III-67)

III-2, 4-Phenyl-4-pentenoic acid[3]
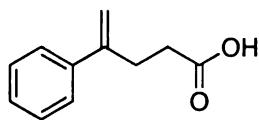
^{1}H NMR (300 MHz, acetone-d_6): δ 7.46 (m, 2H), 7.37-7.27 (m, 3H), 5.32 (m, 1H), 5.12 (m, 1H), 2.82 (m, 2H), 2.46 (m, 2H); ^{13}C NMR (75 MHz, acetone-d_6): δ 171.2, 148.1, 141.5, 129.2, 128.4, 126.8, 112.7, 33.2, 30.9.

III-60, 4-(4-Methoxypheny)-4-pentenoic acid[70]
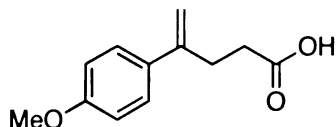
^{1}H NMR (300 MHz, CDCl$_3$): δ 7.33 (m, 2H), 6.85 (m, 2H), 5.23 (s, 1H), 5.00 (m, 1H), 3.80 (s, 3H), 2.80 (m, 2H), 2.51 (m, 2H); ^{13}C NMR (75 MHz, DMSO-d_6): δ 173.9, 158.9, 145.8, 132.4, 126.9, 113.8, 110.6, 55.1, 32.7, 29.7.

III-61, 4-(4-Chlorophenyl)-4-pentenoic acid[70,44]
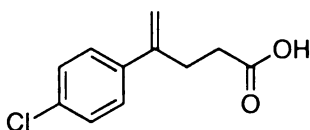
^{1}H NMR (300 MHz, CDCl$_3$): δ 7.30 (m, 4H), 5.30 (s, 1H), 5.10 (m, 1H), 2.80 (t, J = 7.2 Hz, 2H), 2.51 (m, 2H); ^{13}C NMR (75 MHz, CDCl$_3$): δ 179.2, 145.4, 138.8, 133.5, 128.6, 127.4, 113.5, 32.8, 30.0.

III-62, 4-(4-Methylphenyl)-4-pentenoic acid[70]
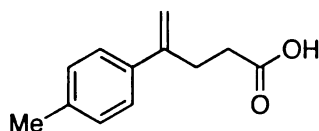
^{1}H NMR (300 MHz, CDCl$_3$): δ 7.31 (d, J = 8.0 Hz, 2H), 7.15 (d, J = 8.0 Hz, 2H), 5.31 (s, 1H), 5.08 (s, 1H), 2.85 (t, J = 7.2 Hz, 2H), 2.54 (t, J = 7.2 Hz, 2H), 2.36

(s, 3H); ^{13}C NMR (75 MHz, CDCl$_3$): δ 179.8, 146.2, 137.42, 137.37, 129.1, 125.9, 112.1, 33.0, 30.1, 21.0.

III-63, 4-(4-Fluorophenyl)-4-pentenoic acid[71]
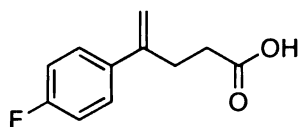
^{1}H NMR (300 MHz, CDCl$_3$): δ 7.35 (m, 2H), 7.01 (m, 2H), 5.25 (s, 1H), 5.08 (s, 1H), 2.80 (t, J = 6.9 Hz, 2H), 2.51 (m, 2H); ^{13}C NMR (75 MHz, CDCl$_3$): δ 179.4, 162.4 (d, $^1J_{C,F}$ = 245.3 Hz), 145.5, 136.5, 127.7 (d, $^3J_{C,F}$ = 8.0 Hz), 115.2 (d, $^2J_{C,F}$ = 21.2 Hz), 112.9, 32.8, 30.2.

III-64, 4-(Naphthalen-2-yl)-4-pentenoic acid
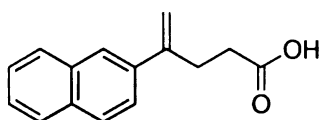
^{1}H NMR (300 MHz, CDCl$_3$): δ 7.82 (m, 4H), 7.55 (m, 1H), 7.46 (m, 2H), 5.47 (s, 1H), 5.21 (m, 1H), 2.96 (t, J = 7.5 Hz, 2H), 2.58 (m, 2H); ^{13}C NMR (75 MHz, CDCl$_3$): δ 179.3, 146.3, 137.6, 133.3, 132.9, 128.2, 128.0, 127.5, 126.2, 126.0, 124.7, 124.5, 113.5, 33.0, 30.1; IR (vcm^{-1}, KBr): 3054, 1699; HRMS (C$_{15}$H$_{14}$O$_2$), Calc. (M+H): 227.1072, Found (M+H): 227.1065; mp = 116-118 °C.

III-65, 4-(Biphenyl-4-yl)-4-pentenoic acid
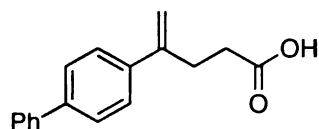
^{1}H NMR (300 MHz, DMSO-d_6): δ 7.70-7.30 (br m, 9H), 5.41 (s, 1H), 5.11 (s, 1H), 2.76 (m, 2H), 2.34 (m, 2H); ^{13}C NMR (75 MHz, DMSO-d_6): δ 173.8, 145.9, 139.6, 139.3, 139.0, 129.0, 127.5, 126.7, 126.5, 126.3, 112.5, 32.7, 29.6; IR (vcm^{-1}, KBr): 3048, 1895; HRMS ($C_{17}H_{16}O_2$), Calc. (M+H): 253.1229, Found (M+H): 253.1222; mp = 180-182 °C.

III-66, 4-(4-Trifluoromethylphenyl)-4-pentenoic acid[70,44]
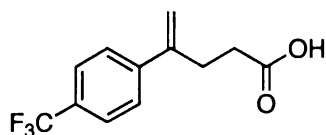
^{1}H NMR (300 MHz, CDCl$_3$): δ 7.65 (m, 2H), 7.55 (m, 2H), 5.45 (s, 1H), 5.27 (s, 1H), 2.91 (m, 2H), 2.59 (m, 2H); ^{13}C NMR (75 MHz, CDCl$_3$): δ 179.4, 145.4, 144.4, 129.7 (q, $^2J_{C,F}$ = 32 Hz), 126.4, 125.4 (q, $^3J_{C,F}$ = 4 Hz), 124.1 (q, $^1J_{C,F}$ = 270 Hz), 114.9, 32.7, 29.9.

III-67, 4-Cyclohexyl-4-pentenoic acid
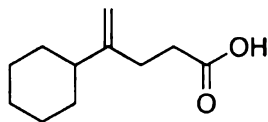
^{1}H NMR (300 MHz, CDCl$_3$): δ 4.75 (m, 1H), 4.66 (m, 1H), 2.50 (m, 2H), 2.35 (m, 2H), 1.72 (m, 6H), 1.15 (m, 5H); ^{13}C NMR (75 MHz, CDCl$_3$): δ 180.2, 153.1, 107.2, 44.5, 32.8, 32.3, 29.1, 26.7, 26.4; IR (νcm^{-1}, KBr): 3090, 1716; HRMS (C$_{11}$H$_{18}$O$_2$), Calc. (M+H): 183.1385, Found (M+H): 183.1379.

3.5: References

1. Ahmad, S. M.; Braddock, D. C.; Cansell, G.; Hermitage, S. A. *Tetrahedron Lett.* **2007,** *48*, 915-918.

2. Ahmad, S. M.; Braddock, D. C.; Cansell, G.; Hermitage, S. A.; Redmond, J. M.; White, A. J. P. *Tetrahedron Lett.* **2007,** *48*, 5948-5952.

3. Braddock, D. C.; Cansell, G.; Hermitage, S. A. *Chem. Commun.* **2006,** 2483-2485.

4. Braddock, D. C.; Cansell, G.; Hermitage, S. A.; White, A. J. P. *Chem. Commun.* **2006,** 1442-1444.

5. Kizirian, J. C. *Chem. Rev.* **2008,** *108*, 140-205.

6. Corey, E. J.; Imwinkelried, R.; Pikul, S.; Xiang, Y. B. *J. Am. Chem. Soc.* **1989,** *111*, 5493-5495.

7. Brown, K. J.; Berry, M. S.; Murdoch, J. R. *J. Org. Chem.* **1985,** *50*, 4345-4349.

8. Enders, D.; Kipphardt, H.; Gerdes, P.; Brenavalle, L. J.; Bhushan, V. *Bull. Soc. Chim. Belg.* **1988,** *97*, 691-704.

9. Bailey, D. J.; Ohagan, D.; Tavasli, M. *Tetrahedron: Asymmetry* **1997,** *8*, 149-153.

10. Dalko, P. I.; Moisan, L. *Angew. Chem., Int. Ed.* **2001,** *40*, 3726-3748.

11. Dalko, P. I.; Moisan, L. *Angew. Chem., Int. Ed.* **2004,** *43*, 5138-5175.

12. Kolb, H. C.; Vannieuwenhze, M. S.; Sharpless, K. B. *Chem. Rev.* **1994,** *94*, 2483-2547.

13. Kacprzak, K.; Gawronski, J. *Synthesis* **2001,** 961-998.

14. France, S.; Guerin, D. J.; Miller, S. J.; Lectka, T. *Chem. Rev.* **2003,** *103*, 2985-3012.

15. Lowenthal, R. E.; Abiko, A.; Masamune, S. *Tetrahedron Lett.* **1990,** *31*, 6005-6008.

16. Evans, D. A.; Woerpel, K. A.; Hinman, M. M.; Faul, M. M. *J. Am. Chem. Soc.* **1991,** *113*, 726-728.

17. Nishiyama, H.; Sakaguchi, H.; Nakamura, T.; Horihata, M.; Kondo, M.; Itoh, K. *Organometallics* **1989,** *8*, 846-848.

18. Miyashita, A.; Yasuda, A.; Takaya, H.; Toriumi, K.; Ito, T.; Souchi, T.; Noyori, R. *J. Am. Chem. Soc.* **1980,** *102*, 7932-7934.

19. Noyori, R. *Acta Chem. Scand.* **1996,** *50*, 380-390.

20. Seebach, D.; Beck, A. K.; Heckel, A. *Angew. Chem., Int. Ed.* **2001,** *40*, 92-138.

21. Kyba, E. P.; Gokel, G. W.; Dejong, F.; Koga, K.; Sousa, L. R.; Siegel, M. G.; Kaplan, L.; Sogah, G. D. Y.; Cram, D. J. *J. Org. Chem.* **1977,** *42*, 4173-4184.

22. Noyori, R.; Tomino, I.; Tanimoto, Y.; Nishizawa, M. *J. Am. Chem. Soc.* **1984,** *106*, 6709-6716.

23. Noyori, R.; Tomino, I.; Yamada, M.; Nishizawa, M. *J. Am. Chem. Soc.* **1984,** *106*, 6717-6725.

24. Bao, J. M.; Wulff, W. D.; Dominy, J. B.; Fumo, M. J.; Grant, E. B.; Rob, A. C.; Whitcomb, M. C.; Yeung, S. M.; Ostrander, R. L.; Rheingold, A. L. *J. Am. Chem. Soc.* **1996,** *118*, 3392-3405.

25. Zhang, Y.; Yeung, S. M.; Wu, H. Q.; Heller, D. P.; Wu, C. R.; Wulff, W. D. *Org. Lett.* **2003,** *5*, 1813-1816.

26. Su, Y.; Rabalakos, C.; Mitchell, W. D.; Wulff, W. D. *Org. Lett.* **2005,** *7*, 367-369.

27. Katsuki, T. *Synlett* **2003**, 281-297.

28. Uccello-Barretta, G.; Di Bari, L.; Salvadori, P. *Magn. Reson. Chem.* **1992,** *30*, 1054-1063.

29. Williams, T.; Pitcher, R. G.; Bommer, P.; Gutzwill.J; Uskokovi.M. *J. Am. Chem. Soc.* **1969,** *91*, 1871-1872.

30. Oliveto, E. P.; C., G. *Org. Synth. Coll.* **1963,** *4*, 104.

31. Zajc, B. *Synth. Commun.* **1999,** *29*, 1779-1784.

32. de Souza, S. P. L.; da Silva, J. F. M.; de Mattos, M. C. S. *Synth. Commun.* **2003**, *33*, 935-939.

33. Iranpoor, N.; Firouzabadi, H.; Shaterian, H. R. *J. Org. Chem.* **2002**, *67*, 2826-2830.

34. Iranpoor, N.; Firouzabadi, H.; Shaterian, H. R. *Tetrahedron Lett.* **2003**, *44*, 4769-4773.

35. Nonhebel, D. C. *J. Chem. Soc.* **1963**, 1216-1220.

36. Zhong, P.; Guo, M. P.; Huang, N. P. *Synth. Commun.* **2002**, *32*, 175-179.

37. Shaabani, A.; Teimouri, M. B.; Safaei, H. R. *Synth. Commun.* **2000**, *30*, 265-271.

38. Bosshard, H. H.; Mory, R.; Schmid, M.; Zollinger, H. *Helv. Chim. Acta* **1959**, *42*, 1653-1658.

39. Lopez-Cantarero, J.; Cid, M. B.; Poulsen, T. B.; Bella, M.; Ruano, J. L. G.; Jorgensen, K. A. *J. Org. Chem.* **2007**, *72*, 7062-7065.

40. Vogl, E. M.; Groger, H.; Shibasaki, M. *Angew. Chem., Int. Ed.* **1999**, *38*, 1570-1577.

41. Whitehead, D. C.; Staples, R. J.; Borhan, B. *Tetrahedron Lett.* **2009**, *50*, 656-658.

42. Prelog, V.; Wilhelm, M. *Helv. Chim. Acta* **1954**, *37*, 1634-1660.

43. Riant, O.; Kagan, H. B.; Ricard, L. *Tetrahedron* **1994**, *50*, 4543-4554.

44. Haas, J.; Bissmire, S.; Wirth, T. *Chem., Eur. J.* **2005**, *11*, 5777-5785.

45. Berkessel, A.; Groger, H. *Asymmetric Organocatalysis - From Biomimmetic Concepts to Applications in Asymmetric Synthesis*; Wiley-VCH: Morlenbach, 2005.

46. Ojima, I., Ed. *Catalytic Asymmetric Synthesis*, 2 ed.; Wiley-VCH: New York, 2000.

47. Corral, R. A.; Orazi, O. O. *J. Org. Chem.* **1963**, *28*, 1100-1104.

48. Tilstam, U.; Weinmann, H. *Org. Process Res. Dev.* **2002**, *6*, 384-393.

49. Hart, R. M.; Whitehead, M. A. *Trans. Faraday Soc.* **1971**, *67*, 1569-1575.

50. Nagao, Y.; Katagiri, S. *Chem. Lett.* **1991**, 1857-1858.

51. Nagao, Y.; Katagiri, S. *Chem. Lett.* **1993**, 1169-1170.

52. Nagao, Y. Katagiri, S. *Sci. Rep. Hirosaki Univ.* **1991,** *38*, 20-23.

53. Poleshchuk, O. K.; Makiej, K.; Ostafin, M.; Nogaj, B. *Magn. Reson. Chem.* **2001,** *39*, 329-333.

54. Taylor, M. S.; Jacobsen, E. N. *Angew. Chem., Int. Ed.* **2006,** *45*, 1520-1543.

55. Garnier, J. M.; Robin, S.; Rousseau, G. *Eur. J. Org. Chem.* **2007**, 3281-3291.

56. Peretto, I.; Forlani, R.; Fossati, C.; Giardina, G. A. M.; Giardini, A.; Guala, M.; La Porta, E.; Petrillo, P.; Radaelli, S.; Radice, L.; Raveglia, L. F.; Santoro, E.; Scudellaro, R.; Scarpitta, F.; Bigogno, C.; Misiano, P.; Dondio, G. M.; Rizzi, A.; Armani, E.; Amari, G.; Civelli, M.; Villetti, G.; Patacchini, R.; Bergamaschi, M.; Delcanale, M.; Salcedo, C.; Fernandez, A. G.; Imbimbo, B. P. *J. Med. Chem.* **2007,** *50*, 1571-1583.

57. Rodgers, T. R.; Lamontagne, M. P.; Markovac, A.; Ash, A. B. *J. Med. Chem.* **1977,** *20*, 591-594.

58. Ware, E. *Chem. Rev.* **1950,** *46*, 403-470.

59. Zaitsev, A. B.; Adolfsson, H. *Synthesis* **2006**, 1725-1756.

60. Corey, E. J.; Noe, M. C. *J. Am. Chem. Soc.* **1996,** *118*, 11038-11053.

61. Corey, E. J.; Noe, M. C.; Sarshar, S. *J. Am. Chem. Soc.* **1993,** *115*, 3828-3829.

62. Becker, H.; King, S. B.; Taniguchi, M.; Vanhessche, K. P. M.; Sharpless, K. B. *J. Org. Chem.* **1995,** *60*, 3940-3941.

63. Arrington, M. P.; Bennani, Y. L.; Gobel, T.; Walsh, P.; Zhao, S. H.; Sharpless, K. B. *Tetrahedron Lett.* **1993,** *34*, 7375-7378.

64. Bennani, Y. L.; Vanhessche, K. P. M.; Sharpless, K. B. *Tetrahedron: Asymmetry* **1994,** *5*, 1473-1476.

65. Kolb, H. C.; Bennani, Y. L.; Sharpless, K. B. *Tetrahedron: Asymmetry* **1993,** *4*, 133-141.

66. Corey, E. J.; Noe, M. C.; Lin, S. Z. *Tetrahedron Lett.* **1995,** *36*, 8741-8744.

67. Corey, E. J.; Zhang, J. H. *Org. Lett.* **2001,** *3*, 3211-3214.

68. Corey, E. J.; Noe, M. C. *J. Am. Chem. Soc.* **1993,** *115*, 12579-12580.

69. Lohray, B. B.; Singh, S. K.; Bhushan, V. *Indian J. Chem. Sect B-Org. Chem. Incl. Med. Chem.* **2002,** *41*, 1226-1233.

70. Haas, J.; Piguel, S.; Wirth, T. *Org. Lett.* **2002,** *4*, 297-300.

71. Takemiya, A.; Hartwig, J. F. *J. Am. Chem. Soc.* **2006,** *128*, 6042-6043.

Chapter 4: A TCCA-Mediated Preparation of N-Chlorinated Hydantoins

4.1: Introduction

Several reagents have been developed for use as organic sources of chlorenium ion (Cl$^+$) in lieu of employing elemental chlorine. The operational advantages of such an approach include ease of handling, more precise control of chlorenium stoichiometry relative to substrate, reduced toxicity, and attenuated reactivity relative to molecular chlorine. Four examples of organochlorenium sources are N-chlorosuccinimide (NCS, **IV-1**), chloramine-T **(IV-2)**, trichloroisocyanuric acid (TCCA, **IV-3**), and 1,3-dichloro-5,5-dimethylhydantoin (DCDMH, **IV-4**).

Figure IV-1. Various organochlorenium sources: NCS, chloramine-T, TCCA, and DCDMH

IV-1   IV-2   IV-3   IV-4
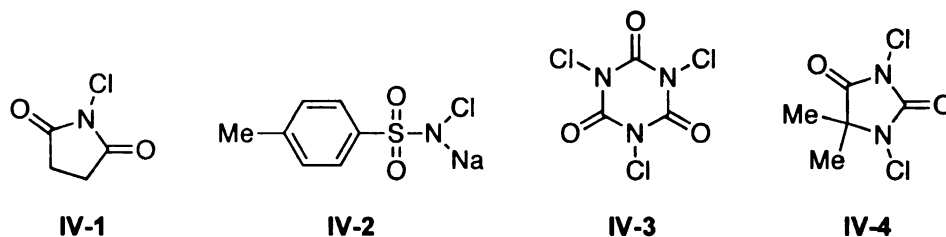
Of the four, NCS has undoubtedly been the most popular organic chlorenium equivalent, finding use in a wide range of chlorination and oxidation reactions.[1] Although primarily employed as an oxidant or nucleophilic nitrogen source, chloramine-T has been employed in a few reports as a source of chlorenium ion in acid.[2] The use of TCCA has been recently reviewed, but its wide-spread use as a chlorenium source is somewhat tempered by its enhanced reactivity relative to NCS. For example, TCCA is known to chlorinate esters and cyclic ethers such as THF and dioxane. Furthermore, it oxidizes aliphatic ethers

to their corresponding esters. This reactivity profile limits the application of TCCA in a number of common solvents.[3] DCDMH has been employed much less frequently than NCS, and reports of its use as an chlorenium source and oxidant in organic transformations have begun to emerge only relatively recently.

With respect to reactivity, DCDMH is couched in between TCCA and NCS. In fact, the enhanced reactivity of DCDMH relative to NCS proved crucial in the optimization of the $(DHQD)_2PHAL$ mediated chlorolactonization reaction discussed earlier (See Chapter 3). The magnitude of the ^{35}Cl nuclear quadrupole resonance (NQR) frequency has been invoked as a quantitative marker for the chlorenium (Cl^+) character of an N-Cl covalent bond (i.e. a larger NQR frequency corresponds to a larger Cl^+ character).[4-7]

In 1991, Nagao and Katagiri measured the ^{35}Cl NQR frequencies for NCS, DCDMH, and TCCA (Scheme IV-1). TCCA was found to have the largest NQR frequency (58.902 MHz), indicating that its N-Cl bond possessed the most chlorenium character. DCDMH, possessing two non-equivalent N-Cl moieties, resonated at 55.960 MHz and 53.639 MHz. The larger of these two values is due to the imide N-Cl bond (N-3), and is larger than the frequency of the imide N-Cl bond of NCS (54.095 MHz). This result is indicative of the fact that the chlorine atom at N-3 of DCDMH possesses a larger degree of chlorenium character, and should therefore be more reactive than that found in NCS. Supposing that more chlorenium character would translate into an enhanced Cl donation ability, the authors correctly predicted that TCCA ought to serve as a chlorine source for the halogenation of succinimide (IV-5) and 5,5-

dimethylhydantoin (**IV-6**). In the event, NCS and DCDMH were produced in 92

and 87% yield, respectively, on treatment with TCCA.[6]

Scheme IV-1. 35-Cl NQR measurements and TCCA chlorinations
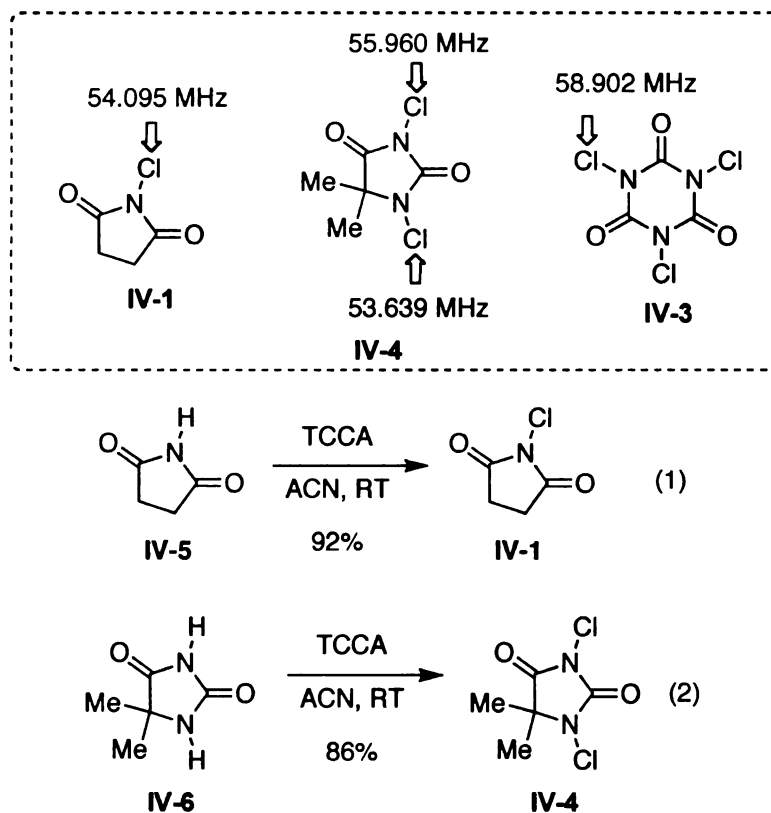
The use of N-chlorinated hydantoins in organic synthesis has been

relatively limited as compared to the more frequently employed NCS. What

follows is a brief review of several applications of N-chlorinated hydantoins.

DCDMH is currently the only commercially available member of this reagent

class, and as such has received the largest amount of attention from the

synthetic community.

DCDMH has been employed as a chlorenium source for various

transformations including the α-chlorination of acetophenones[8], the α-

221

chlorination of 1-aryl-2-pyrazolin-5-ones,[9] the preparation of chlorohydrin

derivatives of corticosteroids,[10] and the benzylic chlorination of 2-

methylpyrazine.[11] Moreover, DCDMH was employed to trap an enolate resulting

from dimethylzinc attack on an α,β-unsaturated ketone thus generating an α-

chloro-β-methyl ketone functionality *en route* to a building block of Amphotericin

B.[12]

Researchers at Abbott Laboratories successfully utilized DCDMH for a

late stage, selective chlorination of a heavily functionalized quinolone derivative

during the preparation of the antibiotic ABT-492 (Scheme IV-2, eq. 1).[13] Initially,

sulfuryl chloride was employed for the transformation, but the researchers

deferred to the milder DCDMH in order to circumvent the formation of a small,

Scheme IV-2. Select examples of DCDMH mediated chlorinations.
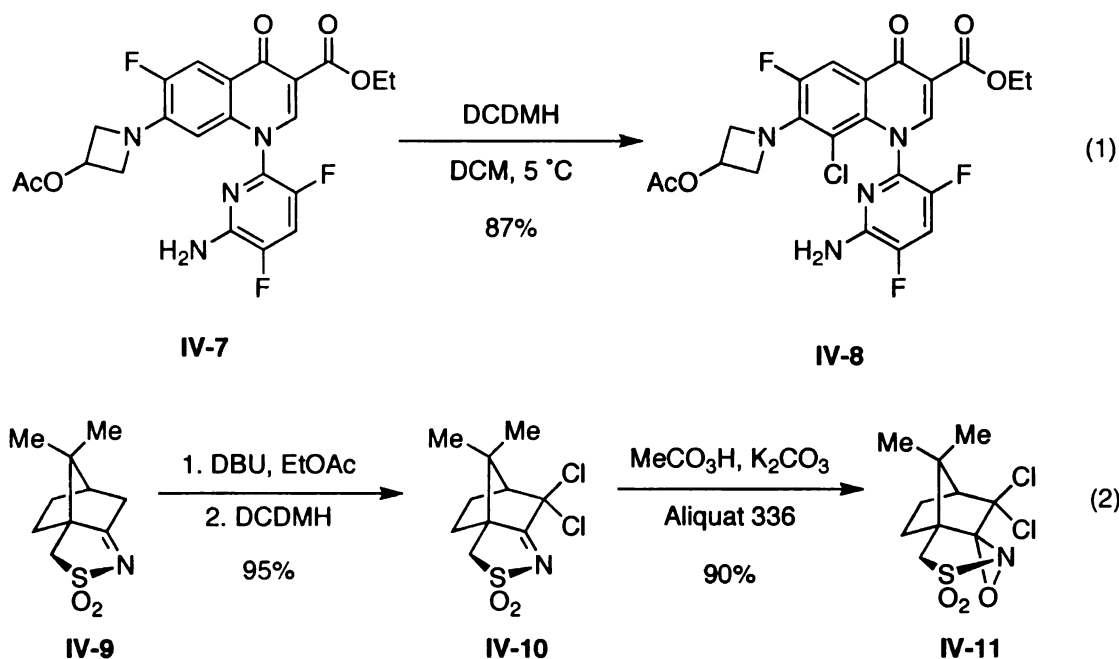
albeit inseperable portion of a by-product resulting from the ring opening of the azetidine.

Researchers at Schering Plough exploited the enhanced reactivity of DCDMH relative to NCS to improve upon the large-scale preparation of Davis' oxaziridine **IV-11** (Scheme IV-2, eq. 2).[14,15] Employing DCDMH in lieu of NCS allowed for the reaction to be conducted at room temperature in ethyl acetate, while employing DBU as the base. This protocol represented a significant operational improvement over the established methodology, whereby **IV-9** was deprotonated by NaHMDS at -78 ˚C in dilute anhydrous THF, and then cannulated into a -78 ˚C THF solution of NCS. The authors go on to note that the use of DCDMH significantly reduced the formation of multi-chlorinated by-products, thus obviating the necessity for chromatographic purification of **IV-10**.

In addition to its use as a chlorenium equivalent, DCDMH has also been employed as an oxidant for a number of transformations including the halodeboronation of aryl boronic acids,[16] the oxidation of urazoles to provide triazolinediones,[17] the microwave-assisted cleavage of oximes,[18] and the preparation of dialkyl chlorophosphates.[19] The compound can also serve as a mild oxidant in the presence of wet silica gel in the sodium nitrite-mediated nitration of phenols[20] and in the preparation of N-nitrosoamines.[21]

If chloramine-T is replaced with DCDMH as the terminal oxidant during the course of the Sharpless asymmetric aminohydroxylation (SAA)[22-24] one can produce chiral carbamate protected amino alcohols or oxazolidinones directly (Scheme IV-3). This is accomplished by utilizing DCDMH as the terminal oxidant

along with the appropriate urethane nitrogen source. Historically, when

carbamate based nitrogen nucleophiles were employed in the SAA reaction, *tert*-

butyl hypochlorite (*t*-BuOCl) was employed as the terminal oxidant.[22-24] Barta

and co-workers utilized DCDMH instead of *t*-BuOCl due to the fact that DCDMH

was a commercially available solid, whereas *t*-BuOCl had to be freshly prepared

each time prior to use.[25] Importantly, they noted that other more common

chlorenium based co-oxidants such as NCS and TCCA were unsuccessful. After

arriving at DCDMH as a suitable substitute for *t*-BuOCl, the conventional SAA

reaction was extended to a one-pot preparation of chiral oxazolidinones (Scheme

IV-3, eq. 1). Subsequently, McLeod and co-workers used a similar strategy to

prepare carbamate protected 4-amino-3-hydroxybutyric acid (GABOB)

precursors such as **IV-16** (eq. 2).[26]

Scheme IV-3. Application of DCDMH in the Sharpless asymmetric aminohydroxylation

224
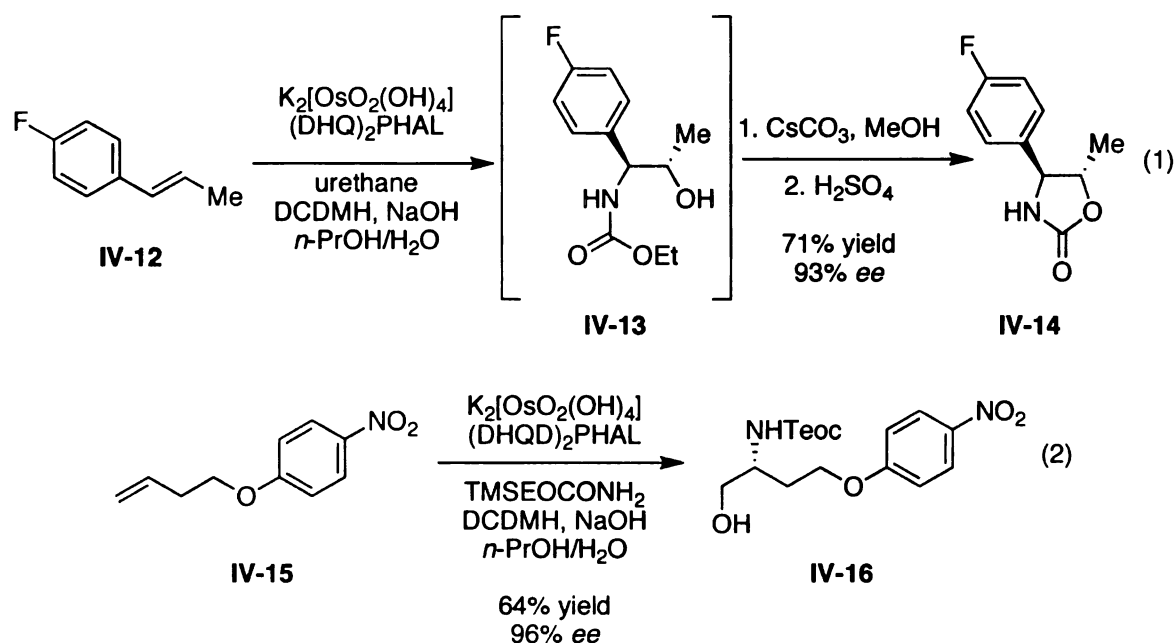
Furthermore, DCDMH has emerged as the reagent of choice for the activation, prior to loading, of silyl linkers for solid-phase organic synthesis.[27-30] Finally, DCDMH has been used as an oxidative activator of an iridium catalyst designed for the asymmetric hydrogenation of substituted quinolines.[31] Other uses for DCDMH include employment as redox titrants in non-aqueous media,[32] and as a cheap yet safe disinfectant and bactericide for municipal water sources.[33]

N-chlorinated hydantoins have also received attention from the pharmacological community. The myriad of adverse side-effects associated with hydantoin-based drugs such as the anti-convulsant Dilantin and the aldose reductase inhibitor Sorbinil have been attributed to N-chloro metabolites **IV-17** and **IV-18** generated *in vivo* via chlorination by myeloperoxidase and hydrogen peroxide (Figure IV-2).[34-36]

Figure IV-2. N-chloro metabolites of the hydantoin-based drugs Dilantin and Sorbinil.

Dilantin (Phenytoin)   **IV-17**   Sorbinil   **IV-18**
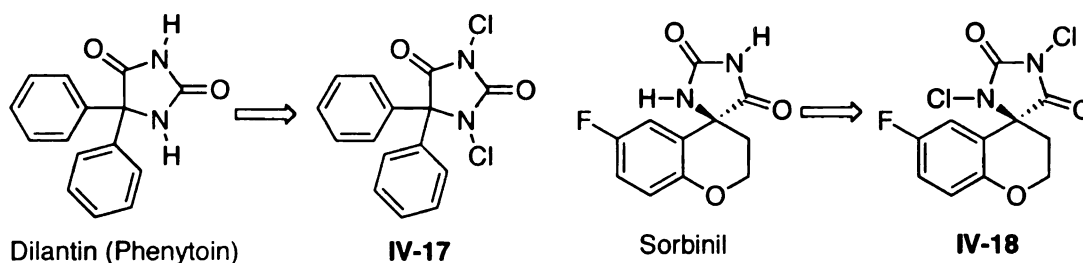
The relative lack of processes employing N-chlorinated hydantoins in organic synthesis is somewhat surprising. When one considers the structural features of N-chloro hydantoins, it becomes apparent that they offer at least the potential for exquisite tuning of the chlorenium source. Considering the generic N-chlorohydantoin represented in the dashed box of Scheme IV-4, one

recognizes that the potential exists for electronic or steric tuning of the chlorenium source by changing either or both substituents at C-5 (R^1 or R^2). Further tuning is available by electing to either alkylate or chlorinate the N-1 substituent (R^3). One can also imagine the preparation of chiral chlorenium sources for asymmetric applications via the utilization of C-5 chiral hydantoin starting materials.

Scheme IV-4. Structural diversity and preparation of N-chlorohydantoins
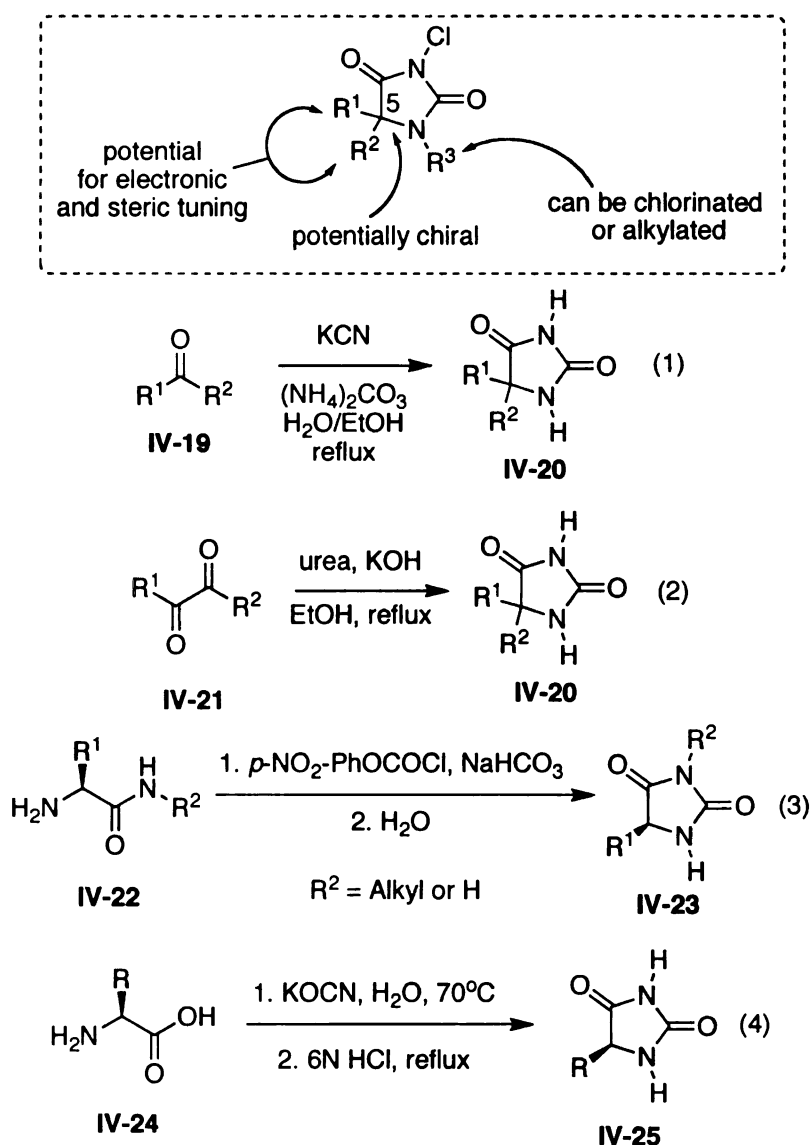
The preparation of the requisite hydantoin precursors is straightforward and has been known for nearly a century. Hydantoins that are disubstituted at C-5 (where R^1 and R^2 are not necessarily the same) can be prepared by the Bucher-Bergs methodology, whereby diaryl ketone **IV-19** is heated in the presence of potassium cyanide and ammonium carbonate (eq. 1).[37] Alternatively, C5 disubstituted hydantoins **IV-20** are prepared by refluxing 1,2-diketones with urea and potassium hydroxide (eq. 2).[38] The preparation of chiral hydantoins is also trivial, originating from readily available amino acid and amide starting materials. Chiral primary or secondary amino amides (**IV-22**) can be treated with *p*-nitrophenylchloroformate in dry acetonitrile, followed by the addition of water to provide chiral hydantoins (eq. 3).[39] Secondary amide starting materials return N-3 alkylated hydantoins such as **IV-23**, leaving the remaining N-1 for subsequent chlorination. In a different approach, chiral amino acids can be converted into their corresponding chiral hydantoin congeners **IV-25** on treatment with potassium cyanate followed by 6 N HCl (eq. 4).[40-42]

Realizing the potential for chlorenium source tunability inherent in the structural features of N-chlorinated hydantoins, we sought an operationally simple and high yielding preparation of these compounds. Moreover, having demonstrated the superiority of DCDMH relative to NCS in terms of both conversion at low temperature and enantiomeric excess in the course of our development of a new asymmetric chlorolactonization methodology, we were excited to prepare and evaluate other non-commercial N-chlorinated hydantoins in that transformation (See Chapter 3). We also noted that prior to our report[43]

discussed herein, there were no examples of the preparation of chiral N-chlorinated hydantoins, except for the preparation of the Sorbinil metabolite **IV-18** (Figure IV-2).[34]

A literature scan revealed that there are two classical methods for the preparation of N-chlorinated hydantoins (Scheme IV-5). One approach involves passing chlorine gas through an aqueous alkaline solution of hydantoin.[44] The toxicity and reactivity of elemental chlorine make this approach somewhat undesirable. In addition, this approach may not be amenable to the preparation of C-5 chiral N-chlorohydantoins due to the possibility of racemization. The second method involves treatment of the hydantoin with an aqueous sodium hypochlorite solution (Chlorox) followed by extraction.[45,34]

Scheme IV-5. Classical methods for the preparation of N-chlorhydantoins.

From elemental chlorine:
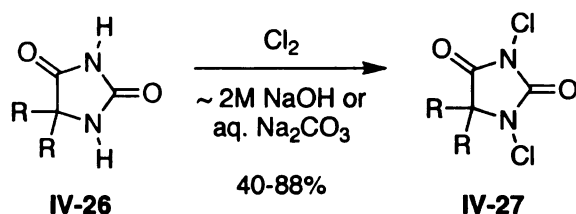
From bleach (NaOCl):
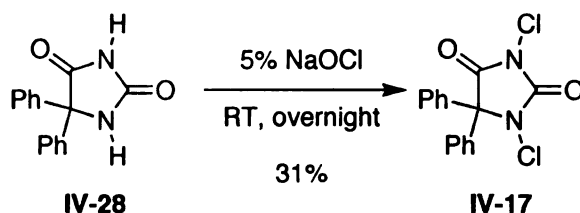
In initial experiments, the latter approach was met with difficulties when less substituted, more water-soluble hydantoins were employed. Dichloromethane extraction of the aqueous layer returned either starting material

or simply no recovered organic material. Given our desire to avoid the use of molecular chlorine, along with the difficulties encountered with the bleach protocol, we sought an alternative method for the chlorination of hydantoins.

Detailed below is account of these efforts which culminated in the development of an efficient protocol that allowed for the preparation of a number of N-chlorinated hydantoins, including some of the first examples of chiral N-chlorohydantoins. In addition we have assembled a compendium of hitherto scarce physical data for these compounds. Whereas historically, these compounds have been characterized only by melting point, elemental analysis, and sometimes ^{13}C NMR,[45,34] we decided to fully characterize these compounds, collecting ^1H and ^{13}C NMR, IR, elemental analysis, melting point, and optical rotation data (where appropriate) for all of the products isolated in this study. Importantly, we were also able to secure X-ray crystal structures for nine of the ten products presented herein (see Section 4.4 for details).

4.2: Results and Discussion

Faced with the difficulties of the classical methods depicted in Scheme IV-5 (*vide supra*), we returned to the isolated report by Nagao and Katagiri published in 1991 (Scheme IV-1, eq. 2).[6] As discussed above, these authors correctly predicted that compounds possessing N-Cl bonds with smaller ^{35}Cl NQR frequencies than that of TCCA, ought to suffer chlorination by action of the latter. Indeed, DCDMH was prepared in 87% yield on treatment with TCCA (Scheme IV-1, eq. 2). We elected to evaluate the scope and limitations of this

229

transformation, given that the initial report contained this singular example. It is also noteworthy that TCCA has been employed previously in the chlorination of various amides and carbamates, although hydantoins were not included in these studies.[46,47]

Close inspection of Nagao and Katagiri's experimental protocol revealed several operational complications including the purification of TCCA by recrystallization prior to use, employing distilled acetonitrile as the solvent, and purifying the product DCDMH by column chromatography followed by a subsequent recrystallization. At the outset, we sought to simplify the operation by shortening the reaction time (from 3 hours to 30 minutes) and by employing unpurified TCCA and undistilled acetonitrile. In addition, cognizant of the crystalline nature of N-chlorohydantoins,[34] we set out to avoid chromatographic purification, instead opting for product purification by recrystallization.

As indicated in Table IV-1, compound **IV-4** was isolated in 87% yield by adding TCCA (Aldrich) to a slurry of 5,5-dimethylhydantoin in undistilled acetonitrile, followed by stirring for 30 minutes and subsequent concentration. We found that the reduced byproducts of TCCA were readily removed on trituration of the isolate in chloroform followed by filtration of the filtrate through a 1 cm-thick pad of silica gel. On concentration, this crude isolate was easily purified by recrystallization from chloroform and hexanes. We found this methodology to be general, returning the desired chlorinated hydantoin products **IV-30** in good yields.

In addition to several examples of 5,5-disubstituted hydantoins (**IV-17**, **IV-31**, **IV-33**, and **IV-34**), 5-monosubstituted hydantoins (**IV-35** through **IV-38**) and unsusbstituted hydantoin **IV-32** were chlorinated without incident. The preparation of trialkylated compound **IV-33** confirms the ability to affect a mono-chlorination by employing one equivalent of TCCA. Of note is the fact that the relatively labile α-C5 of unsubstituted hydantoin **IV-32** as well as the benzylic positions of compounds **IV-34** and **IV-36** were not chlorinated under the reaction conditions.

Table IV-1. TCCA mediated chlorination of hydantoins
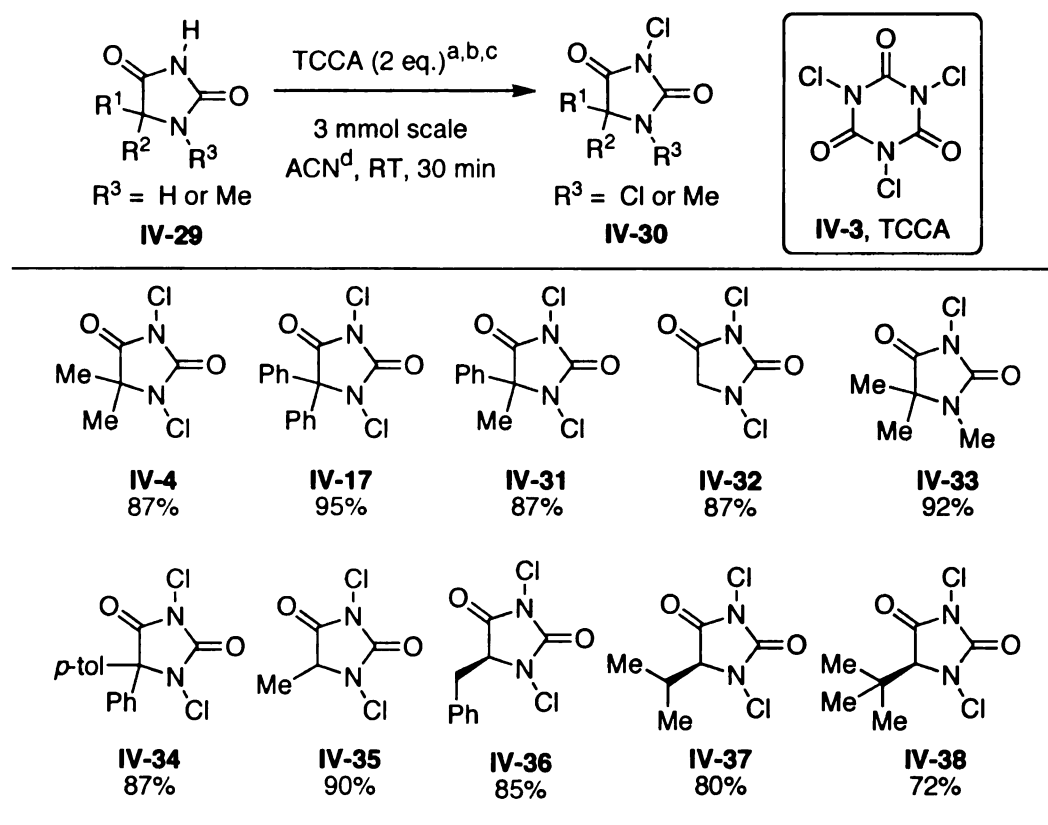
231

It is also noteworthy that in our hands compounds **IV-32** and **IV-33** were not isolated using the bleach protocol described in Scheme IV-5. The attempted chlorination of unsubstituted hydantoin led to the recovery of no organic material after extraction, while the starting 1,5,5-timethylhydantoin was recovered unchanged in the attempted preparation of **IV-33**.

Additionally, this methodology is compatible with chiral hydantoin starting materials, returning the desired chiral N,N-dichlorohydantoins (**IV-36**, **IV-37**, and **IV-38**). The parent chiral hydantoins were prepared in high enantiomeric purity (confirmed by optical rotation) from the corresponding chiral α-amino acids by known methodology (Scheme IV-6).[40-42] Electing to employ the potassium cyanate mediated cyclization of chiral amino acids, chiral hydantoins **IV-39**, **IV-40**, and **IV-41** were prepared from L-phenylalanine, L-valine, and L-*tert*-leucine, respectively. Importantly, reduction of the chiral N,N-dichlorohydantoins with

Scheme IV-6. The preparation of chiral hydantoins.

IV-24

IV-25

IV-39

91% yield
99% ee

IV-40

45% yield
99% ee

IV-41

79% yield
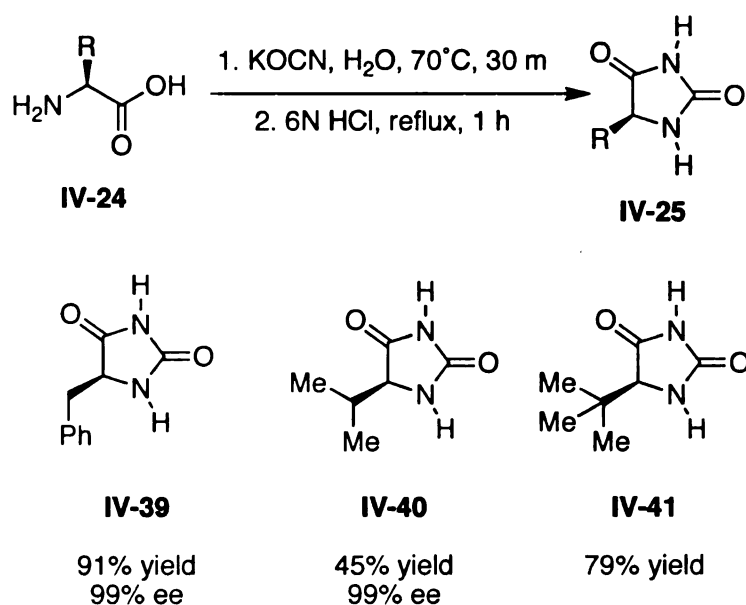
aqueous sodium sulfite returned enantiomerically pure parent hydantoins as judged by optical rotation (see Section 4.4 for details). The ready preparation of chiral hydantoin-based chlorenium sources may facilitate the discovery of new asymmetric halogenation reactions.

Realizing that one molar equivalent of TCCA harbors three chlorenium equivalents (Scheme IV-7, eq. 1), the net 3-fold excess of chlorenium source relative to the parent hydantoin when 2 molar equivalents of TCCA was employed seemed unnecessary. Hence, we set out to explore the fate of the reaction when substantially less TCCA was employed. As indicated in Scheme IV-7, equation 2, the amount of TCCA can be reduced as low as 0.7 molar equivalents (a 1:1 ratio of chlorenium relative to the number of hydantoin nitrogens) without substantial loss of yield. Given these results, we are in a position to recommend employing less than 1 molar equivalent of TCCA relative to the parent hydantoin.

Scheme IV-7. TCCA equivalency study.

TCCA	yield
2 eq.	95%
1 eq.	92%
0.7 eq.	90%
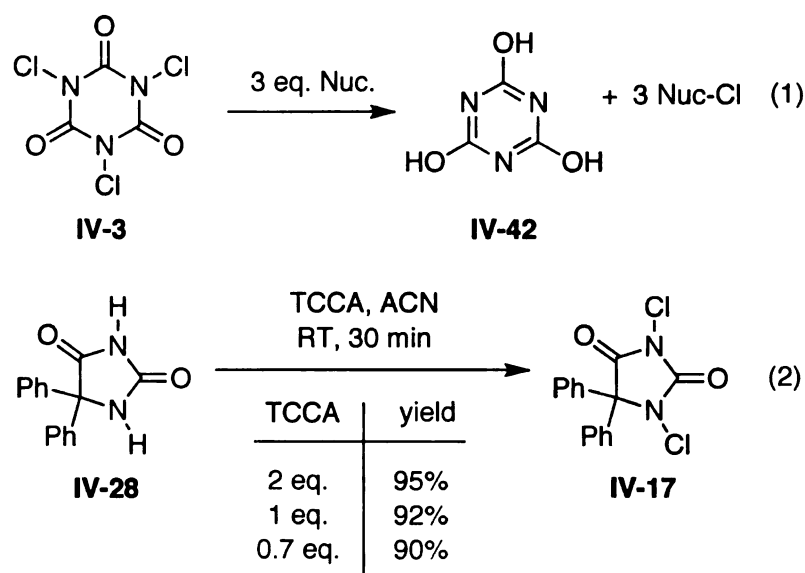
Additionally, these reactions can be conducted on large scale, as shown in Scheme IV-8. Diphenylhydantoin **IV-28** was chlorinated on a 33 mmole scale to return 8.72 g (82%) of 1,3-dichloro-5,5-diphenylhydantoin **IV-17**.

Scheme IV-8. Scaled preparation of **IV-17**.

IV-28

33 mmol

IV-17

82% yield
8.72 g isolated
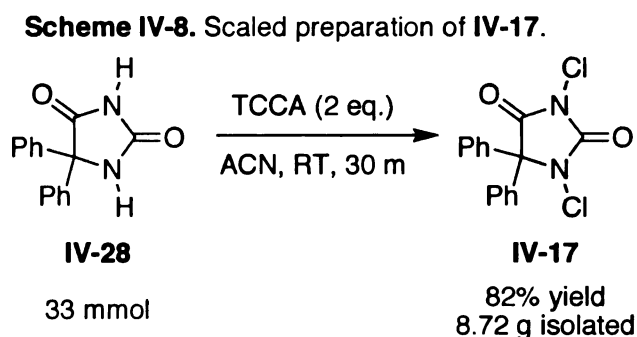
4.3. Conclusions and Future Directions

In conclusion, an operationally simple method for the preparation of a number of N-chlorinated hydantoins has been developed, using unpurified, commercially available TCCA in undistilled solvents. This methodology returns crystalline products in high yield without recourse to chromatographic purification, save a simple filtration step. The most exciting future direction of this project encompasses the development of new chiral N-chlorohydantoins for asymmetric applications. One can imagine several hydantoin-based scaffolds that incorporate a chlorenium equivalent couched within a chiral framework. The obivous starting point for this strategy will be utilizing the available chiral amino acid pool. Several potential scaffolds are delineated in Scheme IV-9. Scaffold **IV-43** is accessible by the sodium cyanate mediated cyclization of chiral amino acids (vide supra, Scheme IV-4, eq. 4).[40-42] This strategy has already been implemented, returning chiral N-chlorohydantoins **IV-36**, **IV-37**, and **IV-38**. This

particular arrangement may not be best suited for chiral applications since the most reactive N-3 chlorine is distal from the C-5 chiral center, while the proximal N-1 chlorine is less reactive (*i.e.* this N-Cl is approximately as labile as that found in NCS according to NQR resonance frequencies).[6] We envision two strategies to correct this issue. First, one could employ the *p*-nitrophenylchloroformate cyclization strategy to prepare reagents of the general scaffold described in structure **IV-44** by cyclizing chiral secondary amino amides (*vide supra*, Scheme IV- 4, eq. 3)[39] Alternatively, one could prepare scaffolds such as **IV-45** and **IV-46**, based upon known bicyclic proline derivatives.[48-50] These scaffolds take

Scheme IV-9. Potential scaffolds for chiral hydantoin-based chlorenium sources.
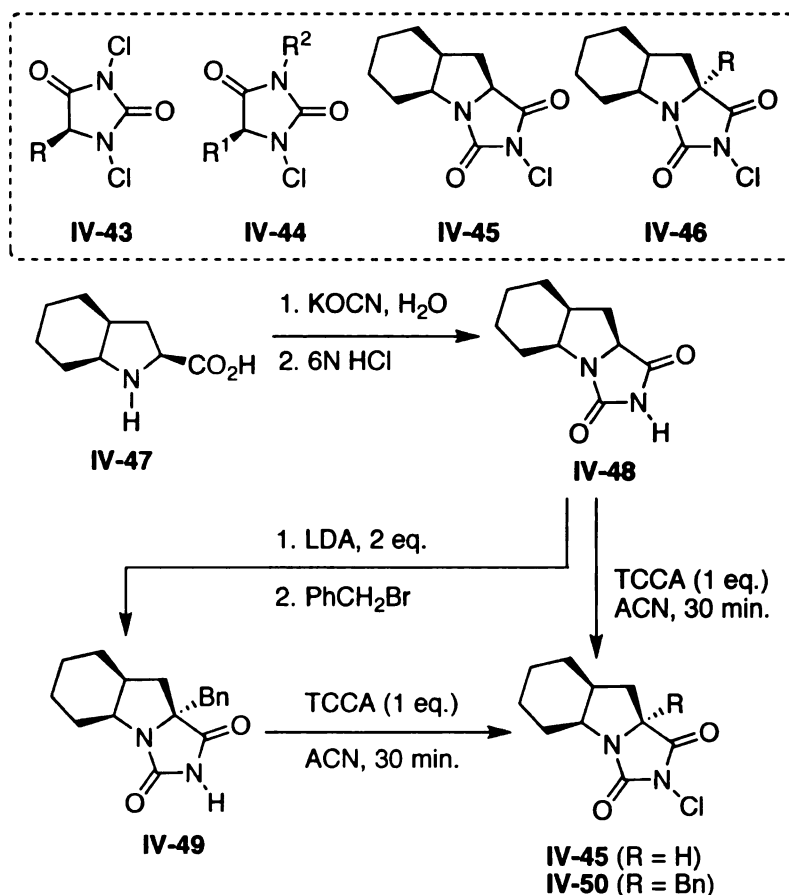
advantage of the concave nature of the 6,5-cis bicyclic system that should shield one enantioface of the N-Cl bond on the more labile N-3 position of the hydantoin. The incorporation of an additional alkyl group in **IV-46**, might also provide an additional steric driver on the convex face of the reagent. Compound **IV-45** is available in two synthetic operations from the known proline analogue **IV-47**.[50] Alternatively, **IV-46** might be accessed by incorporating an additional alkylation step. We envision this step proceeding with stereocontrol, thus incorporating the alkyl group (here represented as a benzyl moiety) from the more accessible convex face of the dianion of hydantoin **IV-48** resulting from LDA-mediated deprotonation.

Current efforts in the Borhan group will include exploiting these new chlorinating reagents for organic synthesis. Particular attention will be given to asymmetric transformations employing chiral N-chlorinated hydantoins as described above.

4.4: Experimental Details

General Information:

All commercially available hydantoins and trichloroisocyanuric acid (TCCA) were purchased from Aldrich and used without purification. Chiral hydantoin starting materials **IV-39, IV-40,** and **IV-41** were prepared by known methods.[40,42,41] Solvents were purchased from either Fisher Scientific or other commercial sources and used without purification. ^{1}H and ^{13}C NMR spectra were collected on a 300 MHz NMR spectrometer (VARIAN INOVA) using

CD_3CN, or CD_3Cl. Chemical shifts are reported in parts per million (ppm). Spectra are referenced to residual solvent peaks. Infrared spectra were collected on a Mattson Galaxy Series FTIR 3000. Samples were prepared as KBr pellets. Elemental analyses were performed on a Perkin Elmer Series II CHNS/O analyzer 2400. Melting points were measured on a Mel-Temp II capillary apparatus and are uncorrected. Optical rotations were measured on a Perkin Elmer Polarimeter 341. Flash silica gel (32-63 mm) from Dynamic Adsorbents, Inc. was used for filtration. In all cases, X-ray quality crystals were obtained directly from the recrystallization crop from chloroform/hexanes, with the exception of compound **IV-34**. X-ray quality crystals for compound **IV-34** were obtained on slow evaporation from benzene and hexanes.

General Procedure for the N-Chlorination of Hydantoins:

The appropriate hydantoin (3 mmol) was suspended in acetonitrile (10 mL) in a 20 mL screw-top vial equipped with a magnetic stir bar. TCCA (6 mmol, 2 equiv) was added in one portion and the resulting slurry was stirred for 30 min, during which time the mixture became uniform and clear. The acetonitrile was removed by rotary evaporation to give a white solid, which was triturated in hot chloroform. The remaining solids were removed by filtration with suction, and the filtrate was then filtered with suction through a 1-cm thick pad of silica gel packed with chloroform in a 50 mL fritted funnel. The silica gel pad was subsequently washed with chloroform and the combined organics were concentrated by rotary evaporation to provide the crude chlorinated product. The crude isolate was

purified by recrystallization from chloroform/hexanes. The mother liquor was then concentrated and the residue was re-subjected to recyrstallization to provide a second crop of products.

Analytical data for IV-4, IV-17, and IV-31 through IV-38:

IV-4, 1,3-Dichloro-5,5-dimethylhydantoin:
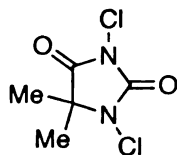
^{1}H NMR (300 MHz, CD$_3$CN): δ 1.48 (s, 6H); ^{13}C NMR (75 MHz, CD$_3$CN): δ 171.3, 151.6, 68.7, 22.4; IR (KBr, vcm^{-1}): 1755, 1734; Elemental Analysis: Calc.: C: 30.48%, H: 3.07%, N: 14.22%; Found: C: 30.47%, H: 2.96%, N: 14.06%; mp = 133-135 °C.

IV-17, 1,3-Dichloro-5,5-phenylhydantoin:
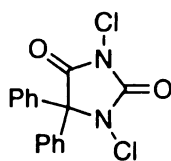
^{1}H NMR (300 MHz, CD$_3$CN): δ 7.51 (m, 6H), 7.35 (m, 4H); ^{13}C NMR (75 MHz, CD$_3$CN): δ 168.5, 151.5, 135.5, 130.5, 129.8, 129.4; IR (KBr, vcm^{-1}): 1797, 1746; Elemental Analysis: Calc.: C: 56.10%, H: 3.14%, N: 8.72%; Found: C: 55.96%, H: 2.92%, N: 8.69%; mp = 159-161 °C.

IV-31, 1,3-Dichloro-5-methyl-5-phenylhydantoin:
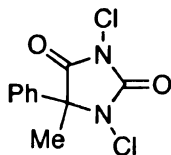
^{1}H NMR (300 MHz, CD$_3$CN): δ 7.45 (s, 5H), 1.95 (s, 3H); ^{13}C NMR (75 MHz, CD$_3$CN): δ 169.6, 151.9, 130.6, 130.1, 127.3, 72.3, 21.1; IR (KBr, vcm^{-1}): 1794, 1747; Elemental Analysis: Calc.: C: 46.36%, H: 3.11%, N: 10.81%; Found: C: 46.13%, H: 3.15%, N: 10.80%; mp = 127-128 °C.

IV-32, 1,3-Dichlorohydantoin:
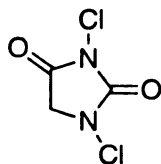
^{1}H NMR (300 MHz, CD$_3$CN): δ 4.26 (s, 2H); ^{13}C NMR (75 MHz, CD$_3$CN): δ 165.1, 154.6, 57.6; IR (KBr, vcm^{-1}): 1740; Elemental Analysis: Calc.: C: 21.33%, H: 1.19%, N: 16.58%; Found: C: 21.41%, H: 1.16%, N: 16.60%; mp = 115-117 °C.

IV-33, 3-Chloro-1,5,5-trimethylhydantoin:
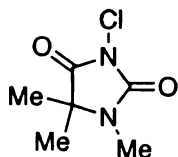
^{1}H NMR (300 MHz, CD$_3$Cl): δ 2.91 (s, 3H), 1.43 (s, 6H); ^{13}C NMR (75 MHz, CD$_3$Cl): δ 172.2, 151.1, 62.8, 25.3, 22.3; IR (KBr, vcm^{-1}): 1744, 1725; Elemental

Analysis: Calc.: C: 40.81%, H: 5.14%, N: 15.86%; Found: C: 40.73%, H: 5.34%, N: 15.94%; mp = 165-168 °C.

IV-34, 1,3-Dichloro-5-(5-methylphenyl)-5-phenylhydantoin:
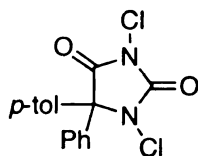
^{1}H NMR (300 MHz, CD$_3$CN): δ 7.46 (m, 3H), 7.32 (m, 2H), 7.26 (m, 2H), 7.18 (m, 2H); ^{13}C NMR (75 MHz, CD$_3$CN): δ 168.6, 151.5, 141.2, 135.5, 132.6, 130.8, 130.4, 129.7, 129.34, 129.32, 79.8, 21.2; IR (KBr, vcm^{-1}): 1796, 1759; Elemental Analysis: Calc.: C: 57.33%, H: 3.61%, N: 8.36%; Found: C: 57.14%, H: 3.63%, N: 8.24%; mp = 130-131 °C.

IV-35, 1,3-Dichloro-5-methylhydantoin:
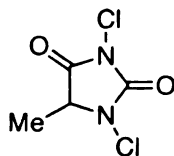
^{1}H NMR (300 MHz, CD$_3$CN): δ 4.34 (q, J = 7.2 Hz, 1H), 1.47 (d, J = 7.2 Hz, 2H),.; ^{13}C NMR (75 MHz, CD$_3$CN): δ 168.3, 156.6, 64.3, 14.6; IR (KBr, vcm^{-1}): 1795, 1756, 1738; Elemental Analysis: Calc.: C: 26.25%, H: 2.20%, N: 15.31%; Found: C: 26.34%, H: 2.20%, N: 15.08%; mp = 94-96 °C.

IV-36, (*S*)-1,3-Dichloro-5-benzylhydantoin:
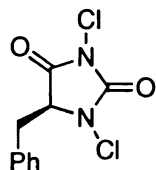
^{1}H NMR (300 MHz, CD$_3$CN): δ 7.29 (m, 3H), 7.21 (m, 2H), 4.60 (m, 1H), 3.24 (m, 2H); ^{13}C NMR (75 MHz, CD$_3$CN): δ 167.1, 153.3, 134.8, 130.7, 129.5, 128.5, 69.0, 34.9; IR (KBr, vcm^{-1}): 1742; Elemental Analysis: Calc.: C: 46.36%, H: 3.11%, N: 10.81%; Found: C: 46.12%, H: 3.13%, N: 10.88%; mp = 114-116 °C; $[\alpha]_D^{20}$ = + 27.5° (c = 1.01, CHCl$_3$).

IV-37, (*S*)-1,3-Dichloro-5-(*iso*-propyl)hydantoin:
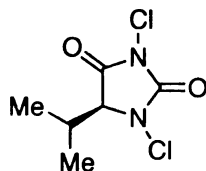
^{1}H NMR (300 MHz, CD$_3$CN): δ 4.21 (d, *J* = 3.3 Hz, 1H), 2.35 (doublet of a septet, J_1 = 3.3 Hz, J_2 = 6.9 Hz, 1H), 1.06 (d, *J* = 6.9 Hz, 3H), 1.00 (d, *J* = 6.9 Hz, 3H); ^{13}C NMR (75 MHz, CD$_3$CN): δ 167.2, 154.3, 73.0, 29.9, 17.2; IR (KBr, vcm^{-1}): 1804, 1740; Elemental Analysis: Calc.: C: 34.15%, H: 3.82%, N: 13.27%; Found: C: 34.42%, H: 3.99%, N: 13.35%; mp = 130-132 °C; $[\alpha]_D^{20}$ = + 23.5° (c = 1.15, CHCl$_3$).

IV-38, (*S*)-1,3-Dichloro-5-(*tert*-butyl)hydantoin:
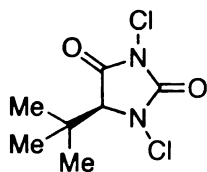
^{1}H NMR (300 MHz, CD$_3$CN): δ 3.99 (s, 1H), 1.10 (s, 9H); ^{13}C NMR (75 MHz, CD$_3$CN): δ 167.4, 155.9, 77.7, 36.7, 26.2; IR (KBr, νcm^{-1}): 1802, 1746; Elemental Analysis: Calc.: C: 37.35%, H: 4.48%, N: 12.45%; Found: C: 37.90%, H: 4.59%, N: 12.57%; mp = 85-87 ˚C; [α]$_D^{20}$ = + 7.2˚ (c = 1.02, CHCl$_3$).

Reduction of Chiral N-Chlorinated Hydantoins to Confirm Optical Purity:

Chiral N-chlorohydantoins **IV-36**, **IV-37**, and **IV-38** were converted back to their parent chiral hydantoins by washing an ethyl acetate solution with saturated aqueous sodium sulfite. The optical rotation of the re-isolated, *non-recrystallized* parent hydantoin was in agreement with that of the starting chiral hydantoins prior to chlorination, thus confirming that the chlorination event does not erode the optical purity of the starting hydantoins (Scheme IV-10).

Scheme IV-10: Dechlorination of chiral N-chlorohydantoins. Verification of optical purity.

IV-39
93% *ee*
$[\alpha]_D^{20} = -95.8°$
c = 0.935, EtOH

IV-36
$[\alpha]_D^{20} = +27.5°$
c = 1.005, CHCl$_3$

IV-39
>99% *ee*
$[\alpha]_D^{20} = -104.5°$
c = 1.015, EtOH

(1)

IV-40
99% *ee*
$[\alpha]_D^{20} = -93.9°$
c = 1.075, EtOH

IV-37
$[\alpha]_D^{20} = +23.5°$
c = 1.15, CHCl$_3$

IV-40
>99% *ee*
$[\alpha]_D^{20} = -96.2°$
c = 0.955, EtOH

(2)

IV-41
$[\alpha]_D^{20} = -74.5°$
c = 0.385, EtOH

IV-38
$[\alpha]_D^{20} = +7.5°$
c = 1.235, CHCl$_3$

IV-41
$[\alpha]_D^{20} = -73.1°$
c = 0.925, EtOH

(3)
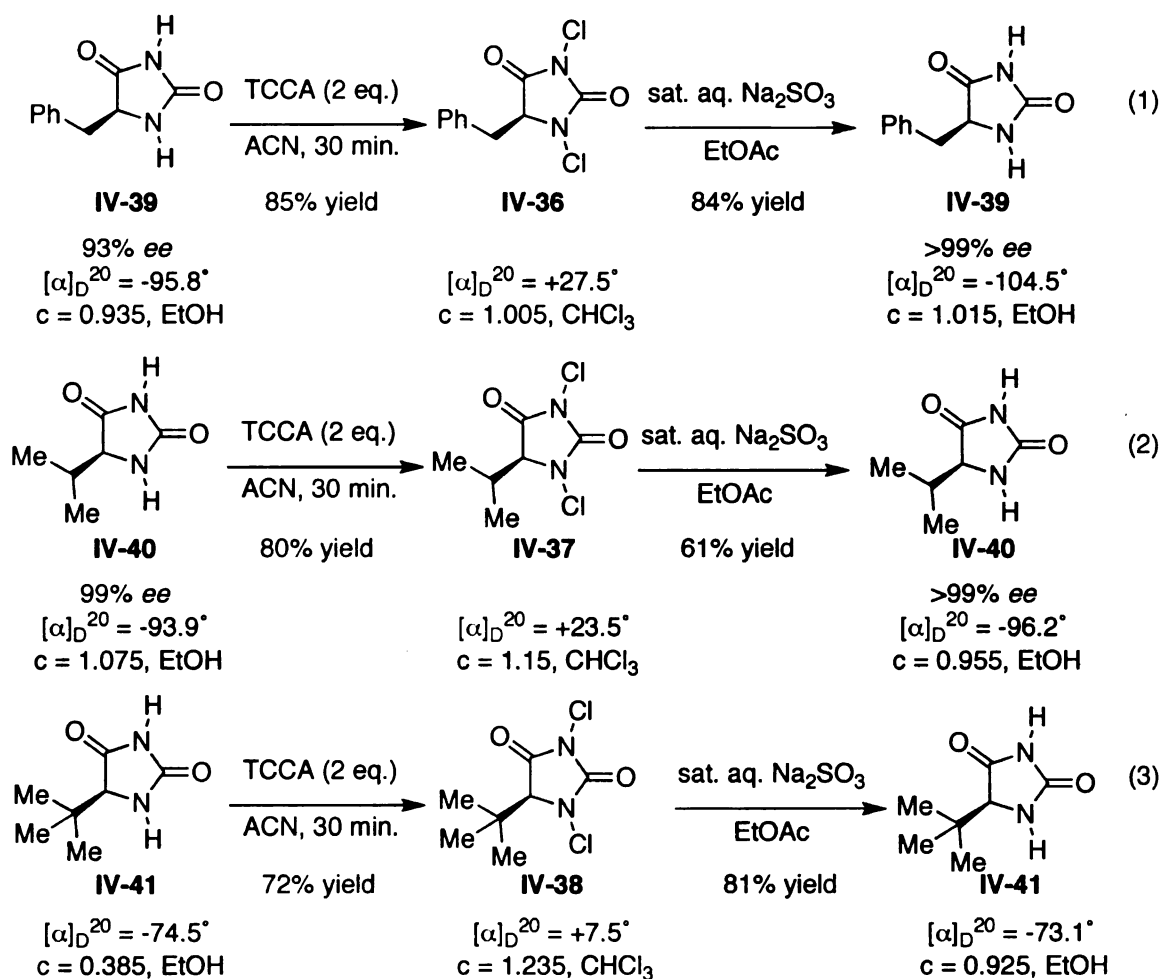
Representative Procedure: Dechlorination of IV-36:

(S)-5-Benzyl-1,3-dichlorohydantoin **IV-36** (100 mg, 0.39 mmol) was

dissolved in ethyl acetate (5 mL) in a 60 mL separatory funnel and washed with

saturated aqueous sodium sulfite (5 mL) followed by saturated brine (5 mL). The

organics were then dried over anhydrous sodium sulfate and concentrated to

give 62 mg (84%) of the reduced (S)-5-benzylhydantoin **IV-39**.

Analytical Data for Recovered Chiral Hydantoins IV-39, IV-40, and IV-41:

IV-39, (S)-5-Benzylhydantoin:[42]
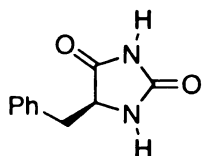
^{1}H NMR (300 MHz, CD$_3$CN): δ 8.43 (br s, 1H), 7.34 (m, 5H), 6.21 (br s, 1H), 4.29

(m, 1H), 3.00 (m, 2H); ^{13}C NMR (75 MHz, CD$_3$CN): δ 175.3, 157.5, 136.9, 130.6,

129.3, 127.9, 60.2, 37.8; $[\alpha]_D^{20}$ = - 104.5° (c = 1.02, EtOH), synthetic (S)-5-

benzylhydantoin (93% ee): -95.8° (c = 0.935, EtOH).

IV-40, (S)-5-(iso-propyl)hydantoin:[42]
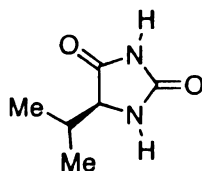
^{1}H NMR (300 MHz, CD$_3$CN): δ 8.75 (br s, 1H), 6.35 (m, 5H), 3.93 (dd, J_1 = 1.5

Hz, J_2 = 3.6 Hz, 1H), 2.08 (septet of doublets, J_1 = 3.6 Hz, J_2 = 6.6 Hz, 1H), 0.977

(d, J = 6.6 Hz, 3H), 0.863 (d, J = 6.6 Hz, 3H); ^{13}C NMR (75 MHz, CD$_3$CN): δ

175.8, 158.7, 64.4, 30.9, 18.9, 16.3; $[\alpha]_D^{20}$ = - 96.2° (c = 0.955, EtOH), synthetic

(S)-5-(*iso*-propyl)hydantoin (99% ee): - 93.9° (c = 1.08, EtOH).

IV-41, (S)-5-(tert-butyl)hydantoin:[41]
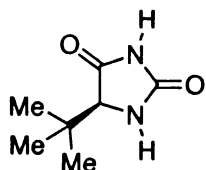
^{1}H NMR (300 MHz, CD$_3$CN): δ 8.37 (br s, 1H), 6.18 (br s, 1H), 3.70 (d, J = 1.8

Hz, 1H), 0.98 (s, 9H); ^{13}C NMR (75 MHz, CD$_3$CN): δ 174.9, 157.9, 67.5, 35.0,

25.7; $[\alpha]_D^{20}$ = - 73.1° (c = 0.925, EtOH), synthetic (S)-5-(*tert*-butyl)hydantoin:

- 74.5° (c = 0.385, EtOH).

X-Ray Crystal Structure for N-Chlorohydantoins

Figure IV-3. X-ray struture of **IV-4**.
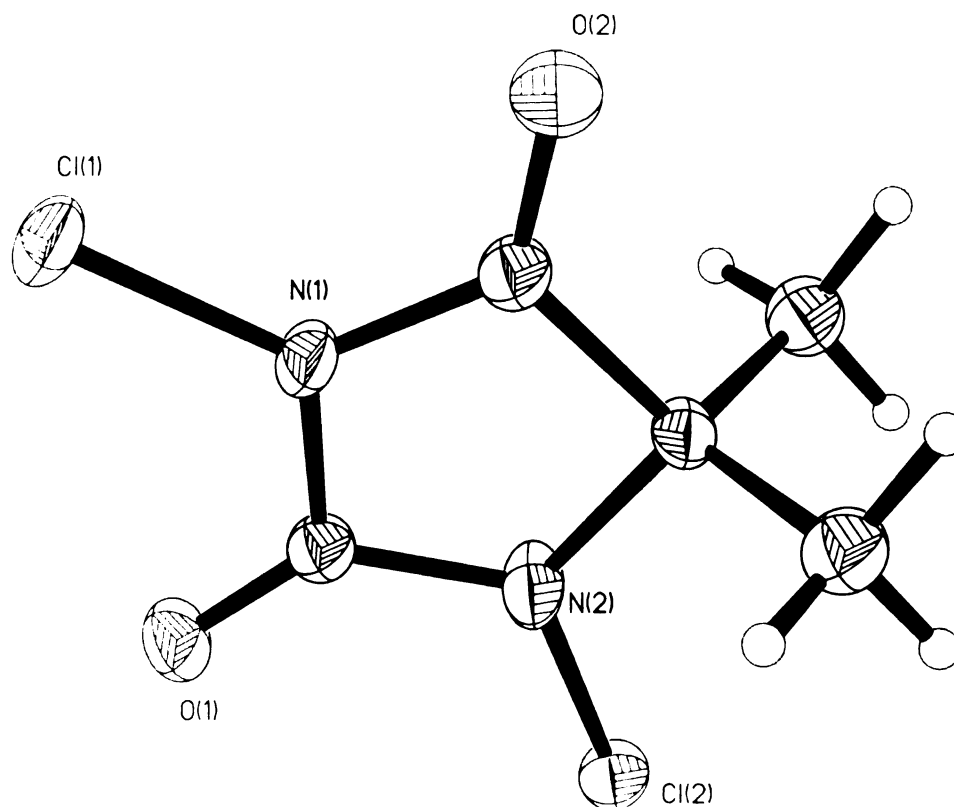
Table IV-2. Crystal data and structure refinement for **IV-4**.

Identification code	bb14	
Empirical formula	C5 H8 Cl2 N2 O2	
Formula weight	199.03	
Temperature	173(2) K	
Wavelength	0.71073 Å	
Crystal system	Orthorhombic	
Space group	Pnma	
Unit cell dimensions	a = 7.9704(3) Å	a= 90°.
	b = 7.3884(3) Å	b= 90°.
	c = 13.1168(5) Å	g = 90°.
Volume	772.43(5) Å^3	
Z	4	
Density (calculated)	1.712 Mg/m^3	
Absorption coefficient	0.789 mm^{-1}	

Table IV-2. (Cont'd)

F(000)	408
Crystal size	0.28 x 0.22 x 0.14 mm^3
Theta range for data collection	2.99 to 27.58°.
Index ranges	-10<=h<=10, -9<=k<=9, -17<=l<=17
Reflections collected	8209
Independent reflections	956 [R(int) = 0.0216]
Completeness to theta = 25.00°	99.9 %
Absorption correction	Numerical
Max. and min. transmission	0.9010 and 0.8100
Refinement method	Full-matrix least-squares on F^2
Data / restraints / parameters	956 / 0 / 77
Goodness-of-fit on F^2	1.056
Final R indices [I>2sigma(I)]	R1 = 0.0215, wR2 = 0.0568
R indices (all data)	R1 = 0.0236, wR2 = 0.0586
Extinction coefficient	0.0055(10)
Largest diff. peak and hole	0.385 and -0.193 e.Å^{-3}

Table IV-3. Atomic coordinates (x 10^4) and equivalent isotropic displacement parameters (Å^{2}x 10^3) for **IV-4**. U(eq) is defined as one third of the trace of the orthogonalized U^{ij} tensor.

	x	y	z	U(eq)
Cl(1)	5397(1)	2500	6472(1)	27(1)
Cl(2)	11171(1)	2500	4453(1)	24(1)
O(1)	9174(2)	2500	6427(1)	28(1)
O(2)	4806(2)	2500	4149(1)	36(1)
N(1)	6708(2)	2500	5473(1)	23(1)
N(2)	9094(2)	2500	4664(1)	32(1)
C(1)	8468(2)	2500	5622(1)	20(1)
C(2)	6219(2)	2500	4467(1)	23(1)
C(3)	7841(2)	2500	3836(1)	22(1)
C(4)	7952(2)	4205(2)	3193(1)	28(1)

Table IV-4. Bond lengths [Å] and angles [°] for **IV-4**.

Cl(1)-N(1)	1.6765(14)
Cl(2)-N(2)	1.6792(15)
O(1)-C(1)	1.197(2)
O(2)-C(2)	1.201(2)
N(1)-C(2)	1.376(2)
N(1)-C(1)	1.416(2)
N(2)-C(1)	1.352(2)
N(2)-C(3)	1.475(2)
C(2)-C(3)	1.535(2)
C(3)-C(4)	1.5180(16)
C(3)-C(4)#1	1.5180(16)
C(4)-H(4A)	0.923(17)
C(4)-H(4B)	0.961(16)

247

Table IV-4. (cont'd)

C(4)-H(4C)	0.948(16)
C(2)-N(1)-C(1)	114.42(13)
C(2)-N(1)-Cl(1)	124.96(11)
C(1)-N(1)-Cl(1)	120.61(11)
C(1)-N(2)-C(3)	115.79(14)
C(1)-N(2)-Cl(2)	121.13(12)
C(3)-N(2)-Cl(2)	123.07(11)
O(1)-C(1)-N(2)	130.30(16)
O(1)-C(1)-N(1)	126.02(15)
N(2)-C(1)-N(1)	103.68(13)
O(2)-C(2)-N(1)	126.80(15)
O(2)-C(2)-C(3)	127.02(15)
N(1)-C(2)-C(3)	106.18(13)
N(2)-C(3)-C(4)	111.67(9)
N(2)-C(3)-C(4)#1	111.67(9)
C(4)-C(3)-C(4)#1	112.16(14)
N(2)-C(3)-C(2)	99.93(12)
C(4)-C(3)-C(2)	110.40(9)
C(4)#1-C(3)-C(2)	110.40(9)
C(3)-C(4)-H(4A)	111.4(10)
C(3)-C(4)-H(4B)	109.0(10)
H(4A)-C(4)-H(4B)	110.7(14)
C(3)-C(4)-H(4C)	108.1(10)
H(4A)-C(4)-H(4C)	108.5(15)
H(4B)-C(4)-H(4C)	109.0(12)

Table IV-5. Anisotropic displacement parameters ($Å^2 \times 10^3$) for **IV-4**. The anisotropic displacement factor exponent takes the form: $-2p^2[h^2a^{*2}U^{11} + ... + 2 h k a^* b^* U^{12}]$

	U^{11}	U^{22}	U^{33}	U^{23}	U^{13}	U^{12}
Cl(1)	24(1)	35(1)	23(1)	0	10(1)	0
Cl(2)	13(1)	36(1)	23(1)	0	1(1)	0
O(1)	25(1)	42(1)	17(1)	0	-4(1)	0
O(2)	15(1)	63(1)	28(1)	0	-2(1)	0
N(1)	16(1)	37(1)	16(1)	0	4(1)	0
N(2)	12(1)	69(1)	16(1)	0	0(1)	0
C(1)	18(1)	24(1)	19(1)	0	1(1)	0
C(2)	16(1)	33(1)	20(1)	0	1(1)	0
C(3)	13(1)	36(1)	16(1)	0	-1(1)	0
C(4)	24(1)	32(1)	27(1)	1(1)	1(1)	-1(1)

Table IV-6. Hydrogen coordinates (x 10^4) and isotropic displacement parameters (Å^2x 10^3) for **IV-4**.

	x	y	z	U(eq)
H(4A)	7940(20)	5230(20)	3594(11)	33(4)
H(4B)	7040(20)	4220(20)	2716(11)	35(4)
H(4C)	8980(20)	4180(20)	2830(12)	41(4)

Table IV-7. Torsion angles [°] for **IV-4**.

C(3)-N(2)-C(1)-O(1)	180.0
Cl(2)-N(2)-C(1)-O(1)	0.0
C(3)-N(2)-C(1)-N(1)	0.0
Cl(2)-N(2)-C(1)-N(1)	180.0
C(2)-N(1)-C(1)-O(1)	180.0
Cl(1)-N(1)-C(1)-O(1)	0.0
C(2)-N(1)-C(1)-N(2)	0.0
Cl(1)-N(1)-C(1)-N(2)	180.0
C(1)-N(1)-C(2)-O(2)	180.0
Cl(1)-N(1)-C(2)-O(2)	0.0
C(1)-N(1)-C(2)-C(3)	0.0
Cl(1)-N(1)-C(2)-C(3)	180.0
C(1)-N(2)-C(3)-C(4)	116.76(10)
Cl(2)-N(2)-C(3)-C(4)	-63.24(10)
C(1)-N(2)-C(3)-C(4)#1	-116.76(10)
Cl(2)-N(2)-C(3)-C(4)#1	63.24(10)
C(1)-N(2)-C(3)-C(2)	0.0
Cl(2)-N(2)-C(3)-C(2)	180.0
O(2)-C(2)-C(3)-N(2)	180.0
N(1)-C(2)-C(3)-N(2)	0.0
O(2)-C(2)-C(3)-C(4)	62.29(10)
N(1)-C(2)-C(3)-C(4)	-117.71(10)
O(2)-C(2)-C(3)-C(4)#1	-62.29(10)
N(1)-C(2)-C(3)-C(4)#1	117.71(10)

Figure IV-4. X-ray structure of **IV-17**.
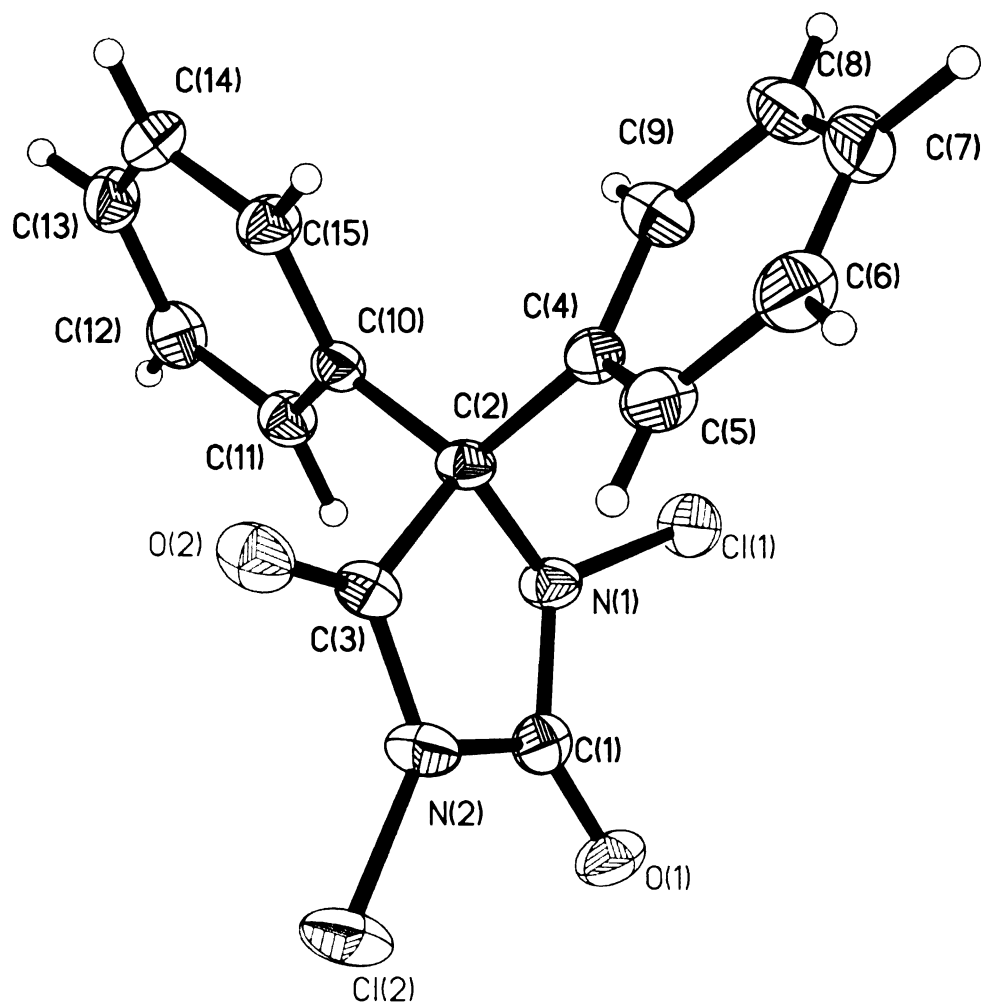
Table VI-8. Crystal data and structure refinement for **IV-17**.

Identification code	bb12m
Empirical formula	C15 H10 Cl2 N2 O2
Formula weight	321.15
Temperature	173(2) K
Wavelength	0.71073 Å
Crystal system	Monoclinic
Space group	P2(1)/n
Unit cell dimensions	a = 8.809(2) Å a= 90°.
	b = 20.693(6) Å b= 117.871(3)°.
	c = 8.859(2) Å g = 90°.
Volume	1427.5(7) Å^3
Z	4

250

Table IV-8. (Cont'd)

Density (calculated)	1.494 Mg/m^3
Absorption coefficient	0.459 mm^{-1}
F(000)	656
Crystal size	$0.23 \times 0.20 \times 0.16 \text{ mm}^3$
Theta range for data collection	1.97 to 28.13°.
Index ranges	$-11<=h<=11, -27<=k<=26, -11<=l<=11$
Reflections collected	7724
Independent reflections	2284 [R(int) = 0.0312]
Completeness to theta = 25.00°	66.3 %
Absorption correction	Semi-empirical from equivalents
Max. and min. transmission	0.9301 and 0.9017
Refinement method	Full-matrix least-squares on F^2
Data / restraints / parameters	2284 / 0 / 230
Goodness-of-fit on F^2	1.033
Final R indices [I>2sigma(I)]	R1 = 0.0363, wR2 = 0.0929
R indices (all data)	R1 = 0.0491, wR2 = 0.0985
Largest diff. peak and hole	$0.231 \text{ and } -0.184 \text{ e.Å}^{-3}$

Table IV-9. Atomic coordinates (x 10^4) and equivalent isotropic displacement parameters ($Å^2$x 10^3) for **IV-17**. U(eq) is defined as one third of the trace of the orthogonalized U^{ij} tensor.

	x	y	z	U(eq)
Cl(1)	3297(1)	-16(1)	6383(1)	30(1)
Cl(2)	6330(1)	1714(1)	11371(1)	40(1)
O(1)	6299(2)	406(1)	9713(2)	31(1)
O(2)	2899(2)	2199(1)	8670(2)	32(1)
N(1)	3523(2)	629(1)	7631(2)	23(1)
N(2)	4860(2)	1369(1)	9565(2)	28(1)
C(1)	5052(2)	740(1)	9036(3)	24(1)
C(2)	2369(2)	1198(1)	6988(2)	20(1)
C(3)	3360(3)	1675(1)	8478(2)	23(1)
C(4)	2258(3)	1449(1)	5314(3)	22(1)
C(5)	3357(3)	1932(1)	5306(3)	30(1)
C(6)	3262(3)	2133(1)	3761(3)	39(1)
C(7)	2107(3)	1854(1)	2250(3)	40(1)
C(8)	1006(4)	1378(1)	2248(3)	38(1)
C(9)	1074(3)	1178(1)	3778(3)	31(1)
C(10)	625(2)	1074(1)	6911(2)	20(1)
C(11)	377(3)	563(1)	7794(3)	25(1)
C(12)	-1221(3)	485(1)	7741(3)	30(1)
C(13)	-2545(3)	912(1)	6820(3)	30(1)
C(14)	-2276(3)	1423(1)	5971(3)	31(1)
C(15)	-695(3)	1508(1)	6021(3)	26(1)

251

Table IV-10. Bond lengths [Å] and angles [°] for **IV-17**.

Cl(1)-N(1)	1.6844(17)
Cl(2)-N(2)	1.6758(19)
O(1)-C(1)	1.195(2)
O(2)-C(3)	1.197(2)
N(1)-C(1)	1.359(3)
N(1)-C(2)	1.485(2)
N(2)-C(3)	1.372(3)
N(2)-C(1)	1.421(3)
C(2)-C(10)	1.528(2)
C(2)-C(4)	1.530(2)
C(2)-C(3)	1.549(3)
C(4)-C(9)	1.388(3)
C(4)-C(5)	1.395(3)
C(5)-C(6)	1.395(3)
C(5)-H(5)	0.93(3)
C(6)-C(7)	1.373(4)
C(6)-H(6)	0.93(3)
C(7)-C(8)	1.382(4)
C(7)-H(7)	1.07(4)
C(8)-C(9)	1.392(3)
C(8)-H(8)	0.87(3)
C(9)-H(9)	0.96(3)
C(10)-C(15)	1.388(3)
C(10)-C(11)	1.391(3)
C(11)-C(12)	1.395(3)
C(11)-H(11)	1.01(3)
C(12)-C(13)	1.384(3)
C(12)-H(12)	0.94(3)
C(13)-C(14)	1.382(3)
C(13)-H(13)	0.91(3)
C(14)-C(15)	1.384(3)
C(14)-H(14)	0.84(3)
C(15)-H(15)	0.91(3)
C(1)-N(1)-C(2)	115.09(16)
C(1)-N(1)-Cl(1)	119.87(13)
C(2)-N(1)-Cl(1)	121.81(13)
C(3)-N(2)-C(1)	114.49(18)
C(3)-N(2)-Cl(2)	122.36(15)
C(1)-N(2)-Cl(2)	123.15(15)
O(1)-C(1)-N(1)	130.3(2)
O(1)-C(1)-N(2)	126.0(2)
N(1)-C(1)-N(2)	103.76(16)
N(1)-C(2)-C(10)	112.14(15)
N(1)-C(2)-C(4)	111.26(14)
C(10)-C(2)-C(4)	113.99(16)
N(1)-C(2)-C(3)	99.58(15)
C(10)-C(2)-C(3)	107.43(14)
C(4)-C(2)-C(3)	111.45(15)
O(2)-C(3)-N(2)	126.6(2)
O(2)-C(3)-C(2)	127.2(2)
N(2)-C(3)-C(2)	106.20(16)
C(9)-C(4)-C(5)	119.36(18)
C(9)-C(4)-C(2)	119.43(17)

Table IV-10. (Cont'd)

C(5)-C(4)-C(2)	121.18(19)
C(4)-C(5)-C(6)	119.7(2)
C(4)-C(5)-H(5)	120.5(16)
C(6)-C(5)-H(5)	119.8(16)
C(7)-C(6)-C(5)	120.6(2)
C(7)-C(6)-H(6)	124.6(17)
C(5)-C(6)-H(6)	114.8(17)
C(6)-C(7)-C(8)	120.0(2)
C(6)-C(7)-H(7)	114(2)
C(8)-C(7)-H(7)	126(2)
C(7)-C(8)-C(9)	120.0(2)
C(7)-C(8)-H(8)	122.7(19)
C(9)-C(8)-H(8)	117.3(19)
C(4)-C(9)-C(8)	120.3(2)
C(4)-C(9)-H(9)	121.0(17)
C(8)-C(9)-H(9)	118.7(17)
C(15)-C(10)-C(11)	120.13(17)
C(15)-C(10)-C(2)	118.28(16)
C(11)-C(10)-C(2)	121.47(17)
C(10)-C(11)-C(12)	119.28(19)
C(10)-C(11)-H(11)	122.1(14)
C(12)-C(11)-H(11)	118.6(14)
C(13)-C(12)-C(11)	120.38(19)
C(13)-C(12)-H(12)	122.2(16)
C(11)-C(12)-H(12)	117.4(16)
C(14)-C(13)-C(12)	119.84(19)
C(14)-C(13)-H(13)	122.7(19)
C(12)-C(13)-H(13)	117.4(19)
C(13)-C(14)-C(15)	120.4(2)
C(13)-C(14)-H(14)	118.6(16)
C(15)-C(14)-H(14)	121.0(16)
C(14)-C(15)-C(10)	119.94(19)
C(14)-C(15)-H(15)	118.9(15)
C(10)-C(15)-H(15)	121.0(15)

Table IV-11. Anisotropic displacement parameters (Å^2x 10^3)for **IV-17**. The anisotropic displacement factor exponent takes the form: $-2p^2[\,h^2a^{*2}U^{11} + ... + 2\,h\,k\,a^*\,b^*\,U^{12}\,]$

	U^{11}	U^{22}	U^{33}	U^{23}	U^{13}	U^{12}
Cl(1)	34(1)	24(1)	31(1)	-4(1)	13(1)	4(1)
Cl(2)	31(1)	48(1)	25(1)	-6(1)	1(1)	-11(1)
O(1)	21(1)	38(1)	31(1)	12(1)	9(1)	7(1)
O(2)	38(1)	23(1)	27(1)	-4(1)	9(1)	0(1)
N(1)	22(1)	20(1)	23(1)	0(1)	6(1)	3(1)
N(2)	25(1)	28(1)	22(1)	-2(1)	3(1)	-2(1)
C(1)	24(1)	27(1)	24(1)	6(1)	13(1)	-1(1)
C(2)	20(1)	17(1)	18(1)	0(1)	5(1)	1(1)
C(3)	25(1)	23(1)	19(1)	-1(1)	8(1)	-4(1)
C(4)	23(1)	23(1)	21(1)	4(1)	10(1)	5(1)
C(5)	23(1)	34(1)	29(1)	6(1)	10(1)	1(1)
C(6)	33(1)	46(1)	42(2)	17(1)	22(1)	4(1)

253

Table IV-11. (Cont'd)

C(7)	45(2)	51(1)	31(1)	16(1)	23(1)	18(1)
C(8)	45(1)	42(1)	20(1)	1(1)	11(1)	9(1)
C(9)	35(1)	30(1)	23(1)	0(1)	10(1)	0(1)
C(10)	20(1)	21(1)	17(1)	-3(1)	6(1)	0(1)
C(11)	28(1)	23(1)	23(1)	1(1)	11(1)	2(1)
C(12)	36(1)	29(1)	29(1)	2(1)	20(1)	-3(1)
C(13)	26(1)	38(1)	31(1)	-5(1)	16(1)	-2(1)
C(14)	25(1)	33(1)	32(1)	3(1)	12(1)	10(1)
C(15)	25(1)	25(1)	27(1)	4(1)	11(1)	3(1)

Table IV-12. Hydrogen coordinates (x 10^4) and isotropic displacement parameters ($Å^2$x 10^3) for **IV-17**.

	x	y	z	U(eq)
H(5)	4120(40)	2130(12)	6320(40)	37(7)
H(6)	4020(30)	2464(12)	3850(30)	36(7)
H(7)	2110(50)	2060(18)	1150(50)	79(11)
H(8)	260(40)	1187(14)	1320(40)	47(8)
H(9)	290(40)	851(13)	3750(40)	39(7)
H(11)	1310(40)	235(14)	8440(40)	38(7)
H(12)	-1340(30)	143(12)	8370(40)	33(6)
H(13)	-3550(40)	848(13)	6840(40)	48(8)
H(14)	-3080(40)	1683(11)	5440(30)	30(6)
H(15)	-560(30)	1835(12)	5400(30)	29(6)

Table IV-13. Torsion angles [°] for **IV-17**.

C(2)-N(1)-C(1)-O(1)	-170.26(17)
Cl(1)-N(1)-C(1)-O(1)	-10.2(3)
C(2)-N(1)-C(1)-N(2)	9.57(19)
Cl(1)-N(1)-C(1)-N(2)	169.64(12)
C(3)-N(2)-C(1)-O(1)	174.24(17)
Cl(2)-N(2)-C(1)-O(1)	-6.1(3)
C(3)-N(2)-C(1)-N(1)	-5.6(2)
Cl(2)-N(2)-C(1)-N(1)	174.06(13)
C(1)-N(1)-C(2)-C(10)	-122.81(17)
Cl(1)-N(1)-C(2)-C(10)	77.55(18)
C(1)-N(1)-C(2)-C(4)	108.19(18)
Cl(1)-N(1)-C(2)-C(4)	-51.5(2)
C(1)-N(1)-C(2)-C(3)	-9.44(18)
Cl(1)-N(1)-C(2)-C(3)	-169.08(12)
C(1)-N(2)-C(3)-O(2)	178.36(17)
Cl(2)-N(2)-C(3)-O(2)	-1.3(3)
C(1)-N(2)-C(3)-C(2)	-0.1(2)
Cl(2)-N(2)-C(3)-C(2)	-179.79(12)
N(1)-C(2)-C(3)-O(2)	-173.24(18)
C(10)-C(2)-C(3)-O(2)	-56.3(2)
C(4)-C(2)-C(3)-O(2)	69.3(2)

Table IV-13. (Cont'd)

N(1)-C(2)-C(3)-N(2)	5.24(17)
C(10)-C(2)-C(3)-N(2)	122.22(16)
C(4)-C(2)-C(3)-N(2)	-112.24(17)
N(1)-C(2)-C(4)-C(9)	86.0(2)
C(10)-C(2)-C(4)-C(9)	-42.0(2)
C(3)-C(2)-C(4)-C(9)	-163.84(18)
N(1)-C(2)-C(4)-C(5)	-92.3(2)
C(10)-C(2)-C(4)-C(5)	139.72(19)
C(3)-C(2)-C(4)-C(5)	17.9(2)
C(9)-C(4)-C(5)-C(6)	-0.6(3)
C(2)-C(4)-C(5)-C(6)	177.69(18)
C(4)-C(5)-C(6)-C(7)	-0.5(3)
C(5)-C(6)-C(7)-C(8)	1.0(4)
C(6)-C(7)-C(8)-C(9)	-0.4(4)
C(5)-C(4)-C(9)-C(8)	1.2(3)
C(2)-C(4)-C(9)-C(8)	-177.07(19)
C(7)-C(8)-C(9)-C(4)	-0.8(3)
N(1)-C(2)-C(10)-C(15)	-167.18(17)
C(4)-C(2)-C(10)-C(15)	-39.6(2)
C(3)-C(2)-C(10)-C(15)	84.4(2)
N(1)-C(2)-C(10)-C(11)	16.9(2)
C(4)-C(2)-C(10)-C(11)	144.43(18)
C(3)-C(2)-C(10)-C(11)	-91.6(2)
C(15)-C(10)-C(11)-C(12)	1.4(3)
C(2)-C(10)-C(11)-C(12)	177.30(18)
C(10)-C(11)-C(12)-C(13)	0.0(3)
C(11)-C(12)-C(13)-C(14)	-1.0(3)
C(12)-C(13)-C(14)-C(15)	0.6(3)
C(13)-C(14)-C(15)-C(10)	0.8(3)
C(11)-C(10)-C(15)-C(14)	-1.8(3)
C(2)-C(10)-C(15)-C(14)	-177.85(19)

Figure IV-5. X-Ray structure of **IV-31**.
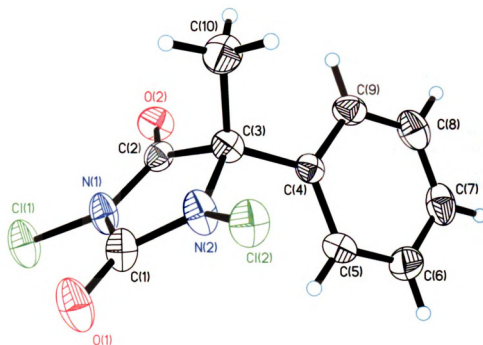
Table IV-14. Crystal data and structure refinement for **IV-31**.

Identification code	bb17
Empirical formula	C10 H8 Cl2 N2 O2
Formula weight	259.08
Temperature	173(2) K
Wavelength	0.71073 Å
Crystal system	Triclinic
Space group	P-1
Unit cell dimensions	a = 7.749(2) Å a= 92.508(5)°.
	b = 7.890(2) Å b= 112.860(3)°.
	c = 9.927(4) Å g = 98.318(4)°.
Volume	550.0(3) Å^3
Z	2
Density (calculated)	1.564 Mg/m^3
Absorption coefficient	0.575 mm^{-1}
F(000)	264
Crystal size	0.15 x 0.10 x 0.10 mm^3
Theta range for data collection	2.24 to 28.19°.
Index ranges	-10<=h<=10, -10<=k<=10, -12<=l<=12
Reflections collected	6080
Independent reflections	2451 [R(int) = 0.0306]
Completeness to theta = 25.00°	99.7 %
Absorption correction	Semi-empirical from equivalents

Table IV-14. (Cont'd)

Max. and min. transmission	0.7457 and 0.6885
Refinement method	Full-matrix least-squares on F^2
Data / restraints / parameters	2451 / 0 / 177
Goodness-of-fit on F^2	1.015
Final R indices [I>2sigma(I)]	R1 = 0.0369, wR2 = 0.0826
R indices (all data)	R1 = 0.0559, wR2 = 0.0911
Largest diff. peak and hole	0.300 and -0.365 e.Å^{-3}

Table IV-15. Atomic coordinates (x 10^4) and equivalent isotropic displacement parameters (Å^2x 10^3) for **IV-31**. U(eq) is defined as one third of the trace of the orthogonalized U^{ij} tensor.

	x	y	z	U(eq)
Cl(1)	8241(1)	3268(1)	5612(1)	42(1)
Cl(2)	686(1)	1970(1)	3080(1)	34(1)
O(1)	4377(2)	3364(2)	5695(2)	43(1)
O(2)	6819(2)	1567(2)	2463(2)	34(1)
N(1)	6043(2)	2616(2)	4306(2)	31(1)
N(2)	2957(2)	2289(3)	3233(2)	32(1)
C(1)	4396(3)	2826(3)	4553(2)	30(1)
C(2)	5675(3)	1878(2)	2932(2)	24(1)
C(3)	3497(3)	1530(3)	2106(2)	25(1)
C(4)	2959(2)	2500(2)	747(2)	22(1)
C(5)	2635(3)	4171(3)	797(3)	35(1)
C(6)	2276(4)	5051(3)	-429(3)	44(1)
C(7)	2254(3)	4285(3)	-1707(3)	39(1)
C(8)	2569(3)	2627(3)	-1769(3)	38(1)
C(9)	2920(3)	1733(3)	-552(2)	30(1)
C(10)	2822(4)	-418(3)	1798(3)	37(1)

Table IV-16. Bond lengths [Å] and angles [°] for **IV-31**.

Cl(1)-N(1)	1.6786(17)
Cl(2)-N(2)	1.6863(17)
O(1)-C(1)	1.199(3)
O(2)-C(2)	1.199(2)
N(1)-C(2)	1.364(3)
N(1)-C(1)	1.421(2)
N(2)-C(1)	1.349(3)
N(2)-C(3)	1.470(3)
C(2)-C(3)	1.539(3)
C(3)-C(4)	1.525(3)
C(3)-C(10)	1.527(3)
C(4)-C(5)	1.380(3)
C(4)-C(9)	1.388(3)
C(5)-C(6)	1.381(3)
C(5)-H(5)	0.86(2)
C(6)-C(7)	1.374(4)
C(6)-H(6)	0.88(3)

Table IV-16. (Cont'd.)

C(7)-C(8)	1.368(4)
C(7)-H(7)	0.92(3)
C(8)-C(9)	1.380(3)
C(8)-H(8)	0.93(3)
C(9)-H(9)	0.89(2)
C(10)-H(10A)	0.96(3)
C(10)-H(10B)	0.95(3)
C(10)-H(10C)	0.98(3)
C(2)-N(1)-C(1)	114.39(16)
C(2)-N(1)-Cl(1)	123.98(14)
C(1)-N(1)-Cl(1)	121.61(14)
C(1)-N(2)-C(3)	115.56(16)
C(1)-N(2)-Cl(2)	120.09(14)
C(3)-N(2)-Cl(2)	121.85(13)
O(1)-C(1)-N(2)	130.61(19)
O(1)-C(1)-N(1)	125.81(19)
N(2)-C(1)-N(1)	103.58(17)
O(2)-C(2)-N(1)	126.85(18)
O(2)-C(2)-C(3)	126.97(18)
N(1)-C(2)-C(3)	106.18(16)
N(2)-C(3)-C(4)	111.86(16)
N(2)-C(3)-C(10)	111.70(18)
C(4)-C(3)-C(10)	115.03(18)
N(2)-C(3)-C(2)	99.89(15)
C(4)-C(3)-C(2)	108.99(15)
C(10)-C(3)-C(2)	108.19(17)
C(5)-C(4)-C(9)	118.7(2)
C(5)-C(4)-C(3)	121.71(18)
C(9)-C(4)-C(3)	119.42(18)
C(4)-C(5)-C(6)	120.2(2)
C(4)-C(5)-H(5)	119.7(16)
C(6)-C(5)-H(5)	120.1(16)
C(7)-C(6)-C(5)	120.7(2)
C(7)-C(6)-H(6)	121.0(19)
C(5)-C(6)-H(6)	118.3(19)
C(8)-C(7)-C(6)	119.6(2)
C(8)-C(7)-H(7)	119.4(17)
C(6)-C(7)-H(7)	121.0(17)
C(7)-C(8)-C(9)	120.2(2)
C(7)-C(8)-H(8)	120.5(15)
C(9)-C(8)-H(8)	119.3(15)
C(8)-C(9)-C(4)	120.6(2)
C(8)-C(9)-H(9)	120.1(15)
C(4)-C(9)-H(9)	119.2(15)
C(3)-C(10)-H(10A)	111.1(15)
C(3)-C(10)-H(10B)	109.8(15)
H(10A)-C(10)-H(10B)	108(2)
C(3)-C(10)-H(10C)	110.6(14)
H(10A)-C(10)-H(10C)	107(2)
H(10B)-C(10)-H(10C)	111(2)

Table IV-17. Anisotropic displacement parameters ($\mathring{A}^2$x 10^3)for **IV-31**. The anisotropic displacement factor exponent takes the form: $-2p^2[\, h^2a^{*2}U^{11} + ... + 2\, h\, k\, a^*\, b^*\, U^{12}\,]$

	U^{11}	U^{22}	U^{33}	U^{23}	U^{13}	U^{12}
Cl(1)	21(1)	68(1)	30(1)	5(1)	4(1)	1(1)
Cl(2)	19(1)	49(1)	38(1)	7(1)	16(1)	6(1)
O(1)	34(1)	76(1)	24(1)	4(1)	16(1)	7(1)
O(2)	22(1)	40(1)	42(1)	-2(1)	15(1)	9(1)
N(1)	16(1)	51(1)	23(1)	3(1)	5(1)	5(1)
N(2)	16(1)	56(1)	26(1)	1(1)	11(1)	6(1)
C(1)	22(1)	44(1)	26(1)	10(1)	11(1)	6(1)
C(2)	20(1)	24(1)	29(1)	5(1)	9(1)	5(1)
C(3)	18(1)	30(1)	28(1)	1(1)	11(1)	3(1)
C(4)	15(1)	25(1)	25(1)	0(1)	7(1)	1(1)
C(5)	39(1)	30(1)	30(1)	-5(1)	9(1)	7(1)
C(6)	46(1)	27(1)	45(1)	4(1)	4(1)	6(1)
C(7)	31(1)	43(1)	32(1)	12(1)	4(1)	-6(1)
C(8)	33(1)	53(2)	26(1)	0(1)	13(1)	2(1)
C(9)	29(1)	30(1)	32(1)	-2(1)	14(1)	6(1)
C(10)	31(1)	34(1)	44(1)	9(1)	14(1)	0(1)

Table IV-18. Hydrogen coordinates (x 10^4) and isotropic displacement parameters ($\mathring{A}^2$x 10^3) for **IV-31**.

	x	y	z	U(eq)
H(5)	2700(30)	4680(30)	1610(30)	40(7)
H(6)	2080(40)	6120(40)	-360(30)	60(9)
H(7)	2060(40)	4880(30)	-2520(30)	53(8)
H(8)	2550(30)	2090(30)	-2630(30)	43(7)
H(9)	3090(30)	640(30)	-600(20)	36(6)
H(10A)	3380(40)	-930(30)	1200(30)	48(7)
H(10B)	3200(30)	-920(30)	2700(30)	46(7)
H(10C)	1440(40)	-690(30)	1250(30)	40(7)

Table IV-19. Torsion angles [°] for **IV-31**.

C(3)-N(2)-C(1)-O(1)	-173.6(2)
Cl(2)-N(2)-C(1)-O(1)	-11.2(4)
C(3)-N(2)-C(1)-N(1)	6.5(2)
Cl(2)-N(2)-C(1)-N(1)	168.88(15)
C(2)-N(1)-C(1)-O(1)	176.1(2)
Cl(1)-N(1)-C(1)-O(1)	-4.8(3)
C(2)-N(1)-C(1)-N(2)	-4.0(2)
Cl(1)-N(1)-C(1)-N(2)	175.05(15)
C(1)-N(1)-C(2)-O(2)	-179.9(2)
Cl(1)-N(1)-C(2)-O(2)	1.1(3)
C(1)-N(1)-C(2)-C(3)	0.2(2)
Cl(1)-N(1)-C(2)-C(3)	-178.78(14)
C(1)-N(2)-C(3)-C(4)	-121.46(19)

Table IV-19 (Cont'd)

Cl(2)-N(2)-C(3)-C(4)	76.5(2)
C(1)-N(2)-C(3)-C(10)	108.0(2)
Cl(2)-N(2)-C(3)-C(10)	-54.1(2)
C(1)-N(2)-C(3)-C(2)	-6.3(2)
Cl(2)-N(2)-C(3)-C(2)	-168.31(14)
O(2)-C(2)-C(3)-N(2)	-176.6(2)
N(1)-C(2)-C(3)-N(2)	3.3(2)
O(2)-C(2)-C(3)-C(4)	-59.3(3)
N(1)-C(2)-C(3)-C(4)	120.64(18)
O(2)-C(2)-C(3)-C(10)	66.5(3)
N(1)-C(2)-C(3)-C(10)	-113.63(19)
N(2)-C(3)-C(4)-C(5)	20.5(3)
C(10)-C(3)-C(4)-C(5)	149.3(2)
C(2)-C(3)-C(4)-C(5)	-89.0(2)
N(2)-C(3)-C(4)-C(9)	-164.00(17)
C(10)-C(3)-C(4)-C(9)	-35.2(3)
C(2)-C(3)-C(4)-C(9)	86.5(2)
C(9)-C(4)-C(5)-C(6)	0.1(3)
C(3)-C(4)-C(5)-C(6)	175.7(2)
C(4)-C(5)-C(6)-C(7)	-0.6(4)
C(5)-C(6)-C(7)-C(8)	0.8(4)
C(6)-C(7)-C(8)-C(9)	-0.5(3)
C(7)-C(8)-C(9)-C(4)	0.0(3)
C(5)-C(4)-C(9)-C(8)	0.2(3)
C(3)-C(4)-C(9)-C(8)	-175.45(19)

Table IV-19 (Cont'd)

Cl(2)-N(2)-C(3)-C(4)	76.5(2)
C(1)-N(2)-C(3)-C(10)	108.0(2)
Cl(2)-N(2)-C(3)-C(10)	-54.1(2)
C(1)-N(2)-C(3)-C(2)	-6.3(2)
Cl(2)-N(2)-C(3)-C(2)	-168.31(14)
O(2)-C(2)-C(3)-N(2)	-176.6(2)
N(1)-C(2)-C(3)-N(2)	3.3(2)
O(2)-C(2)-C(3)-C(4)	-59.3(3)
N(1)-C(2)-C(3)-C(4)	120.64(18)
O(2)-C(2)-C(3)-C(10)	66.5(3)
N(1)-C(2)-C(3)-C(10)	-113.63(19)
N(2)-C(3)-C(4)-C(5)	20.5(3)
C(10)-C(3)-C(4)-C(5)	149.3(2)
C(2)-C(3)-C(4)-C(5)	-89.0(2)
N(2)-C(3)-C(4)-C(9)	-164.00(17)
C(10)-C(3)-C(4)-C(9)	-35.2(3)
C(2)-C(3)-C(4)-C(9)	86.5(2)
C(9)-C(4)-C(5)-C(6)	0.1(3)
C(3)-C(4)-C(5)-C(6)	175.7(2)
C(4)-C(5)-C(6)-C(7)	-0.6(4)
C(5)-C(6)-C(7)-C(8)	0.8(4)
C(6)-C(7)-C(8)-C(9)	-0.5(3)
C(7)-C(8)-C(9)-C(4)	0.0(3)
C(5)-C(4)-C(9)-C(8)	0.2(3)
C(3)-C(4)-C(9)-C(8)	-175.45(19)

Figure IV-6. X-Ray structure of **IV-32**.
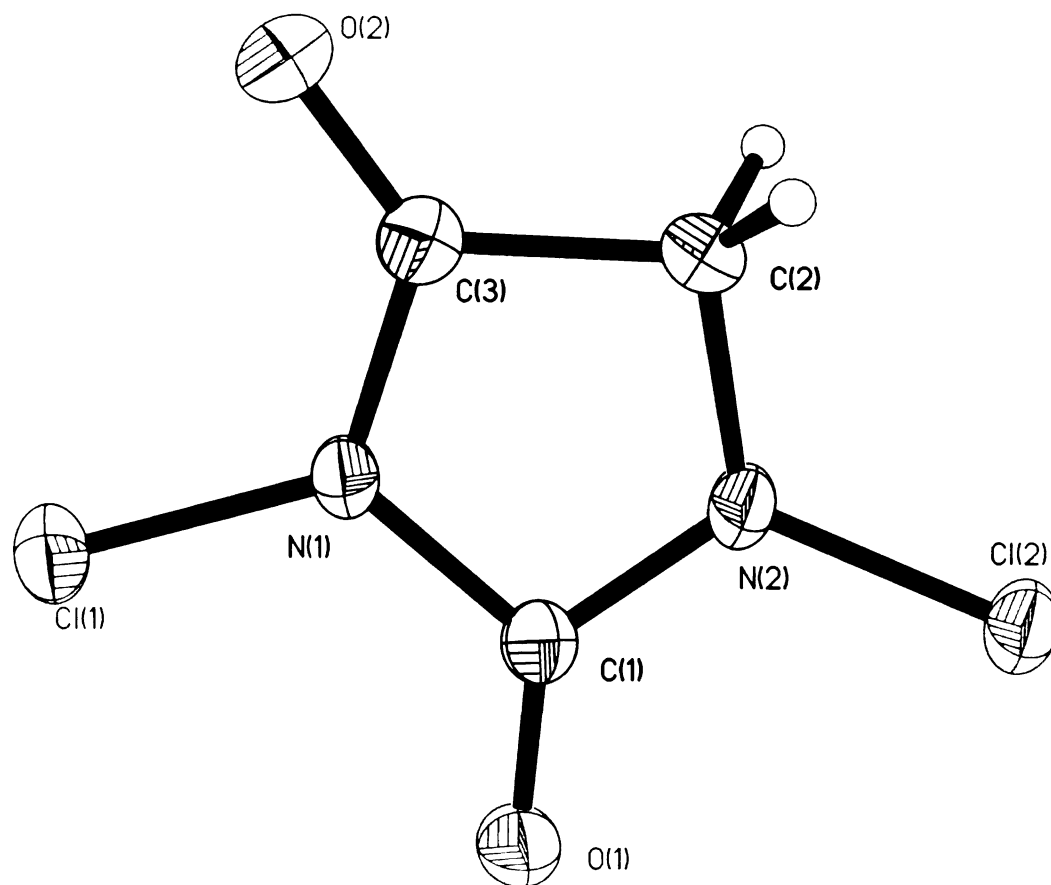
Table IV-20. Crystal data and structure refinement for **V-32**.

Identification code	bb16	
Empirical formula	C3 H2 Cl2 N2 O2	
Formula weight	168.97	
Temperature	173(2) K	
Wavelength	0.71073 Å	
Crystal system	Monoclinic	
Space group	P2(1)/c	
Unit cell dimensions	a = 5.1494(4) Å	a= 90°.
	b = 6.3796(4) Å	b= 92.052(5)°.
	c = 17.3292(13) Å	g = 90°.
Volume	568.92(7) Å^3	
Z	4	
Density (calculated)	1.973 Mg/m^3	
Absorption coefficient	1.052 mm^{-1}	
F(000)	336	
Crystal size	0.27 x 0.05 x 0.05 mm^3	

Table IV-20. (Cont'd)

Theta range for data collection	2.35 to 27.41°.
Index ranges	-6<=h<=6, 0<=k<=8, 0<=l<=22
Reflections collected	2321
Independent reflections	2321 [R(int) = 0.0000]
Completeness to theta = 25.00°	100.0 %
Absorption correction	Semi-empirical from equivalents
Max. and min. transmission	0.9522 and 0.7629
Refinement method	Full-matrix least-squares on F^2
Data / restraints / parameters	2321 / 0 / 91
Goodness-of-fit on F^2	1.032
Final R indices [I>2sigma(I)]	R1 = 0.0425, wR2 = 0.0832
R indices (all data)	R1 = 0.0605, wR2 = 0.0914
Largest diff. peak and hole	0.425 and -0.315 e.Å^{-3}

Table IV-21. Atomic coordinates (x 10^4) and equivalent isotropic displacement parameters (Å^2x 10^3) for **IV-32**. U(eq) is defined as one third of the trace of the orthogonalized U^{ij} tensor.

	x	y	z	U(eq)
Cl(1)	12951(1)	6387(1)	679(1)	27(1)
Cl(2)	5728(1)	2307(1)	2226(1)	26(1)
O(1)	8573(3)	6362(3)	1833(1)	27(1)
O(2)	12928(3)	1721(3)	321(1)	32(1)
N(2)	8021(4)	2823(3)	1587(1)	31(1)
N(1)	11082(4)	4436(3)	990(1)	22(1)
C(1)	9100(4)	4746(4)	1527(1)	21(1)
C(2)	9314(5)	1175(4)	1175(2)	27(1)
C(3)	11372(5)	2373(4)	761(1)	24(1)

Table IV-22. Bond lengths [Å] and angles [°] for **IV-32**.

Cl(1)-N(1)	1.674(2)
Cl(2)-N(2)	1.679(2)
O(1)-C(1)	1.195(3)
O(2)-C(3)	1.201(3)
N(2)-C(1)	1.352(3)
N(2)-C(2)	1.447(3)
N(1)-C(3)	1.384(3)
N(1)-C(1)	1.420(3)
C(2)-C(3)	1.508(3)
C(2)-H(2A)	0.98(3)
C(2)-H(2B)	0.98(3)
C(1)-N(2)-C(2)	115.1(2)
C(1)-N(2)-Cl(2)	121.94(18)
C(2)-N(2)-Cl(2)	121.98(17)
C(3)-N(1)-C(1)	114.04(19)
C(3)-N(1)-Cl(1)	123.07(17)
C(1)-N(1)-Cl(1)	122.88(16)
O(1)-C(1)-N(2)	130.4(2)
O(1)-C(1)-N(1)	126.3(2)

Table IV-22. (Cont'd)

N(2)-C(1)-N(1)	103.4(2)
N(2)-C(2)-C(3)	102.1(2)
N(2)-C(2)-H(2A)	113.2(16)
C(3)-C(2)-H(2A)	112.3(15)
N(2)-C(2)-H(2B)	111.4(16)
C(3)-C(2)-H(2B)	111.3(16)
H(2A)-C(2)-H(2B)	107(2)
O(2)-C(3)-N(1)	126.4(2)
O(2)-C(3)-C(2)	128.5(2)
N(1)-C(3)-C(2)	105.1(2)

Table IV-23. Anisotropic displacement parameters ($Å^2$x 10^3)for **IV-32**. The anisotropic displacement factor exponent takes the form: $-2p^2[h^2a^{*2}U^{11} + ... + 2 h k a^* b^* U^{12}]$

	U^{11}	U^{22}	U^{33}	U^{23}	U^{13}	U^{12}
Cl(1)	25(1)	27(1)	30(1)	3(1)	5(1)	-7(1)
Cl(2)	25(1)	27(1)	28(1)	3(1)	9(1)	-2(1)
O(1)	26(1)	21(1)	35(1)	-4(1)	8(1)	0(1)
O(2)	31(1)	31(1)	36(1)	-8(1)	14(1)	-1(1)
N(2)	35(1)	20(1)	39(1)	-1(1)	24(1)	-3(1)
N(1)	21(1)	18(1)	26(1)	1(1)	7(1)	-3(1)
C(1)	18(1)	22(1)	22(1)	1(1)	1(1)	-1(1)
C(2)	33(2)	18(1)	31(2)	-3(1)	9(1)	-3(1)
C(3)	23(1)	24(1)	24(1)	-1(1)	2(1)	-1(1)

Table IV-24. Hydrogen coordinates (x 10^4) and isotropic displacement parameters ($Å^2$x 10^3) for **IV-32**.

	x	y	z	U(eq)
H(2A)	10050(50)	90(50)	1514(15)	27(7)
H(2B)	8120(50)	470(50)	809(16)	41(8)

Table IV-25. Torsion angles [°] for **IV-32**.

C(2)-N(2)-C(1)-O(1)	-175.1(3)
Cl(2)-N(2)-C(1)-O(1)	-6.4(4)
C(2)-N(2)-C(1)-N(1)	5.5(3)
Cl(2)-N(2)-C(1)-N(1)	174.19(17)
C(3)-N(1)-C(1)-O(1)	176.2(2)
Cl(1)-N(1)-C(1)-O(1)	-2.2(4)
C(3)-N(1)-C(1)-N(2)	-4.3(3)
Cl(1)-N(1)-C(1)-N(2)	177.25(17)
C(1)-N(2)-C(2)-C(3)	-4.6(3)
Cl(2)-N(2)-C(2)-C(3)	-173.31(18)
C(1)-N(1)-C(3)-O(2)	-179.1(2)

Table IV-25. (Cont'd)

Cl(1)-N(1)-C(3)-O(2)	-0.7(4)
C(1)-N(1)-C(3)-C(2)	1.6(3)
Cl(1)-N(1)-C(3)-C(2)	-179.95(17)
N(2)-C(2)-C(3)-O(2)	-177.7(3)
N(2)-C(2)-C(3)-N(1)	1.6(3)

Figure IV-7. X-Ray structure of **IV-33**.
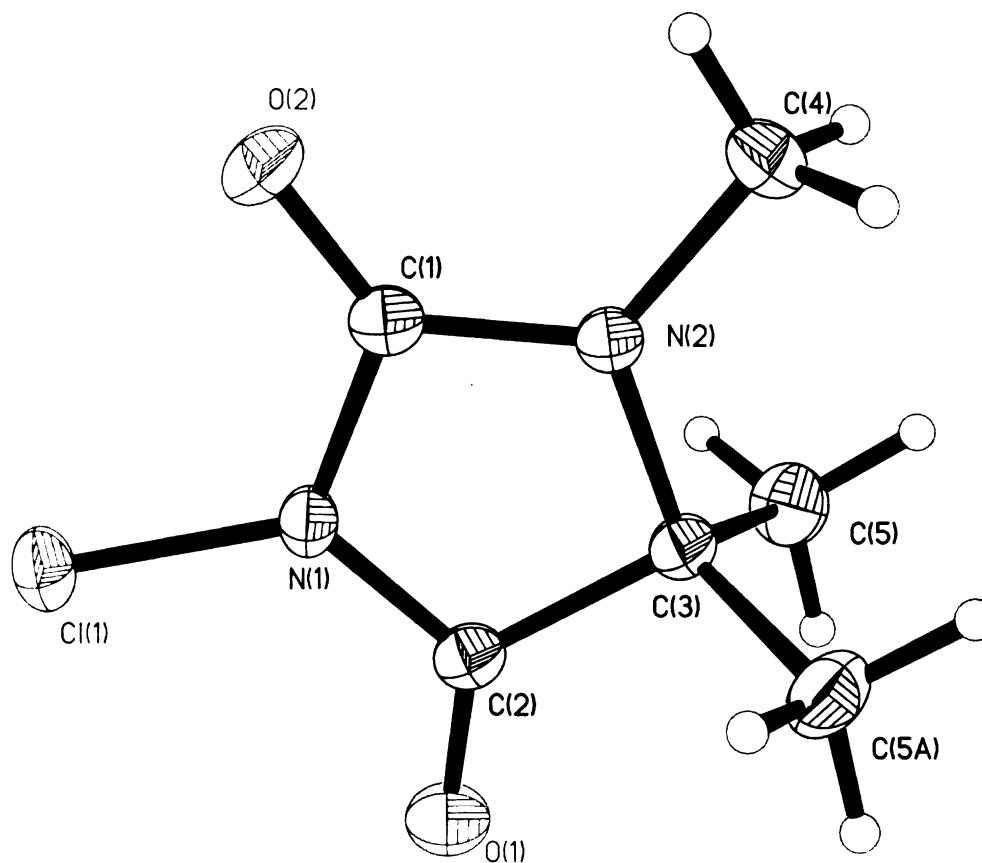
Table IV-26. Crystal data and structure refinement for **IV-33**.

Identification code	bb15
Empirical formula	C6 H9 Cl N2 O2
Formula weight	176.60
Temperature	173(2) K
Wavelength	0.71073 Å
Crystal system	Orthorhombic
Space group	Pnma
Unit cell dimensions	a = 10.8647(17) Å $\quad$ a= 90°.
	b = 6.7327(11) Å $\quad$ b= 90°.
	c = 10.7494(17) Å $\quad$ g = 90°.
Volume	786.3(2) Å^3
Z	4
Density (calculated)	1.492 Mg/m^3
Absorption coefficient	0.436 mm^{-1}
F(000)	368
Crystal size	0.20 x 0.14 x 0.10 mm^3

265

Table IV-26 (Cont'd.)

Theta range for data collection	2.67 to 28.15°.
Index ranges	-14<=h<=14, -8<=k<=8, -13<=l<=13
Reflections collected	8151
Independent reflections	1001 [R(int) = 0.0400]
Completeness to theta = 25.00°	100.0 %
Absorption correction	Semi-empirical from equivalents
Max. and min. transmission	0.9577 and 0.9179
Refinement method	Full-matrix least-squares on F^2
Data / restraints / parameters	1001 / 0 / 83
Goodness-of-fit on F^2	1.058
Final R indices [I>2sigma(I)]	R1 = 0.0295, wR2 = 0.0782
R indices (all data)	R1 = 0.0367, wR2 = 0.0816
Largest diff. peak and hole	0.383 and -0.211 e.$Å^{-3}$

Table IV-27. Atomic coordinates (x 10^4) and equivalent isotropic displacement parameters ($Å^2$x 10^3) for **IV-33**. U(eq) is defined as one third of the trace of the orthogonalized U^{ij} tensor.

	x	y	z	U(eq)
Cl(1)	4604(1)	2500	6770(1)	25(1)
O(1)	7435(1)	2500	6795(1)	30(1)
O(2)	4258(1)	2500	3981(1)	29(1)
N(1)	5657(1)	2500	5628(1)	21(1)
N(2)	6373(1)	2500	3713(1)	19(1)
C(1)	5315(2)	2500	4343(2)	20(1)
C(2)	6904(2)	2500	5810(2)	20(1)
C(3)	7474(2)	2500	4508(2)	19(1)
C(4)	6428(2)	2500	2359(2)	27(1)
C(5)	8234(1)	613(2)	4332(2)	29(1)

Table IV-28. Bond lengths [Å] and angles [°] for **IV-33**.

Cl(1)-N(1)	1.6787(16)
O(1)-C(2)	1.206(2)
O(2)-C(1)	1.212(2)
N(1)-C(2)	1.368(2)
N(1)-C(1)	1.430(2)
N(2)-C(1)	1.335(2)
N(2)-C(4)	1.456(2)
N(2)-C(3)	1.470(2)
C(2)-C(3)	1.530(2)
C(3)-C(5)#1	1.5271(17)
C(3)-C(5)	1.5271(17)
C(4)-H(4A)	0.91(2)
C(4)-H(4B)	0.89(4)
C(5)-H(5A)	0.966(18)
C(5)-H(5B)	0.970(18)
C(5)-H(5C)	0.934(18)
C(2)-N(1)-C(1)	113.31(15)
C(2)-N(1)-Cl(1)	124.80(13)

Table IV-28. (Cont'd)

C(1)-N(1)-Cl(1)	121.89(13)
C(1)-N(2)-C(4)	122.85(16)
C(1)-N(2)-C(3)	113.94(15)
C(4)-N(2)-C(3)	123.21(15)
O(2)-C(1)-N(2)	130.75(18)
O(2)-C(1)-N(1)	123.85(17)
N(2)-C(1)-N(1)	105.40(15)
O(1)-C(2)-N(1)	126.79(17)
O(1)-C(2)-C(3)	127.54(16)
N(1)-C(2)-C(3)	105.67(15)
N(2)-C(3)-C(5)#1	111.57(10)
N(2)-C(3)-C(5)	111.57(10)
C(5)#1-C(3)-C(5)	112.59(17)
N(2)-C(3)-C(2)	101.68(14)
C(5)#1-C(3)-C(2)	109.42(10)
C(5)-C(3)-C(2)	109.42(10)
N(2)-C(4)-H(4A)	110.7(13)
N(2)-C(4)-H(4B)	110(2)
H(4A)-C(4)-H(4B)	110.6(18)
C(3)-C(5)-H(5A)	110.4(11)
C(3)-C(5)-H(5B)	109.9(11)
H(5A)-C(5)-H(5B)	108.5(14)
C(3)-C(5)-H(5C)	109.2(10)
H(5A)-C(5)-H(5C)	110.8(14)
H(5B)-C(5)-H(5C)	108.0(14)

Table IV-29. Anisotropic displacement parameters (Å^2x 10^3)for **IV-33**. The anisotropic displacement factor exponent takes the form: $-2p^2[h^2a^{*2}U^{11} + ... + 2 h k a^* b^* U^{12}]$

	U^{11}	U^{22}	U^{33}	U^{23}	U^{13}	U^{12}
Cl(1)	23(1)	29(1)	23(1)	0	7(1)	0
O(1)	26(1)	42(1)	22(1)	0	-7(1)	0
O(2)	15(1)	42(1)	29(1)	0	-4(1)	0
N(1)	15(1)	30(1)	17(1)	0	2(1)	0
N(2)	16(1)	27(1)	16(1)	0	-1(1)	0
C(1)	20(1)	19(1)	20(1)	0	-2(1)	0
C(2)	18(1)	20(1)	21(1)	0	-2(1)	0
C(3)	15(1)	24(1)	18(1)	0	-2(1)	0
C(4)	27(1)	37(1)	17(1)	0	0(1)	0
C(5)	23(1)	32(1)	33(1)	-3(1)	0(1)	9(1)

Table IV-30. Hydrogen coordinates (x 10^4) and isotropic displacement parameters (Å^2x 10^3) for **IV-33**.

	x	y	z	U(eq)
H(4A)	6870(20)	1430(30)	2077(19)	69(7)
H(4B)	5670(30)	2500	2040(30)	66(10)

Table IV-30. (Cont'd)

H(5A)	8569(15)	560(30)	3500(17)	38(5)
H(5B)	8911(16)	590(30)	4921(17)	35(5)
H(5C)	7739(16)	-490(30)	4488(15)	32(5)

Table IV-31. Torsion angles [°] for **IV-33**.

C(4)-N(2)-C(1)-O(2)	0.0
C(3)-N(2)-C(1)-O(2)	180.0
C(4)-N(2)-C(1)-N(1)	180.0
C(3)-N(2)-C(1)-N(1)	0.0
C(2)-N(1)-C(1)-O(2)	180.0
Cl(1)-N(1)-C(1)-O(2)	0.0
C(2)-N(1)-C(1)-N(2)	0.0
Cl(1)-N(1)-C(1)-N(2)	180.0
C(1)-N(1)-C(2)-O(1)	180.0
Cl(1)-N(1)-C(2)-O(1)	0.0
C(1)-N(1)-C(2)-C(3)	0.0
Cl(1)-N(1)-C(2)-C(3)	180.0
C(1)-N(2)-C(3)-C(5)#1	-116.54(12)
C(4)-N(2)-C(3)-C(5)#1	63.46(12)
C(1)-N(2)-C(3)-C(5)	116.54(12)
C(4)-N(2)-C(3)-C(5)	-63.46(12)
C(1)-N(2)-C(3)-C(2)	0.0
C(4)-N(2)-C(3)-C(2)	180.0
O(1)-C(2)-C(3)-N(2)	180.0
N(1)-C(2)-C(3)-N(2)	0.0
O(1)-C(2)-C(3)-C(5)#1	-61.90(10)
N(1)-C(2)-C(3)-C(5)#1	118.10(10)
O(1)-C(2)-C(3)-C(5)	61.90(10)
N(1)-C(2)-C(3)-C(5)	-118.10(10)

Figure IV-8. X-Ray structure of **IV-34**.
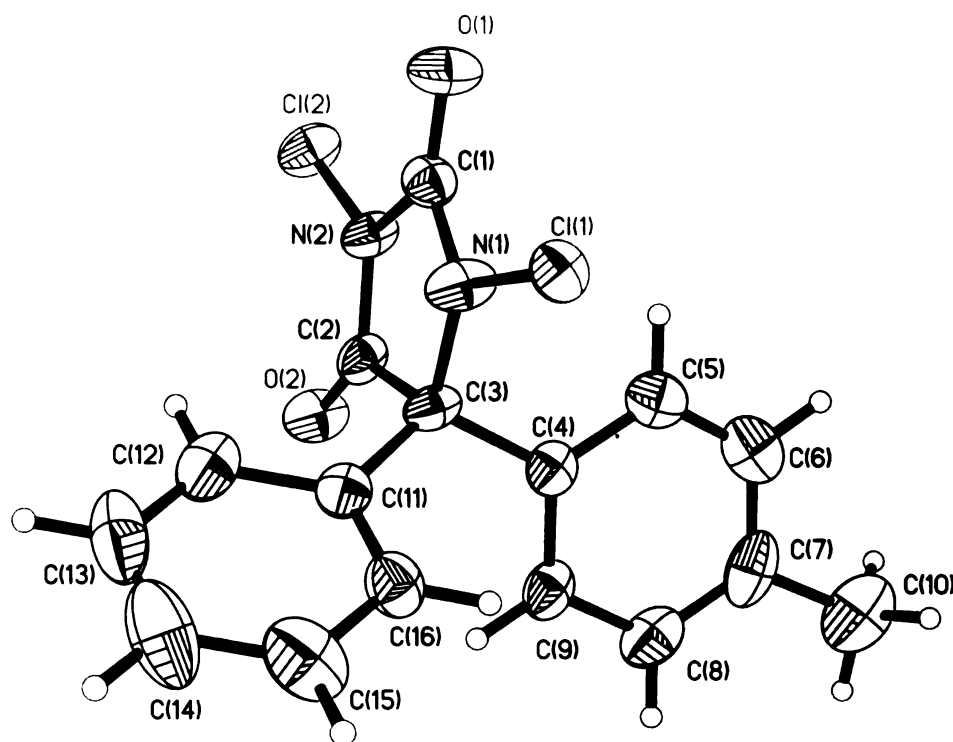
Table IV-32. Crystal data and structure refinement for **IV-34**.

Identification code	bb19_0m
Empirical formula	C16 H12 Cl2 N2 O2
Formula weight	335.18
Temperature	173(2) K
Wavelength	0.71073 Å
Crystal system	Orthorhombic
Space group	P2(1)2(1)2(1)
Unit cell dimensions	a = 7.8122(12) Å a= 90°.
	b = 12.4926(18) Å b= 90°.
	c = 15.579(3) Å g = 90°.
Volume	1520.4(4) Å^3
Z	4
Density (calculated)	1.464 Mg/m^3
Absorption coefficient	0.435 mm^{-1}
F(000)	688
Crystal size	0.27 x 0.24 x 0.08 mm^3
Theta range for data collection	2.09 to 25.34°.
Index ranges	-9<=h<=9, -10<=k<=15, -18<=l<=16
Reflections collected	4533
Independent reflections	2692 [R(int) = 0.0406]
Completeness to theta = 25.00°	99.2 %

269

Table IV-32. (Cont'd)

Absorption correction	Semi-empirical from equivalents
Max. and min. transmission	0.9669 and 0.8924
Refinement method	Full-matrix least-squares on F^2
Data / restraints / parameters	2692 / 0 / 200
Goodness-of-fit on F^2	1.028
Final R indices [I>2sigma(I)]	R1 = 0.0567, wR2 = 0.1265
R indices (all data)	R1 = 0.0731, wR2 = 0.1358
Absolute structure parameter	0.14(12)
Largest diff. peak and hole	0.716 and -0.261 e.Å^{-3}

Table IV-33. Atomic coordinates (x 10^4) and equivalent isotropic displacement parameters (Å^2x 10^3) for **IV-34**. U(eq) is defined as one third of the trace of the orthogonalized U^{ij} tensor.

	x	y	z	U(eq)
Cl(1)	2395(2)	4080(1)	-293(1)	34(1)
Cl(2)	8566(2)	2796(1)	-1342(1)	42(1)
O(1)	4697(5)	2575(3)	-1313(3)	44(1)
O(2)	8836(4)	4715(3)	-134(3)	45(1)
N(1)	4551(5)	3998(3)	-363(3)	39(1)
N(2)	7073(5)	3543(3)	-847(3)	32(1)
C(1)	5293(7)	3281(4)	-897(3)	33(1)
C(2)	7430(6)	4384(3)	-304(3)	33(1)
C(3)	5695(6)	4813(3)	12(3)	31(1)
C(4)	5426(6)	5911(4)	-411(3)	31(1)
C(5)	4677(7)	5995(4)	-1214(3)	40(1)
C(6)	4513(8)	6948(5)	-1608(4)	49(2)
C(7)	5075(7)	7880(4)	-1209(4)	48(2)
C(8)	5849(7)	7815(4)	-424(4)	45(1)
C(9)	6054(6)	6825(4)	-8(4)	38(1)
C(10)	4803(10)	8917(5)	-1686(5)	70(2)
C(11)	5561(6)	4758(4)	993(3)	32(1)
C(12)	6493(7)	3980(4)	1444(4)	46(1)
C(13)	6228(10)	3861(5)	2320(5)	63(2)
C(14)	5096(9)	4463(6)	2759(5)	70(2)
C(15)	4183(8)	5229(6)	2316(4)	60(2)
C(16)	4407(7)	5380(4)	1435(4)	39(1)

Table IV-34. Bond lengths [Å] and angles [°] for **IV-34**.

Cl(1)-N(1)	1.691(4)
Cl(2)-N(2)	1.681(4)
O(1)-C(1)	1.190(5)
O(2)-C(2)	1.203(6)
N(1)-C(1)	1.353(6)
N(1)-C(3)	1.475(6)
N(2)-C(2)	1.377(6)
N(2)-C(1)	1.431(6)
C(2)-C(3)	1.539(7)
C(3)-C(11)	1.534(7)
C(3)-C(4)	1.537(6)

Table IV-34. (Cont'd)

C(4)-C(5)	1.385(7)
C(4)-C(9)	1.393(7)
C(5)-C(6)	1.345(8)
C(5)-H(5)	0.9500
C(6)-C(7)	1.392(8)
C(6)-H(6)	0.9500
C(7)-C(8)	1.366(8)
C(7)-C(10)	1.509(8)
C(8)-C(9)	1.405(7)
C(8)-H(8)	0.9500
C(9)-H(9)	0.9500
C(10)-H(10A)	0.9800
C(10)-H(10B)	0.9800
C(10)-H(10C)	0.9800
C(11)-C(16)	1.374(7)
C(11)-C(12)	1.403(7)
C(12)-C(13)	1.388(9)
C(12)-H(12)	0.9500
C(13)-C(14)	1.348(10)
C(13)-H(13)	0.9500
C(14)-C(15)	1.379(9)
C(14)-H(14)	0.9500
C(15)-C(16)	1.398(8)
C(15)-H(15)	0.9500
C(16)-H(16)	0.9500
C(1)-N(1)-C(3)	116.1(4)
C(1)-N(1)-Cl(1)	120.4(3)
C(3)-N(1)-Cl(1)	122.4(3)
C(2)-N(2)-C(1)	113.9(4)
C(2)-N(2)-Cl(2)	124.4(3)
C(1)-N(2)-Cl(2)	121.5(3)
O(1)-C(1)-N(1)	131.2(5)
O(1)-C(1)-N(2)	125.4(5)
N(1)-C(1)-N(2)	103.4(4)
O(2)-C(2)-N(2)	125.6(5)
O(2)-C(2)-C(3)	127.9(4)
N(2)-C(2)-C(3)	106.5(4)
N(1)-C(3)-C(11)	108.8(4)
N(1)-C(3)-C(4)	111.3(4)
C(11)-C(3)-C(4)	117.3(4)
N(1)-C(3)-C(2)	99.6(3)
C(11)-C(3)-C(2)	111.3(4)
C(4)-C(3)-C(2)	107.1(4)
C(5)-C(4)-C(9)	119.6(5)
C(5)-C(4)-C(3)	120.8(4)
C(9)-C(4)-C(3)	119.4(4)
C(6)-C(5)-C(4)	121.3(5)
C(6)-C(5)-H(5)	119.4
C(4)-C(5)-H(5)	119.4
C(5)-C(6)-C(7)	120.5(5)
C(5)-C(6)-H(6)	119.8
C(7)-C(6)-H(6)	119.8
C(8)-C(7)-C(6)	119.3(5)

271

Table IV-34. (Cont'd)

C(8)-C(7)-C(10)	123.7(6)
C(6)-C(7)-C(10)	117.0(6)
C(7)-C(8)-C(9)	121.1(5)
C(7)-C(8)-H(8)	119.5
C(9)-C(8)-H(8)	119.5
C(4)-C(9)-C(8)	118.2(5)
C(4)-C(9)-H(9)	120.9
C(8)-C(9)-H(9)	120.9
C(7)-C(10)-H(10A)	109.5
C(7)-C(10)-H(10B)	109.5
H(10A)-C(10)-H(10B)	109.5
C(7)-C(10)-H(10C)	109.5
H(10A)-C(10)-H(10C)	109.5
H(10B)-C(10)-H(10C)	109.5
C(16)-C(11)-C(12)	118.8(5)
C(16)-C(11)-C(3)	121.2(5)
C(12)-C(11)-C(3)	119.6(5)
C(13)-C(12)-C(11)	119.3(6)
C(13)-C(12)-H(12)	120.4
C(11)-C(12)-H(12)	120.4
C(14)-C(13)-C(12)	122.5(6)
C(14)-C(13)-H(13)	118.8
C(12)-C(13)-H(13)	118.8
C(13)-C(14)-C(15)	118.2(7)
C(13)-C(14)-H(14)	120.9
C(15)-C(14)-H(14)	120.9
C(14)-C(15)-C(16)	121.4(7)
C(14)-C(15)-H(15)	119.3
C(16)-C(15)-H(15)	119.3
C(11)-C(16)-C(15)	119.8(6)
C(11)-C(16)-H(16)	120.1
C(15)-C(16)-H(16)	120.1

Table IV-35. Anisotropic displacement parameters (Å^2x 10^3)for **IV-34**. The anisotropic displacement factor exponent takes the form: $-2p^2[h^2a^{*2}U^{11} + ... + 2 h k a^* b^* U^{12}]$

	U^{11}	U^{22}	U^{33}	U^{23}	U^{13}	U^{12}
Cl(1)	17(1)	41(1)	45(1)	0(1)	-1(1)	-4(1)
Cl(2)	35(1)	35(1)	54(1)	-7(1)	12(1)	4(1)
O(1)	39(2)	41(2)	52(2)	-16(2)	5(2)	-12(2)
O(2)	18(2)	45(2)	73(3)	-17(2)	-2(2)	-2(2)
N(1)	18(2)	35(2)	65(3)	-15(2)	7(2)	-5(2)
N(2)	19(2)	28(2)	48(3)	-9(2)	6(2)	2(2)
C(1)	30(3)	33(3)	35(3)	1(2)	-1(2)	-6(2)
C(2)	22(2)	28(2)	49(3)	-3(2)	-3(3)	4(2)
C(3)	20(2)	26(2)	47(3)	-9(2)	2(2)	0(2)
C(4)	17(2)	33(2)	42(3)	1(2)	2(2)	-2(2)
C(5)	39(3)	45(3)	37(3)	-3(3)	6(3)	-2(3)
C(6)	41(3)	66(4)	41(3)	3(3)	2(3)	-3(3)
C(7)	33(3)	54(3)	57(4)	19(3)	20(3)	16(3)
C(8)	32(3)	32(2)	72(4)	0(3)	6(3)	-6(2)

Table IV-35. (Cont'd)

C(9)	23(3)	33(2)	58(4)	2(2)	-4(2)	1(2)
C(10)	62(5)	59(4)	90(6)	10(4)	19(4)	4(4)
C(11)	26(3)	27(2)	44(3)	2(2)	-5(2)	-9(2)
C(12)	30(3)	35(3)	73(4)	4(3)	-8(3)	-5(3)
C(13)	54(4)	64(4)	70(5)	32(3)	-29(4)	-21(4)
C(14)	39(4)	113(6)	57(5)	27(4)	-7(4)	-9(4)
C(15)	37(4)	90(5)	52(4)	-6(4)	2(3)	-6(4)
C(16)	30(3)	50(3)	38(3)	0(3)	-2(3)	3(3)

Table IV-36. Hydrogen coordinates (x 10^4) and isotropic displacement parameters ($Å^2$x 10^3) for **IV-34**.

	x	y	z	U(eq)
H(5)	4272	5368	-1493	48
H(6)	4009	6984	-2162	59
H(8)	6255	8449	-155	54
H(9)	6606	6781	535	46
H(10A)	3575	9073	-1718	105
H(10B)	5270	8853	-2268	105
H(10C)	5387	9499	-1382	105
H(12)	7296	3539	1153	56
H(13)	6870	3335	2621	75
H(14)	4930	4361	3358	83
H(15)	3386	5664	2617	72
H(16)	3763	5911	1141	47

Table IV-37. Torsion angles [°] for **IV-34**.

C(3)-N(1)-C(1)-O(1)	-176.6(5)
Cl(1)-N(1)-C(1)-O(1)	-7.8(8)
C(3)-N(1)-C(1)-N(2)	4.8(6)
Cl(1)-N(1)-C(1)-N(2)	173.6(4)
C(2)-N(2)-C(1)-O(1)	-178.7(5)
Cl(2)-N(2)-C(1)-O(1)	-4.1(7)
C(2)-N(2)-C(1)-N(1)	0.1(6)
Cl(2)-N(2)-C(1)-N(1)	174.6(3)
C(1)-N(2)-C(2)-O(2)	176.8(5)
Cl(2)-N(2)-C(2)-O(2)	2.4(8)
C(1)-N(2)-C(2)-C(3)	-4.4(6)
Cl(2)-N(2)-C(2)-C(3)	-178.8(3)
C(1)-N(1)-C(3)-C(11)	-123.7(5)
Cl(1)-N(1)-C(3)-C(11)	67.8(5)
C(1)-N(1)-C(3)-C(4)	105.6(5)
Cl(1)-N(1)-C(3)-C(4)	-63.0(6)
C(1)-N(1)-C(3)-C(2)	-7.1(6)
Cl(1)-N(1)-C(3)-C(2)	-175.6(4)
O(2)-C(2)-C(3)-N(1)	-174.8(5)
N(2)-C(2)-C(3)-N(1)	6.4(5)
O(2)-C(2)-C(3)-C(11)	-60.2(7)

Table IV-37. (Cont'd)

N(2)-C(2)-C(3)-C(11)	121.0(4)
O(2)-C(2)-C(3)-C(4)	69.2(7)
N(2)-C(2)-C(3)-C(4)	-109.6(4)
N(1)-C(3)-C(4)-C(5)	-20.8(6)
C(11)-C(3)-C(4)-C(5)	-147.0(5)
C(2)-C(3)-C(4)-C(5)	87.1(5)
N(1)-C(3)-C(4)-C(9)	163.8(4)
C(11)-C(3)-C(4)-C(9)	37.6(6)
C(2)-C(3)-C(4)-C(9)	-88.4(5)
C(9)-C(4)-C(5)-C(6)	-1.3(8)
C(3)-C(4)-C(5)-C(6)	-176.7(5)
C(4)-C(5)-C(6)-C(7)	-0.9(8)
C(5)-C(6)-C(7)-C(8)	2.1(8)
C(5)-C(6)-C(7)-C(10)	-178.6(6)
C(6)-C(7)-C(8)-C(9)	-1.3(8)
C(10)-C(7)-C(8)-C(9)	179.5(5)
C(5)-C(4)-C(9)-C(8)	2.1(7)
C(3)-C(4)-C(9)-C(8)	177.6(5)
C(7)-C(8)-C(9)-C(4)	-0.8(7)
N(1)-C(3)-C(11)-C(16)	-91.7(5)
C(4)-C(3)-C(11)-C(16)	35.7(7)
C(2)-C(3)-C(11)-C(16)	159.5(4)
N(1)-C(3)-C(11)-C(12)	81.2(5)
C(4)-C(3)-C(11)-C(12)	-151.3(4)
C(2)-C(3)-C(11)-C(12)	-27.5(6)
C(16)-C(11)-C(12)-C(13)	-0.2(8)
C(3)-C(11)-C(12)-C(13)	-173.2(5)
C(11)-C(12)-C(13)-C(14)	0.4(9)
C(12)-C(13)-C(14)-C(15)	-0.6(10)
C(13)-C(14)-C(15)-C(16)	0.5(10)
C(12)-C(11)-C(16)-C(15)	0.0(8)
C(3)-C(11)-C(16)-C(15)	173.0(5)
C(14)-C(15)-C(16)-C(11)	-0.2(9)

Figure IV-9. X-Ray structure of **IV-35**.
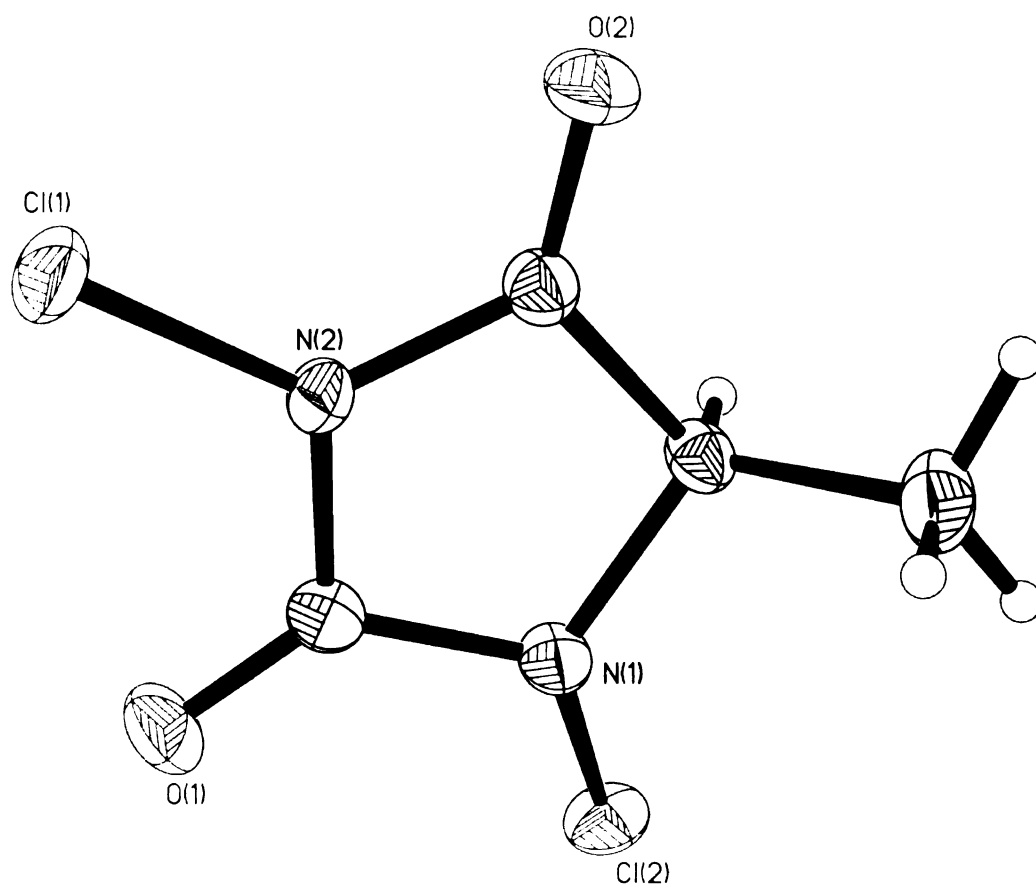
Table IV-38. Crystal data and structure refinement for **IV-35**.

Identification code	bb18m
Empirical formula	C4 H4 Cl2 N2 O2
Formula weight	182.99
Temperature	173(2) K
Wavelength	0.71073 Å
Crystal system	Monoclinic
Space group	P2(1)/c
Unit cell dimensions	a = 7.3843(9) Å a= 90°.
	b = 7.7305(9) Å b= 96.122(2)°.
	c = 24.564(3) Å g = 90°.
Volume	1394.2(3) Å^3
Z	8
Density (calculated)	1.744 Mg/m^3
Absorption coefficient	0.866 mm^{-1}
F(000)	736
Crystal size	0.12 x 0.10 x 0.08 mm^3
Theta range for data collection	1.67 to 28.30°.

Table IV-38. (Cont'd)

Index ranges	-9<=h<=9, -9<=k<=9, -32<=l<=30
Reflections collected	11179
Independent reflections	3126 [R(int) = 0.0334]
Completeness to theta = 25.00°	99.6 %
Absorption correction	Semi-empirical from equivalents
Max. and min. transmission	0.9340 and 0.9032
Refinement method	Full-matrix least-squares on F^2
Data / restraints / parameters	3126 / 0 / 213
Goodness-of-fit on F^2	1.052
Final R indices [I>2sigma(I)]	R1 = 0.0298, wR2 = 0.0705
R indices (all data)	R1 = 0.0426, wR2 = 0.0760
Largest diff. peak and hole	0.391 and -0.263 e.Å^{-3}

Table IV-39. Atomic coordinates (x 10^4) and equivalent isotropic displacement parameters (Å^2x 10^3) for **IV-35.** U(eq) is defined as one third of the trace of the orthogonalized U^{ij} tensor.

	x	y	z	U(eq)
Cl(1)	13504(1)	3786(1)	2200(1)	26(1)
Cl(2)	9856(1)	9599(1)	1803(1)	25(1)
O(1)	13000(2)	7618(2)	2379(1)	30(1)
O(2)	9974(2)	3185(2)	1438(1)	30(1)
N(1)	10086(2)	7436(2)	1916(1)	20(1)
N(2)	11802(2)	5106(2)	1960(1)	19(1)
C(1)	11788(2)	6860(2)	2116(1)	20(1)
C(2)	10300(2)	4613(2)	1617(1)	20(1)
C(3)	9149(2)	6232(2)	1515(1)	19(1)
C(4)	7179(3)	5921(3)	1599(1)	30(1)
Cl(1A)	3366(1)	3988(1)	541(1)	33(1)
Cl(2A)	1584(1)	-2083(1)	-341(1)	36(1)
O(1A)	2386(2)	1714(2)	-447(1)	39(1)
O(2A)	2573(2)	-2368(2)	914(1)	32(1)
N(1A)	3513(2)	1805(2)	475(1)	23(1)
N(2A)	2354(2)	-642(2)	143(1)	26(1)
C(1A)	2697(3)	1082(2)	0(1)	25(1)
C(2A)	2714(3)	-991(2)	694(1)	22(1)
C(3A)	3328(3)	720(2)	958(1)	20(1)
C(4A)	5064(3)	574(3)	1340(1)	27(1)

Table IV-40. Bond lengths [Å] and angles [°] for **IV-35**.

Cl(1)-N(2)	1.6766(14)
Cl(2)-N(1)	1.7002(15)
O(1)-C(1)	1.200(2)
O(2)-C(2)	1.203(2)
N(1)-C(1)	1.373(2)
N(1)-C(3)	1.474(2)
N(2)-C(2)	1.374(2)
N(2)-C(1)	1.410(2)
C(2)-C(3)	1.519(2)
C(3)-C(4)	1.510(3)

Table IV-40. (Cont'd)

C(3)-H(3)	0.96(2)
C(4)-H(4A)	0.92(2)
C(4)-H(4B)	0.95(3)
C(4)-H(4C)	0.99(2)
Cl(1A)-N(1A)	1.7000(16)
Cl(2A)-N(2A)	1.6833(15)
O(1A)-C(1A)	1.202(2)
O(2A)-C(2A)	1.203(2)
N(1A)-C(1A)	1.373(2)
N(1A)-C(3A)	1.472(2)
N(2A)-C(2A)	1.378(2)
N(2A)-C(1A)	1.408(2)
C(2A)-C(3A)	1.520(2)
C(3A)-C(4A)	1.509(3)
C(3A)-H(3B)	0.936(19)
C(4A)-H(4D)	0.97(2)
C(4A)-H(4E)	0.93(3)
C(4A)-H(4F)	0.92(2)
C(1)-N(1)-C(3)	112.38(14)
C(1)-N(1)-Cl(2)	116.66(12)
C(3)-N(1)-Cl(2)	118.67(11)
C(2)-N(2)-C(1)	113.93(14)
C(2)-N(2)-Cl(1)	124.95(12)
C(1)-N(2)-Cl(1)	121.09(12)
O(1)-C(1)-N(1)	129.49(17)
O(1)-C(1)-N(2)	126.15(16)
N(1)-C(1)-N(2)	104.32(14)
O(2)-C(2)-N(2)	126.58(16)
O(2)-C(2)-C(3)	127.59(16)
N(2)-C(2)-C(3)	105.82(14)
N(1)-C(3)-C(4)	113.53(16)
N(1)-C(3)-C(2)	101.32(13)
C(4)-C(3)-C(2)	112.09(15)
N(1)-C(3)-H(3)	108.9(12)
C(4)-C(3)-H(3)	112.8(12)
C(2)-C(3)-H(3)	107.4(12)
C(3)-C(4)-H(4A)	108.4(14)
C(3)-C(4)-H(4B)	109.2(16)
H(4A)-C(4)-H(4B)	108(2)
C(3)-C(4)-H(4C)	110.3(13)
H(4A)-C(4)-H(4C)	109.8(19)
H(4B)-C(4)-H(4C)	111(2)
C(1A)-N(1A)-C(3A)	112.47(15)
C(1A)-N(1A)-Cl(1A)	117.28(13)
C(3A)-N(1A)-Cl(1A)	118.47(12)
C(2A)-N(2A)-C(1A)	114.13(15)
C(2A)-N(2A)-Cl(2A)	125.42(13)
C(1A)-N(2A)-Cl(2A)	120.45(13)
O(1A)-C(1A)-N(1A)	129.37(19)
O(1A)-C(1A)-N(2A)	126.20(18)
N(1A)-C(1A)-N(2A)	104.38(15)
O(2A)-C(2A)-N(2A)	126.60(17)
O(2A)-C(2A)-C(3A)	127.98(17)

Table IV-40. (Cont'd)

N(2A)-C(2A)-C(3A)	105.42(15)
N(1A)-C(3A)-C(4A)	113.41(16)
N(1A)-C(3A)-C(2A)	101.64(14)
C(4A)-C(3A)-C(2A)	113.24(16)
N(1A)-C(3A)-H(3B)	107.8(12)
C(4A)-C(3A)-H(3B)	112.8(12)
C(2A)-C(3A)-H(3B)	107.2(12)
C(3A)-C(4A)-H(4D)	110.9(12)
C(3A)-C(4A)-H(4E)	107.3(15)
H(4D)-C(4A)-H(4E)	110(2)
C(3A)-C(4A)-H(4F)	108.7(12)
H(4D)-C(4A)-H(4F)	109.1(17)
H(4E)-C(4A)-H(4F)	110.5(19)

Table IV-41. Anisotropic displacement parameters ($\text{Å}^2 \times 10^3$) for **IV-35**. The anisotropic displacement factor exponent takes the form: $-2p^2[\,h^2 a^{*2} U^{11} + ... + 2\,h\,k\,a^*\,b^*\,U^{12}\,]$

	U^{11}	U^{22}	U^{33}	U^{23}	U^{13}	U^{12}
Cl(1)	22(1)	28(1)	27(1)	3(1)	-1(1)	9(1)
Cl(2)	29(1)	13(1)	32(1)	0(1)	6(1)	1(1)
O(1)	26(1)	29(1)	34(1)	-7(1)	-7(1)	-7(1)
O(2)	32(1)	17(1)	37(1)	-7(1)	-6(1)	1(1)
N(1)	21(1)	11(1)	26(1)	0(1)	-2(1)	-1(1)
N(2)	18(1)	17(1)	22(1)	0(1)	-3(1)	4(1)
C(1)	22(1)	18(1)	20(1)	0(1)	2(1)	-2(1)
C(2)	20(1)	19(1)	19(1)	0(1)	0(1)	0(1)
C(3)	20(1)	15(1)	21(1)	1(1)	-2(1)	-1(1)
C(4)	19(1)	23(1)	46(1)	0(1)	-2(1)	-2(1)
Cl(1A)	46(1)	17(1)	36(1)	4(1)	1(1)	-4(1)
Cl(2A)	36(1)	35(1)	36(1)	-18(1)	-2(1)	-3(1)
O(1A)	60(1)	36(1)	20(1)	5(1)	-2(1)	8(1)
O(2A)	45(1)	18(1)	36(1)	3(1)	9(1)	-1(1)
N(1A)	32(1)	16(1)	21(1)	2(1)	0(1)	-1(1)
N(2A)	33(1)	22(1)	22(1)	-6(1)	-2(1)	-2(1)
C(1A)	26(1)	25(1)	23(1)	-1(1)	3(1)	4(1)
C(2A)	22(1)	21(1)	25(1)	-1(1)	6(1)	2(1)
C(3A)	23(1)	18(1)	20(1)	2(1)	5(1)	2(1)
C(4A)	31(1)	27(1)	22(1)	-2(1)	-2(1)	5(1)

Table IV-42. Hydrogen coordinates ($\times 10^4$) and isotropic displacement parameters ($\text{Å}^2 \times 10^3$) for **IV-35**.

	x	y	z	U(eq)
H(3)	9300(30)	6630(30)	1153(9)	26(5)
H(4A)	6710(30)	5100(30)	1350(10)	41(6)
H(4B)	6510(30)	6960(30)	1528(10)	52(7)
H(4C)	7080(30)	5510(30)	1977(10)	38(6)

278

Table IV-42. (Cont'd)

H(3B)	2350(30)	1150(20)	1131(8)	19(5)
H(4D)	6010(30)	30(30)	1158(8)	31(6)
H(4E)	4800(30)	-80(30)	1639(10)	47(7)
H(4F)	5440(30)	1670(30)	1449(8)	24(5)

Table IV-43. Torsion angles [°] for **IV-35**.

C(3)-N(1)-C(1)-O(1)	167.63(18)
Cl(2)-N(1)-C(1)-O(1)	25.7(3)
C(3)-N(1)-C(1)-N(2)	-14.48(18)
Cl(2)-N(1)-C(1)-N(2)	-156.42(12)
C(2)-N(2)-C(1)-O(1)	-174.27(18)
Cl(1)-N(2)-C(1)-O(1)	7.5(3)
C(2)-N(2)-C(1)-N(1)	7.75(19)
Cl(1)-N(2)-C(1)-N(1)	-170.45(12)
C(1)-N(2)-C(2)-O(2)	-178.10(18)
Cl(1)-N(2)-C(2)-O(2)	0.0(3)
C(1)-N(2)-C(2)-C(3)	1.6(2)
Cl(1)-N(2)-C(2)-C(3)	179.72(12)
C(1)-N(1)-C(3)-C(4)	135.54(16)
Cl(2)-N(1)-C(3)-C(4)	-83.36(18)
C(1)-N(1)-C(3)-C(2)	15.16(18)
Cl(2)-N(1)-C(3)-C(2)	156.27(12)
O(2)-C(2)-C(3)-N(1)	170.17(18)
N(2)-C(2)-C(3)-N(1)	-9.52(18)
O(2)-C(2)-C(3)-C(4)	48.8(3)
N(2)-C(2)-C(3)-C(4)	-130.91(17)
C(3A)-N(1A)-C(1A)-O(1A)	169.0(2)
Cl(1A)-N(1A)-C(1A)-O(1A)	26.5(3)
C(3A)-N(1A)-C(1A)-N(2A)	-13.6(2)
Cl(1A)-N(1A)-C(1A)-N(2A)	-156.09(13)
C(2A)-N(2A)-C(1A)-O(1A)	-175.30(19)
Cl(2A)-N(2A)-C(1A)-O(1A)	5.1(3)
C(2A)-N(2A)-C(1A)-N(1A)	7.1(2)
Cl(2A)-N(2A)-C(1A)-N(1A)	-172.49(13)
C(1A)-N(2A)-C(2A)-O(2A)	-178.05(18)
Cl(2A)-N(2A)-C(2A)-O(2A)	1.6(3)
C(1A)-N(2A)-C(2A)-C(3A)	1.7(2)
Cl(2A)-N(2A)-C(2A)-C(3A)	-178.73(13)
C(1A)-N(1A)-C(3A)-C(4A)	136.21(17)
Cl(1A)-N(1A)-C(3A)-C(4A)	-81.74(18)
C(1A)-N(1A)-C(3A)-C(2A)	14.32(19)
Cl(1A)-N(1A)-C(3A)-C(2A)	156.37(12)
O(2A)-C(2A)-C(3A)-N(1A)	170.64(19)
N(2A)-C(2A)-C(3A)-N(1A)	-9.07(18)
O(2A)-C(2A)-C(3A)-C(4A)	48.6(3)
N(2A)-C(2A)-C(3A)-C(4A)	-131.07(17)

Figure IV-10. X-Ray structure of **IV-37**.
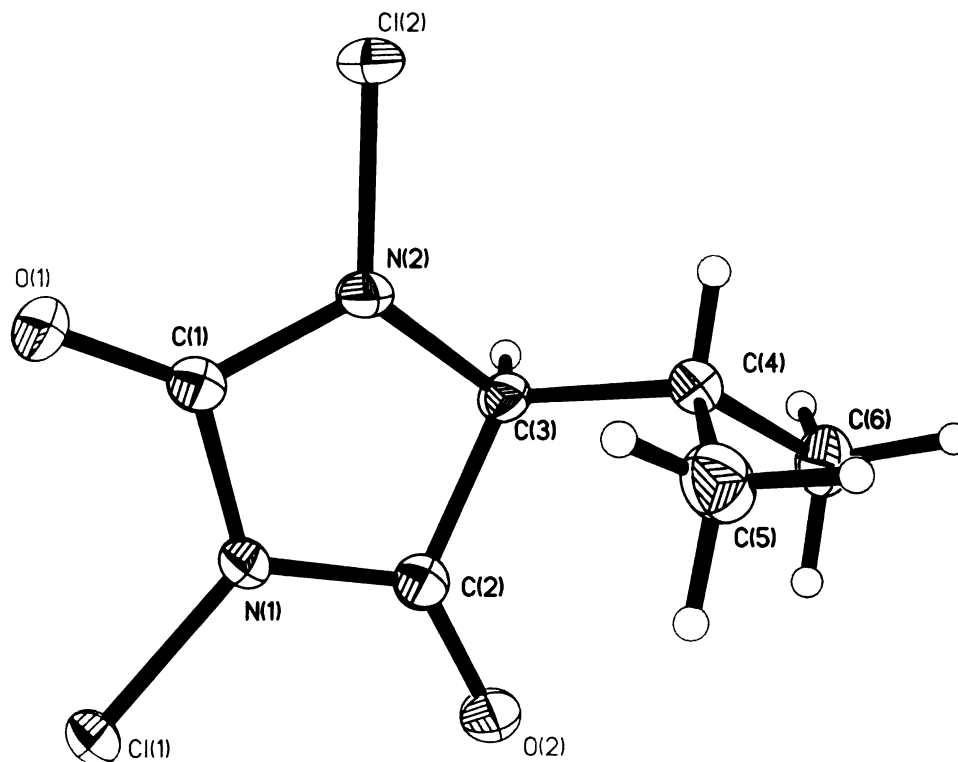
Table IV-44. Crystal data and structure refinement for **IV-37**.

Identification code	bb21_0m
Empirical formula	C6 H8 Cl2 N2 O2
Formula weight	211.04
Temperature	173(2) K
Wavelength	0.71073 Å
Crystal system	Monoclinic
Space group	P 21
Unit cell dimensions	a = 5.2296(10) Å a= 90°.
	b = 5.7248(11) Å b= 99.332(3)°.
	c = 14.455(3) Å g = 90°.
Volume	427.03(14) Å³
Z	2
Density (calculated)	1.641 Mg/m³
Absorption coefficient	0.719 mm⁻¹
F(000)	216
Crystal size	0.31 x 0.27 x 0.06 mm³
Theta range for data collection	2.86 to 27.82°.
Index ranges	-6<=h<=6, -7<=k<=6, -18<=l<=15
Reflections collected	2915
Independent reflections	1764 [R(int) = 0.0174]

Table IV-44. (Cont'd)

Completeness to theta = 25.00°	99.9 %
Absorption correction	Semi-empirical from equivalents
Max. and min. transmission	0.9582 and 0.7675
Refinement method	Full-matrix least-squares on F^2
Data / restraints / parameters	1764 / 1 / 142
Goodness-of-fit on F^2	1.107
Final R indices [I>2sigma(I)]	R1 = 0.0186, wR2 = 0.0562
R indices (all data)	R1 = 0.0191, wR2 = 0.0568
Absolute structure parameter	-0.01(5)
Extinction coefficient	0.041(6)
Largest diff. peak and hole	0.211 and -0.155 e.Å^{-3}

Table IV-45. Atomic coordinates (x 10^4) and equivalent isotropic displacement parameters ($Å^2$x 10^3) for **IV-37**. U(eq) is defined as one third of the trace of the orthogonalized U^{ij} tensor.

	x	y	z	U(eq)
Cl(1)	5061(1)	7449(1)	4371(1)	19(1)
Cl(2)	12340(1)	2515(1)	3048(1)	20(1)
O(1)	8685(2)	3221(2)	4477(1)	23(1)
O(2)	6388(2)	9562(2)	2576(1)	24(1)
N(1)	7228(2)	6663(2)	3688(1)	18(1)
N(2)	9838(2)	4382(2)	3055(1)	19(1)
C(1)	8653(3)	4547(3)	3835(1)	17(1)
C(2)	7555(3)	7847(3)	2890(1)	18(1)
C(3)	9664(2)	6518(3)	2489(1)	16(1)
C(4)	9054(3)	6022(3)	1431(1)	20(1)
C(5)	6391(3)	4915(4)	1144(1)	30(1)
C(6)	9398(4)	8242(3)	875(1)	30(1)

Table IV-46. Bond lengths [Å] and angles [°] for **IV-37**.

Cl(1)-N(1)	1.6807(12)
Cl(2)-N(2)	1.6908(13)
O(1)-C(1)	1.1968(19)
O(2)-C(2)	1.2051(19)
N(1)-C(2)	1.3712(19)
N(1)-C(1)	1.4202(19)
N(2)-C(1)	1.3753(19)
N(2)-C(3)	1.4666(19)
C(2)-C(3)	1.529(2)
C(3)-C(4)	1.536(2)
C(3)-H(3)	0.966(18)
C(4)-C(5)	1.525(2)
C(4)-C(6)	1.530(2)
C(4)-H(4)	0.85(2)
C(5)-H(5A)	0.95(3)
C(5)-H(5B)	0.98(2)
C(5)-H(5C)	0.93(2)
C(6)-H(6A)	1.01(2)
C(6)-H(6B)	0.94(2)

Table IV-46. (Cont'd)

C(6)-H(6C)	0.93(2)
C(2)-N(1)-C(1)	114.47(11)
C(2)-N(1)-Cl(1)	123.32(10)
C(1)-N(1)-Cl(1)	121.82(10)
C(1)-N(2)-C(3)	113.88(12)
C(1)-N(2)-Cl(2)	120.04(10)
C(3)-N(2)-Cl(2)	120.14(9)
O(1)-C(1)-N(2)	129.83(14)
O(1)-C(1)-N(1)	126.78(13)
N(2)-C(1)-N(1)	103.33(12)
O(2)-C(2)-N(1)	126.49(13)
O(2)-C(2)-C(3)	127.91(13)
N(1)-C(2)-C(3)	105.60(12)
N(2)-C(3)-C(2)	100.74(11)
N(2)-C(3)-C(4)	112.67(13)
C(2)-C(3)-C(4)	115.04(11)
N(2)-C(3)-H(3)	108.3(11)
C(2)-C(3)-H(3)	108.2(12)
C(4)-C(3)-H(3)	111.2(10)
C(5)-C(4)-C(6)	112.47(14)
C(5)-C(4)-C(3)	112.37(12)
C(6)-C(4)-C(3)	110.26(14)
C(5)-C(4)-H(4)	109.9(13)
C(6)-C(4)-H(4)	108.5(13)
C(3)-C(4)-H(4)	102.8(13)
C(4)-C(5)-H(5A)	109.2(16)
C(4)-C(5)-H(5B)	109.3(13)
H(5A)-C(5)-H(5B)	106(2)
C(4)-C(5)-H(5C)	110.7(13)
H(5A)-C(5)-H(5C)	118(2)
H(5B)-C(5)-H(5C)	103.8(18)
C(4)-C(6)-H(6A)	110.5(17)
C(4)-C(6)-H(6B)	107.1(15)
H(6A)-C(6)-H(6B)	108.4(19)
C(4)-C(6)-H(6C)	108.9(15)
H(6A)-C(6)-H(6C)	108(2)
H(6B)-C(6)-H(6C)	114(2)

Table IV-47. Anisotropic displacement parameters ($\text{Å}^2 \times 10^3$)for **IV-37**. The anisotropic displacement factor exponent takes the form: $-2p^2[\, h^2 a^{*2} U^{11} + ... + 2\, h\, k\, a^*\, b^*\, U^{12}\,]$

	U^{11}	U^{22}	U^{33}	U^{23}	U^{13}	U^{12}
Cl(1)	22(1)	21(1)	16(1)	-2(1)	7(1)	4(1)
Cl(2)	18(1)	16(1)	25(1)	0(1)	4(1)	5(1)
O(1)	25(1)	23(1)	22(1)	8(1)	6(1)	3(1)
O(2)	30(1)	20(1)	25(1)	5(1)	9(1)	10(1)
N(1)	21(1)	18(1)	16(1)	1(1)	7(1)	5(1)
N(2)	20(1)	17(1)	22(1)	4(1)	8(1)	7(1)
C(1)	16(1)	17(1)	18(1)	-2(1)	3(1)	0(1)
C(2)	20(1)	15(1)	17(1)	-2(1)	3(1)	0(1)

Table IV-47. (Cont'd)

C(3)	16(1)	15(1)	18(1)	3(1)	4(1)	2(1)
C(4)	20(1)	24(1)	17(1)	2(1)	6(1)	5(1)
C(5)	26(1)	38(1)	25(1)	-7(1)	3(1)	-2(1)
C(6)	37(1)	33(1)	23(1)	9(1)	10(1)	5(1)

Table IV-48. Hydrogen coordinates (x 10^4) and isotropic displacement parameters ($\AA^2$x 10^3) for **IV-37**.

	x	y	z	U(eq)
H(3)	11270(30)	7370(40)	2648(12)	22(4)
H(4)	10230(40)	5050(40)	1349(13)	21(4)
H(5A)	6090(50)	4660(60)	480(20)	62(9)
H(5B)	5050(40)	6020(40)	1265(15)	35(5)
H(5C)	6180(40)	3650(40)	1528(15)	35(6)
H(6A)	9270(40)	7870(50)	184(16)	54(7)
H(6B)	8040(40)	9250(50)	952(15)	37(5)
H(6C)	11030(40)	8850(40)	1084(17)	43(6)

Table IV-49. Torsion angles [°] for **IV-37**.

C(3)-N(2)-C(1)-O(1)	-171.43(15)
Cl(2)-N(2)-C(1)-O(1)	-18.5(2)
C(3)-N(2)-C(1)-N(1)	11.29(15)
Cl(2)-N(2)-C(1)-N(1)	164.19(10)
C(2)-N(1)-C(1)-O(1)	179.96(14)
Cl(1)-N(1)-C(1)-O(1)	-7.1(2)
C(2)-N(1)-C(1)-N(2)	-2.65(16)
Cl(1)-N(1)-C(1)-N(2)	170.33(10)
C(1)-N(1)-C(2)-O(2)	173.16(15)
Cl(1)-N(1)-C(2)-O(2)	0.3(2)
C(1)-N(1)-C(2)-C(3)	-6.23(16)
Cl(1)-N(1)-C(2)-C(3)	-179.09(10)
C(1)-N(2)-C(3)-C(2)	-14.59(15)
Cl(2)-N(2)-C(3)-C(2)	-167.46(9)
C(1)-N(2)-C(3)-C(4)	-137.69(12)
Cl(2)-N(2)-C(3)-C(4)	69.44(14)
O(2)-C(2)-C(3)-N(2)	-167.64(15)
N(1)-C(2)-C(3)-N(2)	11.73(14)
O(2)-C(2)-C(3)-C(4)	-46.2(2)
N(1)-C(2)-C(3)-C(4)	133.17(13)
N(2)-C(3)-C(4)-C(5)	64.32(17)
C(2)-C(3)-C(4)-C(5)	-50.40(19)
N(2)-C(3)-C(4)-C(6)	-169.35(12)
C(2)-C(3)-C(4)-C(6)	75.94(16)

283

Figure IV-11. X-Ray crystal structure of **IV-38**.
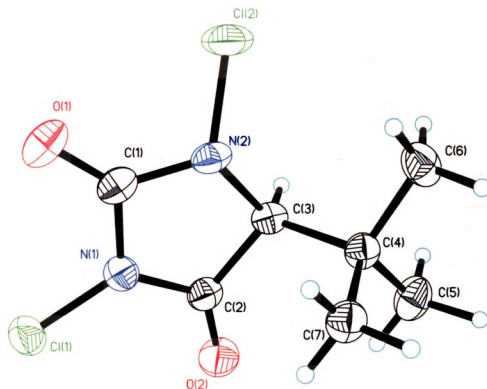
Table IV-50. Crystal data and structure refinement for **IV-38**.

Identification code	bb22_0m
Empirical formula	C7 H10 Cl2 N2 O2
Formula weight	225.07
Temperature	173(2) K
Wavelength	0.71073 Å
Crystal system	Orthorhombic
Space group	P 21 21 21
Unit cell dimensions	a = 7.7735(2) Å a= 90°.
	b = 10.5816(3) Å b= 90°.
	c = 12.0657(3) Å g = 90°.
Volume	992.48(5) Å^3
Z	4
Density (calculated)	1.506 Mg/m^3
Absorption coefficient	0.623 mm^{-1}
F(000)	464
Crystal size	0.40 x 0.34 x 0.19 mm^3
Theta range for data collection	2.56 to 27.89°.

Table IV-50. (Cont'd)

Index ranges	-10<=h<=9, -13<=k<=13, -15<=l<=15
Reflections collected	13556
Independent reflections	2369 [R(int) = 0.0192]
Completeness to theta = 25.00°	99.9 %
Absorption correction	Semi-empirical from equivalents
Max. and min. transmission	0.8907 and 0.7877
Refinement method	Full-matrix least-squares on F^2
Data / restraints / parameters	2369 / 0 / 158
Goodness-of-fit on F^2	1.139
Final R indices [I>2sigma(I)]	R1 = 0.0221, wR2 = 0.0656
R indices (all data)	R1 = 0.0229, wR2 = 0.0661
Absolute structure parameter	0.06(4)
Largest diff. peak and hole	0.255 and -0.130 e.$Å^{-3}$

Table IV-51. Atomic coordinates (x 10^4) and equivalent isotropic displacement parameters ($Å^2$x 10^3) for **IV-38**. U(eq) is defined as one third of the trace of the orthogonalized U^{ij} tensor.

	x	y	z	U(eq)
Cl(1)	836(1)	2012(1)	6938(1)	39(1)
Cl(2)	-2716(1)	5846(1)	5441(1)	46(1)
O(1)	-1355(1)	4360(1)	7339(1)	40(1)
O(2)	1392(2)	2366(1)	4493(1)	42(1)
N(1)	277(1)	3197(1)	6090(1)	28(1)
N(2)	-879(1)	4978(1)	5514(1)	28(1)
C(1)	-764(2)	4204(1)	6431(1)	28(1)
C(2)	594(2)	3170(1)	4960(1)	27(1)
C(3)	-225(2)	4376(1)	4498(1)	24(1)
C(4)	1054(2)	5212(1)	3841(1)	27(1)
C(5)	1464(2)	4547(2)	2743(1)	38(1)
C(6)	202(2)	6483(1)	3585(1)	36(1)
C(7)	2705(2)	5426(1)	4515(1)	32(1)

Table IV-52. Bond lengths [Å] and angles [°] for **IV-38**.

Cl(1)-N(1)	1.6762(10)
Cl(2)-N(2)	1.6991(11)
O(1)-C(1)	1.1991(15)
O(2)-C(2)	1.1945(15)
N(1)-C(2)	1.3847(15)
N(1)-C(1)	1.4004(15)
N(2)-C(1)	1.3797(16)
N(2)-C(3)	1.4723(15)
C(2)-C(3)	1.5317(15)
C(3)-C(4)	1.5491(16)
C(3)-H(3)	0.962(17)
C(4)-C(6)	1.5308(18)
C(4)-C(5)	1.5326(18)
C(4)-C(7)	1.5361(17)

Table IV-52. (Cont'd)

C(5)-H(5A)	0.93(2)
C(5)-H(5B)	1.08(2)
C(5)-H(5C)	0.95(2)
C(6)-H(6A)	0.933(19)
C(6)-H(6B)	1.047(15)
C(6)-H(6C)	0.968(19)
C(7)-H(7A)	0.953(19)
C(7)-H(7B)	0.909(18)
C(7)-H(7C)	0.99(2)
C(2)-N(1)-C(1)	114.06(10)
C(2)-N(1)-Cl(1)	122.63(8)
C(1)-N(1)-Cl(1)	122.68(8)
C(1)-N(2)-C(3)	112.86(9)
C(1)-N(2)-Cl(2)	114.60(8)
C(3)-N(2)-Cl(2)	118.75(9)
O(1)-C(1)-N(2)	128.79(12)
O(1)-C(1)-N(1)	126.47(12)
N(2)-C(1)-N(1)	104.68(9)
O(2)-C(2)-N(1)	124.89(11)
O(2)-C(2)-C(3)	129.55(11)
N(1)-C(2)-C(3)	105.53(9)
N(2)-C(3)-C(2)	101.57(9)
N(2)-C(3)-C(4)	113.62(9)
C(2)-C(3)-C(4)	113.29(10)
N(2)-C(3)-H(3)	106.1(10)
C(2)-C(3)-H(3)	110.7(9)
C(4)-C(3)-H(3)	111.0(9)
C(6)-C(4)-C(5)	108.60(11)
C(6)-C(4)-C(7)	109.80(10)
C(5)-C(4)-C(7)	110.60(11)
C(6)-C(4)-C(3)	109.07(10)
C(5)-C(4)-C(3)	108.26(10)
C(7)-C(4)-C(3)	110.46(10)
C(4)-C(5)-H(5A)	106.9(11)
C(4)-C(5)-H(5B)	106.7(11)
H(5A)-C(5)-H(5B)	115.0(15)
C(4)-C(5)-H(5C)	107.5(11)
H(5A)-C(5)-H(5C)	114.0(16)
H(5B)-C(5)-H(5C)	106.4(15)
C(4)-C(6)-H(6A)	106.0(11)
C(4)-C(6)-H(6B)	111.7(8)
H(6A)-C(6)-H(6B)	100.4(15)
C(4)-C(6)-H(6C)	109.7(11)
H(6A)-C(6)-H(6C)	117.1(14)
H(6B)-C(6)-H(6C)	111.5(15)
C(4)-C(7)-H(7A)	111.6(10)
C(4)-C(7)-H(7B)	108.5(12)
H(7A)-C(7)-H(7B)	104.8(14)
C(4)-C(7)-H(7C)	114.5(12)
H(7A)-C(7)-H(7C)	110.4(15)
H(7B)-C(7)-H(7C)	106.4(16)

Table IV-53. Anisotropic displacement parameters ($\text{Å}^2 \times 10^3$)for **IV-38**. The anisotropic displacement factor exponent takes the form: $-2p^2[\, h^2 a^{*2} U^{11} + \ldots + 2\,h\,k\,a^*\,b^*\,U^{12}\,]$

	U^{11}	U^{22}	U^{33}	U^{23}	U^{13}	U^{12}
Cl(1)	33(1)	43(1)	42(1)	15(1)	0(1)	0(1)
Cl(2)	35(1)	37(1)	66(1)	0(1)	12(1)	14(1)
O(1)	39(1)	48(1)	34(1)	-12(1)	11(1)	-8(1)
O(2)	54(1)	29(1)	44(1)	-2(1)	14(1)	13(1)
N(1)	29(1)	27(1)	30(1)	2(1)	1(1)	1(1)
N(2)	25(1)	24(1)	36(1)	-5(1)	7(1)	2(1)
C(1)	23(1)	29(1)	32(1)	-6(1)	3(1)	-6(1)
C(2)	26(1)	23(1)	33(1)	-1(1)	4(1)	-1(1)
C(3)	23(1)	21(1)	30(1)	-5(1)	0(1)	-2(1)
C(4)	23(1)	30(1)	28(1)	1(1)	-2(1)	-5(1)
C(5)	40(1)	49(1)	26(1)	-3(1)	2(1)	-7(1)
C(6)	32(1)	30(1)	47(1)	9(1)	-7(1)	-7(1)
C(7)	25(1)	39(1)	32(1)	1(1)	-4(1)	-7(1)

Table IV-54. Hydrogen coordinates ($\times 10^4$) and isotropic displacement parameters ($\text{Å}^2 \times 10^3$) for **IV-38**.

	x	y	z	U(eq)
H(3)	-1220(20)	4177(14)	4057(13)	29(4)
H(5A)	1930(20)	3759(19)	2922(15)	36(4)
H(5B)	2310(30)	5160(20)	2290(17)	55(6)
H(5C)	420(30)	4505(19)	2326(16)	55(6)
H(6A)	1020(20)	6957(17)	3202(15)	44(5)
H(6B)	60(20)	7035(15)	4299(12)	34(4)
H(6C)	-890(20)	6343(18)	3219(15)	41(4)
H(7A)	3220(20)	4647(18)	4730(15)	34(4)
H(7B)	2420(20)	5810(15)	5163(15)	37(4)
H(7C)	3570(30)	5979(18)	4150(17)	52(5)

Table IV-55. Torsion angles [°] for **IV-38**.

C(3)-N(2)-C(1)-O(1)	-170.78(12)
Cl(2)-N(2)-C(1)-O(1)	-30.69(17)
C(3)-N(2)-C(1)-N(1)	11.83(13)
Cl(2)-N(2)-C(1)-N(1)	151.92(8)
C(2)-N(1)-C(1)-O(1)	172.10(12)
Cl(1)-N(1)-C(1)-O(1)	0.99(18)
C(2)-N(1)-C(1)-N(2)	-10.43(14)
Cl(1)-N(1)-C(1)-N(2)	178.46(8)
C(1)-N(1)-C(2)-O(2)	-176.92(12)
Cl(1)-N(1)-C(2)-O(2)	-5.81(19)
C(1)-N(1)-C(2)-C(3)	5.03(14)
Cl(1)-N(1)-C(2)-C(3)	176.14(8)
C(1)-N(2)-C(3)-C(2)	-8.82(12)

Table IV-55. (Cont'd)

Cl(2)-N(2)-C(3)-C(2)	-147.12(8)
C(1)-N(2)-C(3)-C(4)	-130.84(11)
Cl(2)-N(2)-C(3)-C(4)	90.87(11)
O(2)-C(2)-C(3)-N(2)	-175.78(13)
N(1)-C(2)-C(3)-N(2)	2.14(12)
O(2)-C(2)-C(3)-C(4)	-53.54(17)
N(1)-C(2)-C(3)-C(4)	124.38(11)
N(2)-C(3)-C(4)-C(6)	-55.29(13)
C(2)-C(3)-C(4)-C(6)	-170.55(10)
N(2)-C(3)-C(4)-C(5)	-173.29(11)
C(2)-C(3)-C(4)-C(5)	71.44(13)
N(2)-C(3)-C(4)-C(7)	65.47(13)
C(2)-C(3)-C(4)-C(7)	-49.79(13)

4.5: References

1.   Golebiewski, W. M.; Gucma, M. *Synthesis* **2007**, 3599-3619.

2.   Agnihotri, G. *Synlett* **2005**, 2857-2858.

3.   Tilstam, U.; Weinmann, H. *Org. Proc. Res. Dev.* **2002,** *6*, 384-393.

4.   Hart, R. M.; Whitehead, M. A. *Trans. Faraday Soc.* **1971,** *67*, 1569-1575.

5.   Nagao, Y.; Katagiri, S. *Chem. Lett.* **1993**, 1169-1170.

6.   Nagao, Y.; Katagiri, S. *Sci. Rep. Hirosaki Univ.* **1991,** *38*, 20-23.

7.   Poleshchuk, O. K.; Makiej, K.; Ostafin, M.; Nogaj, B. *Magn. Res. Chem.* **2001,** *39*, 329-333.

8.   Xu, Z. J.; Zhang, D. Y.; Zou, X. Z. *Synth. Commun.* **2006,** *36*, 255-258.

9.   Spitulnik, M. J. *Synthesis* **1985**, 299-300.

10.   Shapiro, E. L.; Gentles, M. J.; Tiberi, R. L.; Popper, T. L.; Berkenkopf, J.; Lutsky, B.; Watnick, A. S. *J. Med. Chem.* **1987,** *30*, 1581-1588.

11.   Karmazin, L.; Mazzanti, M.; Bezombes, J. P.; Gateau, C.; Pecaut, J. *Inorg. Chem.* **2004,** *43*, 5147-5158.

12.   Miesch, L.; Gateau, C.; Morin, F.; Franck-Neumann, M. *Tetrahedron Lett.* **2002,** *43*, 7635-7638.

13.   Barnes, D. M.; Christesen, A. C.; Engstrom, K. M.; Haight, A. R.; Hsu, M. C.; Lee, E. C.; Peterson, M. J.; Plata, D. J.; Raje, P. S.; Stoner, E. J.; Tedrow, J. S.; Wagaw, S. *Org. Proc. Res. Dev.* **2006,** *10*, 803-807.

14.   Chen, B. C.; Murphy, C. K.; Kumar, A.; Reddy, R. T.; Clark, C.; Zhou, P.; Lewis, B. M.; Gala, D.; Mergelsberg, I.; Scherer, D.; Buckley, J.; DiBenedetto, D.; Davis, F. A. In *Organic Synthesis, Vol 73*, 1996; pp. 159-173.

15.   Mergelsberg, I.; Gala, D.; Scherer, D.; Dibenedetto, D.; Tanner, M. *Tetrahedron Lett.* **1992,** *33*, 161-164.

16.   Szumigala, R. H.; Devine, P. N.; Gauthier, D. R.; Volante, R. P. *J. Org. Chem.* **2004,** *69*, 566-569.

17. Zolfigol, M. A.; Nasr-Isfahani, H.; Mallakpour, S.; Safaiee, M. *Synlett* **2005**, 761-764.

18. Khazaei, A.; Manesh, A. A. *Synthesis* **2005**, 1929-1931.

19. Shakya, P. D.; Dubey, D. K.; Pardasani, D.; Palit, M.; Gupta, A. K. *Org. Prep. Proced. Int.* **2005,** *37*, 569-574.

20. Zolfigol, M. A.; Ghaemi, E.; Madrakian, E.; Choghamarani, A. G. *Mendeleev Commun.* **2006**, 41-42.

21. Niknam, K.; Zolfigol, M. A. *J. Iran. Chem. Soc.* **2006,** *3*, 59-63.

22. Nilov, D.; Reiser, O. *Adv. Synth. Catal.* **2002,** *344*, 1169-1173.

23. Bodkin, J. A.; McLeod, M. D. *J. Chem. Soc.-Perkin Trans. 1* **2002**, 2733-2746.

24. O'Brien, P. *Angew. Chem., Int. Edit.* **1999,** *38*, 326-329.

25. Barta, N. S.; Sidler, D. R.; Somerville, K. B.; Weissman, S. A.; Larsen, R. D.; Reider, P. J. *Org. Lett.* **2000,** *2*, 2821-2824.

26. Harding, M.; Bodkin, J. A.; Hutton, C. A.; McLeod, M. D. *Synlett* **2005**, 2829-2831.

27. DiBlasi, C. M.; Macks, D. E.; Tan, D. S. *Org. Lett.* **2005,** *7*, 1777-1780.

28. Grela, K.; Tryznowski, M.; Bieniek, M. *Tetrahedron Lett.* **2002,** *43*, 9055-9059.

29. Kobori, A.; Miyata, K.; Ushioda, M.; Seio, K.; Sekine, M. *Chem. Lett.* **2002**, 16-17.

30. Komatsu, M.; Okada, H.; Akaki, T.; Oderaotoshi, Y.; Minakata, S. *Org. Lett.* **2002,** *4*, 3505-3508.

31. Zhou, Y. G. *Acc. Chem. Res.* **2007,** *40*, 1357-1366.

32. Radhamma, M. P.; Indrasenan, P. *Talanta* **1983,** *30*, 49-50.

33. Rao, Z. M.; Zhang, X. R.; Baeyens, W. R. G. *Talanta* **2002,** *57*, 993-998.

34. Lipinski, C. A.; Bordner, J.; Butterfield, G. C.; Marinovic, L. C. *J. Hetercyclic Chem.* **1990,** *27*, 1793-1799.

35. Mays, D. C.; Pawluk, L. J.; Apseloff, G.; Davis, W. B.; She, Z. W.; Sagone, A. L.; Gerber, N. *Biochem. Pharmacol.* **1995,** *50*, 367-380.

36. Uetrecht, J.; Zahid, N. *Chem. Res. Toxicol.* **1988,** *1*, 148-151.

37. Ware, E. *Chem. Rev.* **1950,** *46*, 403-470.

38. Muccioli, G. G.; Poupaert, J. H.; Wouters, J.; Norberg, B.; Poppitz, W.; Scriba, G. K. E.; Lambert, D. M. *Tetrahedron* **2003,** *59*, 1301-1307.

39. Yamaguchi, J.; Harada, M.; Kondo, T.; Noda, T.; Suyama, T. *Chem. Lett.* **2003,** *32*, 372-373.

40. Anteunis, M. J. O.; Spiessens, L.; Dewitte, M.; Callens, R.; Reyniers, F. *Bull. Soc. Chim. Belg.* **1987,** *96*, 459-465.

41. Lickefett, H.; Krohn, K.; Konig, W. A.; Gehrcke, B.; Syldatk, C. *Tetrahedron-Asymmetry* **1993,** *4*, 1129-1135.

42. Reist, M.; Carrupt, P. A.; Testa, B.; Lehmann, S.; Hansen, J. J. *Helv. Chim. Acta* **1996,** *79*, 767-778.

43. Whitehead, D. C.; Staples, R. J.; Borhan, B. *Tetrahedron Lett.* **2009,** *50*, 656-658.

44. Corral, R. A.; Orazi, O. O. *J. Org. Chem.* **1963,** *28*, 1100-1104.

45. Derosa, M.; Melenski, E.; Holder, A. J. *Heterocycles* **1993,** *36*, 1059-1064.

46. De Luca, L.; Giacomelli, G.; Nieddu, G. *Synlett* **2005**, 223-226.

47. Hiegel, G. A.; Hogenauer, T. J.; Lewis, J. C. *Synth. Commun.* **2005,** *35*, 2099-2105.

48. Pyne, S. G.; Javidan, A.; Skelton, B. W.; White, A. H. *Tetrahedron* **1995,** *51*, 5157-5168.

49. Martens, J.; Lubben, S. *J. Prakt. Chem.* **1990,** *332*, 1111-1117.

50. Urbach, H.; Henning, R. *Heterocycles* **1989,** *28*, 957-965.

PLACE IN RETURN BOX to remove this checkout from your record.
TO AVOID FINES return on or before date due.
MAY BE RECALLED with earlier due date if requested.

DATE DUE	DATE DUE	DATE DUE

THE DEVELOPMENT OF A NOVEL ASYMMETRIC HALOLACTONIZATION
AND THE INVESTIGATION OF PEPTIDIC LIGANDS FOR OSMIUM
TETROXIDE MEDIATED TRANSFORMATIONS

VOLUME II

By

Daniel Charles Whitehead

A DISSERTATION

Submitted to
Michigan State University
in partial fulfillment of the requirements
for the degree of

DOCTOR OF PHILOSOPHY

Chemistry

2009

Chapter 5: Investigation of Peptide Scaffolds as Chiral Ligands for Osmium Tetroxide

5.1: Introduction
5.1.1: Peptidic Ligands for Metal Mediated Reactions

Small peptidic sequences have recently emerged as a powerful and highly modular source of viable ligands[1-6] and organocatalysts[7-10] for a number of organic transformations. For a detailed discussion of the use of peptide scaffolds as organocatalysts, see Chapter 1. The modularity of peptide sequences, afforded by the large pool of both natural and unnatural amino acid building blocks, along with the relative ease of synthesis by solid-phase techniques[11] facilitates the preparation and screening of a large number of ligand structures. Furthermore, the advent of several high-throughput screening methods have made the quick evaluation of peptidic libraries as potential asymmetric catalysts and ligands quite facile in some cases.[7,12-30] The recent development of split-and-pool solid-phase synthesis techniques have made it possible to synthesize literally thousands of unique sequences at once.[20,31,32] Such high-throughput techniques for the design of ligands and organocatalysts have an obvious advantage over conventional approaches toward ligand design, which rely on (typically time-consuming) step-by-step modification of an initial scaffold. Many examples of this combinatorial approach toward ligand design have appeared in the literature. A brief review follows that will highlight several pertinent examples.

The first example of peptide-mediated asymmetric induction in a metal catalyzed organic transformation was reported in 1956. Researchers at Osaka University were able to generate a chiral hydrogenation catalyst by reducing a

peptide/metal complex that had been generated by the adsorption of palladium

chloride onto silk fibroin fibers. Using this catalyst, several acylated oximes were

hydrogenated to generate the corresponding α-amino acids. For example, the

reduction of diethyl α-acetoximinoglutarate V-1 returned L-glutamic acid

hydrochloride V-2 after a subsequent acid hydrolysis (Scheme V-1).[33]
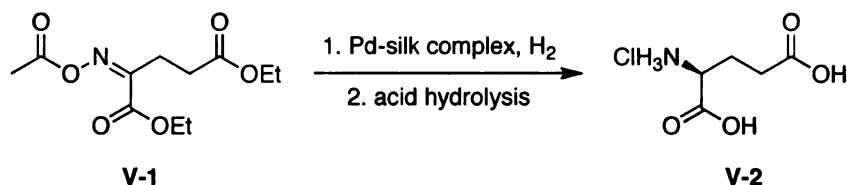
Since this initial historic disclosure, a number of groups have developed

peptide-based scaffolds for asymmetric metal-mediated transformations. The

contemporary approach often entails the generation of a library of potential

ligands through a combinatorial approach, followed by iterative modification of

the initial "hit" scaffold that ultimately results in the development of a superior

ligand for a particular metal-mediated transformation. The collaborative efforts of

Hoveyda and Snapper have been perhaps the most prolific in the field. Over the

course of longer than a decade, these researchers have developed a battery of

peptide imine ligands like structures V-3, V-4, V-5, and V-6 (Figure V-1) for a

number of transition metal mediated organic transformations. Phenolic Schiff

base peptides like V-3 were initially employed for the titanium mediated

enantioselctive addition of TMSCN to *meso* epoxides.[34,35] Subsequently, this

scaffold was found to promote the asymmetric Strecker reaction (i.e. addition of

cyanide to imines),[36-38] the formation of chiral cyanohydrins,[39] the copper

mediated S_N2' displacement of allylic phosphates with alkylzinc reagents,[40] the zirconium catalyzed alkylation of imines using alkylzinc reagents,[41-43] and the aluminum catalyzed alkylation of α-ketoesters with alkylzinc reagents.[44]

Figure V-1. Various peptide imine ligand scaffolds from Hoveyda and Snapper.
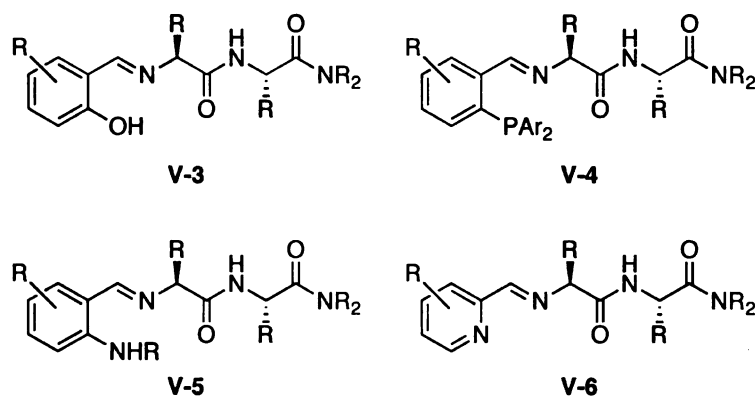
Phosphine Schiff base catalysts of the general scaffold V-4 were developed in order to promote reactions mediated by late transition metals. Phosphine V-4 has been applied to the copper mediated asymmetric 1,4 alkylation and arylation of cyclic[45] and acyclic[46,47] enones and cyclic[48] and acyclic[49,50] nitroalkenes. Here again, alkyl and aryl zinc reagents were employed as the carbon nucleophile. The development of anilinic Schiff base V-5 was required in order to extend this methodology to the copper promoted 1,4-alkylation of cyclic unsaturated β-ketoesters.[51]

Finally, ligand V-6, equipped with a pyridine moiety, was developed for copper mediated asymmetric allylic substitutions[52] and the silver mediated asymmetric addition of enolsilanes to α-ketoesters.[53]

A closer look at the development of the titanium mediated asymmetric ring-opening of *meso* epoxides will serve to highlight the nuances of their overall approach to peptide ligand design.[2,4,34,35] It is noteworthy that a similar approach was applied for the other transformations alluded to above as well as those described subsequently. The optimal peptide ligand **V-13** for the ring opening of cyclohexene oxide **V-8** was arrived at after a systematic positional scanning of each of the structural elements in the general peptide scaffold **V-7**.

Scheme V-2. Interative optimization of peptide ligands for the preparation of **V-9**.
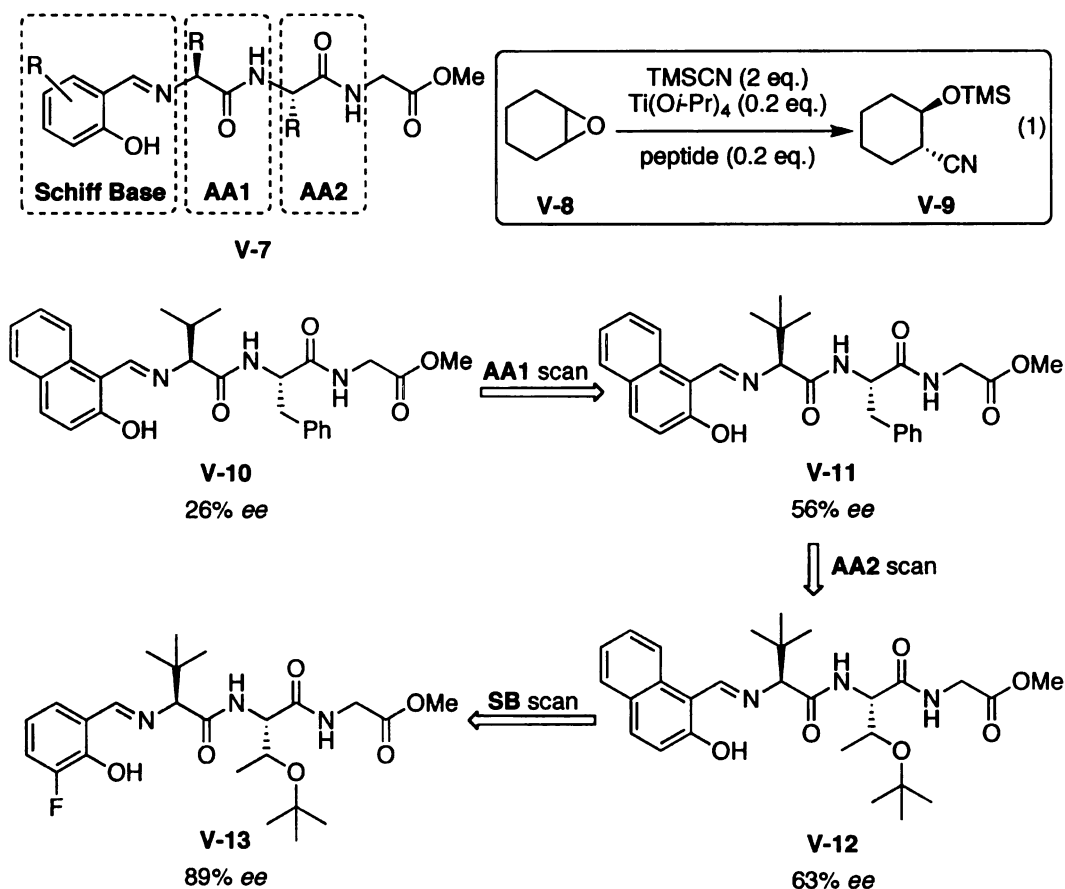
More specifically, the randomly generated initial scaffold **V-10** returned the ring opened product **V-9** in 26% *ee*. Positional scanning of the first amino acid

295

unit (AA1, see **V-7**) generated peptide **V-11** which produced **V-9** in 56% *ee*.

Positional scanning of AA2 followed by the Schiff base moiety returned peptides

that produced **V-9** in 63 and 89% *ee*, respectively. The advantage of this

systematic approach, relying on the iterative scanning of each unit of the

scaffold, is one of economy. In this example, only 60 potential ligands were

prepared (simply by solid phase synthesis) in order to develop an effective

ligand. This number pales in comparison to the 8000 (20^3) potential ligands

available by randomly combining the 20 natural amino acids and 20 phenolic

aldehydes.

Scheme V-3 illustrates another interesting nuance of this approach to

ligand design. Namely, seemingly subtle changes in the peptide scaffold can

have a profound effect on the enantioselectivity of the transformation.

Furthermore, these effects can be difficult to predict and rationalize.   For

instance, by substituting a tritylated asparagine moeity for the *t*-butylthreonine

unit at the AA2 position, a complete reversal of enantioselectivity was observed

without changing the absolute stereochemistry of the ligand at that position! In

the event, peptide **V-12**, with a Thr(*t*-Bu) residue in the AA2 position returned the

(*S,R*) product **V-15** in 83% *ee*. In sharp contrast, peptide **V-17** containing an

Asn(Trt) residue in the same position returned the (*R,S*) enantiomer **V-16** in 58%

ee. It warrants emphasis that this stereochemical reversal of the product is due

to a change in ligand constitution without altering the absolute stereochemistry of

the AA2 position. This result serves to underscore the fact that a rational

approach to ligand optimization can be difficult with peptide scaffolds, and as such one must defer to a more combinatorial screening approach to optimization.

Scheme V-3. Small changes in the peptide ligands have profound effects on selectivity.
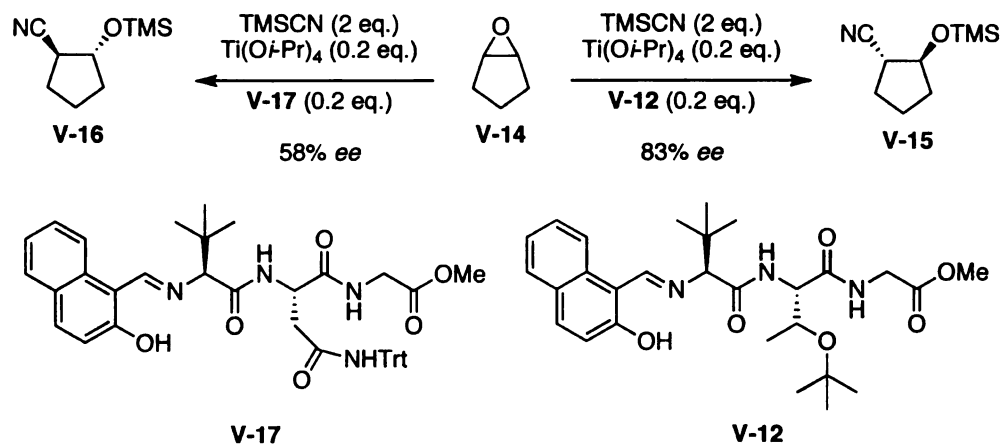
A final consequence of this combinatorial approach for peptide ligand design is that one often finds that substrates of even very similar structures will have different optimal catalysts. For example, if one considers several *meso* epoxides, Hoveyda and Snapper have discovered that they each require a different ligand within the same general scaffold to achieve the highest enantioselectivity (Scheme V-4). In this instance, small changes within the Schiff base region of the general scaffold (**V-7**, Scheme V-2) produced a small family of peptide ligands, each of which performed best with a particular substrate (Scheme V-4). Perhaps the knee-jerk reaction to these data would be to assume that the methodology lacks generality, requiring a new ligand for every substrate. Instead, one must take care to appreciate the exquisite tunability and potential for ligand optimization inherent in the strategy. That different yet structurally similar

ligands from the same general scaffold can promote a specific transformation offers the intriguing possibility to optimize and tune the ligand scaffold. In principle, even the most stubborn substrate might surrender after a targeted optimization around an initial ligand "hit". In that vein, one might view the requirement for a collection of catalysts of a general scaffold to be an advantage rather than a limitation. The facile preparation of a library of potential ligands by high throughput solid phase synthesis underscores this conclusion.

Scheme V-4. Different substrates require unique ligands within the same scaffold.
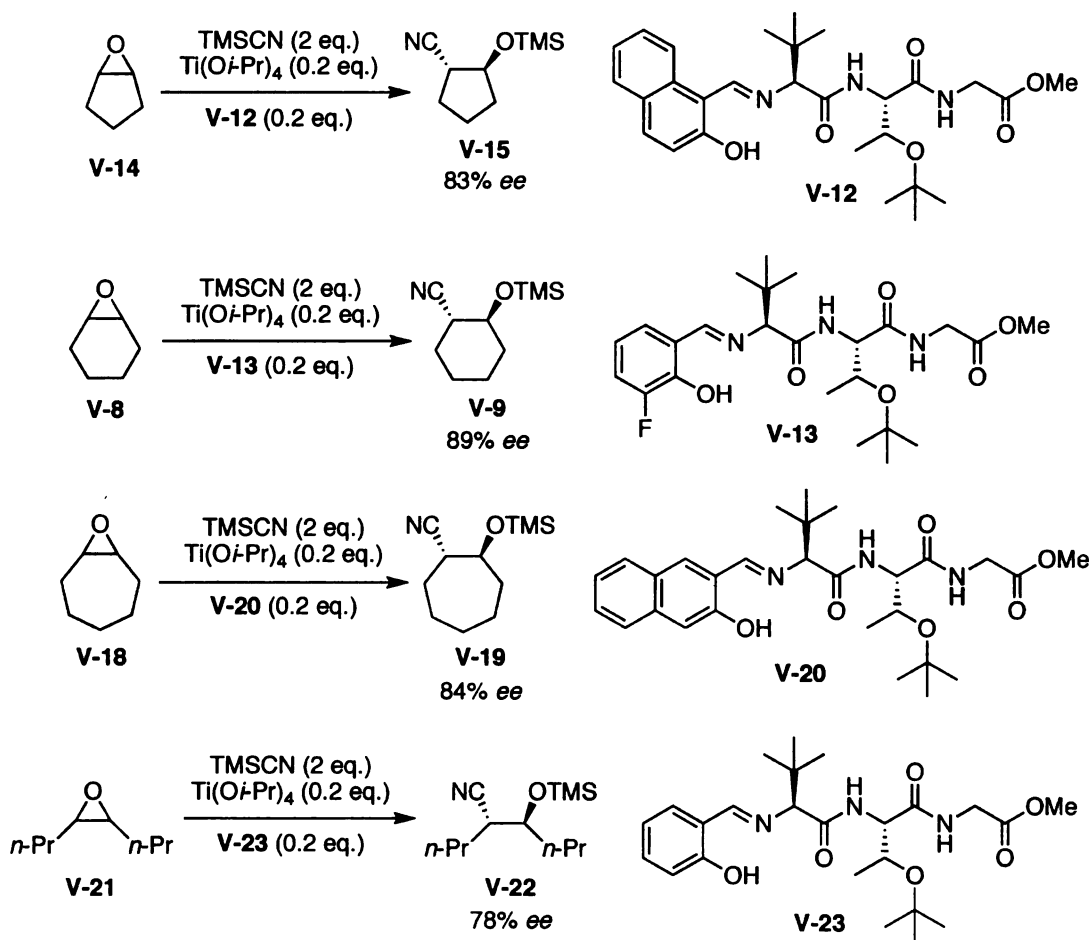
In addition to the efforts on behalf of Hoveyda and Snapper described above, others have sought to apply a similar strategy to peptide ligand design. In particular, the Gilbertson group has designed a number of peptidic diphosphine ligands (e.g. peptide V-26) that have proven effective in several applications of the palladium-mediated enantioselective allylic alkylation reaction.[5] After developing elegant methodology aimed at facilitating the straightforward preparation of chiral phosphine containing amino acids,[54-56] this group set out to incorporate these ligating moieties within peptide ligand scaffolds. Initially, they developed a helical peptide scaffold comprised of eleven amino acids including two diphenylphosphinoserine residues that was capable of binding a cationic rhodium species.[57-60] This chiral complex was used to reduce methyl 2-acetamidoacrylate to give N-acetyl alanine methyl ester with marginal enantioselectivity (>40% ee). Subsequently, they developed β-turn peptide scaffolds again incorporating phosphine ligation sites that facilitated several palladium catalyzed transformations of allylic acetates (Scheme V-5). Specifically, peptide V-26 was found to effectively promote the addition of dimethyl malonate to cyclopentene acetate V-24, returning V-25 in excellent yield and enantiopurity.[61-65] A similar β-turn scaffold allowed for the desymmetrization of 1,3-diphenylprop-2-enyl acetate by the addition of dimethyl malonate.[66] Finally, peptide V-29 was effective for the palladium catalyzed desymmetrization of meso-2,4-pentenediol derivative V-27 by generating oxazolidinone V-28 in up to 76% ee.[67] In these examples, the rapid screening of a number of potential ligands was further accelerated by screening the ligands on bead, directly after

preparation by solid phase synthesis. In addition, Meldal[68], Landis[69], van

Koten[70], and Alper[71] have also investigated peptide ligands for palladium

transformations, with varying degrees of success.

Scheme V-5. Various applications of peptido-phosphine ligands from the Gilbertson group.

$$\text{V-24} \xrightarrow[\substack{\textbf{V-22} \text{ (0.04 eq.)} \\ \text{dimethyl malonate} \\ \text{BSA, TBAF} \\ \text{THF, 0 °C}}]{[\text{Pd(allyl)Cl}]_2 \text{ (0.02 eq.)}} \text{V-25} \qquad (1)$$

V-25
91% yield
95% ee

V-26

$$\text{V-27} \xrightarrow[\text{TBAF, THF, RT}]{\text{Pd}_2(\text{dba})_3 \cdot 2\text{L} \text{ (0.05 eq.)}} \text{V-28} \qquad (2)$$

V-28
76% ee

V-29
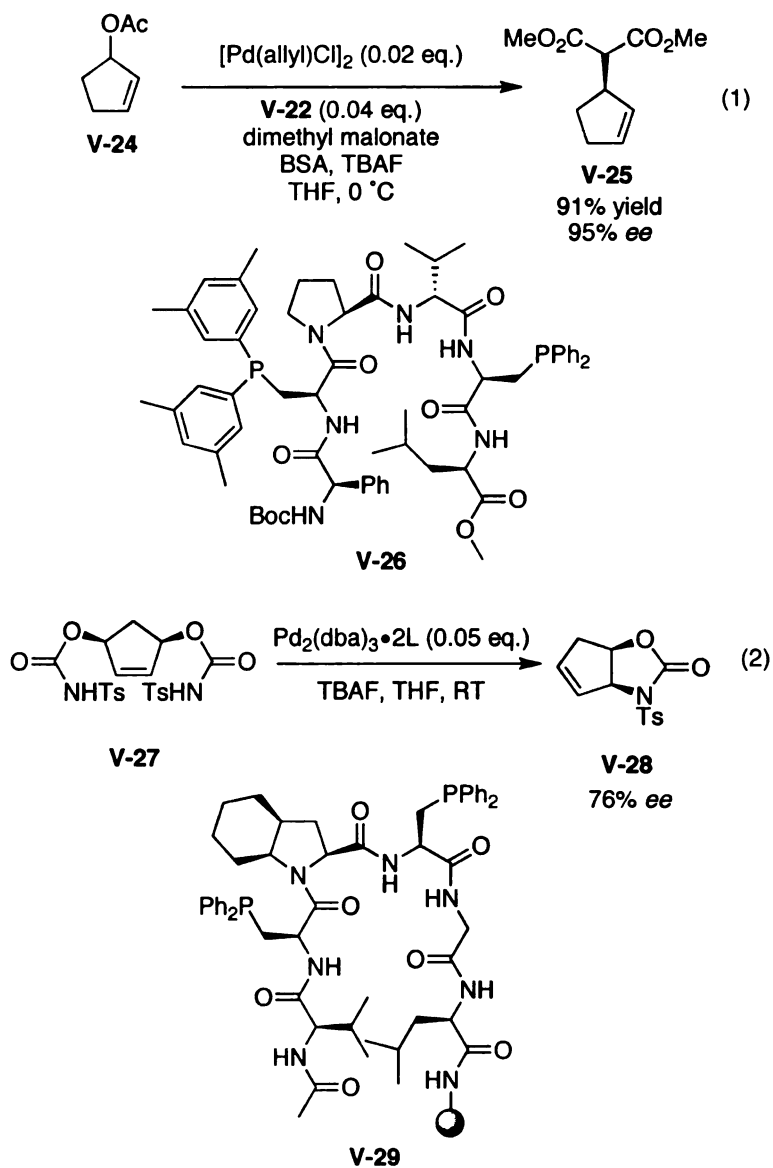
Recently, Shi and coworkers have disclosed a Simmons-Smith

cyclopropanation employing a chiral dipeptide ligand.[72-74] In the presence of

diethyl zinc and diiodomethane, unfunctionalized olefins **V-30** are converted into

their corresponding cyclopropanes **V-31** with enantiomeric excesses ranging

from 72 to 91% when peptide dimer **V-32** is employed (Scheme V-6). These

authors do not report the absolute stereochemical course of the reaction.

Scheme V-6. Shi's peptide ligand for the asymmetric Simmons-Smith reaction.
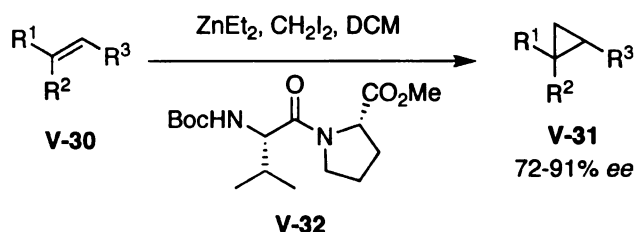
A final compelling example of the application of peptidic ligands to achieve

asymmetric induction in metal mediated processes is Wool-Osmium. These

samples of osmium tetroxide ligated to strands of wool have been shown to be

mildly effective in the catalytic asymmetric dihydroxylation reaction of allylic

alcohols and amines.[75]

It warrants emphasis again that all of the ligands described above were

generated by a common strategy. A combinatorial approach was applied

whereby the optimal ligand was discovered by employing a randomized

screening of a library of peptide candidates. The best ligands from this initial

screen were then optimized by generating directed libraries by which the initial

"hits" were modified until the result for the test reaction was acceptable.

Oftentimes a pool of less than 100 unique ligands was sufficient to drive the enantioselectivity to synthetically useful levels for the desired transformation.

5.1.2: Strategy for Application of Peptide Ligands for OsO₄

We sought to use a similar approach to develop peptidic ligands for several osmium tetroxide-mediated oxidative processes. One such transformation from our laboratory is the oxidative cleavage of olefins under OsO_4-catalytic conditions. This reaction (Scheme V-7, equation 1) utilizes a catalytic amount of OsO_4 in conjunction with several equivalents of Oxone as a co-oxidant to effect the cleavage.[76-78] One could imagine, with the appropriate ligand, applying the oxidative cleavage chemistry to either kinetic resolutions (Scheme V-7, equation 3) or desymmetrizations (Scheme V-7, equation 4). A second osmium tetroxide-mediated methodology developed in our lab is an OsO_4/Oxone mediated oxidative cyclization of 1,4-dienes to give 2,3,5-trisubstituted tetrahydrofuran-diols (Scheme V-7, equation 2).[79] In the case of the oxidative cyclization protocol, since the diastereoselectivity is mediated by the initial formation of the osmate ester prior to cyclization, one could imagine rendering the process enantioselecitive if the initial osmylation is made asymmetric with the aid of an appropriate ligand.

302

Scheme V-7. Potential asymmetric applications of osmium tetroxide from the Borhan group.

$$
\begin{array}{c}
R^1 \overset{R^2}{\underset{}{=}} R^3 \\
\textbf{V-33}
\end{array}
\xrightarrow[\text{DMF, 3h, RT}]{\substack{\text{OsO}_4\ (0.01\ \text{eq.}) \\ \text{Oxone (4 eq.)}}}
\quad
R^1 \overset{O}{\underset{}{\Vert}} R^2
\ +\
HO \overset{O}{\underset{}{\Vert}} R^3
\qquad (1)
$$

$$
\begin{array}{c}
\textbf{V-34} \qquad \qquad \textbf{V-35}
\end{array}
$$

V-36 $\xrightarrow[\text{DMF, 3h, RT}]{\substack{\text{OsO}_4\ (0.01\ \text{eq.}) \\ \text{Oxone (4 eq.)}}}$ V-37 + V-38 (2)

$$
\begin{array}{c}
R^1 \overset{R^2}{\underset{}{\diagup}} \diagup \\
\textbf{V-39}
\end{array}
\xrightarrow[\text{Oxone}]{\substack{\text{OsO}_4 \\ \text{L*}}}
\quad
R^1 \overset{R^2}{\underset{}{\diagup}} \diagup
\ +\
R^1 \overset{R^2}{\underset{}{\diagup}} \overset{OH}{\underset{O}{\diagdown}}
\qquad (3)
$$

$$
\begin{array}{c}
\textbf{V-40} \qquad \textbf{V-41}
\end{array}
$$

$$
\begin{array}{c}
\diagup\diagdown \overset{}{\underset{R}{\diagdown}}\diagup \\
\textbf{V-42}
\end{array}
\xrightarrow[\text{Oxone}]{\substack{\text{OsO}_4 \\ \text{L*}}}
\quad
HO \overset{O}{\underset{R}{\diagdown}}\diagup
\qquad (4)
$$

$$
\textbf{V-43}
$$
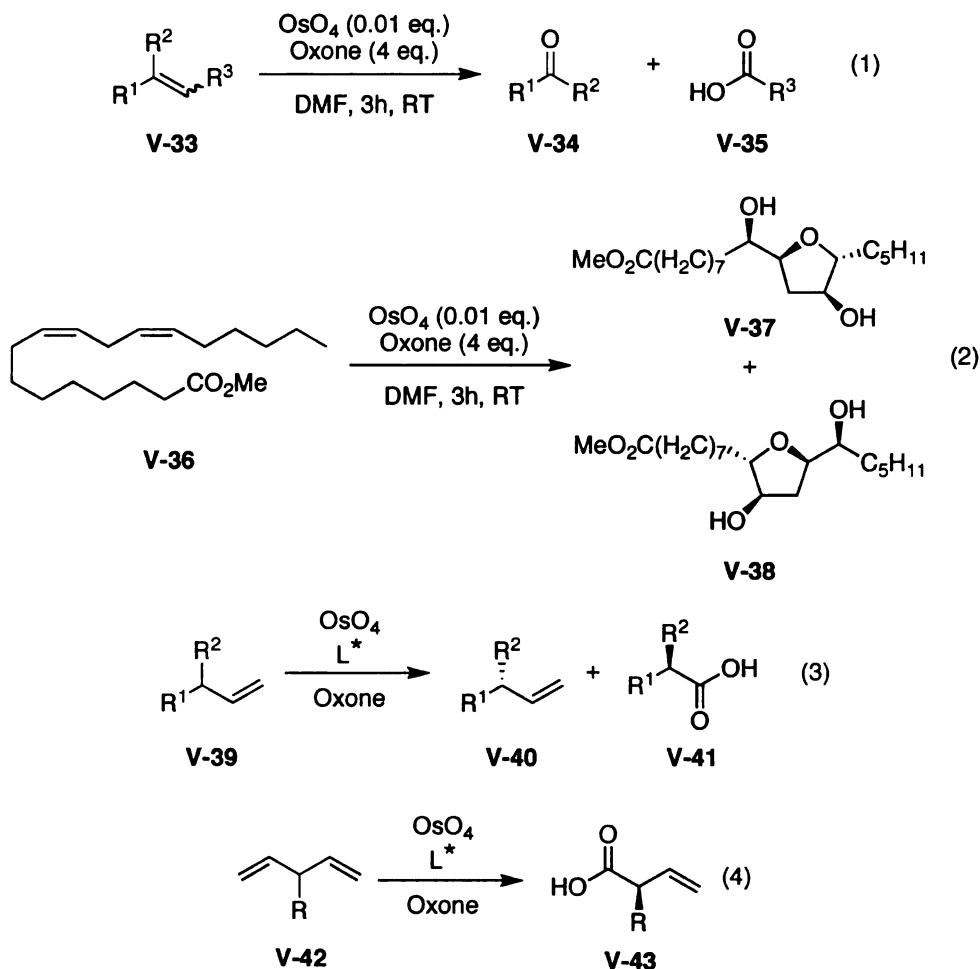
Along with the osmium tetroxide-mediated chemistry from our laboratory, we also sought to apply these peptidic ligands as a complement to the well-known Sharpless Asymmetric Dihydroxylation (SAD) reaction.[80] One can easily argue that the SAD protocol is one of the most reliable and widely applicable transition metal-mediated processes known to organic chemists. That said, the methodology is not without its limitations in certain niches of asymmetric

dihydroxylation. Perhaps the most obvious limitation is the relative inability of the

SAD to provide synthetically useful asymmetric induction for the dihydroxylation

of *cis* olefins.[80] The SAD protocol also exhibits a relatively lackluster

performance in the arenas of desymmetrization and kinetic resolution of

appropriate olefin precursors. Although sparse reports of desymmetrizations[81-84]

and kinetic resolutions[85-90] mediated by the *Cinchona*-based SAD ligands have

appeared in the literature (with varying degrees of success), this particular aspect

of asymmetric dihydroxylation is markedly underdeveloped.

The problem of coupling peptidic ligands with osmium tetroxide distilled to

the need to quickly develop and screen a number of peptides that contain

sequences appropriately placed to induce binding to the osmium site, thus

creating a chiral environment. Studies by both Miller[8,10] and Gilbertson[5] as

described above indicated that some element of secondary peptide structure is

optimal for an effective asymmetric ligand or catalyst. Following their precedent

we set out to investigate peptides containing the well-characterized β-turn

structural motif as an element of secondary structure. Several sequence

combinations have been identified that bias a peptide to adopt the β-turn.

Namely, Pro-D-Aaa (where Aaa is any D amino acid), D-Pro-Gly, and Pro-Aib all

have the ability to cause a peptide to adopt a β-turn secondary structure.[91-101]

One might argue that, for our purposes, the Pro-D-Aaa strategy might be the

most pertinent since it would add another element of diversity to the ligand pool.

Pursuant to the goals outlined above we undertook the synthesis of a

number of peptide ligands based on the three scaffolds outlined below in Figure

V-2. The two key features of these three scaffolds are first, the presence of the β-turn-inducing motif, and second the strategically-placed residues that might provide a ligating site for OsO_4.

Figure V-2. Potential β-turn ligand scaffolds for osmium tetroxide with one or two ligation sites.
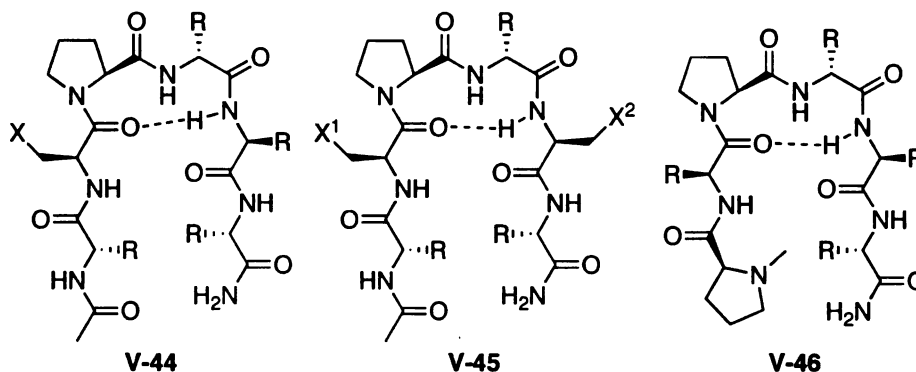
For **V-44** and **V-45**, possible ligating residues represented as X, X^1, and X^2 respectively, might include glutamine, asparagine, lysine, serine, threonine, along with any number of unnatural amino acids containing for instance, tertiary amines or pyridyl moieties. Peptides of the general structure **V-44** would presumably behave as monodentate ligands, whereas sequence **V-45** mimics Gilbertson's bidentate phosphine ligands (**V-26**, Scheme V-5). In this particular sequence, one can envision incorporating, for example, two amide-containing sequences in the X^1 and X^2 positions or a combination of an amine and an amide. Diamino variants were pursued with reservations, however, as they are known to render the dihydroxylation reaction stoichiometric in osmium tetroxide in some cases.[102-121] Scaffold **V-46** incorporates a cyclic tertiary amine residue, represented here but not limited to an N-methylproline moiety. The installation of the cyclic tertiary

amine structure necessitates the inclusion of this residue at the N-terminus of the β-turn scaffold.

A second strategy for the incorporation of osmium tetroxide onto a peptidic backbone involves the use of recently developed methodology for harnessing osmium tetroxide on tetra-substituted olefins, via the formation of the osmate ester.[122-126] These osmate esters have been used effectively for the catalytic dihydroxylation of olefins, presumably via the bis-osmate ester. Although the phenomenon is not well understood, the osmate resulting from the less-substituted olefin is hydrolyzed preferentially to the tetra-substituted olefin. Four such peptides that would incorporate a tetra-substituted olefin are shown in Figure V-3.

Figure V-3. Potential Scaffolds relying on covalent harnessing of osmium tetroxide on tetra-substituted olefins.

V-47

V-48

V-49

V-50
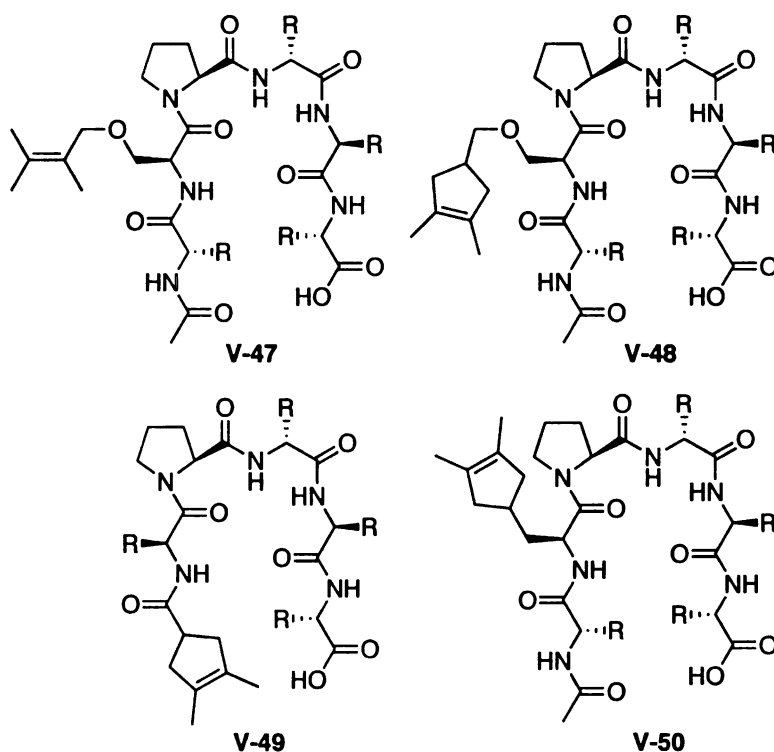
Peptides **V-47** and **V-48** require a serine moiety to introduce the tetra-substituted olefin. Several strategies for alkylating the serine hydroxyl group are known.[127-130] Structure **V-49**, perhaps the simplest to prepare, would result from the capping of the N-terminus of the growing peptide chain with the appropriate tetra-substituted olefin containing carboxylic acid. Peptide **V-50** would introduce the tetra-substituted olefin via the incorporation of an unnatural amino acid. It should be mentioned that, if successful, this strategy would mark the first example of an asymmetric catalyst that relies on a tetra-substituted olefin for harnessing osmium tetroxide.

Presented below is a detailed report of the efforts towards the goals detailed above. As an initial focal point we decided to pursue the development of a peptidic ligand that is effective in an asymmetric *cis*-dihydroxylation of α-methylstryrene, an olefin that performs well under conventional SAD conditions. It was thought that developing this system first would allow us use the SAD protocol as a benchmark standard for the dihydroxylation reaction. Although a selective peptide-based ligand was never realized, important lessons learned are discussed below which will hopefully direct future efforts towards the development of a viable peptide ligand class for various osmium tetroxide applications.

5.2: Results and Discussion

5.2.1: General Peptide Synthesis

The first task at hand was the mastery of solid-phase peptide synthesis (SPPS). For this project we chose to rely on the Fmoc solid phase synthesis

variant. This technique was easily learned by closely following the wealth of tried-and-true procedures available in the literature.[11] Scheme V-8 gives a detailed schematic of the course of a general SPPS sequence. The strategy discussed below was applied for the generation of each of the peptide ligands discussed in this chapter.

Scheme V-8. General schematic for Fmoc SPPS.
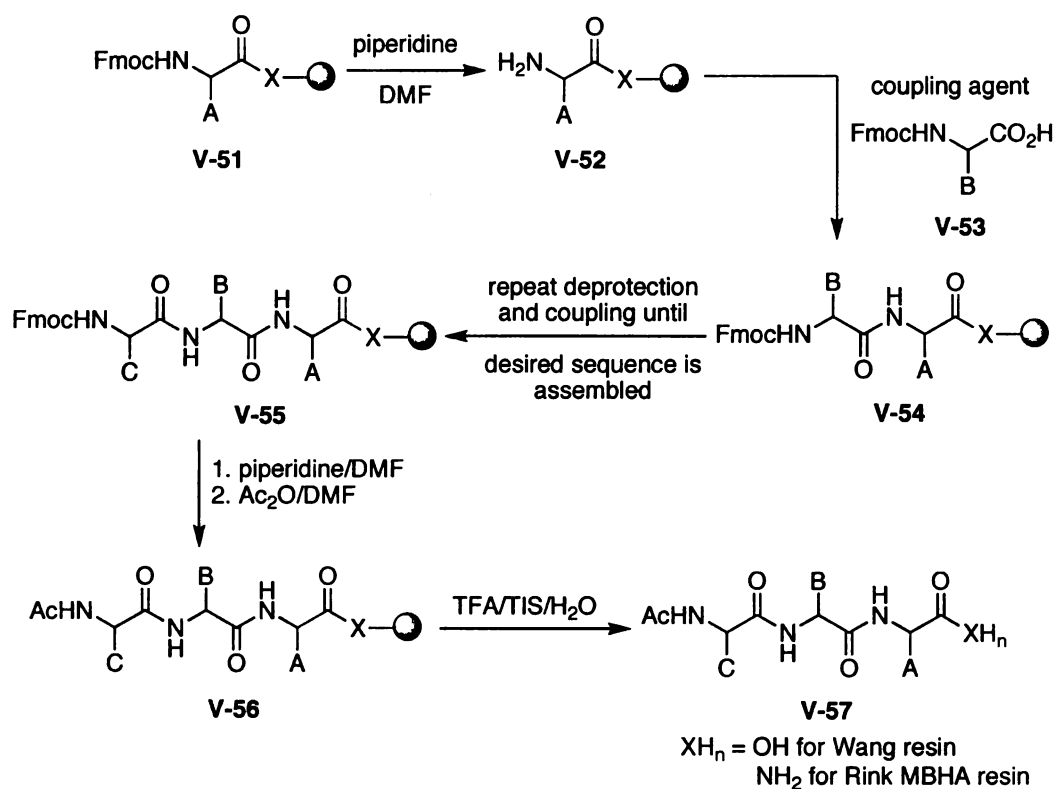
The typical sequence involves first, deblocking the pre-loaded resin **V-51**, followed by a coupling step with an activated Fmoc-amino acid partner to give resin-bound dipeptide **V-54**. After a series of wash steps, this sequence is then repeated, hence deblocking now the second amino acid in the sequence followed by coupling with the next Fmoc-amino acid. The series of steps is repeated until

308

the desired sequence **V-55** has been assembled. The resultant on-bead peptide

sequence is then N-deprotected and capped to produce the bead-harnessed N-

acylated peptide **V-56**. Subsequent cleavage of the peptide from the solid

support returns the target peptide **V-57**.

For the peptides discussed in this chapter, each synthesis began either

with preloaded Wang resin (loaded with Fmoc-Gly) or Rink Amide MBHA resin.

Fmoc deprotection was accomplished with the standard 20% piperidine in DMF

recipe (**V-51** to **V-52**). After initially experiencing some difficulties with DIC

activation, we settled on the HOBt activated ester methodology for the activation

prior to loading of the Fmoc-protected amino acids (i.e. **V-52** to **V-54**). The

completed on-bead peptide sequence was then N-deprotected and capped as

the acetamide in some cases by treatment with a 5% solution of acetic anhydride

in DMF. The completed peptide sequence was then cleaved from the resin using

a TFA/H_2O/TIS mixture to yield the peptide carboxylate (Wang Resin) or the C-

terminal amide (Rink Amide MBHA). The identity of each peptide was evaluated

by MALDI-MS analysis. Given the reliability of Fmoc-SPPS, we elected to

characterize the peptides so generated only by mass spectrometry to facilitate a

high-throughput approach to ligand generation. This level of characterization is

in keeping with other practitioners in the field. By employing the HOBt coupling

methodology, we were able to routinely synthesize hexapeptides of varying

sequences. Full experimental procedures for the synthesis of a generic peptide

sequence using the HOBt coupling methodology can be found in the

experimental section of this chapter (Section 5.5).

5.2.2: Initial Results Towards Asymmetric Dihydroxylation

Peptides **V-58** to **V-64** were synthesized using Fmoc solid phase peptide synthesis as described above. The peptides were isolated as C-terminal carboxylic acids and their identity was confirmed by MALDI-TOF mass spectrometry. Peptide **V-58** was prepared as an initial foray into solid phase peptide synthesis, and does not contain a potential ligation site. Peptides **V-59**, **V-61**, **V-63**, and **V-64** contain an asparagine moiety one residue removed from the N-terminus as a potential ligation site, and differ only in the selection of the D-amino acid (or Aib residue for **V-59**) that serves to induce the β-turn. Conversely, **V-60** and **V-62** incorporate two asparagine residues, and would presumably behave as potential bidentate ligands.

Figure V-4. Peptides **V-58** through **V-64**.

V-58

V-59

V-60

V-61

V-62

V-63

V-64
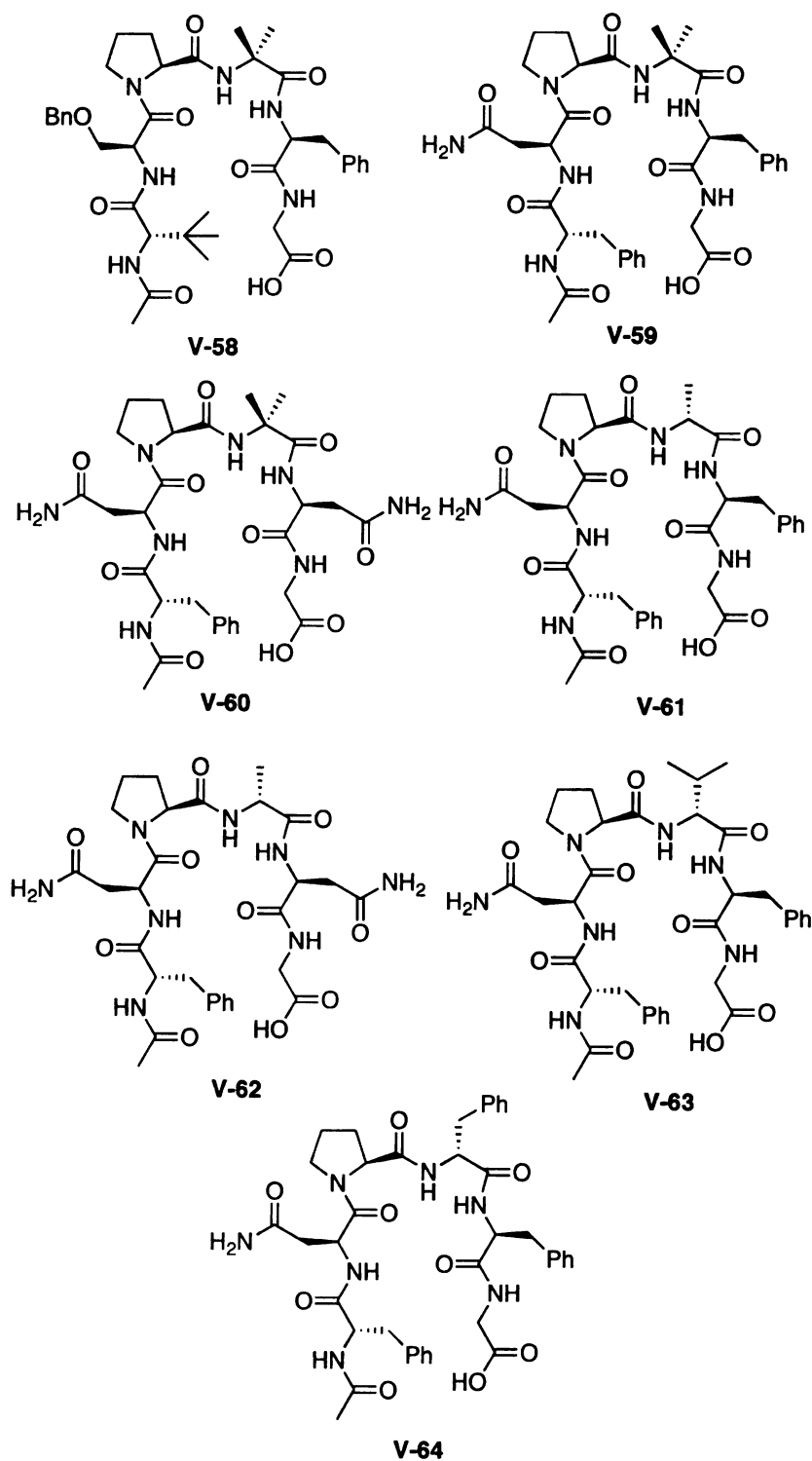
In a intial set of experiments, each of the above peptides were screened

as possible ligands for the asymmetric dihydroxylation of α-methylstyrene. The

ligands were screened using the well-known Ogino-Sharpless potassium

ferricyanide/potassium carbonate co-oxidant system[80,131,132] in a 1:1 mixture of t-

butyl alcohol and water (equation 9, Table 1). For comparison, the

dihydroxylation of α-methylstyrene was performed using standard SAD

conditions with AD-mix-α to give the desired diol in 86% ee.

Table V-1. Screen of peptide **V-59** through **V-64** in the dihydroxylation of
α-methylstyrene.

Peptide (0.025 eq.)
OsO$_4$ (0.01 eq.)

K$_3$Fe(CN)$_6$ (3 eq.)
K$_2$CO$_3$ (3 eq.)
t-BuOH/H$_2$O (1:1)

Ph — **V-65** → Ph — **V-66**
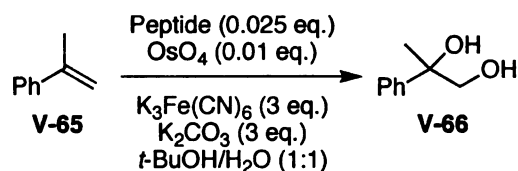
Peptide	% yield	% ee
V-59	60	0
V-60	97	0
V-61	100	0
V-62	47	0
V-63	100	0
V-64	93	0

These initial experiments returned the desired diol **V-66** in each case,

providing fair to excellent yields depending on which peptide was used. While

the yields of the desired diol were acceptable in most cases, the extent of

stereoinduction was non-existent. One can speculate several possible reasons

for the lack of induction. First, perhaps peptides **V-59** through **V-64** do not contain sites that bind osmium tightly enough. Also, one could argue that the peptides (as terminal carboxylates) might be more soluble in the water layer of the biphasic reaction conditions than the corresponding organic layer. A final scenario would be that the peptides could be coordinating to osmium tetroxide in the organic layer, but do not maintain their secondary structure due to the high polarity of the solvent system. Each of these questions were addressed to some degree, as described below.

A new series of ligands were synthesized (Figure V-5, peptides **V-67** through **V-70**) containing a lysine residue one residue removed from the β-turn sequence. Due to the presence of the amine side chain in lysine, one might argue that these ligands could present a better binding site for osmium tetroxide than the primary amide sites contained within ligands **V-59** through **V-64**.

Figure V-5. Peptides **V-67** through **V-70** containing lysine residues.

V-67

V-68

V-69

V-70
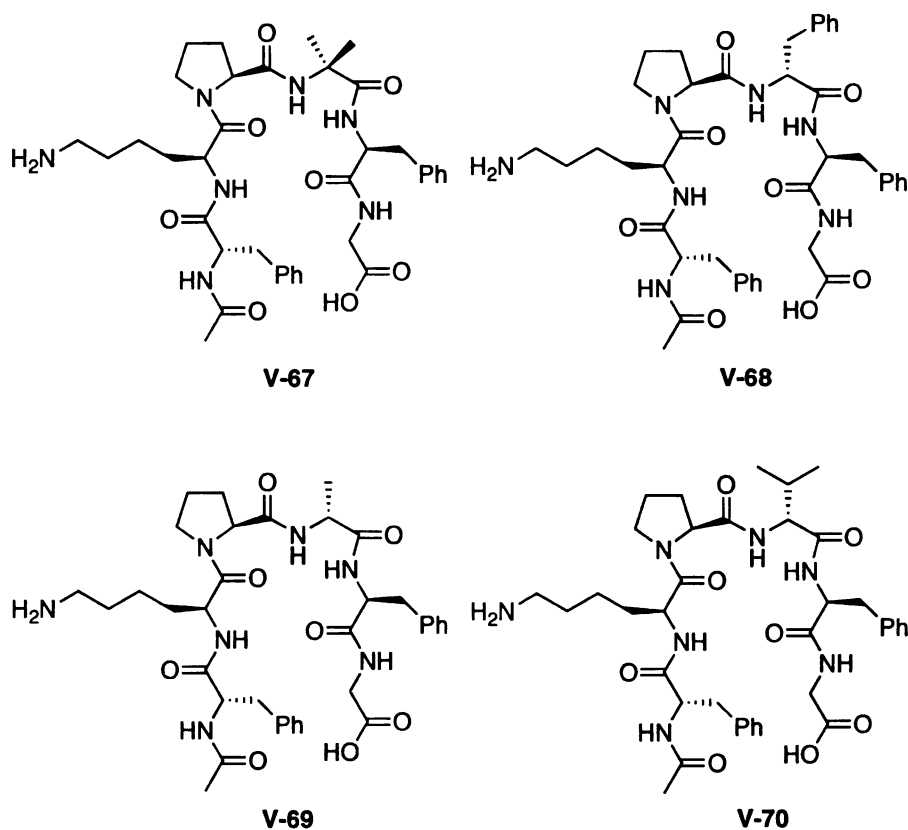
The amine-containing peptides **V-67** through **V-70** were screened as

ligands for the asymmetric dihydroxylation reaction, and again, acceptable yields

were realized, but no detectable enantioselectivity resulted.   Table V-2 shows

the results from this set of experiments.

At this point, we speculated that several issues might be contributing to

the lack of stereoinduction in these initial experiments. If the lack of induction is

due to the solubility of the ligand in the water layer, two possible solutions

present themselves. First, the presence of the peptides as their sodium salts

might contribute significantly to the solubility of the peptides in the water layer as

alluded to earlier. This situation could be alleviated by either producing

314

analogous peptide methyl esters or amides by known methodology. Peptide methyl esters are prepared by altering the cleavage protocol after assembly of the peptide scaffold on solid phase. Conversely, C-terminal peptide amides are readily available upon TFA cleavage from the Rink amide MBHA resin.

Table V-2. Screen of peptide **V-67** through **V-70** in the dihydroxylation of α-methylstyrene.

Peptide (0.025 eq.)
OsO$_4$ (0.01 eq.)

K$_3$Fe(CN)$_6$ (3 eq.)
K$_2$CO$_3$ (3 eq.)
t-BuOH/H$_2$O (1:1)

V-65 → V-66
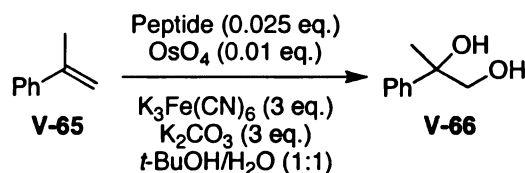
Peptide	% yield	% ee
V-67	100	0
V-68	97	0
V-69	100	0
V-70	77	0

We envisioned that employing the monophasic Upjohn[133] conditions might also address our concerns about the water solubility of the ligands. This option also presents the intriguing possibility that these peptide ligands might prove to be effective Fokin-Sharpless second cycle ligands.[134] Ligands of this class are purported to maintain complete bidentate coordination to the osmium center throughout the catalytic cycle. An example of a Fokin-Sharpless second cycle ligand is shown below in Scheme V-9. Fokin and Sharpless argue that the presence of the carboxylate in **V-73** is crucial in aiding in hydrolysis of the

olefin/OsO$_4$-L* complex.[134,135] One might argue that the peptide carboxylates might act in a similar manner.

Scheme V-9. Asymmetric dihydroxylation mediated by Fokin-Sharpless second cycle ligand **V-73**.

Ph— (V-71) → V-73 (0.05 eq.) / OsO$_4$ (0.02 eq.) / NMO (1.1 eq.) / tBuOH/H$_2$O (1:1) → Ph—CH(OH)—CH$_2$OH (V-72) >99% conv. 42 % *ee* | Ph—C(NHTs)(CO$_2$H)—CH(OH)— (V-73)
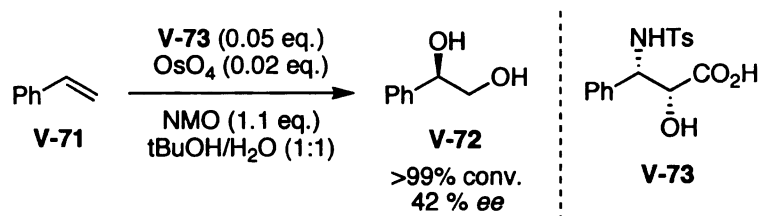
Another possible explanation for the lack of stereoinduction could be that the peptides are not efficient binders of osmium tetroxide. The results in Tables V-1 and V-2 might be due to the action on non-ligated, freely solvated osmium tetroxide. One might alleviate this problem by producing peptides with substituents that have a stronger affinity for osmium tetroxide, such as tertiary amines or pyridyl groups.

The strategies discussed above for correcting the poor results shown in Tables V-1 and V-2 have all been explored to some extent. Let us first turn to exploring other oxidation conditions with the two groups of peptides described above (**V-59** through **V-64** and **V-67** through **V-70**). Table V-3, shown below shows the results for the NMO-mediated dihydroxylation (Upjohn conditions) of α-methylstyrene for a representative sample of these peptides. Overall, the monophasic Upjohn conditions did not provide any additional induction when compared to the Ogino-Sharpless conditions. Those entries that provided a non-zero enantiomeric excess are probably not within the range of experimental error. It is interesting, however, that those peptides containing a lysine side chain (**V-67**

to **V-70**) seemed to have deleterious effect upon the course of the Upjohn

dihydroxylation. None of the four lysine-containing peptides returned the desired

diol in greater than 33% yield, and one of the peptides, compound **V-67**, seemed

to completely shut down the dihydroxylation under Upjohn conditions. This result

is particularly intriguing when one considers that peptide **V-67** returned the

desired diol in quantitative yield under Ogino-Sharpless conditions. The reason

for this disparity, and for the overall poor performance of all of the peptides with

lysine residues in the Upjohn dihydroxylation is not clear.

Table V-3. Screen of Upjohn conditions with peptides **V-59** through **V-64** and **V-67** through **V-70**.
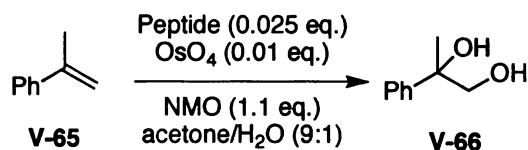
Peptide	% yield	% ee
V-59	87	0
V-60	77	1
V-61	100	1
V-62	70	0
V-63	70	0
V-64	50	0
V-67	0	-
V-68	33	1
V-69	30	0
V-70	33	0

Once it seemed clear that the performance of the peptides described above could not be optimized to any large extent by changing the reaction conditions, attention was then focused on synthesizing a new group of peptides with different C-termini. These peptides served to further probe the theory that the C-terminal carboxylates might prove to be too water soluble to facilitate catalysis in the organic layer of the Ogino-Sharpless protocol.

Peptides **V-74**, **V-75**, and **V-76** were prepared by assembling the desired sequence on the Fmoc-Gly-Wang resin and then cleaving the peptide from the bead with a 9:1:1 mixture of TEA/MeOH/DMF for four days to release the fully protected peptide methyl ester. These structures were meant to be fully protected, methyl ester analogues of peptides **V-59**, **V-60**, and **V-68**. Likewise, by building the peptide off of the Rink Amide MBHA resin, peptides **V-78**, **V-79**, and **V-80** provided C-terminal peptide amide analogues similar to **V-60**, **V-64**, and **V-68**. Finally, peptide **V-77**, containing three carboxylic acid residues, was prepared in order to investigate the potential of a peptide acting as a Fokin-Sharpless second cycle ligand[134] (*vide supra*).
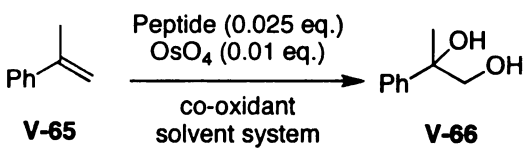
These seven ligands were screened for stereoinduction in the dihydroxylation of α-methylstyrene under both the Ogino-Sharpless and Upjohn dihydroxlation protocols. Table V-4 presents the data for the Ogino-Sharpless dihydroxylation as well as the data for the Upjohn protocol.

Figure V-6. Peptides **V-74** through **V-80**, peptide methyl esters and amides.

V-74

V-75

V-76

V-77

V-78

V-79

V-80
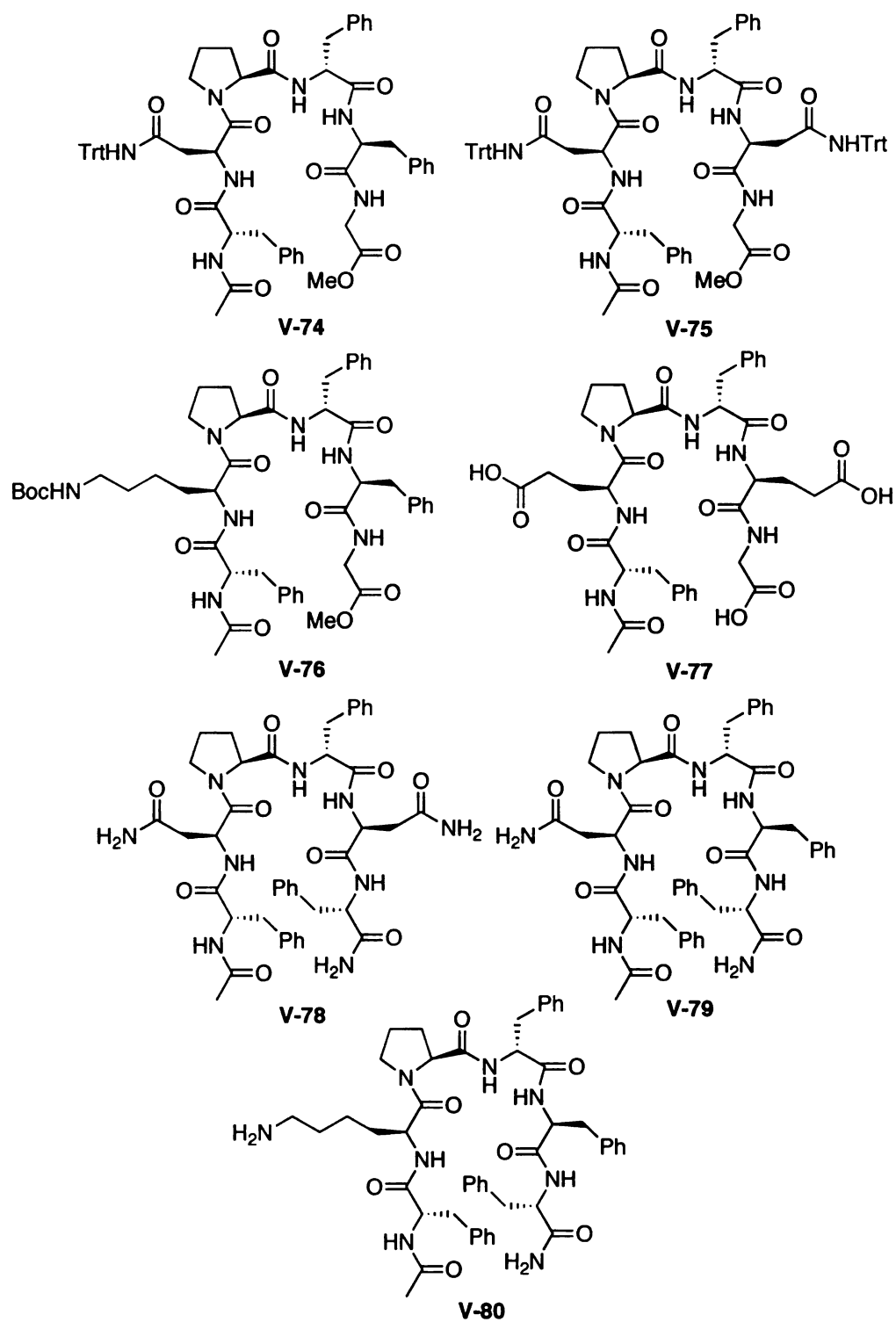
The results from these peptides were also discouraging. For the most part, under the Ogino-Sharpless protocol, each peptide allowed for (or at least did not hinder) the conversion to the desired diol in good to excellent yield. The product diols, however, were virtually racemic. The best result for the Ogino-Sharpless dihydroxylation of α-methylstyrene, with regards to enantioselectivity, was with peptide **V-80**, a Pro-D-Phe induced β-turn with a pendant lysine residue as the putative site of coordination.

Table V-4. Screen of peptides **V-74** through **V-80** with the Ogino-Sharpless and Upjohn conditions.

Ogino-Sharpless (K$_3$Fe(CN)$_6$)			Upjohn (NMO)		
Peptide	% yield	% ee	Peptide	% yield	% ee
V-74	87	0	V-74	100	0
V-75	100	0	V-75	100	0
V-76	90	0	V-76	100	2
V-77	80	1	V-77	90	1
V-78	100	0	V-78	100	0
V-79	60	0	V-79	77	1
V-80	70	3	V-80	100	0

Similarly discouraging results were obtained for the dihydroxylation of α-methylstyrene under Upjohn conditions in the presence of peptides **V-74** through

V-80. The dihydroxylation again proceeded in high yield, but returned virtually racemic diol products.

Unsure of whether or not the 3% *ee* observed for peptide **V-80** under Ogino-Sharpless conditions was a "real", believable result, an eight member group of analogous peptides was synthesized that differ from peptide **V-80** at the N-terminal amino acid (Figure V-7). This particular position was altered under the important assumption that this residue, neighboring the putative ligation site (lysine) would have the largest potential to influence the binding of osmium tetroxide. This systematic screening of an initial "hit" peptide is well precedented.[2,3,10] It was assumed that if the 3% *ee* observed for peptide **V-80** was a legitimate result, that the single point mutations should show some influence on the enantioselectivity of the dihydroxylation reaction. If, however, the result presented in Table V-4 was within the experimental error of the HPLC apparatus, then one might expect for the point mutations in the eight structures analogous to **V-80** to produce diol products that had no discernable enantiomeric excess. The particular residues that were selected for incorporation onto the N-terminus were judiciously chosen to provide a wide range of structural variability. Ideally, by varying the structural elements at the C-terminal position with a wide range of different types of functionalities, one of the focused group might return a second generation scaffold that drastically perturbed the initial 3% *ee* value (*i.e.* +/- 10 % *ee*).

Figure V-7. N-terminal analogues of peptide **V-80**. **V-81** through **V-88**.

V-81

V-82

V-83

V-84

V-85

V-86

V-87

V-88
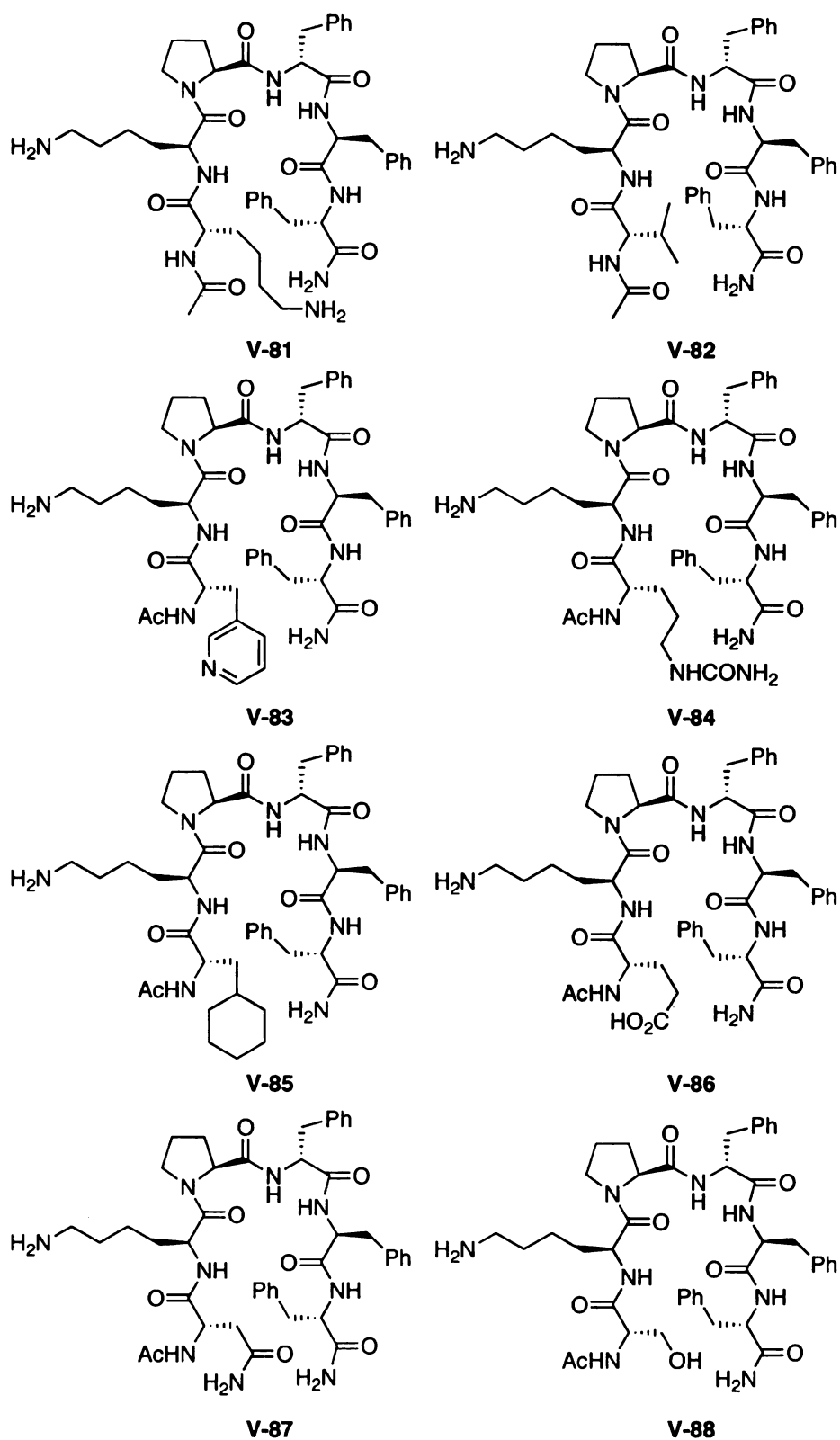
Frustratingly, peptides **V-81** through **V-88** provided only racemic samples of the desired diol in good yields under the Ogino-Sharpless protocol. Two possible conclusions can be drawn from this result: either the N-terminal amino acid is not important in altering the extent of stereoinduction (which seems unlikely), or the result shown in Table V-4 above is an artifact. It seems likely that the result for peptide **V-80** in Table V-4 was not a real "hit".

At this point, it was decided to pursue the synthesis of a series of peptides that contained other potentially stronger binding sites. In that vein, a series of eleven peptides designed around the Pro-D-Phe β-turn sequence were synthesized and screened for stereoinduction in the dihydroxylation of α-methylstyrene using the Ogino-Sharpless protocol.

Peptides **V-89** through **V-93** were designed as putative monodentate ligands for osmium tetroxide (Figure V-8). The potential binding sites were surmised to be the various nitrogen-containing heterocyclic side chains: namely the indole ring of tryptophan (**V-89**), the pyrrolidine ring of proline (**V-90**), the imidazole ring of histidine (**V-91**), and the pyridine rings of the unnatural 3- and 4-pyridylalanine residues (**V-92** and **V-93** respectively). In each case, however, the dihydroxylation of α-methylstyrene returned virtually racemic diol products. In each case, the desired diol was isolated in nearly quantitative yield.

Figure V-8. Monodentate ligands **V-89** through **V-93**.

V-89, 0% *ee*

V-90, 0% *ee*

V-91, 0% *ee*

V-92, 2% *ee*

V-93, 0% *ee*
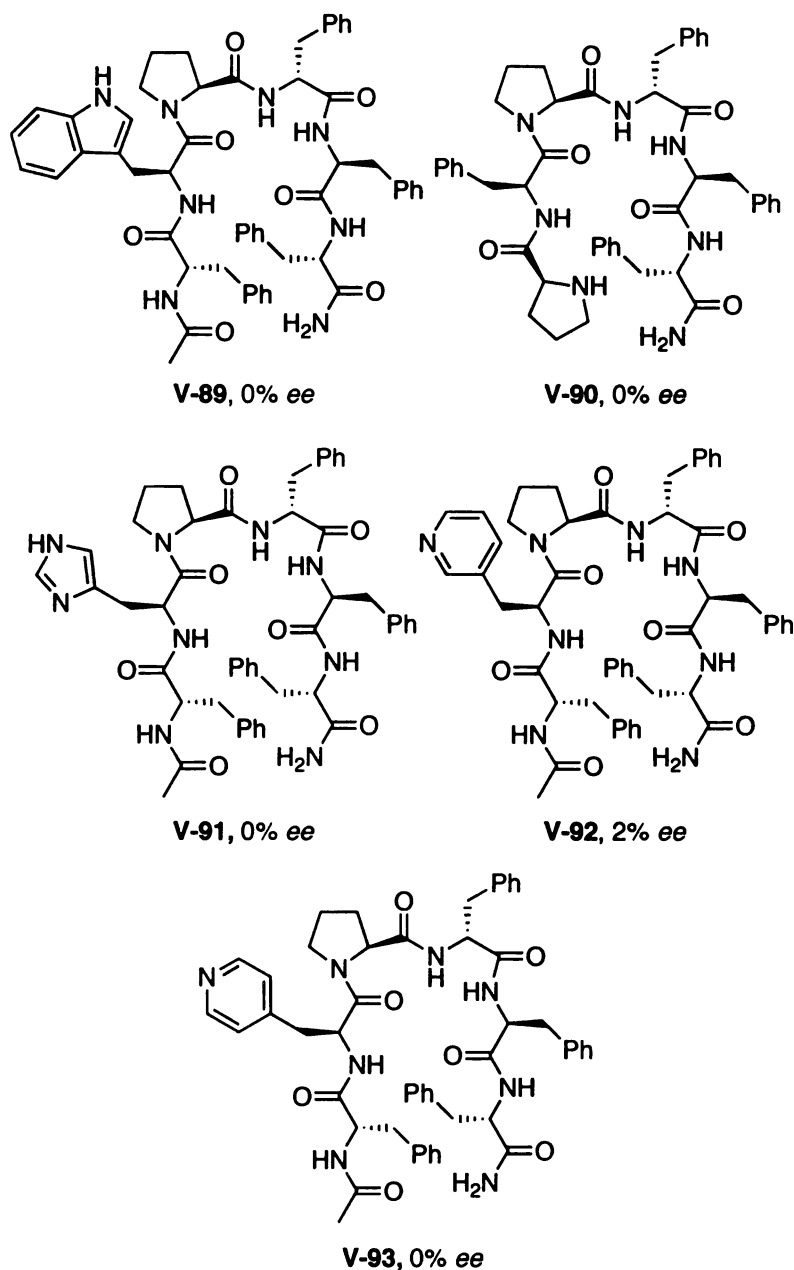
Peptides **V-94** through **V-99** were designed to be possible bidentate ligands by combining either two strategically placed pyridine rings or a pyridine ring and a primary amine residue from either lysine or ornithine residues flanking each side of the D-Phe-Pro β-turn inducing motif.

Figure V-9. Bidentate peptides **V-94** through **V-99**.
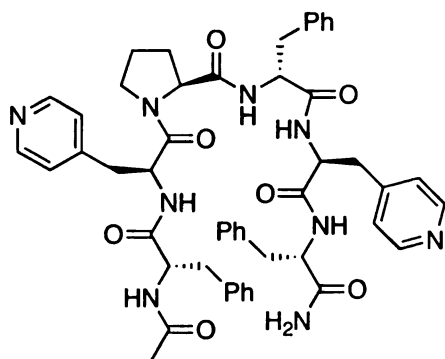
V-94, 3% *ee*
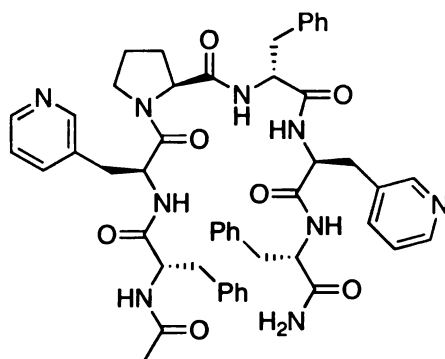
V-95, 1% *ee*
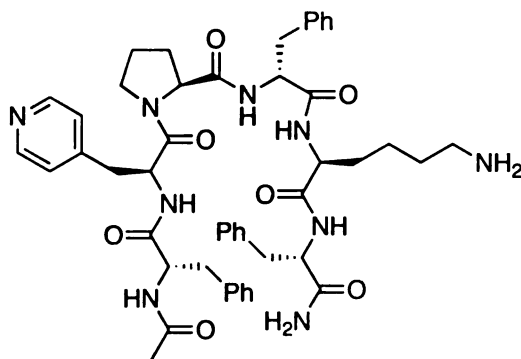
V-96, 0% *ee*
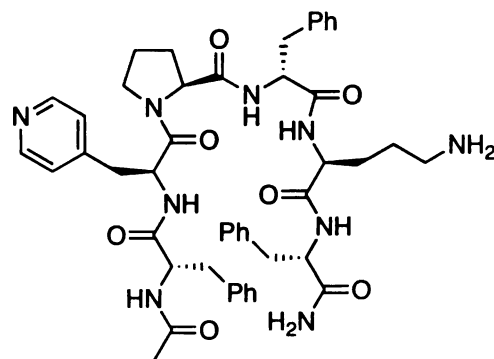
V-97, 1% *ee*
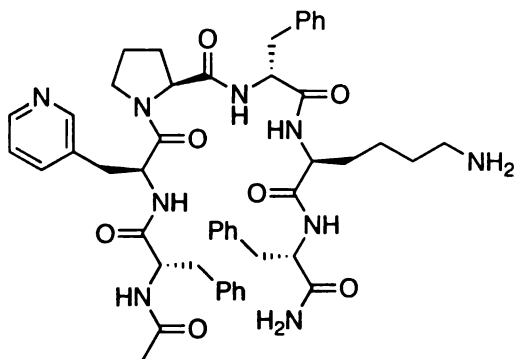
V-98, 1% *ee*
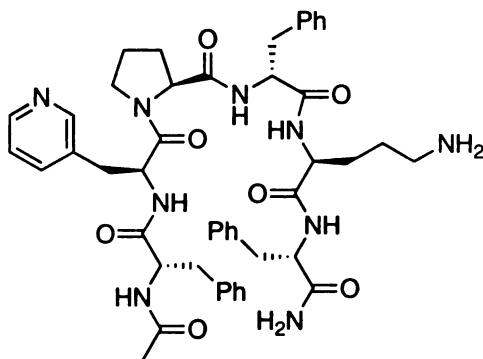
V-99, 0% *ee*

Unfortunately, all of the compounds shown in Figure V-9 also returned the desired diol product with enantiomeric excess lower than 3% *ee*. Again, the desired diol was isolated in nearly quantitative yields.

Subsequently compound **V-94** was used in an exploration of reaction

conditions for the dihydroxylation of α-methylstyrene. As can be seen in Scheme

V-10 below, the room temperature dihydroxylation of α-methylstyrene returned

diol of 3% *ee*, whereas cooling the reaction to 4°C (which one would suggest

ought to improve *ees* as shown by Sharpless and others in the SAD reaction)

returned racemic diol. By employing the less polar, *tert*-butyl methyl ether as the

organic solvent, a diol product of 0% *ee* was returned. Similar to the positional

scanning study presented in Figure V-7, these incongruous results further

confirm the necessity to establish a threshold of at least 10% *ee* as a

requirement for a credible, workable initial "hit" scaffold.

Scheme V-10. Condition screen with peptide **V-94**.
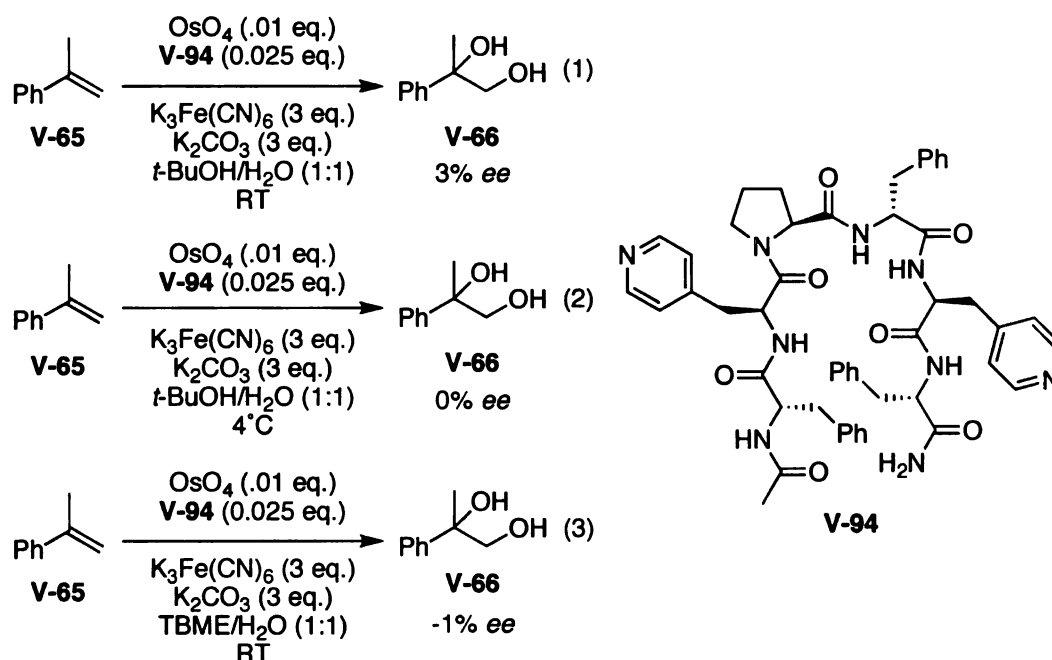
5.2.3: Stoichiometric Study

Since the catalytic dihydroxylation protocols employed up to this point had provided poor stereoinduction, a few of the peptide ligands were evaluated in the context of a stoichiometric asymmetric dihydroxylation. It was surmised that perhaps the ligands could be quite effective in imparting selectivity, but were being out-competed by a faster, non-ligated, and thus racemic background dihydroxylation. It warrants emphasis that there is no guarantee that peptidic ligands will benefit from the well-known ligand accelerated catalysis that so exquisitely governs the efficacy of the normal SAD protocol.[80] With this in mind, peptides **V-87** and **V-92** were screened in a small scale (0.02 mmol) stoichiometric dihydroxylation of α-methylstyrene in toluene (Scheme V-11).

Scheme V-11. Stoichiometric dihydroxylation of **V-65** in the presence of **V-87** and **V-92**.
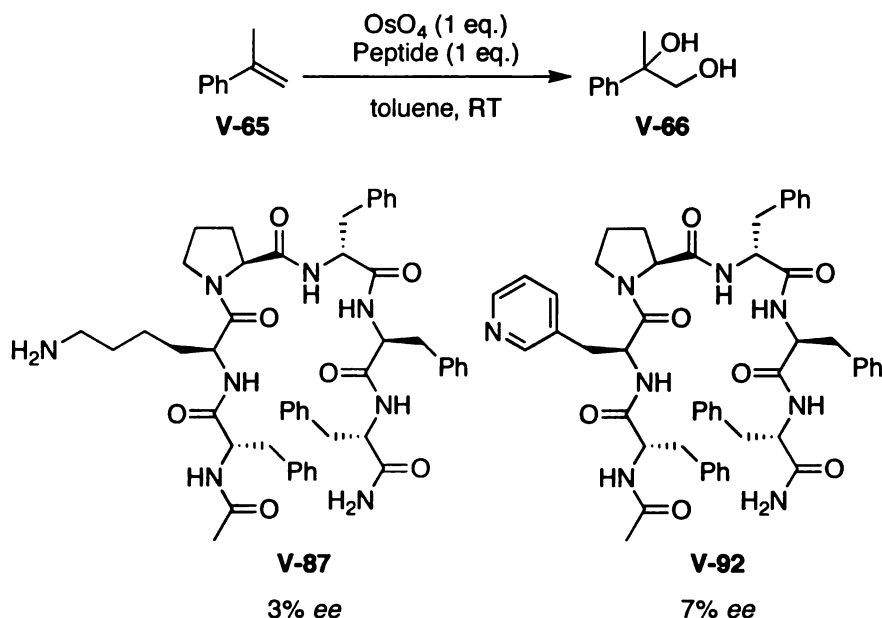
In the event, peptide **V-92** provided diol in 7% *ee*, while peptide **V-87** provided the diol in 3% *ee*. It is difficult to argue whether or not these data are reliable given the small scale of the experiment and the poor level of asymmetric induction. Given that both peptides returned diol products with enantiomeric excess below 10% *ee*, coupled with the large amount of peptide required for a scale-up experiment, this approach was not pursued any further. The main conclusion drawn from these data is that the peptides do not behave as appreciably more selective ligands in the stoichiometric dihydroxylation reaction.

5.2.4: Investigation of Cyclic Peptides

Given the failure of various acyclic β-turn scaffolds in the dihydroxylation of α-methylstyrene, we next set out to develop a new scaffold that would be more robust in the highly polar solvents conducive to the dihydroxylation reaction. Cyclic peptides offered an intriguing alternative to the β-turn motif, since their secondary structure is maintained by covalent bonds. Furthermore, peptide macrocycles are readily prepared by standard solid phase peptide synthesis (Scheme V-12). This is accomplished by attaching a doubly protected initial residue to the bead via its side chain (see **V-100**), building the sequence on the N-terminal end (**V-100** to **V-101**), deblocking the C-terminus and then cyclizing the final product on the bead (**V-102** to **V-103**). The cyclic peptide is then cleaved from the resin using standard procedures.[136-140]

Scheme V-12. General schematic for the on-bead preparation of cyclic peptide ligands.

V-100

assemble sequence

via Fmoc SPPS

V-101

1. 20% piperidine in DMF

2. Pd(PPh$_3$)$_4$ (0.1 eq.)
   DMSO/THF/aq. HCl/morpholine
   (2:2:1:0.1), 2h

V-102

PyBOP (5 eq.)
HOBt (5 eq.)

DIEA (5 eq.)
DMF
8 hr

V-103

TFA/H$_2$O/TIS

(95:2.5:2.5)
2 h

V-104
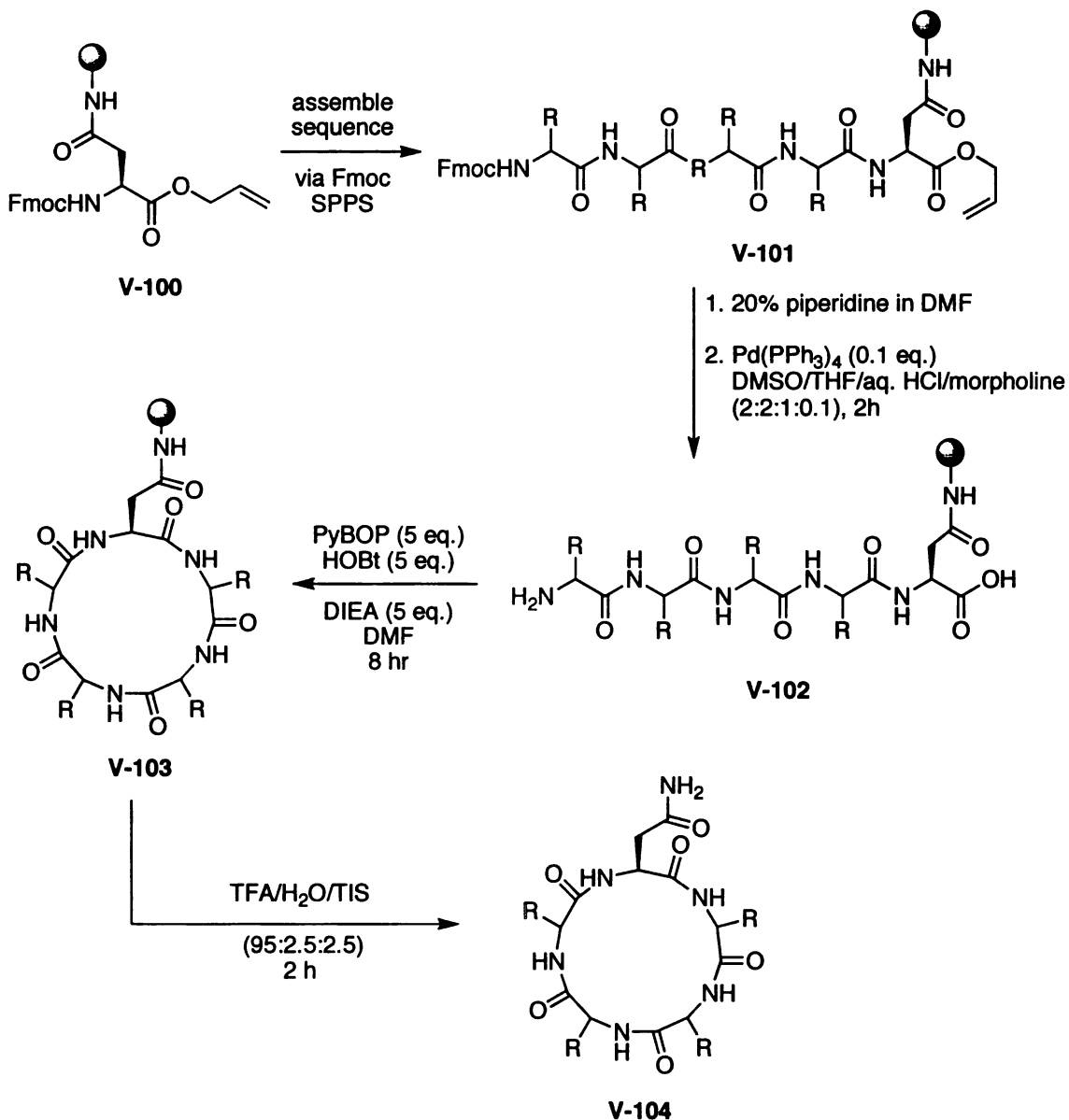
Using this strategy, a new scaffold was selected, that was designed about

a cyclic heptapeptide containing the same Pro-D-Aaa feature of the acyclic

peptides (see scaffold **V-105**, Figure V-10).

Figure V-10. Cyclic peptides based on scaffold **V-105**.

V-105

V-106

V-107

V-108

V-109
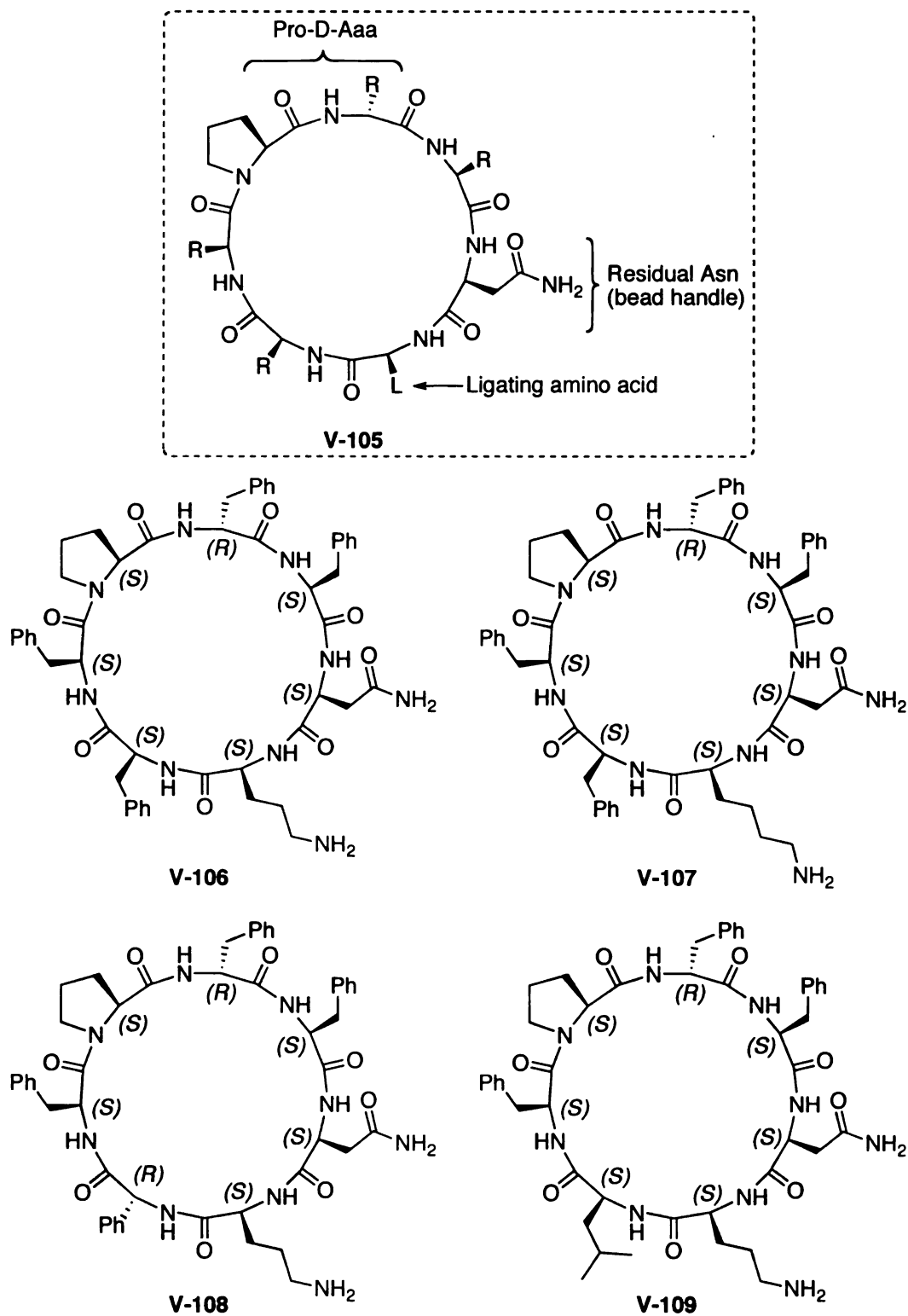
Figure V-10 continued.

V-110

V-111

V-112

V-113
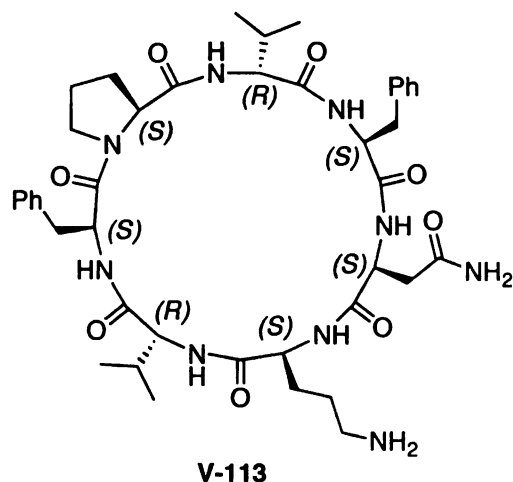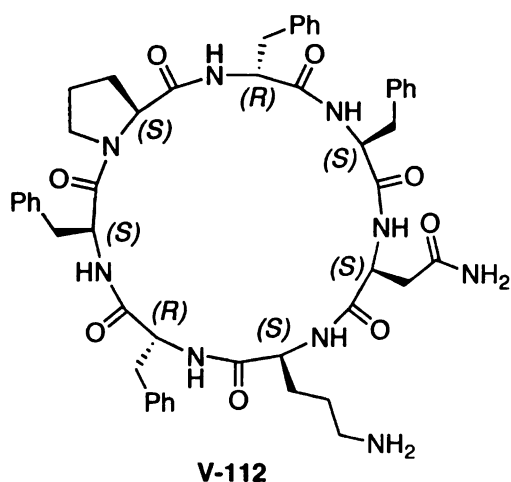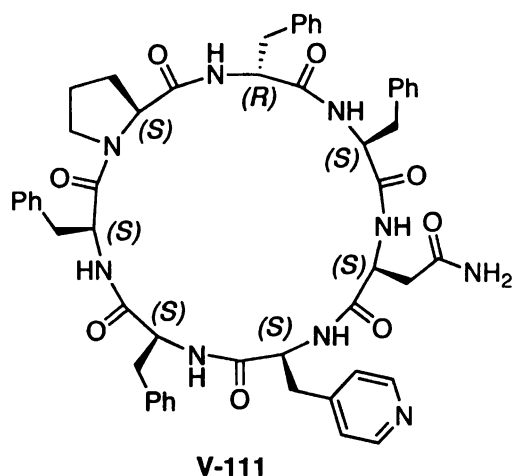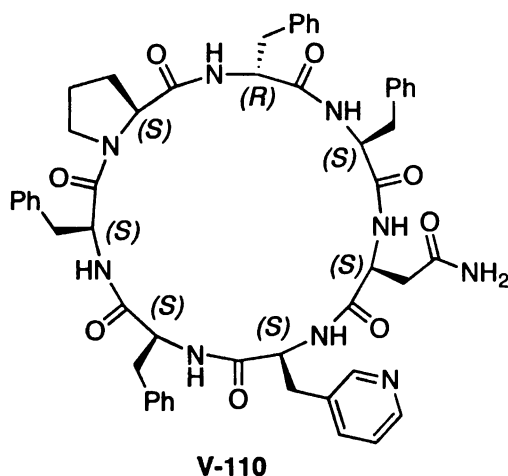
Scaffold **V-105** maintains the Pro-D-Aaa β-turn motif, but incorporates this group into a cyclic structure, thus restricting it from potentially unwinding. In this scaffold, the putative ligating residue was installed two positions away from the proline N-terminus instead of one, thus placing the ligating residue proximal to the residual Asn residue. This was done to potentially facilitate a bidentate binding regime between the Asn amide and the ligating residue functionality. Using this scaffold **V-105** as a template, eight cyclic heptapeptides were synthesized. Peptides **V-106** through **V-113** were synthesized by attaching the

331

C-terminal allyl ester of Fmoc-aspartic acid (Fmoc-Asp-OAll) to Rink Amide

MBHA resin via the aspartate side chain carboxylic acid. Then, the peptide chain

was elongated using standard Fmoc-SPPS techniques. Finally, the C-terminal

allyl protecting group was cleaved by action of $Pd(PPh_3)_4$ in the presence of

morpholine (allyl scavenger). The final stage of the synthesis entailed stitching

the ring closed by a PyBop/HOBt-mediatied coupling. The cyclic peptides were

then liberated from the beads by treatment with a 95:2.5:2.5 mixture of

trifluoroacetic acid, triethylsilane, and water (See Scheme V-11).

Overall, the synthesis of these cyclic peptides was facile, but there was

some evidence for competing dimerization to make the analogous 14-mer. For

example, the MALDI-TOF mass spectrum of cyclic peptide **V-106**. contained

along with the desired M+Na ion (m/z = 936.33) a smaller contribution from a

2M+Na ion (m/z = 1850.69). Dimerization of the desired peptide is a common

problem with the synthesis of cyclic peptides. Given the cyclic peptides were the

only ligands synthesized in the study that showed evidence of contaminants in

the MALDI mass spectrum, we elected to screen these crude samples and purify

them further by HPLC if the extent of stereoinduction was promising.

Peptides **V-106** through **V-113** were screened in the catalytic

dihydroxylation of α-methylstyrene under the Ogino-Sharpless conditions, again

returning diol products in excellent yields but virtually no stereoinduction (Table

V-5). Given these poor results in the initial screen of the cyclic peptide of this

scaffold, this strategy was abandoned in lieu of an extensive screen of a new

oxidation protocol with the more simply prepared acyclic ligand (*vide infra*).

Table V-5. Screen of cyclic ligands **V-106** through **V-113** under the Ogino-Sharpless conditions.

$$\text{Ph} \diagup \!\!= \quad \begin{array}{c} \text{Peptide (0.025 eq.)} \\ \text{OsO}_4 \text{ (0.01 eq.)} \\ \xrightarrow{\hspace{3cm}} \\ \text{K}_3\text{Fe(CN)}_6 \text{ (3 eq.)} \\ \text{K}_2\text{CO}_3 \text{ (3 eq.)} \\ t\text{-BuOH/H}_2\text{O (1:1)} \end{array} \quad \text{Ph} \diagup \!\! \begin{array}{c} \text{OH} \\ \text{OH} \end{array}$$

V-65   V-66
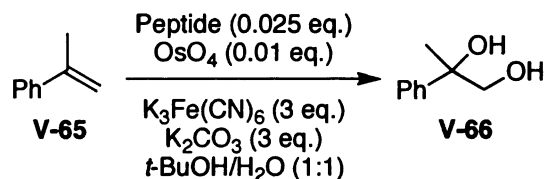
Peptide	% ee
V-106	1
V-107	2
V-108	3
V-109	0
V-110	0
V-111	1
V-112	0
V-113	0

5.2.5: Investigation of the Anhydrous Narasaka Dihydroxylation Protocol

After considering the failed scaffolds described above, two main concerns emerged that we envisioned might be the root cause of the lack of stereoinduction. First, all of the initial experiments under both the Ogino-Sharpless (K$_3$Fe(CN)$_6$/K$_2$CO$_3$) and the Upjohn (NMO) co-oxidant systems were conducted in highly polar solvent systems (mixtures of t-butyl alcohol/water and acetone/water, respectively). The acyclic ligands might have some difficulty nucleating the β-turn, a process governed by hydrogen bonding between the amide NH and carbonyls across the turn, due to competitive hydrogen bonding

333

with the polar solvent system. We therefore sought a method by which we could effect a dihydroxylation event in relatively non-polar media, preferably in the absence of water. In the late 1980s, Narasaka reported the facile conversion of olefins into their corresponding cyclic boronic esters via an osmium tetroxide-mediated *syn* dihydroxylation (NMO as co-oxidant) in *dry* DCM that employed phenyl boronic acid to facilitate the collapse of the osmate ester instead of water.[141] Narasaka (Scheme V-13, equation 1), and later Sharpless[142] (Scheme V-13, equation 2) applied this protocol under strictly anhydrous conditions in dichloromethane. Some years later, Muniz showed that this novel method for decomposing the osmate ester did not require anhydrous conditions at all, rather the modification could yield the desired phenyl boronic esters in good yield under normal Upjohn and Ogino-Sharpless conditions in aqueous solvent systems (H_2O/*t*-BuOH) (Scheme V-13, equation 3). In his report, he also confirmed that this methodology is compatible with conventional SAD ligands, allowing for the direct preparation of chiral boronic esters from olefins.[143]

This protocol, especially that described by Narasaka, was very intriguing since it allowed for a dihydroxylation event that was catalytic in osmium tetroxide and yet importantly, could be conducted in non-aqueous solvents. We surmised that the ability to use phenyl boronic acid as a "hydrolyzing" surrogate in dry solvents might provide a dihydroxylation event in a solvent more conducive for the maintenance of the β-turn secondary structure of the acyclic peptides described above. Furthermore, Sharpless[142] and Muniz[143] have shown that the

resulting boronic esters can be readily converted to the corresponding diols by treatment with a 30% hydrogen peroxide solution.

Scheme V-13. The Narasaka protocol for an anhydrous dihydroxylation event.

Narasaka:

(1)

V-114   V-116
93%

Sharpless:

(2)

V-117   V-118

Muniz:

(3)

V-119   V-120
up to 99 % yield
up to 99 % ee
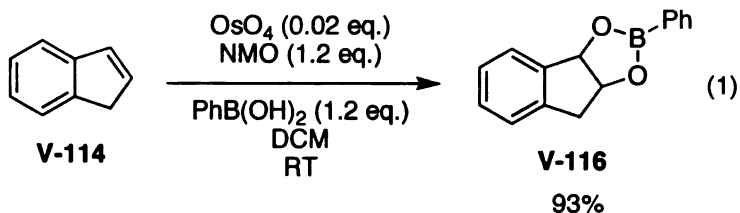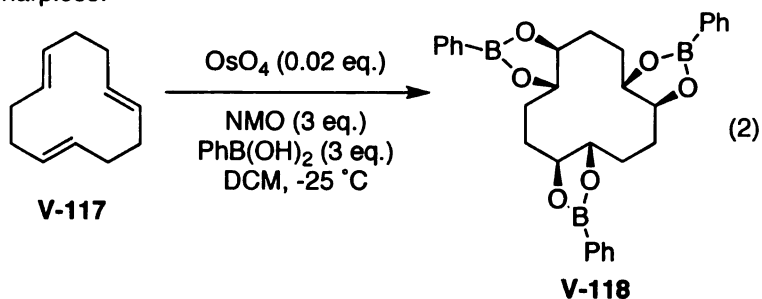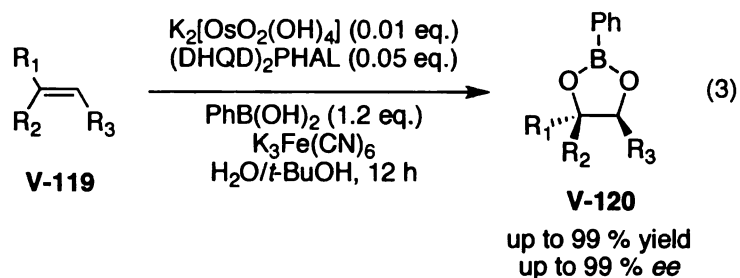
A second concern arose after considering the failed peptide scaffolds presented above. Namely, none of the ligands discussed so far contain a tertiary amine moiety. It warrants emphasis that the selectivity of the SAD methodology is governed by the binding of osmium tetroxide with a tertiary amine (i.e. the quinuclidine moiety of the *Cinchona* alkaloids).[80] We surmised that the most direct avenue for incorporating a tertiary amine motif into the peptide scaffold

would be to append an N-alkyl proline residue on the N-terminus of the β-turn scaffold (see **V-46**). N-methyl proline **V-122** was readily prepared by reductive amination of proline as reported previously (Scheme V-14).[144] What follows is an account of results obtained after considering the two strategies delineated above in tandem.

Scheme V-14. Tertiary amine scaffold **V-46** and the preparation of N-methyl proline **V-122**.
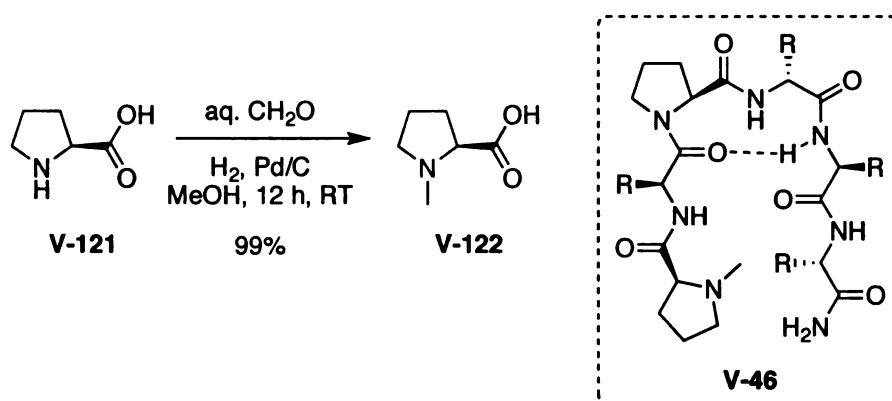
As an initial excursion into the Narasaka protocol, a series of six previously synthesized ligands (**V-80**, **V-83**, **V-92**, **V-95**, **V-98**, and **V-99**) were screened in the dihydroxylation of α-methylstyrene. In addition, three peptides designed around the general scaffold **V-46** were prepared and screened. In each case, the olefin was treated with a catalytic amount of osmium tetroxide (NMO co-oxidant) and 3 mol % of peptide in the presence of phenylboronic acid in dry DCM. The isolated phenylboronic esters were then cleaved to the desired diols using the cleavage protocol described by both Sharpless[142] and Muniz.[143] Enantiomeric excess was measured at the stage of the free diol.

Figure V-11. Peptide ligands screened under the anhydrous Narasaka protocol.
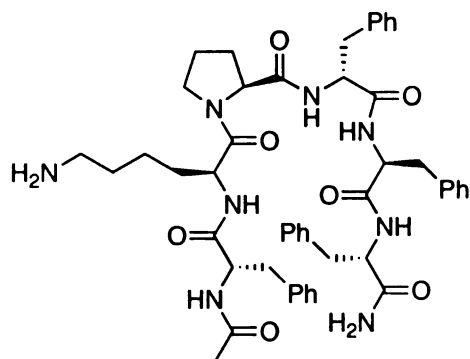
V-80
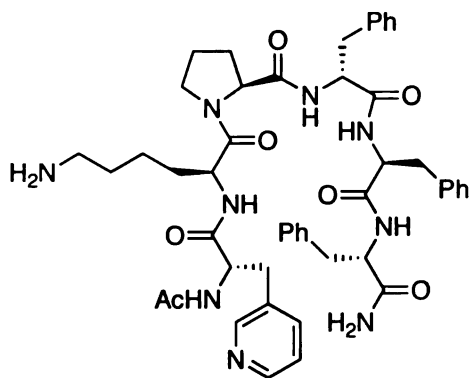
V-83
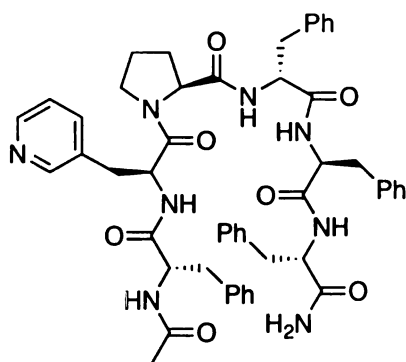
V-92
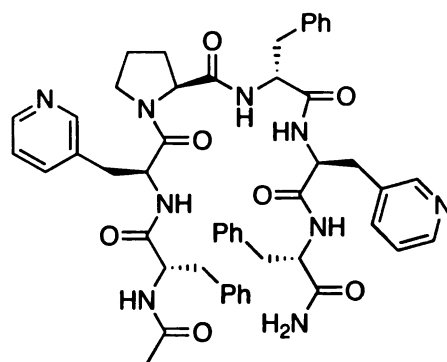
V-95
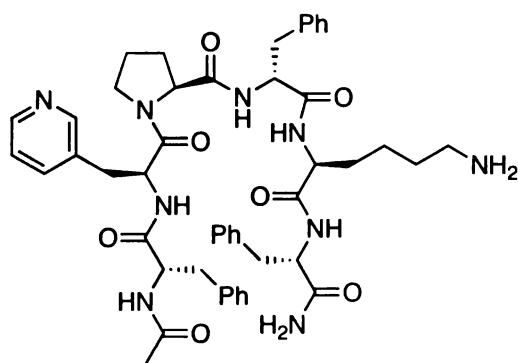
V-98
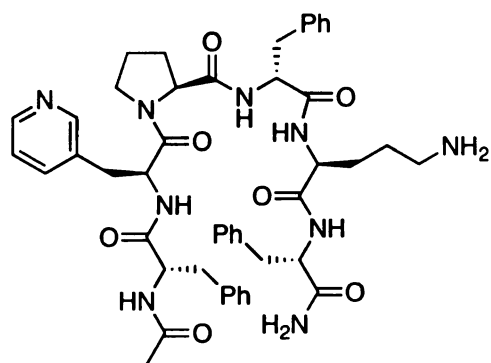
V-99

Figure V-11 (Cont'd).

V-123

V-124

V-125
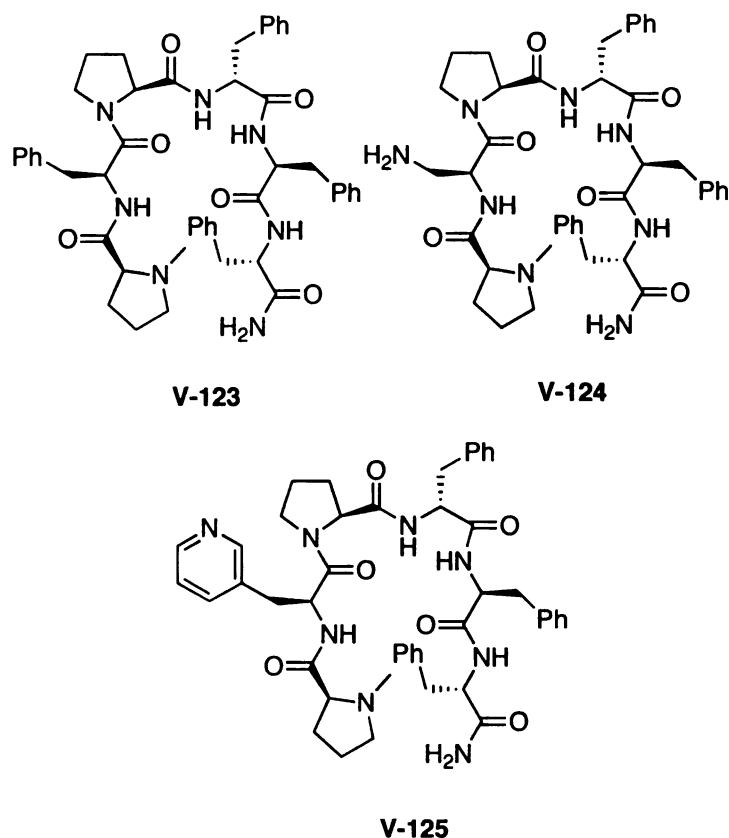
The peptides from the initial library were chosen to reflect several different potential binding motifs. Ligands **V-80** and **V-92** were putative monodentate ligands with either a primary amine functionality or a pyridyl moiety, respectively. Peptides **V-83**, **V-98**, and **V-99** provided the opportunity for bidentate binding by the strategic placement of a pyridylalanine residue and a lysine or ornithine residue within the β-turn scaffold. Similarly, **V-95** incorporates two pyridylalanine units on either side of the β-turn motif. In addition to these peptides, already in hand, peptides **V-123** through **V-125** were prepared as an initial foray into scaffold **V-46**. These peptides were easily synthesized by capping the N-

338

terminus of the peptide with an N-methylproline unit in lieu of the acetate cap.

Ligands **V-123** provides the N-terminal methylproline as the only potential ligating

site. Alternatively, **V-124** and **V-125** also incorporate neighboring Dab or

pyridylalanine residues proximal to the N-terminal methylproline in order to

potentially establish a bidentate binding regime. The results from this initial

screening of the Narasaka protocol are presented in Table V-6.

Table V-6. Screen of assorted peptides under the Narasaka protocol.

Peptide	% yield (V-126)	% yield (V-66)	% ee (V-66)
V-80	100	83	2
V-83	94	50	3
V-92	94	80	0
V-95	100	87	2
V-98	81	13	0
V-99	83	53	0
V-123	100	100	7
V-124	100	100	4
V-125	100	100	2

While all of the peptides screened in this initial event returned the desired

diol **V-66** in poor enantiomeric excess, even under anhydrous conditions, peptide

V-123 returned the desired diol with an enantiomeric excess of 7%. At this point, ligand **V-123** was employed in a number of Narasaka oxidations in an attempt to discover optimal reaction conditions for the transformation. As an initial avenue into the optimization protocol a solvent screen was undertaken. Table V-7 lists the various conditions and results from this initial investigation. In essence, solvents that had proven useful for others in peptide catalyzed asymmetric reactions were screened in our system. Also, in one solvent system (tol:DCM 3:1) the effect of colder temperatures and a base additive were investigated.

According to Table V-7, performing the reaction in a 3:1 mixture of toluene and dichloromethane appears to have no effect upon the observed *ee* value when compared to using only dichloromethane. All other solvent systems perform poorly (entries 6-12) with the notable exception of benzene (entry 10). Cooling the reaction further below 4 °C did not improve the enantiomeric excess as predicted. At -20 °C the reaction is impractically slow, but upon warming to -10 °C the reaction proceeds to completion, providing nearly racemic diol. Similarly, lowering the temperature to -50 °C in DCM returned the racemate as well. These results were somewhat disconcerting and may suggest that the initial 7% *ee* observed for **V-123** might not lie within the range of experimental error of the HPLC analysis. The addition of an inorganic base, potassium carbonate, did not improve the selectivity of the reaction (entry 3). It was thought that the relatively basic tertiary methylproline pyrrolidine nitrogen might be protonated under the reaction conditions. What might be concluded from this initial screen is that DCM, toluene/DCM (3:1), and benzene are all potentially

effective solvent systems for the peptide-based Narasaka protocol. Although

benzene returned a diol with 7% *ee*, it did not allow for complete conversion to

the desired phenylboronic ester product, even after prolonged reaction times (>

40 h). Therefore, either DCM or a 3:1 mixture of toluene and DCM seem to be

the best solvent system of those described. Finally, it seems unnecessary to run

Table V-7. Condition screen with peptide **V-123**.
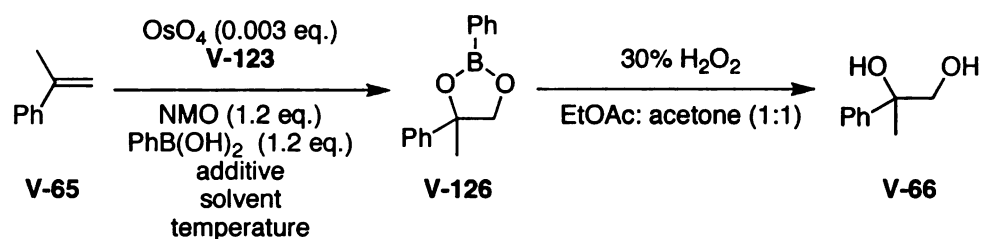
Entry	Solvent	Temp. (°C)	Additive	eq. V-123	% *ee* (V-66)
1	tol:DCM (3:1)	4	-	0.03	7
2	tol:DCM (3:1)	-20 to -10	-	0.03	1
3	tol:DCM (3:1)	4	4 eq. K_2CO_3	0.03	2
4	tol:DCM (3:1)	4	-	0.1	1
5	tol:DCM (9:1)	4	-	0.03	2
6	toluene	4	-	0.03	3
7	ACN	4	-	0.03	0
8	THF	4	-	0.03	0
9	chloroform	4	-	0.03	2
10	benzene	4	-	0.03	7
11	1,4-dioxane	20	-	0.03	0
12	DCE	4	-	0.03	0
13	DCM	-50	-	0.03	0

341

the reaction colder than 4 °C. At this point we elected to prepare a few analogs of the N-alkyl proline-terminal β-turn hexapeptide scaffold **V-46** (Scheme V-13) to probe whether or not the 7% *ee* result from the initial lead peptide **V-123** could be optimized. Peptides **V-127** through **V-131** were designed to investigate several nuances of scaffold **V-46** (Figure V-12).

First, ligands **V-127** and **V-128** were prepared to modulate the structural features of the residue proximal to the N-terminal methylproline. Specifically, **V-127** was generated in order to increase the size of the aryl subsitutent relative to the phenyl ring in **V-123**. Peptides **V-128** was meant to assess the effects of installing a bulkier substituent such as the *tert*-butyl group resident in the *tert*-leucine residue. Peptides **V-129** and **V-130** incorporated different tertiary amine binders. Ligand **V-129** was capped on its N-terminus with N-methylpipecolinic acid, prepared analogously to N-methylproline. Alternatively, **V-130** was capped with commercially available 1-piperidine propionic acid. Finally, ligand **V-131** incorporates the requisite methylproline at the N-terminus of a peptide sequence whose turn is nucleated by the presence of a gabapentin residue.[145]

Figure V-12. Analogues of **V-123**.

V-127

V-128

V-129

V-130
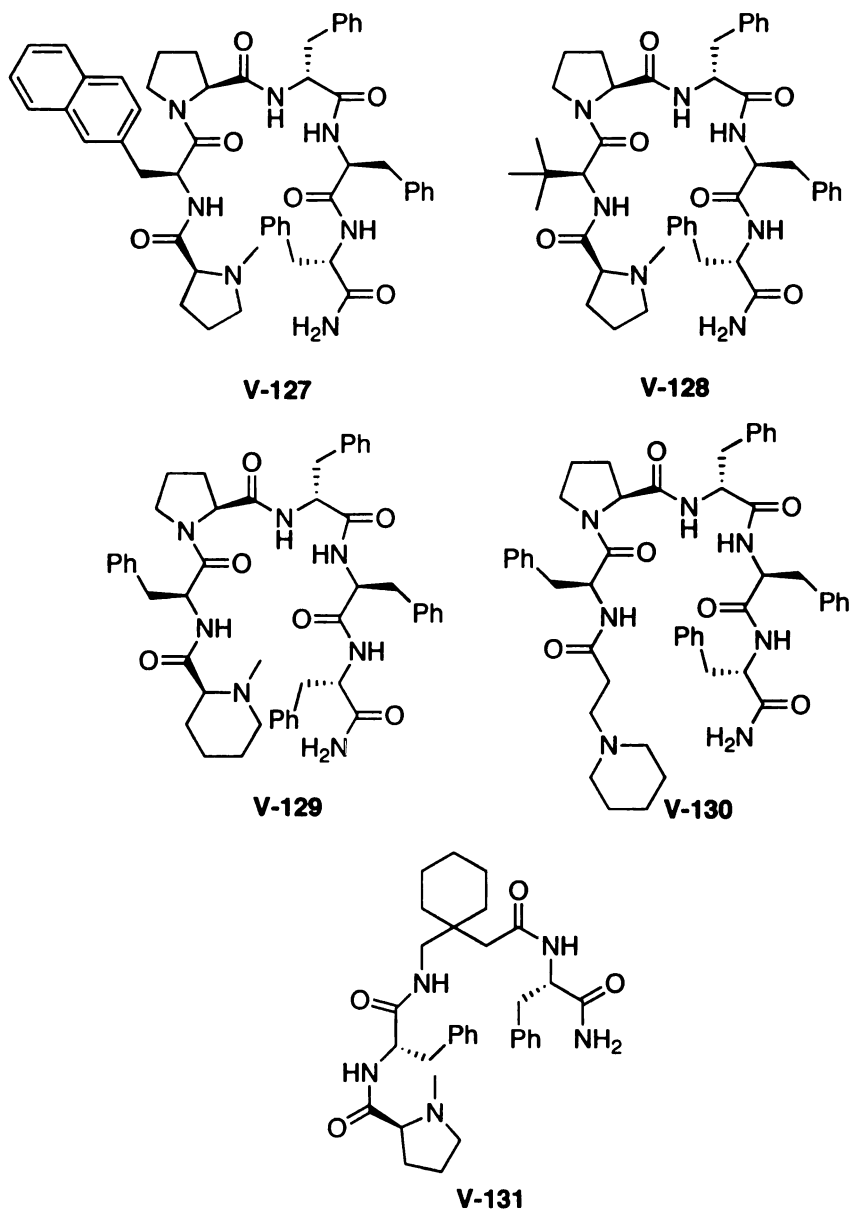
V-131

In the event, peptides **V-127** through **V-131** were screened in the

dihydroxylation of α-methylstyrene under both the anhydrous Narasaka and the

Ogino-Sharpless co-oxidant systems. Again as before, the enantiomeric

excesses were measured at the diol stage for those products prepared via the

intermediacy of the boronic ester. Peptides **V-127** through **V-131** performed

poorly under the Narasaka conditions (Table V-8). All of these analogues of **V-123** returned the diol in acceptable yields, but with enantiomeric excesses no

higher than 2%. Similarly, the ligands returned virtually racemic diol products

under the Ogino-Sharpless protocol (Table V-9).

Table V-8. Screen of peptide analogues of **V-123** under Narasaka conditions.
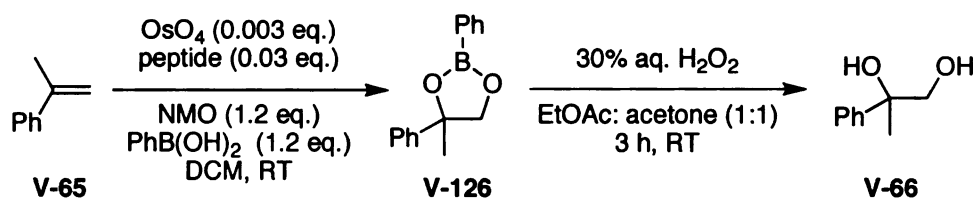
Peptide	% yield (V-126)	% yield (V-66)	% ee (V-66)
V-127	100	100	1
V-128	100	100	1
V-129	100	67	0
V-130	100	77	0
V-131	100	97	2

Table V-9. Screen of peptide analogues of **V-123** under Ogino-Sharpless conditions.

Peptide (0.03 eq.)
OsO$_4$ (0.003 eq.)

K$_3$Fe(CN)$_6$ (3 eq.)
K$_2$CO$_3$ (3 eq.)
t-BuOH/H$_2$O (1:1)

V-65 → V-66
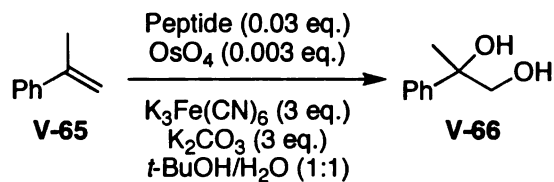
Peptide	% yield	% ee
V-127	100	0
V-128	100	2
V-129	100	2
V-130	100	0
V-131	87	0

In addition to the β-turn analogues of **V-123** (i.e. **V-127** through **V-131**), two potentially bidentate ligands, containing two terminal N-methyl proline residues were designed based on appending amino acids off of both amino residues contained within a bis-Fmoc protected lysine (**V-132**). After harnessing **V-132** onto the Rink amide MBHA resin via its carboxylate, subsequent treatment with piperidine in DMF liberated both amines which simultaneously suffer amidation in the following coupling steps. In this manner, bis-pyrrolidine ligands **V-133** and **V-134** were readily prepared (Figure V-13). Finally, seven linear tripeptides, each capped with a N-terminal methyl proline were generated (**V-135** through **V-141**).

Figure V-13. Bis N-methylproline and linear N-methylproline ligands.

346
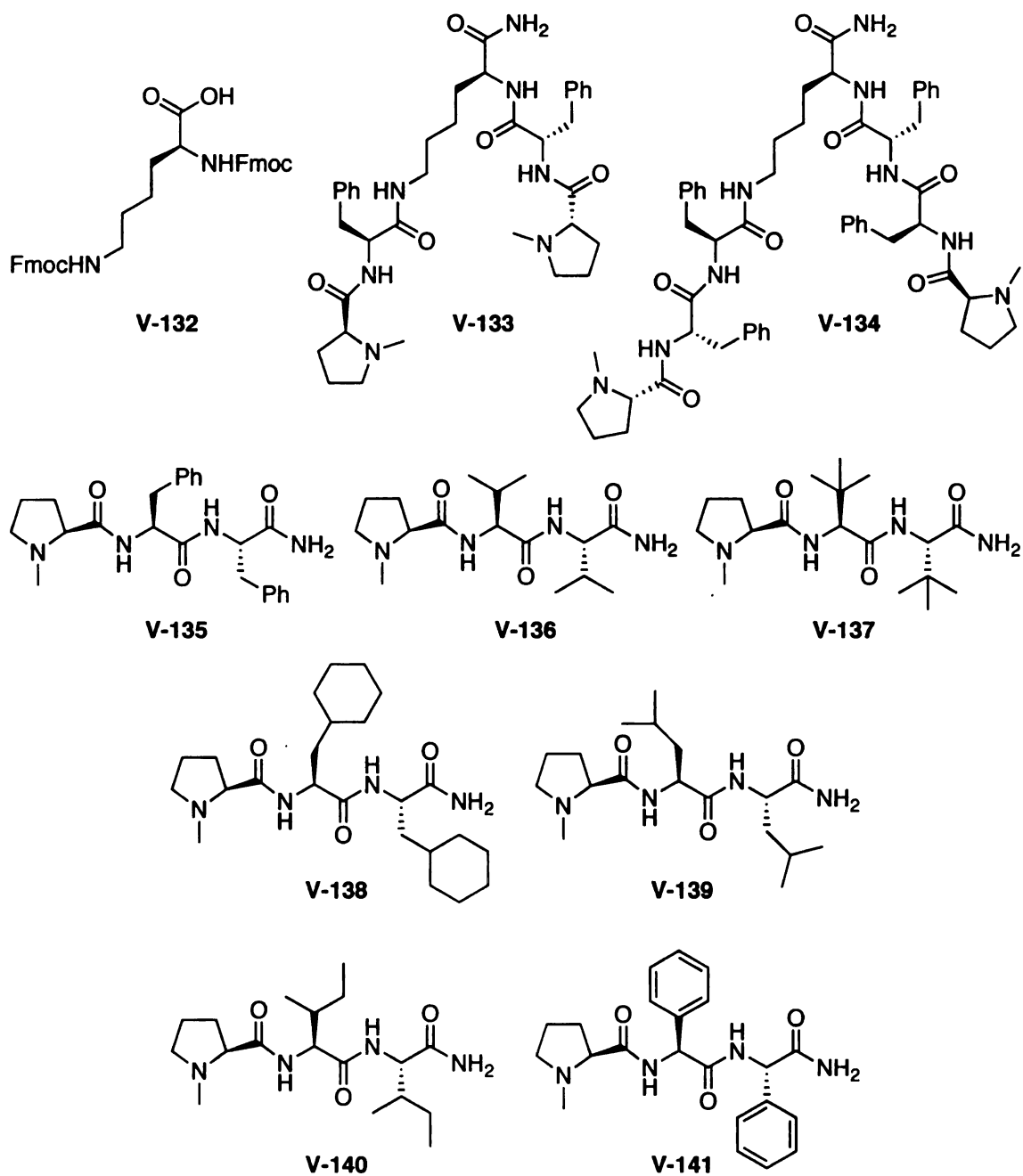
Bis-pyrrolidine ligands **V-133** and **V-134**, along with the linear tripeptides

V-135 through **V-141** were screened in the dihydroxylation of α-methylstyrene

under both the Narasaka (Table V-10) and the Ogino-Sharpless conditions

(Table V-11).

Table V-10. Screen of ligands **V-133** through **V-141** under the Narasaka protocol.
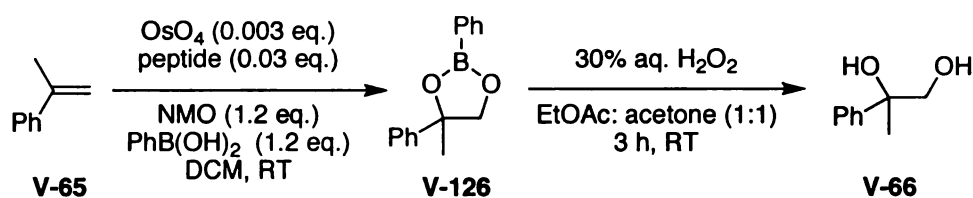
Peptide	% yield (V-126)	% yield (V-66)	% ee (V-66)
V-133	100	83	0
V-134	100	83	0
V-135	100	70	4
V-136	100	87	2
V-137	100	100	0
V-138	100	90	2
V-139	100	100	4
V-140	100	83	0
V-141	100	93	3

Table V-11. Screen of ligands **V-133** through **V-141** under the Ogino-Sharpless conditions.

$$\text{Ph}\diagup\diagdown \quad \xrightarrow[\substack{K_3Fe(CN)_6 \text{ (3 eq.)} \\ K_2CO_3 \text{ (3 eq.)} \\ t\text{-BuOH/H}_2O \text{ (1:1)}}]{\substack{\text{Peptide (0.03 eq.)} \\ OsO_4 \text{ (0.003 eq.)}}} \quad \text{Ph}\diagup\diagdown^{OH}_{OH}$$

V-65 → **V-66**
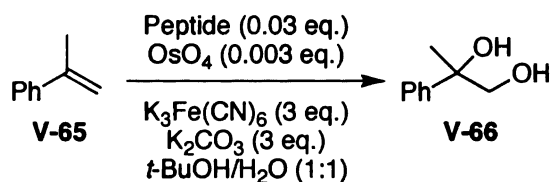
Peptide	% yield	% ee
V-133	83	0
V-134	57	1
V-135	37	2
V-136	90	1
V-137	100	1
V-138	43	0
V-139	43	2
V-140	90	3
V-141	67	4

The bis-pyrrolidine ligands **V-133** and **V-134**, as well as the linear tripeptides **V-135** through **V-141** returned unsatisfactory results overall. None returned diol **V-66** with higher than 4% *ee* under both the anhydrous Narasaka conditions or the aqueous Ogino-Sharpless protocol. In sum, fourteen analogues were prepared in order to improve upon the initial 7% *ee* observed under the Narasaka protocol with peptide **V-123** (*vide supra*, Figure V-11 and Table V-6). Given the inability to improve upon this initially observed selectivity for peptide **V-**

123 by tuning either reaction conditions or modulating the gross structure of the ligand, it seems unlikely that **V-123** should be considered a legitimate hit scaffold for the dihydroxylation of α-methylstyrene. These final experiments with peptides **V-133** through **V-141** were contemporaries of the initial discoveries that lead to the development of a novel asymmetric halolactonization methodology (See Chapters 2 and 3). Given this fact, coupled with the poor results described in this chapter that were the culmination of roughly one and one half years of work, this project was abandoned in order to facilitate development of the lactonization methodology.

5.3: Conclusions and Future Directions

Over sixty peptides were prepared and screened for asymmetric induction in the dihydroxylation of α-methylstyrene. The ligands were screened under three separate co-oxidant systems in both aqueous and non-aqueous media. The results overall were disappointing, never returning the target diol with larger than 7% *ee*. Although the objectives of this research project were never realized, the data collected during my efforts might be useful for future attempts at applying peptidic ligands to osmium tetroxide mediated processes. For instance, one might argue that, the adherence to a pre-established scaffold (*i.e.* the β-turn motif) might be partially responsible for the failure of the approach. If one truly desires to develop a combinatorial approach to the problem, it might have been more appropriate to generate a completely randomized library of hexapeptides and screen those against a battery of olefin substrates rather than just one

example. In retrospect two years after the termination of these efforts, this approach might have been better served by the generation of a much larger (500-1000 member), truly random peptide library over the course of a few months of effort. A subsequent screen of this much larger library with several test substrates under the three co-oxidant systems might then result in the discovery of an initial hit scaffold. A more iterative, logic-driven approach to the optimization of that initially discovered scaffold would then be appropriate. After a year of rumination, it seems as though the structural iterations of the peptide library generated in this study explore a relatively limited area of structural space. One could rightly argue that the project was hamstrung by an over-adherence to a pre-ordained scaffold.

With regards to the design of potential residues to be incorporated within the peptide framework that preferentially bind osmium tetroxide, one area that was under-explored during the course of my efforts was the development of those structures that contain tetra-substituted olefins (*vide supra*, Figure V-3). These particular scaffolds offer the distinct advantage of securing the metal catalyst to the chiral peptide backbone *covalently* via the formation of an osmate ester. This approach would remove from consideration any trepidation about how strongly or poorly a particular peptide scaffold binds to the catalyst, as well as assuring the existence of a metal-ligand complex regardless of solvent system. Several β-turn scaffolds were shown in Figure V-3 that incorporate a tetra-substituted olefin. Any resurgence in effort towards the goals outlined in this chapter ought to focus largely on the exploration of these scaffolds as well.

In that vein, Scheme V-15 describes another potential scaffold that incorporates the tetra-substituted olefin motif that was conceptualized after the efforts described herein were abandoned. This scaffold couples a pseudo C2 symmetric tetra-substituted olefin with a strategically placed tertiary amine residue (See **V-143**). This strategy relies upon the facile SPPS of non-β-turn scaffolds that tether the tertiary amino moiety to the tetra-substituted olefin by way of commercially available amino acids that contain an orthogonally protected amine side chain. Scaffold **V-143** requires an Mtt protected Dpr residue **V-142** (Mtt = methytrityl). The analogous Mtt protected lysine, ornithine, and diaminobutane systems are also commercially available.

These ligands are proposed based upon the assumption that once the ligand is osmylated, the pendant amine will serve as a resting-state "gating" ligand for osmium, creating a chiral osma-heterocycle (see **V-144**), until such time that the osmium is oxidized to the catalytically active species (**V-145**). Alternatively, the tertiary amino ligand may remain bound to osmium during the course of the oxidation generating an oxidized and catalytically active gated complex **V-147**. (Coincidentally, one also cannot *a priori* rule out an equilibrating mixture of **V-145** and **V-148**.) Furthermore, it is believed that the initial osmylation event onto the tetra-substituted olefin of precatalyst **V-143** will be face-selective for the diastereomer shown below (**V-144**) based upon an initial osmylation *syn* to the pendant amido carbonyl that is directed by the pre-coordination of OsO_4 with the pyrrolidine nitrogen.

Scheme V-15. Proposed gating ligand **V-143**.

V-142
*orthogonally
protected
Dpr amino acid*

V-143

V-144
Resting (Gated) State

V-145
Active (Open Gate) State

V-146
Reduced Open Gate State

V-147
Active (Gated) State
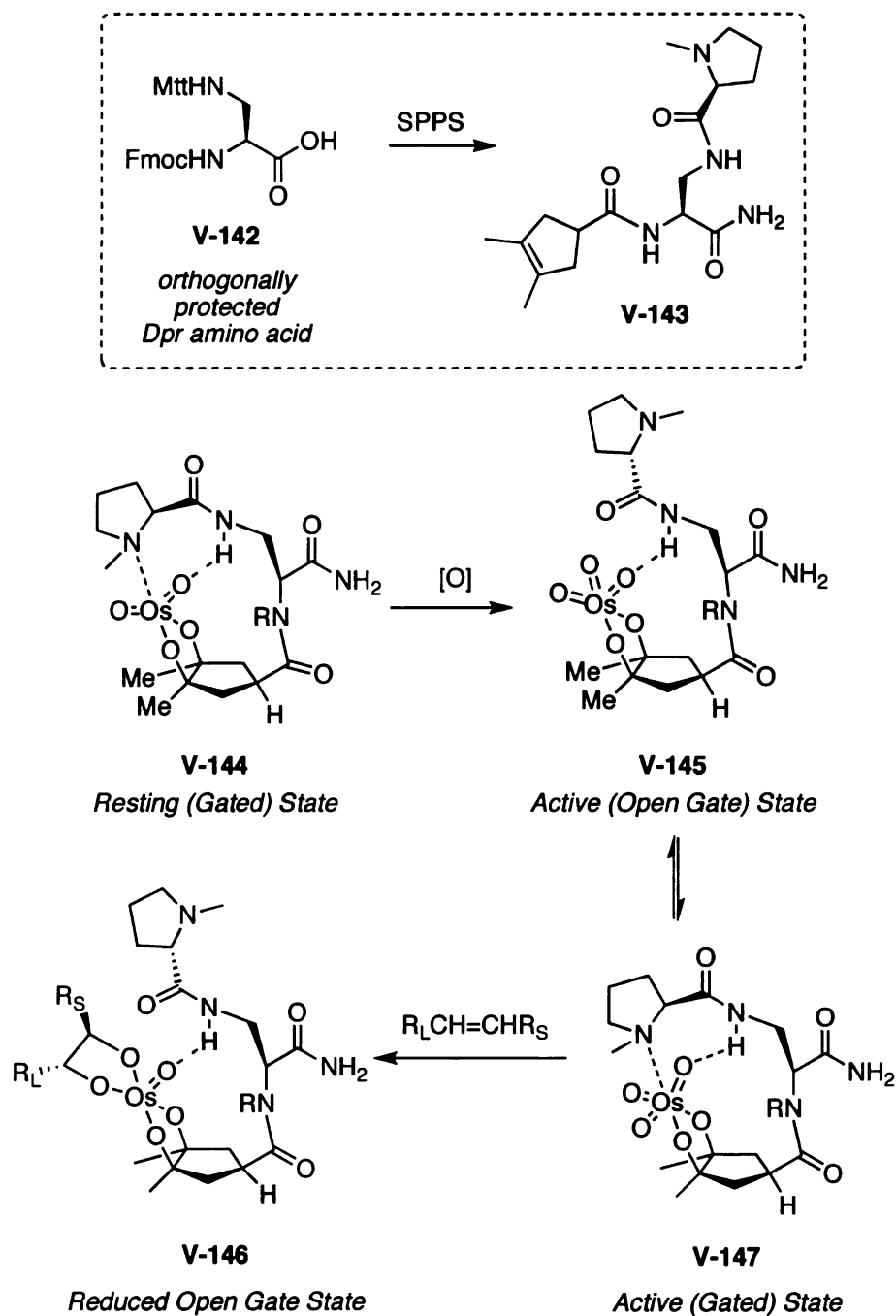
The coordination of the tertiary amine to osmium should be facile and may

also be facilitated by hydrogen-bonding interactions between the osmium oxo

ligands and amide hydrogens along the peptide scaffold. Ideally, if the gated active species **V-147** is formed after the oxidation of resting state **V-144**, then one would expect the chiral environment of **V-147** to be maintained until the substrate olefin is osmylated yielding the reduced open state **V-146**. If, however, the active catalyst exists as **V-145**, a selective osmylation may be less likely, but still possible if the secondary H-oxo hydrogen bonds can maintain a chiral environment even after the tertiary amine has dissociated from the metal. Also, if the active species exists as an equilibrating mixture of **V-145** and **V-147**, an enantioselective osmylation might still be possible if the gated complex **V-147** is more active than the dissociated (open gate) species **V-145**. Scaffold **V-143** should be investigated as either the secondary amide as drawn or the tertiary aryl or alkyl substituted amide (*i.e.* R in **V-144** = methyl or phenyl). The tertiary amides could lead to a higher *syn* adopted conformation of the structure, in which the pyrrolidine ring is situated above the osmate.

These small ligands could be prepared via conventional SPPS techniques by first installing the tetra-substituted olefin upon removal of the Fmoc group (20% piperidine in DMF) in the presence of the base-stable Mtt group. Subsequent removal of the Mtt group on-bead (1% TFA in DCM), would then unveil the side-chain amino group, which would thereafter be coupled with the tertiary amine ligand. The reliance of this putative scaffold on solid phase synthesis would lend itself to extensive screening efforts. For instance, a battery of orthogonally protect amino acids with residual side-chain amines could be assayed simultaneously. Furthermore, the nature of the tertiary amine binder

could be investigated. Finally, the linker between the olefin and the tertiary

amine could be extended by the installation of an intervening amino acid residue.

Should this project be resurrected in the future, I hope this scaffold will receive

some attention.

5.4: Acknowledgement

The efforts described in this chapter were greatly facilitated by the efforts

of Dr. Chrysoula Vasileiou, Mr. Kin-Sing Lee, and Mr. Matt Fhaner. Dr. Vasileiou

or Mr. Lee collected the MALDI-TOF data for the peptides that were prepared in

this study. Mr. Fhaner prepared several of the linear peptides described in

Figure V-13 under my guidance. Their efforts in this regard are highly

appreciated.

5.5: Experimental Details

General Information:

The solid phase peptide synthesis of the peptides described herein was

conducted following well-established protocols that can be found in *Fmoc Solid

Phase Peptide Synthesis: A Practical Approach* by W.C. Chan and P.D. White.[146]

Additional protocols can be found in the appendix of the Novabiochem product

catalogue. Peptides were prepared in disposable 5 or 10 mL fritted syringes

purchased from CSPS Pharmaceuticals, Inc. All Fmoc protected amino acids

were purchased from Novabiochem, CSPS Pharmaceuticals, Inc. or Aldrich and

used without purification. Wang and Rink Amide MBHA resins were purchased

from Novabiochem. All other reagents and solvents were purchased from commercial sources and used without purification. C-terminal carboxylic acid and methyl ester peptides were synthesized using a commercially available Wang resin that was preloaded with Fmoc-glycine (Fmoc-Gly-Wang resin). C-terminal amide peptides and cyclic peptides were synthesized using the Rink Amide MBHA resin which was loaded with the first amino acid of the desired sequence. Peptide ligands were characterized by MALDI-TOF mass spectrometry.

Crude peptides were then screened as ligands for the enantioselective dihydroxylation of α-methylstyrene. HPLC separation of the two enantiomeric diols (Chiralpak AS-H column, 5% IPA/hexane, 1 mL/min, 245 nm UV detection) provided the extent of selectivity imparted by the ligand. Given below is a general protocol for each step in the solid phase synthesis along with a general protocol for the dihydroxylation reaction.

General Procedures for Solid Phase Peptide Synthesis
Bead Loading

Rink Amide MBHA resin (87 mg, 0.06 mmol, 0.69 mmol/g loading) was pre-swelled in a 5 mL disposable syringe equipped with a frit by rotating with DCM (3 mL) for 1h. The resin was then washed with DMF (5 X 4 mL). The Fmoc protecting group on the bead was removed by treatment with 5 bed volumes (*ca.* 4 mL) of a 20% piperidine solution in DMF for 20 minutes.

Meanwhile, Fmoc-Phe-OH (116 mg, 0.3 mmol, 5 eq.) was dissolved in

DMF (3 mL) along with HOBt (41 mg, 0.3 mmol, 5 eq.). Diisopropyl carbodiimide

(DIC) (50 μL, 0.3 mmol, 5 eq.) was then added and the resulting mixture was

stirred at room temperature for 30 min.

After 20 minutes, the resin was washed with DMF (5 X 4 mL). To the

thoroughly washed resin bed, was added the coupling solution (Fmoc-Phe-OH,

HOBt, and DIC), and the resulting mixture was rotated for 12 hours. The loaded

resin was then washed with DMF (5 X 4 mL) and used in subsequent Fmoc solid

phase peptide synthesis as described below.

Fmoc removal

The Fmoc group of terminal amino acid of the growing peptide chain was

deprotected by treating the resin beads (0.69 mmol/g loading) with a 20%

solution of piperidine in DMF (*ca.* 4 mL) with rotation for three minutes. The

deprotection cocktail was then discharged from the syringe and the resin beads

were treated with a fresh portion of 20% piperidine in DMF for three minutes.

This protocol is repeated until the resin beads have been treated with four

aliquots of 20% piperidine in DMF. The final portion is then discharged from the

syringe and the deprotected beads are washed with DMF (5 X 4 mL). The

washed, deprotected resin beads were then immediately coupled with the next

amino acid in the sequence.

HOBt-Mediated Coupling

The next amino acid in a desired sequence was activated as the HOBt ester by dissolving the desired amino acid (0.3 mmol, 5 equivalents relative to the 0.69 mmol/g resin loading) along with HOBt (41 mg, 0.3 mmol, 5 eq.) in DMF/DCM (1:1) (3 mL). To the resulting solution was added DIC (50 μL, 0.3 mmol, 5 eq.) and the resulting solution was stirred at room temperature for twenty minutes (usually while the terminal amino acid of the resin bound sequence is deprotected).

The resulting solution of HOBt ester was added to the N-terminal deprotected, resin-bound, peptide sequence and the mixture was rotated for one hour. The resin beads were then thoroughly washed with DMF (5 X 4 mL). The resulting N-terminal, Fmoc-protected, resin-bound peptide sequence was then resubjected to the Fmoc removal protocol and subsequent HOBt couplings until the desired sequence had been assembled.

N-Terminal Acetate Capping

For acyclic peptides, the N-terminal amino moiety was capped as the acetamide by the following protocol:

After the final desired sequence had been assembled, the N-terminal Fmoc group was removed by the protocol described above. After washing with DMF (5 X 4 mL) the N-terminal deprotected, resin-bound peptide sequence was treated with a freshly prepared 5% acetic anhydride solution in DMF (4 mL) with rotation for thirty minutes. The capping cocktail was then ejected from the

syringe and the acetamide-capped resin-bound peptide was washed thoroughly with DMF (5 X 4 mL).

On-Bead Cyclization Protocol (Peptides V-106 to V-113)

After the linear sequences were assembled on-bead, the N-terminal Fmoc protecting group was removed as described above. Following the requisite DMF washes (5 X 4 mL) and subsequent washes with THF (5 X 4 mL) the C-terminal allyl protecting group was removed by treating the peptide (0.69 mmol/g loading) with a cocktail comprised of palladium (0) tetrakistriphenylphosphine (7 mg, 0.006 mmol, 0.1 eq. relative to bead loading) in 3 mL of a DMSO/THF/0.5N HCl/Morpholine (2:2:1:0.1) solvent system under a positive flow of nitrogen for two hours. The resulting N- and C-terminal deprotected, resin bound peptide was washed with THF (5 X 4 mL), DCM (5 X 4 mL), and DMF (5 X 4 mL).

After washing, the terminally deprotected, resin-bound peptide was treated with a DMF solution (3 mL) of PyBOP (156 mg, 0.3 mmol, 5 eq. relative to bead loading), HOBt (50 mg, 0.3 mmol, 5 eq.), and diisopropyl ethyl amine (52 μL, 0.3 mmol, 5 eq.). The resulting mixture was rotated for eight hours to yield the resin-bound, cyclic peptides.

TFA Cleavage/Global Side-chain Deprotection of Peptides

Peptides were cleaved from the resin beads by employing the following protocol:

The fully assembled, resin-bound peptides were prepared for cleavage by washing the beads with DMF (5 X 4 mL), DCM (5 X 4 mL), and methanol (5 X 4

mL). The syringe plunger was removed from the barrel and the resin beads were dried overnight in the vacuum oven at 25 °C. The following day, the resin was treated with a cleavage cocktail comprised of a mixture of TFA/H$_2$O/TIS (95:2.5:2.5) (3 mL) for 2.5 hours with minimal, intermittent agitation. The cleavage cocktail, containing the solvated, resin-free peptide was then ejected into a 5 mL pear-shaped flask and the solvent was removed under a stream of nitrogen to give a thick oil. The crude peptide was then precipitated by the addition of ice-cold diethyl ether. The solid peptide was then isolated by vacuum filtration and washed with copious amounts (*ca.* 15-20 mL) of cold ethyl ether. The solid peptide was then dried *in vacuo*. The identity of the desired sequence was verified by MALDI-TOF mass spectroscopy.

MeOH/TEA/DMF Cleavage of Peptides (methyl esters V-74 through V-76)

The fully assembled, side-chain protected, resin-bound peptides were readied for cleavage by washing the beads with DMF (5 X 4 mL), DCM (5 X 4 mL), and methanol (5 X 4 mL). The syringe plunger was removed from the barrel and the resin beads were dried overnight in the vacuum oven at 25 °C. The following day, the resin was treated with a cleavage cocktail comprising methanol/TEA/DMF (9:1:1) (3 mL) with rotation for four days. The cleavage cocktail, containing the solvated, resin-free peptide was then ejected into a 5 mL pear-shaped flask and the solvent was removed under a stream of nitrogen to give a thick oil. The crude peptide was then precipitated by the addition of ice-cold ethyl ether. The solid peptide was then isolated by vacuum filtration and

washed with copious amounts (*ca.* 15-20 mL) of cold ethyl ether. The solid

peptide was then dried *in vacuo*. The identity of the desired sequence was

verified by MALDI-TOF mass spectroscopy (Figure V-14).

Figure V-14. MALDI-TOF data for peptides.
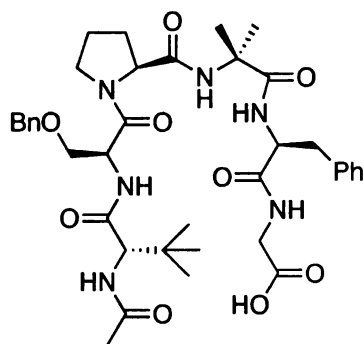
V-58

Calc.: 736.85   Found: 760.0 (M+Na)
759.84 (M+Na)
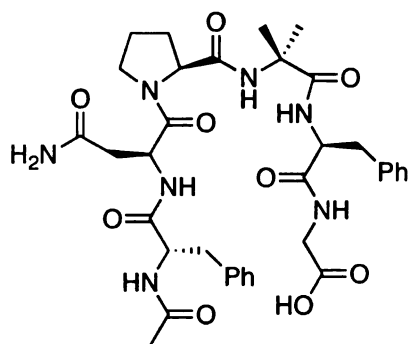
V-59

Calc.: 707.77   Found: 730.1 (M+Na)
730.67 (M+Na)
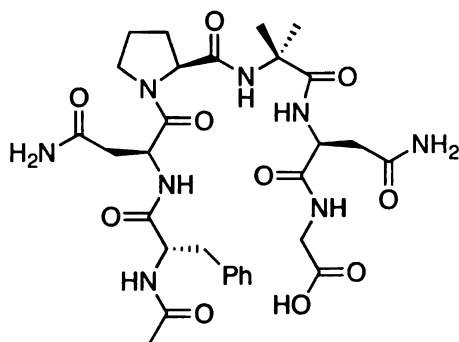
V-60

Calc.: 674.70   Found: 696.7 (M+Na)
697.69 (M+Na)
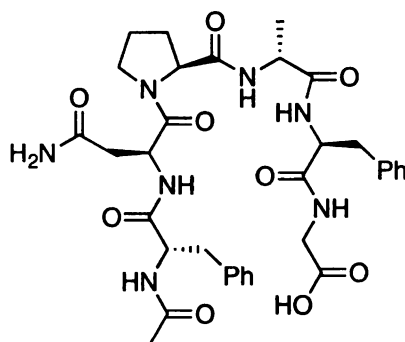
V-61

Calc.: 693.75   Found: 715.6 (M+Na)
716.74 (M+Na)
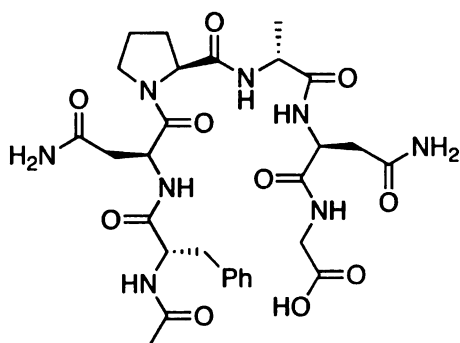
V-62

Calc.: 660.68   Found: 683.1 (M+Na)
683.67 (M+Na)
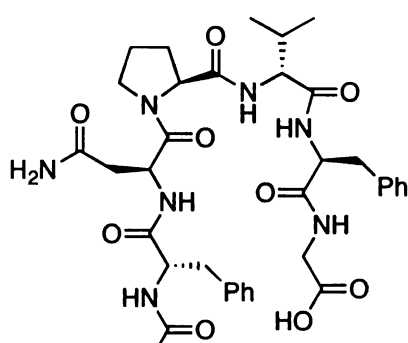
V-63

Calc.: 721.80   Found: 743.6 (M+Na)
744.79 (M+Na)

Figure V-14. (Cont'd)

V-64

Calc.: 769.80   Found: 791.6 (M+Na)
792.8 (M+Na)

V-67
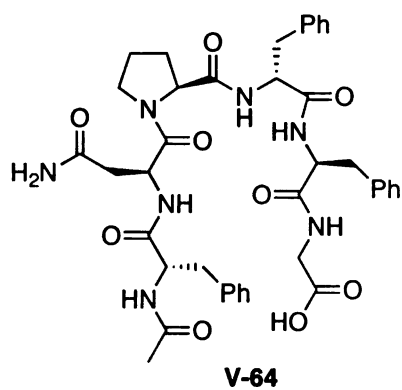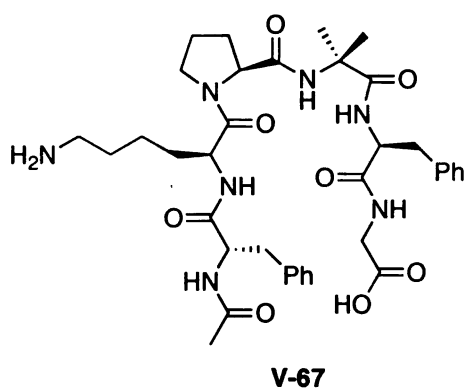
Calc.: 721.89   Found: 722.0

V-68
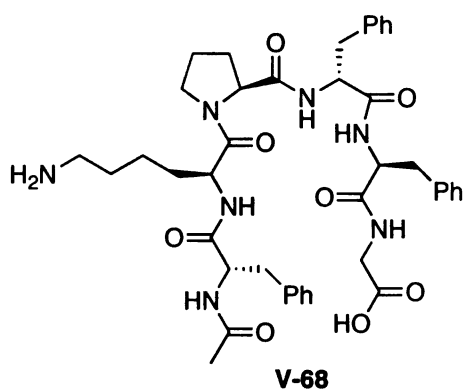
Calc.: 783.91   Found: 784.1

V-69
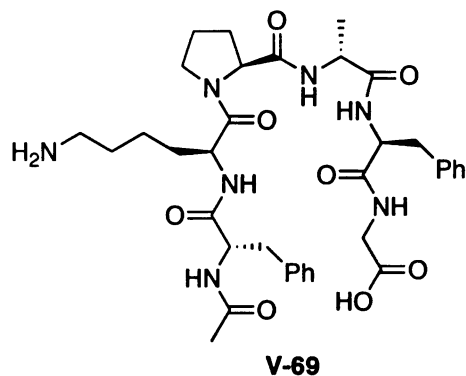
Calc.: 707.82   Found: 708.1

V-70

Calc.: 735.87   Found: 758.3 (M+Na)
758.86 (M+Na)

V-74
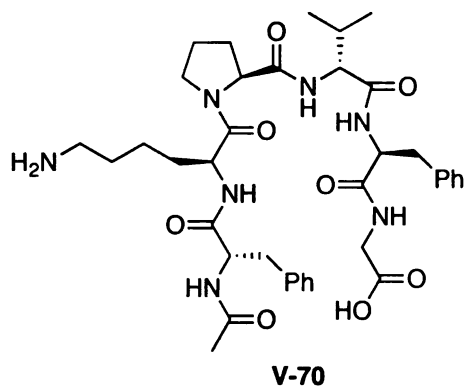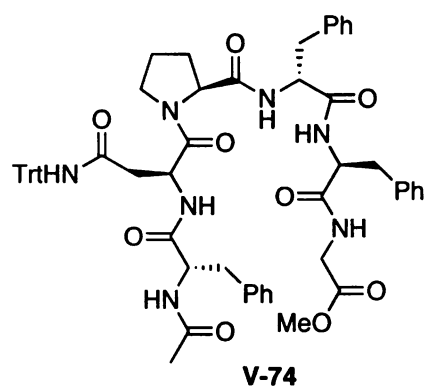
Calc.: 1026.18   Found: 1048.1 (M+Na)
1049.17 (M+Na)

Figure V-14. (Cont'd)

V-75
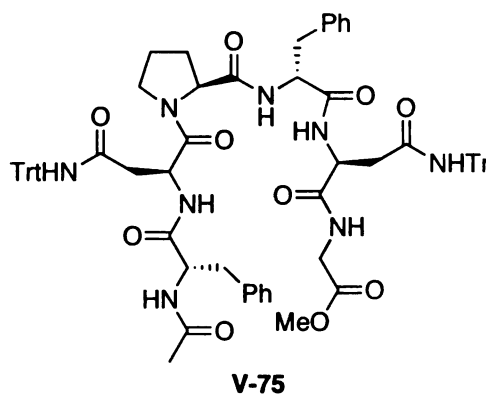
Calc.: 1235.43   Found: 1235.4

V-76
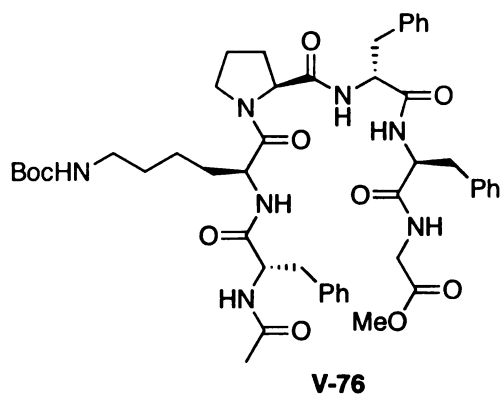
Calc.: 898.05   Found: 920.3 (M+Na)
921.04 (M+Na)

V-77
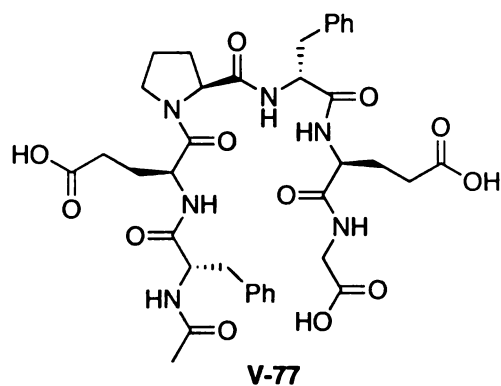
Calc.: 766.79   Found: 789.0 (M+Na)
789.8 (M+Na)

V-78
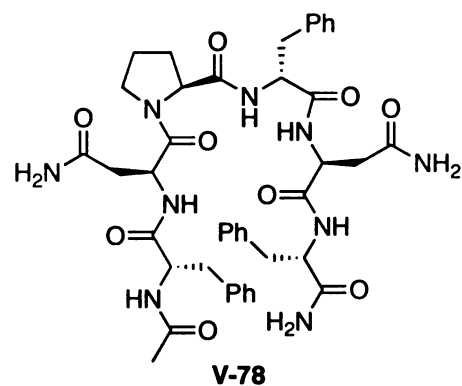
Calc.: 825.91   Found: 848.3 (M+Na)
848.90 (M+Na)

V-79
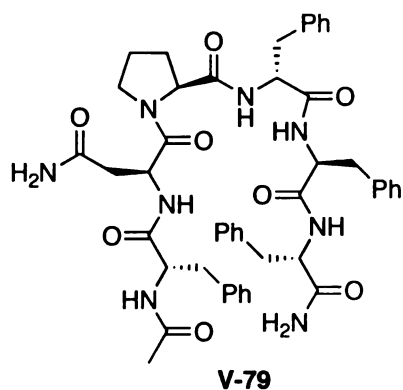
Calc.: 858.98   Found: 882.0 (M+Na)
881.97 (M+Na)

V-80
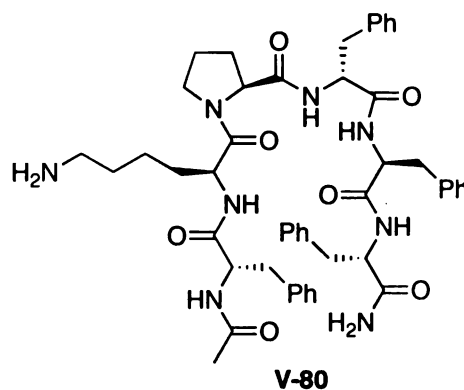
Calc.: 873.05   Found: 873.1

363

Figure V-14. (Cont'd)
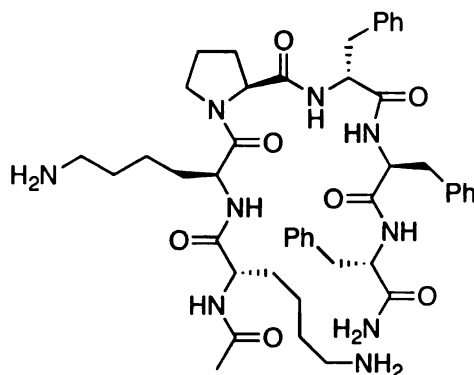
V-81

Calc.: 854.05   Found: 854.1
877.0 (M+Na)   876.2 (M+Na)
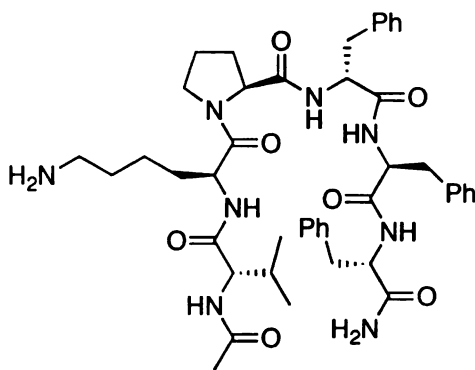
V-82

Calc.: 825.01   Found: 847,2 (M+Na)
848.00 (M+Na)   863.2 (M+K)
864.1 (M+K)
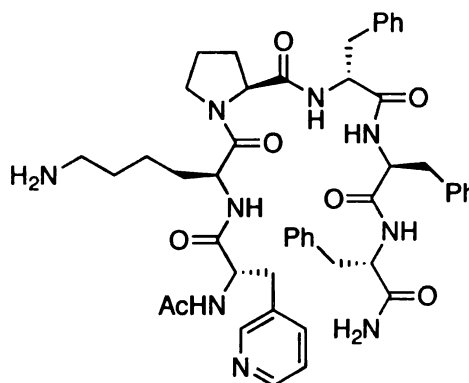
V-83

Calc.: 873.45   Found: 874.2
896.44 (M+Na)   896.2 (M+Na)
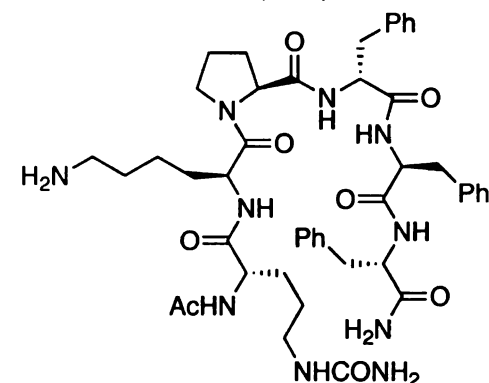
V-84

Calc.: 883.05   Found: 883.2
906.04 (M+Na)   905.4 (M+Na)
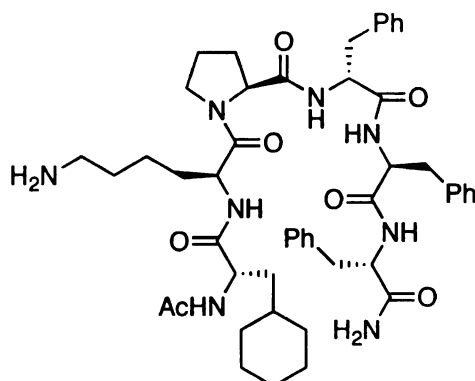
V-85

Calc.: 879.1   Found: 901.2 (M+Na)
902.09 (M+Na)   917.1 (M+K)
918.2 (M+K)
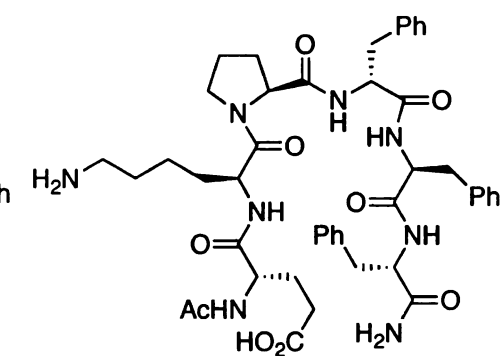
V-86

Calc.: 854.99   Found: 855.0

364

Figure V-14. (Cont'd)
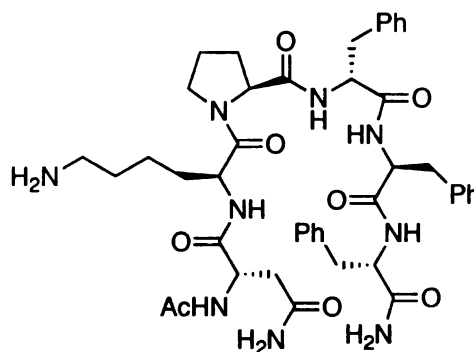
V-87

Calc.: 839.98   Found: 840.1
862.97 (M+Na)   862.1(M+Na)
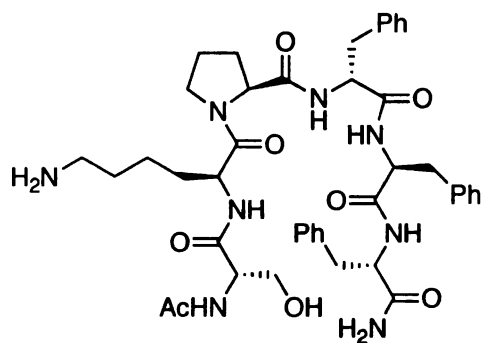
V-88

Calc.: 812.95   Found: 813.2
835.94 (M+Na)   835.31 (M+Na)
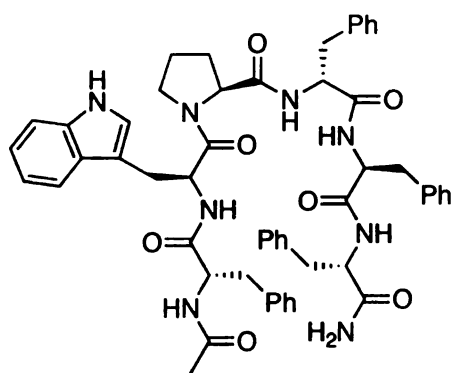
V-89

Calc.: 931.09   Found: 953.3 (M+Na)
954.0 (M+Na)
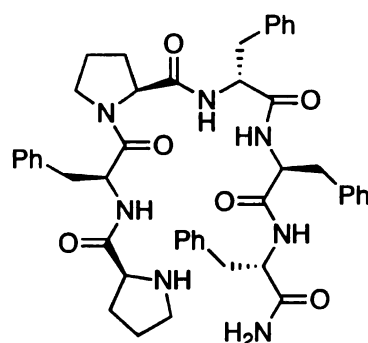
V-90

Calc.: 799.96   Found: 800.01
822.95 (M+Na)   822.0 (M+Na)
839.06 (M+K)   838.1(M+K)
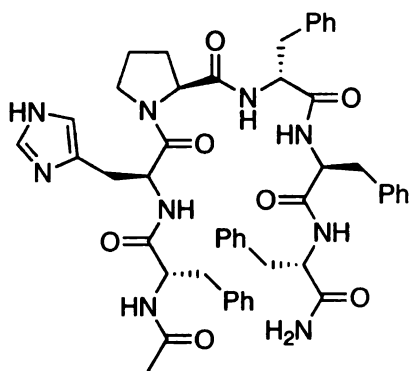
V-91

Calc.: 882.02   Found: 882.1
905.0 (M+Na)   904.2 (M+Na)
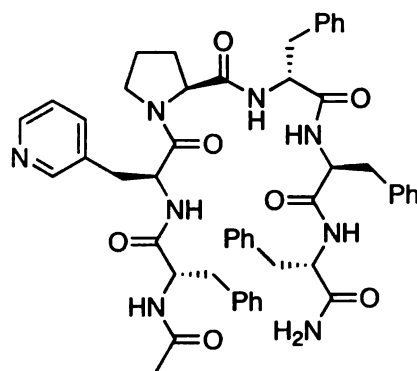
V-92

Calc.: 893.04   Found: 893.2
916.0 (M+Na)   915.2 (M+Na)
932.1 (M+K)   931.4 (M+K)

Figure V-14. (Cont'd)

V-93
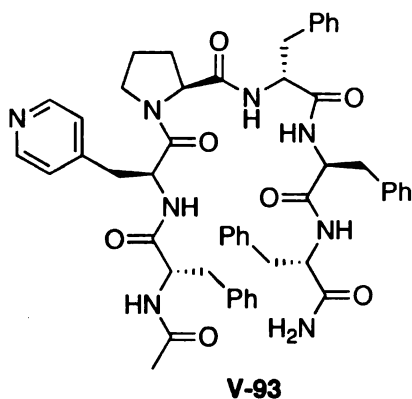
Calc.: 893.04   Found: 893.2
916.03 (M+Na)   914.9 (M+Na)
932.14 (M+K)   931.0 (M+K)

V-94
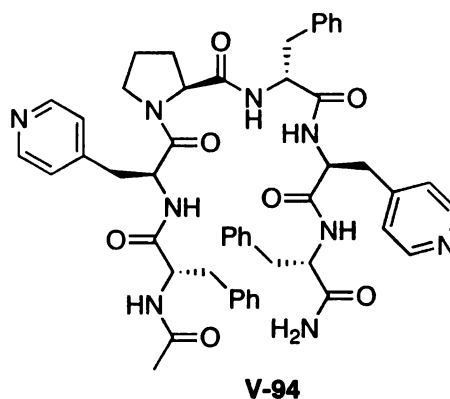
Calc.: 894.03   Found: 894.1

V-95
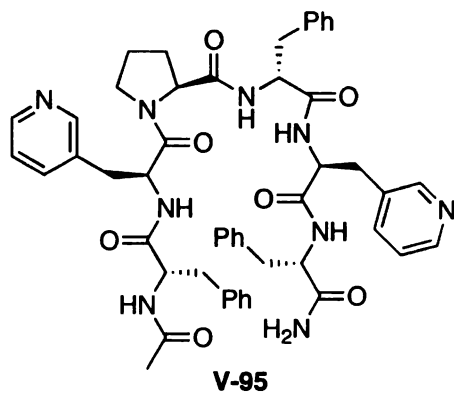
Calc.: 894.03   Found: 894.2

V-96
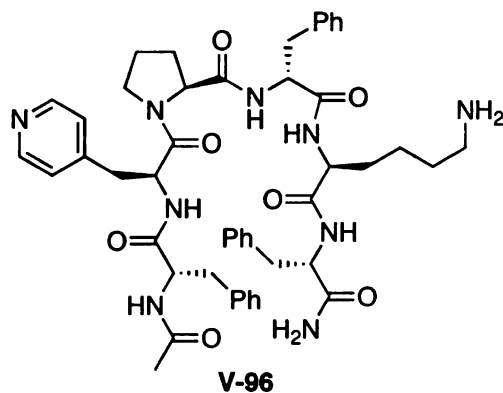
Calc.: 874.05   Found: 874.1
897.04 (M+Na)   896.1 (M+Na)
913.15 (M+K)   912.1 (M+K)

V-97
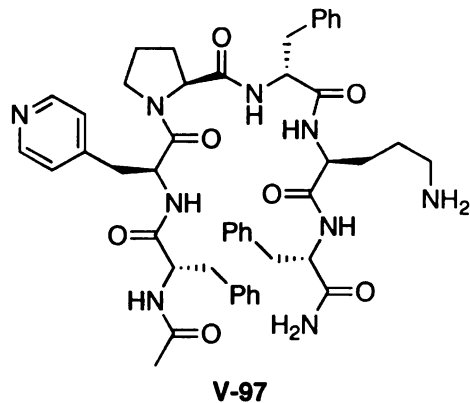
Calc.: 860.01   Found: 860.2
883.00 (M+Na)   882.2 (M+Na)

V-98
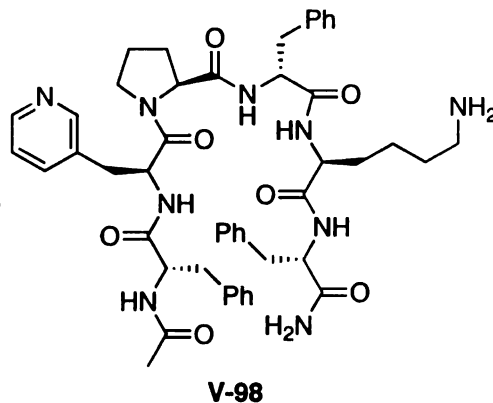
Calc.: 874.05   Found: 874.1
897.04 (M+Na)   896.2 (M+Na)

366

Figure V-14. (Cont'd)
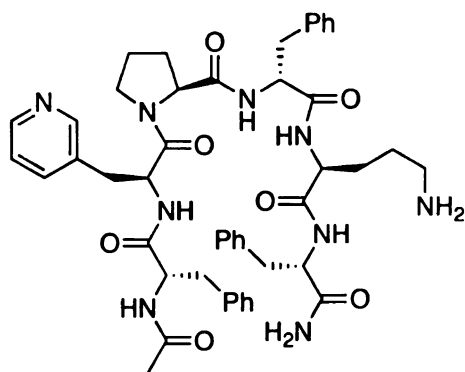
V-99

Calc.: 860.01   Found: 860.21
     883.00 (M+Na)   882.2 (M+Na)
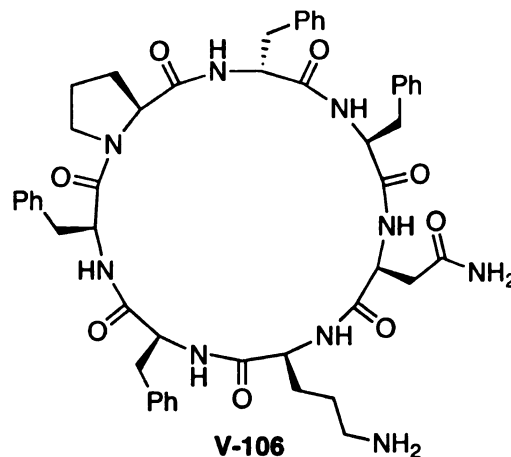
V-106

Calc.: 914.06   Found: 936.4 (M+Na)
     937.07 (M+Na)   952.3 (M+K)
     953.16 (M+K)   1850.7 (2M+Na)
     1851.11 (2M+Na)
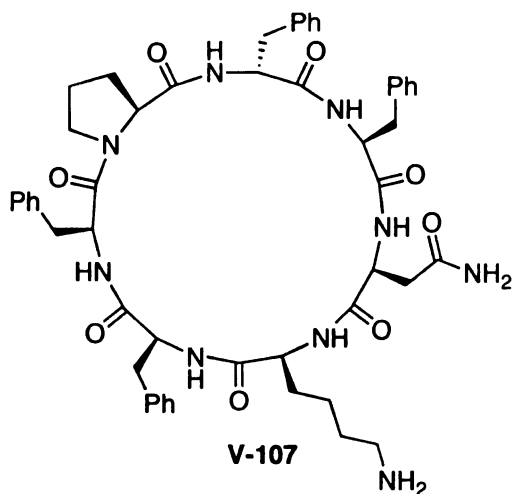
V-107

Calc.: 928.09   Found: 950.4 (M+Na)
     951.08 (M+Na)   966.4 (M+K)
     967.19 (M+K)   1878.9 (2M+Na)
     1879.17 (2M+Na)
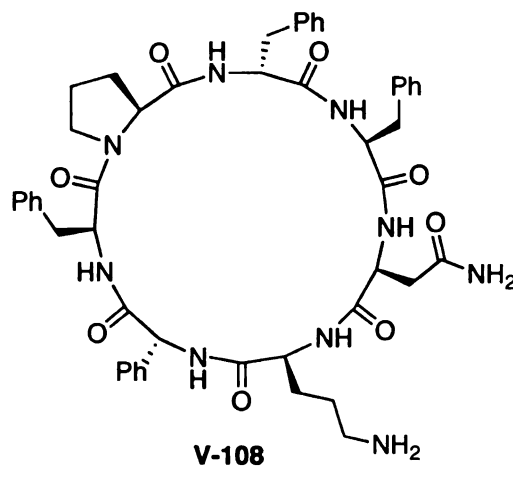
V-108

Calc.: 900.03   Found: 922.1 (M+Na)
     923.02 (M+Na)   938.1 (M+K)
     939.13 (M+K)   1822.4 (2M+Na)
     1823.05 (2M+Na)

367

Figure V-14. (Cont'd)

V-109
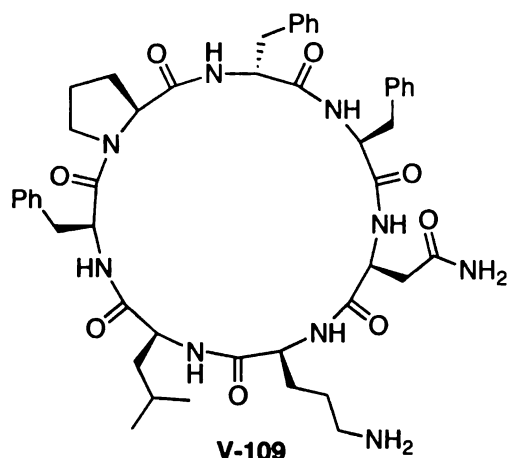
Calc.: 880.04   Found: 902.4 (M+Na)
      903.03 (M+Na)   918.3 (M+K)
      919.14 (M+K)   1798.9 (2M+K)
      1799.1 (2M+K)

V-110
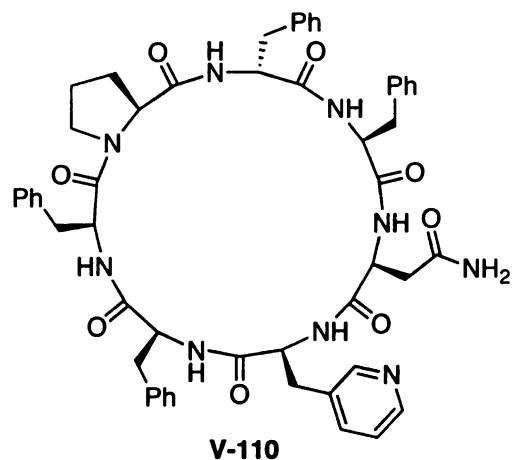
Calc.: 948.08   Found: 970.2 (M+Na)
      971.07 (M+Na)   986.3 (M+K)
      987.18 (M+K)   1918.8 (2M+Na)
      1919.15 (2M+Na)

V-111
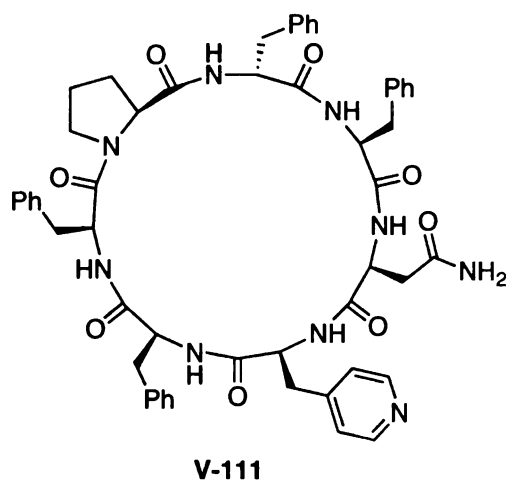
Calc.: 948.08   Found: 970.3 (M+Na)
      971.07 (M+Na)   986.3 (M+K)
      987.18 (M+K)   1918.9 (2M+Na)
      1919.15 (2M+Na)

V-112
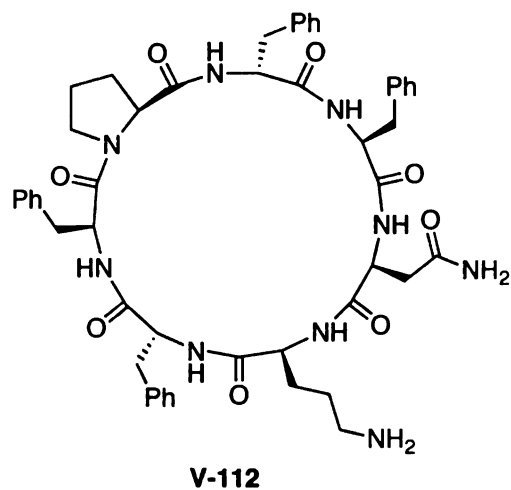
Calc.: 914.06   Found: 936.3 (M+Na)
      937.05 (M+Na)   952.3 (M+K)
      953.16 (M+K)   1850.7 (2M+Na)
      1851.11 (2M+Na)

Figure V-14. (Cont'd)

V-113
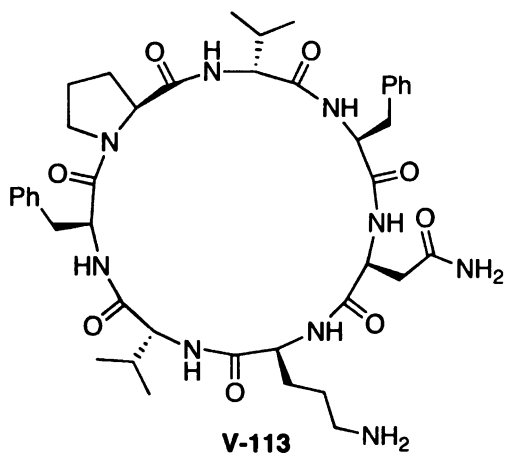
Calc.: 817.96   Found: 840.5 (M+Na)
   840.95 (M+Na)   856.5 (M+K)
   857.06 (M+K)   1658.9 (2M+Na)
   1658.91 (2M+Na)

V-123
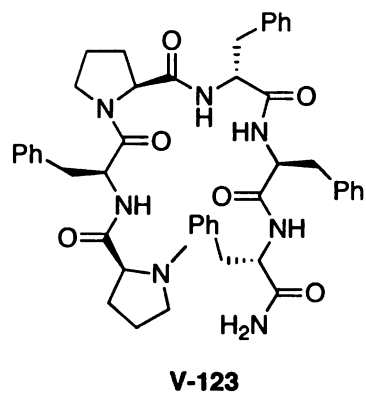
Calc.: 813.98   Found: 814.2
   836.97 (M+Na)   836.5 (M+Na)
   853.1 (M+K)   852.4 (M+K)
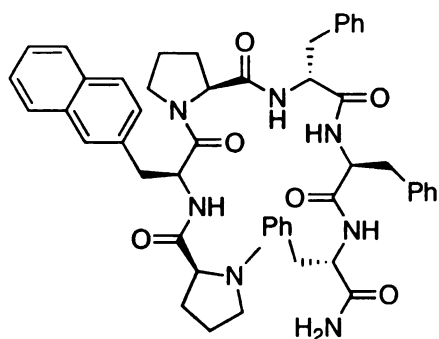
V-124
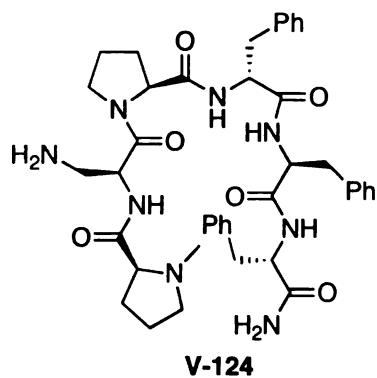
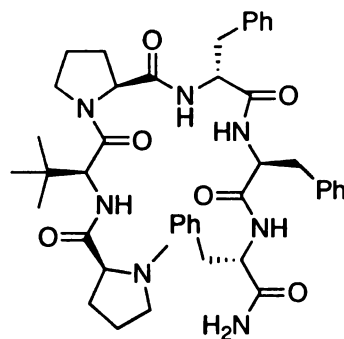Calc.: 752.90   Found: 753.5
   775.89 (M+Na)   775.4 (M+Na)

V-125
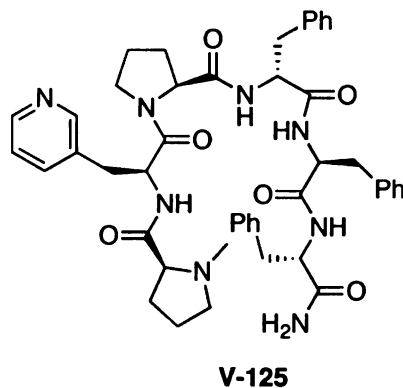
Calc.: 814.97   Found: 815.0
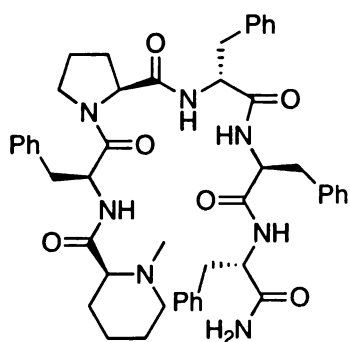   837.96 (M+Na)   837.7 (M+Na)

Figure V-14. (Cont'd)

V-127

Calc.: 864.04   Found: 864.0
    887.03 (M+Na)   886.9 (M+Na)
    903.14 (M+K)   903.8 (M+K)
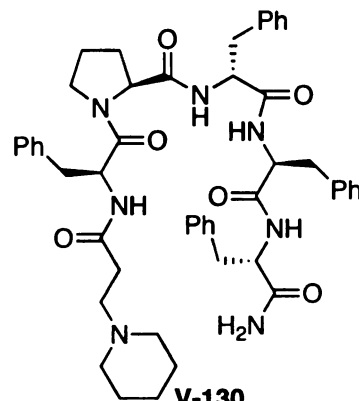
V-128

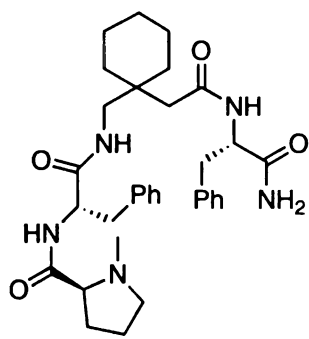Calc.: 779.97   Found: 779.9
    819.07 (M+K)   818.8 (M+K)

V-129

Calc.: 828.01   Found: 828.0
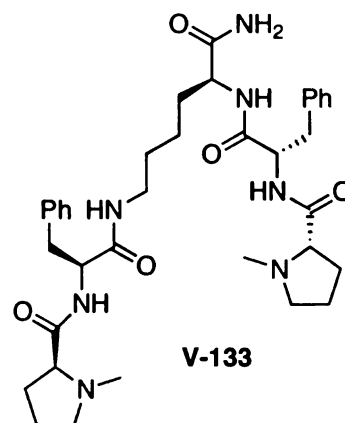   851.00 (M+Na)   850.2 (M+Na)
    867.11 (M+K)   866.1 (M+K)

V-130

Calc.: 842.04   Found: 841.9

V-131

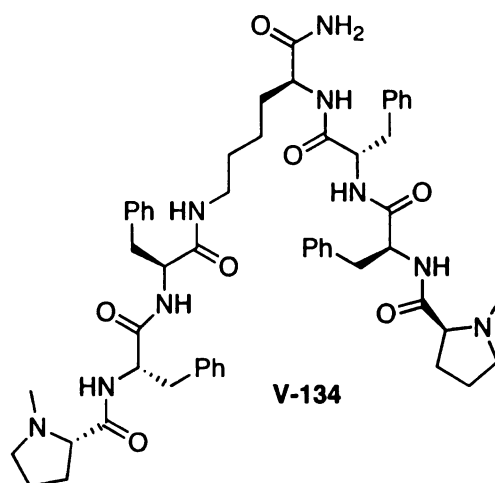Calc.: 576.54   Found: 575.7
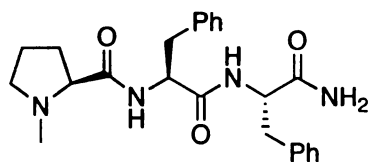   599.73 (M+Na)   598.3 (M+Na)
    614.84 (M+K)   614.2 (M+K)

V-133

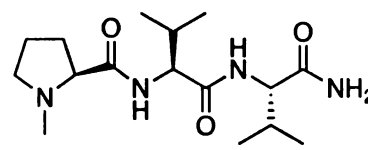Calc.: 661.83   Found: 662.1

370

Figure V-14. (Cont'd)

V-134

Calc.: 956.18   Found: 956.1
979.17 (M+Na)   979.1 (M+Na)

V-135

Calc.: 422.52   Found: 422.7

V-136

Calc.: 326.43   Found: 326.9
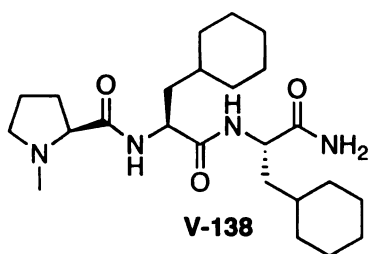

V-137
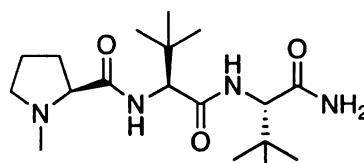
Calc.: 354.49   Found: 355.5
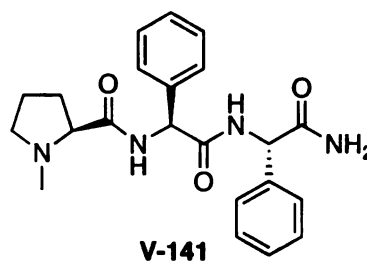377.48 (M+Na)   377.5 (M+Na)

Figure V-14. (Cont'd)

V-138

Calc.: 434.61   Found: 435.0

V-139

Calc.: 354.49   Found: 354.9

V-140

Calc.: 354.49   Found: 354.9

V-141
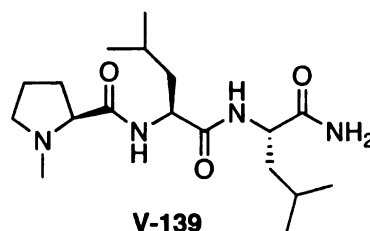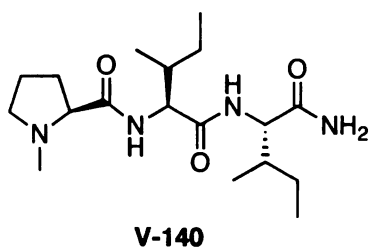
Calc.: 394.49   Found: 394.8

General Protocol For Screening Peptides in the Dihydroxylation of Olefins (Ogino-Sharpless Conditions)

To a 3 mL screw-top vial equipped with a magnetic stir bar was added peptide (usually *ca.* 5 mg, 0.005 mmol, 0.03 eq. with respect to olefin), potassium ferricyanide (III) (196 mg, 0.6 mmol, 3 eq.), and potassium carbonate (83 mg, 0.6 mmol, 3 eq.). The resulting mixture was dissolved in a 1:1 mixture of *t*-butyl alcohol and water (2 mL) with stirring. Osmium (VI) tetroxide (10 μL of a 0.2 M solution in toluene, 0.002 mmol, 0.01 eq.) was added via syringe and the resulting yellow solution was stirred for 15 minutes. The desired olefin (0.2

mmol, 1 eq.) was added in one portion and the reaction mixture was stirred at room temperature overnight and monitored by TLC (20% EtOAc in hexanes).

The reaction was quenched by the addition of solid sodium sulfite (300 mg). The resulting solution was allowed to stir for one hour. The reaction mixture was then diluted with 10 mL of water and extracted with DCM (3 X 10 mL). The combined organics were then dried (anhydrous Na_2SO_4), concentrated via rotory evaporation, and dried further *in vacuo*. The resulting crude diol products were screened for enantiomeric excess without further purification (Chiralpak AS-H, 5% IPA in hexanes, 1 mL/min, 254 nm).

General Protocol For Screening Peptides in the Dihydroxylation of Olefins (Upjohn Conditions)

To a 3 mL screw-top vial equipped with a magnetic stir bar was added peptide (usually *ca.* 5 mg, 0.005 mmol, 0.03 eq. with respect to olefin and NMO (26 mg, 0.22 mmol, 1.1 eq.). The resulting mixture was dissolved in a 9:1 mixture of acetone and water (2 mL) with stirring. Osmium (VI) tetroxide (10 μL of a 0.2 M solution in toluene, 0.002 mmol, 0.01 eq.) was added via syringe and the resulting solution was stirred for 15 minutes. The desired olefin (0.2 mmol, 1 eq.) was added in one portion and the reaction mixture was stirred at room temperature overnight and monitored by TLC (20% EtOAc in hexanes).

The reaction was quenched by the addition of solid sodium sulfite (300 mg). The resulting solution was allowed to stir for one hour. The reaction mixture was then diluted with 10 mL of water and extracted with DCM (3 X 10

mL). The combined organics were then dried (anhydrous Na_2SO_4), concentrated

via rotary evaporation, and dried further *in vacuo*. The resulting crude diol

products were screened for enantiomeric excess without further purification.

General Protocol For Screening Peptides in the Dihydroxylation of Olefins (Narasaka Conditions)

To a 3 mL screw-top vial equipped with a magnetic stir bar was added peptide

(usually *ca.* 5 mg, 0.005 mmol, 0.03 eq. with respect to olefin, NMO (26 mg, 0.22

mmol, 1.1 eq.), and phenyl boronic acid (29 mg, 0.24 mmol, 1.2 eq.). The

resulting mixture was dissolved in dichloromethane (2 mL) with stirring. Osmium

(VI) tetroxide (10 µL of a 0.2 M solution in toluene, 0.002 mmol, 0.01 eq.) was

added via syringe and the resulting solution was stirred for 15 minutes. The

desired olefin (0.2 mmol, 1 eq.) was added in one portion and reaction mixture

was stirred at room temperature overnight and monitored by TLC (20% EtOAc in

hexanes).

The reaction was quenched by the addition of solid sodium sulfite (300

mg). The resulting solution was allowed to stir for one hour. The reaction

mixture was then diluted with 10 mL of water and extracted with DCM (3 X 10

mL). The combined organics were then dried (anhydrous Na_2SO_4), concentrated

via rotary evaporation, and dried further *in vacuo*. The resulting crude

phenylboronic ester products were treated immediately with hydrogen peroxide

as described below to liberate the free glycol.

Peroxide Mediated Removal of the Phenyl Boronic Ester

The phenyl boronic ester (0.2 mmol) was dissolved in a 1:1 mixture of ethyl acetate and acetone (2 mL) in a 3 mL screw-top vial. To this stirred solution was added 1.2 eq. of a solution of H_2O_2 (35% in H_2O). The resulting mixture was stirred at room temperature for 3 hours. The reaction mixture was extracted twice with ethyl acetate (5 mL), and the combined organics were washed with 1 M NaOH (5 mL). The organics were dried over anhydrous sodium sulfate and concentrated via rotary evaporation. The crude glycol, so isolated, was immediately subjected to HPLC analysis.

Analytical Data

V-66, 2-phenyl-1,2-propanediol[147]
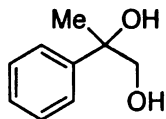
^{1}H NMR (300 MHz, CD_3Cl): δ 7.4-7.2 (m, 5H), 3.69 (d, J = 11.1 Hz, 1H), 3.53 (d, J = 11.1 Hz, 1H), 3.10 (br s, 1H), 2.65 (br s, 1H), 1.46 (s, 3H); ^{13}C NMR (75 MHz, CD_3Cl): δ 144.7, 128.0, 126.8, 124.8, 74.6, 70.6, 25.6.

5.6: References

1. Shimizu, K. D.; Snapper, M. L.; Hoveyda, A. H. *Chem.-Eur. J.* **1998**, *4*, 1885-1889.

2. Hoveyda, A. H. *Chem. Biol.* **1998,** *5,* R187-R191.

3. Hoveyda, A. H.; Hird, A. W.; Kacprzynski, M. A. *Chem. Commun.* **2004,** 1779-1785.

4. Kuntz, K. W.; Snapper, M. L.; Hoveyda, A. H. *Curr. Opin. Chem. Biol.* **1999,** *3*, 313-319.

5. Agarkov, A.; Greenfield, S.; Xie, D. J.; Pawlick, R.; Starkey, G.; Gilbertson, S. R. *Biopolymers* **2006,** *84,* 48-73.

6. Licini, G.; Scrimin, P. *Angew. Chem Int. Ed.* **2003,** *42,* 4572-4575.

7. Berkessel, A. *Curr. Opin. Chem. Biol.* **2003,** *7,* 409-419.

8. Blank, J. T.; Miller, S. J. *Biopolymers* **2006,** *84,* 38-47.

9. Jarvo, E. R.; Miller, S. J. *Tetrahedron* **2002,** *58,* 2481-2495.

10. Miller, S. J. *Acc. Chem. Res.* **2004,** *37,* 601-610.

11. Fields, G. B.; Noble, R. L. *Int. J. Pept. Protein Res.* **1990,** *35,* 161-214.

12. Berkessel, A.; Ashkenazi, E.; Andreae, M. R. M. *Appl. Catal. A-Gen.* **2003,** *254,* 27-34.

13. Berkessel, A.; Herault, D. A. *Angew. Chem Int. Ed.* **1999,** *38,* 102-105.

14. Jarvo, E. R.; Evans, C. A.; Copeland, G. T.; Miller, S. J. *J. Org. Chem.* **2001,** *66,* 5522-5527.

15. Copeland, G. T.; Miller, S. J. *J. Am. Chem. Soc.* **1999,** *121,* 4306-4307.

16. Harris, R. F.; Nation, A. J.; Copeland, G. T.; Miller, S. J. *J. Am. Chem. Soc.* **2000,** *122,* 11270-11271.

17. Copeland, G. T.; Miller, S. J. *J. Am. Chem. Soc.* **2001,** *123,* 6496-6502.

18. Evans, C. A.; Miller, S. J. *Curr. Opin. Chem. Biol.* **2002,** *6,* 333-338.

19. Abato, P.; Seto, C. T. *J. Am. Chem. Soc.* **2001,** *123,* 9206-9207.

20. Lam, K. S.; Salmon, S. E.; Hersh, E. M.; Hruby, V. J.; Kazmierski, W. M.; Knapp, R. J. *Nature* **1991,** *354,* 82-84.

21. Song, A. M.; Zhang, J. H.; Lebrilla, C. B.; Lam, K. S. *J. Am. Chem. Soc.* **2003,** *125,* 6180-6188.

22. Taylor, S. J.; Morken, J. P. *Science* **1998,** *280,* 267-270.

23. Johansson, K. J.; Andreae, M. R. M.; Berkessel, A.; Davis, A. P. *Tetrahedron Lett.* **2005,** *46,* 3923-3926.

24. Muller, M.; Mathers, T. W.; Davis, A. P. *Angew. Chem Int. Ed.* **2001,** *40,* 3813-3815.

25. Krattiger, P.; McCarthy, C.; Pfaltz, A.; Wennemers, H. *Angew. Chem Int. Ed.* **2003,** *42,* 1722-1724.

26. Reetz, M. T.; Becker, M. H.; Liebl, M.; Furstner, A. *Angew. Chem Int. Ed.* **2000,** *39,* 1236-1239.

27. Reetz, M. T.; Hermes, M.; Becker, M. H. *Appl. Microbiol. Biotechnol.* **2001,** *55,* 531-536.

28. Reetz, M. T. *Angew. Chem Int. Ed.* **2002,** *41,* 1335-1338.

29. Korbel, G. A.; Lalic, G.; Shair, M. D. *J. Am. Chem. Soc.* **2001,** *123,* 361-362.

30. van Delden, R. A.; Feringa, B. L. *Angew. Chem Int. Ed.* **2001,** *40,* 3198-3200.

31. Furka, A.; Sebestyen, F.; Asgedom, M.; Dibo, G. *Int. J. Pept. Protein Res.* **1991,** *37,* 487-493.

32. Houghten, R. A.; Pinilla, C.; Blondelle, S. E.; Appel, J. R.; Dooley, C. T.; Cuervo, J. H. *Nature* **1991,** *354,* 84-86.

33. Akabori, S.; Sakurai, S.; Izumi, Y.; Fujii, Y. *Nature* **1956,** *178,* 323-324.

34. Cole, B. M.; Shimizu, K. D.; Krueger, C. A.; Harrity, J. P. A.; Snapper, M. L.; Hoveyda, A. H. *Angew. Chem. Int. Ed.* **1996,** *35,* 1668-1671.

35. Shimizu, K. D.; Cole, B. M.; Krueger, C. A.; Kuntz, K. W.; Snapper, M. L.; Hoveyda, A. H. *Angew. Chem. Int. Ed.* **1997,** *36,* 1703-1707.

36. Josephsohn, N. S.; Kuntz, K. W.; Snapper, M. L.; Hoveyda, A. H. *J. Am. Chem. Soc.* **2001,** *123*, 11594-11599.

37. Krueger, C. A.; Kuntz, K. W.; Dzierba, C. D.; Wirschun, W. G.; Gleason, J. D.; Snapper, M. L.; Hoveyda, A. H. *J. Am. Chem. Soc.* **1999,** *121*, 4284-4285.

38. Porter, J. R.; Wirschun, W. G.; Kuntz, K. W.; Snapper, M. L.; Hoveyda, A. H. *J. Am. Chem. Soc.* **2000,** *122*, 2657-2658.

39. Deng, H. B.; Isler, M. R.; Snapper, M. L.; Hoveyda, A. H. *Angew. Chem Int. Ed.* **2002,** *41*, 1009-1012.

40. Murphy, K. E.; Hoveyda, A. H. *Org. Lett.* **2005,** *7*, 1255-1258.

41. Porter, J. R.; Traverse, J. F.; Hoveyda, A. H.; Snapper, M. L. *J. Am. Chem. Soc.* **2001,** *123*, 10409-10410.

42. Porter, J. R.; Traverse, J. F.; Hoveyda, A. H.; Snapper, M. L. *J. Am. Chem. Soc.* **2001,** *123*, 984-985.

43. Fu, P.; Snapper, M. L.; Hoveyda, A. H. *J. Am. Chem. Soc.* **2008,** *130*, 5530-5541.

44. Wieland, L. C.; Deng, H. B.; Snapper, M. L.; Hoveyda, A. H. *J. Am. Chem. Soc.* **2005,** *127*, 15453-15456.

45. Degrado, S. J.; Mizutani, H.; Hoveyda, A. H. *J. Am. Chem. Soc.* **2001,** *123*, 755-756.

46. Kacprzynski, M. A.; Kazane, S. A.; May, T. L.; Hoveyda, A. H. *Org. Lett.* **2007,** *9*, 3187-3190.

47. Mizutani, H.; Degrado, S. J.; Hoveyda, A. H. *J. Am. Chem. Soc.* **2002,** *124*, 779-781.

48. Luchaco-Cullis, C. A.; Hoveyda, A. H. *J. Am. Chem. Soc.* **2002,** *124*, 8192-8193.

49. Mampreian, D. M.; Hoveyda, A. H. *Org. Lett.* **2004,** *6*, 2829-2832.

50. Wu, J.; Mampreian, D. M.; Hoveyda, A. H. *J. Am. Chem. Soc.* **2005,** *127*, 4584-4585.

51. Hird, A. W.; Hoveyda, A. H. *J. Am. Chem. Soc.* **2005,** *127*, 14988-14989.

52. Luchaco-Cullis, C. A.; Mizutani, H.; Murphy, K. E.; Hoveyda, A. H. *Angew. Chem Int. Ed.* **2001,** *40,* 1456-1460.

53. Akullian, L. C.; Snapper, M. L.; Hoveyda, A. H. *J. Am. Chem. Soc.* **2006,** *128,* 6532-6533.

54. Gilbertson, S. R.; Chen, G. H.; McLoughlin, M. *J. Am. Chem. Soc.* **1994,** *116,* 4481-4482.

55. Gilbertson, S. R.; Pawlick, R. V. *Angew. Chem. Int. Ed.* **1996,** *35,* 902-904.

56. Greenfield, S. J.; Gilbertson, S. R. *Synthesis* **2001,** 2337-2340.

57. Gilbertson, S. R.; Chen, G. H.; Kao, J.; Beatty, A.; Campana, C. F. *J. Org. Chem.* **1997,** *62,* 5557-5566.

58. Gilbertson, S. R.; Wang, X. F. *Tetrahedron Lett.* **1996,** *37,* 6475-6478.

59. Gilbertson, S. R.; Wang, X. F. *Tetrahedron* **1999,** *55,* 11609-11618.

60. Gilbertson, S. R.; Wang, X. F.; Hoge, G. S.; Klug, C. A.; Schaefer, J. *Organometallics* **1996,** *15,* 4678-4680.

61. Agarkov, A.; Gilbertson, S. R. *Tetrahedron Lett.* **2005,** *46,* 181-183.

62. Agarkov, A.; Greenfield, S. J.; Ohishi, T.; Collibee, S. E.; Gilbertson, S. R. *J. Org. Chem.* **2004,** *69,* 8077-8085.

63. Gilbertson, S. R.; Collibee, S. E.; Agarkov, A. *J. Am. Chem. Soc.* **2000,** *122,* 6522-6523.

64. Gilbertson, S. R.; Yamada, S. *Tetrahedron Lett.* **2004,** *45,* 3917-3920.

65. Greenfield, S. J.; Agarkov, A.; Gilbertson, S. R. *Org. Lett.* **2003,** *5,* 3069-3072.

66. Gilbertson, S. R.; Lan, P. *Org. Lett.* **2001,** *3,* 2237-2240.

67. Agarkov, A.; Uffman, E. W.; Gilbertson, S. R. *Org. Lett.* **2003,** *5,* 2091-2094.

68. Christensen, C. A.; Meldal, M. *Chem.-Eur. J.* **2005,** *11,* 4121-4131.

69. Landis, C. R.; Clark, T. P. *Proc. Natl. Acad. Sci. U. S. A.* **2004,** *101,* 5428-5432.

70. Guillena, G.; Rodriguez, G.; van Koten, G. *Tetrahedron Lett.* **2002**, *43*, 3895-3898.

71. Alper, H.; Hamel, N. *J. Chem. Soc.-Chem. Commun.* **1990**, 135-136.

72. Du, H. F.; Long, J.; Shi, Y. *Org. Lett.* **2006**, *8*, 2827-2829.

73. Long, J.; Du, H. F.; Li, K.; Shi, Y. *Tetrahedron Lett.* **2005**, *46*, 2737-2740.

74. Long, J.; Yuan, Y.; Shi, Y. *J. Am. Chem. Soc.* **2003**, *125*, 13632-13633.

75. Miao, J. H.; Yang, J. H.; Chen, L. Y.; Tu, B. X.; Huang, M. Y.; Jiang, Y. Y. *Polym. Adv. Technol.* **2004**, *15*, 221-224.

76. Travis, B. R.; Narayan, R. S.; Borhan, B. *J. Am. Chem. Soc.* **2002**, *124*, 3824-3825.

77. Schomaker, J. M.; Travis, B. R.; Borhan, B. *Org. Lett.* **2003**, *5*, 3089-3092.

78. Whitehead, D. C.; Travis, B. R.; Borhan, B. *Tetrahedron Lett.* **2006**, *47*, 3797-3800.

79. Travis, B.; Borhan, B. *Tetrahedron Lett.* **2001**, *42*, 7741-7745.

80. Kolb, H. C.; Vannieuwenhze, M. S.; Sharpless, K. B. *Chem. Rev.* **1994**, *94*, 2483-2547.

81. Angelaud, R.; Landais, Y. *J. Org. Chem.* **1996**, *61*, 5202-5203.

82. Landais, Y. *Chimia* **1998**, *52*, 104-111.

83. Angelaud, R.; Babot, O.; Charvat, T.; Landais, Y. *J. Org. Chem.* **1999**, *64*, 9613-9624.

84. Landais, Y.; Zekri, E. *Tetrahedron Lett.* **2001**, *42*, 6547-6551.

85. Corey, E. J.; Noe, M. C.; Guzmanperez, A. *J. Am. Chem. Soc.* **1995**, *117*, 10817-10824.

86. Christie, H. S.; Hamon, D. P. G.; Tuck, K. L. *Chem. Commun.* **1999**, 1989-1990.

87. Hamon, D. P. G.; Tuck, K. L.; Christie, H. S. *Tetrahedron* **2001**, *57*, 9499-9508.

88. Burke, S. D.; Jiang, L. *Org. Lett.* **2001**, *3*, 1953-1955.

89. Hawkins, J. M.; Meyer, A.; Solow, M. A. *J. Am. Chem. Soc.* **1993**, *115*, 7499-7500.

90. Hawkins, J. M.; Meyer, A. *Science* **1993**, *260*, 1918-1920.

91. Rose, G. D.; Gierasch, L. M.; Smith, J. A. *Adv. Protein Chem.* **1985**, *37*, 1-109.

92. Venkatachalapathi, Y. V.; Nair, C. M. K.; Vijayan, M.; Balaram, P. *Biopolymers* **1981**, *20*, 1123-1136.

93. Venkatachalapathi, Y. V.; Balaram, P. *Biopolymers* **1981**, *20*, 1137-1145.

94. Prasad, B. V. V.; Balaram, H.; Balaram, P. *Biopolymers* **1982**, *21*, 1261-1273.

95. Ravi, A.; Balaram, P. *Tetrahedron* **1984**, *40*, 2577-2583.

96. Raghothama, S. R.; Awasthi, S. K.; Balaram, P. *J. Chem. Soc.-Perkin Trans. 2* **1998**, 137-143.

97. Imperiali, B.; Fisher, S. L.; Moats, R. A.; Prins, T. J. *J. Am. Chem. Soc.* **1992**, *114*, 3182-3188.

98. Imperiali, B.; Kapoor, T. M. *Tetrahedron* **1993**, *49*, 3501-3510.

99. Haque, T. S.; Little, J. C.; Gellman, S. H. *J. Am. Chem. Soc.* **1996**, *118*, 6975-6985.

100. Stanger, H. E.; Gellman, S. H. *J. Am. Chem. Soc.* **1998**, *120*, 4236-4237.

101. Amblard, M.; Raynal, N.; Averlant-Petit, M. C.; Didierjean, C.; Calmes, M.; Fabre, O.; Aubry, A.; Marraud, M.; Martinez, J. *Tetrahedron Lett.* **2005**, *46*, 3733-3735.

102. Nakajima, M.; Tomioka, K.; Koga, K. *J. Pharm. Sci.* **1987**, *76*, S243-S243.

103. Tomioka, K.; Nakajima, M.; Koga, K. *J. Am. Chem. Soc.* **1987**, *109*, 6213-6215.

104. Tomioka, K.; Nakajima, M.; Iitaka, Y.; Koga, K. *Tetrahedron Lett.* **1988**, *29*, 573-576.

105. Tomioka, K.; Shinmi, Y.; Shiina, K.; Nakajima, M.; Koga, K. *Chem. Pharm. Bull.* **1990**, *38*, 2133-2135.

106. Tomioka, K.; Nakajima, M.; Koga, K. *Tetrahedron Lett.* **1990,** *31,* 1741-1742.

107. Nakajima, M.; Tomioka, K.; Iitaka, Y.; Koga, K. *Tetrahedron* **1993,** *49,* 10793-10806.

108. Oishi, T.; Hirama, M. *J. Org. Chem.* **1989,** *54,* 5834-5835.

109. Hirama, M.; Oishi, T.; Ito, S. *J. Chem. Soc.-Chem. Commun.* **1989,** 665-666.

110. Oishi, T.; Hirama, M. *Tetrahedron Lett.* **1992,** *33,* 639-642.

111. Oishi, T.; Iida, K.; Hirama, M. *Tetrahedron Lett.* **1993,** *34,* 3573-3576.

112. Imada, Y.; Saito, T.; Kawakami, T.; Murahashi, S. I. *Tetrahedron Lett.* **1992,** *33,* 5081-5084.

113. Haubenstock, H.; Subasinghe, K. *Chirality* **1992,** *4,* 300-301.

114. Fuji, K.; Tanaka, K.; Miyamoto, H. *Tetrahedron Lett.* **1992,** *33,* 4021-4024.

115. Rosini, C.; Tanturli, R.; Pertici, P.; Salvadori, P. *Tetrahedron: Asymmetry* **1996,** *7,* 2971-2982.

116. Hanessian, S.; Meffre, P.; Girard, M.; Beaudoin, S.; Sanceau, J. Y.; Bennani, Y. *J. Org. Chem.* **1993,** *58,* 1991-1993.

117. Illesinghe, J.; Ebeling, R.; Ferguson, B.; Patel, J.; Campi, E. M.; Jackson, W. R.; Robinson, A. J. *Aust. J. Chem.* **2004,** *57,* 167-176.

118. Corey, E. J.; Jardine, P. D.; Virgil, S.; Yuen, P. W.; Connell, R. D. *J. Am. Chem. Soc.* **1989,** *111,* 9243-9244.

119. Corey, E. J.; Sarshar, S.; Azimioara, M. D.; Newbold, R. C.; Noe, M. C. *J. Am. Chem. Soc.* **1996,** *118,* 7851-7852.

120. Tokles, M.; Snyder, J. K. *Tetrahedron Lett.* **1986,** *27,* 3951-3954.

121. Yamada, T.; Narasaka, K. *Chem. Lett.* **1986,** 131-134.

122. Severeyns, A.; De Vos, D. E.; Fiermans, L.; Verpoort, F.; Grobet, P. J.; Jacobs, P. A. *Angew. Chem Int. Ed.* **2001,** *40,* 586-589.

123. Severeyns, A.; De Vos, D. E.; Jacobs, P. A. *Green Chem.* **2002,** *4,* 380-384.

124. Tang, W. J.; Yang, N. F.; Yi, B.; Deng, G. J.; Huang, Y. Y.; Fan, Q. H. *Chem. Commun.* **2004**, 1378-1379.

125. Pescarmona, P. P.; Masters, A. F.; van der Waal, J. C.; Maschmeyer, T. *J. Mol. Catal. A-Chem.* **2004,** *220*, 37-42.

126. Huang, Y. G.; Meng, W. D.; Qing, F. L. *Tetrahedron Lett.* **2004,** *45*, 1965-1968.

127. Palmer, M. J.; Danilewicz, J. C.; Vuong, H. *Synlett* **1994**, 171-172.

128. Barlos, K.; Papaioannou, D.; Cordopatis, P.; Theodoropoulos, D. *Tetrahedron* **1983,** *39*, 475-478.

129. Chen, S. T.; Wu, S. H.; Wang, K. T. *Synth. Commun.* **1989,** *19*, 3589-3593.

130. Chen, S. T.; Wang, K. T. *Synthesis* **1989**, 36-37.

131. Kwong, H. L.; Sorato, C.; Ogino, Y.; Hou, C.; Sharpless, K. B. *Tetrahedron Lett.* **1990,** *31*, 2999-3002.

132. Ogino, Y.; Chen, H.; Kwong, H. L.; Sharpless, K. B. *Tetrahedron Lett.* **1991,** *32*, 3965-3968.

133. Vanrheenen, V.; Kelly, R. C.; Cha, D. Y. *Tetrahedron Lett.* **1976**, 1973-1976.

134. Andersson, M. A.; Epple, R.; Fokin, V. V.; Sharpless, K. B. *Angew. Chem Int. Ed.* **2002,** *41*, 472-475.

135. Dupau, P.; Epple, R.; Thomas, A. A.; Fokin, V. V.; Sharpless, K. B. *Adv. Synth. Catal.* **2002,** *344*, 421-433.

136. Davies, J. S. *J. Pept. Sci.* **2003,** *9*, 471-501.

137. Trzeciak, A.; Bannwarth, W. *Tetrahedron Lett.* **1992,** *33*, 4557-4560.

138. Kates, S. A.; Sole, N. A.; Johnson, C. R.; Hudson, D.; Barany, G.; Albericio, F. *Tetrahedron Lett.* **1993,** *34*, 1549-1552.

139. Thieriet, N.; Alsina, J.; Giralt, E.; Guibe, F.; Albericio, F. *Tetrahedron Lett.* **1997,** *38*, 7275-7278.

140. Yan, L. Z.; Edwards, P.; Flora, D.; Mayer, J. P. *Tetrahedron Lett.* **2004,** *45*, 923-925.

141. Iwasawa, N.; Kato, T.; Narasaka, K. *Chem. Lett.* **1988**, 1721-1724.

142. Gypser, A.; Michel, D.; Nirschl, D. S.; Sharpless, K. B. *J. Org. Chem.* **1998,** *63*, 7322-7327.

143. Hovelmann, C. H.; Muniz, K. *Chem.-Eur. J.* **2005,** *11*, 3951-3958.

144. Han, Z. J.; Wang, R.; Zhou, Y. F.; Liu, L. *Eur. J. Org. Chem.* **2005**, 934-938.

145. Vasudev, P. G.; Ananda, K.; Chatterjee, S.; Aravinda, S.; Shamala, N.; Balaram, P. *J. Am. Chem. Soc.* **2007,** *129*, 4039-4048.

146. Chan, W. C.; White, P. D. *Fmoc Solid Phase Peptide Synthesis*; Oxford University Press: Oxford, 2004.

147. Sharpless, K. B.; Akashi, K. *J. Am. Chem. Soc.* **1976,** *98*, 1986-1987.

Chapter 6: The OsO₄/Oxone Oxidative Cleavage of Olefins with Alternative Osmium Sources

6.1: Introduction

In 2002, our group reported on an osmium tetroxide-promoted catalytic oxidative cleavage of olefins.[1] This reaction employs a catalytic portion of osmium tetroxide in conjunction with several equivalents of Oxone as a co-oxidant to effect the cleavage of a variety of olefins VI-1 (Scheme VI-1, eq. 1). For mono- and vicinal disubstituted alkenes VI-1, this methodology provides easy access to the corresponding carboxylic acid cleavage products VI-2 and VI-3. Higher order alkenes VI-4 (or geminal disubstituted olefins) grant access to the corresponding ketones VI-5 (Scheme VI-1, eq. 2). The reactions usually proceed in excellent yields for the cleavage of a number of different alkene substrates.

Scheme VI-1. Oxidative cleavage of olefins with osmium tetroxide and oxone.
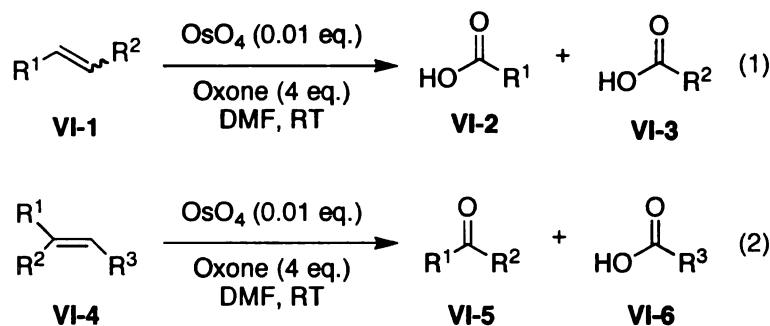
The reaction is suggested to initiate by the formation of the osmate ester VI-7 via the accepted[2,3] [3+2] osmylation mechanism (Scheme VI-2). Subsequent oxidation of the Os (VI) glycolate by action of Oxone provides the corresponding Os (VIII) species. Attack on this intermediate by the peroxysulfate anion provides intermediate VI-8. This intermediate might then undergo facile

385

oxidative cleavage to provide aldehyde (or ketone) cleavage products **VI-9**, thus

regenerating the catalytic portion of OsO_4. The aldehyde cleavage products then

undergo facile oxidation to their corresponding carboxylic acids **VI-10** via a

Baeyer-Villeger-type process by action of residual Oxone.[4-6]

**Scheme VI-2.** Proposed mechanism for the cleaveage of olefins with osmium
tetroxide/oxone.
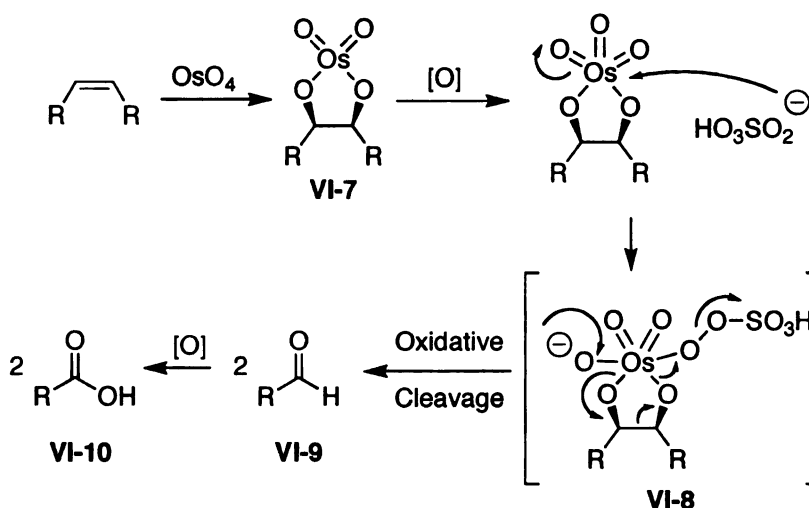
An important distinction between this proposed mechanism and the well-

known Johnson-Lemieux[7,8] oxidative cleavage is apparent. The Lemieux-

Johnson protocol is proposed to proceed through the initial formation of glycol

intermediates which subsequently suffer cleavage by periodate anion. In

contrast the Oxone-mediated cleavage is presumably the result of the

fragmentation of the initial osmium glycolate **VI-7** *without* the intermediacy of

vicinal diols. In fact, treatment of glycols with the reaction conditions described in

Scheme VI-1 returns unchanged starting material.[1]

The OsO_4/Oxone methodology represents a significant departure from the

more common reactivity profile of catalytic OsO_4 and co-oxidant which results in

the generation vicinal diols. Racemic diols are most readily prepared by action

of the OsO$_4$/NMO reagent combination (historically referred to as the Upjohn[9]

conditions).[10] Scalemic diols are accessible via the Sharpless Asymmetric

Dihydroxylation (SAD) methodology, where OsO$_4$/K$_3$Fe(CN)$_6$ is employed in

conjunction with various *Cinchona* alkaloid derivatives.[11,12] Aside from the

Lemieux-Johnson methodology alluded to above, oxidative cleavages mediated

by OsO$_4$ have historically carried the stigma of undesired side reactions,

producing the olefin cleavage products in low yields.[13,14] Prior to the report from

our lab, there was only one account detailing the direct oxidative cleavage of

olefins (without the intermediacy of diols) by action of OsO$_4$ that proceeded in

synthetically useful yields. Tsui and Paquette noted the scission of the olefin

functionality in compound **IV-11** on heating with a stoichiometric quantity of OsO$_4$

in pyridine to 90°C, followed by a sodium dithionate reductive work-up.[15] Keto-

aldehyde **IV-12** was returned in 41% yield (Scheme VI-3).

**Scheme VI-3.** Oxidative cleavage of **IV-11** with osmium tetroxide.

VI-11   VI-12
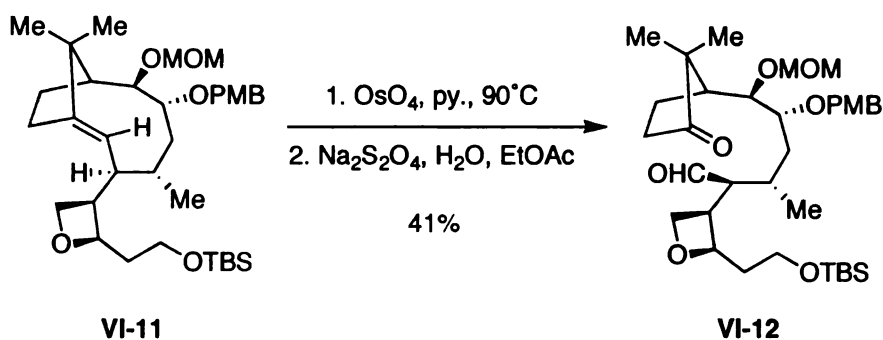
Since the initial disclosure, the OsO$_4$/Oxone methodology has been

extended to include the direct formation of lactones by way of the oxidative

cleavage of alkenols (Scheme VI-4, eq. 1)[16] This transformation was highlighted

387

as the key transformation leading to the efficient total synthesis of (+)-tanikolide

VI-16 (Scheme VI-4, eq. 2).[17] Furthermore, the Martin group has employed the

OsO$_4$/Oxone methodology in the very late stages of their elegant total synthesis

of Erythromycin B.[18]

Scheme VI-4. Oxidative lactonization with osmium tetroxide and oxone.
Application to the total synthesis of (+)-tanikolide **VI-16**.
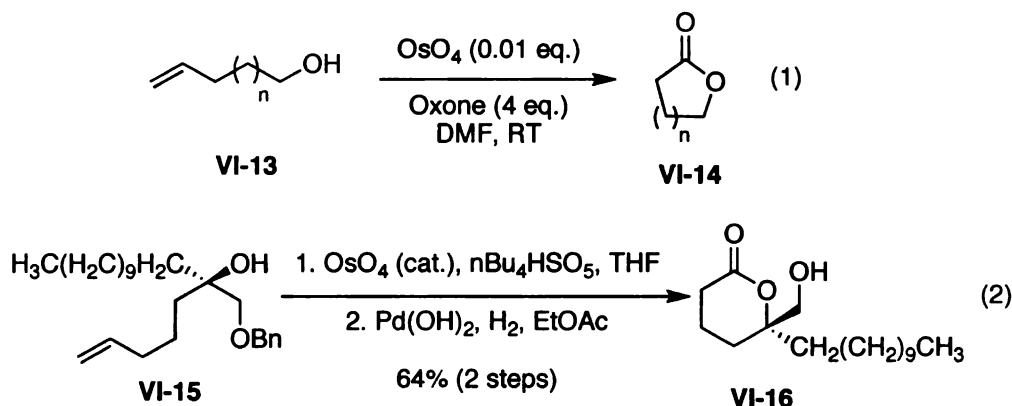
6.2: Results and Discussion

Given the apparent success of this methodology, we set out to explore the

use of alternate sources of the osmium catalyst. Namely, presented herein is an

account of the investigation of the integrity of this methodology when cheaper,

less toxic, and easier-to-handle osmium sources are employed.[19] Four different

sources of osmium were chosen for this study, each offering its own advantages

over osmium tetroxide. Both osmium trichloride and potassium osmate are

cheaper, less volatile osmium sources, which can be handled safely in their solid

state, a considerable advantage to preparing organic solutions of osmium

tetroxide. Commercially available polymer-bound osmium tetroxide (1 wt. % on

poly(4-vinylpyridine))[20,21] also provides a catalyst source that is easier to handle

and less volatile than standard samples of osmium tetroxide. A final osmium

source, OsEnCat™, was kindly provided by the Ley laboratory. OsEnCat™ is

osmium tetroxide that has been microencapsulated in polyurea

microcapsules.[22,23] The Ley group has shown that this catalyst system is highly

effective in both the catalytic dihydroxylation of olefins under Upjohn conditions[9]

and in the oxidative cleavage of olefins by the Lemiuex-Johnson reaction.[7,8] This

particular osmium source offers the intriguing opportunity of recycling the catalyst

for use in subsequent reactions. Ley and coworkers have shown that a sample

of OsEnCat™ can be used for five iterations without any detectable leaching of

osmium tetroxide or loss of catalytic activity.

Each of the four sources of osmium were screened for activity in the

oxidative cleavage and oxidative lactonization reactions. Reactions were carried

out for 12 hours using a 0.1 M solution of substrate in DMF, with 4 equivalents of

Oxone and 0.01 equivalents of catalyst when osmium trichloride or potassium

osmate were employed. A lower catalyst loading of 0.001 equivalents of

polymer-bound and 0.0025 equivalents of encapsulated osmium tetroxide were

used for some substrates in order to avoid adding an impractically large mass of

substance to achieve the desired catalyst loading. Other substrates, however,

proved too sluggish when the lower catalyst loading was used, so for those

substrates, the use of 0.01 equivalents of either polymer-bound osmium tetroxide

or OsEnCat™ is recommended. Control experiments with 0.01 equivalents of

osmium tetroxide were run for comparisons. The results from this study are

given in Table VI-1.

Table VI-1. The oxidative cleavage of olefins with alternative osmium sources.

Entry	Substrate	Product	A	B	C	D	E
1[a,b]	Ph⌒=⌒Ph **VI-17**	$PhCO_2H$ **VI-18**	84%	84%	80%	79%	84%
2	Me-(⌒)₇-/= **VI-19**	Me-(⌒)₇-CO_2H **VI-20**	100%	96%	100%	75%	97%
3	Ph⌒=⌒CO_2H **VI-21**	$PhCO_2H$ **VI-18**	84%	79%	30% 96%[c]	96%[c]	74%
4[d,e]	Me / Ph⌒=⌒ **VI-22**	Me / Ph⌒C=O **VI-23**	90%	95%	82%	71%	84%
5	Ph⌒=⌒Me Me **VI-24**	$PhCO_2H$ **VI-18**	96%	67%	79%[c]	55%	88%
6	Me ... Me **VI-25**	Me-(⌒)₇-CO_2H **VI-20**	97%	85%	91%[c]	97%[c]	82%
7	Ph—≡ **VI-26**	$PhCO_2H$ **VI-18**	21%	38%	16%	8%	42%
8	⌒-(⌒)₇-O-⌒≡ **VI-27**	HO_2C-(⌒)₇-O-⌒≡ **VI-28**	76%	82%	48% 93%[c]	51% 95%[c]	75%
9	**VI-29**	**VI-30**	98%	93%	95%[c]	95%[c]	98%

Condition A: 0.01 equiv. of osmium trichloride was used as the catalyst.
Condition B: 0.01 equiv. of potassium osmate was used as the catalyst.
Condition C: 0.001 equiv. of polymer-bound osmium tetroxide was used as the catalyst.
Condition D: 0.0025 equiv. of OsEnCat was used as the catalyst.
Condition E: 0.01 equiv. of osmium tetroxide was used as the catalyst.
[a]Reactions were carried out at RT for 12 h using a 0.1 M solution of substrate in DMF with 4 equiv. of Oxone employed as co-oxidant. [b]All yields are isolated yields unless otherwise specified. [c]0.01 equiv. of either polymer-bound OsO_4 or OsEnCat was used. [d]GC yield. [e]Diol and acid products were also formed (*vide infra*).

Entries 1 and 2 showcase the ability of each osmium source to efficiently cleave both aromatic (**VI-17**) and aliphatic (**VI-19**) olefins. Cinnamic acid (entry 3) serves as an example of an electron deficient system. All osmium sources performed on a comparable level with osmium tetroxide, but 0.01 equivalents of both polymer-bound osmium tetroxide and OsEnCat™ were needed to efficiently promote cleavage of **VI-21**.

The cleavage of α-methylstyrene **VI-22** gave the desired acetophenone cleavage product with all five sources of osmium in yields ranging from 71 to 95% (entry 4). In each case, however, the acetophenone product was contaminated with other oxidation products (*vide infra*). Entries 5 and 6 highlight the ability of this methodology to efficiently promote the oxidative cleavage of higher order olefins **VI-24** and **VI-25**. As described previously,[1] the use of sodium bicarbonate (4 equiv) as an additive is necessary to suppress side reactions.

The sluggish oxidation of phenyl acetylene **VI-26** under the prescribed reaction conditions (entry 7: only 8-42% yield of benzoic acid after 12 hours) suggested that one might be able to garner some selectivity for the cleavage of olefins in the presence of alkynes. To test this hypothesis, an ene-yne substrate **VI-27** was prepared by alkylation of the lithium alkoxide of 9-decene-1-ol **VI-31** (Scheme VI-5). The facile cleavage of the olefin in **VI-27** was achieved with each of the five osmium sources while preserving the propargylic alkyne functionality. This selectivity, coupled with the immunity of other sensitive functionalities such

as alcohols and vicinal diols, makes this methodology an attractive strategy for the oxidative cleavage of olefins within highly functionalized intermediates.

Scheme VI-5. Preparation of ene-yne substrate **VI-27**.
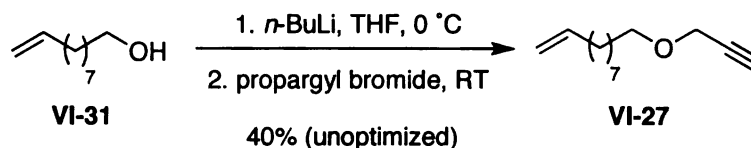
With the final entry in Table VI-1, the alternative forms of osmium tetroxide were utilized for the oxidative lactonization protocol. Alkenol **VI-29** depicted in entry 9 was readily prepared as previously reported (Scheme VI-6).[16] Namely, commercially available diol **VI-32** was mono-TBS protected to provide alcohol **VI-33**. Ley oxidation[24] followed by methylenation of the resultant aldehyde returned alkene **VI-34**. Compound **VI-34** was then deprotected by action of TBAF to generated alkenol substrate **VI-29**.
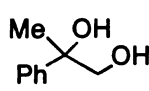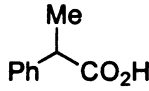
Scheme VI-6. Preparation of lactonization substrate **VI-29**.
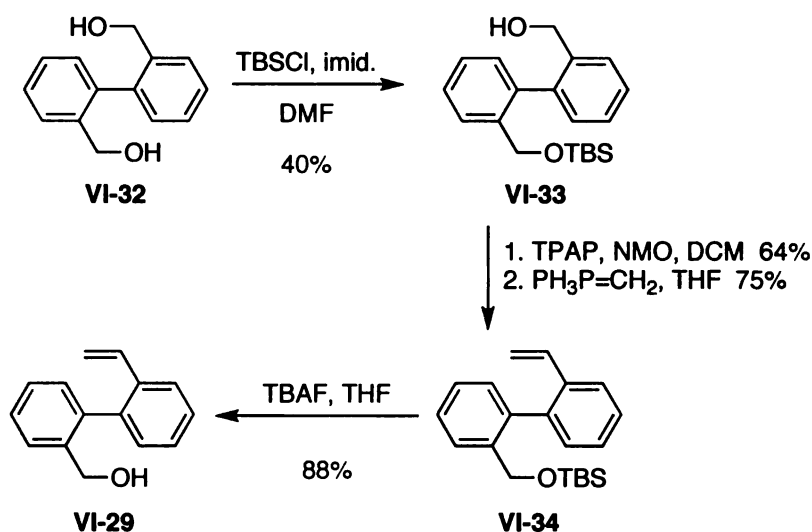
We initially envisioned the cyclization of protected **VI-34** to give lactone **VI-30** directly via a single deprotection/lactonization event, but the TBS deprotection by the mildly acidic reaction conditions proved to be too sluggish. In the event, the desired lactone **VI-30** was returned as the sole product with all five osmium sources in yields ranging from 27 to 43% after 12 hours. On the other hand, treatment of the free alcohol **VI-29** with the oxidative reaction conditions described above, generated in all cases the desired lactone product in excellent yields (93-98% yield, entry 9).

As mentioned above, the presence of other oxidative side products in the cleavage of α-methylstyrene warrant some comment. For all five osmium sources (Table VI-1, Entry 4), the cleavage of this substrate produced predominantly the desired acetophenone (**VI-23**) cleavage product. We were surprised, however, to see evidence for the dihydroxylation product, 2-phenyl-1,2-propanediol (**VI-35**), along with 2-phenylpropanoic acid (**VI-36**) in addition to the desired acetophenone. In order to verify the presence of these two side products in the ^{1}H NMR spectrum and GC traces, the diol and carboxylic acid products were prepared independently (see Section 6.3). With pure samples of the two byproducts in hand, their presence in the crude ^{1}H NMR spectra and GC traces of the cleavage reaction for α-methylstyrene was verified. GC analysis of the reaction mixture obtained from the cleavage reaction for each of the five osmium sources is listed in Table VI-2.

Table VI-2. GC analysis of the observed products from the oxidative cleavage of **VI-22**.

Osmium Source[a]	Me Ph—C(=O) **VI-23**	Me OH Ph—C—CH$_2$OH **VI-35**	Me Ph—CH—CO$_2$H **VI-36**
OsCl$_3$	90%	3%	7%
K$_2$[OsO$_2$(OH)$_4$]	95%	2%	3%
P.B. OsO$_4$	82%	2%	16%
OsEnCat	71%	3%	26%
OsO$_4$	84%	3%	12%

[a]GC yields.

The presence of diol **VI-35**, resulting from hydrolysis of the osmate ester, was minimal regardless of the osmium source. The presence of 2-phenylpropanoic acid **VI-36**, however, varied depending on the osmium source, with as little as 3% formed when potassium osmate was employed to 26% when OsEnCat™ was used. It is interesting to speculate about the origin of this particular side product. The initial product from the fragmentation of the osmate ester is most likely the 2-phenylpropionaldehyde **VI-37**. This substance (not observed by ^{1}H NMR or GC of the product mixtures) would be readily oxidized to the observed carboxylic acid **VI-36** by action of Oxone.[6] Scheme VI-7 shows three possible routes to 2-phenylpropionaldehyde **VI-37**. Equation 1 invokes a 1,2-hydride shift from the osmate ester intermediate (transition state **VI-38**) that would lead to the aldehyde by way of a concerted process. One can also imagine the formation of the aldehyde intermediate **VI-37** by two different two-step pathways. Equation 2 suggests the intermediacy of carbocation **VI-40** resulting from initial dissociation of the osmate ester **VI-39** followed by hydride shift. Equation 3 suggests the intermediacy of enolate species **VI-42** resulting

from the deprotonation of the initial osmate ester intermediate **VI-41**. While at this point, none of these possibilities can be ignored, one can speculate on the merits of each case. Equations 1 and 2 are similar in that they both rely on a 1,2-hydride transfer. The formation of the stable tertiary benzylic carbocation **VI-40** may in fact be necessary to allow for a 1,2-hydride shift. One might expect that if the hydride migration readily occurs without carbocation formation, that the problem of forming undesired products would be more systemic. The deprotonation/reprotonation sequence described equation 3 is perhaps less likely given that the generation of enolate **VI-42** under the relatively acidic reaction conditions seems suspect. Finally, none of these mechanisms account for the fact the product ratios are osmium source dependant.

Scheme VI-7. Plausible mechanisms for the formation of **VI-37** leading to **VI-36**.

395
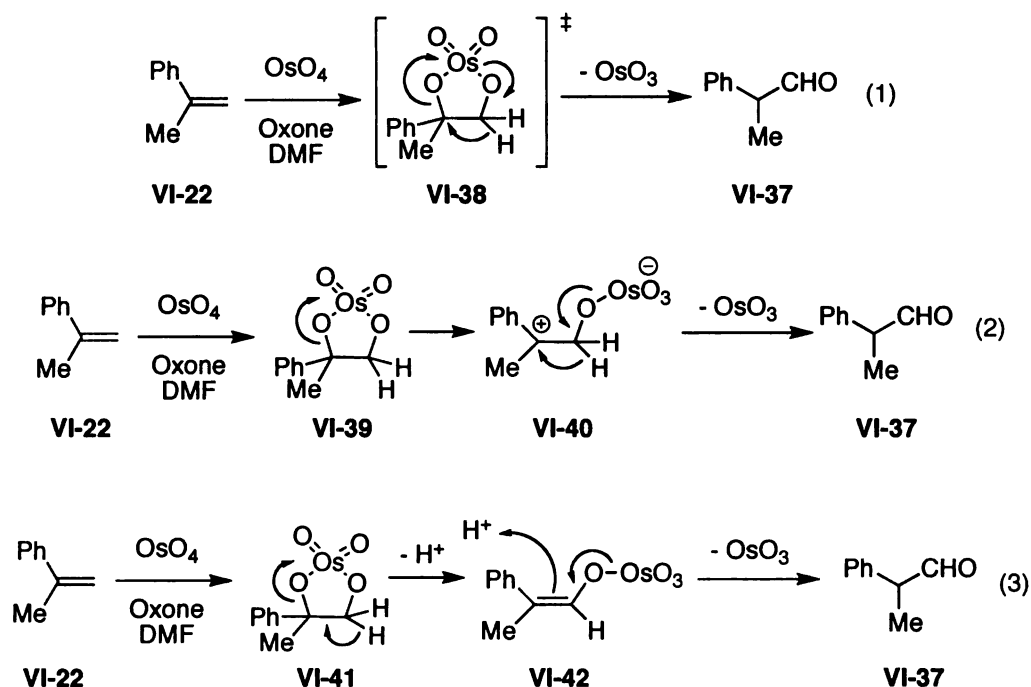
Finally, we also evaluated the ability to recycle the encapsulated osmium

tetroxide, OsEnCat™ when employed as the catalyst in our methodology. When

0.02 equivalents of OsEnCat™ was employed in successive cleavage runs with

trans-stilbene (Table VI-3), the catalyst was readily recycled, allowing for the

same sample of OsEnCat™ to be employed in up to three sequential reactions.

The immobilized catalyst was easily recovered by vacuum filtration, followed by

washing with water and ethyl acetate to remove residual salts and cleavage

product. While the catalyst proved non-recyclable at lower catalyst loadings, it is

noteworthy that OsEnCat™ performs amiably at a remarkably low 0.0025

equivalent catalyst loading in the oxidative cleavage of activated substrates (*e.g.*,

trans-stilbene (Table VI-1, Entry 1)).

Table VI-3. OsEnCat recyclability study.

Run	eq. OsEnCat™	Yield
1	0.02	73%
2	0.02	85%
3	0.02	56%
4	0.02	inc.

Note: Inc. = reaction was incomplete after 12 h.
Yields are isolated yields. The catalyst was
recovered and used without modification after each
run.

In summary, the osmium-mediated oxidative cleavage of olefins is

compatible with various different osmium sources. The ability to employ less

volatile and more innocuous osmium sources without sacrificing yield or purity of

the desired product should serve to enhance the usefulness of this mild and effective method for the oxidative cleavage of olefins.

6.3: Experimental Details

General Information:

All commercially available reagents were purchased from Aldrich and used without purification. Solvents were purchased from either Fisher Scientific or Mallinckrodt Chemicals and used without purification. The ^{1}H and ^{13}C NMR spectra were collected on a 300 MHz NMR spectrometer (VARIAN INOVA) using CD_3Cl or acetone-d_6. Chemical shifts are reported in parts per million (ppm). Spectra are referenced to residual solvent peaks. Infrared spectra were collected on a Mattson Galaxy Series FTIR 3000. Samples were prepared using KBr discs.

All known products were characterized by ^{1}H and ^{13}C NMR. ^{1}H and ^{13}C NMR data for all samples of benzoic acid, nonanoic acid, and acetophenone were in full agreement with commercial samples of the same compound. The ^{1}H and ^{13}C NMR for lactone VI-30 were in full agreement with an authentic sample previously prepared in our group.[16] The ^{1}H and ^{13}C NMR data for substrate VI-25,[25] diol VI-35,[26] and acid VI-36[27] were in full agreement with data published elsewhere.

General Procedure for the Oxidative Cleavage of Olefins:

The osmium source and Oxone (4 mmol, 4 equiv. relative to the olefin) were added to DMF (10 mL) at RT. Osmium loadings varied as follows: 0.01 equiv. was employed when osmium tetroxide, osmium trichloride, or potassium osmate were used. Polymer-bound osmium tetroxide was used in either 0.001 equiv. or 0.01 equiv. depending on the substrate as indicated in Table VI-1. OsEnCat™ was employed in either 0.0025 equiv. or 0.01 equiv. depending on the substrate as indicated in Table VI-1. When osmium trichloride or potassium osmate were employed, the resulting mixture was stirred for 0.5 h prior to addition of olefin to allow for the pre-oxidation of the catalyst, after which time the olefin (1 mmol, 1 equiv.) was added in one portion and the resultant mixture was stirred for 12 h. For all other osmium sources the olefin was added directly after the addition of the osmium source and Oxone. After the reaction was judged to be complete by TLC, the resulting mixture was poured into a separatory funnel and the remaining Os (VIII) was reduced by adding an equal volume of saturated sodium sulfite solution. The resulting slurry was then extracted with ethyl acetate (3X). The combined organics were then washed with 1N HCl (3X) and brine, dried over anhydrous sodium sulfate, and concentrated by rotary evaporation. The crude products were then purified by silica gel chromatography or recrystallization where necessary.
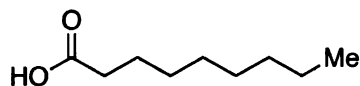
Analytical Data for the products of Table VI-1:

**VI-18**, Benzoic acid (product from the cleavage of **VI-17**, **VI-21**, **VI-24** and **VI-26**)
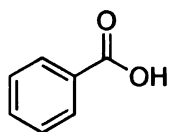
^{1}H NMR (300 MHz, CD₃Cl): δ 11.8 (br s, 1H), 8.13 (m, 2H), 7.61 (m, 1H), 7.47 (m, 2H); ^{13}C NMR (75 MHz, CD₃Cl): δ 172.5, 133.8, 130.2, 129.3, 128.5.

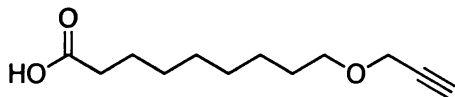**VI-20**, Nonanoic acid (product from the cleavage of **VI-20** and **VI-25**)

^{1}H NMR (300 MHz, CD₃Cl): δ 9.8 (br s, 1H), 2.30 (t, J = 7.5 Hz, 2H), 1.59 (pentet, J = 7.5 Hz, 2H), 1.1-1.3 (m, 8H), 0.84 (t, J = 6.9 Hz, 3H); ^{13}C NMR (75 MHz, CD₃Cl): δ 180.2, 34.1, 31.8, 29.17, 29.06, 29.03, 24.7, 22.6, 14.0.

VI-23, Acetophenone
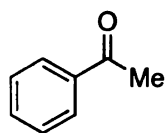
^{1}H NMR (300 MHz, CD₃Cl): δ 7.94 (m, 2H), 7.54 (m, 1H), 7.61 (m, 1H), 7.44 (m, 2H), 2.59 (s, 3H); ^{13}C NMR (75 MHz, CD₃Cl): δ 198.2, 137.1, 133.1, 128.5, 128.3, 26.6.

VI-28, 9-(Prop-2-ynloxy)nonanoic acid

^{1}H NMR (300 MHz, CD$_3$Cl): δ 4.12 (d, J = 2.3 Hz, 2H), 3.48 (t, J = 6.6 Hz, 2H),

2.39 (t, J = 2.3 Hz, 1H), 2.32 (t, J = 7.2 Hz), 1.59 (m, 4H), 1.4-1.2 (br m, 8H);

HRMS (C$_{11}$H$_{20}$O$_3$), Calc. (M+H): 213.1491, Found (M+H): 213.1490.

VI-30, Dibenzo[c,e]oxepin-5(7H)-one[16]
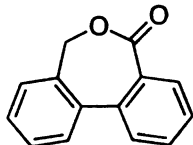
^{1}H NMR (300 MHz, acetone-d$_6$): δ 7.91 (m, 1H), 7.73 (m, 2H), 7.59 (m, 2H), 7.48

(m, 1H), 5.06 (s, 2H); ^{13}C NMR (75 MHz, acetone-d$_6$): δ 170.1, 139.7, 137.8,

136.4, 133.4, 132.4, 132.0, 130.9, 129.56, 129.54, 129.4, 129.3, 129.2, 69.4.

Preparation of Substrates

**Preparation of Substrate VI-25, 2-Methyl-2-dodecene[25]**
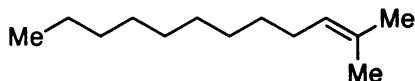
To a flame-dried 250 mL three-neck flask equipped with a magenetic stir

bar was added *iso*-propyltriphenylphosphonium iodide (4.76 g, 11 mmol, 1.1

equiv.). The necks were sealed with rubber septa and equipped with a nitrogen

inlet. Freshly distilled THF (50 mL) was added to the mixture was cooled to 0 °C

on an ice bath. A 7.5 mL portion (12 mmol, 1.2 equiv.) of *n*-butyl lithium (1.6 M in hexanes) was added dropwise to the stirred mixture via syringe. The resulting solution was stirred on the ice bath for 20 minutes, at which time nonanal (1.72 mL, 10 mmol, 1 equiv.) was added dropwise via syringe. The resulting mixture was stirred overnight while warming to room temperature. The reaction mixture was then diluted with diethyl ether (50 mL) and washed with water (2 X 100 mL) and saturated brine (100 mL). The organics were then dried (anhydrous Na₂SO₄) and concentrated by rotary evaporation. The desired product was isolated (1.31 g, 78 % yield) after purification by silica gel column chromatography (1% ethyl acetate in hexanes). The product so isolated had ¹H and ¹³C NMR data in full agreement with literature data for a sample prepared by other means.[25]

¹H NMR (300 MHz, CD₃Cl): δ 5.10 (m, 1H), 1.94 (m, 2H), 1.67 (s, 3H), 1.58 (s, 3H), 1.38-1.20 (m, 10H), 0.86 (t, *J* = 6.6 Hz, 3H); ¹³C NMR (75 MHz, CD₃Cl): δ 131.1, 125.0, 31.9, 29.9, 29.6, 29.4, 29.3, 28.1, 25.7, 22.7, 17.6, 14.1.

**Preparation of VI-27, 10-(Prop-2-ynyloxy)dec-1-ene**
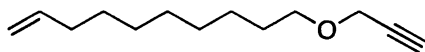
To a flame-dried 100 mL round-bottom flask equipped with a magnetic stir bar was added freshly distilled THF (20 mL) and 9-decen-1-ol (3.6 mL, 20 mmol,

1 equiv.). The resulting solution was cooled to 0 °C on an ice bath. An 8 mL

portion (20 mmol, 1 equiv.) of n-butyl lithium (2.5 M in hexanes) was added

dropwise via syringe. The resulting solution was stirred at 0 °C for 30 minutes.

Propargyl bromide (5.35 mL, 48 mmol, 2.4 equiv.) was added dropwise via

syringe, and the resulting mixture was stirred overnight while warming to room

temperature. The reaction mixture was then diluted with diethyl ether (20 mL)

and washed with water (2 X 50 mL) and saturated brine (50 mL). The organics

were dried (anhydrous Na_2SO_4) and concentrated by rotary evaporation. The

crude product was then purifed by silica gel column chromatography (10% ethyl

acetate in hexanes) to return 1.56 g of the desired product (40% yield) as a pale

yellow oil.

^{1}H NMR (300 MHz, CD_3Cl): δ 5.78 (m, 1H), 4.94 (m, 2H), 4.1 (m, 2H), 3.48 (t, J =

6.6 Hz, 2H), 2.39 (m, 1H), 2.01 (m, 2H), 1.56 (m, 2H), 1.4-1.2 (m, 10H); ^{13}C NMR

(75 MHz, CD_3Cl): δ 139.2, 114.1, 80.0, 74.0, 70.2, 58.0, 33.8, 29.5, 29.4, 29.3,

29.0, 28.9, 26.0; IR (KBr discs, νcm^{-1}): 3310, 3079, 2930, 2857, 2251; HRMS

(C13H22O), Calc: (M+H): 195.1749, Found (M+H): 195.1744.

Preparation of VI-35, 2-Phenyl-1,2-propanediol[26]
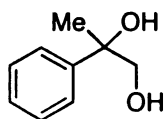
A 20 mL screw-top vial was charged with α-methylstyrene (260 μL, 2 mmol, 1 equiv.), N-methylmorpholine N-oxide (281 mg, 2.4 mmol, 1.2 equiv.), and 10 mL of a 9:1 acetone/water mixture. To this stirred solution was added 10 μL of a solution of osmium tetroxide (1M in toluene). The resulting mixture was stirred for three days at room temperature. The mixture was poured into a separatory funnel and quenched by addition of 10 mL of a saturated sodium sulfite solution. The aqueous layer was then extracted with ethyl acetate (3X 20 mL). The combined organics were washed with water (100 mL) followed by saturated brine (100 mL) and dried over anhydrous sodium sulfate. On concentration by rotary evaporation the desired product was isolated in 67% yield (205 mg).

^{1}H NMR (300 MHz, CD$_3$Cl): δ 7.4-7.2 (m, 5H), 3.69 (d, J = 11.1 Hz, 1H), 3.53 (d, J = 11.1 Hz, 1H), 3.10 (br s, 1H), 2.65 (br s, 1H), 1.46 (s, 3H); ^{13}C NMR (75 MHz, CD$_3$Cl): δ 144.7, 128.0, 126.8, 124.8, 74.6, 70.6, 25.6.

Preparation of VI-36, 2-Phenylpropanoic acid[27]
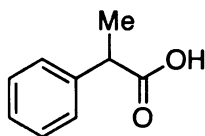
A 20 mL screw-top vial equipped with a stir bar was charged with 2-phenylpropionaldehyde (265 μL, 2 mmol, 1 equiv.) and 10 mL of DMF. Oxone (1.35 g, 2.2 mmol, 1.1 equiv.) was added and the resulting slurry was stirred

overnight at room temperature. The reaction mixture was poured into a separatory funnel and diluted with 25 mL of water. The aqueous layer was then extracted with ethyl acetate (3X 25 mL). The combined organics were washed with 1N HCl (3X 100 mL) and saturated brine (100 mL). The organics were then dried over anhydrous sodium sulfate and concentrated by rotary evaporation to return 265 mg (88% yield) of the desired carboxylic acid.

^{1}H NMR (300 MHz, CD$_3$Cl): δ 7.35-7.20 (m, 5H), 3.76 (q, J = 7.2 Hz, 1H), 1.53 (d, J = 7.2 Hz, 3H); ^{13}C NMR (75 MHz, CD$_3$Cl): δ 180.9, 139.4, 128.4, 127.3, 127.1, 45.1, 17.8.

6.4: References

1.   Travis, B. R.; Narayan, R. S.; Borhan, B. *J. Am. Chem. Soc.* **2002**, *124*, 3824-3825.

2.   DelMonte, A. J.; Haller, J.; Houk, K. N.; Sharpless, K. B.; Singleton, D. A.; Strassner, T.; Thomas, A. A. *J. Am. Chem. Soc.* **1997**, *119*, 9907-9908.

3.   Deubel, D. V.; Frenking, G. *Acc. Chem. Res.* **2003**, *36*, 645-651.

4.   Travis, B.; Borhan, B. *Tetrahedron Lett.* **2001**, *42*, 7741-7745.

5.   Travis, B. R.; Ciaramitaro, B. P.; Borhan, B. *Eur. J. Org. Chem.* **2002**, 3429-3434.

6.   Travis, B. R.; Sivakumar, M.; Hollist, G. O.; Borhan, B. *Org. Lett.* **2003**, *5*, 1031-1034.

7.   Pappo, R.; Allen, D. S.; Lemieux, R. U.; Johnson, W. S. *J. Org. Chem.* **1956**, *21*, 478-479.

8.   Yu, W. S.; Mei, Y.; Kang, Y.; Hua, Z. M.; Jin, Z. D. *Org. Lett.* **2004**, *6*, 3217-3219.

9.   Vanrheenen, V.; Kelly, R. C.; Cha, D. Y. *Tetrahedron Lett.* **1976**, 1973-1976.

10. Schroder, M. *Chem. Rev.* **1980**, *80*, 187-213.

11. Kolb, H. C.; Vannieuwenhze, M. S.; Sharpless, K. B. *Chem. Rev.* **1994**, *94*, 2483-2547.

12. Zaitsev, A. B.; Adolfsson, H. *Synthesis* **2006**, 1725-1756.

13. Milas, N. A.; Trepagnier, J. H.; Nolan, J. T.; Iliopulos, M. I. *J. Am. Chem. Soc.* **1959**, *81*, 4730-4733.

14. Sharpless, K. B.; Akashi, K. *J. Am. Chem. Soc.* **1976**, *98*, 1986-1987.

15. Tsui, H. C.; Paquette, L. A. *J. Org. Chem.* **1998**, *63*, 8071-8073.

16. Schomaker, J. M.; Travis, B. R.; Borhan, B. *Org. Lett.* **2003**, *5*, 3089-3092.

17. Schomaker, J. M.; Borhan, B. *Org. Biomol. Chem.* **2004**, *2*, 621-624.

18. Hergenrother, P. J.; Hodgson, A.; Judd, A. S.; Lee, W. C.; Martin, S. F. *Angew. Chem., Int. Ed.* **2003**, *42*, 3278-3281.

19. Whitehead, D. C.; Travis, B. R.; Borhan, B. *Tetrahedron Lett.* **2006**, *47*, 3797-3800.

20. Cainelli, G.; Contento, M.; Manescalchi, F.; Plessi, L. *Synthesis* **1989**, 45-47.

21. Cainelli, G.; Contento, M.; Manescalchi, F.; Plessi, L. *Synthesis* **1989**, 47-48.

22. Lee, A. L.; Ley, S. V. *Org. Biomol. Chem.* **2003**, *1*, 3957-3966.

23. Ley, S. V.; Ramarao, C.; Lee, A. L.; Ostergaard, N.; Smith, S. C.; Shirley, I. M. *Org. Lett.* **2003**, *5*, 185-187.

24. Ley, S. V.; Norman, J.; Griffith, W. P.; Marsden, S. P. *Synthesis* **1994**, 639-666.

25. Rao Volla, C. M.; Vogel, P. *Angew. Chem., Int. Ed.* **2008**, *47*, 1305-1307.

26. Sharpless, K. B.; Amberg, W.; Bennani, Y. L.; Crispino, G. A.; Hartung, J.; Jeong, K. S.; Kwong, H. L.; Morikawa, K.; Wang, Z. M.; Xu, D. Q.; Zhang, X. L. *J. Org. Chem.* **1992**, *57*, 2768-2771.

27. Ito, R.; Umezawa, N.; Higuchi, T. *J. Am. Chem. Soc.* **2005**, *127*, 834-835.